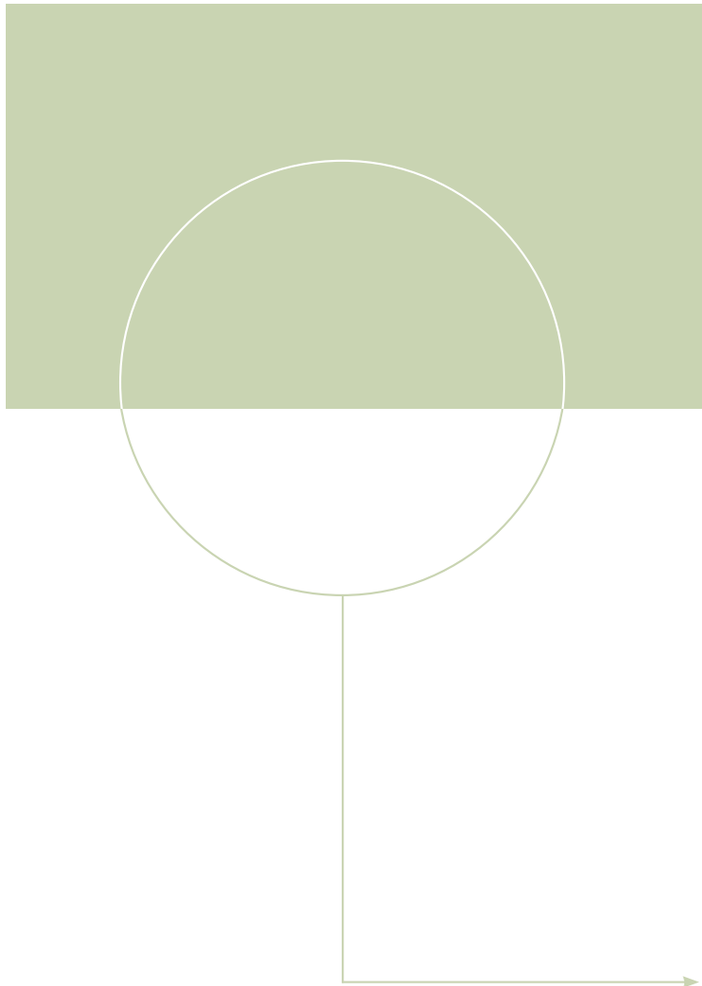

Master's thesis

2020

Mahmoud Kenawi

NTNU
Norwegian University of
Science and Technology
Faculty of Engineering
Department of Civil and Environmental Engineering

Mahmoud Kenawi

Flow Ramping from Hydropower Operation

Evaluation of Trends and Mitigation of Peak Supply and Environmental Impacts in Norway

June 2020

NTNU
Norwegian University of
Science and Technology

NTNU
Norwegian University of
Science and Technology

NTNU
Norwegian University of
Science and Technology

Flow Ramping from Hydropower Operation

Evaluation of Trends and Mitigation of Peak Supply and Environmental Impacts in Norway

Mahmoud Kenawi

MSc. Environmental Engineering and Management
Submission date: June 2020
Supervisor: Knut Alfredssen
Co-supervisor: Jo Halvard Halleraker

Norwegian University of Science and Technology
Department of Civil and Environmental Engineering

NTNU
Norwegian University of
Science and Technology

Flow Ramping from Hydropower Operation

Evaluation of Trends and Mitigation of Peak Supply and Environmental Impacts in Norway

Mahmoud Kenawi

MSc. Environmental Engineering and Management
Submission Date: June 2020
Supervisor: Knut Alfredssen
Co-Supervisor: Jo Halvard Halleraker

Norwegian University of Science and Technology
Department of Civil and Environmental Engineering

ACKNOWLEDGMENT

I would like to express my deepest gratitude to my supervisors Prof.Knut and Jo, for their unconditional support and their guidance throughout this work. Their ideas, recommendations, and contributions were very beneficial and very well-acknowledged to this work and me as a person. For their support and motivations despite all the circumstances that occurred during this work.

To my friends, Ahmed, Helena and Mahmoud who showed generous support and motivation for me while working on my thesis.

To my mother, the most important person in my life for everything she did and keeps doing to support me. I wouldn’t reach this point in my life without you. Thank you for being in my life.

ABSTRACT

Increased flexibility is vital in hydropower systems to meet future market demands, and work is undertaken to improve hydropower machinery to handle larger ramping rates and more frequent starts and stops. This increased flexibility simultaneously can cause rapid changes in the flow rate known to be as flow ramping. The impacts of flow ramping on downstream rivers due to hydropower operation are documented in several studies and expected to increase in the future that it would require mitigation measures to provide an environmentally friendly production regime.

This work aims for two main tasks. First, to put a grasp on the current level and characteristics of the flow ramping in Norway by analyzing the hourly turbine discharge data for various hydropower plants using various hydrological indicators and tools used to quantify this impact and assessing the efficiency of the provided environmental legislation and restrictions to eliminate this impact. Second, to evaluate this flow ramping impact and mitigation measures in future production scenarios with the implementation of the HydroFlex production scenario using hydraulic modeling on the river Nidelva in Norway.

Results show that the occurred flow ramping varies in terms of level and characteristics depending on the type and operational pattern of the power plant itself. Additionally, the provided measures and environmental legislation to restrict this ramping showed some efficiency in reducing the magnitude of this ramping, yet; they did not cover all potentially ecologically power plants. On the contrary, the intensity of flow ramping is expected to increase severely due to the implementation of the HydroFlex production scenario, and the provided traditional measures are not feasible solutions for mitigating this increased impact in the investigated river Nidelva. It can be concluded that it is crucial to further assess the efficiency of innovative technologies to coop with this increasing ramping ratio. Lastly, using hydraulic modeling can be a very efficient tool for mapping out the impact of flow ramping, and its recommended to use for further assessment of such impact from different production scenarios.

CONTENTS

LIST OF FIGURES

LIST OF TABLES

ABBREVIATIONS

IPCC . . . . . Intergovernmental Panel on Climate Change

MW . . . . . Megawatt

GW . . . . . Gigawatt

kWh . . . . . Kilowatt hour

TWh . . . . . Terawatt hour

HP . . . . . Hydropower Plant

IHA . . . . . International Hydropower Association

WFD . . . . . Water Framework Directive

JRC . . . . . Joint Research Centre

EU . . . . . European Union

HMWB . . . . . Heavily Modified Water Bodies

ACUR . . . . . Air Cushion Underground Cavern

BESS . . . . . Battery Energy Storage System

LCA . . . . . Life Cycle Assessment

NVE . . . . . The Norwegian Water Resources and Energy Directorate

EIA . . . . . Environmental Impact Assessment

NTNU . . . . . Norwegian University of Science and Technology

VOL . . . . . Volume

R . . . . . River

L . . . . . Lake

F . . . . . Fjord

Env . . . . . Environmental

RoR . . . . . Run of River

COSH . . . . . Characterization of rapid fluctuations of flow and stage in rivers in consequence of hydropeaking

SINTEF . . . . . Stiftelsen for industriell og teknisk forskning (The Foundation for Industrial and Technical Research)

Inc . . . . . Increase

Dec . . . . . Decrease

RoC . . . . . Rate of Change

M-K . . . . . Mann Kendall trend test

LiDAR . . . . . Light Detection and Ranging

HEC-RAS . . . . Hydrologic Engineering Center's River Analysis System

WSE . . . . . Water Surface Elevation

S . . . . . Mann Kendal test value

VAR . . . . . Variance

Cap . . . . . Capacity

CEDERN . . . . Centre for Environmental Design of Renewable Energy

Q . . . . . Discharge value in m^3/s

Avg . . . . . Average

Max . . . . . Maximum

R^2 . . . . . Coefficient of determination

GIS . . . . . Geographic Information System

M.A.S.L . . . . . Meter Above Sea Level

FFR . . . . . Flow Fluctuation Ratio

1. INTRODUCTION

Hydropower is a clean, efficient source for energy production that has an advantage over other renewable energy sources for providing the flexibility of usage (IHA, 2019; Beckitt et al., 2019). It is subsequently considered to be a key component for mitigating the climate effect and transition into a fully green production scenario relying on its flexibility (Beckitt et al., 2019; Charmasson et al., 2018).

This flexibility is expected to increase in hydropower systems to meet the future market demands to coop with the changes in the market demands in a sub-daily time interval and to provide additional balancing for other renewable energy sources to provide a fully integrated, efficient, cheap and green energy production scenario (Graabak and Korpås, 2016; Siemonsmeier et al., 2018).

However, it can also cause severe environmental impacts that affect the ecosystem and biodiversity. One crucial consequence that emerges as a consequence of the flexibility is the rapid artificial change in the discharge or as known flow ramping, which can cause severe impacts on the riverine biota (Moog, 1993; Meile et al., 2011; Sauterleute and Charmasson, 2014; Carolli et al., 2015).

Flow ramping poses threats to the environment downstream of the power plant, and negative impacts have been observed on fish, invertebrates, aquatic plants, and riparian vegetation (Halleraker et al., 2003; Chen et al., 2015; Bejarano et al., 2018). It is also expected that the intensity of this impact will increase in future production scenarios where hydropower provides flexibility and power balancing for other renewable energy sources (Charmasson et al., 2018). Therefore, mitigation measures are needed to eliminate the impacts of the flow variability in the current as well as future production scenarios.

Norway possesses more than 50% of Europe reservoir capacity and relies on more than 95% of its electricity production on hydropower (Graabak and Korpås, 2016; IHA, 2019). The potential hydropower capacity provided by Norway is considered in every green production scenario where this potential can work as a green battery for almost the whole of Europe (Charmasson et al., 2018; Graabak and Korpås, 2016). Hence, it is essential to have an overview of the current potential environmental impact that is resulted from the operational pattern of the hydropower there in the current situation as well as in these future production scenarios.

In Norway, the new energy law in 1991 changed how the power market was organized

(Thaulow et al., 2016; Charmasson and Zinke, 2011), and the incentives for more variability in power production followed the development of the free power market. The short-term price variations and an increasing need for load balancing are all factors that drive a more frequent ramping operation of hydropower plants . Moreover, and based on the projected need for future short term balancing power, the European Union-funded the Hydroflex project (https://www.h2020hydroflex.eu), which aims at developing a turbine with high operational flexibility with up to 30 starts and stops per day (Siemonsmeier et al., 2018). Such an operational pattern will severely increase the level of flow ramping and requires innovative measure for this impact.

The potential negative consequences of flexible operation are acknowledged by the HydroFlex project, and a part of the project aims at developing mitigation measures (Juarez et al., 2019). The focus is on using AirCushion Underground Cavern(ACUR) propsed by Storli and Lundström (2019) to eliminate rapid changes in the outflow from the power plant.

The purpose of this thesis is twofold. The first part evaluates current operational patterns in Norwegian hydropower plants by investigating the following:

- Evaluate the resulted flow ramping in sub-daily time interval from the current operational pattern and assess its characteristics.
- Linking this flow ramping evaluation results with the ecological conditions around the investigated hydropower plants
- Assess the efficiency of the environmental legislation and measures provided to mitigate this impact
- Investigate the relation between the resulted flow ramping and properties of hydropower plants using linear regression
- Determine the existence of any trending of flow ramping in some of the investigated power plants throughout their production time.

Then the second part is focused on the evaluation of mitigation measures. This will have a particular focus on the mitigation related to the Hydroflex project in the river Nidelva. The main objectives of this part are as follows:

- Investigate the ecological impact that will result from the HydroFlex scenario.
- Evaluate the efficiency of traditional mitigation measures to eliminate this impact.
- Investigate the feasibility of ACUR as a mitigation measure for the HydroFlex scenario

2. BACKGROUND

2.1. Flow ramping, hydropeaking and flexible hydropower

Global warming is considered on of the major issues that are related to environmental science nowadays. According to IPCC 5th assessment report, Energy production contributes to more than 35% of the overall CO_2eq emissions (Schrader et al., 2019).

2.1.1 Value of hydropower in electricity system

Hydropower plays a very significant rule in reduction of the level of CO_2-eq since its a renewable source of electricity production with a low-carbon footprint with a median value of 18.5 gCO_2-eq/kWh (IHA, 2019). In addition to its advantages as a clean source of electricity, hydropower has a natural advantage over other renewable energy sources as its water storage can work as energy storage, which can be naturally built or man-made. Storage reservoirs can provide very flexible variable ways of energy production and can also be used for other purposes, such as flood protection, irrigation, and other water management applications. Even though it requires a high initial investment for construction procedures, HP still offers a relatively low price for the electricity that can be with an average of 0.047$ per kWh (IHA, 2019). Additionally, hydropower also provides a very efficient way of generating electricity that can reach up to 90% depending on the head and the turbine type.

As a consequence of its flexibility, hydropower is a key component in every future scenario where other renewable energy sources can be integrated with hydropower to provide a clean, sustainable and flexible source of the electricity system. Hydropower can provide not only a flexible source of clean energy but also to other renewable energy sources such as wind and solar power to enhance their contribution to the power system and prevent the rationing of these variable sources of energy. It can provide flexibility and integration of other renewable sources of energy from being used as a clean, efficient source of electricity to manage the problem of surplus and rationing that is very crucial to these sources (Beckitt et al., 2019).

All the above-mentioned reasons are making valid reasons behind the increasing demand for HP installed capacity all over the world. In 2018 only there was more than 21.8 GW

newly installed HP facilities in various places in the world led by China, Brazil, Pakistan accordingly (IHA, 2019). It is also expected that this growth will expand in the future due to the demand for social and economic development. Figure 2.1 (IHA, 2019) shows the hydropower worldwide growth rate.

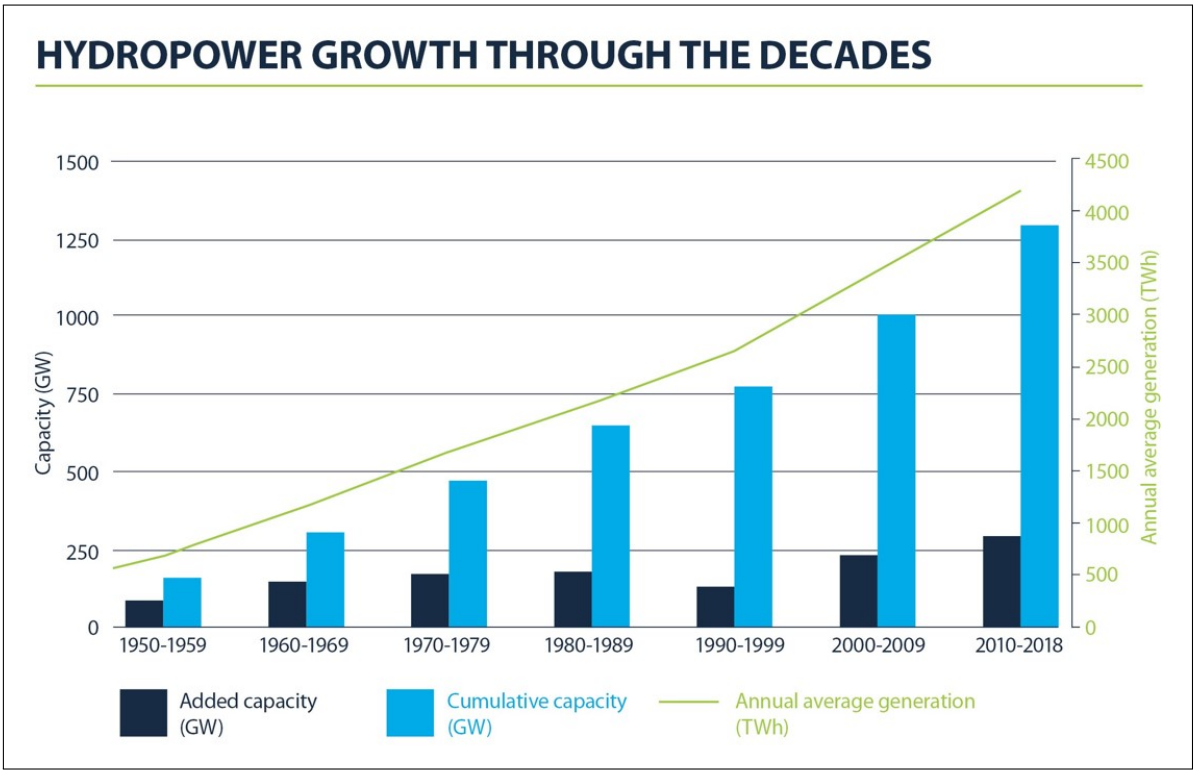

Figure 2.1: HP growth rate worldwide (IHA, 2019).

On the contrary, hydropower can also have a significant potential environmental and social impact during its construction and operation. The increasing growth of HP will axiomatically increase this impact on the ecosystem and the loss of biological diversity. One significant environmental impact that has been noticeably increased due to the increasing demand and growth of the electricity market is **the artificial discharge fluctuation in the rivers downstream** from the way of operation of the HP (Sauterleute and Charmasson, 2014). This can cause ecological damage to the river biota and ecosystem yet can be mitigated by modern measures. This chapter will specify in detail how we can characterize these unnatural fluctuations and evaluate its threshold for causing ecological damage.

2.1.2 Definition of flow ramping

The natural operation of hydropower works by converting the mechanical energy that results from the movement of water into electrical energy. This is done by releasing

high-velocity water through the water turbine then to a downstream outlet in the river. The advantage of hydropower providing a flexible way of operation to meet the electricity supply variation has a drawback as it causes variation in the amount of water released to the outlet depending on the amount of electricity needed.

Flow ramping refers to the rapid artificial increase and decrease of the discharge in the river reach that is resulted from the change in the demand of electricity supply from the hydropower, which alter the hydro-morphological properties in the river downstream such as water lever, velocity and temperature (Sauterleute and Charmasson, 2014). Although that term was defined and recognized as major environmental impact that affects the river ecosystem by many researchers and journals (Moog, 1993; Meile et al., 2011; Sauterleute and Charmasson, 2014), there is a problem identifying the threshold weather this rapid artificial increase and decrease is considered flow ramping or closer to natural increase and decrease that can happen due to rapid snow melt or intensive precipitation. This is because the ecological impact resulted from this way of operation widely varies depending on the river's hydrological and geometrical characteristics, the level of change in the river morphology and the response from the river biota itself to this change which can be determined case-by-case for each river and it can vary within river reaches itself.

Building from that, it is essential to distinguish between the resulted variation of discharge from the change of the market and demand, which is known as hydropeaking (Sauterleute and Charmasson, 2014) and the ecological impact that is resulted from this way of operation whether it exists or not which is flow ramping.

As mentioned above, one of the main advantages of hydropower as a renewable source of energy is its ability to provide flexibility in operation. The rate of electricity production can be adjusted to the amount needed by increasing/decreasing the amount of released water from the storage. This, by default, causes a variation in the flow regime in the river downstream as a consequence of this operation (Moog, 1993).

Another significant factor that can increase the potential of this flow variation is the liberalization of the energy market, which can cause competence enhancing this flow variation into a sub-daily scale with higher rates based on the conditions (Torabi Haghighi et al., 2019).

2.1.3 Environmental impacts from flow ramping

Impacts of the flow ramping has been very well documented by various studies on the river morphology and ecosystem. It is specified according to the Water Framework Direc-

tive (WFD) as one of the main environmental impacts of hydropower generation (Elefther-ria et al., 2011). From a hydro-morphological perspective, these rapid artificial changes in the flow regime affect the natural flow regime downstream as it changes the hydraulic conditions such as Water level, velocity, and sedimentation (Meile et al., 2011). In addi-tion to the before-mentioned, flow ramping can cause a thermal variation, which alters the natural temperature of the river downstream depending on the conditions upstream and the season of the year (Toffolon et al., 2010).

These anthropogenic changes to the river downstream have a severe ecological impact on the river ecosystem. Several studies and experiments have been conducted to docu-ment and assess this impact on the river ecosystem. For instance, the rapid increasing peaks have been well documented its significant effect of flushing the macroinverte-brates species in the river downstream, depending on ramping velocity and duration (Auer et al., 2017; Pellaud, 2007).

This cause as a consequence of the reduction of the population of the macroinvertebrates in the river (Schülting et al., 2016). On the other hand, the rapid decreases in the flow have been documented its impact causing stranding on the fish and dewatering the spawning areas, which has a big effect on the reduction of its population (Halleraker et al., 2003).

The level of the damage caused by flow ramping has been assessed by several hydro-morphological indicators that relate this unnatural change to the ecological impact on the aquatic biota. For example, Indicators of Hydrological Alteration purposed by Richter et al. (1996) aim to quantify the level of hydro-morphological change on the river based on the daily discharge data in the river before and after the regulation of the river while other indicators can be used to assess the impact level caused by the flow variation in sub-daily scales such as Sauterleute and Charmasson (2014) and Meile et al. (2011). However, as mentioned before, reflecting these hydro-morphological changes in the river to the ecological damage on the river biota require investigations for each river case individually to have a proper assessment of the level of the damage (Tonolla et al., 2017).

Moreover, determining the longitudinal level of the damage that can be caused by either rapid increasing or decreasing of the flow and the resulted drifting or stranding effect caused downstream requires further studies assessing to what longitudinal extent these fluctuations can cause damage to the river biota.

Hauer et al. (2017a) conducted a longitudinal assessment of decreasing peaks in different river reaches in the alpine region. His study shows that the impact of the fast decreasing peak can cause significant stranding damage up to 5 km along downstream the river at

where the impact slightly decreases. Other aspects that affect this longitudinal damage level is dependent on the river morphology itself. Figure 2.2 (Hauer et al., 2017a) shows the longitudinal impact of flow ramping to the river downstream

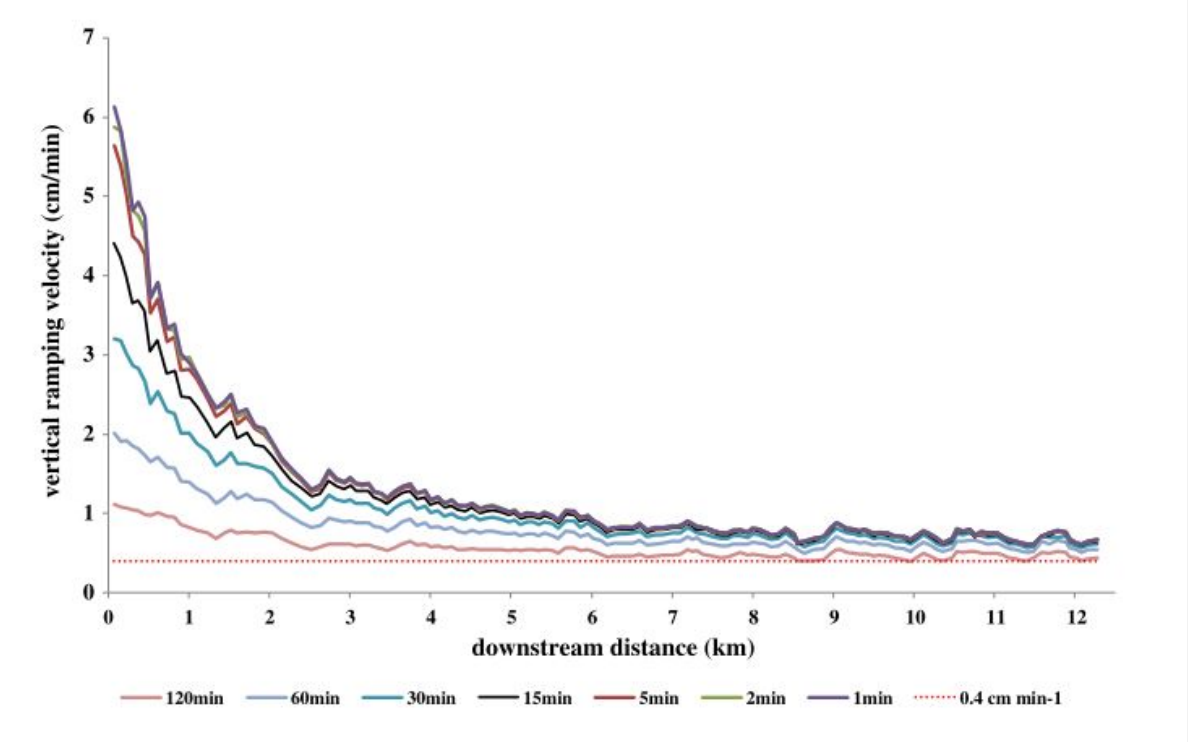

Figure 2.2: Longitudinal ramping velocity downstream (Hauer et al., 2017b)

2.1.4 Current mitigation measures for flow Ramping

Providing mitigation measures to reduce the impact from flow ramping can be rather complex and expensive at the same time (CEN, 2018). The main solution for minimizing this damage to the river biota is by altering the way of operation, which will lead to the economic losses to the power producers and limit their flexibility of renewable sources of energy. However, there have been different mitigation measures provided to reduce this impact. These measures can vary depending on the river characteristics and geometry and which ecological effect that is aimed to achieve. In general, these measures can be categorized into there are 3 main types that can be implemented (CEN, 2018; Charmasson and Zinke, 2011; Greimel et al., 2018) as following:

1. **Operation measures**
2. **Construction measures**
3. **Physical changes in the river geometry**

Operation measures

This method relies mainly on restricting the operational pattern of the HP itself. Depending on the characteristics of aquatic biota and the ecological target needed to be achieved, local studies have to be made to determine the level of damage that needs to be minimized to achieve this target. This can be performed by:

- Applying restrictions on the way of operation of the HP to reduce the magnitude, frequency, and timing of the peak.
- Increasing minimum flow required in the river downstream, which can be either static with a specific discharge amount or can be specified based on the timing of the year.
- Combination between restrictions and applying minimum flow.

All the above-mentioned options need to be determined in case-by-case depending on the river ecosystem and its requirement. However, these kinds of measures usually tend to cause huge economic losses to the hydropower producers since releasing water basically leads to loss of electricity to the producers, and restricting the way of operation on the HP affects the main advantage of hydropower of flexibility of operation.

Construction measures

These type of measures rely on building hydraulic structures to reduce the effect of the peaks such constructions can be:

- Retention ponds
- Multilevel Outlet structures in the reservoir
- Channels to secure water in a specific part of the river

Such hydraulic constructions are also slightly expensive to achieve and in some cases they are neither economically nor technically feasible to use.

Physical modification in the river

This type of mitigation consists of changes in some parts of the river's physical parameters downstream to reduce the impact. Such measures can be :

- River widening to avoid flushing
- Placement of gravel and sediment
- Restoration structures, e.g., Weirs, debris

In addition to the intensive economic cost of finding mitigation for flow ramping, setting up a framework for mitigating the effect of it is rather complex and requires further investigations and assessment of its efficiency. (Tonolla et al., 2017) conducted a general framework for setting up an efficient mitigation measure on a regional scale, Particularly in Switzerland, by connecting the hydro-morphological and ecological indicators in a systematic approach. However, rather few studies have conducted the same approach in different regions. This is because finding mitigation measure varies widely depending on the river characteristics, HP potential ecological scale, and the target that is needed to be achieved, and this requires combinations of field measurements and hydraulic tools to have accurate information on these parameters.

A working group project was conducted by Joint Research Centre (JRC) and under the support of the EU Commission to evaluate the mitigation measures applied for Heavily Modified Water Bodies (HMWB) by hydropower and reservoir operation. The working group investigated the mitigation measures written in each EU state's mitigation measures library. Fifteen countries identified the impact of the rapidly changing flow on the water bodies while eight countries responded that they don't see any need to include any mitigation measures for rapidly changing flow in their library. Six mitigation measures for rapid changing flows were investigated that were reported from the remaining twelve countries. one operational measure, which is reducing the rate of ramping down, three of them were constructional measures while fish stocking was listed as a mitigation measure as well. Results showed that most of these measures provide an efficient ecological response; however, there were some constraints that limit the implementation of these measures. Most of these mitigation measures were reported by EU countries to have either technological or economic costs that constrain from applying them. For instance, the operational measure (reducing ramping rate) was pointed out to be on the top of using water resources among all other flow alteration measures (Halleraker et al., 2016).

2.1.5 Alternative technologies for peak supply

As it was pointed out in the previous section that traditional measures to limit the impact of flow ramping can be rather expensive and technologically infeasible. Some alternative method was introduced to balance between the economic feasibility and ecological protection. Some of these technological aspects are already being implemented, particularly in the alpine region, while others are still in a theoretical approach. In this section, some of these alternative technologies are going to be investigated its efficiency for mitigating the impact that might occur from future scenarios.

Water displacement using air pressure downstream

Storli and Lundström (2019) introduced an alternative technical approach for mitigating the effect of peak supply. This is mainly done by displacing water under air pressure. The study proves the theoretical benefit of giving additional freedom of water management, which in this study focus can be used to flatten the peak of flow fluctuation. Consequently, Storli and Lundström (2019) Introduce using AirCushion Underground Cavern (ACUR) for minimizing the peaking effect by reducing the rate of change of the water going to the downstream. ACUR is basically a cavern filled with specific air pressure from the top and has an intake that allows water to go in and out. ACUR works as a water container with additional pressure from the pressed air that can be used for controlling the velocity of ramping resulted from the natural pattern of the operation.

ACUR has the same concept of air cushion surge chambers that are used to control and minimize water hammer effects. However, there are some limits to this technical approach. Firstly, the size of the excavated cavern relies on the rate of change and how much water needed to be stored to minimize the impact of rapid fluctuation. This can be, in some cases, technologically infeasible to find a suitable location for such volume, or it can have enormous economic costs. Furthermore, the ACUR location must be closer to the water flow, which will make the air pressure inside, not a slightly big difference than the normal atmosphere.

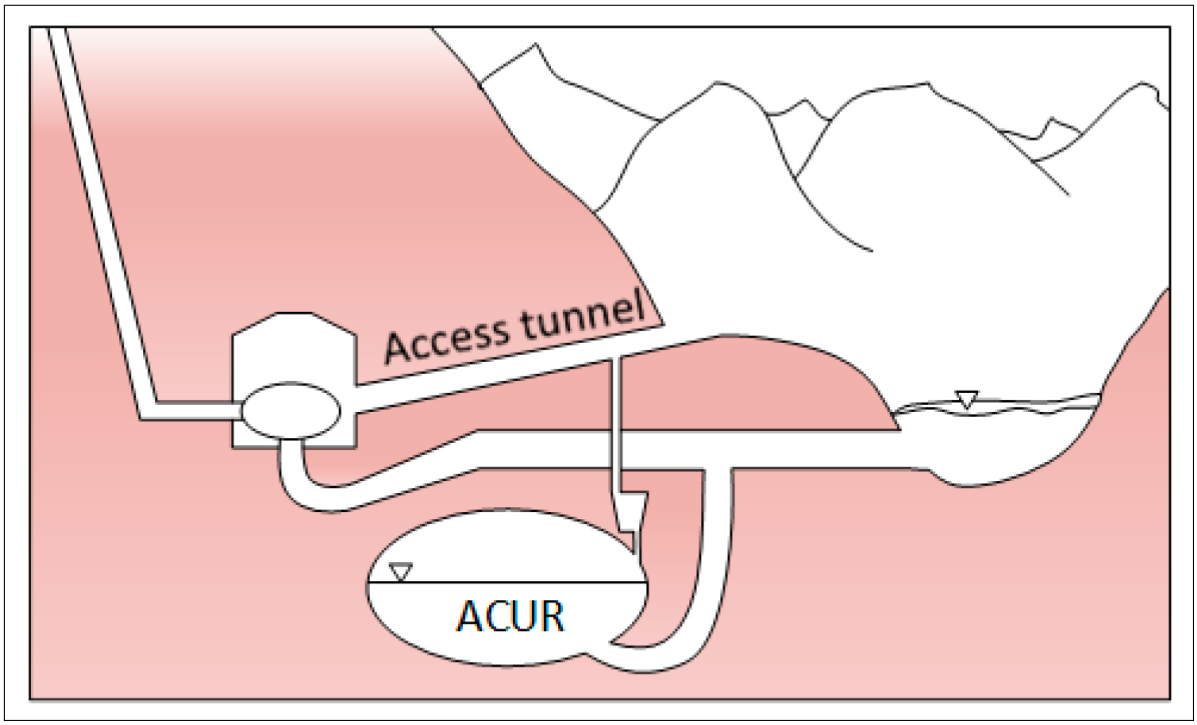

Figure 2.3: Preliminary design for ACUR minimizing flow fluctuations. From Storli and Lundström (2019)

Using Batteries as Storage System

Batteries are already implemented as an energy storage system for balancing the vari-

ability of renewable energy sources. The slightly decreasing costs of manufacturing Lithium-Ion batteries with increasing its efficiency allowed the implementation to increase in the current situation (Alliance for Rural Electrification, 2013). It is even more expected that costs for batteries manufacturing are going to decrease with increasing efficiency more in the future. Furthermore, using batteries as an energy storage system is expected to increase in 100% a response to the increasing demand for the energy storage needed in addition to other different technologies to balance variable renewable resources (Child et al., 2018).

Anindito et al. (2019) proposed an approach where the Battery energy storage system (BESS) can be used to minimize the rate of rapid fluctuations by storing the energy during the low production hours of the power plant and using this energy during the high demand hours. Additionally, Anindito et al. (2019) evaluated the cost efficiency of this approach compared to different approaches where the operational constraints are used to minimize the ramping ratio. Using an interdisciplinary model of hydropower production where economic, technological, and environmental aspects are involved in the model, they evaluated the efficiency of using Batteries as mitigating for flow fluctuation in addition to the usual operational constrains and reservoirs downstream.

His results show that BESS are can mitigate the ramping rate with a slightly lower cost than traditional operational constraints provided that their cost-effectiveness is expected to increase by 10% in the near future. However, his results also show that using reservoirs downstream tends to be more economically efficient and more flexible. Using BESS can be an alternative way of mitigation where it is not possible to construct A reservoir downstream. Furthermore, using batteries as energy storage has additional technological and environmental limitations. Batteries are still limited to their lifetime, and this requires regular maintenance. Additionally, Using Batteries as storage can increase the total carbon footprint of any renewable source of energy. Various Life Cycle Assessment (LCA) studies found out that the GHG emissions of manufacturing batteries can vary widely depending on the location of material extraction and the manufacturing as well as the source of energy used for production (Dai et al., 2019).

Regulation Reservoirs downstream

Using regulation reservoir downstream as mitigation for flow ramping is being implemented and used in the alpine region where the high head of power plant causes severe flow ramping (Tonolla et al., 2017). This measure has proved efficiency in mitigating the measure by various studies (Pérez-Díaz et al., 2012; Tonolla et al., 2017; Halleraker et al., 2016). The central concept of this approach is by providing an artificial lake or reservoir at the river downstream with a controlled discharge rate. This artificial reservoir can be filled with water at the maximum production rate; after that, it can be emptied

during low or no production rate. Figure 2.4 from (Bruder et al., 2016) shows the concept of mitigating the ramping effect using this measure.

In addition to this measure environmental benefits, can also provide more flexibility for HP by implementing a pumped storage system as the downstream reservoir can be used additionally to store water that can be pumped again during low production times (Pérez-Díaz et al., 2012). This measure proved economical and technological efficiency in comparison to using BESS and operational constrains by Anindito et al. (2019). However, such a measure requires intensive construction and changing of the landscape that might result in additional environmental impact. In addition to that, in some cases, such measures cant be feasible to implement as the area needed to regulate this amount of water might not be available at the beginning of the river downstream.

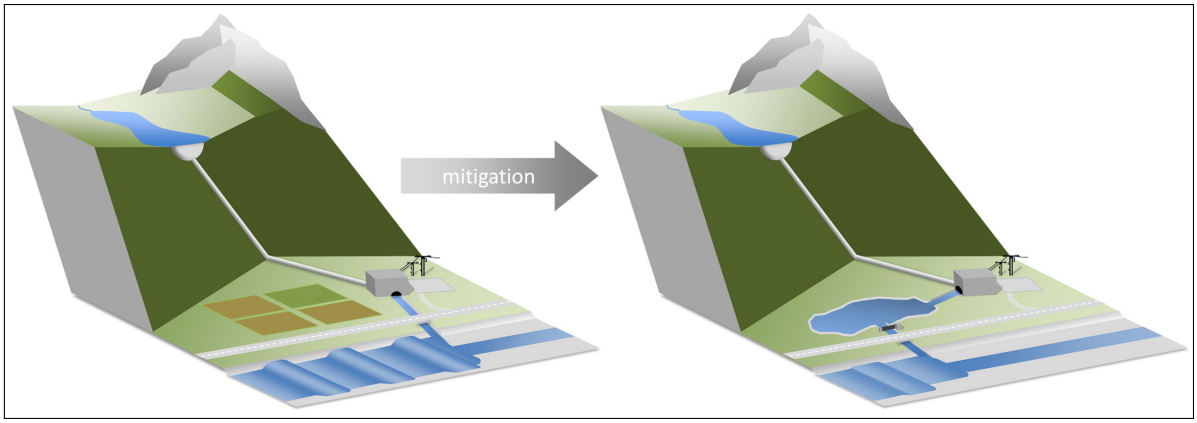

Figure 2.4: Framework of using regulation reservoir as a mitigation measure (Bruder et al., 2016)

2.2. Hydropower operation in Norway

Norway's natural geographic and climatic conditions have made it perfect conditions for hydropower (IHA, 2019). Norway has a widely varied elevation in addition to its natural lake and high precipitation, which made it slightly feasible to rely on such a source of renewable energy. Currently, more than 95% of the electricity produced in Norway is made from hydropower. Norway, by far, the largest hydropower production among EU/EEA countries as it has more than 50% of the storage capacity in Europe. Its additionally expected that this relying on hydropower is going to expand with the connection of the electricity system in the Nordic region and EU (Flataker and Nielsen, 2018).

2.2.1 Overview on the historical way of operation

Norway has been relying on hydropower as a source for energy for industry and society since late 1800. In 1911 the first HP was built for industrial purposes. At that time, the government set up regulations and laws for ensuring the publicity of the hydropower sector and invested heavily in it as a source of energy. During WW2, Germans also invested in the Hydropower sector for Aluminum production. However, the era between 1950 and 1990 witnessed a huge development in the hydropower sector and simultaneously in the transmission and grid system to coop with this huge energy growth. During that time, the potential hydropower capacity increased from 2500 MW to up-to 28000 MW (Thaulow et al., 2016).

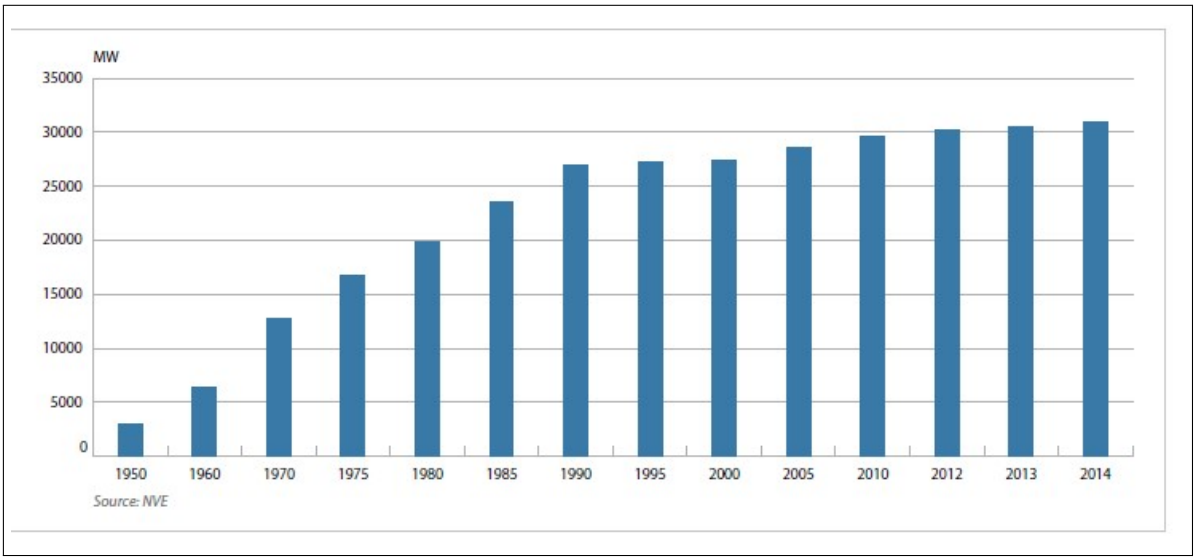

Figure 2.5: Historical Hydropower development in Norway (MPE, 2015).

Despite the fact that environmental science started to gain attention during the 70 ties, hydropower has raised environmental issues since its early development. On a local scale, some waterfalls kept preserved from any hydropower development in the early stage of the development of hydropower. However, hydropower development started to cause more controversy from 1970 till early 1980, where few large HP projects caused debate due to the fear of its environmental impact and the low environmental legislation to have an accurate assessment and minimizing this impact. After that and in the late 1980 ties standard environmental flow was introduced by the legislators whenever new HP is approved (NVE, 2017; Thaulow et al., 2016).

At this time and until 1990, the main environmental impacts that gained the concern were mainly dealing with the effect in the bypass section due to the regulation of the river and how to minimize this impact and in the outlet mainly about thermal change due to the regulation and the sediment problems. The impact of the flow fluctuations

was not widely observed or had any attention or focus (Charmasson and Zinke, 2011).

2.2.2 Energy Act

In 1990, Norway initiated the energy act governing electricity production transition, distribution, and energy price. This act has liberalized the energy market to reach the cheapest and most optimum way of efficient energy use by achieving competition among electricity producers. Under this act, HP owners are entitled to deliver energy to the grid system while consumers can buy the cheapest electricity available (Thaulow et al., 2016; Charmasson and Zinke, 2011; NVE, 2018).

This act, while it made Norway a leading country in a free efficient energy price market, has changed the way of operating the power plant significantly. Many HP operators started to change the rate of production depending on the energy price to achieve the most economic benefit while this caused huge variation in the flow downstream of the river in an irregular seasonally, daily and sub-daily time intervals depending on the highest economic benefit (Charmasson and Zinke, 2011).

Due to this way of operation, the increasing flow ramping started to grasp more attention of the environmental authorities as there has not been any legislation that limits this environmental impact. in 1996 The Norwegian Water Resources and Energy Directorate(NVE) conducted a research project to assess the effect of flow ramping on different aspects of the river morphology and ecology. Its outcome pointed out the negative consequences of flow ramping on the river ecosystem and the reduction of its biota. Further assessment projects have been conducted after that to have a more detailed view of the level of damage caused by this way of operation (Charmasson and Zinke, 2011).

2.2.3 Legislation of Hydropower in Norway and Flow Ramping

In Norway, the Norwegian Water Resources and Energy Directorate (NVE) is the main responsibility for managing the legal matters for the hydropower sector. Its department under the Norwegian ministry of petroleum and energy that is also responsible for managing the country's energy and water resources while water resource management is shared with the Ministry of Climate and Environment. They are the main responsible for issuing and renewing a license for the hydropower operator to ensure the government control on the sector, avoid severe environmental damage from the project during con-

struction and operation and control any means of monopoly services that might occur in the sector. In order to apply for an HP license, the developer has to apply for an application then the volume of the capacity that will be installed determine the licensing authority responsible and the procedures for obtaining the license (Rognstad, 2018; Thaulow et al., 2016).

Small Scale HP < 10 MW

This type of HP is under the responsibility of NVE if the installed capacity is bigger than 1 MW or the installed capacity will have severe environmental/social impact or the expected development is going to affect protected rivers then, in this case, the application must go through NVE then NVE gives its recommendation to the local county for decision. However, in the general case where the HP is bigger than 1 MW, a typical procedure of obtaining the license shall be that the developer submits an application to NVE including simplified EIA and other technical information regarding the development then NVE will make a final decision for this type of development after having a public hearing, consultation with different stakeholders and the field trip to the expected project site.

However, in case of HP that has a capacity less than 1 MW (Micro or Mini) that does not have any severe environmental/social impact or exposed to the protected river, the license can be given directly by the county council with public hearing consultation (Rognstad, 2018; Thaulow et al., 2016).

Large Scale HP > 10 MW

This type of projects has more players involved and more complicated procedures since the Social/Economical/Environmental consequence can be critical. The king in a council with the government has the final decision in issuing the license for the HP or no after several procedures, and steps have to be performed. First, the applicant has to notify the authorities as well as the local people of his interest in the project and provide them with the technical information of the project as well as the environmental impacts from this project and his plan to minimize these impacts. A public hearing has to be made to discuss the social/environmental impacts and the public opinion and worries from the project. All the results from the before mentioned procedures are summed up and included in a full EIA that has to be submitted to NVE, which decides whether the submitted report and the already done procedures are sufficient or require further evaluation and investigation steps. If the EIA is sufficient, then an application has to be sent by the developer to NVE, where it evaluates all the project related information and does a final assessment of it specifying all the related potential environmental/social impacts and possible mitigation measures. Finally, NVE provides a recommendation of whether accepting or rejecting the license to ministry level. The ministry gives the final

recommendation to the parliament, and then the license is granted or rejected by the council that includes the king (Thaulow et al., 2016).

Hydro Power Projects	Installed effect	Licensing authority
Micro	< 100 kW	County Council
Mini	< 1 MW	County Council
Small	< 10 MW	NVE
Large	> 10 MW	King/Government
Special cases	> 20.000 nhp	Parliament

Figure 2.6: Scale of HP and licensing authority (Rognstad, 2018).

When the developer obtains the license, he can proceed with all the construction process for the HP. The license typically contains all the regulation of hydropower operation and specifying all the technical, environmental, and safety procedures related to the hydropower plant (Thaulow et al., 2016). From environmental prescriptive, the license contains all the environmental aspects and policies to ensure that there is no severe damage to the environment during the construction of the hydropower or its operation. Such environmental aspects can be related to the river ecosystem, river morphology, or preventing pollution in general. For example, a minimum flow for the river downstream during the non-operation period has to be specified in the license for each HP if required with the amount and the period of this flow. Also, any means of restriction of the operation of the HP regarding the level of the flow ramping is specified in the license. However, in that case, it is mainly specified with no technical aspect whatsoever, which allows the operators to get over this sort of restrictions (Thaulow et al., 2016).

However, the obtained license has to be revised every 30-50 years to meet the demand for any new technical, social, or environmental aspects that might emerge. In addition to that and with the implementation of the Water Framework Directive (WFD), all the newly granted HP and the revised licenses have to follow all the aims of WFD ensuring the quality of the lightly modified water bodies and aiming for reducing the impact of the heavily modified ones (Thaulow et al., 2016). Nonetheless, modernization of licenses and implementing emerging good practice on relevant mitigation measures seems to be quite slowly being incorporated in management practice.

In conclusion, NVE is considered to be the main responsible for the management, environmental and legal matters related to the hydropower operations in cooperation with environmental authorities. They have a very well established framework for managing this sector; however, they have a limitation on forbidding some specific environmental

impact such as this study goal, which is the flow ramping resulted from the operation of this hydropower on a small and bigger scale.

For instance, Abée-lund and Villar (2017) evaluated the pattern of shutting down and starting the operation of 256 small scales HPs. his study shows that the way of operation has no correlation whether these HPs are permitted to such a way of operation or no. However, the pattern of operation relied more on the average discharge in the river. This shows a clear defect in the interpretation of the legal, environmental requirements, and auditing of the license given to this category of HPs, which require further investigation.

2.3. Future scenarios and energy transition

In addition to what was mentioned in section 2.1.1 regarding the increasing reliability of hydropower, the way of operation of hydropower itself will require more flexibility and variation in production. Consequently, this will lead to more change in the fluctuation of the discharge, which will cause more flow ramping. Further future scenarios will be explained as follows.

2.3.1 EU Green Deal and sustainable hydropower

In 2020, the EU commission has initiated the EU green deal with the aim of becoming a leader in achieving a sustainable way of living for its habitat. The green deal aims towards 4 main goals: 1) Achieving climate neutrality by 2050 2) Ensuring a zero pollution ambition for the environment 3) accelerate towards sustainability 4) Ensure that this transition includes all the EU members (Brussels, 2020).

A key component in achieving these goals is by ensuring the use of clean energy throughout the whole of Europe. As energy production contributes to more than 75% of EU's greenhouse gas emissions (Brussels, 2020; Graabak and Korpås, 2016) EU has set a group of key solutions to achieve climate neutrality and reduce these emissions from the energy sectors. Relying on renewable energy sources is one of the main key components to reaching such a goal. By 2050 its planned that wind and solar shall contribute to 65% of electricity generation (Brussels, 2020). Some balancing technologies were purposed to overcome the variability problem of these renewable sources, which will increase by the increase of the production from such energies (Graabak and Korpås, 2016). Hydropower integration with other renewables, as mentioned in section 2.1.1, is

considered a key solution to this problem where integration can be done on a regional scale.

In various energy scenarios, the potential reservoir's capacity in the Nordic region - where Norway only contain almost half of the storage capacity of the reservoirs with a potential of 85 TWh (Graabak and Korpås, 2016)- is expected to play a significant rule for balancing the energy in northern Europe and gradually to the whole Continent. For instance, (Sauterleute et al., 2015) conducted 4 different scenarios where Nordic hydropower can be used for balancing the electricity from other renewable sources on Short and long time horizon and/or regional or continental scale.

To achieve such integration, two key components shall be developed in the hydropower operation itself. Solar and wind production balancing can be in a sub-hourly time interval, which will require the production of hydropower to be flexible on the same scale. Furthermore, the Seasonal pattern of the Nordic hydropower operation shall change from reservoir filling in spring/summer, and emptying in winter shall change to be more dynamic and irregular to match the uncertainty of the energy production from solar and wind.

Currently, Nordic hydropower works inflexible way depending on the energy demand where it rises during the day and lowers during the night. However, this flexibility is limited on a national scale. There is currently a grid line connection between the northern region; however, the integration between wind solar and hydropower for balancing hasn't been addressed fully (Simensen, 2012). There are some constraints for connecting some of the Nordic hydropower plants to other parts of the Europe grid system (Farahmand et al., 2015). In addition to that, The technology for hydropower to work as pump storage to have the ability to store the surplus energy is rarely existed in the Nordic region and require further development (Graabak and Korpås, 2016).

All the above-mentioned scenarios conducted that the variability of production of HP will become more irregular in the different timescale. However, the environmental impact of such change has been addressed in a quantitative way to show the ecological effect of such change. Charmasson et al. (2018) pointed out the potential environmental impact that will happen due to more rapid and frequent fluctuations will occur. However, they pointed out that further studies need to be addressed to evaluate the ecological damage in the fish population since every river ecological damage can vary significantly yet, they only investigated the water temperature change as an indicator of the river morphological level of change which is not sufficient for assessing the actual ecological damage that might occur from such intense level of flow ramping.

2.3.2 Climate change and hydropower

The climate change effect on Water resources is very well documented. It will also affect the precipitation frequency patterns, frequency of occurrence of extreme conditions, and increase the evaporation rate from the water (Jiménez Cisneros et al., 2015). This will affect the distribution of the water inflow to reservoirs as a result of the influenced hydrological cycle (Chang et al., 2018; Jiménez Cisneros et al., 2015). This change can cause spill loss from reservoirs, which will lead to a loss in energy and economy. Hydropower producers will have to change their way of operation to coop with this change (Tarroja et al., 2016). Introduced more flexibility has been proposed to the producers to avoid or minimize the loss of energy. This flexibility will add additional pressure on water variability as a consequence of the additional needed flexibility.

2.3.3 HydroFlex

Under EU regulation ”H2020-EU.3.3.2 – Low-cost, low-carbon energy supply” EU funded and supported research activities finding innovative technologies to increase relying on renewable energy sources and decrease CO_2 emissions. HydroFlex was initiated in 2018 to increase the flexibility of hydropower operation. The main objective of the project is to create a water turbine that can change its production rate significantly throughout the day. The project has five HPs sites in the Nordic region for practical experiments, and it is coordinated by NTNU (Siemonsmeier et al., 2018).

Reaching such a level of flexibility where the production can change from maximum to zero in 15 minutes will severely increase the ramping ratio in a sub-daily time interval, and proper environmental impact assessment should be conducted for having a proper evaluation of the ecological damage that might occur due to such operation.

Fortunately, the HydroFlex project also considers the environmental consequences of this operation. They conduct environmental assessments simultaneously with technical and management investigations. In their fifth work package, they focus on social and environmental impact assessment. They developed two hydraulic models representing two rivers that are regulated by 2 of the five references HPs, Nidelva and Ume älv. Those two models have been calibrated and validated to evaluate the flow characteristics that will result from different production scenarios (Juarez et al., 2019). In chapter 4, the hydraulic model representing Nidelva will be used to evaluate some mitigation measures and alternative technologies in order to minimize the impact that will occur in their future scenarios.

3. EVALUATION OF FLOW RAMPING IN NORWAY

3.1. Trends in flow ramping from HP operation

To obtain a proper overview on the current level and situation of flow ramping in Norway, It is necessary to evaluate the level of flow ramping that occurs in a different region from a different type of HPs there and to what extent this flow ramping is causing an ecological impact to the riverine ecosystem. Additionally, the environmental legislation and restrictions provided to minimize such impact need to be evaluated. Furthermore, It is required to investigate the existence of a relation between the level of ramping, and some of HP's characteristics such as the head of the HP, type of HP and reservoir capacity as some studies show that the existence of a relation between the level of ramping and the head of HP (Greimel et al., 2018; Bruder et al., 2016). Finally, the historical trend in the level of ramping has to be investigated to evaluate the efficiency of such environmental legislation implemented to restrict it.

3.2. Materials and methods

Hourly and daily turbine discharge data were obtained representing different types of HPs in different time periods from the hydrological department of NVE. Each of HP was evaluated case by case to gain an overview of the HP's technical, hydrological, and geographical characteristics in addition to the legislation specified in their operating license. These details were obtained through NVE Atlas, a portal where all the information regarding the license requirement and characteristics for most HP in Norway are published by law for the public. Additionally, these data from NVE Atlas were combined with WFD database for Norway.

Eventually, and after processing the quality of the obtained data, we ended up having 57 hourly turbine flow data of HPs mostly in the period from 2010-2018 and 117 daily data with various periods, different outlet locations, and different characteristics. Since this chapter aims to investigate the impact caused by flow ramping in a sub-daily time interval, the daily time interval data were excluded from further analysis. Additionally, the quality of the data was checked by removing the irregularities and years with missing data by processing the data through R. R is a free programming language that is

mainly used for data science and statistical analysis. Eventually, the final data that were analyzed are presented in table 3.1. Restrictions on this table refer to the limitation of changing of the rate of production and instant shutdown that is specified in the license of the HP. Additionally, the option of the existing bypass valve in the power plant is an efficient solution for mitigating the severe impact from the instant shut down due to any accidents which can cause severe stranding effect on the river downstream. Various hydrological indicators were used in order to evaluate and quantify the occurred flow ramping from the operation of these HPs. Hourly data was analyses by the methods described in the following sub-chapters.

3.2.1 COSH tool

First, COSH tool was used for the assessment. COSH is a computational tool developed by a collaboration of SINTEF and Centre for Environmental Design of Renewable Energy (CEDREN) (Sauterleute and Charmasson, 2014) for quantifying the effect of hydropeaking in a sub-daily time interval. Using this tool allows having a quantified indicator of the resulted flow ramping behavior on the river downstream. These indicators are similar to indicators of hydrological alteration derived by Richter et al. (1996) categorized into three categories describing magnitude, frequency, the timing of the rapid fluctuations in the river downstream, yet they are modified to coop with the sub-daily time interval.

The tool workflow has three main steps to identify whether the change in the discharge is considered a peaked flow and calculate its effect or neglect it. First, the data series were imported into the software after ensuring there is no irregularity in the time interval. Most of the data series that were obtained are from the period 2010-2018; however, the years with missing data were excluded to ensure the quality of the results. After the data series were loaded, the tool identifies a threshold for considering the change of the discharge in one time step as an increasing or decreasing ramping event is defined.

The threshold values for considering the change of discharge ($\triangle Q_{th}$) in one time step a fast increase or decrease is first defined by multiplying the absolute maximum rate of change in the whole time series by factors of increase and decrease. These factors usually vary between 0.05 to 0.2. Then if the rate of change in the time step $\triangle Q_t > \triangle Q_{th}$ for increase and decrease respectively then this is considered a peak otherwise it is neglected.

Finally, the output from the tool after running through the whole time series for each of the studied HP would be a set of statistical indicators to determine the characteristics of the peaking behavior from each HP to the river downstream. In our investigated results

here we decided to present and further analysis the following indicators:

- Average annual number of increasing/decreasing peak
- Distribution of the number of increasing/decreasing peak throughout the day
- Average number of increasing/decreasing peaks in the day
- Maximum Rate of change that can occur during increasing/decreasing peaks per year

Table 3.1: Overview on the Analyzed HP properties with hourly turbine flow data time interval

Name	Number	Time period	HP type	Outlet	Max Q m3/s	Cap. MW	Head (m)	Vol Mill.M3	Restrictions	Env.Flow m3/s	Bypass valve
Alta	3	2010-2018	Reservoir	R	96.0	150	185	135	Yes	16	T
Bingsfoss	22	2001-2019	RoR	R	820.0	32.5	5	0	-	0	F
Bogna	34	2010-2018	Reservoir	L	23.8	57	290	150	-	0	F
Borgund	35	2010-2018	Reservoir	R	28.0	212	874	74.7	Yes	0	F
Braskereidfoss	37	2000-2019	RoR	R	450.0	35.95	9.5	0.5	-	65	F
Bratsberg krv	38	2010-2018	Reservoir	R	105.0	124	145	366.7	No	30	F
Brattset	40	2010-2018	Reservoir	R	36.0	80	268.9	1.7	No	0	T
Dividal	58	2010-2018	Reservoir	R	11.6	26	278.5	135.7	Yes	0	F
Driva	63	2010-2018	Reservoir	R	30.0	140	565.59	280	Yes	11	T
Eidfoss	68	2011-2018	RoR	R	93.8	13.2	18.89	0	No	0	F
Einunna	75	2008-2019	Reservoir	R	9.0	9	121.69	85	-	-	F
Fjæremsfoss	87	2010-2015	RoR	R	80.3	18.8	27	0	-	0	F
Follafoss	92	2010-2018	Reservoir	F	29.0	48.1	175.3	32	No	0	F
Skagen	94	2010-2018	Reservoir	R	32.5	270	967	28.8	No	0	F
Funnefoss	102	2003-2019	RoR	R	444.4	40	10.5	0	-	-	F
Grana	113	2010-2018	Reservoir	R	19.0	75	455	144	-	0	F
HARPEFOSS	131	2005-2019	RoR	R	400.0	108	34.62	0	No	-	F
Hemsil II	142	2010-2011	Reservoir	R	31.0	98	370	0	Yes	-	F
Hjartal	147	2010-2018	Reservoir	L	32.4	104	592	91.2	No	-	F
Storåni	154	2010-2018	Reservoir	R	299.1	106	308	544	No	0	F
Hunderfossen	164	2010-2018	Reservoir	R	30.6	112	46.4	1312	No	15	F
Kolsvik krv	209	1996 2017	Reservoir	F	7.3	128	519	188.1	No	0	T
Kongsfjord	210	2010-2018	Reservoir	L	510.0	4.4	70.5	88.1	No	0.9	F
Kongsvinger	212	2005-2018	RoR	R	284.0	42.7	10.25	0	-	-	F
Laudal	239	2004-2018	Reservoir	R	30.0	32	36	2	Yes	8	F
Litjfossen	247	2010-2018	Reservoir	L	5.5	75	285	150	-	30	F
Lysebotn krv	256	2008-2013	Reservoir	R	176.0	5.35	106	38.4	No	-	F
Lopet	260	2005-2019	Reservoir	R	12.0	29	18.89	75	No	-	F
Mesna	268	2003-2019	Reservoir	L	20.0	37.5	356	81.4	-	-	F
Mørre	285	2010-2018	Reservoir	F	80.0	13.6	81.3	12.4	No	0	F
Nedre Vinstra	302	2009-2018	Reservoir	L	55.0	308	443.2	31.1	No	-	F
Søre Osa	321	2010-2018	Reservoir	R	2.5	90	200	265	-	-	F
Reinset	334	1998-2003	Reservoir	R	60.0	4.9	263.6	10.5	No	1.5	F
Rendalen	336	2010-2018	RoR	R	1215.0	100.5	209.69	0	No	-	F
Raanaafoss	349	2016-2018	RoR	R	32.0	128.4	12.3	1312	-	-	F
Savalen	363	2002-2019	Reservoir	R	18.5	62	230	61.2	-	-	F
Skibotn	375	2010-2018	Reservoir	R	220.0	70	440	145.6	Yes	6	F
Skjefstadfoss	377	2011-2018	RoR	R	258.3	19.8	12.8	0	No	40	F
Skogfoss	383	2010-2018	Reservoir	L	16.0	48	19.7	2684	No	0	F
Sokna	393	2010-2018	Reservoir	R	110.0	25	185	1	No	0	F
Solhom	396	2010-2018	Reservoir	L	248.0	200	215	336.8	No	-	F
Straumsmo	404	2009-2012	Reservoir	R	70.0	130	229	3.7	No	0	F
Svartelva krv	414	2010-2018	Reservoir	R	16.6	15.5	107.9	74	No	0	F
Svorkmo	422	2000-2018	Reservoir	R	69.1	55	96	-9999	Yes	-	T
Søa	424	2010-2018	Reservoir	F	16.0	37	273.2	67	No	-	F
Tonstad	448	2010-2018	Reservoir	L	36.1	960	442	70.19	No	0	F
Ulset	474	2010-2018	Reservoir	R	253.2	35	151.5304	132	No	-	F
Usta II	480	2010-2011	Reservoir	L	12.0	184	540	385	No	-	F
Øvre Tessa	522	2012-2018	Reservoir	L	11.2	16	175	130	-	Only summer	F
Åna-Sira	528	2010-2018	Reservoir	F	375.4	150	47	155	-	0	F
Årøy	530	2010-2018	Reservoir	R	70.0	90	147	53	Yes	3	F
Dokka	537	2008-2019	Reservoir	L	41.0	44.6	130	-9999	-	-	F
Mel	549	2010-2018	Reservoir	R	7.5	52	810	60.3	Yes	1.5	F
Stuvane	557	2010-2018	Reservoir	R	28.0	38	156.19	7.7	Yes	-	F
Meråker	619	2010-2018	Reservoir	R	36.7	86.8	263.7	4.5	Yes	9.5	T
Solbergfoss	776	2010-2018	RoR	R	1200.0	208	21.29	314	No	-	F
Øyberget	828	2010-2018	Reservoir	R	75.0	99.5	149.6	0.55	Yes	0.3	F
Framrusti	829	2010-2018	Reservoir	R	27.0	75	325.6	166	Yes	0.65	F

Note | *R=River>0.5 km,L=Lake/Reservoir,F=Fjord,C=Cascade, T= True, F= False, - = Missing data*

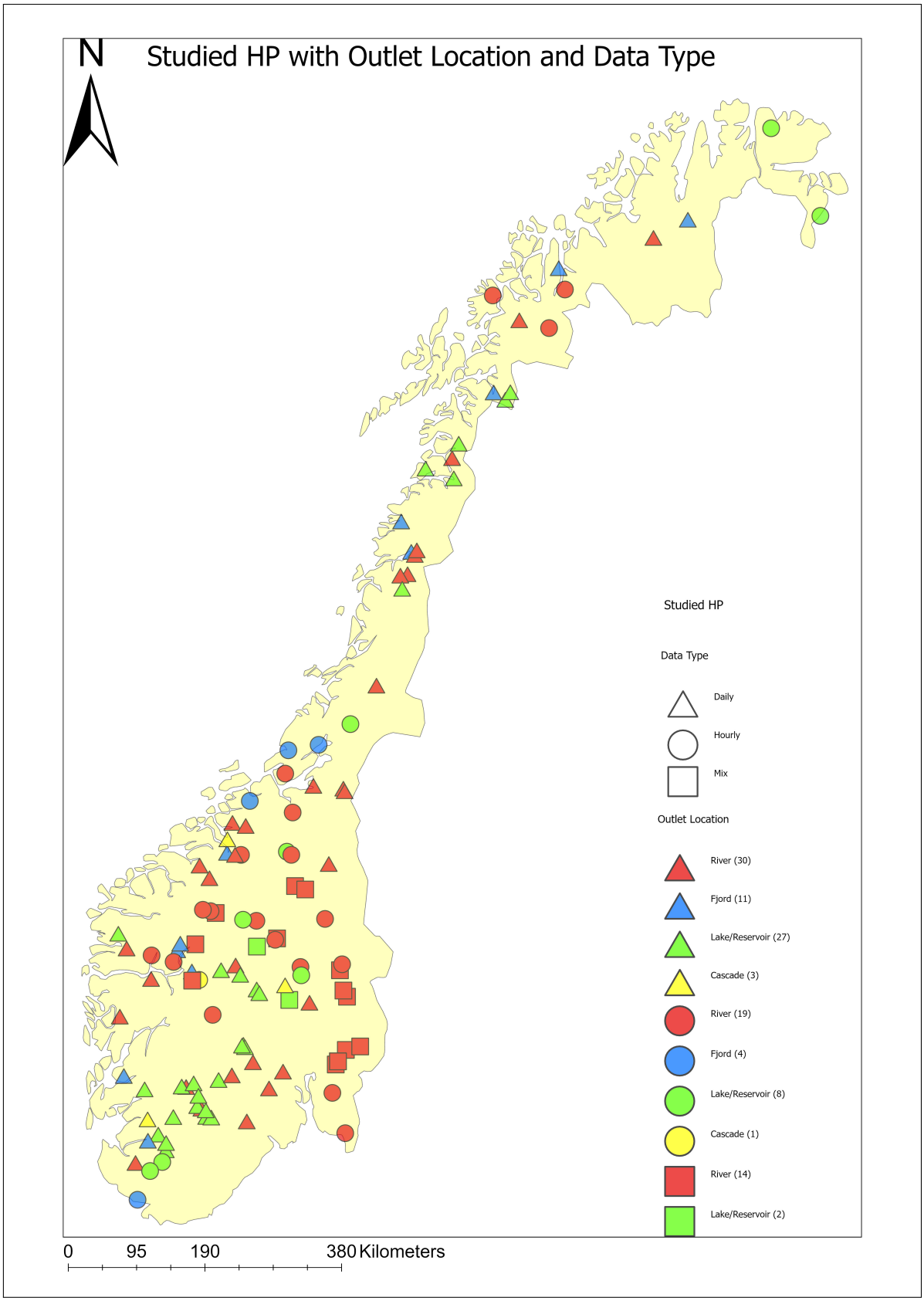

Figure 3.1: Overview of the investigated HP with their outlet location

Alternatively, COSH tool has an option to export all the statistical analysis that is cal-

culated by the software in one Excel file. These Excel files were used and summarized to obtain some of the above mentioned statistical indicators that represent the level of ramping over the time to have a comparison overview on the historical trend in these indicators by processing them through R.

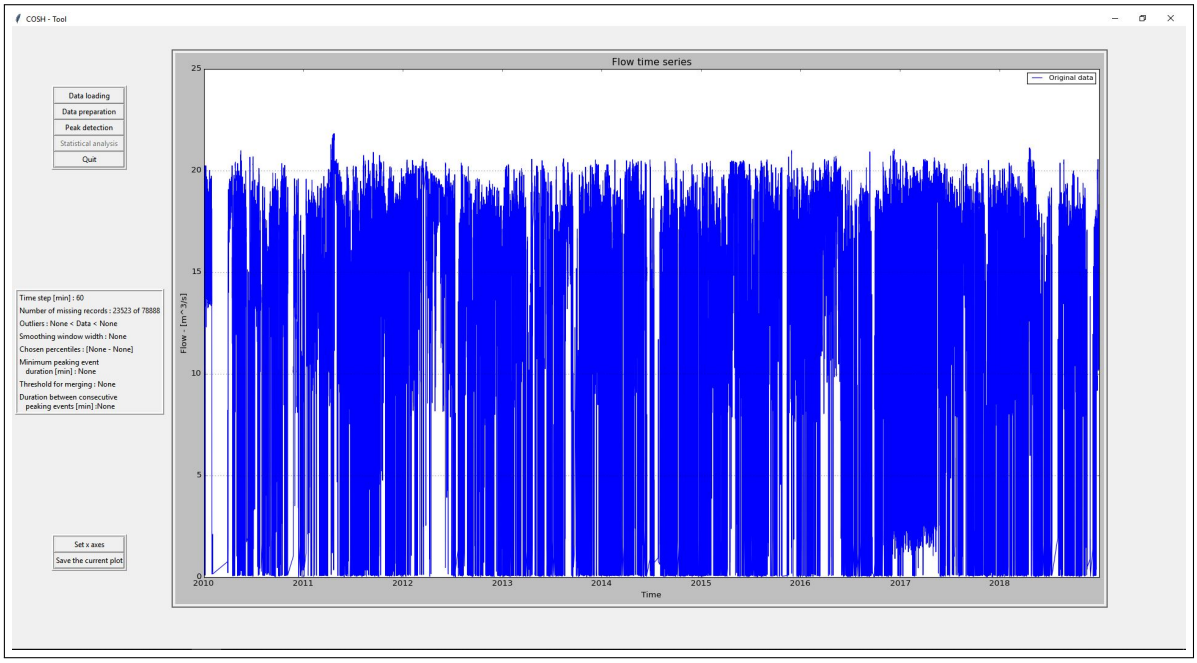

Figure 3.2: COSH tool interface with an example of flow ramping amplitudes over several years.

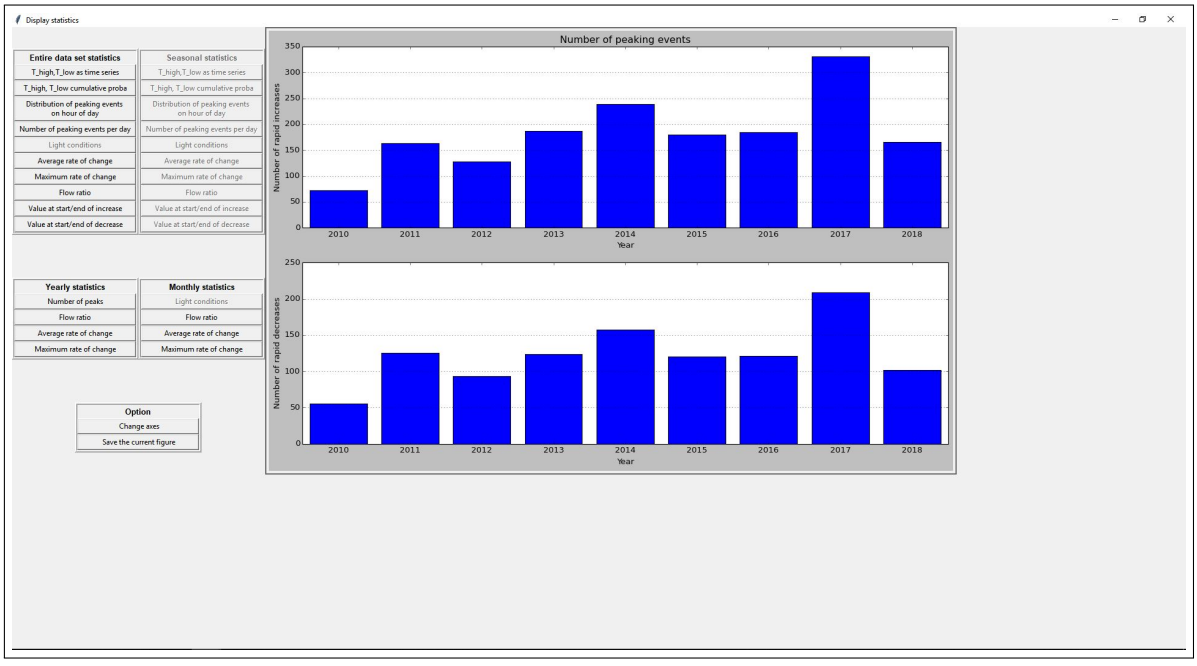

Figure 3.3: Output options from COSH tool showing annual number of (rapid) up ramping and down ramping events per year.

3.2.2 Flow ramping indicators

Carolli et al. (2015) developed two simple indicators for quantifying the level of peaking on a sub-daily time interval. Their indicators were applied to various HPs from a different region in Europe. In their study, two main indicators were purposed to assess the level of ramping that occur. The first indicator is for assessing the magnitude of the peak HP1. HP1 is a dimensionless indicator calculated as following. For each HP, we calculated for each day the difference between maximum discharge (Q_{max}) and minimum discharge (Q_{min}) divided by the average Discharge (Q_{avg}) on the same day. Then HP1 refers to the median of the daily values calculated from the previous process. HP1 was calculated for each HP for each year from 2010 to 2018.

The second indicator HP2 is the rate of change indicator. It refers to the frequency of the occurring peaks. It is calculated by dividing the change of the discharge in every hour, then to exclude the outliers, the 90-percentile of the resulted values were calculated. Finally, HP2 refers to the median of values that were calculated for each year for each HP.

An advantage of using Carolli et al. (2015) Indicators is they provide a preliminary overview of the potential ramping level before any ecological investigations that can happen with a simple procedure. Both Indicators were calculated by processing our data through R.

3.2.3 Statistical and trend analysis

Different types of statistical analyses were carried out on our results due to the following reasons. First, it is essential, as mentioned above, to investigate the relation between the level and frequency of peaking with different HP's characteristics. Such relation, if it exists, can be used for further classifications of HPs potential level of peaking based on HPs characteristics. Additionally, it is also essential to have an overview of the historical trend that might occur in the level of peaking based on each HP. To reach these objectives, the following methods were used:

Visual trend and comparison by groups

After calculating the above-mentioned indicators, it is necessary to have a proper view on the trend of these indicators in relation to the environmental legislation implemented for every HP. By grouping the HPs into two main categories where there are restrictions implied against flow ramping and no restrictions. Using that allows us to evaluate the

efficiency of the environmental legislation and to get a proper comparison between the different patterns of operation.

Multiple linear regression

Multiple linear regression is a statistical approach for investigating a linear relationship between dependent and independent variables. This relation can be used for predicting the values of the independent variable based on this linear relation that is constructed. Furthermore, from the constructed relation, it is possible to investigate which dependent variable has more influence on the predicted one. Mainly a multiple linear regression model formula for i = n number of observations is as follows (Reilly, 1978):

$$y_i = \beta_0 + \beta_1 x_{i1} + \beta_2 x_{i2} + ... + \beta_k x_k + \epsilon \tag{3.1}$$

where:

- y_i: dependent variable
- x_i: explanatory variables
- β_0: constant value referring to the interception value
- β_k: slope coefficients for the dependent variables
- ϵ: the model residuals

Multiple linear regression is based on the following assumptions (Reilly, 1978). First, there must be a linear relationship between the two types of variables. This would be the outcome of our model by testing whether this relation exists or no. To have a proper assessment of this relationship, we must ensure that our variables are normally distributed; therefore, it is essential to test the normality of the analyzed variables and make a transformation in the data if they are not normally distributed. Additionally, any correlation between the explanatory variables cant exist. Furthermore, the normality of residuals must exist. This implies that the residual values are normally distributed with a mean of 0 and a variance of σ^2. It is vital to test the aforementioned conditions before building up our models.

After building the models, it is essential to estimate the goodness of fit for them using the coefficient of determination R^2. R^2 is an indicator that shows how accurate the model fitting is. It Can be calculated as follows:

$$R^2 = 1 - \frac{SS_{res}}{SS_{tot}} \tag{3.2}$$

where: SS_{res} is the sum of the square of values, and it is calculated as follows:

$$SS_{\text{res}} = \sum_i (y_i - f_i)^2 \tag{3.3}$$

where y is the true value, and f is the fitted value through the model.
SS_{tot} is the sum of total squares, and it is calculated as follows:

$$SS_{\text{tot}} = \sum_i (y_i - \hat{y}_i)^2 \tag{3.4}$$

where y is the true value, and $\hat{y}$ is the predicted value through the model.

Two multiple linear regression models were carried out for our results. The first model refers between the relation between our calculated HP1 referring to the magnitude of the peak for every year as a dependent variable (y1) and HP characteristics represented in four variables: 1)reservoir capacity in a million m^3 2)head of the HP in meters 3)outlet location of the HP 4) the installed capacity of HP in MW. Similarly, the second model refers to the relation between the frequency of the peak occurring indicator HP2 as an independent variable (y2) and the before mentioned HP characteristics as explanatory variables.

Mann Kendall trend test

Mann Kendall (M-K) trend test is a statistical test that is often used to analyze the trend in the data over a long time series. It is used to test whether there is a constant increasing or decreasing trend over the tested time period. One advantage of this test that it is a non-linear test that doesn't require my data to be normally distributed (Gilbert Richland, 1987). Furthermore, it is possible to work around any missing data along with the time series. The test evaluates the relative magnitudes of the sample of data instead of the absolute values itself. This test has been used frequently for evaluating the trend in various hydrological and meteorological phenomena (Ahmad et al., 2015; Shadmani et al., 2012).

The test can work in smaller data points; however, in order to show its efficiency, it is recommended to use a longer time series for evaluating the trend. The obtained data included two HPs with longer time series and restriction against flow ramping. In order to have a proper view of the efficiency of these restrictions, it is essential to evaluate the trend in those two HPs using the M-K test. after calculating the above-mentioned indicators representing the magnitude of flow ramping every year using COSH and Carolli et al. (2015) indicators, it is essential to conduct the M-K test for HP1, HP2, and the average annual number of fast increases and decreases throughout every year.

The test consists of two parts that are calculated. The first part is the M-K statistic value (S). (S) is initially assumed to be 0 (no trend exists) then:
for $x_1 ... x_n$ number of data points in time j S is calculated as follows (Gilbert Richland, 1987):

$$S = \sum_{k=1}^{n-1} \sum_{j=k+1}^{n} sign(x_j - x_k) \text{Where :} \tag{3.5}$$

$$\text{sign}(x_j - x_k) = \begin{cases} 1 \text{ if } x_j - x_k > 0 \\ 0 \text{ if } x_j - x_k = 0 \\ -1 \text{ if } x_j - x_k < 0 \end{cases} \tag{3.6}$$

S represents how the trend behaves throughout the time period. If S has a very high positive value, it means the trend is significantly increasing and vice versa. After calculating S, the variance of S, VAR(S) then is calculated using the following:

$$VAR(S) = \frac{1}{18}\left[n(n-1)(2n+5) - \sum_{p=1}^{g} t_p(t_p-1)(2t_p+5)\right] \tag{3.7}$$

Where n is the number of data points, g is the number of sample data that share the same value, and t_p is the number of data points in the p^{th} group. After the variance is calculated, the normalized Z test is calculated by the following:

$$Z = \begin{cases} \frac{S-1}{[VAR(S)]^{\frac{1}{2}}} & \text{if S > 0} \\ 0 & \text{if S = 0} \\ \frac{S+1}{[VAR(S)]^{\frac{1}{2}}} & \text{if S < 0} \end{cases} \tag{3.8}$$

Finally, the probability of Z test is calculated for a normal distribution of an average of 0 and σ^2 of 1 as follows:

$$f(z) = \frac{1}{\sqrt{2\pi}} e^{-\frac{z^2}{2}} \tag{3.9}$$

The null hypothesis (H_0) for the M-K test (p > 0.05) is that there is no consistent trend in the time series. If (H_0) condition is not met, the alternative hypothesis (H_1) is that the trend exists. It can be positive or negative or not null. When the hypothesis conditions are met, there is an existing trend, the magnitude of the trend can be calculated using Sen's Slope as following. The inserted values are first arranged in ordered time series and ensure there is no correlation in the data before it is tested.

Sen's slope estimator

Sen's slope is an often method for determining the magnitude of a trend over a time series. Similarly to the M-K test, it non-linear test which doesn't require the data to be

normally distributed. This estimator is crucial for showing us how big is the trend in our calculated indicators is which will show to what extent the provided restrictions on flow ramping provided for the two HPs are effective for minimizing the level of ramping.

Sen slope estimates the trend of a sample of N pairs of data as follows (Gocic and Trajkovic, 2013):

$$Q_i = \frac{x_j - x_k}{j - k} for i = 1, ..., N \tag{3.10}$$

Where x_j and x_k are data points at the j and k time points, respectively. Consequently, for n data measurements in the timer series will be $N = \frac{n(n-1)}{2}$ slope estimates. Unlike the least square method used for linear regression, Sen slope estimators use the median for the slope estimates Q_i. For the existence of one or more data points in one time period then $N < \frac{n(n-1)}{2}$. After Q_i is calculated, they are ranked, and the median of it is calculated as follows:

$$Q_{med} = \begin{cases} Q_{[(N+1)/2]} & \text{for N is odd} \\ \frac{Q_{[(N/2)]} + Q_{[(N+2)/2]}}{2} & \text{for N is even} \end{cases} \tag{3.11}$$

Q_med represents the trend in the data. The higher the median value is, the steeper the slope is to be. Moreover, the confidence interval is calculated for the slope as follows:

$$C_\alpha = Z_{1-\alpha/2}\sqrt{VAR(S)} \tag{3.12}$$

Where Var(S) is the variance of M-K value and $Z_{1-\alpha/2}$ is a standard normal distribution with a mean of 0 and a standard deviation of 1. All the above mentioned statistical methods and approaches are conducted by processing the data through R using different statistical and plotting packages making it possible to automate all these tests.

3.3. Results

After analyzing the obtained data representing the investigated HPs, results will be shown as follows. Initially, the data were analyzed by being plotted in a categorized box plot based on restriction provided for each HP against flow ramping to investigate the level of variation of flow visually to have a preliminary assessment of the level of ramping that might occur due to each HP. Moreover, a visual quality check was carried out to ensure there are no outliers in the discharge data by plotting the discharge of each HP throughout the year.

Afterward, the data of HP were processed through COSH too. Results obtained from

COSH will be presented to have a view of different characteristics of each flow ramping that occurs from each HP operation. The results will be presented for each HP separately. Additionally, Carolli et al. (2015) indicators HP1 and HP2 results will be presented categorically based on the outlet location and the restrictions provided for each HP to have a proper view on the actual potential ecological damage that can occur from each HP. Furthermore, the indicators are presented in a box plot to show the level of change for each HP operational pattern.

Finally, the statistical analysis results are presented in three ways, as mentioned before. A visual trend in COSH indicators representing the magnitude of peaking throughout the years is plotted categorically based on restrictions against flow ramping. Then, the linear and non-linear results will be shown refereed to the multiple linear regression and M-K test and Sen's slope estimator.

3.3.1 Preliminary visual assessment

Results below show the preliminary investigations of the potential flow ramping that might occurs reflected in box plotting of the discharge Q and the change of discharge ΔQ of each HP. Box plot is a useful plotting way to show the extent of change for each variable between the median and the inner 25 and 75 quantiles. Moreover, it is useful to exclude the outliers of each data series as they will be on the edge of each box plot.

Figure 3.4 represents HP's discharge variation throughout the time represented in the box plot. The variation in the discharge for each HP can be related to the HP and the river characteristics. It is noticeable also that HPs without any restrictions on the license against flow ramping has higher median and variation of discharge than the restricted ones.

Similarly, Figure 3.5 shows the change in the discharge (ΔQ) in a one-time step (1 hour). It can be seen from a preliminary investigation that restricted HPs have lower median value for (ΔQ) except in few cases such as Laudal power plant (239). Moreover, there is no relation between higher median discharge value and greater change in the discharge. The outliers in every HPs represent extreme cases that can be referred to as an accidental shutdown (unplanned due to, e.g., problems in transition line, etc.) of the HP.

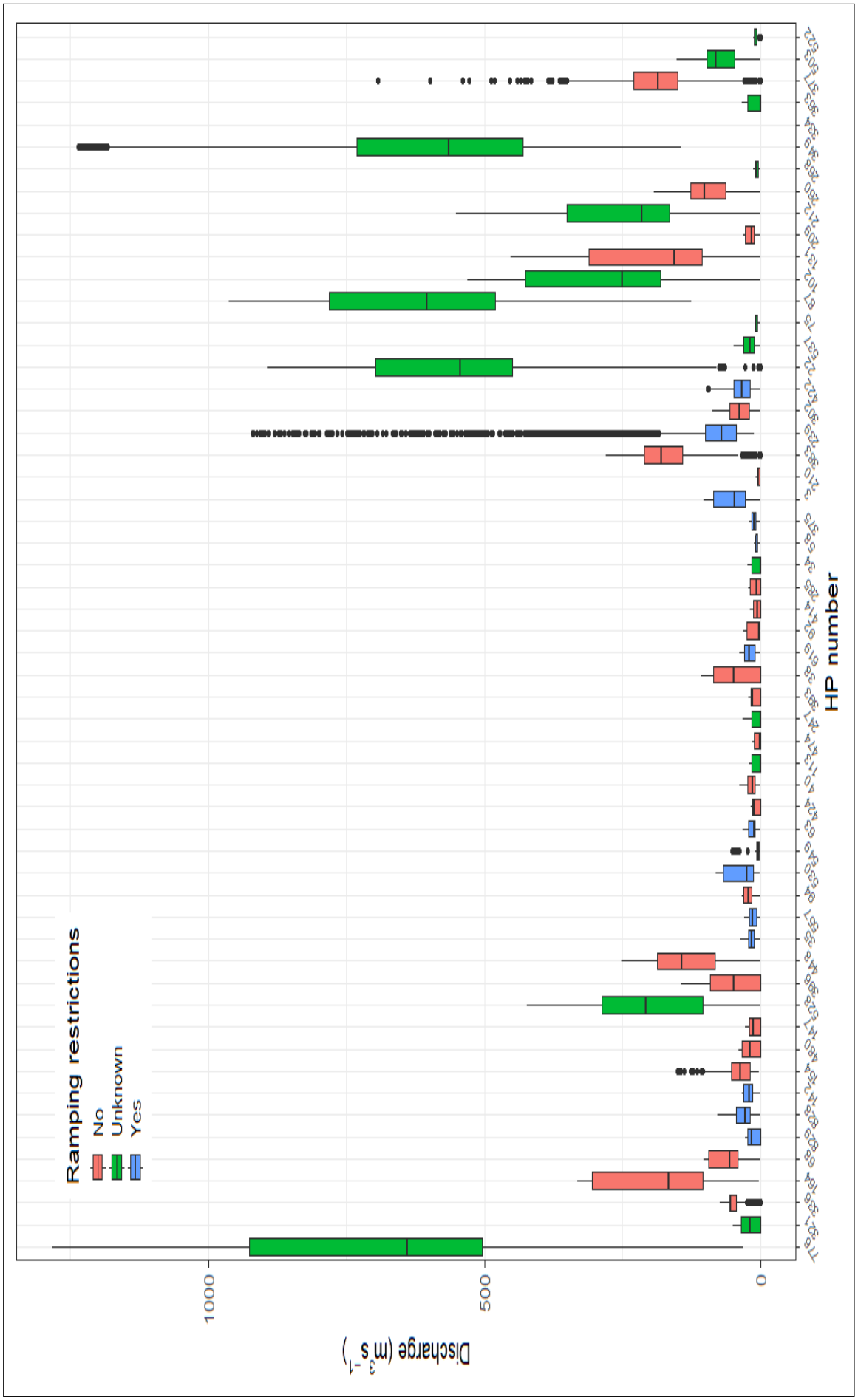

Figure 3.4: Box plot of the discharge for HPs throughout the investigated period. Color illustrate if there are restrictions in license against typical start/stop operation.

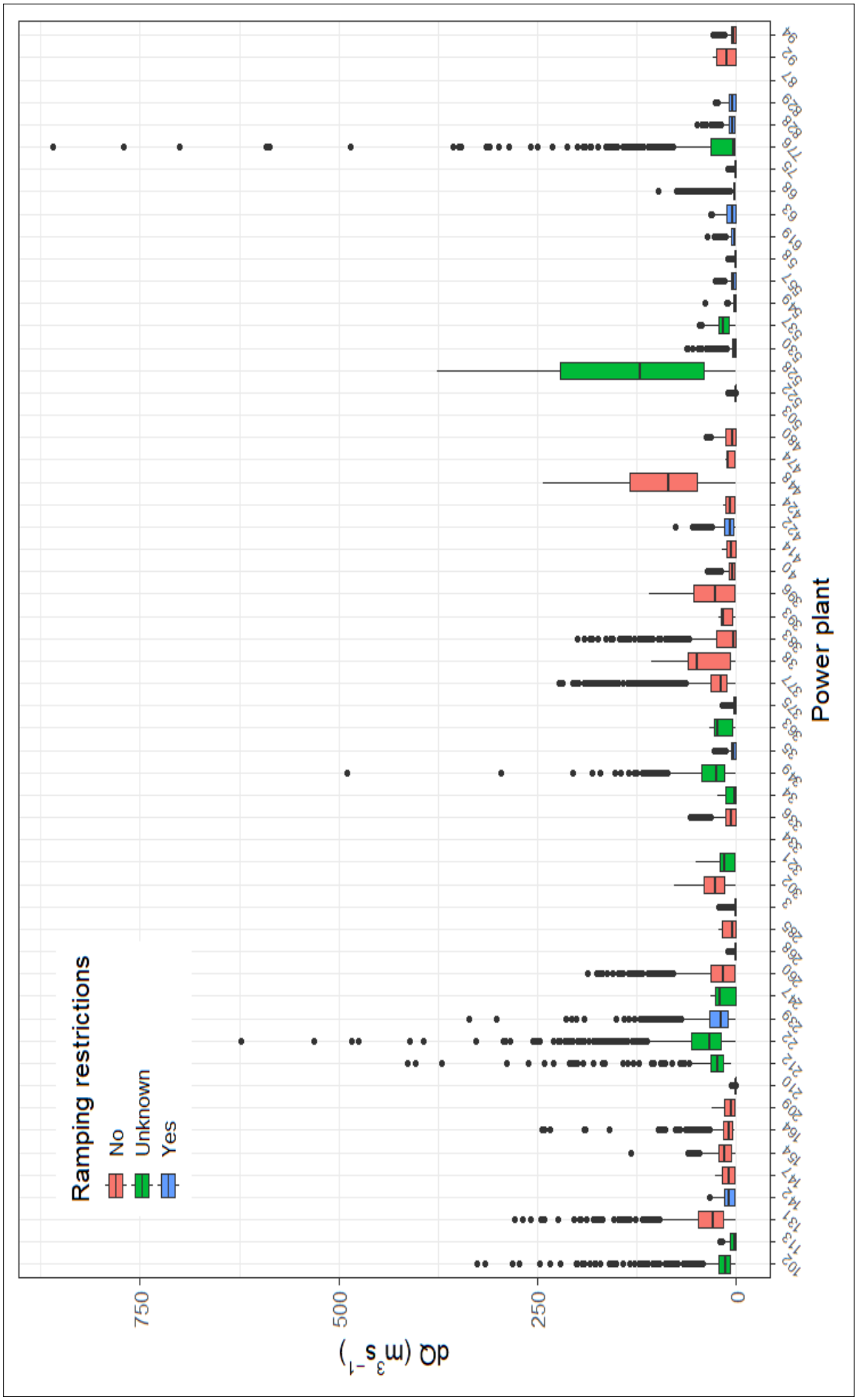

Figure 3.5: box-plot of delta Q (change in flow between consecutive time steps). Color represents restrictions on flow ramping in the license.

3.3.2 COSH tool results

In this section, COSH tool results will be presented. COSH is an efficient tool as it allows representing the results in a graphical way for allowing the comparison and has a preliminary check on any existent trend throughout the time. All the investigated HPs data were processed through COSH after excluding years with missing values.

Eventually, the indicators mentioned in section 3.2.1, referring to Sauterleute and Charmasson (2014), will be presented in graphs in this section. For illustrative purposes of showing how the results are, two HPs will be selected for presenting the results (Laudal 239) and (Bratsberg 38). Both HPs are with the outlet of tail-race into a river. The first power plant has a restriction against flow ramping, and it has a longer time series allowing us to investigate the efficiency of such restriction. The second one Bratsberg is located in the river Nidelva doesn't have any restrictions, and it will be further evaluated for future scenarios with the implementation of the HydroFlex project. However, all the other results from the remaining HPs are gathered and presented in Appendix A.

Number of peaks per year

The number of annual peaks per year will be presented below. The number of peaks refers to the sudden and fast change in the discharge of each HP. Since our data represents the discharge coming from the outlet location of the HP, they are representative of the actual potential of flow ramping, excluding any natural change in the flow that can occur from snow melting, flooding, or precipitation.

Figures 3.6 and 3.7 represent the number of peaks per year throughout the time for Laudal and Bratsberg power plants, respectively. By a first inspection, we can see the number of peaks for both power plants varies throughout the time. The highest number of peaks was calculated in 2008 and 2014 for Laudal and Bratsberg, respectively, with both having an average of 220 number of increasing peaks. However, the highest decreasing number of peaks was estimated to be in 2013 for Bratsberg with an average of 190 number of peaks. It is also noticeable that the restriction in the license provided for Laudal doesn't have any effect on minimizing the level of ramping compared to Bratsberg power plant, which doesn't have any restriction against flow ramping.

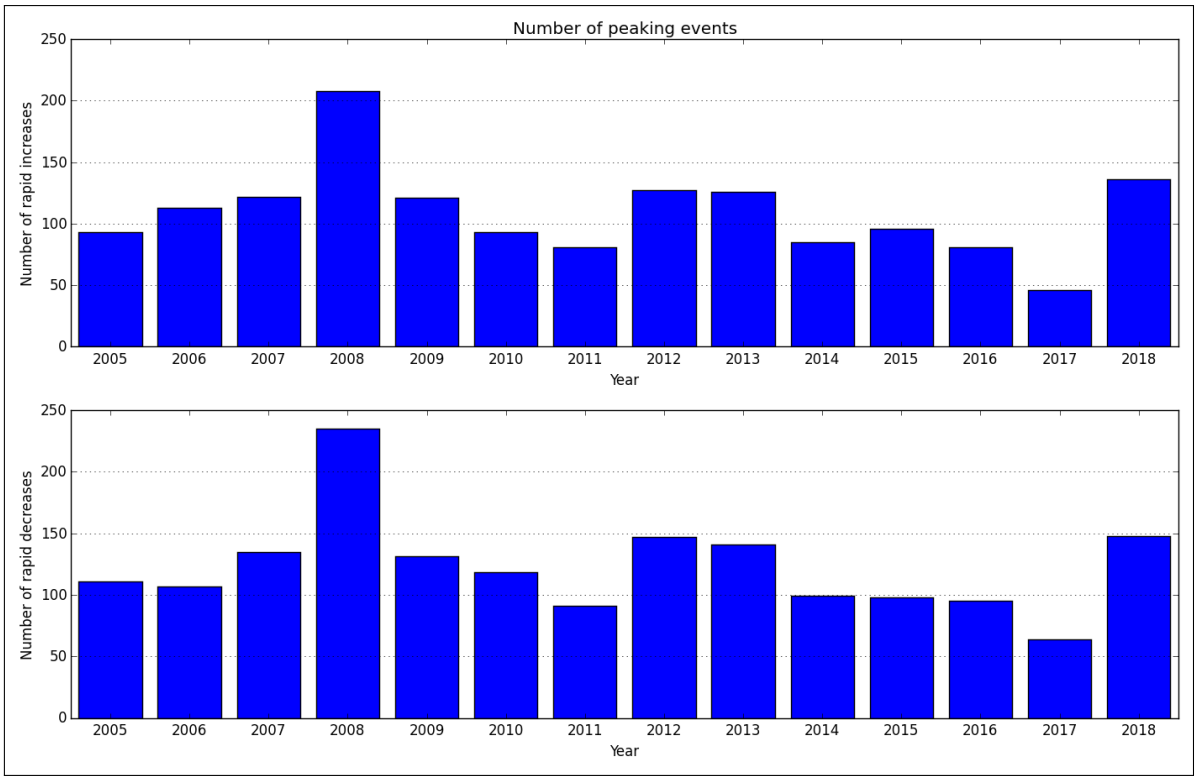

Figure 3.6: Number of Inc/Dec flow ramping events per year for Laudal

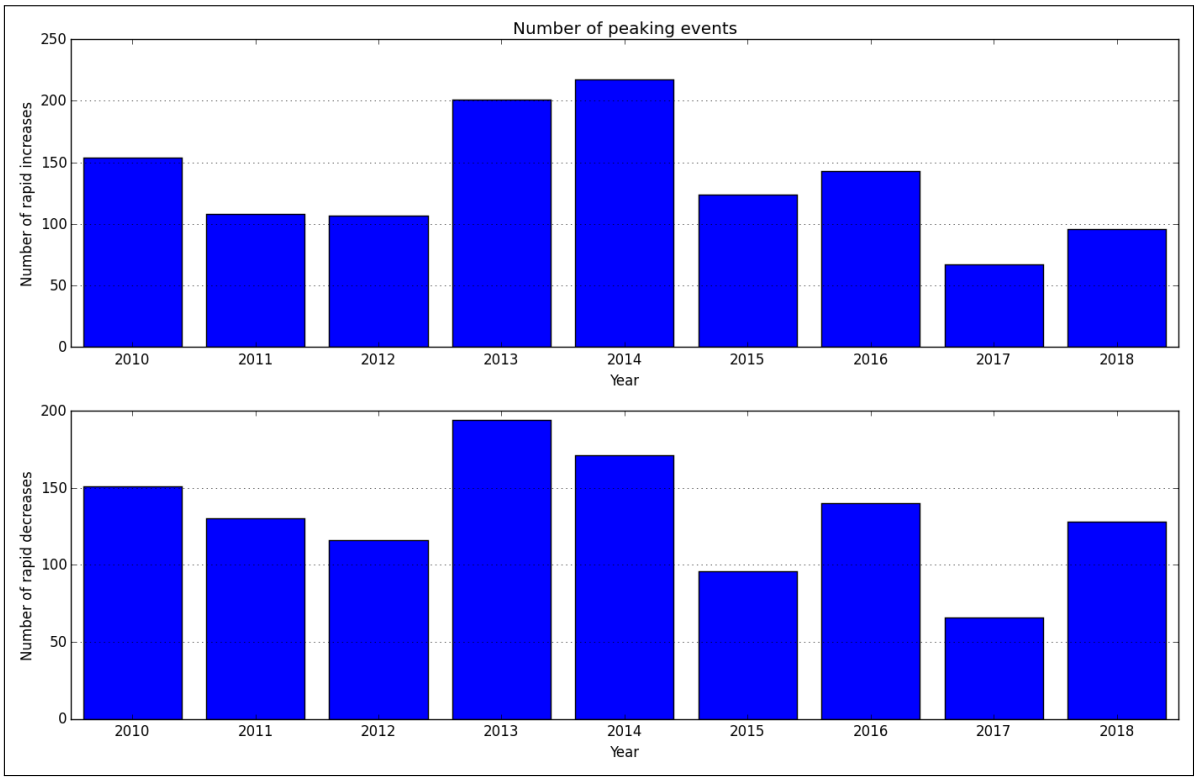

Figure 3.7: Number of Inc/Dec flow ramping events per year for Bratsberg

Distribution of number of increasing/decreasing peak throughout the day

The next results obtained from the COSH tool will be presented here, referring to the frequency distribution of the number of peaks throughout the day. This indicator is useful as it shows how regular flow ramping occurs throughout the day, which refers to the frequency category in (Sauterleute and Charmasson, 2014) indicators for quantification of hydropeaking.

Figure 3.8 and 3.9 shows the distribution of peaks throughout the day for Laudal and Bratsberg, respectively. It can be seen that the regularity of peak occurrence in Laudal is significantly higher than it is in Bratsberg where the peak occurrence shows an irregular pattern. The distribution throughout the day represents the typical daily hydropower operational pattern where the HP is almost shut down at night, and then it starts operating at max capacity at the morning rush hour, then the operation is decreased again, whereas it increases at the evening rush hour. This pattern of operation has more potential impact on the river ecosystem than it is, for example, for Laudal, where the distribution of the peak throughout the day is almost regular.

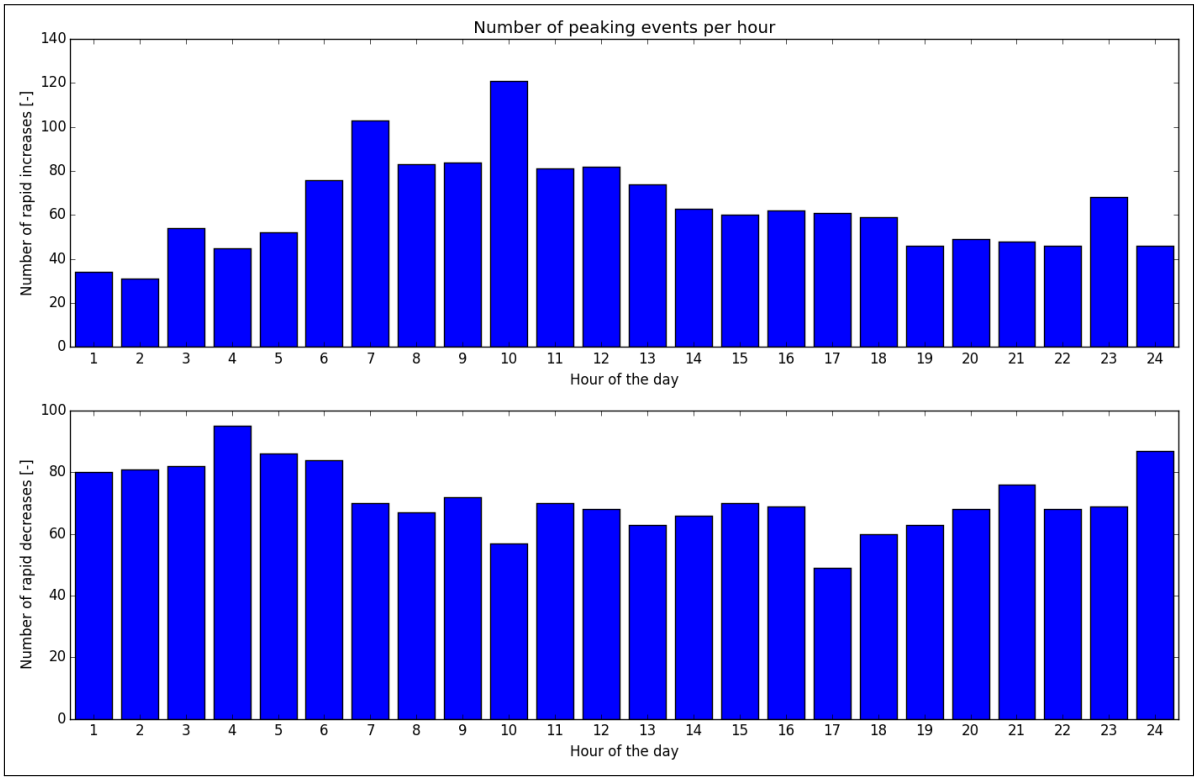

Figure 3.8: Average distribution of the number of Inc/Dec peaks throughout the day for Laudal

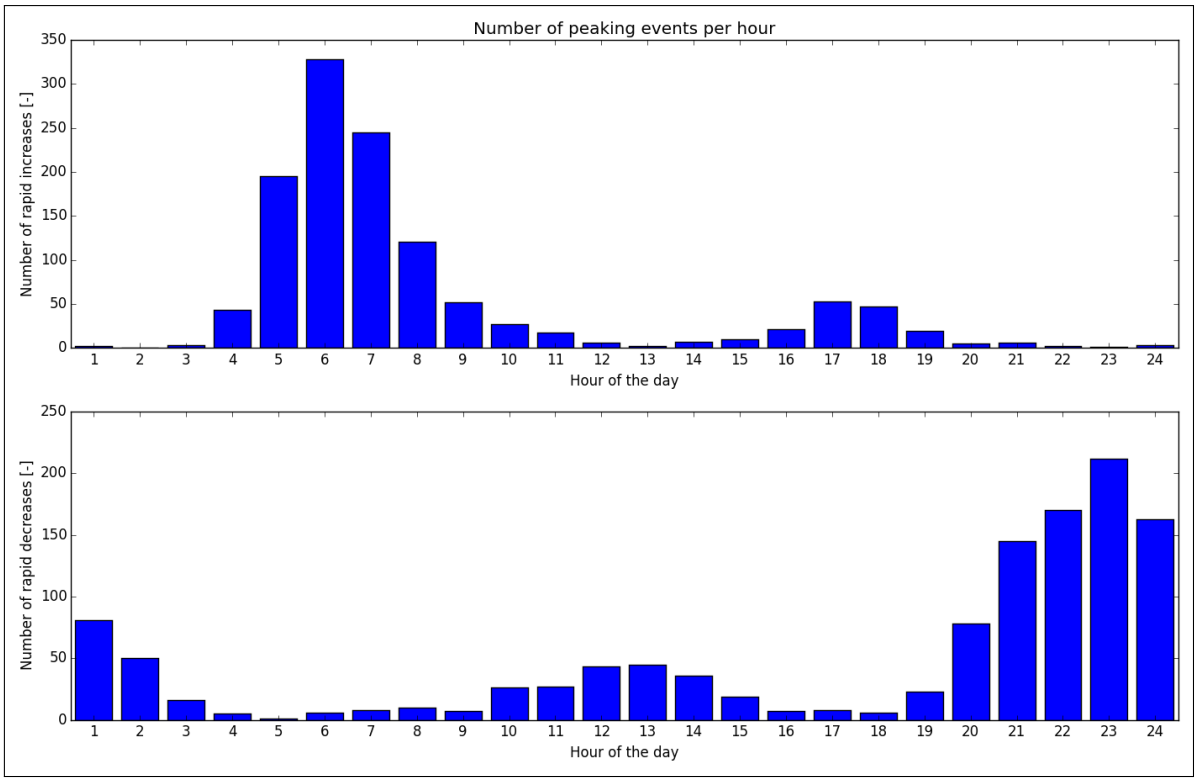

Figure 3.9: Average distribution of the number of Inc/Dec peaks throughout the day for Bratsberg

Maximum rate of change for increase/decrease

In this section, results from COSH tool presenting the maximum Rate of Change (RoC) will be presented. Maximum RoC is a very useful indicator that shows to what extent the HP can change its production rate in a 1-hour time step. It is also a good indicator representing the potential ecological damage that might occur from this operation pattern.

Figure 3.10 and 3.11 represent the maximum RoC for Laudal and Bratsberg for each year during the investigated time period. It can be seen that RoC for Laudal doesn't vary a lot throughout the time period with an approximate median value of 10 m^3/s per hour while it is much bigger for Bratsberg with a median value of 30-35 m^3/s per hour for both increasing and decreasing peak. Further trend analysis will be made to investigate the existence of such a trend in the results for this indicator to have a proper evaluation of this result.

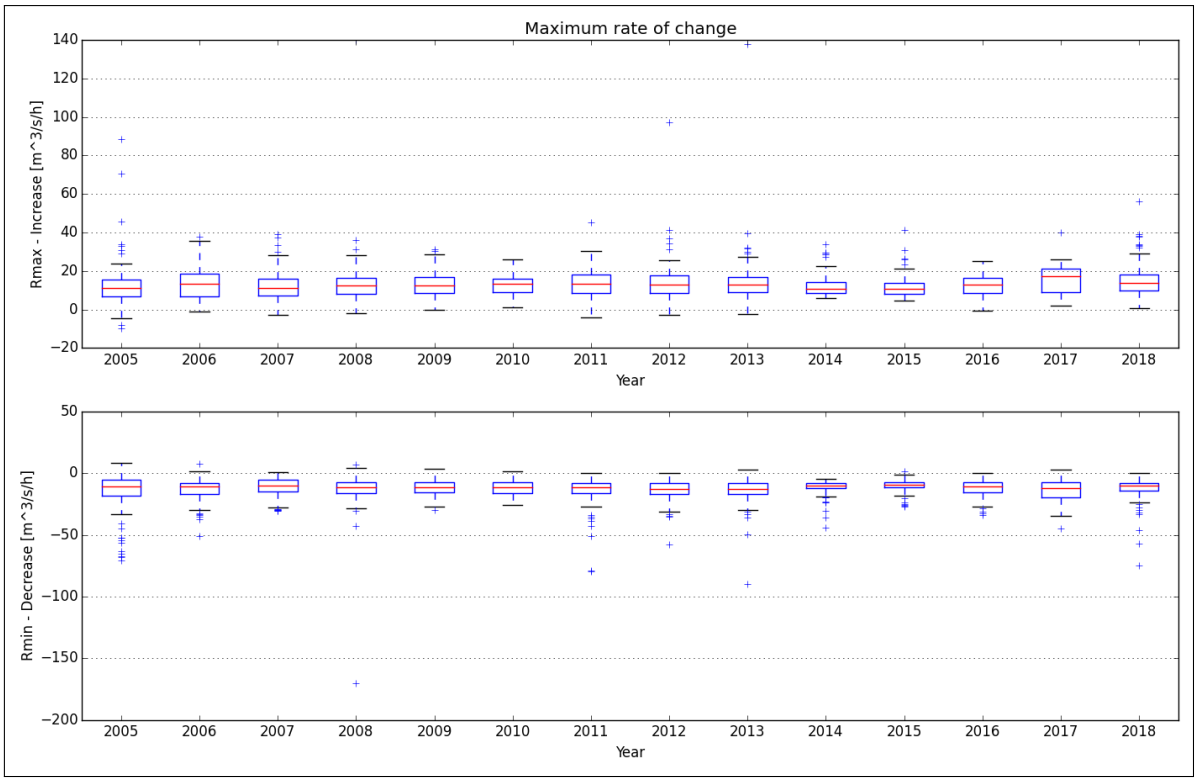

Figure 3.10: Maximum RoC for Inc/Dec per year for Laudal

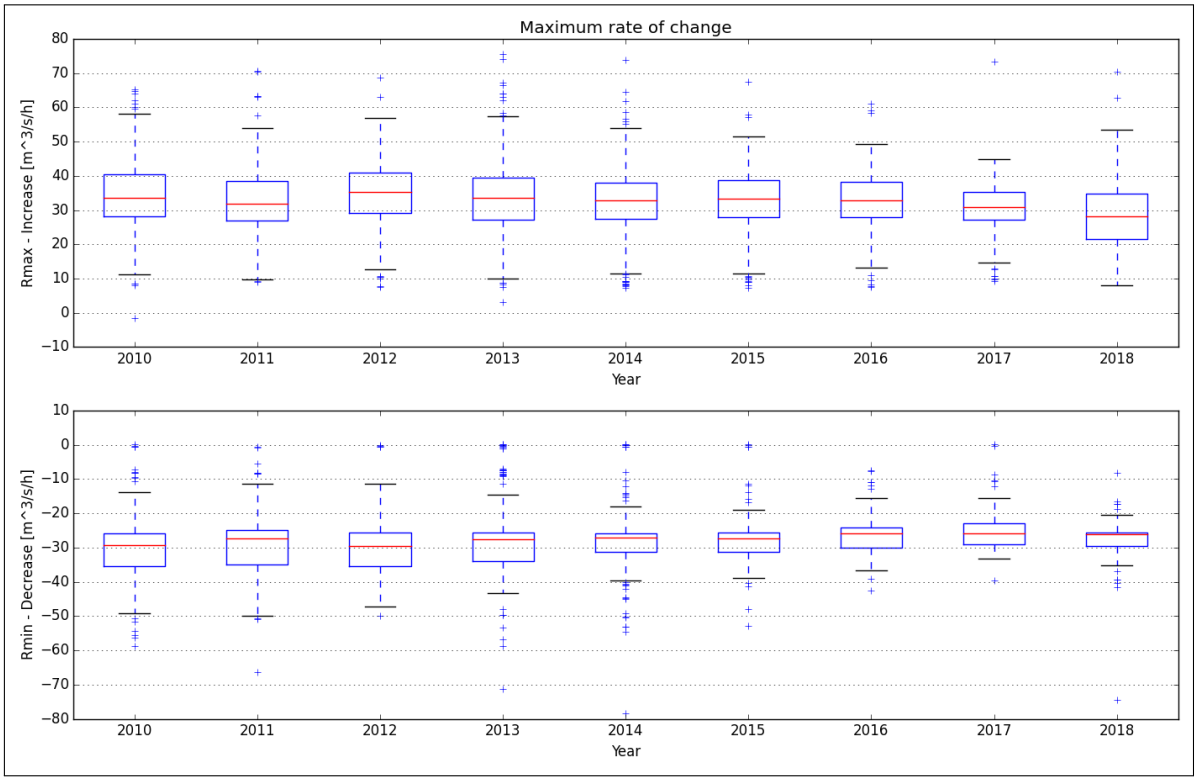

Figure 3.11: Maximum RoC for Inc/Dec per year for Bratsberg

Number of peaks per day

As mentioned above, COSH tool has the possibility to summarize the data into different indicators. In this section, the number of peaks per day for each year will be presented. This indicates how many peaks occur in a single day on average per year. This indicator also represents the frequency of ramping that occurs on a daily basis. The higher number of peaks that happen per day, the more frequent it is per day.

In the following figures, 3.12 and 3.13 show the average annual number of peaks that occur per day for Laudal and Bratsberg, respectively. It can be seen the highest number of peaks has a relation with the first results representing the total number of increasing and decreasing peaks. Hence, it can be seen in 2008 has the highest number of peaks per day with more than 5 increasing and decreasing peaks per day. On the other hand, Bratsberg has a lower average annual number of peaks per day, with almost not exceeding more than 2 peaks per day.

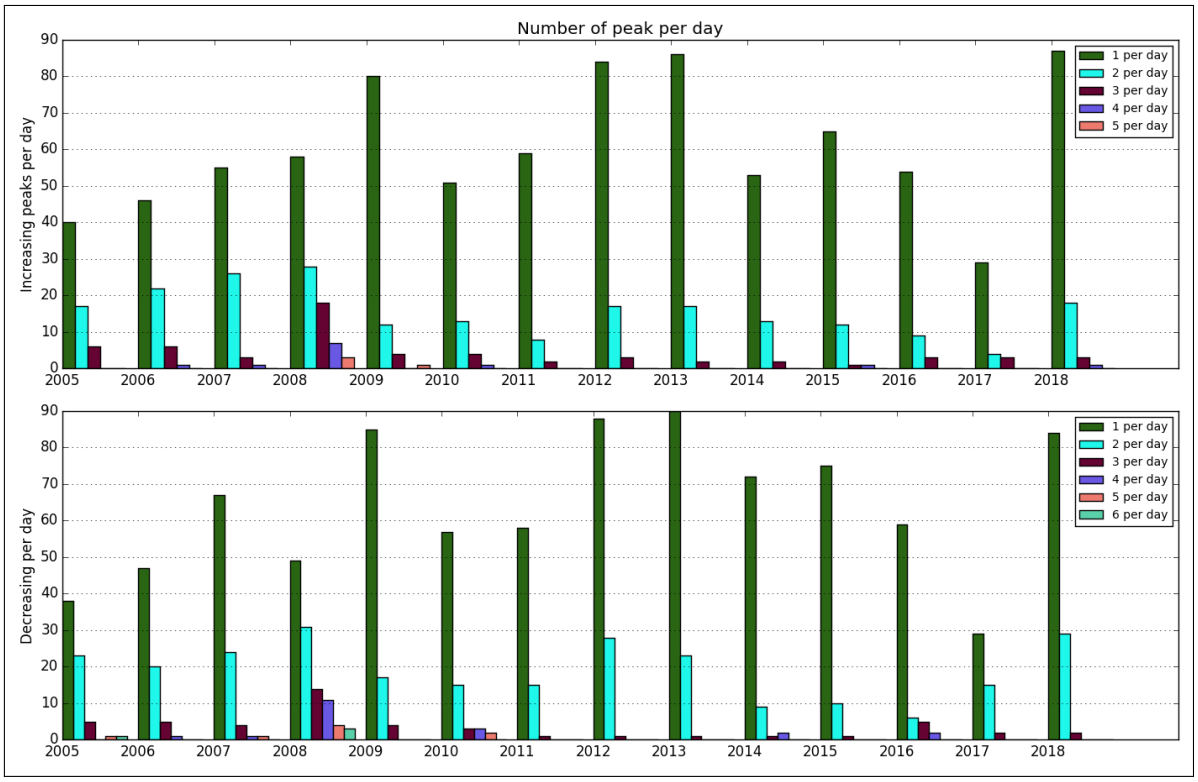

Figure 3.12: Average annual number of peaks per day for Laudal

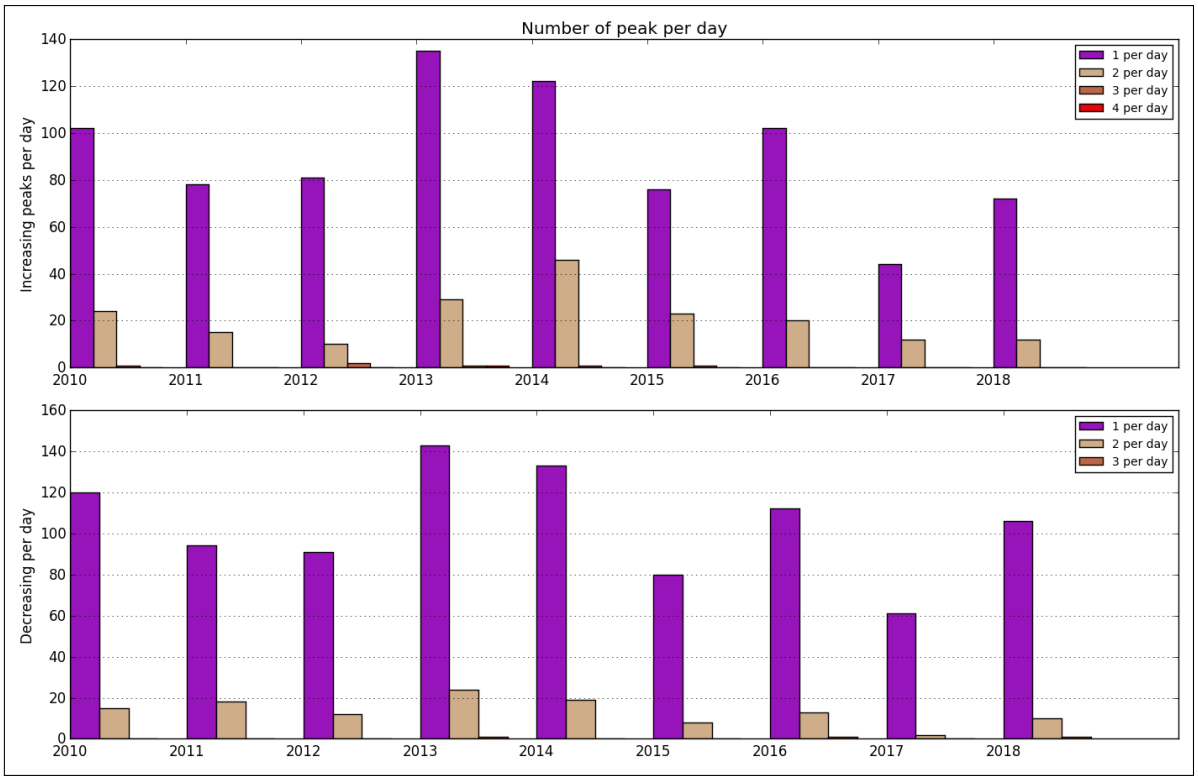

Figure 3.13: Average annual number of peaks per day for Bratsberg

3.3.3 Flow ramping indicators

After processing the data through R to calculate the indicators represented in (Carolli et al., 2015) journal. Results of HP1 and HP2 were obtained for each power plant for every year from 2010 to 2018. Years with missing values were excluded to avoid any outliers. Unlike how the indicators are calculated by (Carolli et al., 2015), there was no threshold definition for HP1 and HP2 to normalize the results. The reason behind this is that the investigated HPs, in their characteristics, will make it inaccurate to set a single threshold for all HPs. In addition to that, we are using the indicator to provide an overview of the potential flow ramping that occurs for every power plant individually; hence, there was no need for setting a threshold.

Results will be presented for HP1 and HP2 in a box plot for each HP representing the median value and inner quantiles throughout the time period. Additionally, to obtain a proper overview, we categorized the results based on the restrictions provided for each HP.

HP1

Figure 3.14 shows the results of HP1 representing the magnitude of flow ramping occurs

in each HP throughout the year. Results show a significant variation in the median values for the investigated HPs. Additionally, it is noticeable that HP1 has a bigger variation in its value throughout the time period for HPs without restrictions than it is for the restricted HPs.

HP2

In figure 3.15, the results of the HP2 are presented. As mentioned above, HP2 indicates the frequency of flow ramping that occurs for every HP, and it is calculated for every year. Results show that power plants without restrictions also have a higher value of HP2 than the restricted ones.

Additionally, it is also noticeable that some of the restricted power plants have a relatively bigger value, which questions the efficiency of the legislation implied for these HPs. Also it can be seen from figure 3.17 that HPs that are located to fjords and lakes have a bigger ramping magintude and frequency represented from their resulted HP1 and HP2 indicators. However, the figure also shows that there is a high potential ramping effect that can result from HPs located across the river and these HPs require further investigations.

Finally, in order to relate our HP1 and HP2 with the potential environmental impact that might occur due to the existing flow ramping, they were plotted in the x-y plot being classified to the outlet location of each HP as it can be seen in figure 3.16. It can be seen that most of the severe ramping occur in HPs with outlet location to lakes and fjords. However, it can also be seen that some HPs with outlet location to rivers cause severe flow ramping with the frequent occurrence, yet there are no restrictions implemented against this behavior. It is noticeable that restricted power plants, in general, have a lower magnitude of peaking than it unrestricted ones, yet they both share the same frequency. Additionally, HP1 and HP2 result plotted in a combination of the outlet location as a box plot.

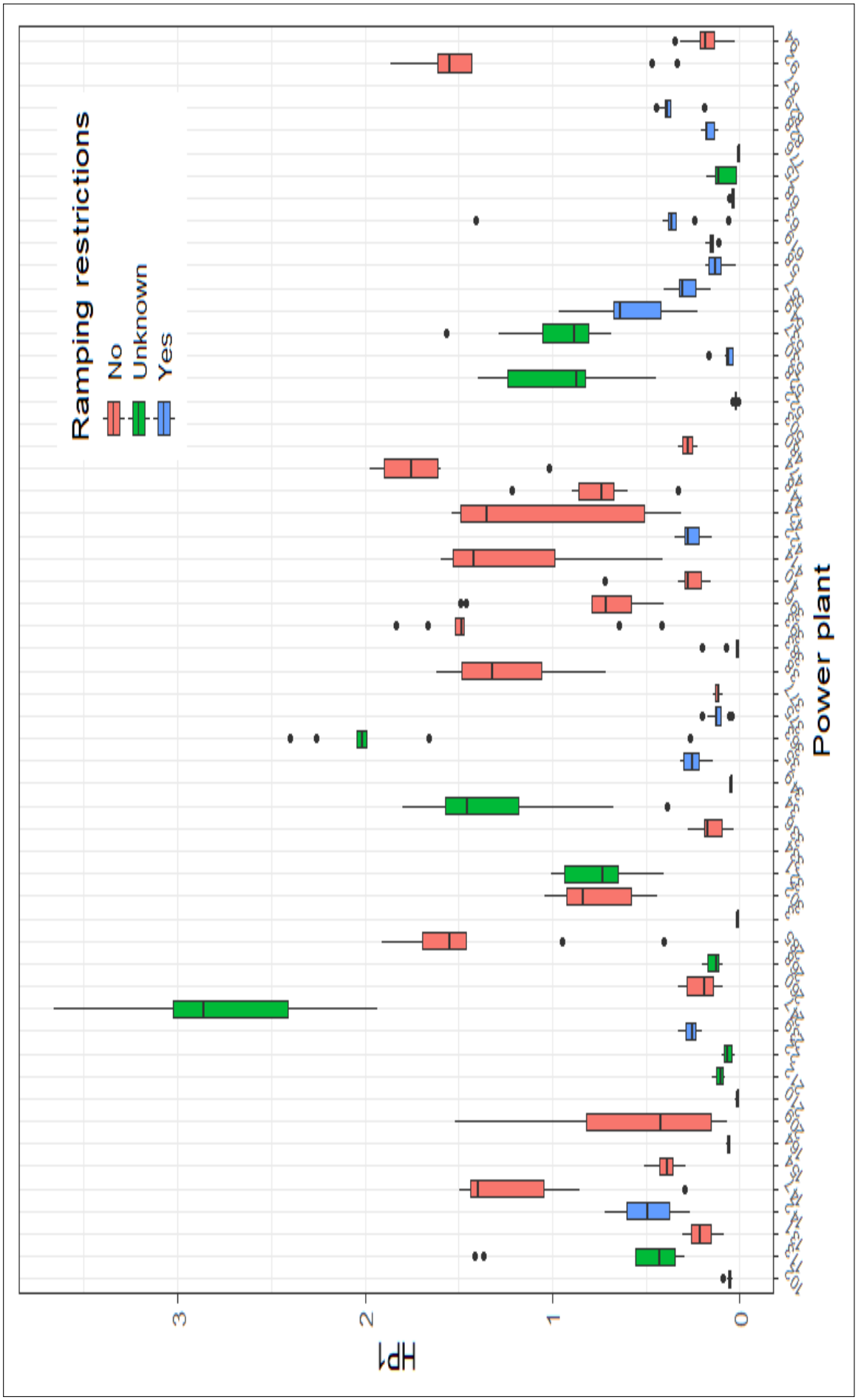

Figure 3.14: Box plot of the resulted HP1 for HPs throughout the investigated period

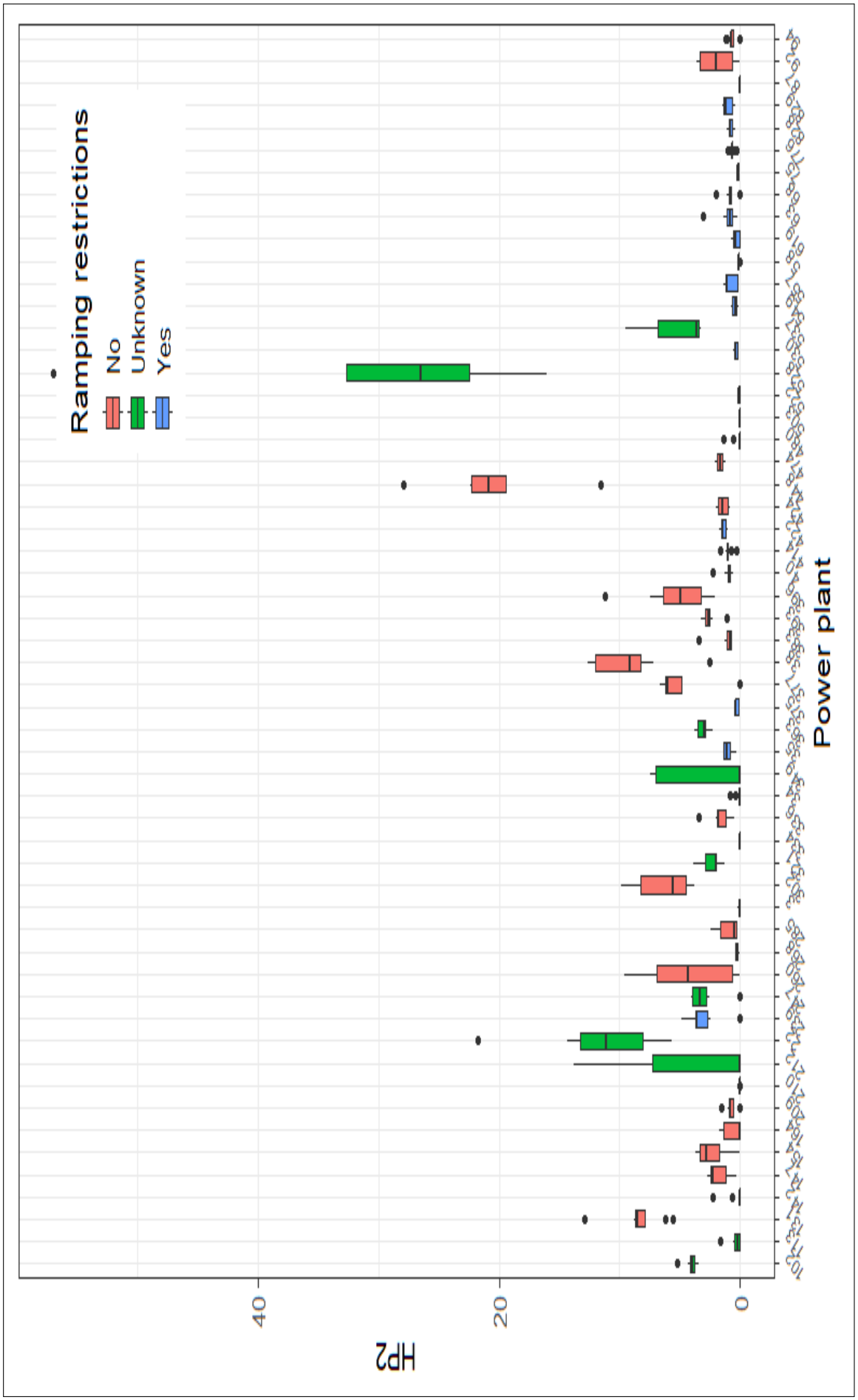

Figure 3.15: Box plot of resulted HP2 throughout the investigated period

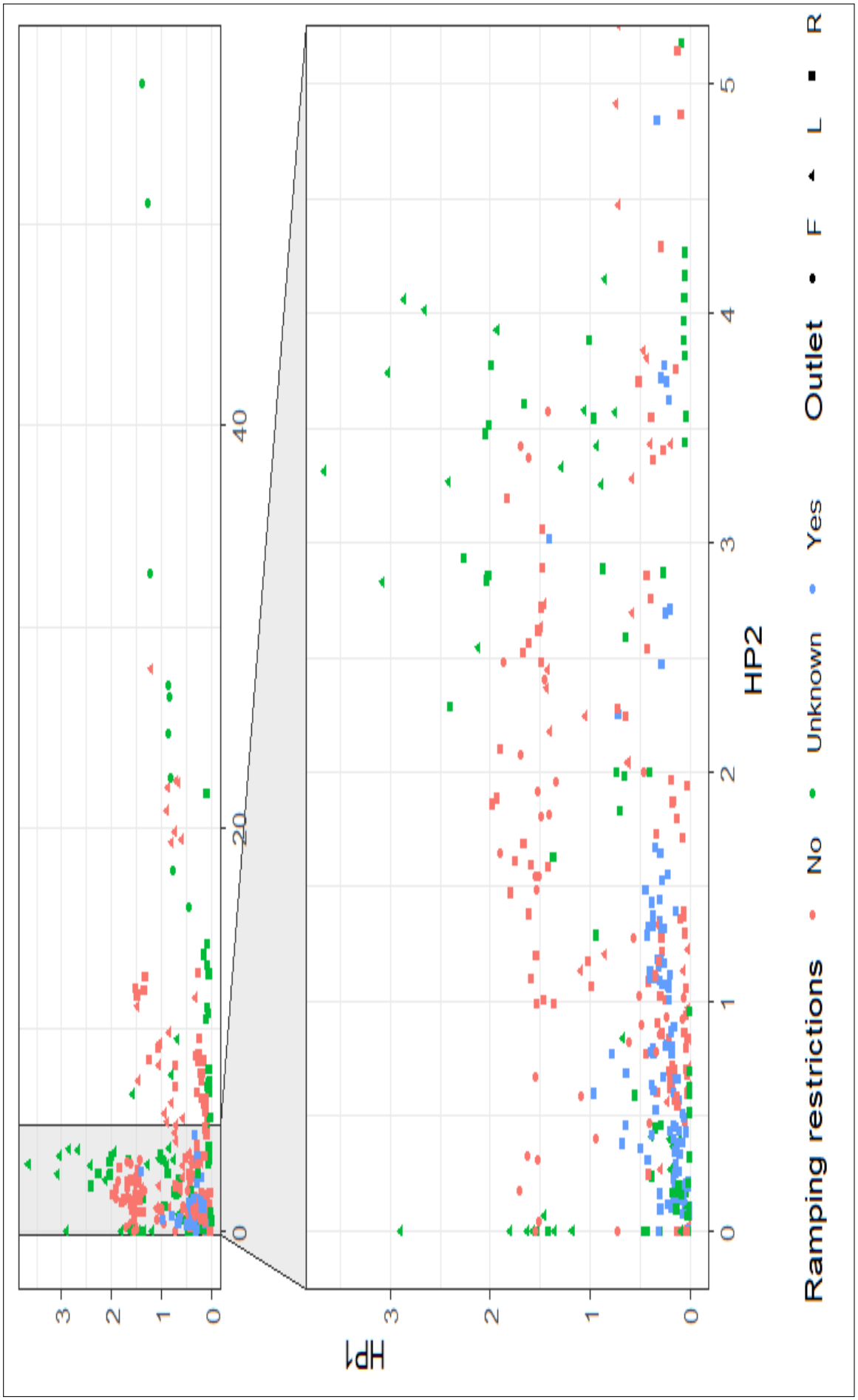

Figure 3.16: x-y plot of resulted HP1 & HP2 throughout the investigated period

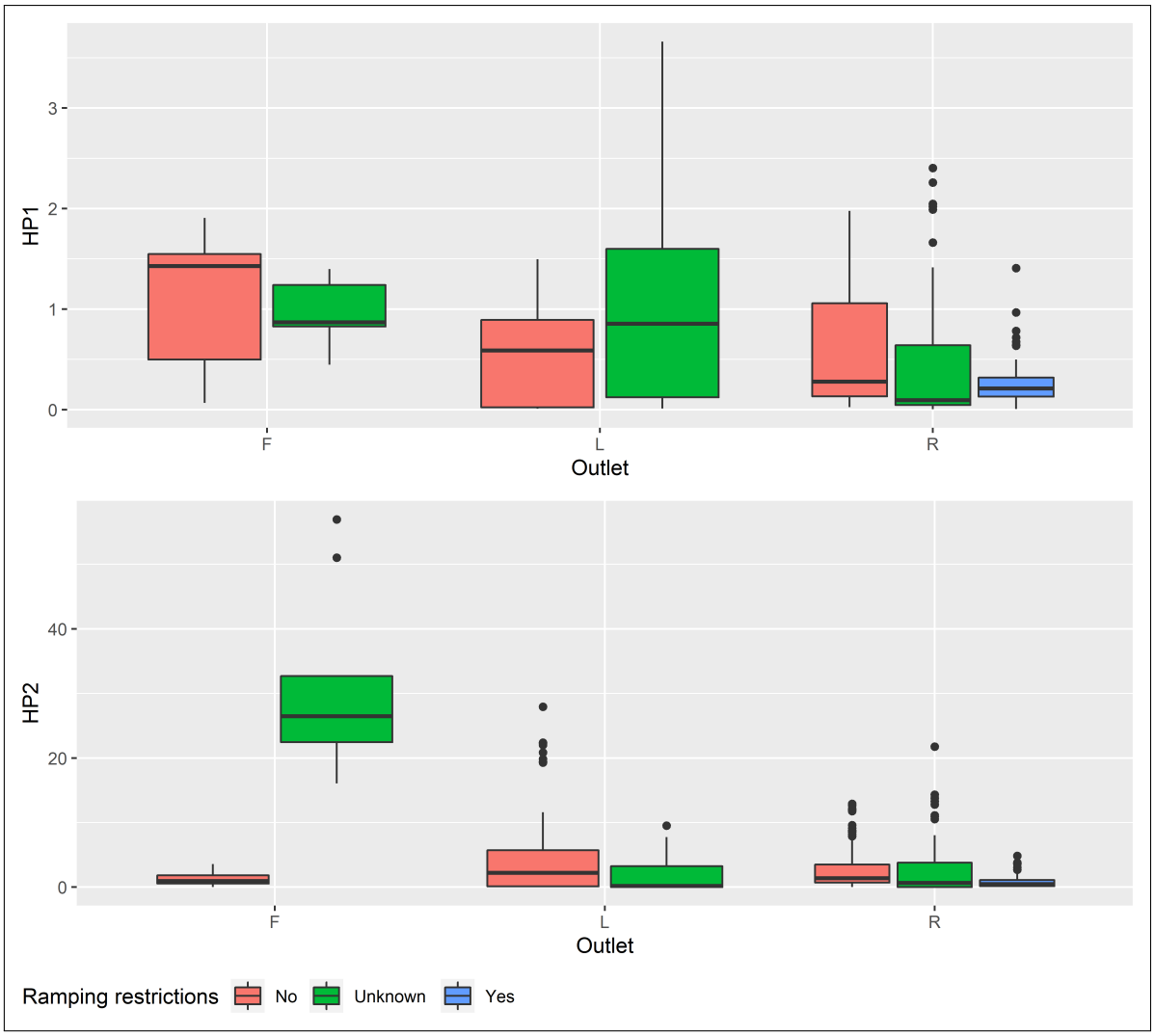

Figure 3.17: Box plot of calculated flow ramping indicators by the outlet location of the power plant

3.4. Statistical analysis results

In this section results of the conducted statistical analysis will be presented. As mentioned before, results will be presented into three parts after post-processing our results from the COSH tool and the indicators calculated using Carolli et al. (2015) approach by using R.

The first part represents the visual trend analysis for different COSH results reflecting the magnitude of flow ramping throughout the investigated period. The purpose behind this is to provide a clear visual inspection of any existing trend for both the rapid increase and decrease in the discharge. Moreover, a linear trend with confidence interval will be plotted for every HP in order to investigate any existence of the linearity of our results.

In the second part, Multiple linear regression models results will be presented. First, check for normality and test for correlation of the investigated variables will be presented, then the model's coefficients and results will be shown.

Eventually, non-linear trend results from the M-K test and its estimator using Sen's slope. as mentioned before, since M-K relies efficiently on longer timer points (Gilbert Richland, 1987), it was decided to investigate only two power plants: Svorkmo and Laudal, which has longer time series and outlet location to river. Indicators from COSH referring to the annual number of peaks and maximum RoC in addition to HP1 and HP2 results will be investigated using this test.

3.4.1 Visual Trend Results

Annual number of increasing/decreasing peaks

Figures 3.18 shows the trend in the number of fast increases and decreases throughout the time for HP with restrictions. By excluding HPs with a shorter time, it can be seen that there is some trending in an annual number of fast increases for HPs with restrictions such as Årøy-530, Skibotn-375, and Framrusti-829 which are all located to a river. However, there is no significant trending in the annual number of decreases per year for restricted HPs except for Laudal-239, Skibotn-375, and Borgund-35.

On the other hand, figure 3.19 shows the trending in the number of increases and decreases for HPs without restrictions. It can be seen that linear trending varies a lot. it can also be seen that for both HPs with and without restrictions that a linear trending doesn't accurately represent the results since it varies non linearly.

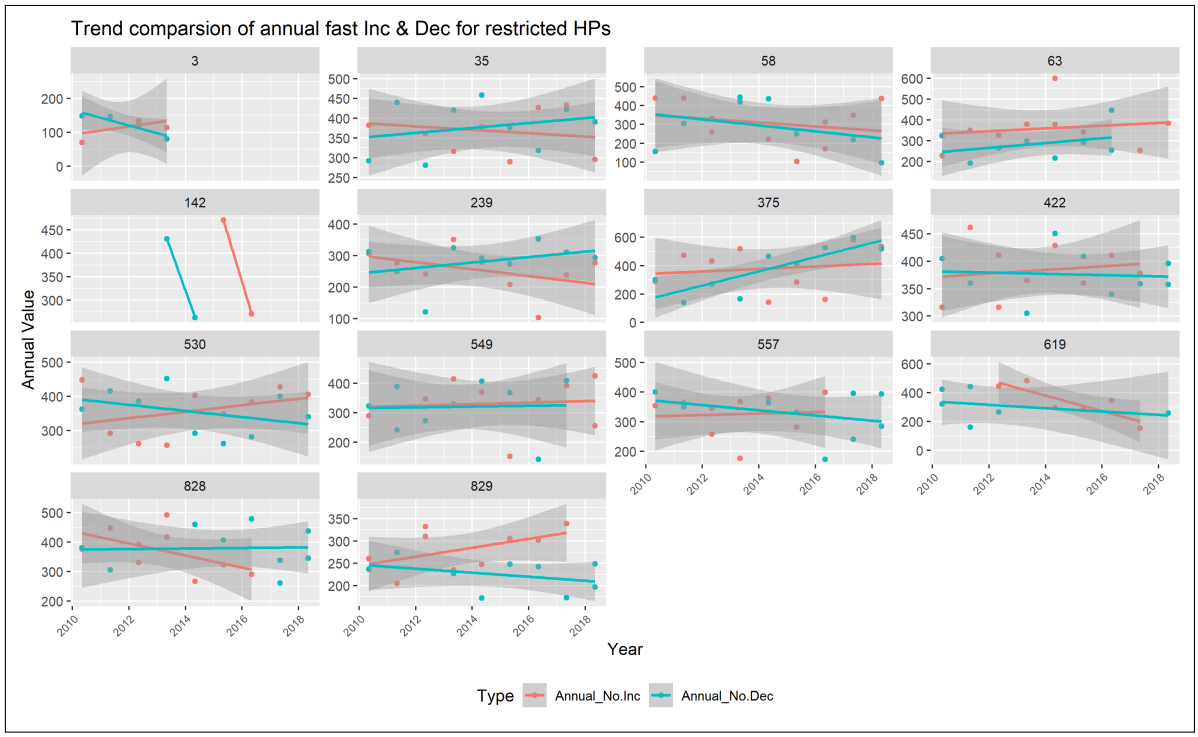

Figure 3.18: Trend for Annual fast Inc/Dec for restricted HPs

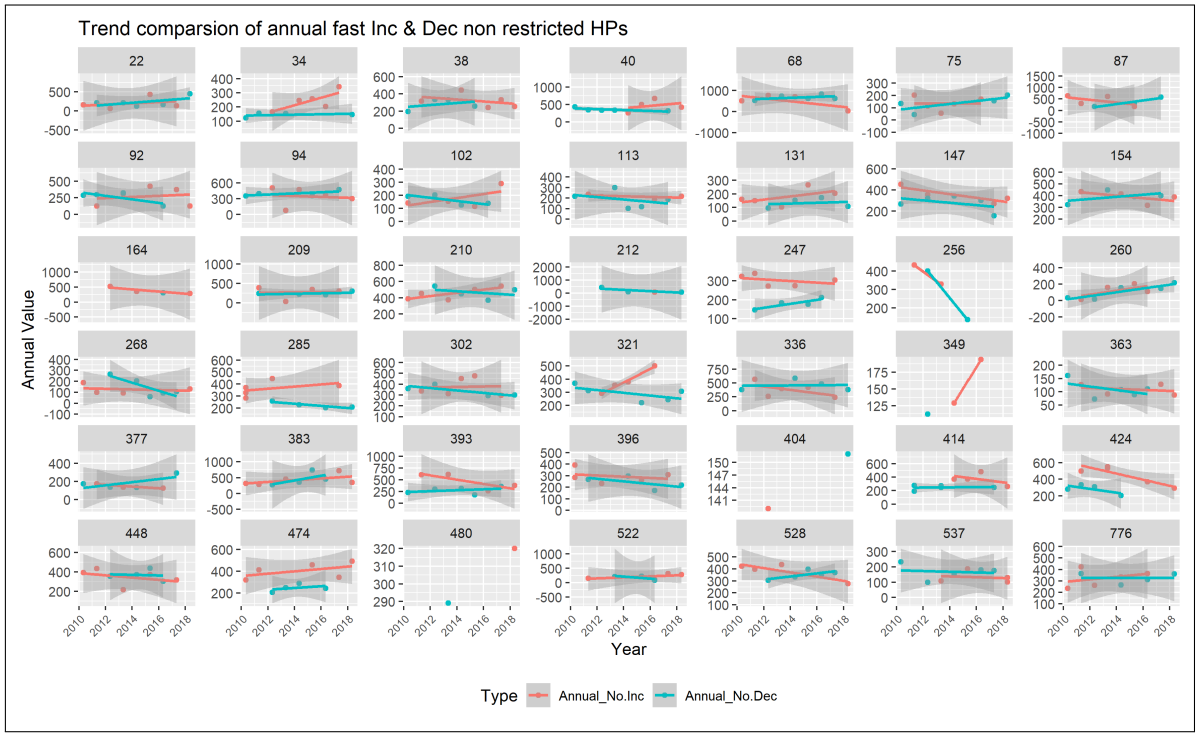

Figure 3.19: Trend for Annual fast Inc/Dec for non-restricted HPs

Annual max RoC of increasing/decreasing peaks

Figures 3.20 and 3.21 show the trend in the annual maximum rate of change during fast increases and decreases for restricted and non-restricted HPs, respectively. Results do not show any significant trending for either restricted or non restricted power plants. This might be because the most drastically ramping event might be accidental shutdowns. However, it can be seen that, on average, the annual maximum rate of change for the majority of non-restricted power plants has a significantly bigger value for the restricted power plants. This implies the fact that the flexibility of power plants without restrictions is significantly bigger as they can change the rate of production based on the market demand without any limitations.

Eventually, COSH results regarding the annual number of fast events and the maximum RoC for both increase and decrease changes were combined and plotted for the outlet location of the HPs in order to link the potential ecological impact with the resulted hydro-morphological indicators. It can be seen from figure 3.22 that RoC is generally bigger for non-restricted HPs; however, it doesn't differ much depending on the outlet location.

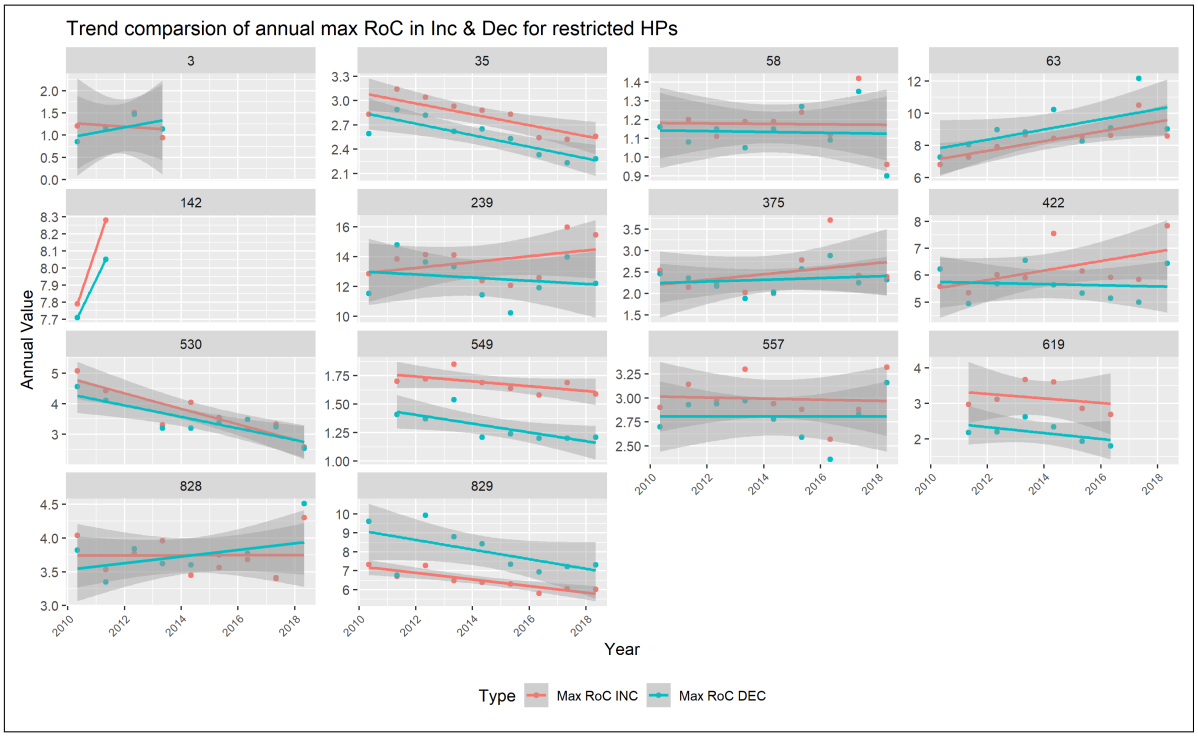

Figure 3.20: Trend for Annual max RoC of fast Inc/Dec for restricted HPs

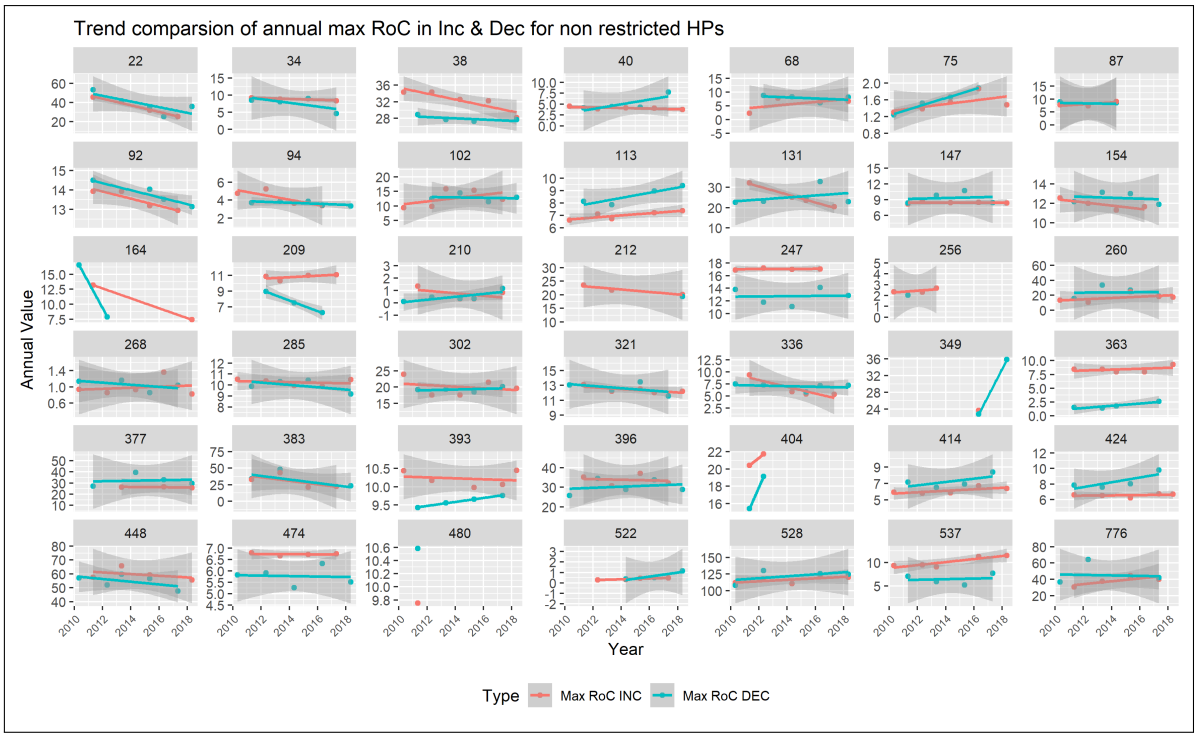

Figure 3.21: Trend for Annual max RoC of fast Inc/Dec for non-restricted HPs

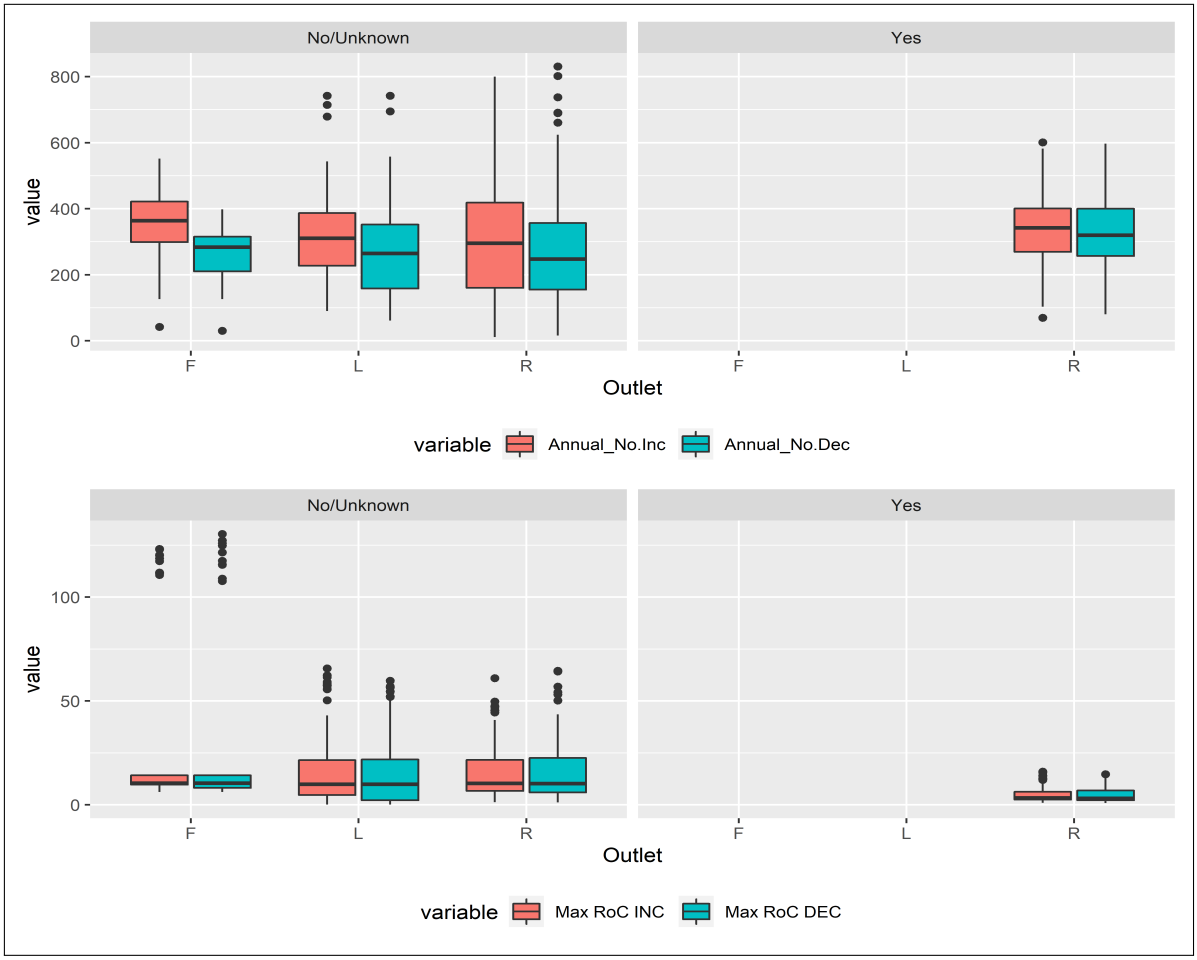

Figure 3.22: Evaluated COSH tool results plotted based on the outlet location and restrictions provided for HPs.

3.4.2 Multiple linear regression

Results representing regression models will be represented here. After checking the normality of distribution of the analyzed variables before building the models it was found out that transformation needs to be carried out to ensure such normality. Procedures and transformations that were carried out can be looked up in Appendix B where the final results showing the normal distribution fitting for regressions variables will be presented.

A very important assumption in linear regression is that there is no correlation between dependent variables. To ensure there is no multicollinearity figure 3.23 shows our visual inspection of the correlation between our investigated variables. It can be seen that there is no significant correlation between variables.

After running the models through R, tables 3.2 and 3.3 show the regression results for HP1 and HP2 respectively. It can be seen that based on R^2 results that there is no significant relation between HP1 and HP2 and HPs parameters.

This interferes with various studies (Greimel et al., 2018; Bruder et al., 2016) which relate the cause of flow ramping to one of HP characteristics such as the head of the power plant.

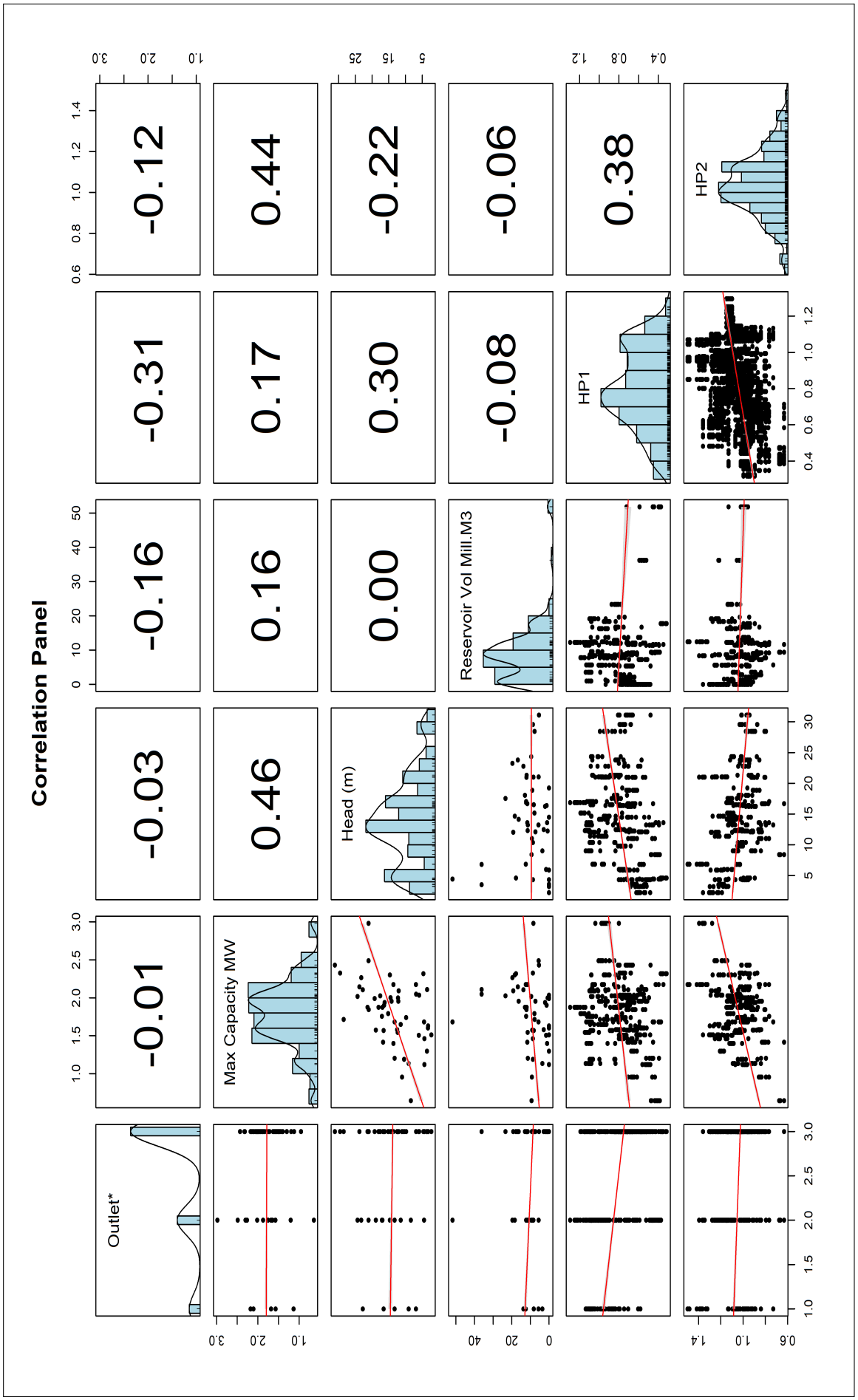

Figure 3.23: Correlation results between the analyzed explanatory and dependent variables

Table 3.2: Regression results for HP1 model

	Dependent variable:
	HP1
OutletL	−0.162***
	(0.014)
OutletR	−0.234***
	(0.011)
'Max Capacity MW'	0.00004
	(0.00003)
'Head (m)'	0.0002***
	(0.00002)
'Reservoir Vol Mill.M3'	−0.0001***
	(0.00001)
Constant	0.958***
	(0.011)
Observations	3,374
R^2	0.186
Adjusted R^2	0.185
Residual Std. Er RoR	0.201 (df = 3368)
F Statistic	154.239*** (df = 5; 3368)
Note:	*p<0.1; **p<0.05; ***p<0.01

Table 3.3: Regression results for HP2 model

	Dependent variable:
	HP2
OutletL	−0.111***
	(0.009)
OutletR	−0.057***
	(0.007)
'Max Capacity MW'	0.001***
	(0.00002)
'Head (m)'	−0.0002***
	(0.00001)
'Reservoir Vol Mill.M3'	0.00000
	(0.00001)
Constant	1.095***
	(0.007)
Observations	3,374
R^2	0.295
Adjusted R^2	0.294
Residual Std. Er RoR	0.131 (df = 3368)
F Statistic	282.397*** (df = 5; 3368)
Note:	*p<0.1; **p<0.05; ***p<0.01

3.4.3 M-K analysis results

Tables 3.4 and 3.5 show M-K test results for different indicators representing Laudal and Svorkmo power plants respectively After processing conducting the M-K test for the indicators related to both power plants. As mentioned before M-K is a hypothesis test where the smaller p-value the more evident that there is an existing trend in the indicator throughout the time.

From the results, it can be seen that HP1 results for both power plants show significant trending with a p-value of 0.002 and 0.05 for Laudal and Svorkmo. However, S results show that trend is negative for Laudal while it is positive for Svorkmo. To investigate more the significant trend that is resulted in HP1, Sen slope estimator was conducted for HP1. Results show there slope estimate for both power plants is not significant however it confirms with the M-K test that the trend exists.

Table 3.4: M-K results for the analyzed indicator for Laudal power plant

Indicator	T-statistic	p-value	S	VAR(S)
HP1	-0.6	0.0021535	-63	408.33
HP2	-0.2952381	0.1376459	-31	408.33
Annual number of Inc	-0.166677	0.4420502	-15	331.66
Annual number of Dec	-0.2087912	0.3244236	-19	333.66
Max RoC during Inc	0.25274724	0.2284398	23	333.66
Max RoC during Dec	-0.0989011	0.6614159	-9	333.66

Table 3.5: M-K results for the analyzed indicators for Svorkmo power plant

Indicator	T-statistic	p-value	S	VAR(S)
HP1	0.33333337	0.0500903	57	817
HP2	0.02923977	0.8887056	5	817
Annual number of Inc	0.20059784	0.2474157	34	814
Annual number of Dec	-0.2136734	0.2191604	-36	811.33
Max RoC during Inc	-0.1812866	0.2939172	-31	817
Max RoC during Dec	-0.0526316	0.779566	-9	817

Table 3.6: Sen slop estimator for HP1 for Laudal power plant

Indicator	Sen's Estimate	T-statistic	p.value	parameter	conf.low	conf.high
HP1	-0.0194	-3.0682	0.0022	15	-0.0273	-0.0066

Table 3.7: Sen slop estimator for HP1 for Svorkmo power plant

Indicator	Sen's Estimate	T-statistic	p.value	parameter	conf.low	conf.high
HP1	0.0065	-3.0682	0.0022	15	-0.0273	-0.0066

3.4.4 Assessment of the potential ecological damage from the investigated HPs

In order to link the calculated results from COSH and Carolli et al. (2015) indicators with the actual ecological damage that can occur to the rivers downstream, it is essential to categorize these calculated results based on different parameters that reflect the characteristics of flow ramping. To do so, the following procedures were followed

First, the power plants located on fjords and lakes were excluded from such classification. This is because such power plants do not possess any potential ramping to rivers. Hence, it is logical to set the focus on the power plants that are located on rivers and map out their results into ramping categories.

Greimel et al. (2016) did a ramping classification for the HPs in the Alpine region. His study classified the ramping into three main categories: 1)Hydro peaking: representing the HPs with storage reservoirs that can be adjusted based on the production demands. 2)Schwellbetrieb: represents RoR power plants with the ability to retain water for a shorter time period and alter the natural flow ratio moderately. 3)Hydro fibrillation: represents those RoR power plants with no ability to retain any water for storage at all; however, they can alter the natural flow change but relatively lower than the second category.

The same classification from Greimel et al. (2016) was used in this work, with additionally classifying the hydropeaking category into three main categories: 1)Low hydropeaking 2)Moderate hydropeaking and 3)Heavy hydropeaking represent the magnitude and the frequency of this type of ramping that occurs.

And to classify the investigated power plants into these categories. First, the resulted indicators were visually assessed for each of these HPs then the same classification table from Greimel et al. (2016) was followed with the two newly added classes. As table 3.8 shows, there are three main parameters define the ramping type along with the HP type. These parameters were calculated as follows.

The first parameter fluctuation rate was defined based on three main indicators. First,

Table 3.8: Classification of the ramping type from HPs operated on the river

HP type	Flow Ramping Type	Fluctuation Rate	Amplitude	Frequency
Reservoir HP	Low Hydropeaking	Low	Low-Moderate	High
Reservoir HP	Moderate Hydropeaking	Moderate	Moderate-High	High
Reservoir HP	Heavy Hydropeaking	High	Moderate High	High
RoR	Hydro fibrillation	Low	Low-Moderate	High
RoR	Schwellbetrieb	Moderate-High	Moderate-High	High

Flow Fluctuation Ratio (FFR) indicator was calculated for those power plants with storage capacity. This indicator is calculated by dividing the max discharge in the power plant Q_{max} by the minimum environmental flow $Q_{Env.}$. This indicator is crucial for setting the amplitude of the ramping ratio that can theoretically occur for each power plant in case there are no restrictions on the operation provided or voluntary limitation on change of operation. Due to the lack of data regarding the minimum flow of some of the HPs, some of the minimum flow was assumed based on an expert judgment from my supervisors. After it was calculated for each HPs, it was classified into five main classes:

$$FFR = \begin{cases} 1-3 & \text{Low FFR} \\ 3-5 & \text{Low-Moderate FFR} \\ 5-10 & \text{Moderate-High FFR} \\ >10 & \text{High FFR} \\ > NotRelevant(N.R) & \text{for RoR power plant} \end{cases}$$

The second indicator that influences the class of the fluctuation rate was the normalized maximum rate of decrease per 1-time step (Max.RoC.Dec.Ratio). This was calculated first by calculating the median of the annual Max decrease RoC from COSH then normalizing it by the minimum flow of each HP. After it was calculated, it was classified into the following categories:

$$MaxRoC.Dec.Ratio = \begin{cases} 0-0.8 & \text{Low} \\ 0.9-4 & \text{Moderate} \\ >4 & \text{High} \end{cases}$$

This indicator differs from FFR as it shows the actual maximum potential ramping magnitude that has occurred occur by the power plant during the investigated time period. Moreover, the median of HP1 for each power plant was calculated for confirmation of the

level of ramping that occurs and then it was classified into 3 main categories as follows:

$$HP1 = \begin{cases} 0 - 0.5 & \text{Low} \\ 0.5 - 1.4 & \text{Moderate} \\ > 1.4 & \text{High} \end{cases}$$

This classification could not be implemented on the RoR power plants for the following reasons. First, RoR has a constant flow that goes through the turbine; hence, neither (FFR) nor (Max.RoC.Dec.Ratio) indicators can be implemented for this scheme of HP. Additionally, the magnitude of ramping for RoR is minimal compared to the storage power plant (Total average HP1 of 0.1); therefore, this cant be used for differentiating the ramping that occurs from this scheme of power plants. To overcome this problem and differentiate between the level of fluctuation rate that occurs from this scheme of the power plant, the absolute maximum rate of change during decrease was used in two main categories as follows

$$Max.RoC.Dec = \begin{cases} 0 - 10 & \text{Low} \\ > 10 & \text{High} \end{cases}$$

Eventually, the flow fluctuation rate class was determined for the reservoir HPs based on the above mentioned three main indicators and for the RoR scheme based on Max Dec Roc indicator.

The frequency category refers to the difference of flow ramping occurrence in comparison to natural floods or intensive precipitation and other natural phenomena, which is generally less frequent to occur compared to those anthropogenic changes (Carolli et al., 2015; Greimel et al., 2016). However, an additional type of frequency was added to classify the peaking power plants into regular or irregular throughout the day. This is mostly done to differentiate between RoR and storage power plants that aim to adjust the production based on the market demands.

As for the Amplitude, it was assessed visually using figure 3.5 representing d.Q throughout the time period for the river located power plants.

After processing all the above-mentioned classifications, the results of the classification are presented in table 3.9. These classifications are crucial in order to map out the power plant with severe ramping and further link this ramping with the impact on the ecosystem in their rivers either by fieldwork, fish indexes, or habitat modeling.

Table 3.9: Classification of the ramping type for the HPs located on rivers

Name	Number	Type	Max Q	Env.Flow	Max.RoC.Dec.Ratio	Freq	HP1	Restrictions	Ramping Type	FFR_CLASS
Alta	3	Reservoir	96.01	16	L	Regular	L	Yes	Low Hydropeaking	5_10
Bingsfoss	22	ROR	820	0	H	Regular	L	-	Schwellbetrieb	N.R
Braskereidfoss	37	ROR	450	65	L	Regular	-	-	Hydro fibrillation	N.R
Bratsberg krv	38	Reservoir	105	30	M	Irregular	M	No	Moderate Hydropeaking	3-5
Brattset	40	Reservoir	36.02	0	M	Irregular	M	No	Moderate Hydropeaking	5_10
Dividal	58	Reservoir	11.59	0	L	Irregular	L	Yes	Low Hydropeaking	5_10
Driva	63	Reservoir	30.01	11	M	Irregular	L	Yes	Low Hydropeaking	3-5
Eidfoss	68	ROR	93.83	0	L	Regular	L	No	Hydro fibrillation	N.R
Einunna	75	Reservoir	8.98	-	M	Regular	L	-	Low Hydropeaking	5_10
Fjæremsfoss	87	ROR	80.33	0	L	Regular	L	-	Hydro fibrillation	N.R
Skagen	94	Reservoir	32.5	0	M	Irregular	L	No	Moderate Hydropeaking	>10
Funnefoss	102	ROR	444.44	-	L	Regular	L	-	Hydro fibrillation	N.R
Grana	113	Reservoir	19.01	0	H	Irregular	L	-	Heavy Hydropeaking	>10
HARPEFOSS	131	ROR	400	-	H	Regular	L	No	Schwellbetrieb	N.R
Hemsil II	142	Reservoir	31	-	H	Irregular	M	Yes	Moderate Hydropeaking	5_10
Storåni	154	Reservoir	32.4	0	H	Irregular	M	No	Heavy Hydropeaking	>10
Hunderfossen	164	RoR	299.14	15	L	Regular	L	No	Hydro fibrillation	N.R
Kongsvinger	212	ROR	510	-	H	Regular	L	-	Schwellbetrieb	N.R
Laudal	239	Reservoir	30.02	8	M	Regular	L	Yes	Moderate Hydropeaking	-
Lysebotn krv	256	Reservoir	5.5	-	M	Irregular	-	No	Moderate Hydropeaking	>10
Lopet	260	Reservoir	176	-	H	Irregular	M	No	Heavy Hydropeaking	>10
Søre Osa	321	Reservoir	54.95	-	H	Irregular	M	-	Heavy Hydropeaking	5_10
Rendalen	336	ROR	60	-	L	Regular	L	No	Hydro fibrillation	N.R
Raanaafoss	349	ROR	1215	-	H	Regular	L	-	Schwellbetrieb	N.R
Savalen	363	Reservoir	32	-	L	Irregular	H	-	Low Hydropeaking	1_3
Skibotn	375	Reservoir	18.5	6	L	Irregular	L	Yes	Low Hydropeaking	3-5
Skjefstadfoss	377	ROR	220	40	H	Regular	L	No	Schwellbetrieb	N.R
Sokna	393	Reservoir	16	0	H	Irregular	H	No	Heavy Hydropeaking	>10
Straumsmo	404	Reservoir	70	0	H	Irregular	-	No	Heavy Hydropeaking	>10
Svartelva krv	414	Reservoir	16.6	0	H	Irregular	M	No	Heavy Hydropeaking	5_10
Svorkmo	422	Reservoir	69.12	-	L	Regular	L	Yes	Low Hydropeaking	>10
Ulset	474	Reservoir	12	-	H	Irregular	H	No	Heavy Hydropeaking	>10
Årøy	530	Reservoir	70.02	3	L	Irregular	L	Yes	Low Hydropeaking	>10
Mel	549	Reservoir	7.5	1.5	L	Irregular	L	Yes	Low Hydropeaking	5_10
Stuvane	557	Reservoir	28	-	L	Irregular	L	Yes	Low Hydropeaking	3-5
Meråker	619	Reservoir	36.7	9.5	L	Irregular	L	Yes	Low Hydropeaking	3-5
Solbergfoss	776	ROR	1200	-	H	Regular	L	No	Schwellbetrieb	N.R
Øyberget	828	Reservoir	75	0.3	M	Irregular	L	Yes	Low Hydropeaking	>10
Framrusti	829	Reservoir	27	0.65	H	Irregular	L	Yes	Heavy Hydropeaking	>10

Note *L: Low, M: Moderate, H: High, N.R: Not Relevant, -: Missing data*
All discharge values in m3/s. Storåni data is measured gauge data

Finally, and to further differentiate between the the different level and characteristics of the occurred flow ramping. a quantile curve was made for those investigated power plants representing the flow fluctuations intensity and the occurrence in percentile. Flow fluctuations intensity is a ratio between the different percentile of the maximum rate of change normalized by the maximum value of this indicator. The important of this is to distinguish between different operational scheme and characteristics of HPs and their characteristics. Due to the fact that it is not possible to obtain the pre-analyzed data from COSH, the calculated percentiles were used for every year for each power plant.

Using these curves show significant differentiation among the categories of ramping. As it can be seen in figure 3.24 that the scheme of the power plant determines the characteristics of the ramping that can occur. for instance, RoR power plants tend to have less than 25% of the maximum RoC for up to 90% of the time while reservoir power plants varies and signficantly reach higher percentage of the maximum RoC for more 50% of the time.

Moreover, figure 3.25 shows the different ratio of the maximum RoC for different ramping classes. It can be seen that hydro fibrillation RoR tend to operate on the lowest ratio from its maximum RoC while heavy hydropeaking plants use up to 75% of the maximum RoC during its operation more than 50% of the time. This curve also shows that there are outliers in the classification of ramping types for the power plants particularly for Schwellbetrieb and heavy hydropeaking classes.

Additionally, the same curve was plotted for the RoR power plants only. Figure 3.26 shows there is difference between the two ramping classes as it can be seen that Schwell-betrieb has higher magnitude of the RoC. It can be also seen that there is some deviations in the curve that does not comply with the classification that was conducted.

Finally to Link the heavily hydropeaking power plants with the ecological impact regrading the effect on the population of the fish, a threshold was used from Schmutz et al. (2015) results as his regression model shows that there is a strong correlation between the reduction of the population of the fish if the number of the annual severe peaks occurs more than 20 times per year. A severe peak is identified by the 90th percentile value of the maximum RoC in one time step. If this value is exceeded then a severe peak event is counted.

Using the same concept, the median of the 90th percentile value of the max decrease RoC was calculated from COSH tool for the heavy hydropeaking power plants and set as a threshold for every time step of the calculation. As it can be seen from table 3.10 that some of these power plants exceed this threshold significantly.

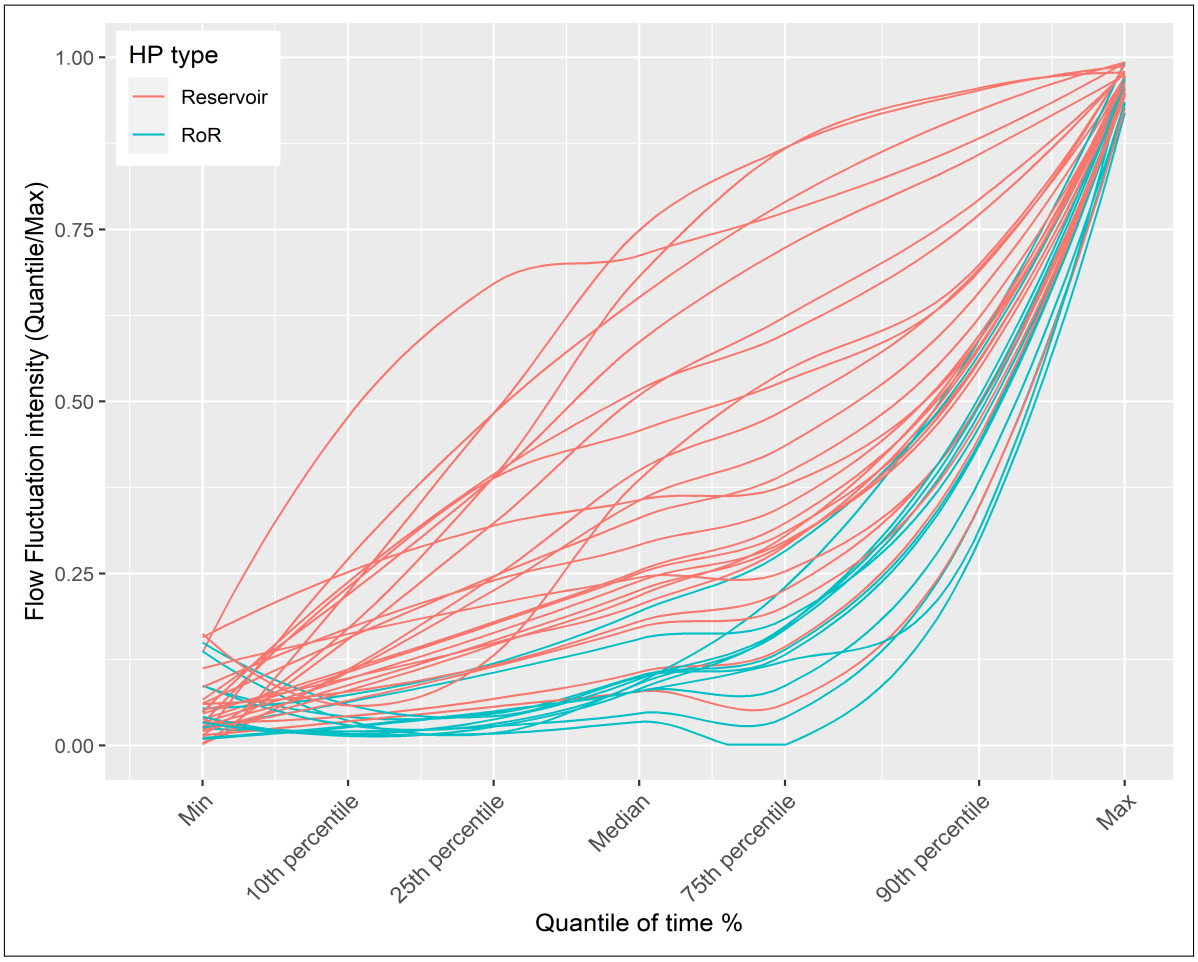

Figure 3.24: Quantile curve for the ratio of max ramping rate for different type of HPs located on the river

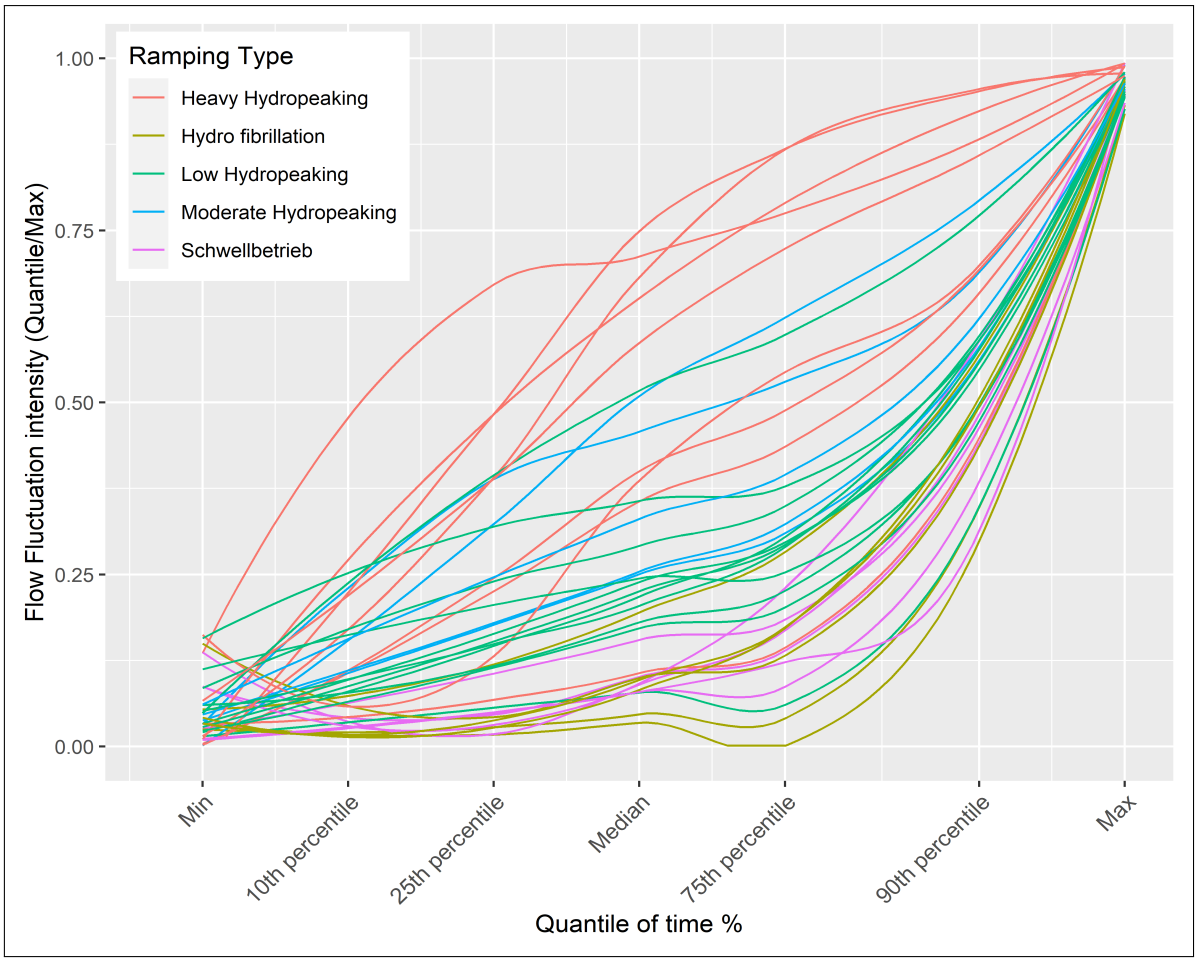

Figure 3.25: Quantile curve for the ratio of max ramping rate for different ramping classes of HPs located on the river

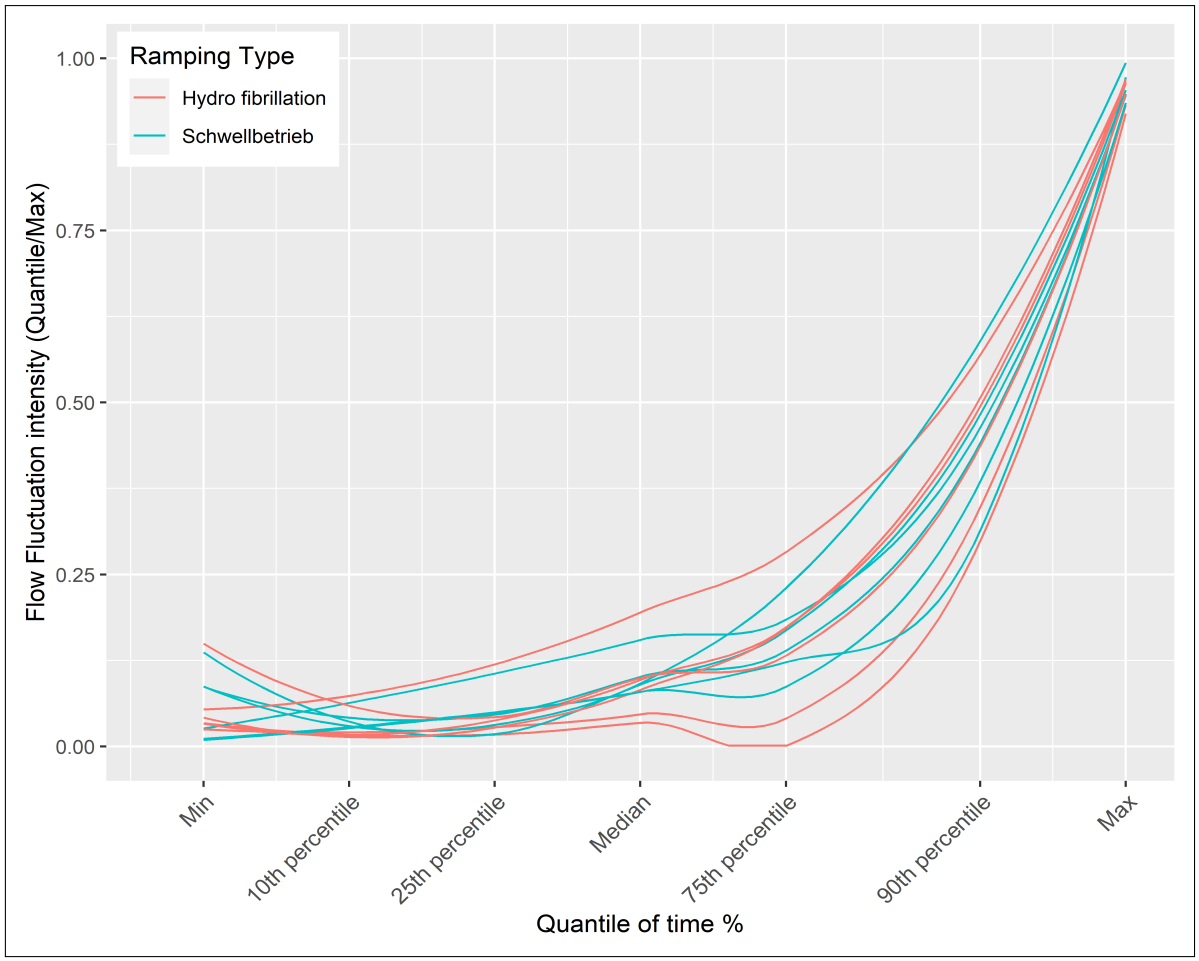

Figure 3.26: Quantile curve for the ratio of max ramping rate for different ramping classes for RoR HPs

Table 3.10: Annual number of severe peaks for heavy hydropeaked power plants

	Name	Grana	Storåni	Sokna	Ulset	Framrusti
	HP Number	113	154	393	474	829
Number of Severe Peaks	2010	-	-	-	4	26
	2011	-	17	12	10	15
	2012	2	25	13	13	23
	2013	4	19	14	12	21
	2014	2	20	10	6	12
	2015	2	21	17	9	8
	2016	0	14	7	13	19
	2017	51	11	41	19	11
	2018	-	-	-	11	-

3.5. Discussion

Flow ramping poses a great threat to the environment as it can cause various negative impacts on the riverine biota. However, the resulted flow ramping effect from HP operation needs to be connected with the geographical and technical aspects of HP itself to have a prior assessment of the potential ecological damage from this ramping. Results show a severe and intensive variation of the flow for some HP; however, their outlet is located on fjords, lakes, or reservoirs. This level of flow ramping from HP located on a fjord can be neglected as it does not pose any ecological threat to any river stream. However, for HPs located to lakes or reservoirs, further assessment needed to determine whether and to what extent the capacity of this reservoir or lake will dampen the magnitude and the frequency of the occurred flow ramping effect on the river downstream.

Additionally, It can be seen from the before-mentioned figures that severe and frequent flow ramping occurs from HPs located on river streams and without any restrictions to limit or minimize this ramping effect. This type of ramping needs further assessment as it poses potential ecological damage to the riverine ecosystem, which also is dependent not only on the level of flow ramping but also the river morphology and characteristics of the riverine biota itself.

On the other hand, it can be seen that in general, restrictions implied on the operation of HPs have lowered the level of flow ramping to the majority of this power plant in comparison to HPs without restriction implemented to limit this operational pattern. It can be seen from the calculated indicators in figure 3.17 and 3.22 that restricted HPs has a relatively lower magnitude of flow ramping represented in RoC and HP1 yet, these restrictions didn't affect the level of frequency represented in the number of ramping events and HP2. Nevertheless, there are some defects in the efficiency of these implied restrictions that require further investigations such as Framusti power plant with significantly bigger RoC compared to other restricted HPs, which can vary between 0-5 $m^3/s/h$.

Furthermore, the results of this chapter show that the occurred flow ramping has different characteristics based on different HPs type and their operational pattern. For instance, it can be seen that the majority of RoR power plants show the same pattern of flow ramping characteristics and can be categorized into two main categories. First, by investigating the COSH results regarding this type of HPs, it can be seen that the majority has a regular distribution of an intensive number of rapid flow ramping events throughout the day with up to 6 -7 number of events per day with small RoC that can be estimated 0-10 $m^3/s/h$. This type of flow ramping has been defined in (Greimel et al., 2016) as hydro fibrillation, which refers to the intensive regular rapid small changes in the discharge. These small

changes are due to minor adjustments for load balancing in the grid system.

Additionally, there is another type of RoR scheme power plant that has the ability to cause relatively higher ramping compared to the hydro fibrillation type. This type of RoR has the same intensive number of rapid changes, yet with a higher magnitude that can be up to 35 m^3/s/h. Greimel et al. (2016) classified this ramping as Schwellbetrieb. This ramping is mainly done due to RoR that has the ability to retain water for a few hours and gives the opportunity to more adjust their production rate with a higher percentage than the hydro fibrillation category.

Greimel et al. (2016) also specifies that the above-mentioned two types of flow ramping exist in the river downstream of RoR power plants, which comply with COSH results for this type of power plant as well as the quantiles curves.

On the contrary, characteristics of the occurred flow ramping from storage HPs differs from the RoR power plants. Based on COSH results, it can be seen that the majority of this type of HPs have relatively less frequent daily peaking events with an average of 2 ramping events per day. Yet, these events are irregularly distributed throughout the day, and significantly higher magnitude than the occurred from RoR plants. These results don't comply with all storage HPs as it can be seen, for instance, that Laudal and Svorkmo power plants have regular, more frequent ramping events. It can be concluded that this type of flow ramping is a result of hydropeaking that occurs due to the change in market price to gain the most revenue of energy production.

It can also be concluded from the results that restrictions implied on the storage HPs have proven, in most cases, efficiency for reducing the magnitude of ramping events. Yet, it didn't affect the frequency and regularity of occurred ramping events. an example of the efficiency of the ramping restrictions can be seen from Alta-3 power plant as results show it has a lower magnitude of the ramping ratio than some of the RoR power plants as it can be seen from figure 3.24 and 3.25.

Subsequently, figure 3.5 shows that there are a significant number of extreme changes in the flow, which indicates the accidental shutdown or fast starting of the power plant. It can be seen that power plants with no restrictions on the operation have more numbers of these extreme events. Such events need to be further taken into consideration as it can cause severe stranding or drifting effect on the riverine biota and should be mitigated. The existence of a bypass valve can be a good solution to mitigate such type of severe flow ramping; however, it doesn't exist in most of the storage power plants.

It is also important to mention the role the environmental flow plays to minimize the level of ramping. A relatively higher environmental flow in reference to the maximum discharge of the power plant can significantly reduce the rate of ramping that occurs

from the HP operation. The existence and the level of the environmental flow compared to the maximum capacity of the power plant plays a very important role in determining the level of the ramping that occurs and also mitigating this ramping.

Additionally, the existence of dampening reservoirs or lakes can also reduce or mitigate the impact from flow ramping depending on the capacity of this lake and the rate of ramping that happens.

Moreover, It can also be seen that A linear trend line does not work efficiently in determining the existence of any trend, whether by increase or decrease in any of the calculated indicators. Figures 3.20 and 3.21 show that the indicators vary a lot non-linearly. Trend tests such as M-K would work more efficiently for assessing the existence of such a trend provided that there is longer time series to be assessed, which was not the case in this study except for a few HPs only.

It can also be seen that the constructed regression models failed to show any significant results between HP parameters and the magnitude and frequency of flow ramping represented in HP1 and HP2. This result does not comply with various studies (Greimel et al., 2018; Bruder et al., 2016) that refer to the existence of a relation between the level of ramping and the head of the power plant, for instance. Besides, the regression results don't comply with the resulted indicators from the COSH tool that differentiate the pattern and the characteristics of flow ramping to some properties of the HP itself. The reason for not showing the existence of such a relationship might be due to the limitation of the number of investigated power plants. Further analysis is required to investigate, map, and categorize the occurred flow ramping from the power plants based on their properties in case additional data would be provided.

Moreover, results regarding the M-K test for the two investigated power plants show that there is a trend in the magnitude of ramping for both power plants (Laudal-239) and (Svorkmo-422). Although the estimated Sen's slope is not significant, the efficiency of the restriction on operation for these two power plants needs further assessment.

Consequently, it can be concluded that severe ecological damage from flow ramping can be resulted based on HP characteristics and the river properties. First, HP with bigger storage capacity and high head with no restrictions on the flow ramping and relatively or low minimum flow can pose the most significant potential of flow ramping. Subsequently, a river morphology with high steep and long reach will extend this ramping effect along the reach in addition to the key species that exist in the riverine itself. On the other hand, an ecologically friendly operational HP can be characterized to be generally RoR and HP with restrictions specified in their license against flow ramping and relatively higher environmental flow.

Based on that, results from table 3.9 provides an indicator for the HPs that are currently causing heavy hydropeaking and should be investigated for further assessment and mitigation. As it can also be seen from table 3.10 that some of these HPs (Grana, Storåni, Sokna, Ulset, and Framrusti) are causing severe ramping that is well documented having a significant effect on the population of the fish. These class of ramping power plants needs to be taken into considerations for further assessment and evaluation of the mitigation measures implemented.

Additionally, the resulted quantile curves in figures 3.24-3.26 proved an efficient way of differentiating the type and pattern of the flow ramping that occurs for different power plants. Also, it complies with Greimel et al. (2016) duration curves for differentiating the type and the magnitude of flow ramping that occurs from RoR than from hydropeaking power plants.

It is also important to mention that this work relied on a fixed time step for the calculation of all the indicators, which is more conservative than other studies such as Schmutz et al. (2015) and Greimel et al. (2016). However, results still show that there are some power plants located in the rivers and causing heavy hydropeaking that require further mitigation.

The ecological effect of the type of flow ramping that occurs in RoR scheme power plants needs further studies to put a grasp on the response from the riverine ecosystem. Also, the impact of flushing due to the rapid increase of the flow needs to be more assessed and link its impact on the small habitats and macroinvertebrates in the river.

4. MITIGATION FOR HYDROFLEX SCENARIOS

4.1. Overview and investigated location

As mentioned in section 2.3.3, HydroFlex is an innovative project providing more flexibility to the operation of HP, allowing it to start and stop in 15 minutes time interval. In order to cover all the project aspects, HydroFlex provided a work package evaluating the social and environmental impacts of the project. Work package developed 2 hydraulic models representing 2 rivers from their five reference HP for further investigation and assessing the environmental impact (Juarez et al., 2019).

4.1.1 Investigated location

The focus of this part of the study shall be on the river Nidelva where HP Bratsberg is operated. The river is located in Trøndelag region in Norway. It is regulated and serves some HPs. The workgroup developed the hydraulic model representing the last 10 km of the river from the very last regulation in Nedre Leirfoss until the drainage location in Trondheim fjord. Water surface level (WSE) varies in the river from 11 to -1 M.A.S.L. The river is considered to be a fish habitat for Atlantic salmon and brown trout. The modeled river reaches from the outlet location of the lowest operating HP Bratsberg till the fjord is considered a reproduction area for the fish. The river has a current minimum flow of 35 m^3/s while the flow can increase up to 135 m^3/s.

The lowest HP operating is called Bratsberg. It has two Francis turbines with a height of 147 meters and a max capacity of 124 MW. A current typical daily operation of the plant is by turning off the plant at night then turning on either one of the two turbines into production from the morning rush hour. Consequently, with 30 m^3/s minimum flow, this exposes the river to a moderate ramping effect (Saltveit et al., 2001). Figure 4.1 shows the level of variation of flow in the last two months in 2018.

4.1.2 Model development

The model terrain was developed through a combination of LiDAR data representing the river banks, previous work surveys, and additional field measurements where there is

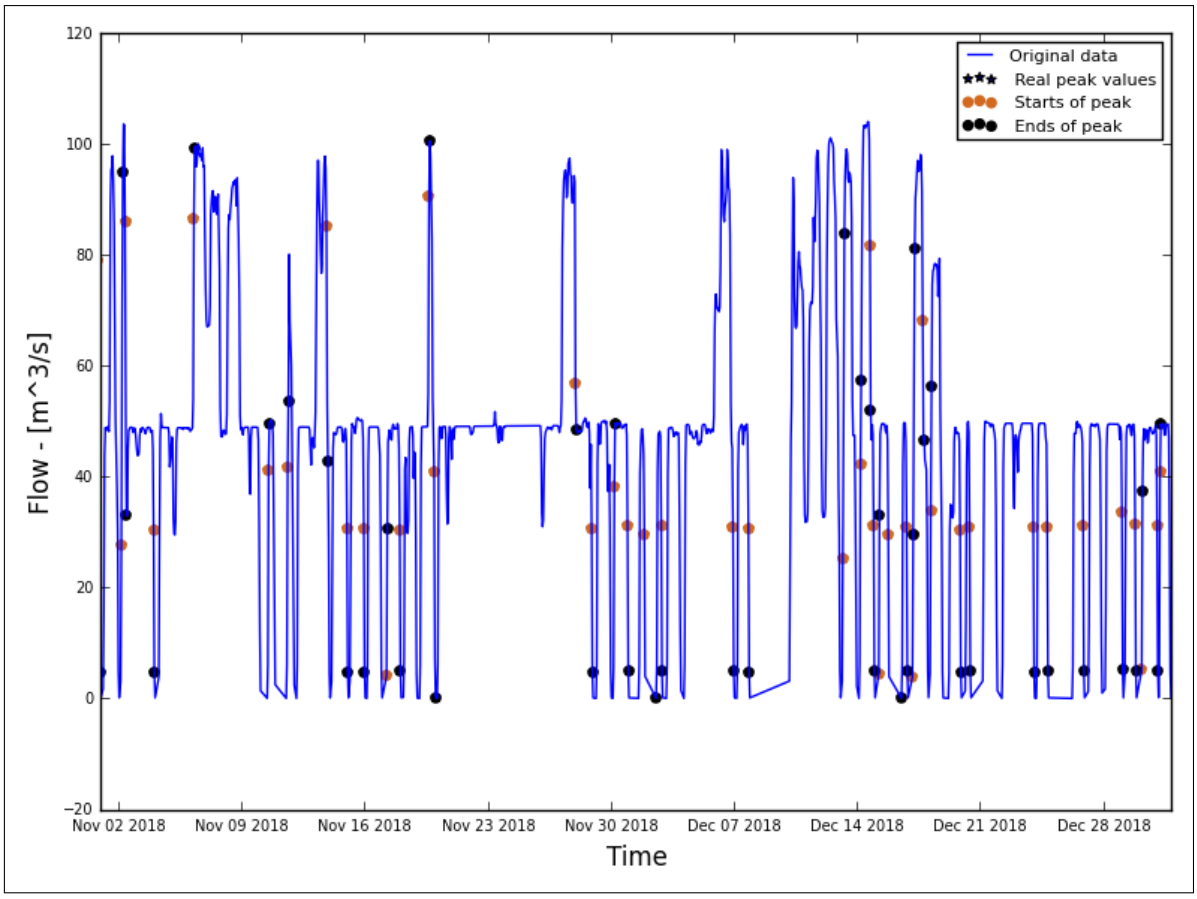

Figure 4.1: Flow hydro-graph for the last two months in 2018 of Bratsberg

no available data. HEC-RAS 2D was then used for building the hydraulic model based on the terrain input. After the model was built and tested, calibration was made by adjusting the manning number by testing different areas and inserting it as a data-set in the model. Different measurements in different areas of the river were taken to compare the modeled WSE to the observed values. Eventually, the model reached a final accuracy of a 6 cm difference between modeled and observed WSE. Additionally, 1D simulations were conducted for modeling temperature. The model error was found out to be 0.18°C (Juarez et al., 2019).

Furthermore, additional work was carried out using the hydraulic model for validation and testing its efficiency representing the flow characteristics in detail by Graf (2019) under the research of the HydroFlex project framework. The first main task of Graf (2019) work is to validate the model by running different simulations scenarios in a different region of the model and compared evaluated the efficiency of the model results working as a whole and working in small parts by measuring the difference between the modeled and observed results. He concluded that the model is verified and validated, resulting in more accuracy when it is working as a whole. It can be used for measuring the dried out areas, the velocity of dewatering and other hydro-morphological parameters that can be used for indicating the ecological impact on the river.

4.1.3 Previous work and environmental Impacts

Fieldwork was carried out by Saltveit et al. (2001) in the area to evaluate the effect of the instant shutdown of the power plant on the amount of mortality of fish. Results show that there is a significant mortality rate of salmonid fish due to the stranding, which is caused by the rapid decrease in the flow discharge in the river. Moreover, journal results show also that the rate of stranding varies a lot not only depending on the rate of dewatering, but also on other parameters such as the water temperature, period of the year, and light condition. Results show that the highest rate of stranding occurs in winter with low water temperature during the daytime. Saltveit et al. (2001) also pointed out the possibility of reducing the stranding effect by increasing the time of shutting down the power plant.

4.2. Method used

In order to assess the environmental impacts from the implementation of the HydroFlex production scenario on the river of Nidelva and evaluate mitigation measures to minimize this impact, the following methods will be used.

4.2.1 Hydraulic simulations

The production scenario of Bratsberg was obtained from the HydroFlex researcher in Aachen research center. Figure 4.2 shows one week from the production scenario of Bratsberg power plant in HydroFlex scenario. The production scenario shows an extreme variation in the rate of production that can vary from maximum production to instant shutdown in less than 15 minutes.

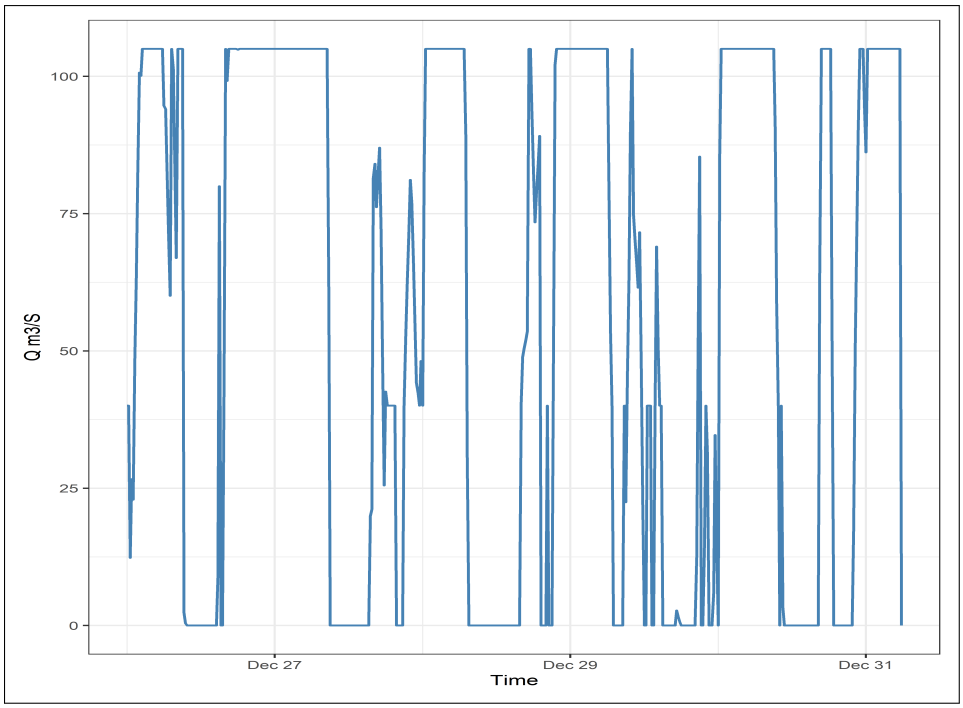

Figure 4.2: Weekly HydroFlex production scenario developed for Bratsberg power plant

After analyzing the HydroFlex production scenario, the hydraulic model representing Nidelva was used in the following plan. First, In order to map out the environmental impact on the river from the above-mentioned production scenario, a simulation has been run using the worst production scenario on the river of Nidelva by running a simulation from the maximum production to the minimum flow that is specified to be 35 m^3/s. And to obtain the dried out areas and the velocity of drying out for these areas, results were processed and presented using GIS software.

After mapping out the most exposed areas and the velocity of dewatering in these areas, different simulations were run using the model to reach out to the most optimum way of operation that will minimize to some extent the stranding effect on the fish downstream. In order to achieve a slow dewatering rate using Halleraker et al. (2003) guidelines for the operation of hydropower, different simulations were conducted to reach the most feasible operation pattern that will reach the before mentioned velocity of drying out.

By plotting out the most severe production scenario from HydroFlex with the environmental guideline simulation, it is possible to obtain the amount of water needed to maintain the rate of ramping to 10-13 cm/h. Using this volume of water, it is possible to evaluate the traditional mitigation measure, and in collaboration with (Storli and Lundström, 2019), it is possible to evaluate the efficiency of ACUR as an innovative solution for this problem. All the above-mentioned methods will be conducted using HEC-RAS-2D for the hydraulic simulations and ArcGISPro as a GIS software in addition to R and Excel to post-process the data.

4.3. Results

Results of the simulations that were run using the hydraulic model, and data processing using GIS will be presented in this section. First, the model response to the river downstream was analyzed in order to set the time boundary. Figure 4.3 shows that the model takes up to 12 hours to fully respond and stabilize from the change in the discharge from the upstream i.e., the change in production from the power plant. Building from that, All the simulations that were done are based on the worst production scenario during 12 hours time period.

The results will be presented in the following order. First, results representing the dried out areas from the HydroFlex scenario be presented then the iterative simulations to reach the optimum production scenario that will not cause a negligible stranding effect on the fish will be shown. Eventually, an evaluation of different mitigation measures will be presented.

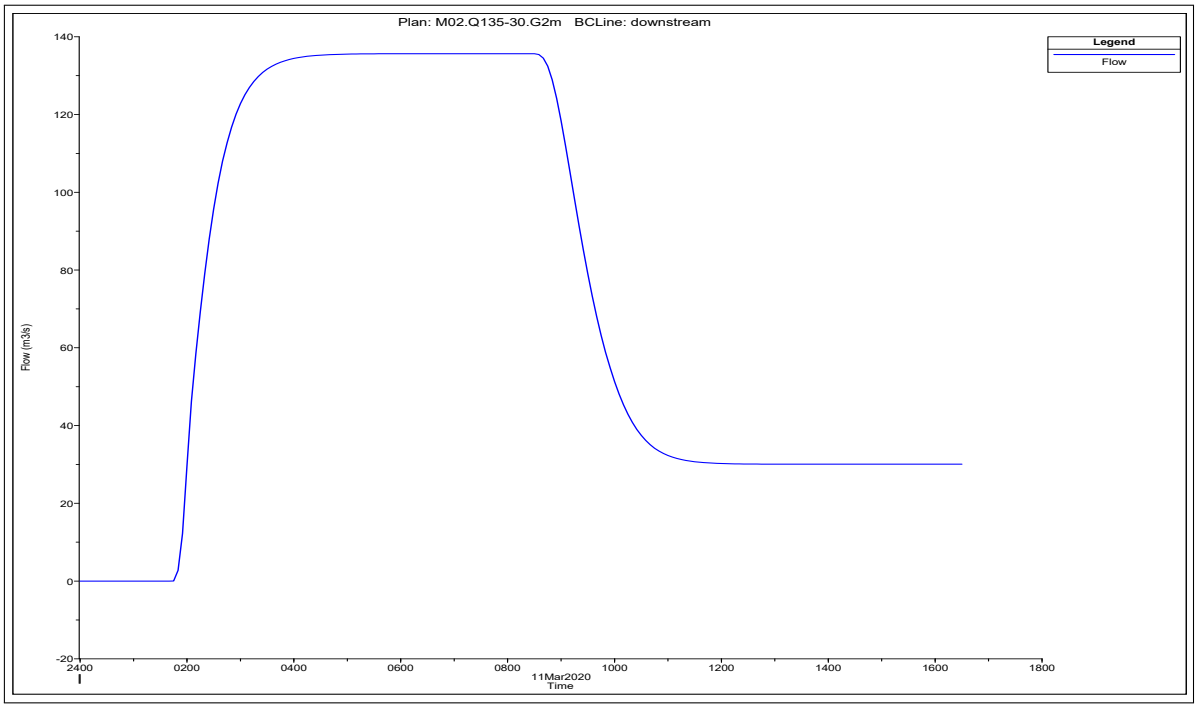

Figure 4.3: Downstream boundary condition reaction time in Nidelva

4.3.1 Dried out areas

After running a simulation based on the HydoFlex production scenario From maximum production to the minimum flow specified in the river regulation (35 m^3/s) and process the results to GIS, it was found out that there are sere dried out area along the

river downstream. This shows the fact that a constant minimum flow of 35 m^3/s is not sufficient for mitigating the impact of stranding areas. Figure 4.4 below shows the summarized dried areas that would result from such a production scenario.

In order to further evaluate the results from this scenario Casas-Mulet et al. (2015) method was used for measuring the dewatering rate, however, instead of using actual fieldwork measurements using piezometers, measurements points were used on the dry, shallow and wet area along with the affected areas through GIS. These points were further used for evaluating the rate of dewatering by being classified into regions, and then the average for each region was computed. This was done by extracting the depth of water at each point every 5 minutes during the simulations, then process the results in excel as it will be shown in the next section.

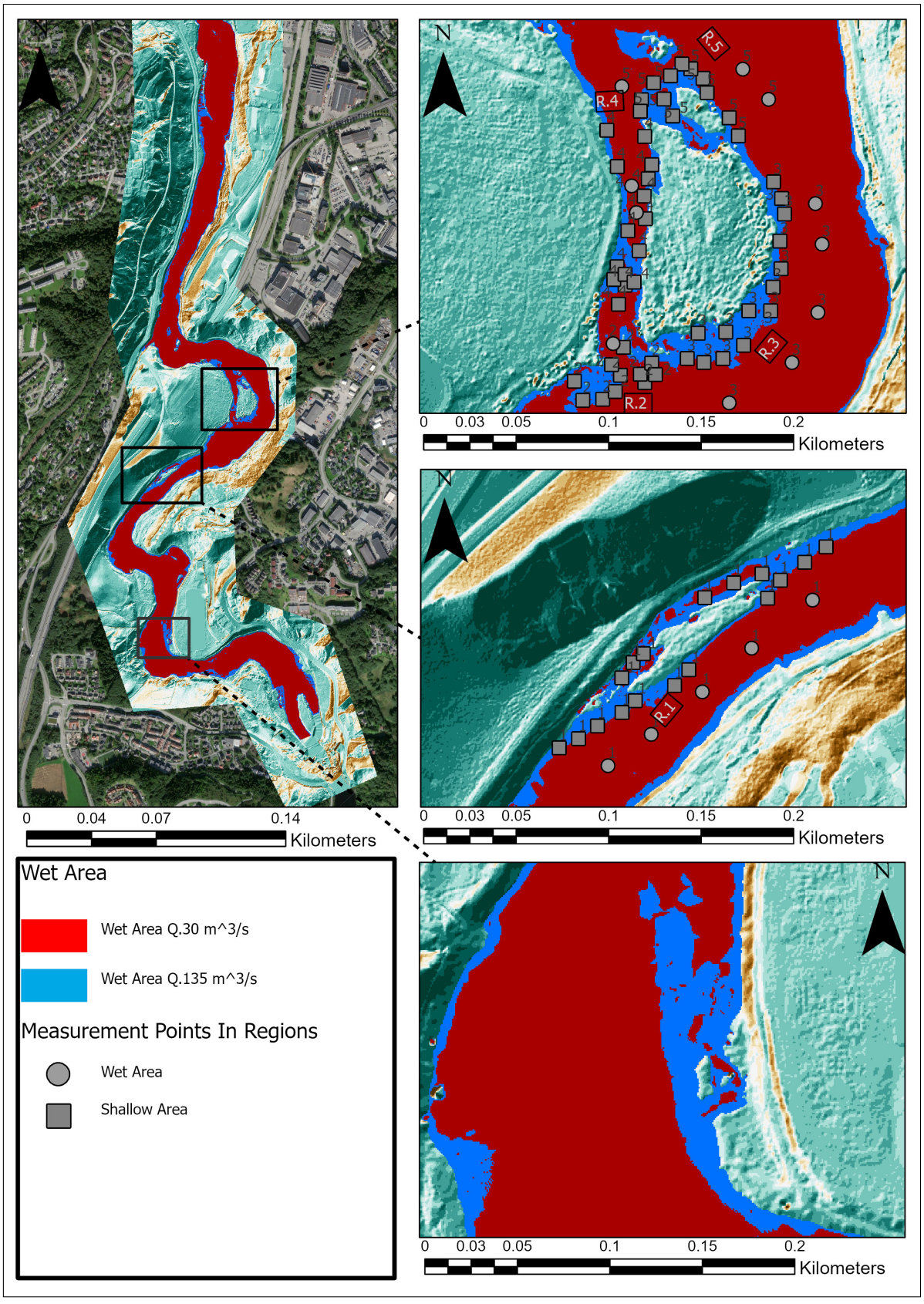

Figure 4.4: Dried out areas due to HydroFlex production scenario. Exposed areas are separated into region numbers.

4.3.2 Dewatering rate

In addition to the drying out areas, the rate of dewatering is considered a crucial aspect for the mortality and stranding rate of fish in the river (Halleraker et al., 2003). Based on Halleraker et al. (2003) field experiment, the rate of dewatering has a great effect on the portions of stranding fish. He classified the dewatering rate into 3 categories; huge stranding effect (dewatering rate > 60 cm/h), moderate stranding effect (dewatering rate $\approx$ 20 cm/hr) and low stranding rate where the dewatering rate is less than 10 cm/hr.

Building from that, the measurement points were used for evaluating the dewatering rate. In every region, different points were used in the hyporheic area as well as the wet area in order to obtain a proper average of the dewatering rate. after extracting the results for the water depth, every 5 minutes results were investigated visually.

Figure 4.5 shows the dewatering rate for the evaluated points. In order to accurate results representing the dewatering rates, measurements taken after reaching a stable water level needs to be excluded. To do that the dewatering rate was calculated as follows:
for every point, the rate of dewatering was calculated for every 5 minutes

$$\text{Dewatering rate}_k = \frac{depth_{i+1} - depth_i}{5} * 60 * 100 = cm/hr \tag{4.1}$$

and then if the dewatering rate is less than 1 cm/hr, it is excluded from the calculation. After that, for each point, the dewatering rate is calculated:

$$\text{Dewatering rate for point n} = Average(Dewatering_k) \tag{4.2}$$

Then to have an overview of the average for each region, the average was calculated for all its representing points. Table 4.1 shows the resulted average dewatering rate for each region. It can be seen that the dewatering rate will result in a big stranding effect on the fish in most of the exposed regions. Additionally, results in regions 2-5 are nearly similar to the fieldwork conducted by Saltveit et al. (2001) for measuring the dewatering rate in the river 1.3 km along with the downstream.

Table 4.1: Dewatering rate for the exposed regions due to HydroFlex production Scenario

Region Number	Region 1	Region 2	Region3	Region 4	Region 5
Avg dewatering rate (cm/h)	53.72	73.22	68.94	70.29	61.02

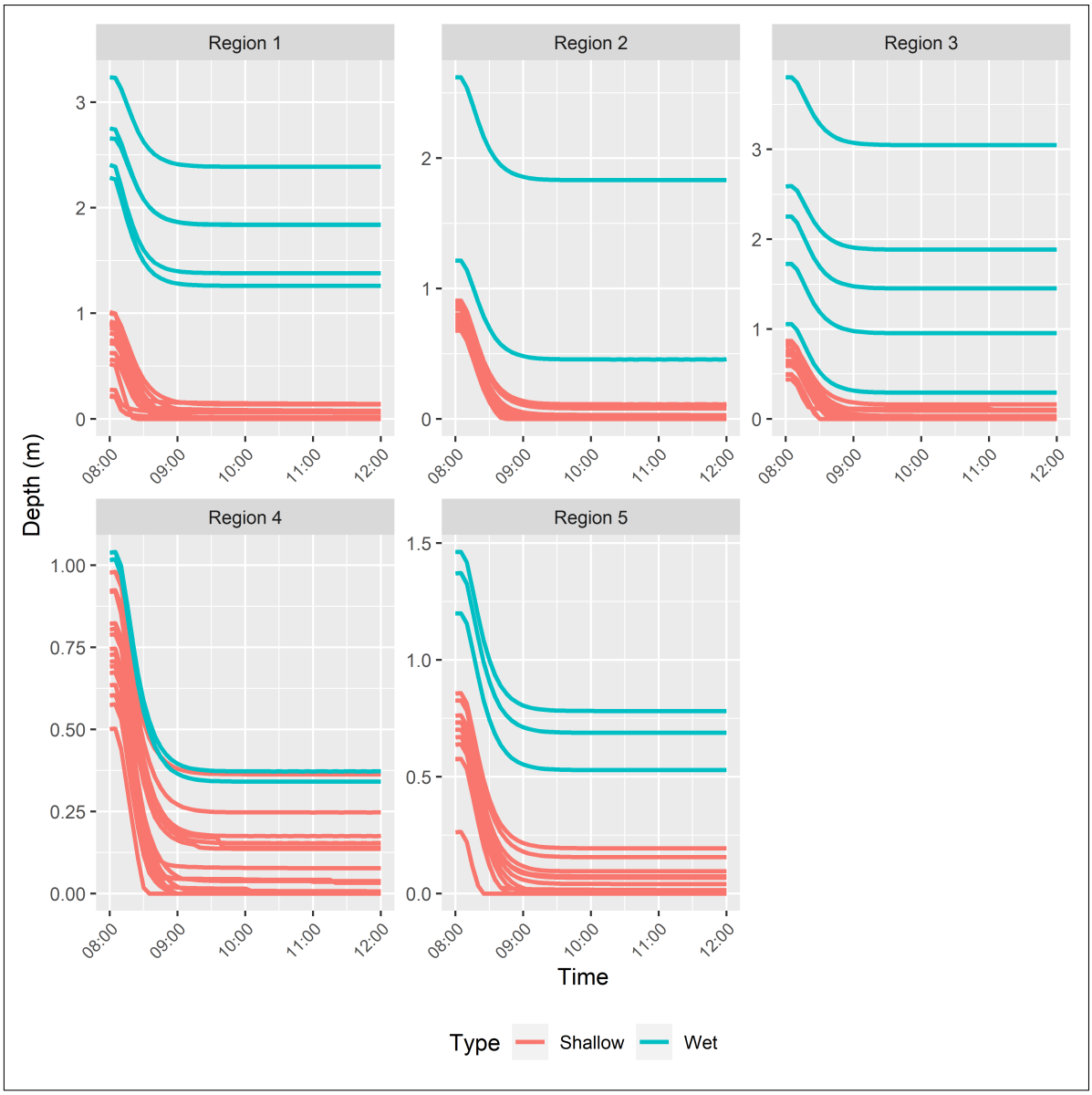

Figure 4.5: Dewatering rate for the measurement points due to HydroFlex scenario

4.3.3 Mitigating the ramping effect

Results from the before section show a severe impact on the riverine ecosystem will occur from the HydroFlex scenario. It is evident that drying out areas with rapid dewatering rate will affect the mortality of the fish habitat in the river. Furthermore, it is also evident that the current environmental legislation will not suffice to minimize this impact while adding operational constraints to limit the ramping rate thoroughly interfere with the concept of HydroFlex aims to provide more flexibility to hydropower operation.

From that concept, it is essential to find flexible mitigation for this impact while not affecting the flexibility of operation. By identifying the main causes, it is possible to set

our goals into two main goals. First, it is essential to reduce the dried out areas as the possible second; it is crucial to minimize the dewatering rate into a low or moderate level. Thereafter it is possible to define an environmentally friendly production scenario where its possible to evaluate different mitigation measures that allow reaching this goal.

To limit the drying out area, different simulations were carried out using the model at different discharge values then results were processed through GIS. Figure 4.6 shows the dried out areas at different discharge rates. It is noticeable that most of the exposed areas are not dried out at Q 105 m^3/s.

Furthermore, to determine a low or moderate dewatering rate. different simulations were carried out using the same change in the discharge upstream, but in different time steps, then the dewatering rate for each region in the exposed area downstream was calculated for every simulation as done before in the previous section.

By using these results, it is possible to establish a correlation between the dewatering rate and the change in production from the power plant. Figure 4.7 shows the resulted relation between the time of change in the HydroFlex scenario upstream in minutes and the dewatering rate for different sections. Building from this correlation, it is possible to reach a dewatering rate by setting the time of the change in production from maximum to shutdown to ≈300-380 minutes. One simulation was tested using the approximated value. Table 4.2 shows the dewatering rate after running simulation by extending the time of the change in maximum production rate to 380 minutes.

Table 4.2: Dewatering rate for investigated regions due to change in the discharge upstream in 380 minutes

Region Number	Region 1	Region 2	Region3	Region 4	Region 5
Avg dewatering rate (cm/h)	12.12	10.48	10.38	9.19	8.5

Based on the combination of the before-explained results, the most possible environmentally friendly simulation was developed as follows. First As it can be seen that reducing the discharge from upstream from max production to 105 m^3/s will not result in almost any dried out areas. Additionally, from the resulted relation between the dewatering rate and the changing rate from the upstream, it is possible to find a rate of change upstream that will cause a low or moderate dewatering rate. Building from that, we purposed the following the production scenario.

After testing the proposed simulation and calculating the resulted dewatering rate, table 4.3 shows the resulted dewatering rate from the proposed production scenario. It can be seen that, on average, the dewatering rate is considered low or moderate, which will cause a low stranding effect on the riverine fish.

Table 4.3: Dewatering rate from the proposed simulation

Region Number	Region 1	Region 2	Region3	Region 4	Region 5
Avg dewatering rate (cm/h)	12.86	12.16	11.40	10.68	10.32

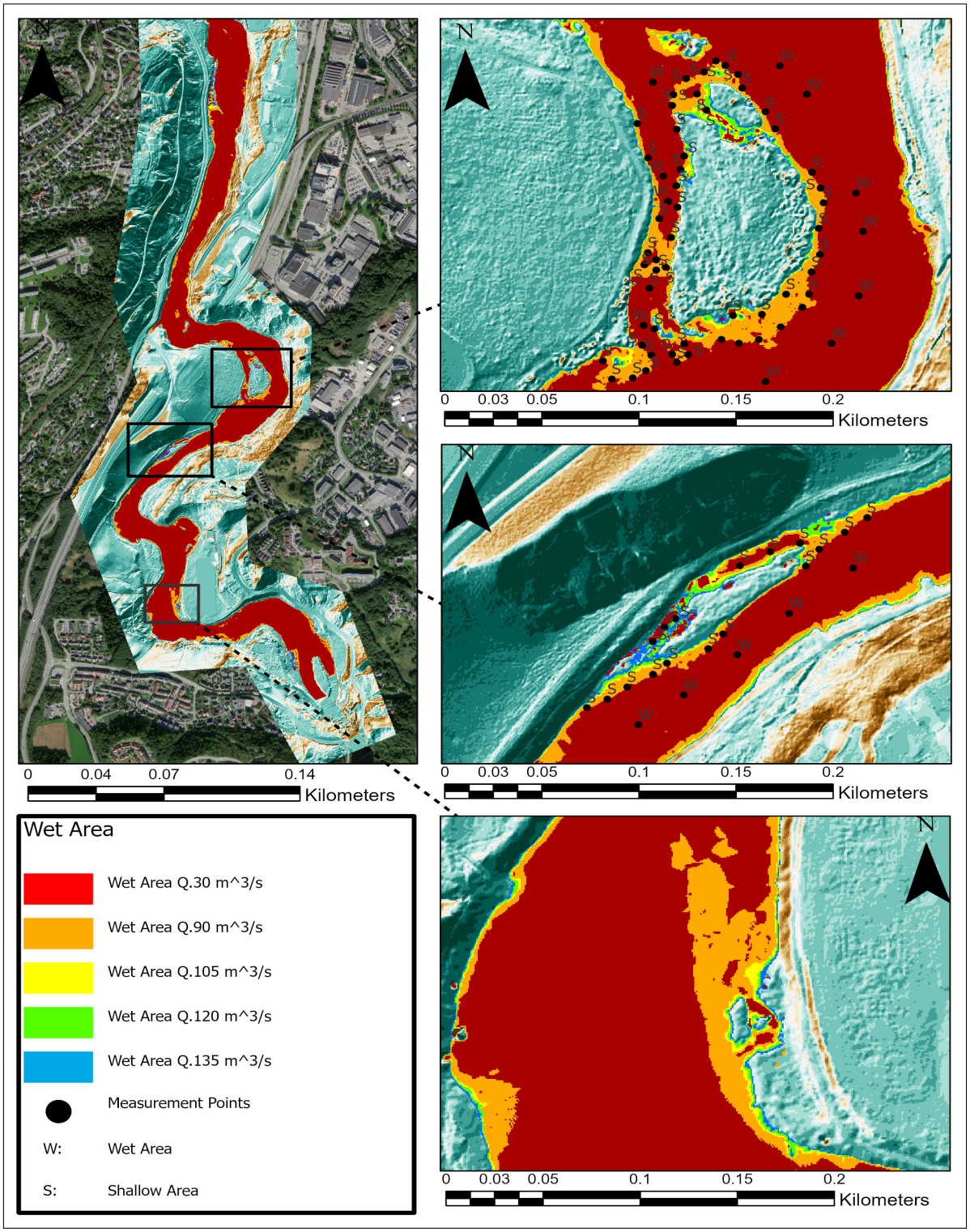

Figure 4.6: Dried Out Areas from different discharge level

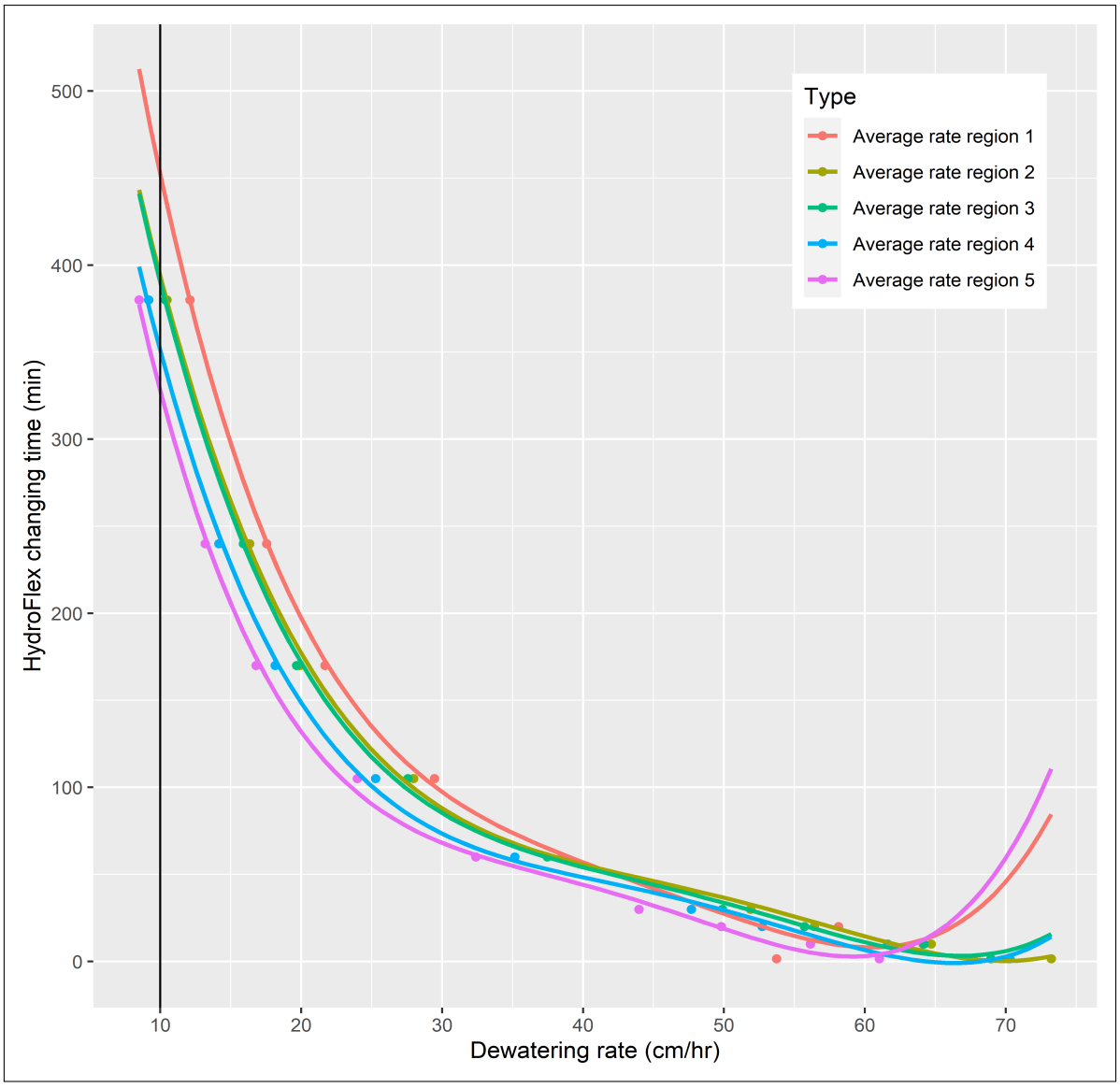

Figure 4.7: Correlation between Change in production upstream and the dewatering rate for different regions downstream

Figure 4.8 shows the proposed simulation in comparison to the HydroFlex production scenario. It is evident that using this scenario is not feasible technically nor economically. However, by plotting both scenarios, it is possible to determine the required amount of water that needs to be stored and regulated to minimize the effect of ramping. Such amount of water can be used further for implementing different mitigation measures as it will be shown in the coming section.

After performing integration between the two scenarios, it was calculated that **0.61 Million m^3** is needed to be controlled for minimizing this impact. This amount of water will be used further for the evaluation of different measures in the following section.

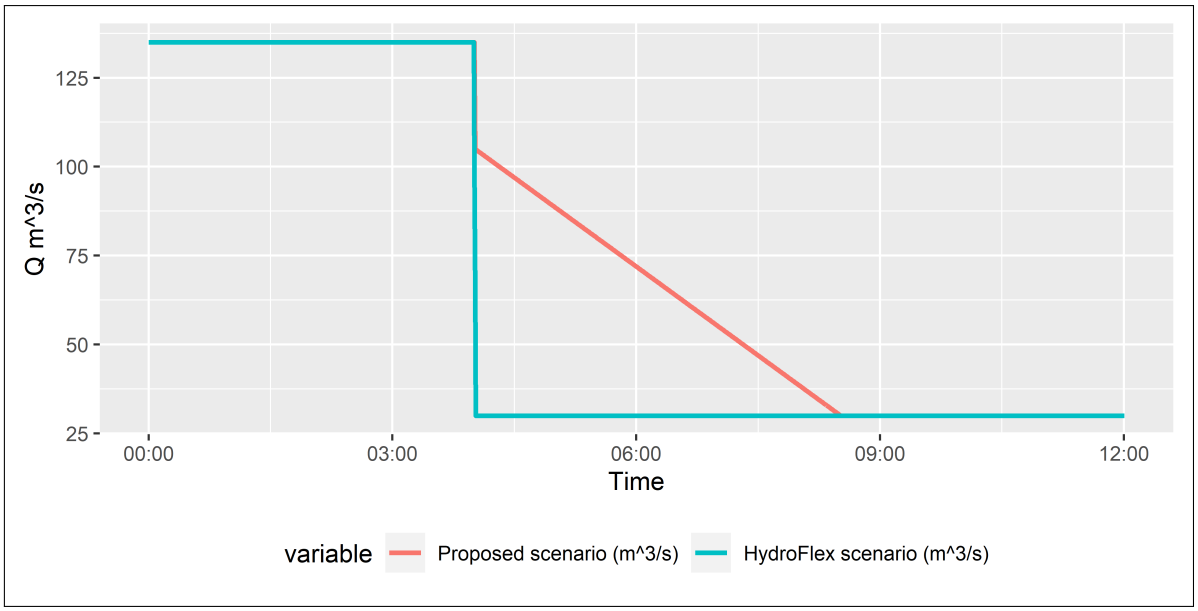

Figure 4.8: Comparison between the proposed production scenario and HydroFlex production scenario

4.3.4 Evaluation of the traditional mitigation measures using a weir

Weirs have been widely used to mitigate some impacts from hydropower development and river regulation for many years. Using weirs have some positive effects as they can control the water velocity, increase the wetted area, and provide suitable conditions for fish to rehabilitate. However, they have also very well documented environmental impacts on the aquatic ecosystem, such as fish migration barriers, reduction of the spawning habitats for the fish, and separation of the river morphology (Brittain, 2003; Mueller et al., 2011). Nevertheless, the effectiveness and feasibility of using weir to limit the ramping effect will be shown in this section.

Based on the calculated volume of water from the previous section, it is possible to estimate the height and the location of the weir at the beginning of the river downstream. Different locations were proposed near the outlet to ensure there is no possible migration barrier that will affect the fish habitat. Eventually, two main locations were preliminary proposed suitable locations for creating an artificial reservoir downstream, as shown in figure 4.9. After preliminary calculation, it was found out that the first location is not suitable for storing the amount of water needed to mitigate the ramping effect. The height of the weir was calculated through two main components as follows.

First, the volume of water before the weir at maximum production was calculated by calculating the river cross-section profiles every specific distance then by summing up

the volume that is located between every two cross-sections, as shown in figure 4.9 the cross-sections that were mapped out in the river. The resulted volume from the river up to the second location of the weir was estimated to be **0.454 million m^3**, which indicates that there is a remaining 0.155 million m^3 needed to reach the required amount of water to be stored for mitigating the ramping.

The additional height of the weir that will result in the needed amount of water was calculated using the contour lines. By multiplying the surface area before the weir at the maximum flow with the surface area of the resulted contour lines from the height that is estimated. Using iterative heights, it was estimated the final height of the weir to be 1.6 meters above the current Water Surface Elevation (WSE) at the weir location. This height will result in an additional **0.152 million m^3**, which will suffice with the initial to the total volume of water that needs to be stored.

Eventually, the height of the weir at the second location is estimated to be 3.8 meters resulted from the initial water depth at the proposed location during maximum discharge in addition to the 1.6 meters. It is noticeable that the proposed height of the weir will result in flooding to the riverside banks, which will affect some already existing structures and roads along the river downstream, as shown in figure 4.9. Additionally, the proposed location will also have an effect on the fish migration to some extent as well as the fishing activity in that area.

4.3.5 Evaluation of alternative technologies using ACUR

In collaboration with (Storli and Lundström, 2019), the resulted amount of regulated water needed was sent to the department of energy and process engineering at NTNU to investigate the size and the amount of excavation needed to be done and evaluate its feasibility and currently it is being investigated.

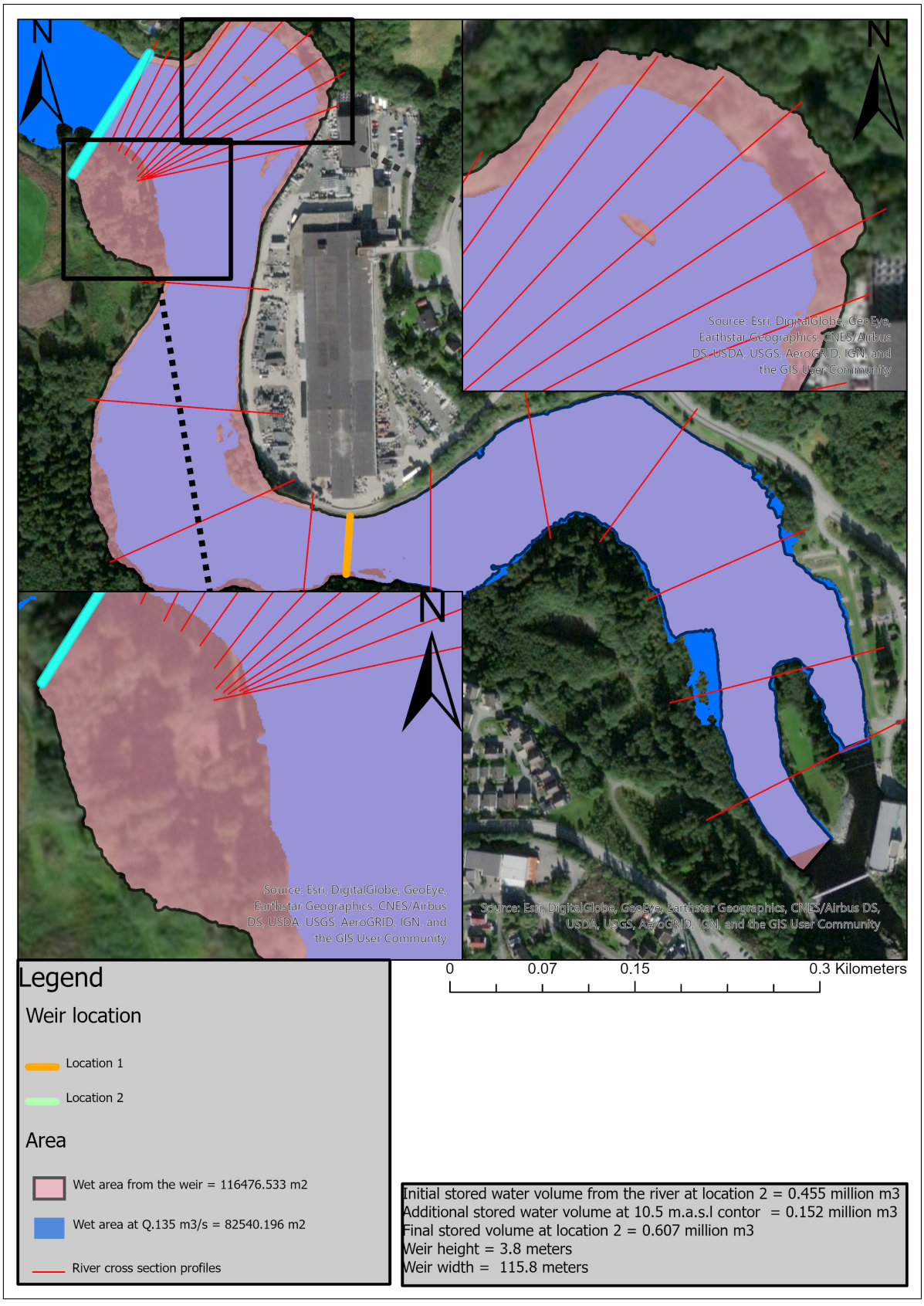

Figure 4.9: Resulted wet area from constructing artificial dam along the river

4.4. Discussion

It was pointed out in the beginning that flow ramping magnitude and frequency will increase in the future due to the increasing need for flexible, clean energy source and integration with other renewable energy sources. As it can be seen from the HydroFlex production scenario in figure 4.2 that the rate of change in the discharge is expected to be severe as it can vary from 135 m^3/s to minimum flow in 15 minutes. This rate of change will increase the ramping effect significantly, which consequently will result in severe hydro-morphological changes in the river downstream that will affect the aquatic biota. Such an impact needs to be considered for any future production scenario to ensure a clean green source of energy production.

It is important to mention that mapping the effect from flow ramping is rather complex and requires intensive investigations in various aspects. Using hydraulic modeling proves to be very efficient for mapping out the resulted hydro-morphological changes in the river from the expected flow ramping. For instance, the resulted dewatering rate in sections 4 and 5 comply with Saltveit et al. (2001) fieldwork experiment for measuring the rate of change of the depth in some regions in Nidelva downstream. Hydraulic modeling can be additionally used for mitigating the impact using a combination of different types of measures.

Moreover, as can be seen from this chapter result that implementing minimum flow with relatively high value is not an effective measure for mitigating the impact of future production scenarios. Results show that in the river of Nidelva that severe hydro-morphological changes will result from implementing the minimum flow only. The dried-out area will be exposed as it can be seen from figure 4.4 with a rapid dewatering rate as it can be seen from table 4.1, which will lead to a huge stranding effect on the riverine fish. On the other hand, providing restriction or increasing the minimum flow is neither technically nor economically feasible as it conflicts with the flexibility provided from HydroFlex implementation.

Additionally, results show that mitigating the ramping effect from the HydroFlex scenario will require a significant amount of water (**0.61 Million m^3**) to be regulated upon the outlet location. Such an amount of water requires a combination of traditional and innovative technologies to provide an efficient feasible measure. For instance, it can be seen from figure 4.6 that providing a physical modification to the river in section one can slightly reduce the required regulated volume of water to reach a low-moderate ramping rate.

It can be concluded that building creating an artificial reservoir using a weir is not a

feasible measure for the river Nidelva for the following reasons. The first proposed location, as it can be seen from figure 4.9, is not feasible as it will increase the WSE to the outlet location water level. Such an impact will reduce the potential net head of the power plant, which consequently will reduce its production capacity. On the contrary, the second proposed location is able to restore the required amount of regulated water, yet; it will cause flooding over banks as it can be seen in figure 4.9. Moreover, the second proposed location is expected to construct a physical barrier on the riverine fish and other aquatic biotas.

Despite that the main hydro-morphological characteristics focus of this work was regarding the dried out areas and dewatering rate, further investigations can be done for evaluating the effect of a severe flow ramping on the water temperature as well. (Halleraker et al., 2003) results show that water temperature has a significant effect on the fish stranding rate as it affects fish behavior and movement prior to the dewatering rate. Such an investigation can lead to a more dynamic production scenario that will reduce the amount of the needed regulated water.

Finally, results from this work can be used to evaluate the size, location, and efficiency of ACUR to provide alternative technologies as measures for severe flow ramping.

5. CONCLUSION

The effect of flow ramping on the riverine ecosystem is evident. It has been documented by various studies that were pointed out at the beginning of this study as it poses a significant threat to the riverine biota in different ways, such as stranding or drifting of macroinvertebrates and require great focus to be mitigated.

This study aims to put a grasp on the level of flow ramping caused by hydropower operational patterns and the expected level in the future. It can be concluded that flow ramping occurs from the operation of HP in Norway with different characteristics depending on the type of HP and its operational pattern.

Using a combination of hydrological indicators and tools proved efficiency for mapping and differentiating the characteristics of this resulted flow ramping; however, Ecological and geographical (e.g., HP location) aspects need to be taken into consideration to determine the actual ecological impact that might occur to the riverine biota.

Additionally, it is possible to conclude that the environmental legislation and measures provided to mitigate the impact proved efficiency, however, it doesn't cover all the impacted river and further assessment and legislation needs to be provided for some power plants that have potential ecological damage with no environmental legislation or measures to limit this damage.

Subsequently, Further work needs to be conducted for having a proper assessment of the potential ecological damage caused by the pattern of flow ramping that occurred from RoR power plants or as known to be hydrofibrilation.

On the contrary, this study proves that it is evident the increasing level of flow ramping is expected to increase significantly due to the implementation of HydroFlex water turbine and the traditional measures to limit this impact is not going to suffice for eliminating this expected impact. Using innovative technologies to eliminate this impact requires further work and assessment to be acquainted with their feasibility. Moreover, Using hydraulic modeling proves efficiency for mapping out the resulted impact from the implementation of the HydroFlex scenario.

Finally, Further hydro-morphological indicators need to be evaluated as a resulted impact from the HydroFlex production scenario, such as the change in water temperature and how it affects the riverine biota.

BIBLIOGRAPHY

Abée-lund, J. H. L. and Villar, J. O. (2017). Start-stop practice in small Norwegian hydropower plants.

Ahmad, I., Tang, D., Wang, T., Wang, M., and Wagan, B. (2015). Precipitation trends over time using Mann-Kendall and spearman's Rho tests in swat river basin, Pakistan. *Adv. Meteorol.*, 2015.

Alliance for Rural Electrification (2013). Using bateries to ensure clean, reliable and affordable universal electricity access. *ARE Energy Storage Campaign*, pages 1–16.

Anindito, Y., Haas, J., Olivares, M., Nowak, W., and Kern, J. (2019). A new solution to mitigate hydropeaking? Batteries versus re-regulation reservoirs. *J. Clean. Prod.*, 210:477–489.

Auer, S., Zeiringer, B., Führer, S., Tonolla, D., and Schmutz, S. (2017). Effects of river bank heterogeneity and time of day on drift and stranding of juvenile European grayling (Thymallus thymallus L.) caused by hydropeaking. *Sci. Total Environ.*, 575:1515–1521.

Beckitt, A., Bockenhauer, S., Botterud, A., Christensen, T. H., Middleton, L., Nielsen, N., and Somani, A. (2019). Flexible hydropower providing value to renewable energy integration. Technical report.

Bejarano, M. D., Jansson, R., and Nilsson, C. (2018). The effects of hydropeaking on riverine plants: a review. *Biol. Rev.*, 93(1):658–673.

Brittain, J. E. (2003). Weirs as a mitigation measure in regulated rivers—the norwegian experience. *Can. Water Resour. J.*, 28(2):217–229.

Bruder, A., Tonolla, D., Schweizer, S. P., Vollenweider, S., Langhans, S. D., and Wüest, A. (2016). A conceptual framework for hydropeaking mitigation. *Sci. Total Environ.*, 568:1204–1212.

Brussels, . (2020). Proposal for a REGULATION OF THE EUROPEAN PARLIAMENT AND OF THE COUNCIL establishing the framework for achieving climate neutrality and amending Regulation (EU) 2018/1999 (European Climate Law) EN. Technical Report 9.

Carolli, M., Vanzo, D., Siviglia, A., Zolezzi, G., Bruno, M. C., and Alfredsen, K. (2015). A simple procedure for the assessment of hydropeaking flow alterations applied to

several European streams. *Aquat. Sci.*, 77(4):639–653.

Casas-Mulet, R., Alfredsen, K., Hamududu, B., and Timalsina, N. P. (2015). The effects of hydropeaking on hyporheic interactions based on field experiments. *Hydrol. Process.*, 29(6):1370–1384.

CEN (2018). EN 14614. Water quality — Guidance standard for assessing the hydromorphological features of rivers. Technical report.

Chang, J., Wang, X., Li, Y., Wang, Y., and Zhang, H. (2018). Hydropower plant operation rules optimization response to climate change. *Energy*, 160:886–897.

Charmasson, J., Belsnes, M., Andersen, O., Eloranta, A., Graabak, I., Korpås, M., Palm Helland, I., Sundt, H., and Wolfgang, O. (2018). Hydrobalance. Roadmap for large-scale balancing and energy storage from Norwegian hydropower. Opportunities, challenges and needs until 2050. Technical report.

Charmasson, J. and Zinke, P. (2011). Mitigation Measures Against Hydropeaking. *EnviPEAK Publ.*, page 51.

Chen, Q., Zhang, X., Chen, Y., Li, Q., Qiu, L., and Liu, M. (2015). Downstream effects of a hydropeaking dam on ecohydrological conditions at subdaily to monthly time scales. *Ecol. Eng.*, 77:40–50.

Child, M., Bogdanov, D., and Breyer, C. (2018). The role of storage technologies for the transition to a 100% renewable energy system in Europe. *Energy Procedia*, 155:44–60.

Dai, Q., Kelly, J. C., Gaines, L., and Wang, M. (2019). Life Cycle Analysis of Lithium-Ion Batteries for Automotive Applications.

Eleftheria, K., von der Weppen, J., and Dworak, T. (2011). Water management , Water Framework Directive & Hydropower Common Implementation Strategy Workshop Brussels , 13-14 September 2011 Issue Paper (final version). Technical Report November.

Farahmand, H., Jaehnert, S., Aigner, T., and Huertas-Hernando, D. (2015). Nordic hydropower flexibility and transmission expansion to support integration of North European wind power. *Wind Energy*, 18(6):1075–1103.

Flataker, O. N. and Nielsen, H. H. N. (2018). National Report 2018. Technical Report 74, NVE.

Gilbert Richland, W. A. U. S. R. O. P. N. N. L. P. (1987). *Statistical Methods for Environmental Pollution Monitoring*.

Gocic, M. and Trajkovic, S. (2013). Analysis of changes in meteorological variables using Mann-Kendall and Sen's slope estimator statistical tests in Serbia. *Glob. Planet. Change*, 100:172–182.

Graabak, I. and Korpås, M. (2016). Balancing of Variable Wind and Solar Production in Continental Europe with Nordic Hydropower - A Review of Simulation Studies. *Energy Procedia*, 87(1876):91–99.

Graf, M. (2019). Internship Report. Technical Report 2.

Greimel, F., Schülting, L., Graf, W., Bondar-Kunze, E., Auer, S., Zeiringer, B., and Hauer, C. (2018). *Hydropeaking Impacts and Mitigation*, pages 91–110. Springer International Publishing, Cham.

Greimel, F., Zeiringer, B., Höller, N., Grün, B., Godina, R., and Schmutz, S. (2016). A method to detect and characterize sub-daily flow fluctuations. *Hydrol. Process.*, 30(13):2063–2078.

Halleraker, J. H., Saltveit, S. J., Harby, A., Arnekleiv, J. V., Fjeldstad, H. P., and Kohler, B. (2003). Factors influencing stranding of wild juvenile brown trout (Salmo trutta) during rapid and frequent flow decreases in an artificial stream. *River Res. Appl.*, 19(5-6):589–603.

Halleraker, J. H., van de Bund, W., Bussettini, M., Gosling, R., Döbbelt-Grüne, S., Hensman, J., Kling, J., Koller-Kreimel, V., and Pollard, P. (2016). Working Group ECOSTAT report on common understanding of using mitigation measures for reaching Good Ecological Potential for heavily modified water bodies. Part 1: Impacted by water storage. Technical report.

Hauer, C., Holzapfel, P., Leitner, P., and Graf, W. (2017a). Longitudinal assessment of hydropeaking impacts on various scales for an improved process understanding and the design of mitigation measures. *Sci. Total Environ.*, 575:1503–1514.

Hauer, C., Siviglia, A., and Zolezzi, G. (2017b). Hydropeaking in regulated rivers – From process understanding to design of mitigation measures.

IHA (2019). Hydropower status report 2019: Sector trends and insights. Technical report.

Jiménez Cisneros, B. E., Oki, T., Arnell, N. W., Benito, G., Cogley, J. G., Döll, P., Jiang, T., Mwakalila, S. S., Kundzewicz, Z., and Nishijima, A. (2015). Freshwater resources. Technical report.

Juarez, A., Alfredsen, K., and Burman, A. (2019). Hydraulic Models. Technical Report

764011.

Meile, T., Boillat, J. L., and Schleiss, A. J. (2011). Hydropeaking indicators for characterization of the Upper-Rhone River in Switzerland. *Aquat. Sci.*, 73(1):171–182.

Moog, O. (1993). Quantification of daily peak hydropower effects on aquatic fauna and management to minimize environmental impacts. *Regul. Rivers Res. Manag.*, 8(1□2):5–14.

MPE (2015). Facts 2015. Energy and water resources in Norway. Technical report.

Mueller, M., Pander, J., and Geist, J. (2011). The effects of weirs on structural stream habitat and biological communities. *J. Appl. Ecol.*, 48(6):1450–1461.

NVE (2017). Overview of Norway's Electricity History. Technical Report November.

NVE (2018). The Norwegian power system. Grid connection and licensing. Technical Report 3.

Pellaud, M. (2007). *Ecological response of a multi-purpose river development project using macro-invertebrates richness and fish habitat value*. PhD thesis.

Pérez-Díaz, J. I., Millán, R., García, D., Guisández, I., and Wilhelmi, J. R. (2012). Contribution of re-regulation reservoirs considering pumping capability to environmentally friendly hydropower operation. *Energy*, 48(1):144–152.

Reilly, P. M. (1978). Probability and Statistics for Engineers and Scientists by Ronald E. Walpole, Raymond H. Myers. Second Edition. Macmillan Publishing Co., Inc., New York, 1978. xii + 580 pp. U.S. $16.95. ISBN 0-02-424110-5. *Can. J. Stat.*, 6(2):283–284.

Richter, B. D., Baumgartner, J. V., Powell, J., and Braun, D. P. (1996). A Method for Assessing Hydrologic Alteration within Ecosystems. *Conserv. Biol.*, 10(4):1163–1174.

Rognstad, A. J. (2018). Hydropower licensing in norway. Technical report, 2018.

Saltveit, S., Halleraker, J., Arnekleiv, J., and Harby, A. (2001). Field experiments on stranding in juvenile atlantic salmon (Salmo salar) and brown trout (Salmo trutta) during rapid flow decreases caused by hydropeaking. *Regul. Rivers Res. Manag.*, 17(45):609–622.

Sauterleute, J., Wolfgang, O., and Graabak, I. (2015). Scenarios for large-scale balancing and storage from Norwegian hydropower. Technical report.

Sauterleute, J. F. and Charmasson, J. (2014). A computational tool for the characterisation of rapid fluctuations in flow and stage in rivers caused by hydropeaking. *Environ.*

Model. Softw., 55:266–278.

Schmutz, S., Bakken, T. H., Friedrich, T., Greimel, F., Harby, A., Jungwirth, M., Melcher, A., Unfer, G., and Zeiringer, B. (2015). Response of Fish Communities to Hydrological and Morphological Alterations in Hydropeaking Rivers of Austria. *River Res. Appl.*, 31(8):919–930.

Schrader, F., Kamolidinov, A., Bekchanov, M., Laldjebaev, M., and Tsani, S. (2019). Hydropower. Technical report.

Schülting, L., Feld, C. K., and Graf, W. (2016). Effects of hydro- and thermopeaking on benthic macroinvertebrate drift. *Sci. Total Environ.*, 573:1472–1480.

Shadmani, M., Marofi, S., and Roknian, M. (2012). Trend Analysis in Reference Evapotranspiration Using Mann-Kendall and Spearman's Rho Tests in Arid Regions of Iran. *Water Resour. Manag.*, 26(1):211–224.

Siemonsmeier, M., Baumanns, P., van Bracht, N., Schönefeld, M., Schönbauer, A., Moser, A., Dahlhaug, O., and Heidenreich, S. (2018). Hydropower Providing Flexibility for a Renewable Energy System : Three European Energy Scenarios. (December):1–79.

Simensen, E. O. (2012). *Norway as Europe's Green Battery: Analysing Functions in Technological Innovation Systems for Renewable*. PhD thesis, University of Oslo.

Storli, P. T. and Lundström, T. S. (2019). A new technical concept for water management and possible uses in future water systems. *Water (Switzerland)*, 11(12):1–16.

Tarroja, B., AghaKouchak, A., and Samuelsen, S. (2016). Quantifying climate change impacts on hydropower generation and implications on electric grid greenhouse gas emissions and operation. *Energy*, 111:295–305.

Thaulow, H., Nesheim, I., and Barkved, L. (2016). Hydropower in Norway. Technical Report December.

Toffolon, M., Siviglia, A., and Zolezzi, G. (2010). Thermal wave dynamics in rivers affected by hydropeaking. *Water Resour. Res.*, 46(8):1–18.

Tonolla, D., Bruder, A., and Schweizer, S. (2017). Evaluation of mitigation measures to reduce hydropeaking impacts on river ecosystems – a case study from the Swiss Alps. *Sci. Total Environ.*, 574:594–604.

Torabi Haghighi, A., Ashraf, F. B., Riml, J., Koskela, J., Kløve, B., and Marttila, H. (2019). A power market-based operation support model for sub-daily hydropower regulation practices. *Appl. Energy*, 255:113905.

Appendices

A. HOURLY DATA RESULTS

A.1. Eidfoss

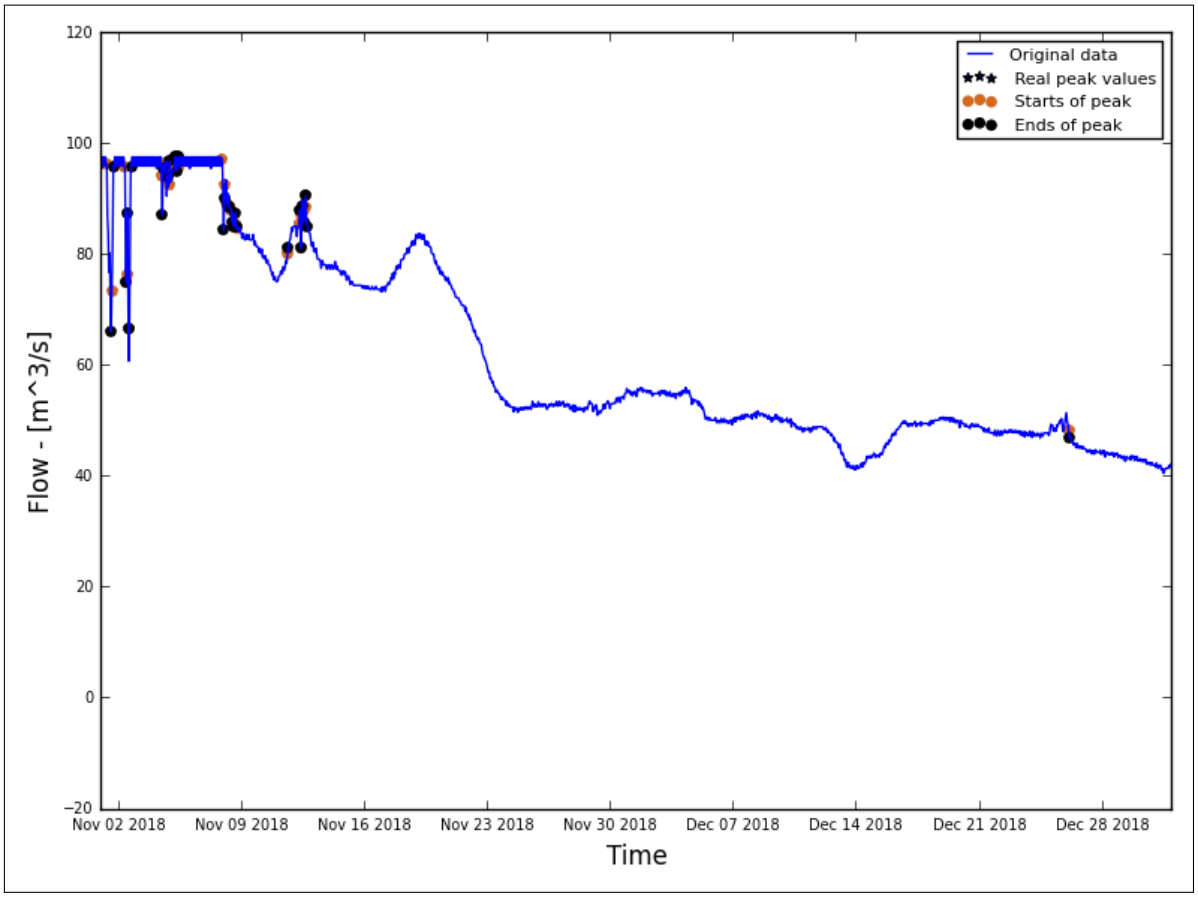

Figure A.1.1: Hydrograph of the last two months of the recorded data

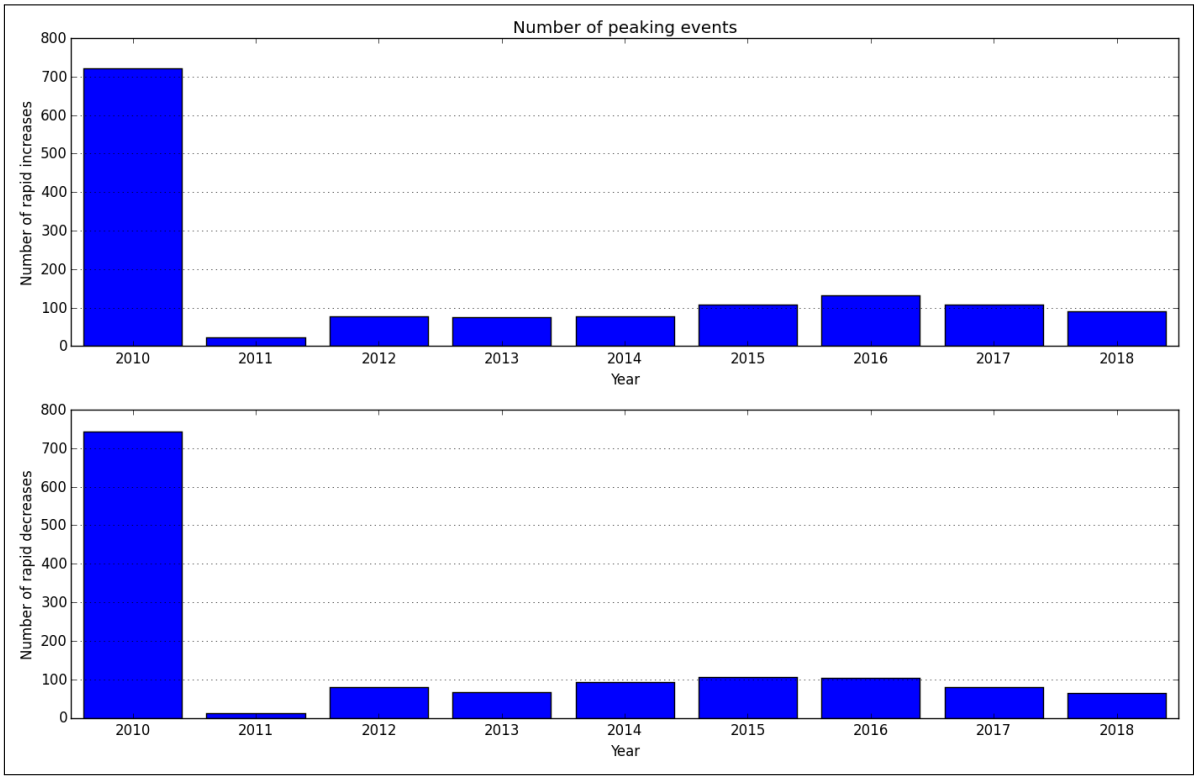

Figure A.1.2: Average annual number of increased/decreased peaks

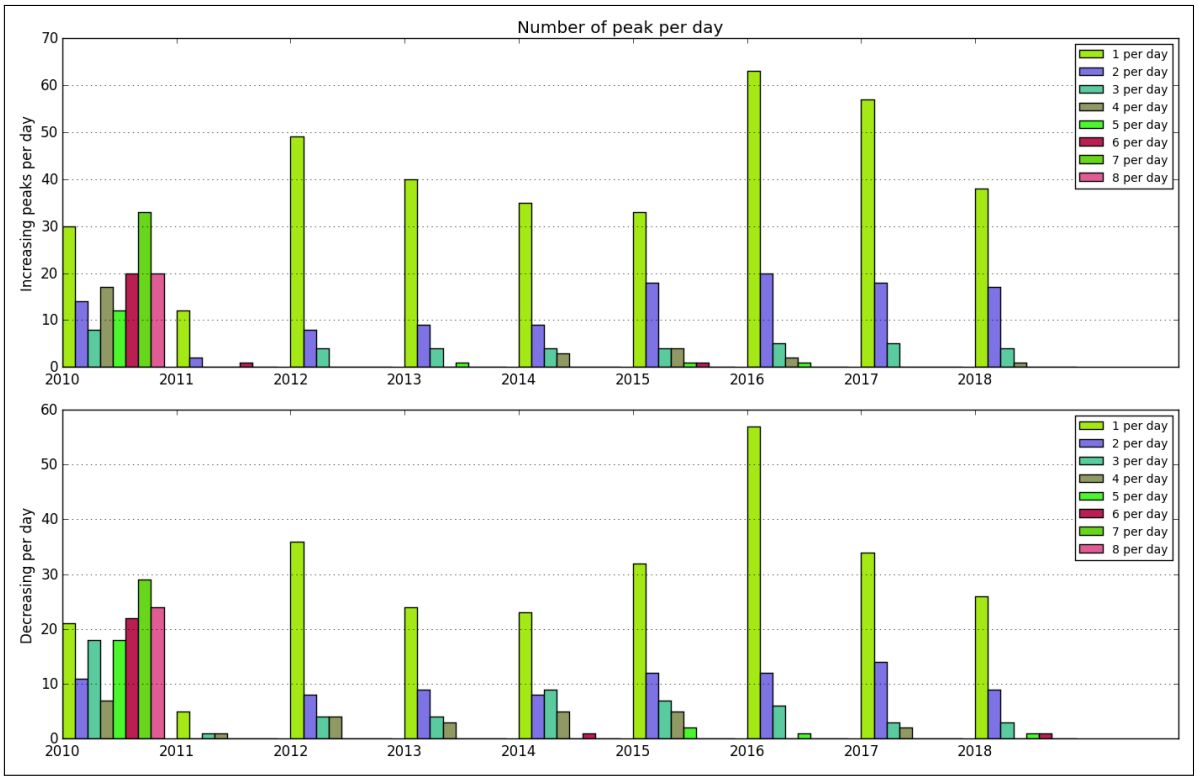

Figure A.1.3: Number of peaks per day

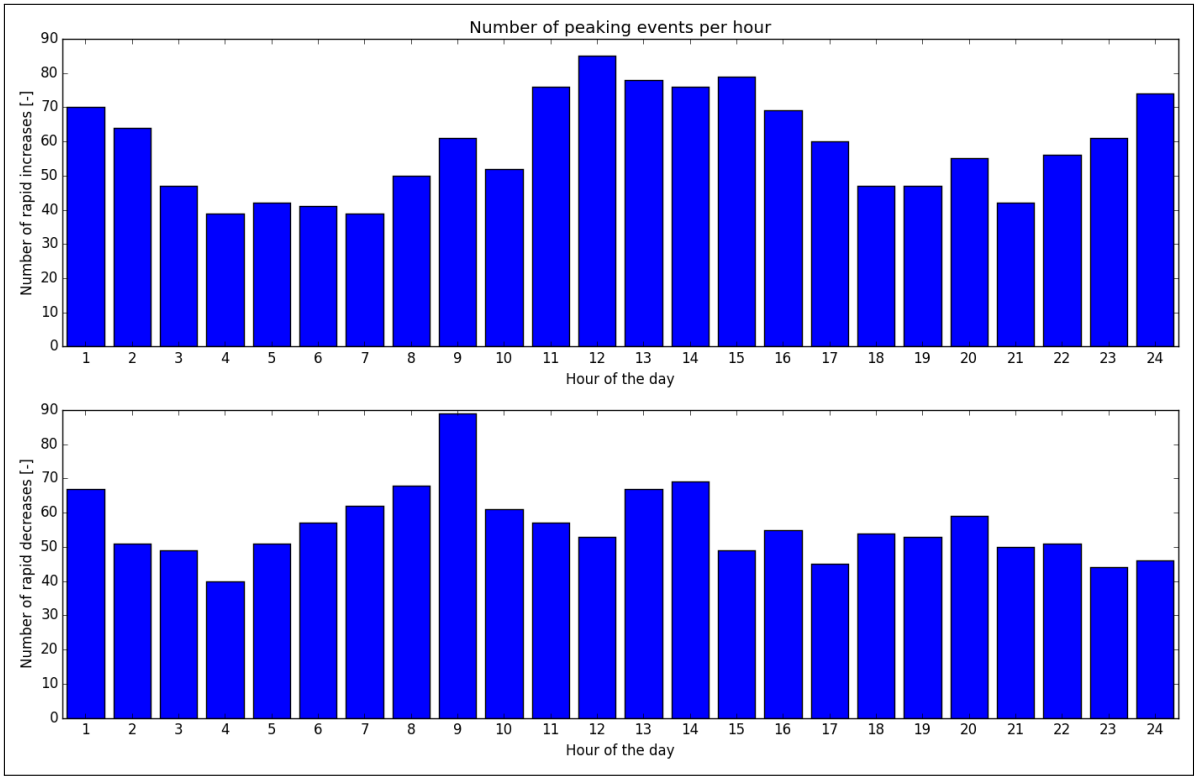

Figure A.1.4: Distribution of peaks throughout day

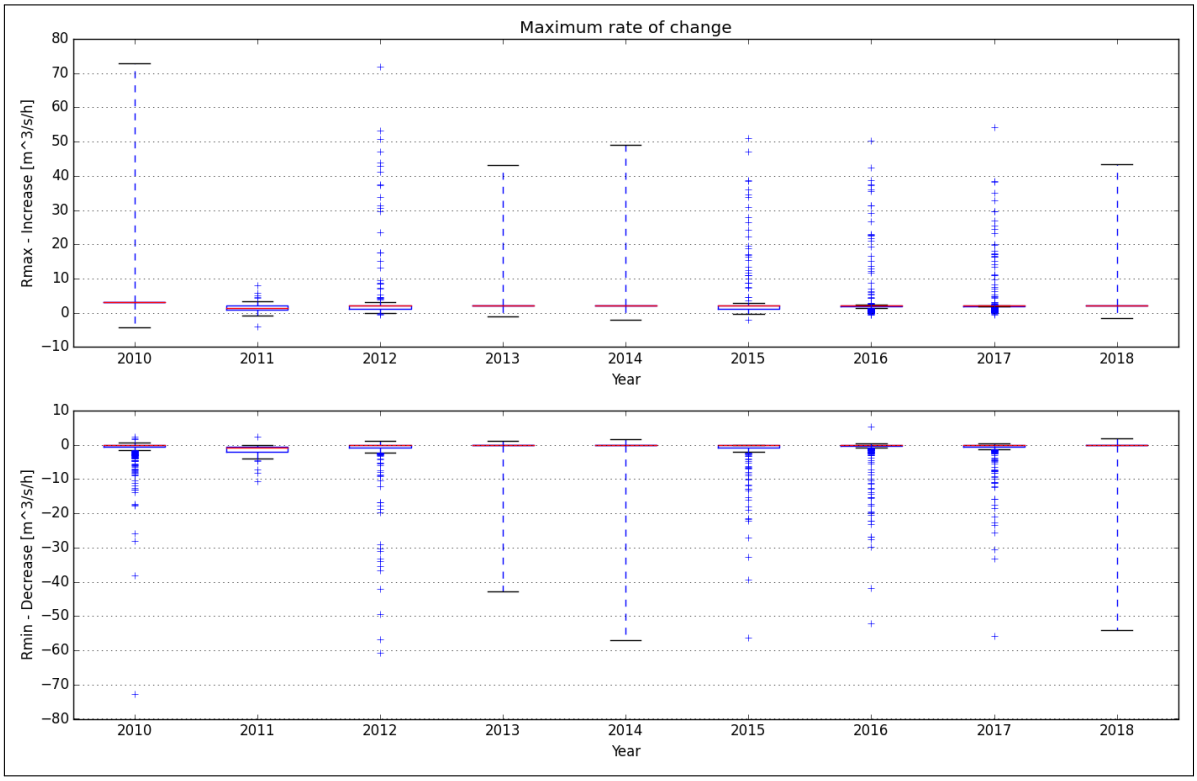

Figure A.1.5: Maximum rate of change

A.2. Hunderfossen

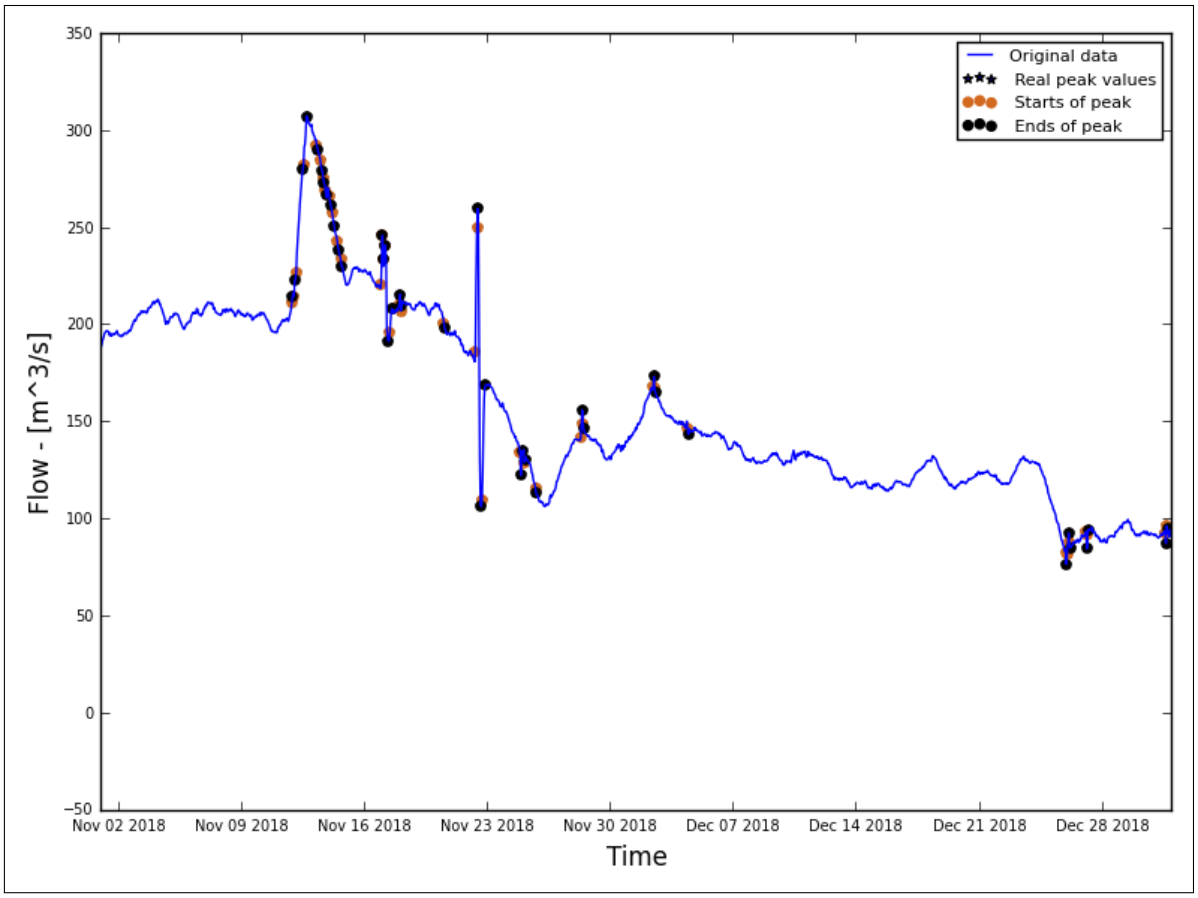

Figure A.2.6: Hydrograph of the last two months of the recorded data

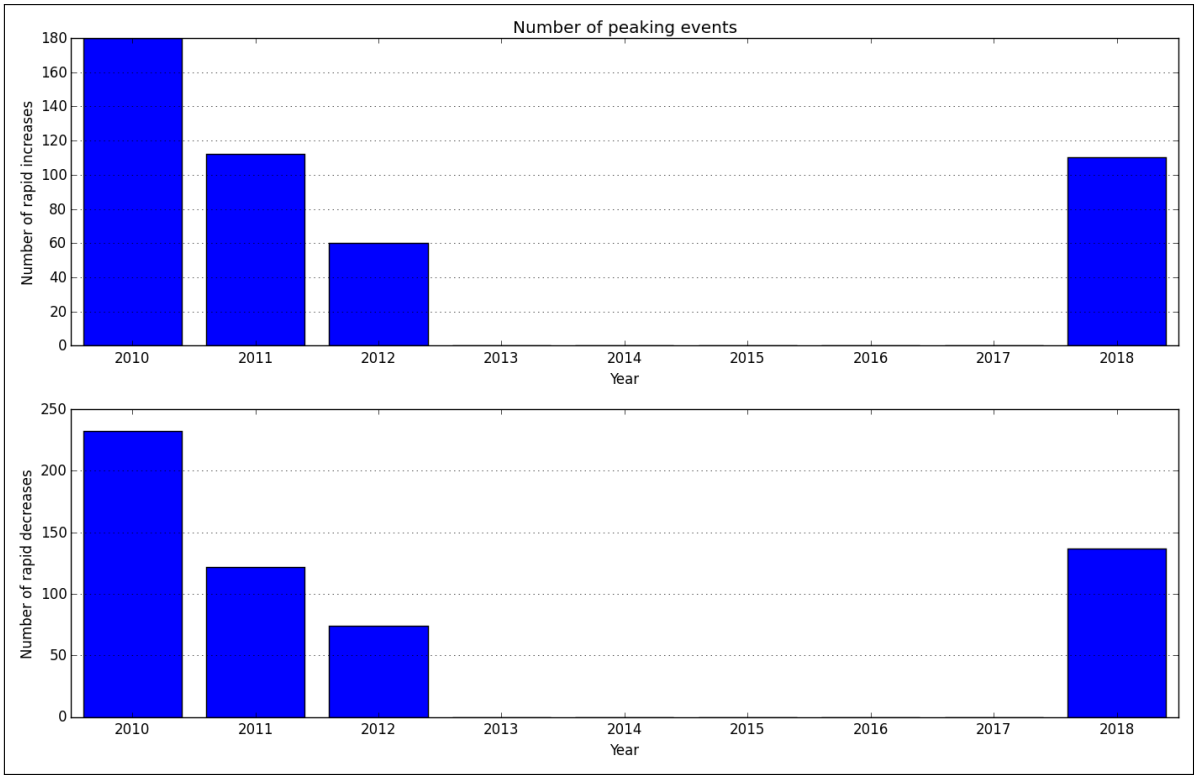

Figure A.2.7: Average annual number of increased/decreased peaks

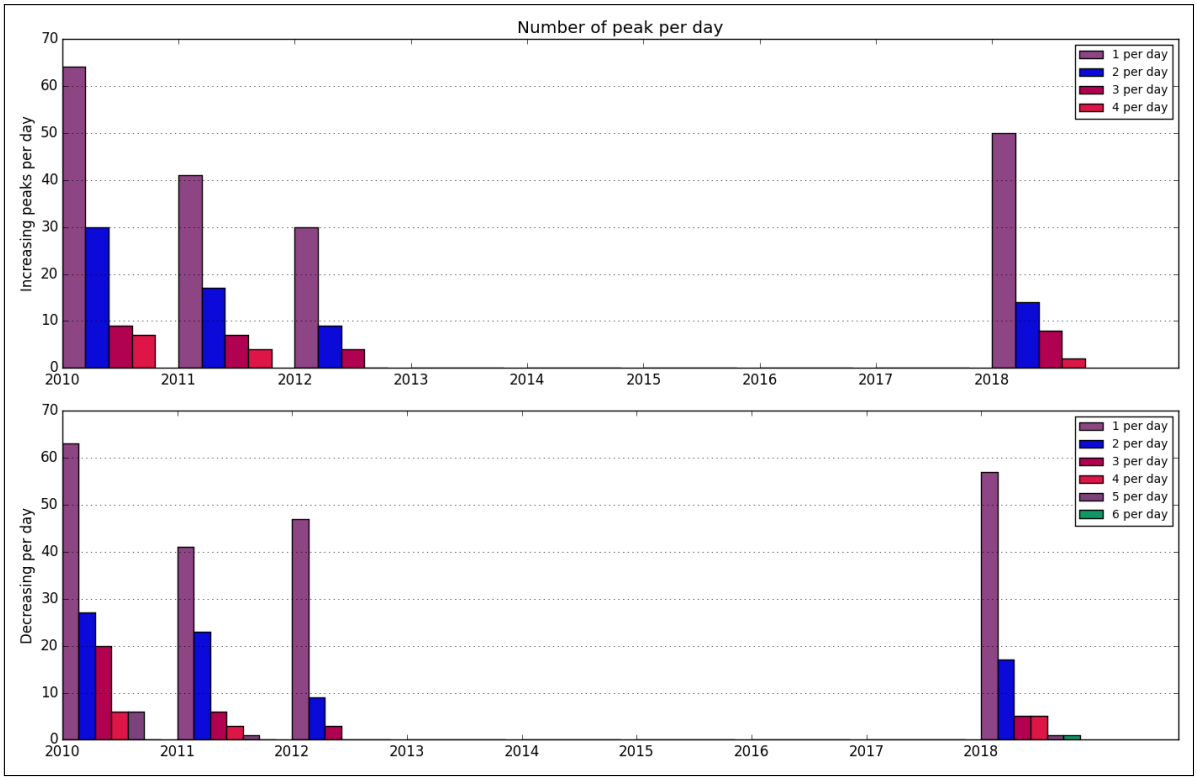

Figure A.2.8: Number of peaks per day

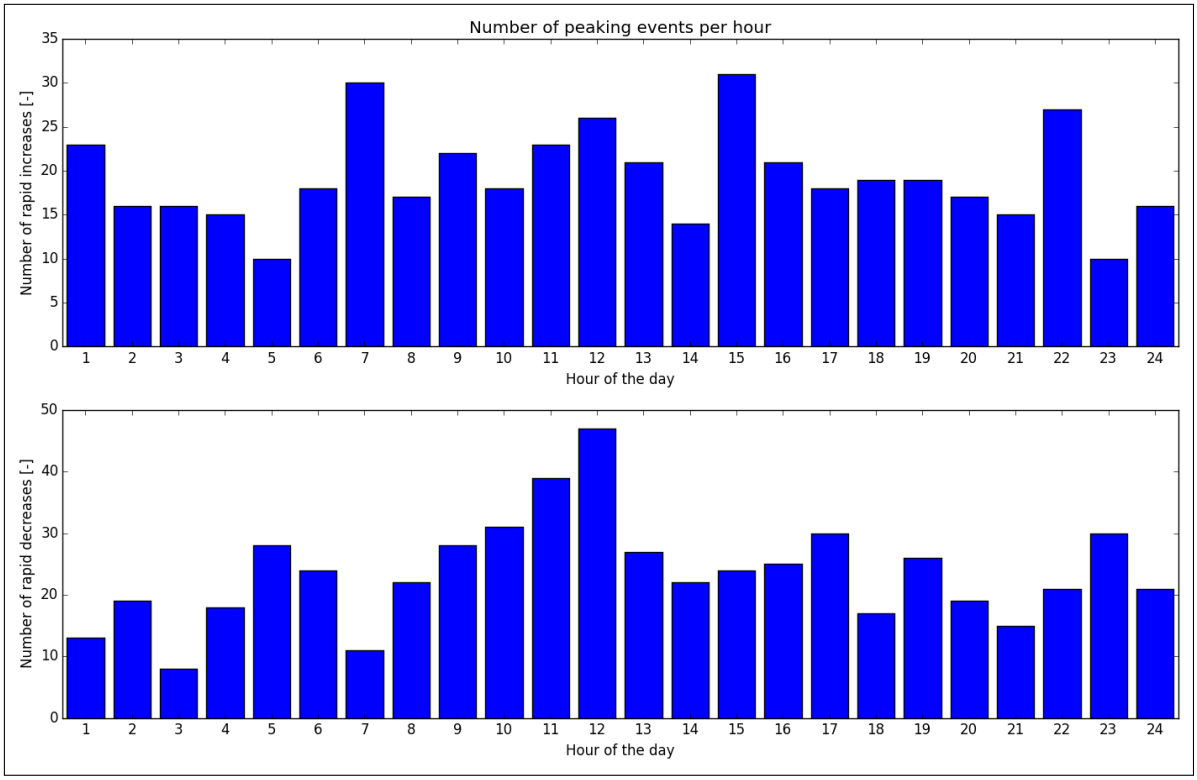

Figure A.2.9: Distribution of peaks throughout day

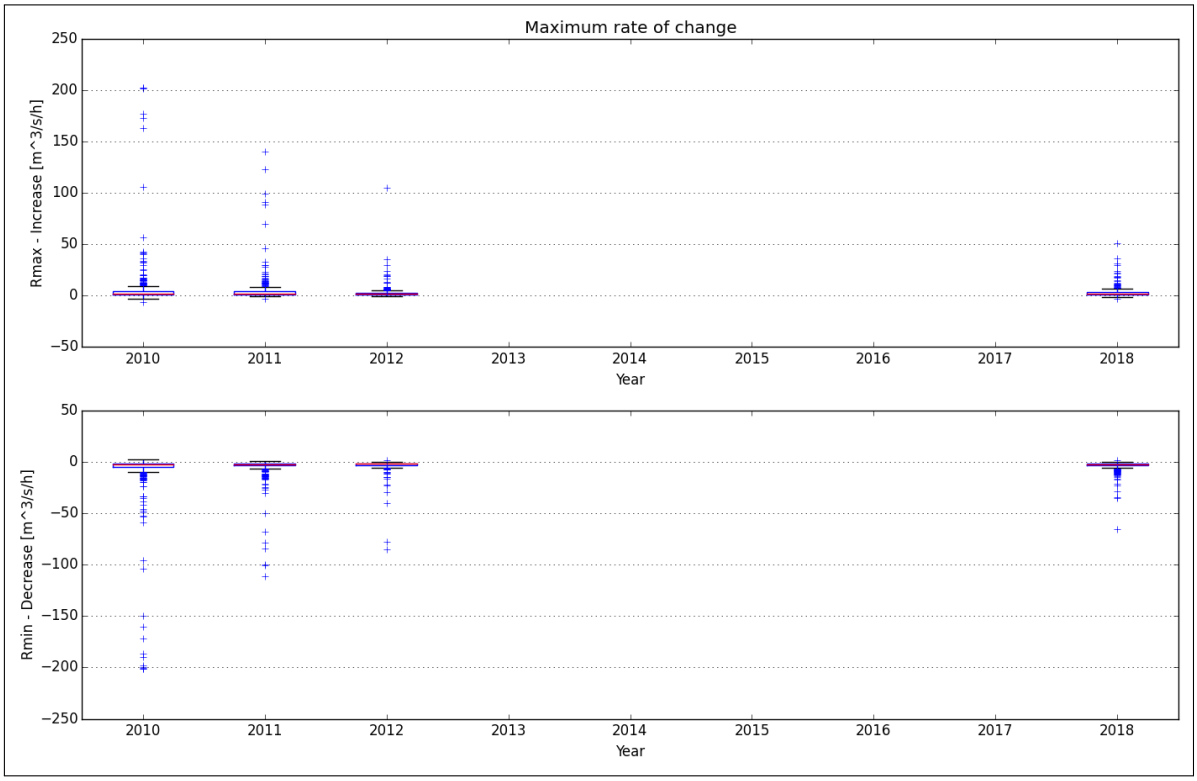

Figure A.2.10: Maximum rate of change

A.3. Rendalen

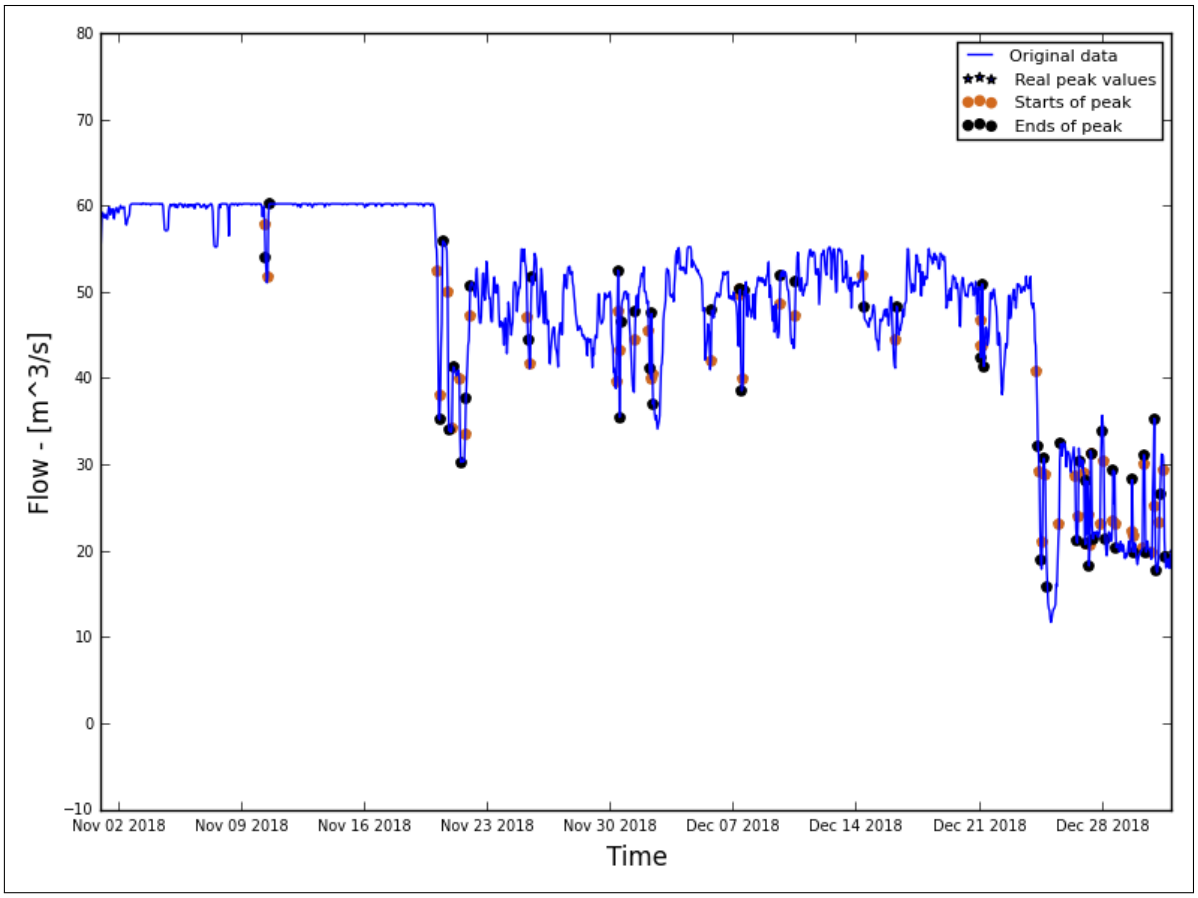

Figure A.3.11: Hydrograph of the last two months of the recorded data

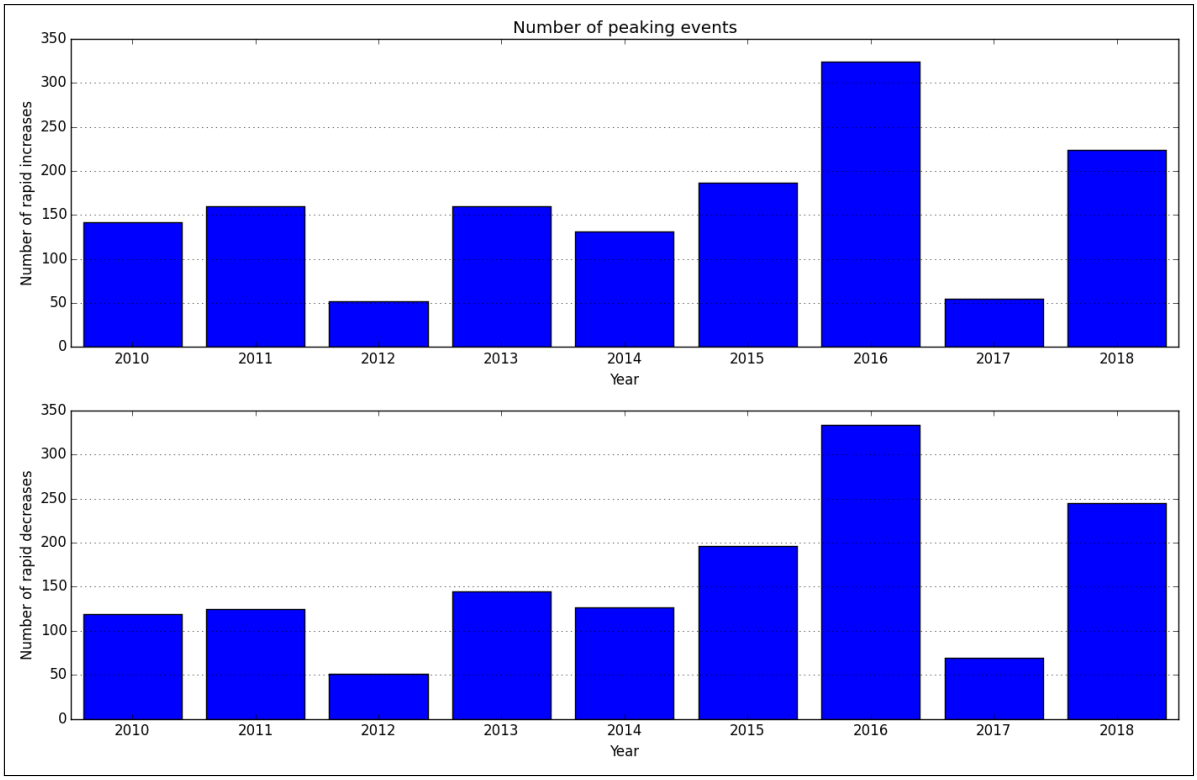

Figure A.3.12: Average annual number of increased/decreased peaks

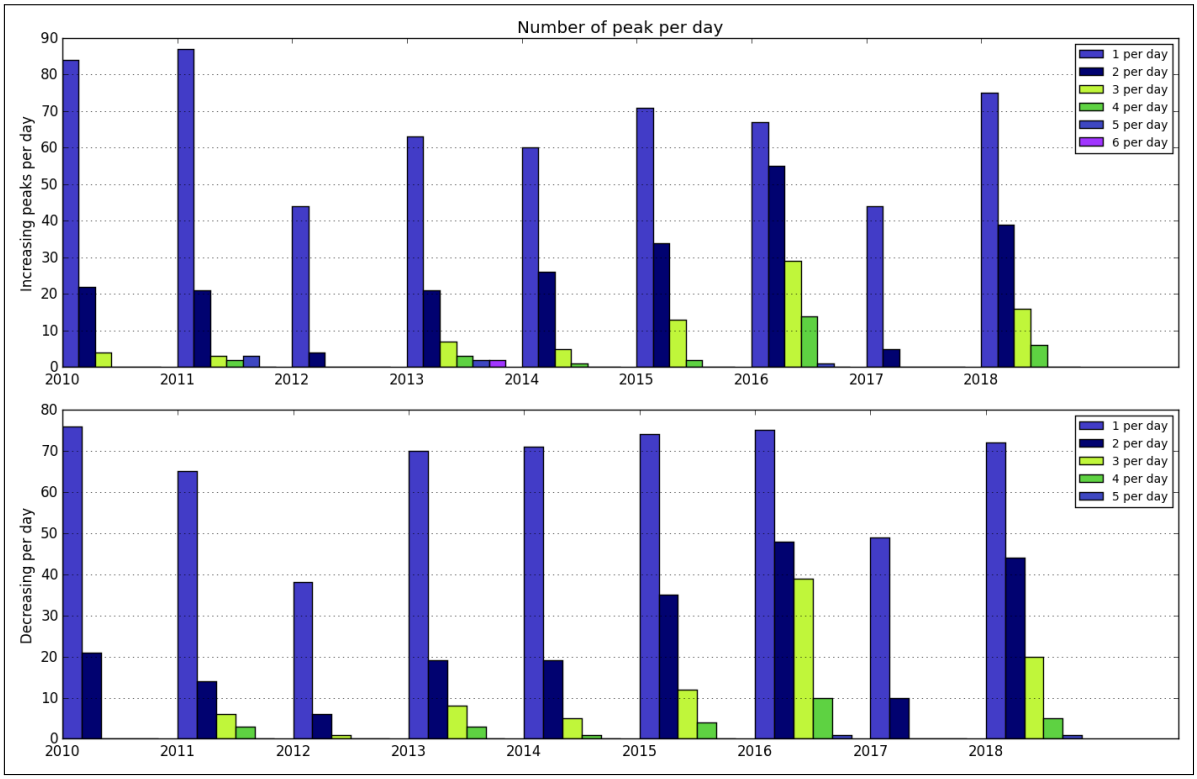

Figure A.3.13: Number of peaks per day

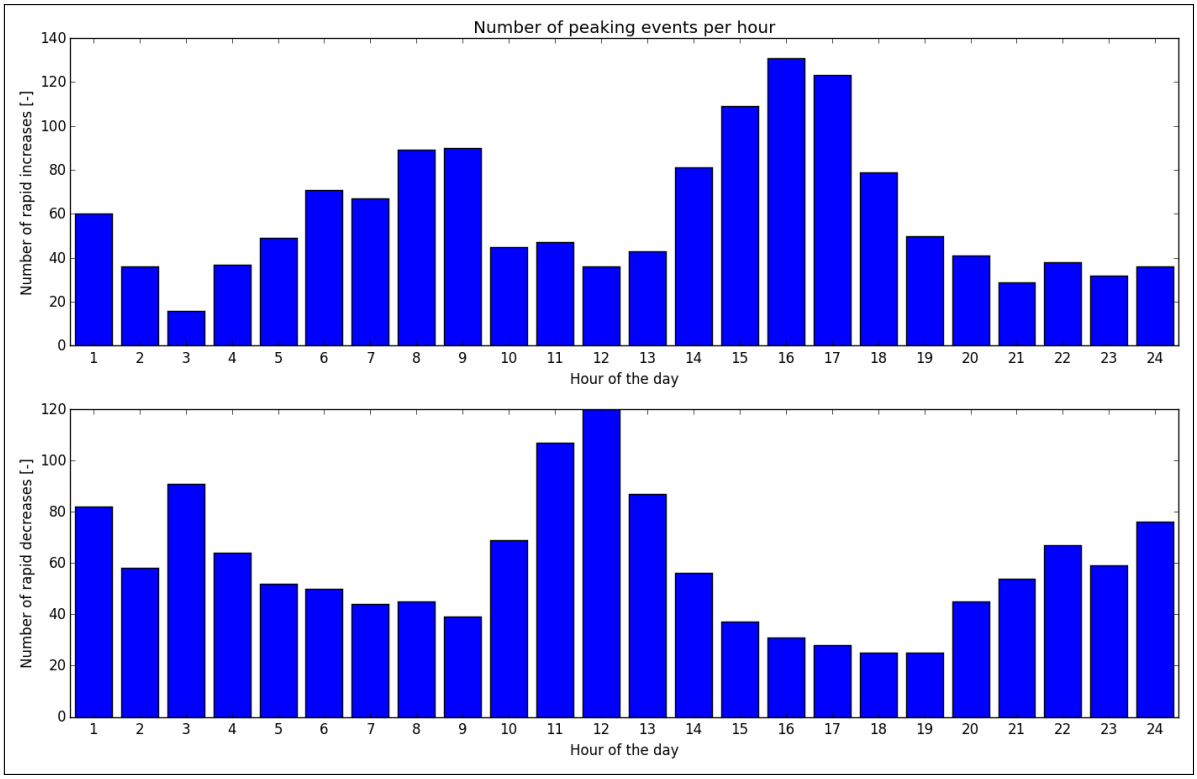

Figure A.3.14: Distribution of peaks throughout day

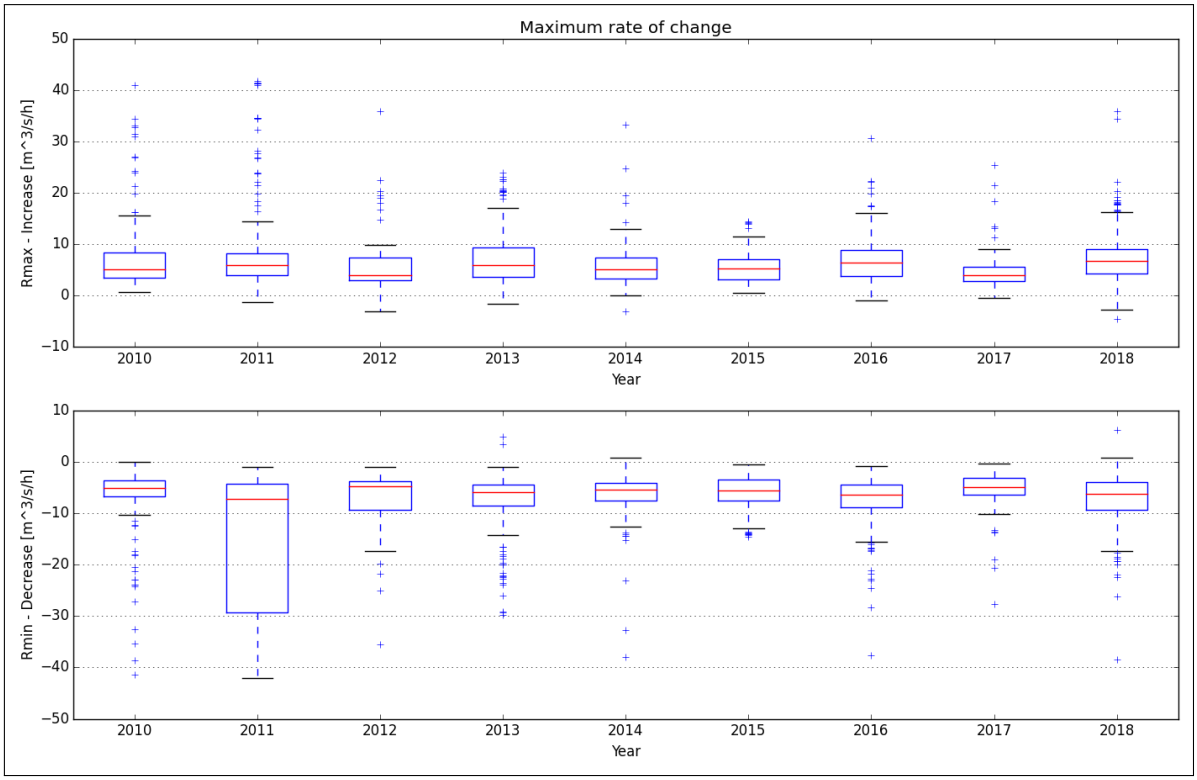

Figure A.3.15: Maximum rate of change

A.4. Framrusti

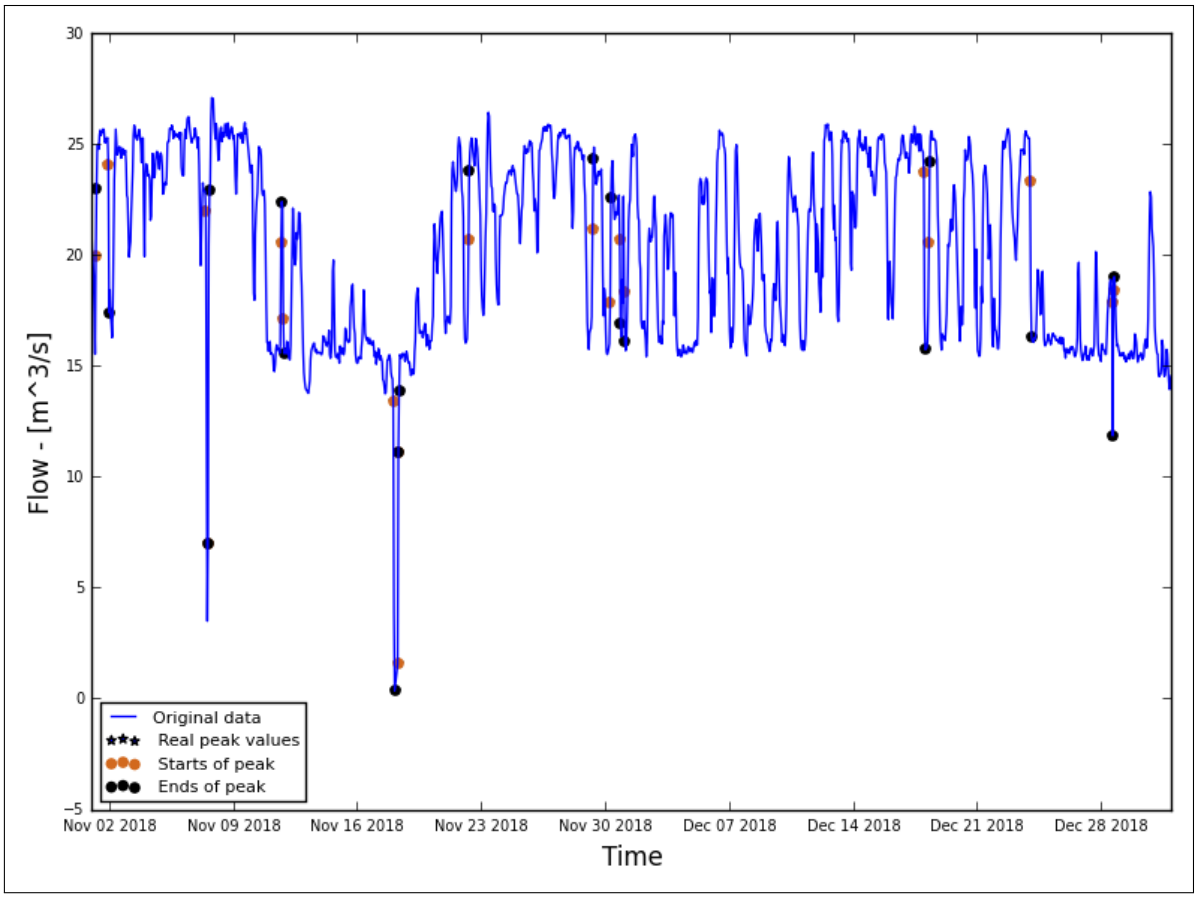

Figure A.4.16: Hydrograph of the last two months of the recorded data

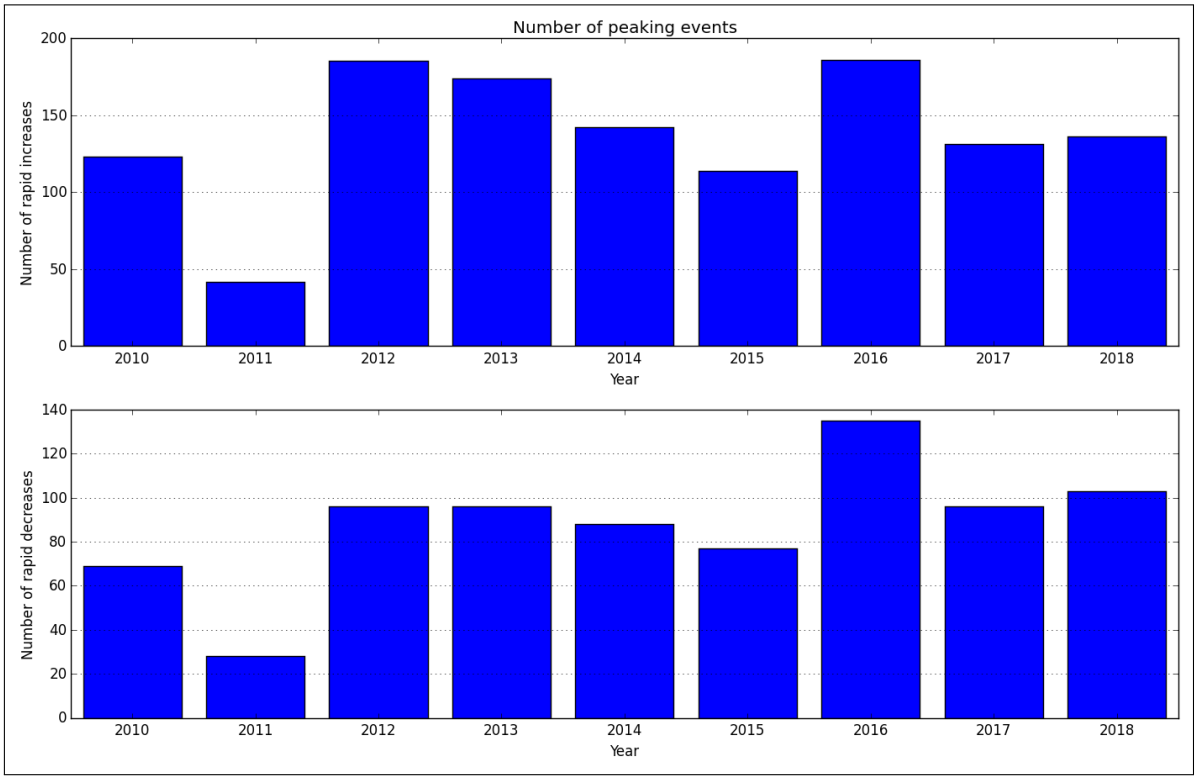

Figure A.4.17: Average annual number of increased/decreased peaks

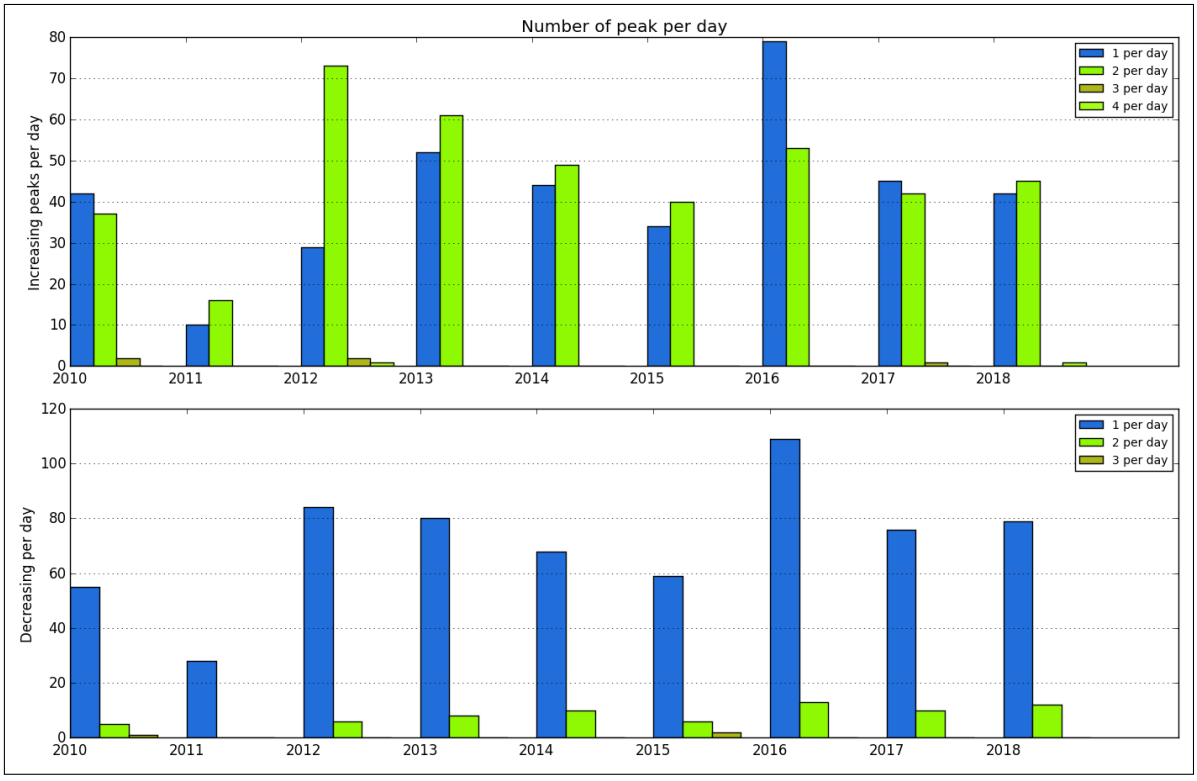

Figure A.4.18: Number of peaks per day

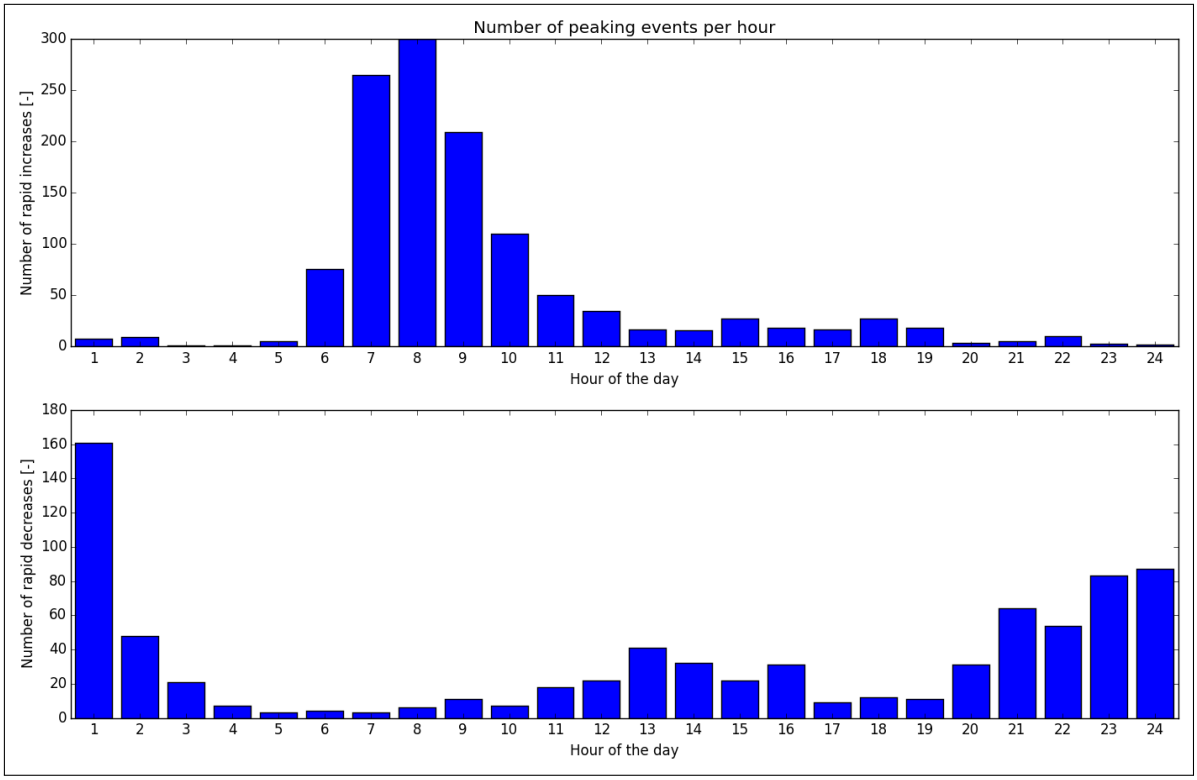

Figure A.4.19: Distribution of peaks throughout day

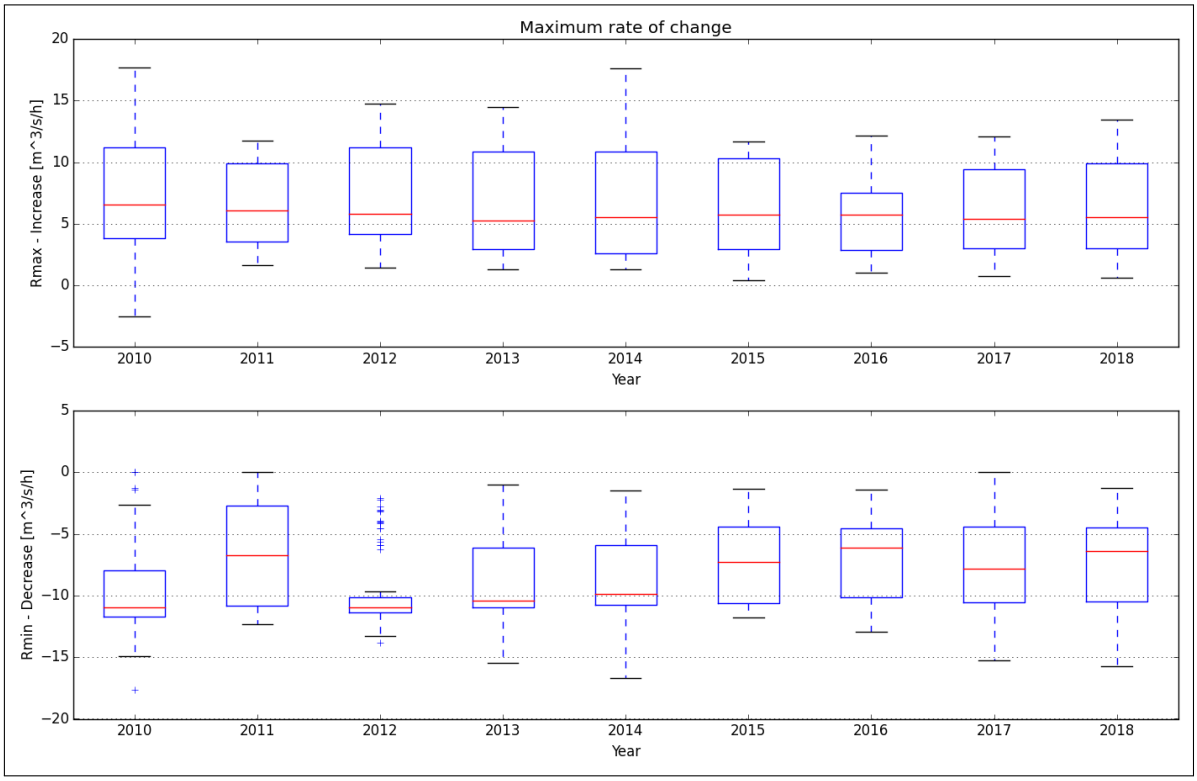

Figure A.4.20: Maximum rate of change

A.5. Øyberget

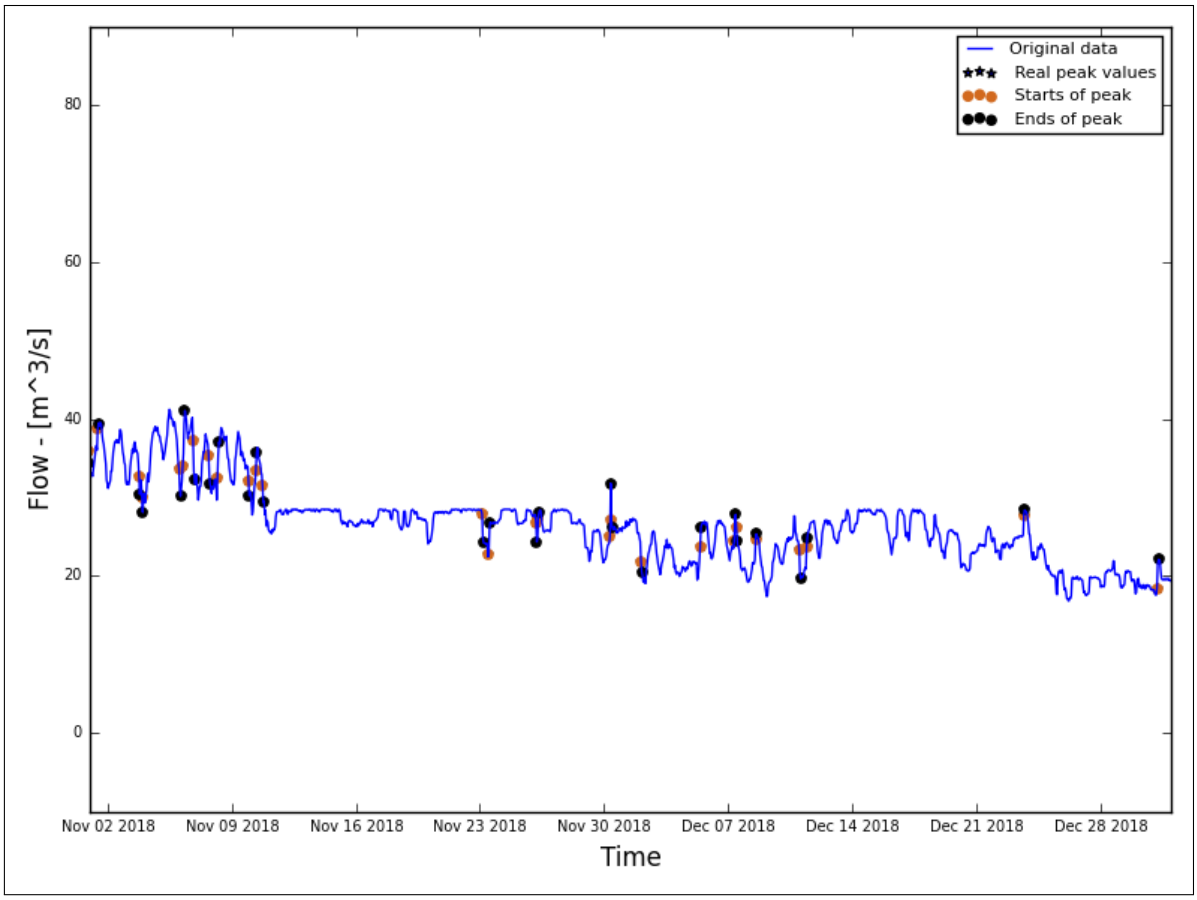

Figure A.5.21: Hydrograph of the last two months of the recorded data

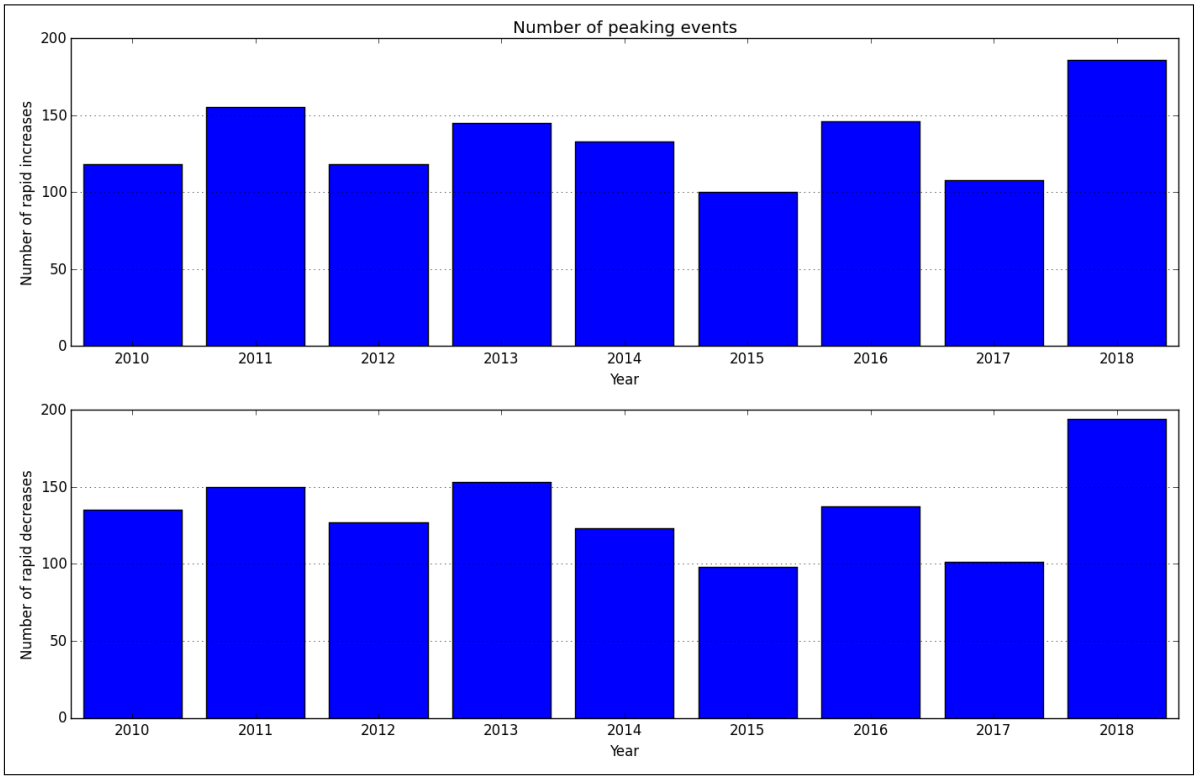

Figure A.5.22: Average annual number of increased/decreased peaks

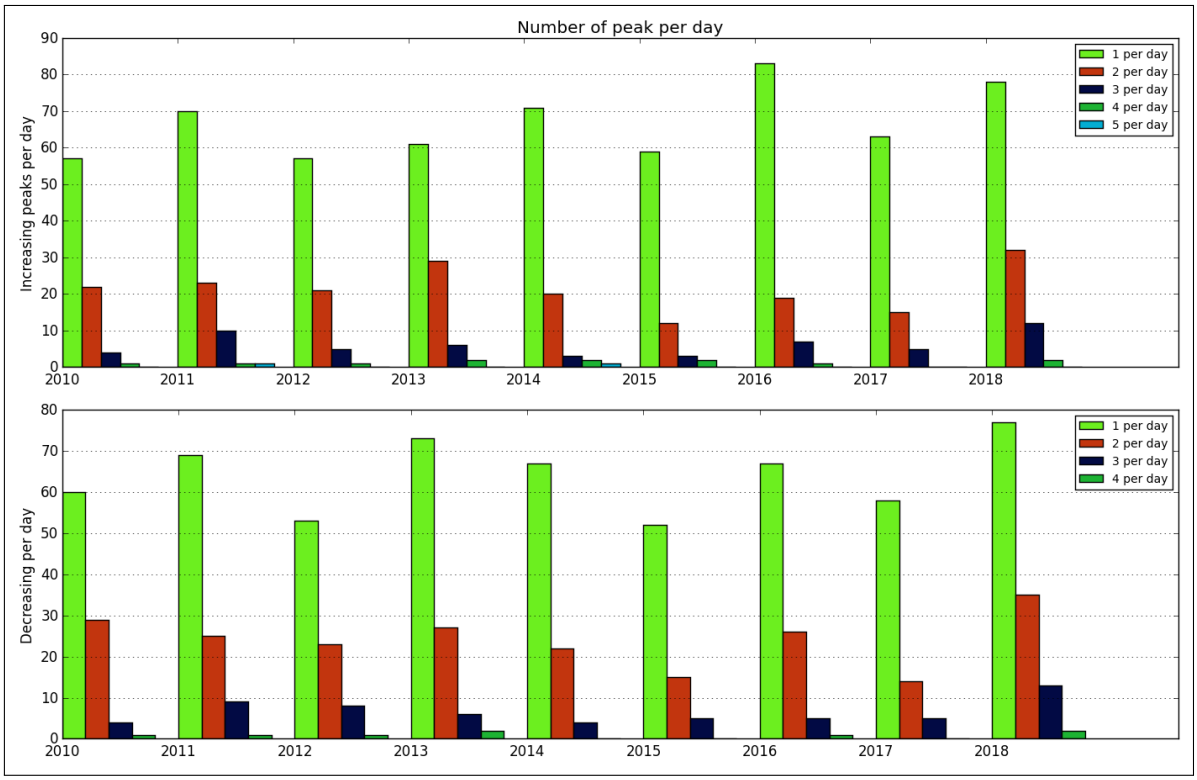

Figure A.5.23: Number of peaks per day

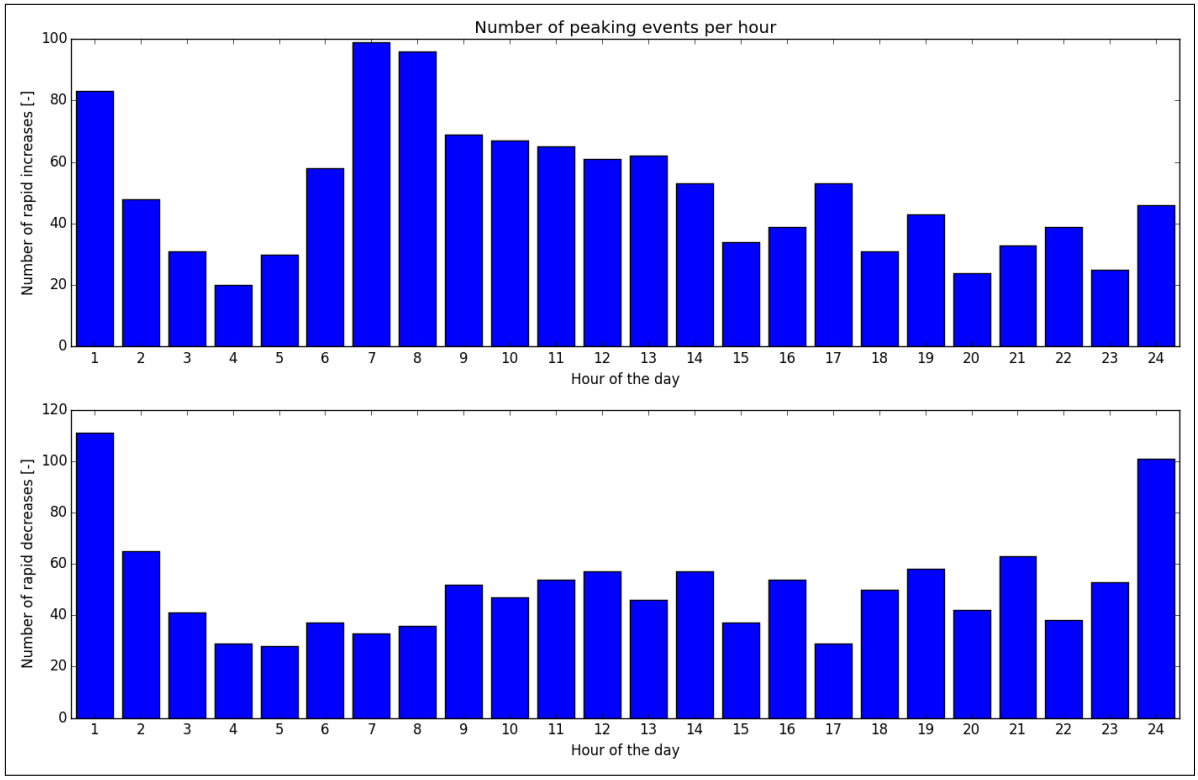

Figure A.5.24: Distribution of peaks throughout day

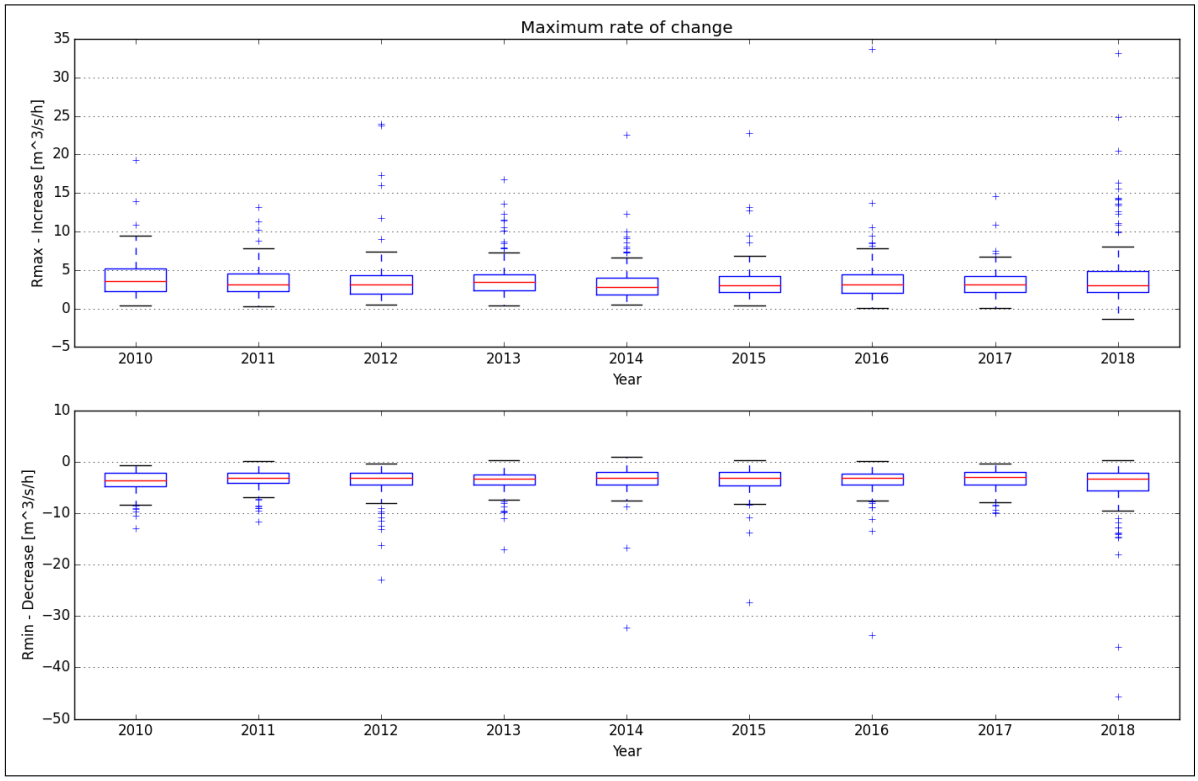

Figure A.5.25: Maximum rate of change

A.6. Solbergfoss

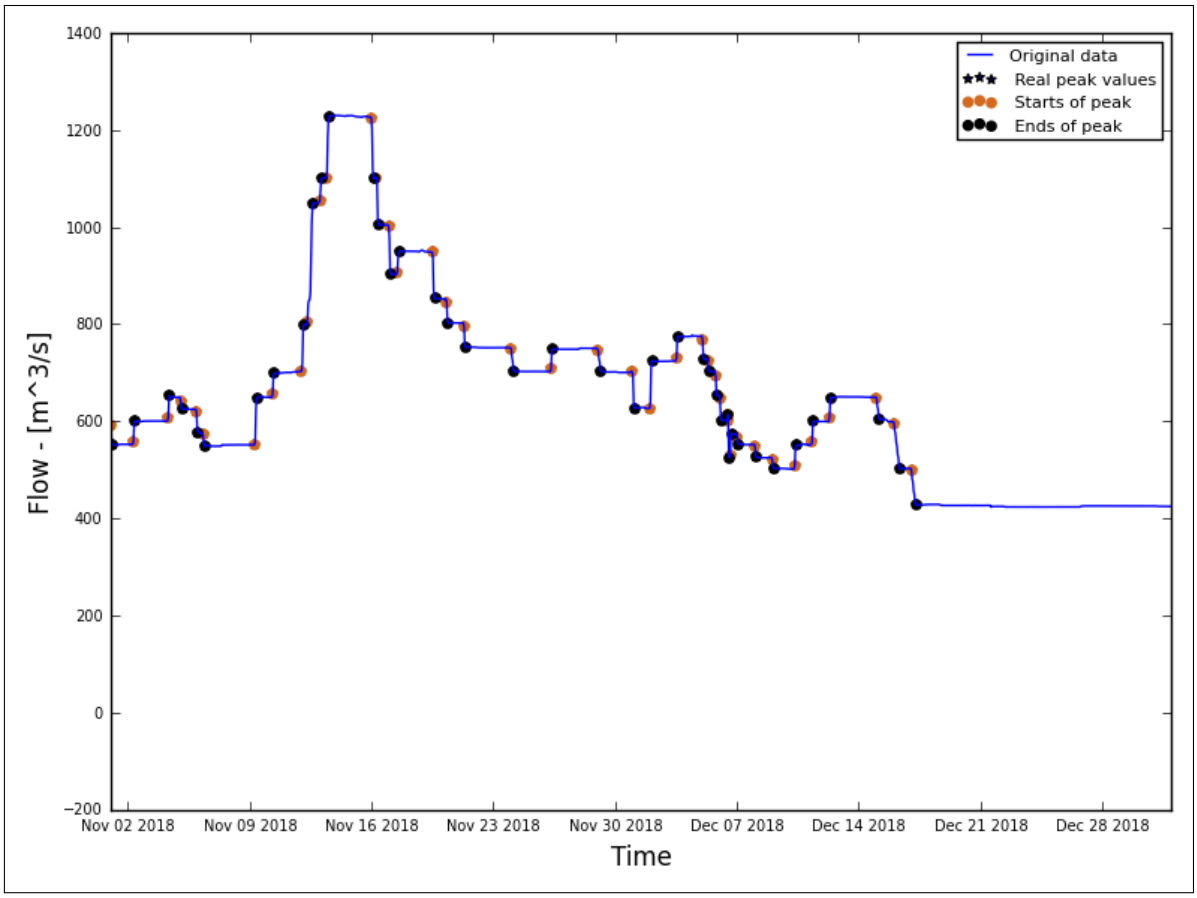

Figure A.6.26: Hydrograph of the last two months of the recorded data

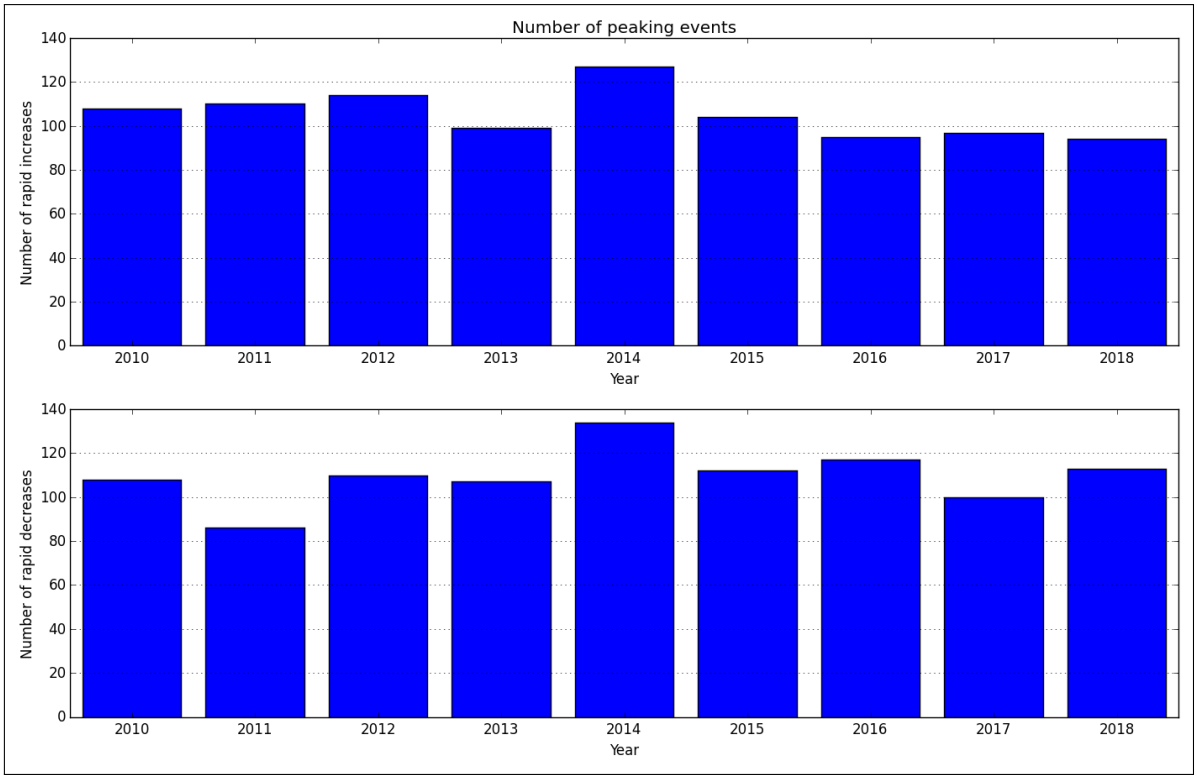

Figure A.6.27: Average annual number of increased/decreased peaks

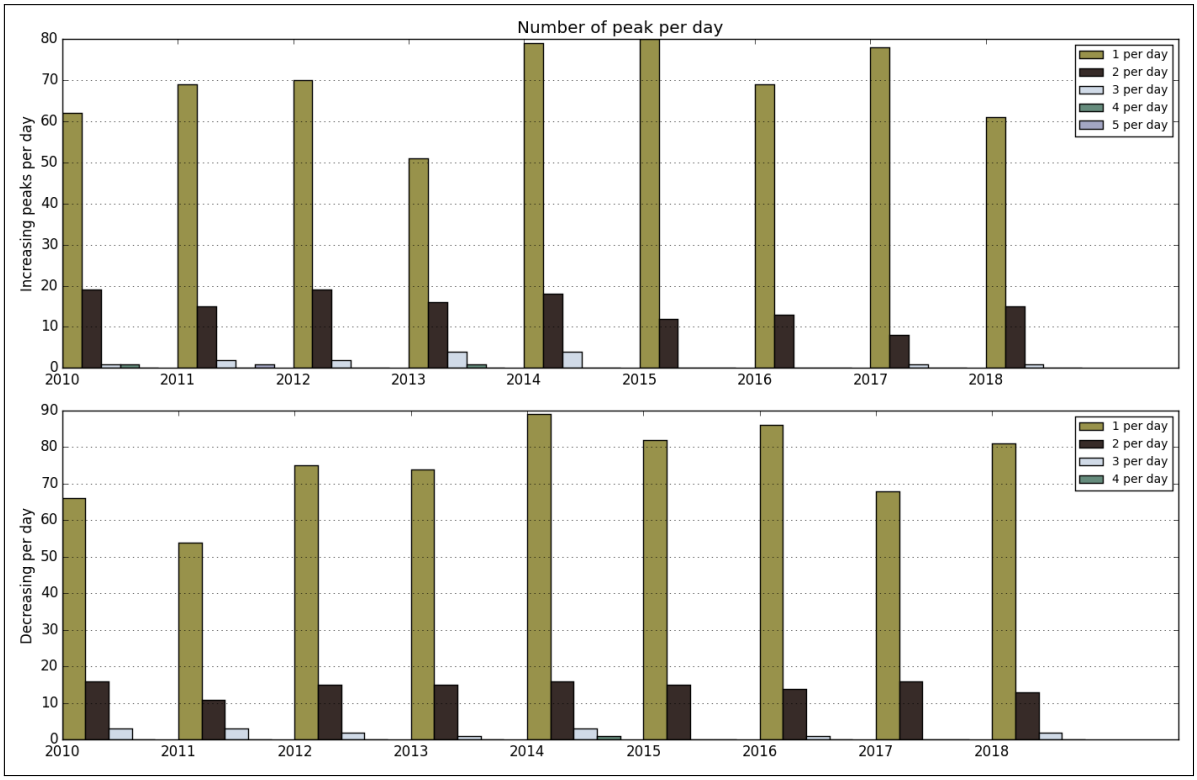

Figure A.6.28: Number of peaks per day

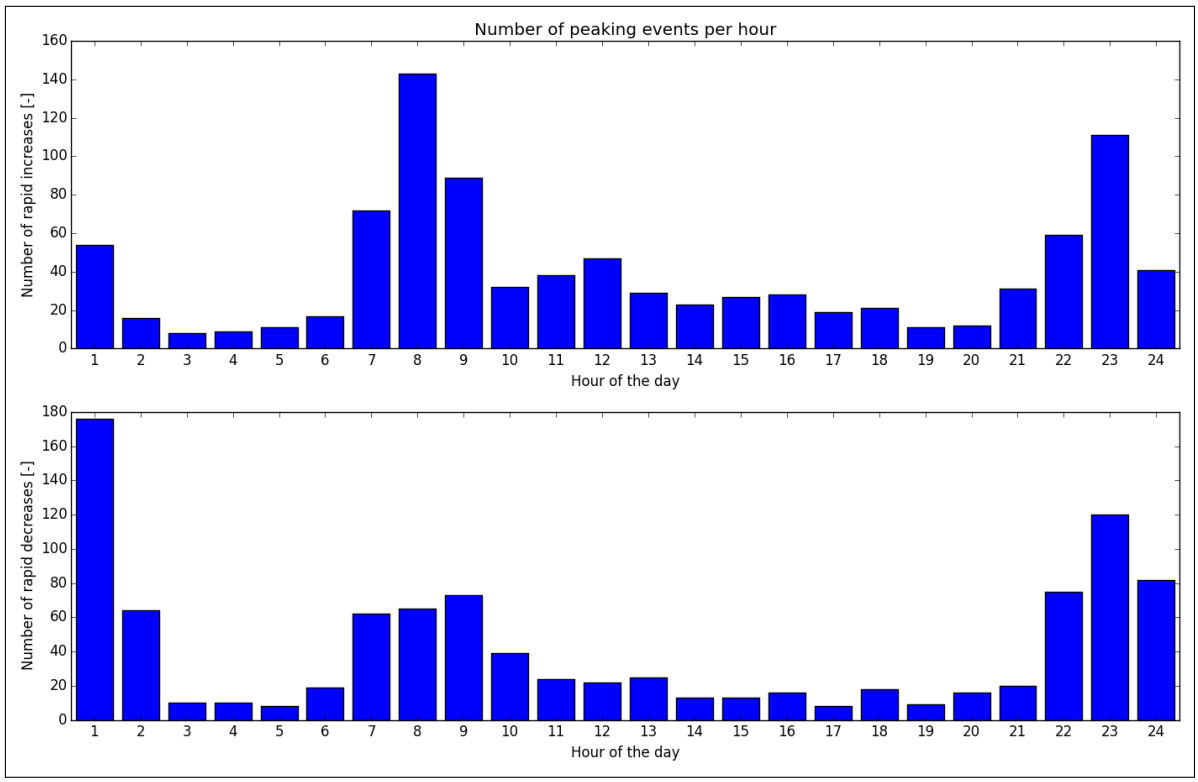

Figure A.6.29: Distribution of peaks throughout day

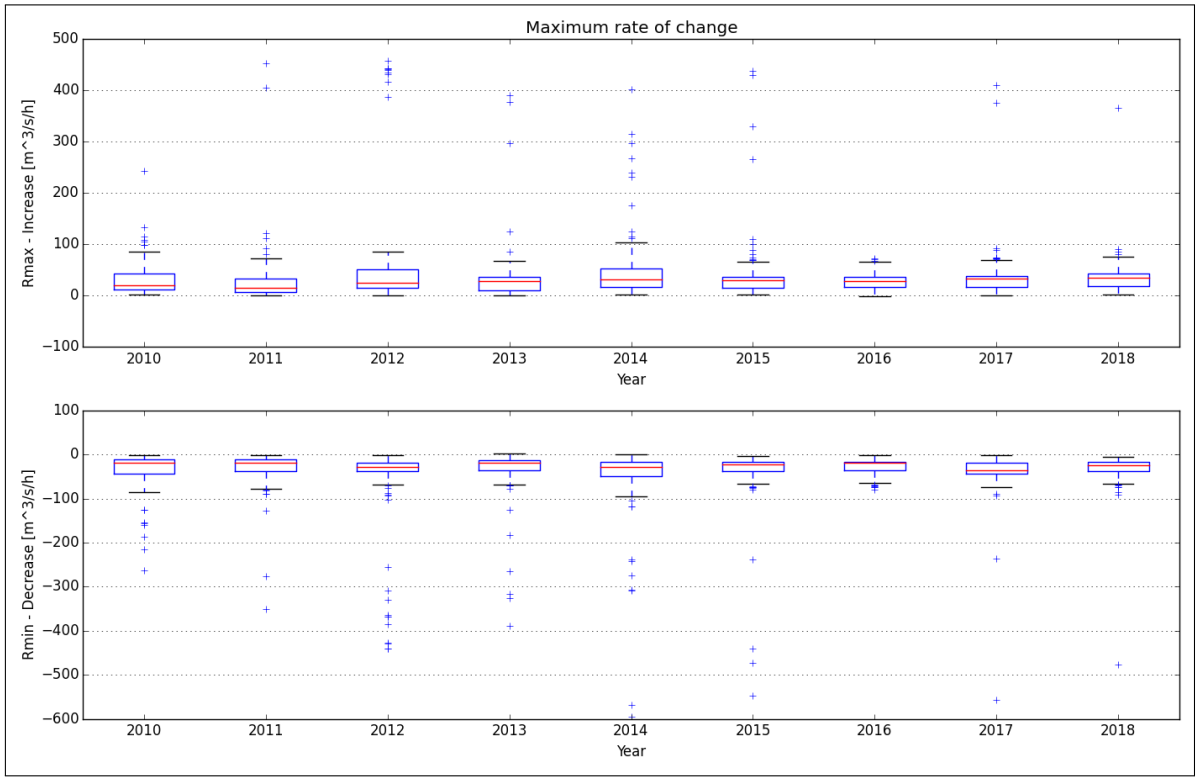

Figure A.6.30: Maximum rate of change

A.7. Søre Osa

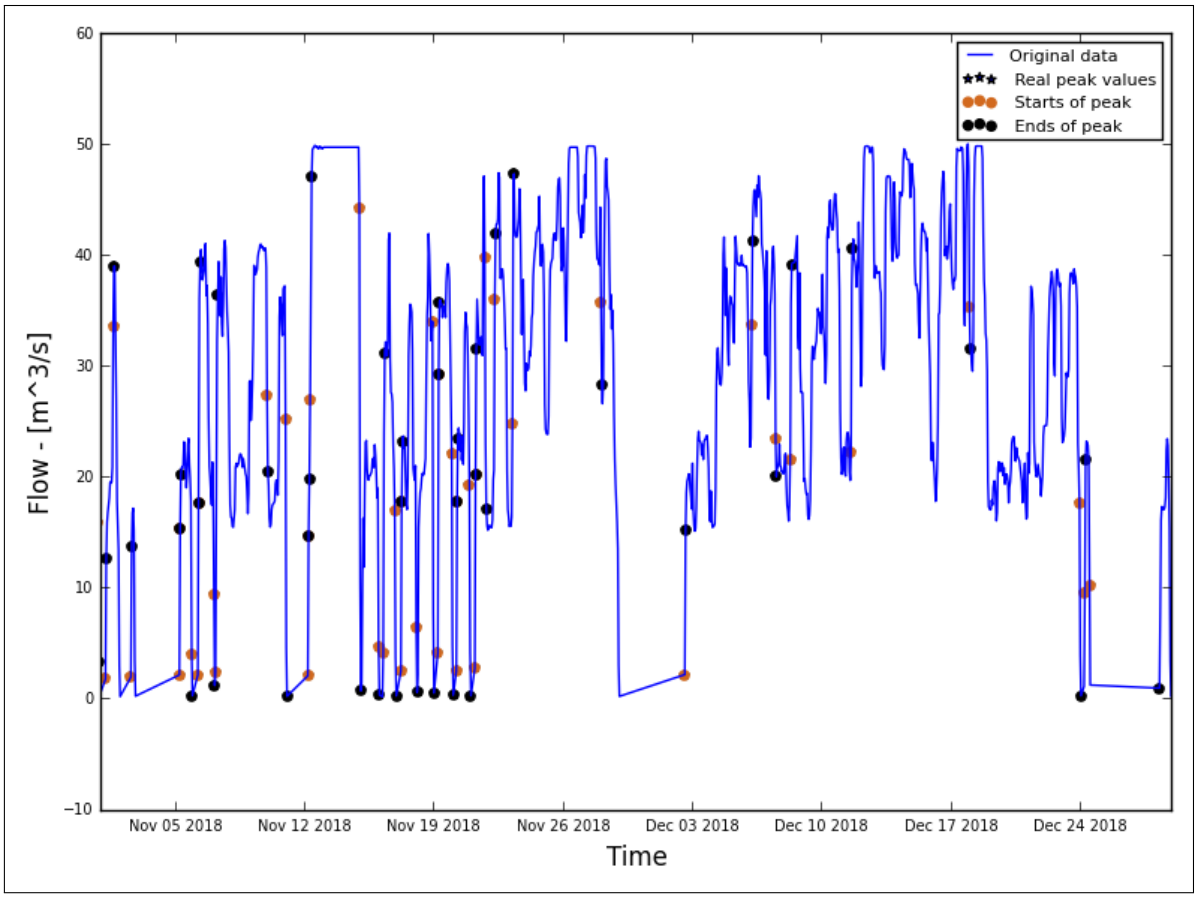

Figure A.7.31: Hydrograph of the last two months of the recorded data

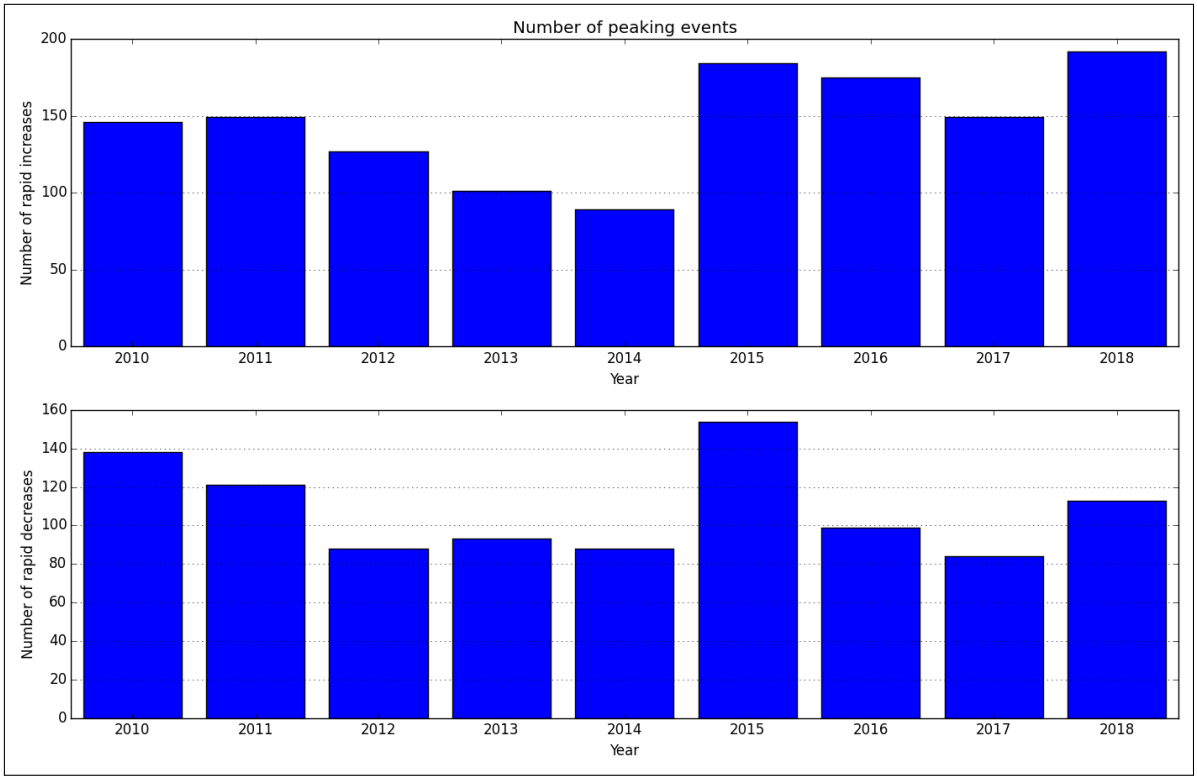

Figure A.7.32: Average annual number of increased/decreased peaks

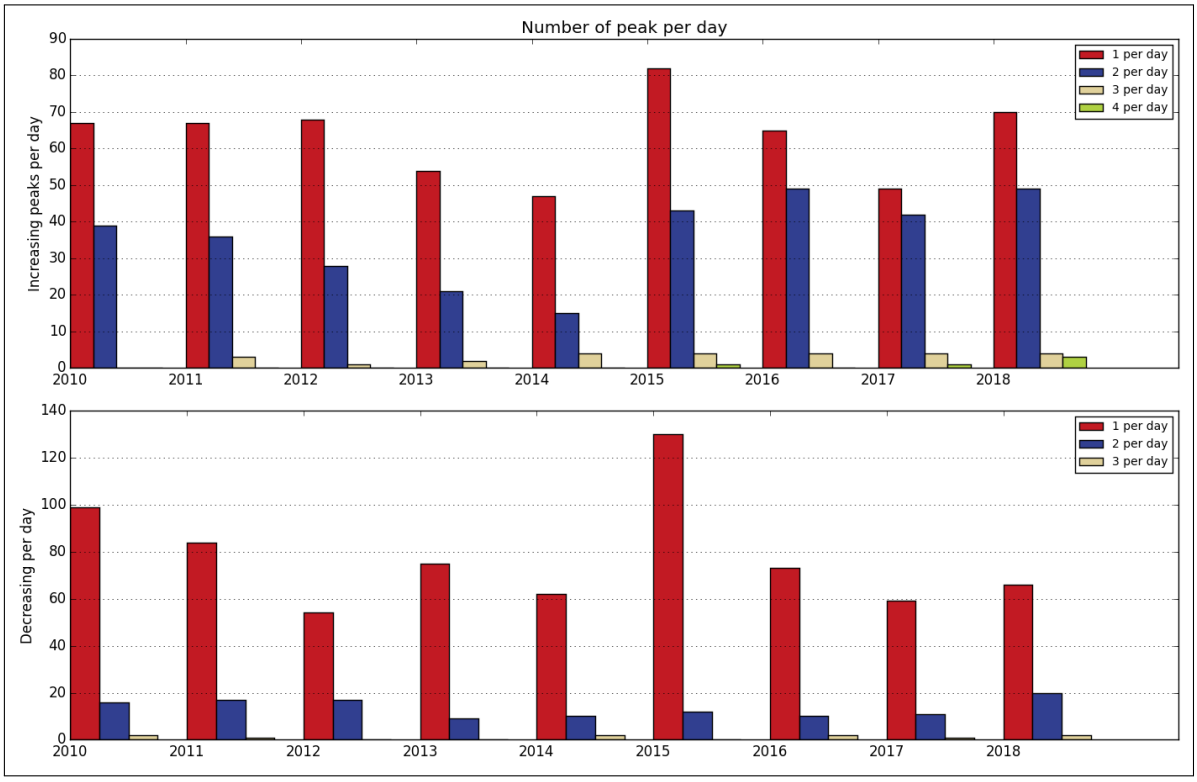

Figure A.7.33: Number of peaks per day

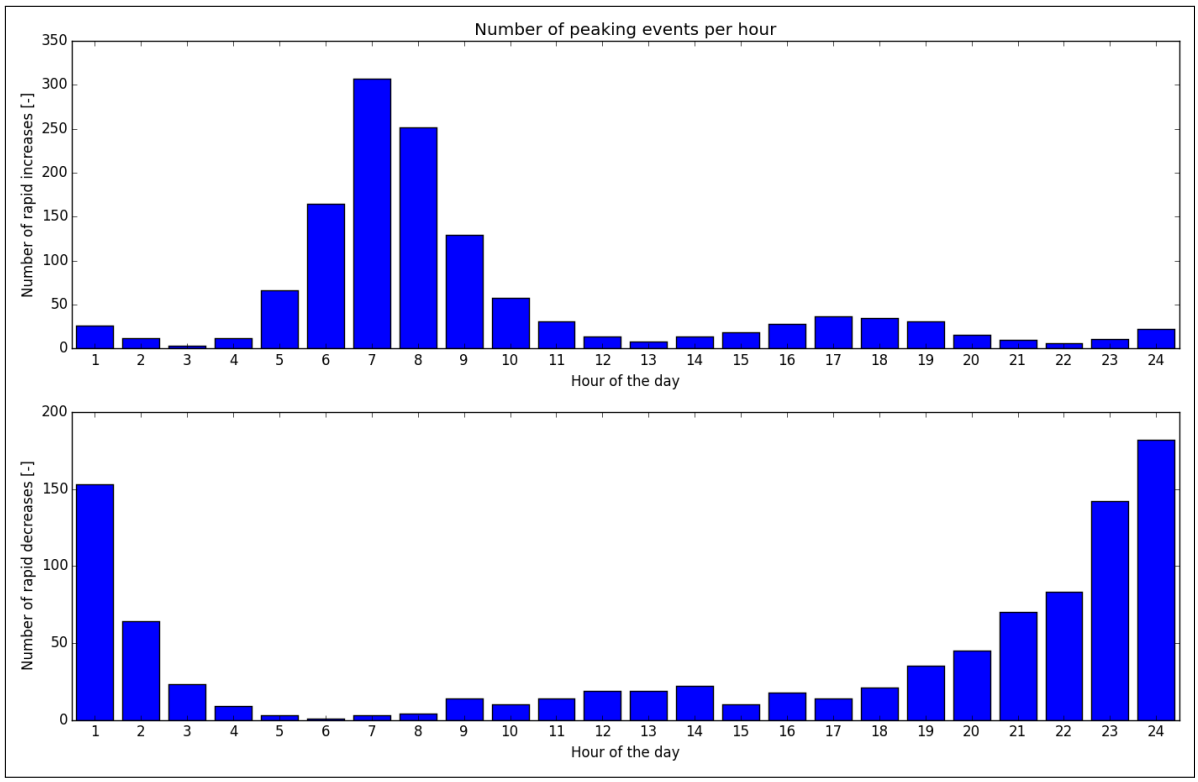

Figure A.7.34: Distribution of peaks throughout day

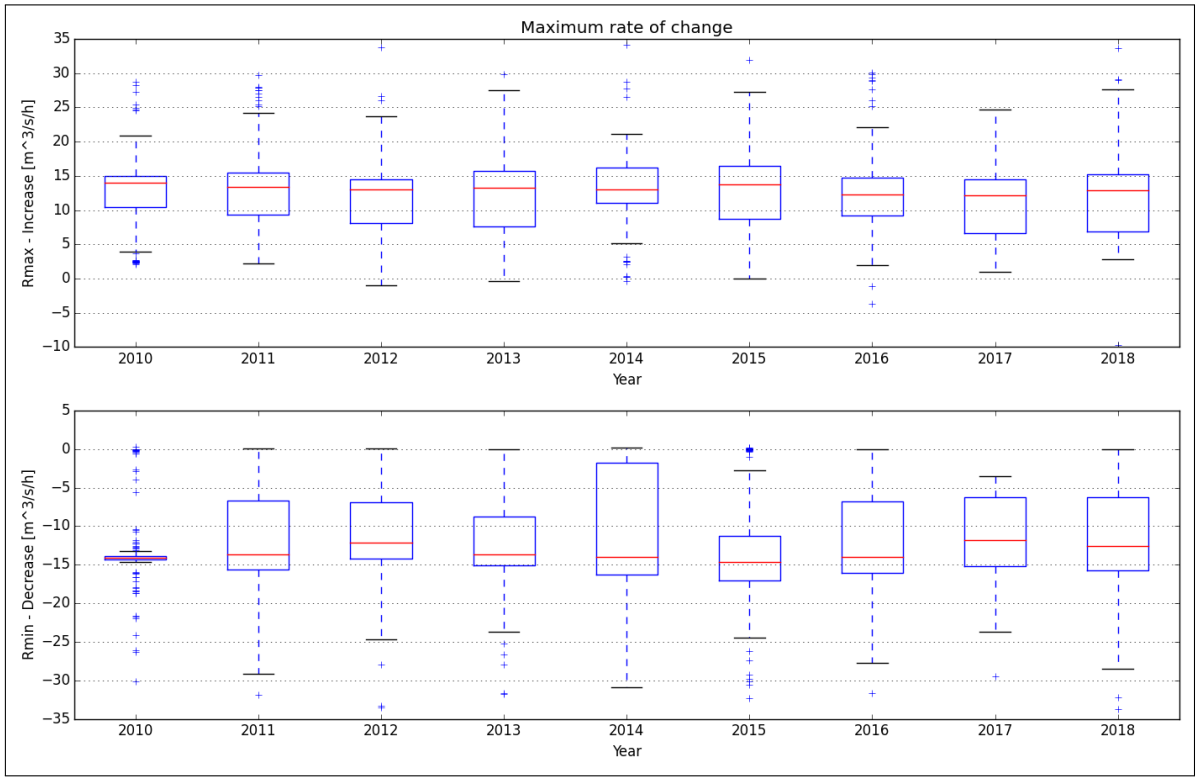

Figure A.7.35: Maximum rate of change

A.8. OvreTessa

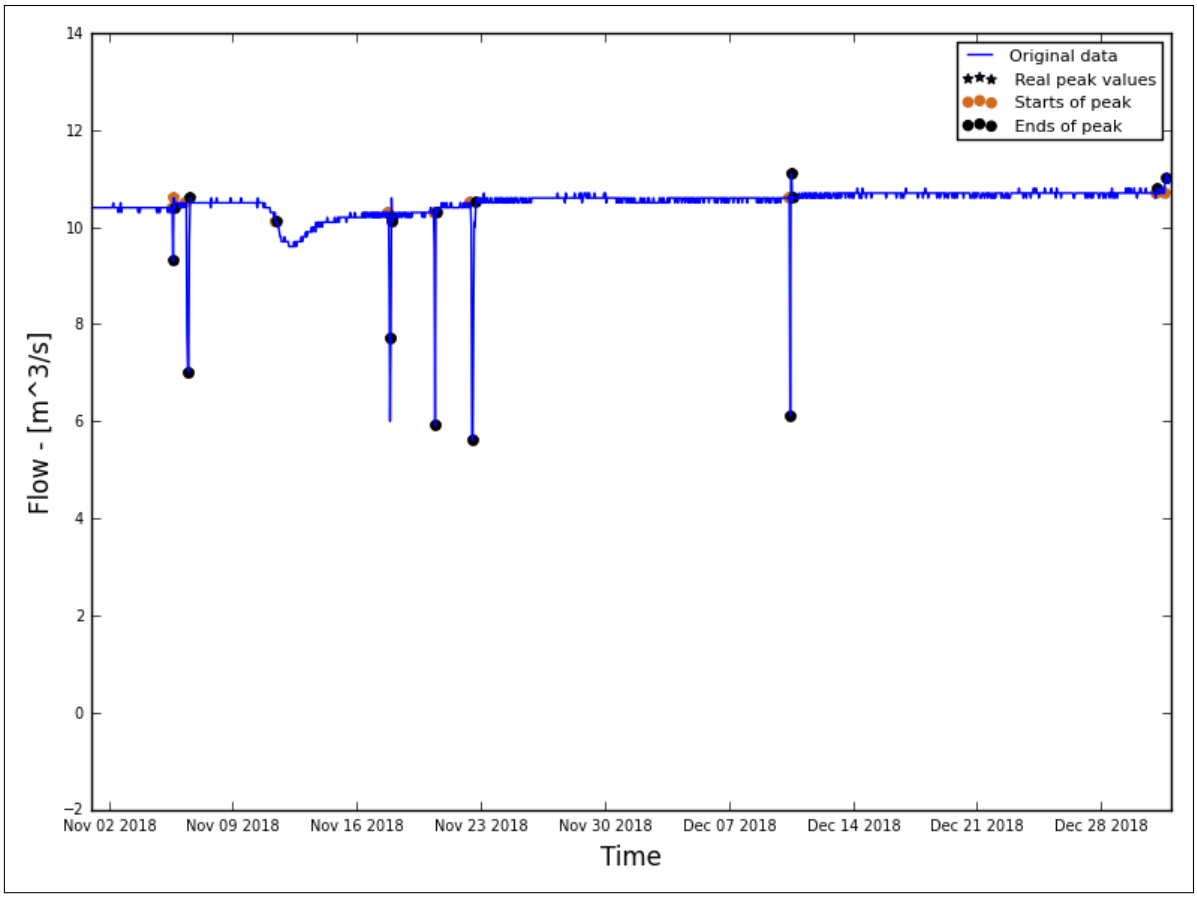

Figure A.8.36: Hydrograph of the last two months of the recorded data

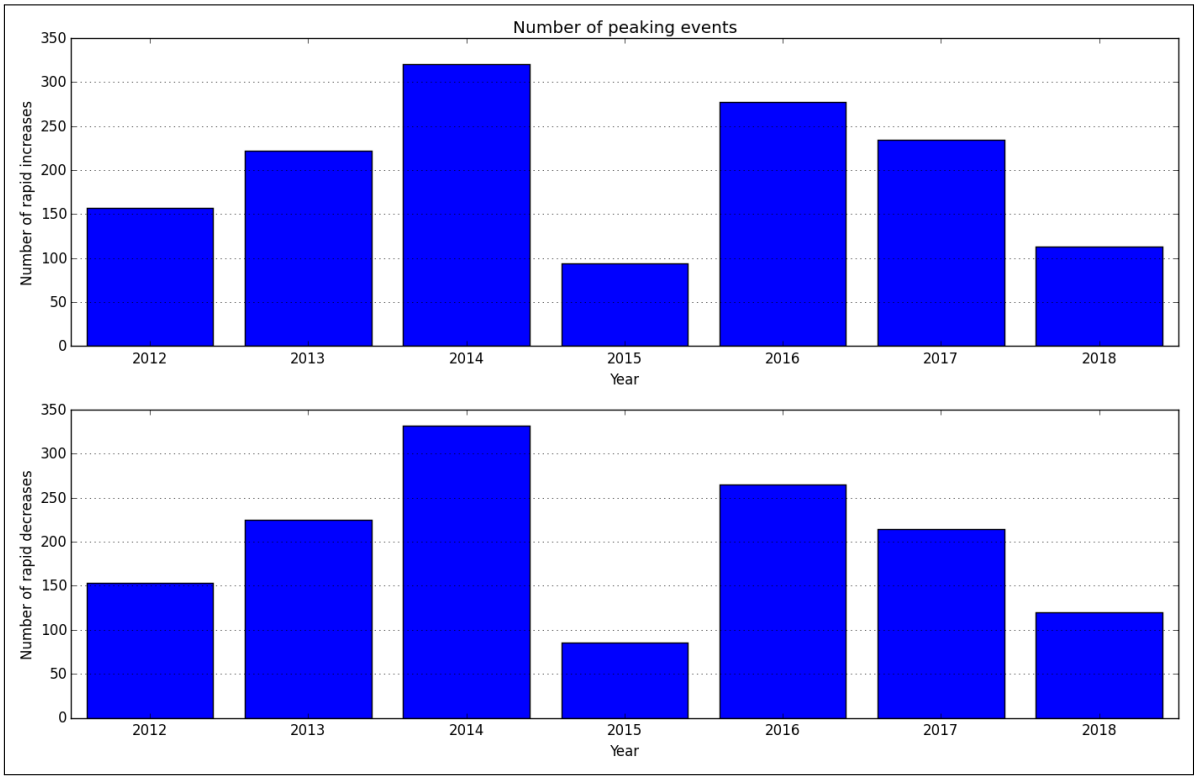

Figure A.8.37: Average annual number of increased/decreased peaks

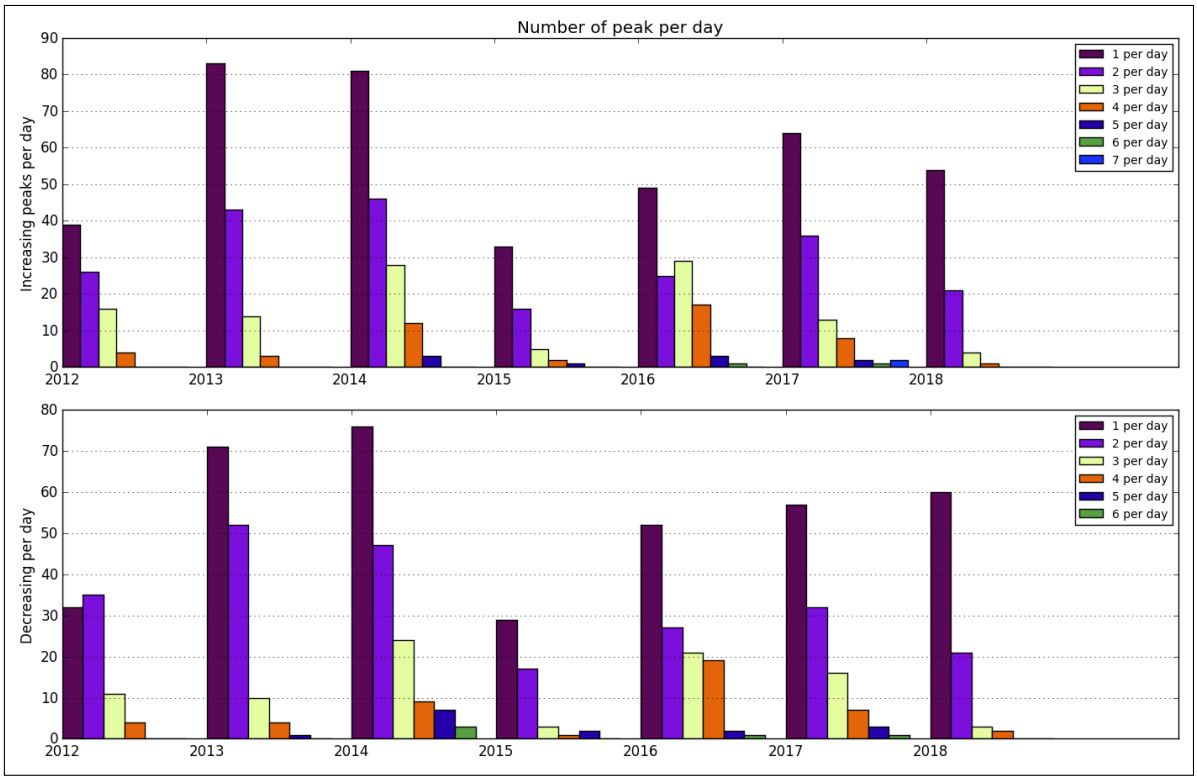

Figure A.8.38: Number of peaks per day

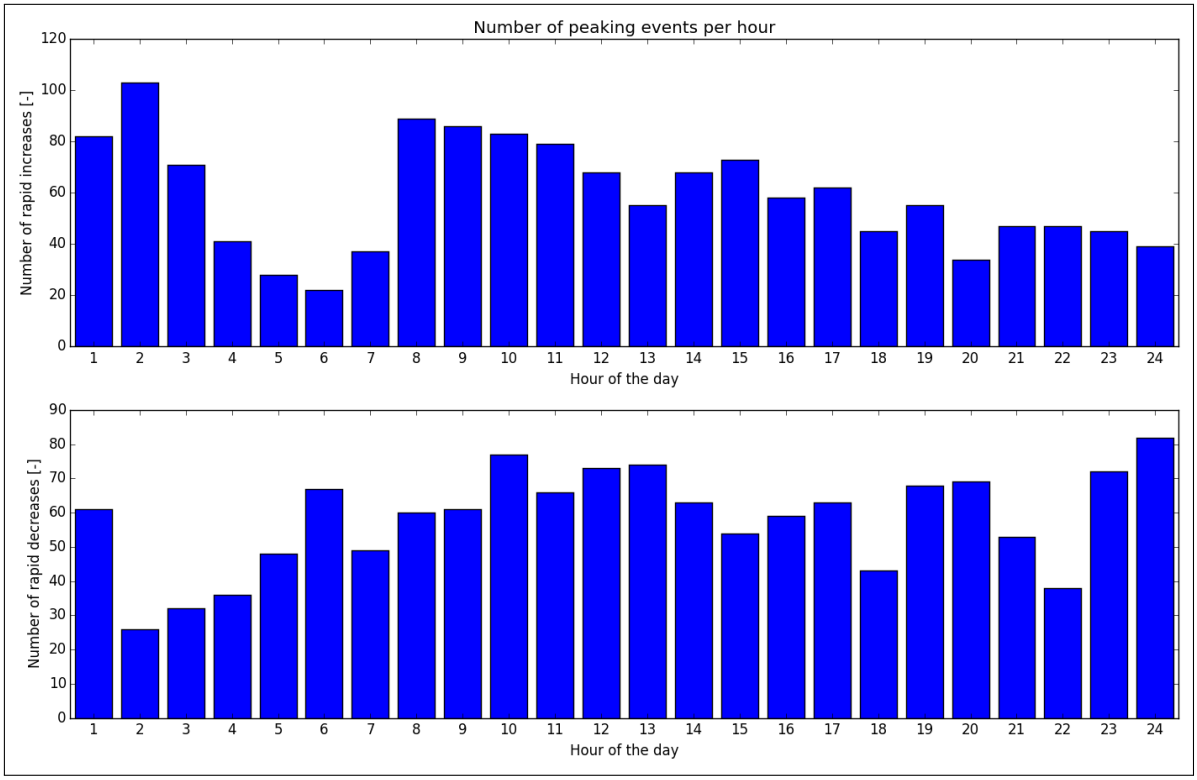

Figure A.8.39: Distribution of peaks throughout day

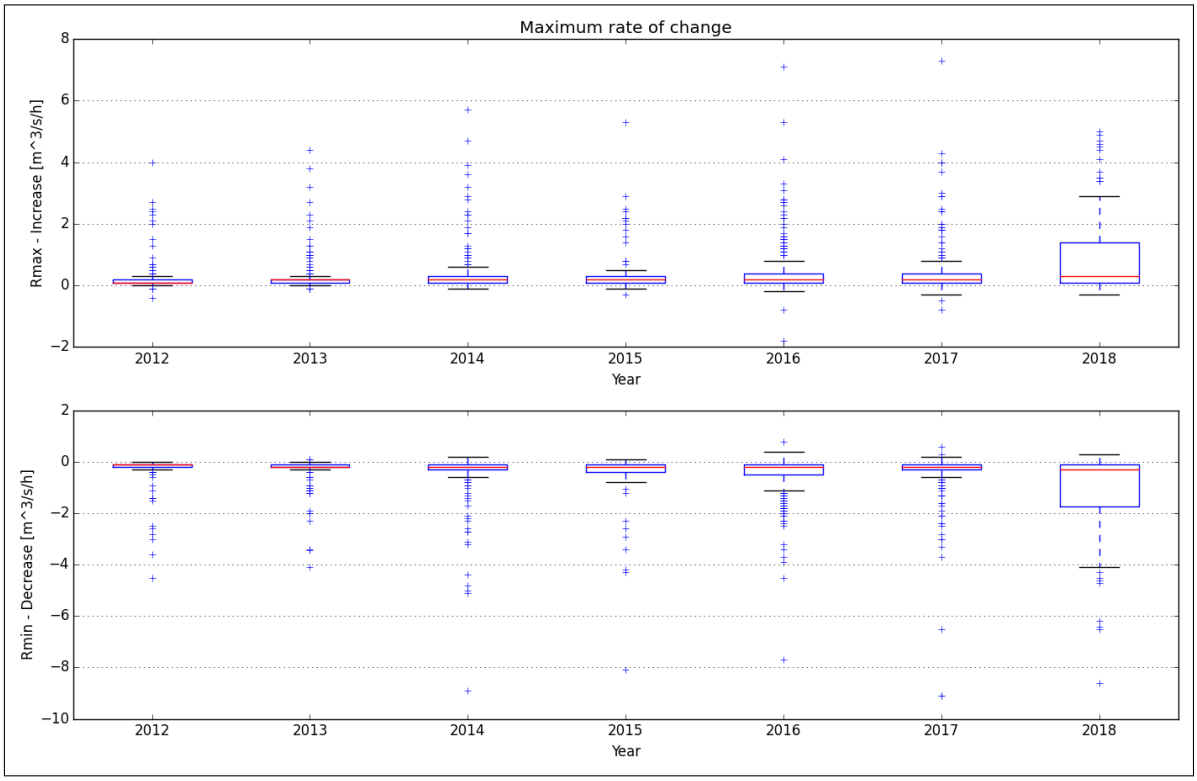

Figure A.8.40: Maximum rate of change

A.9. N.Vinstra

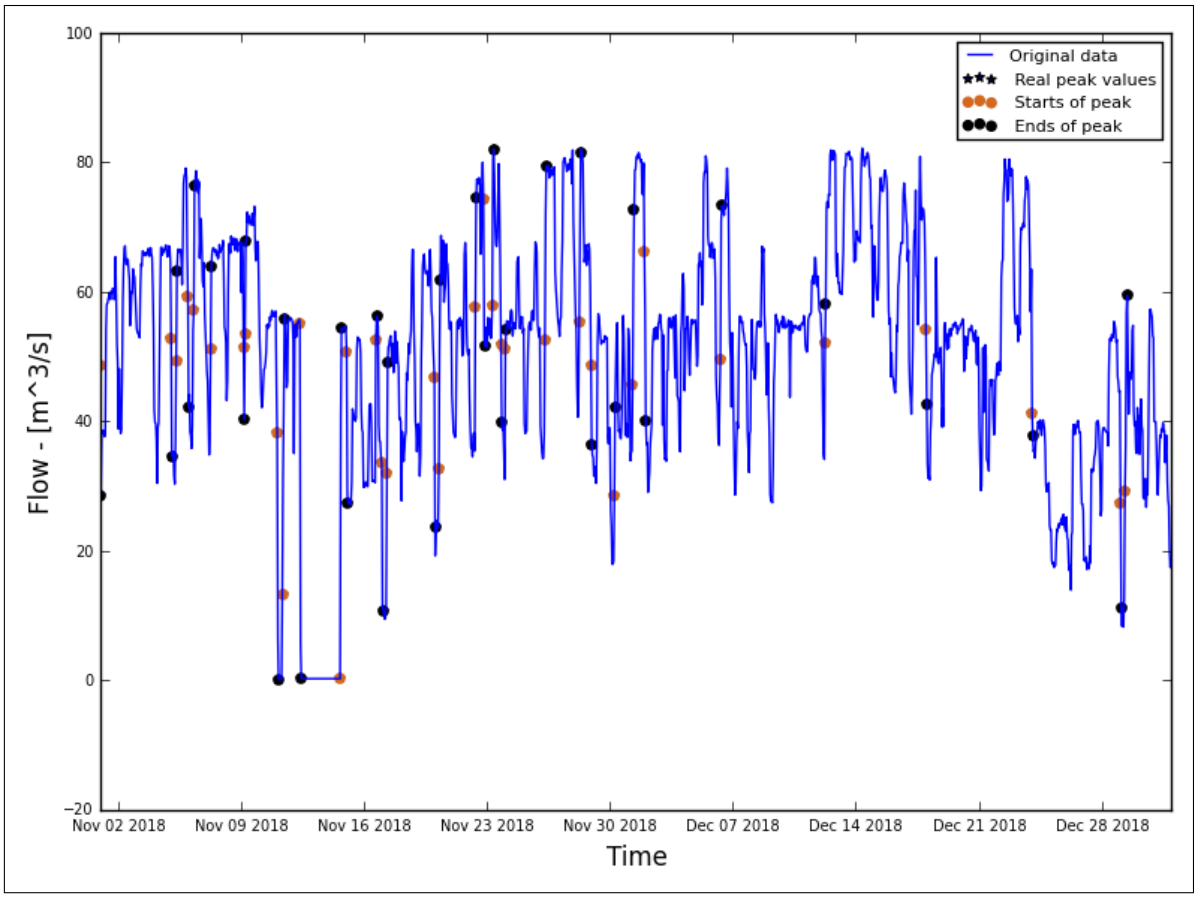

Figure A.9.41: Hydrograph of the last two months of the recorded data

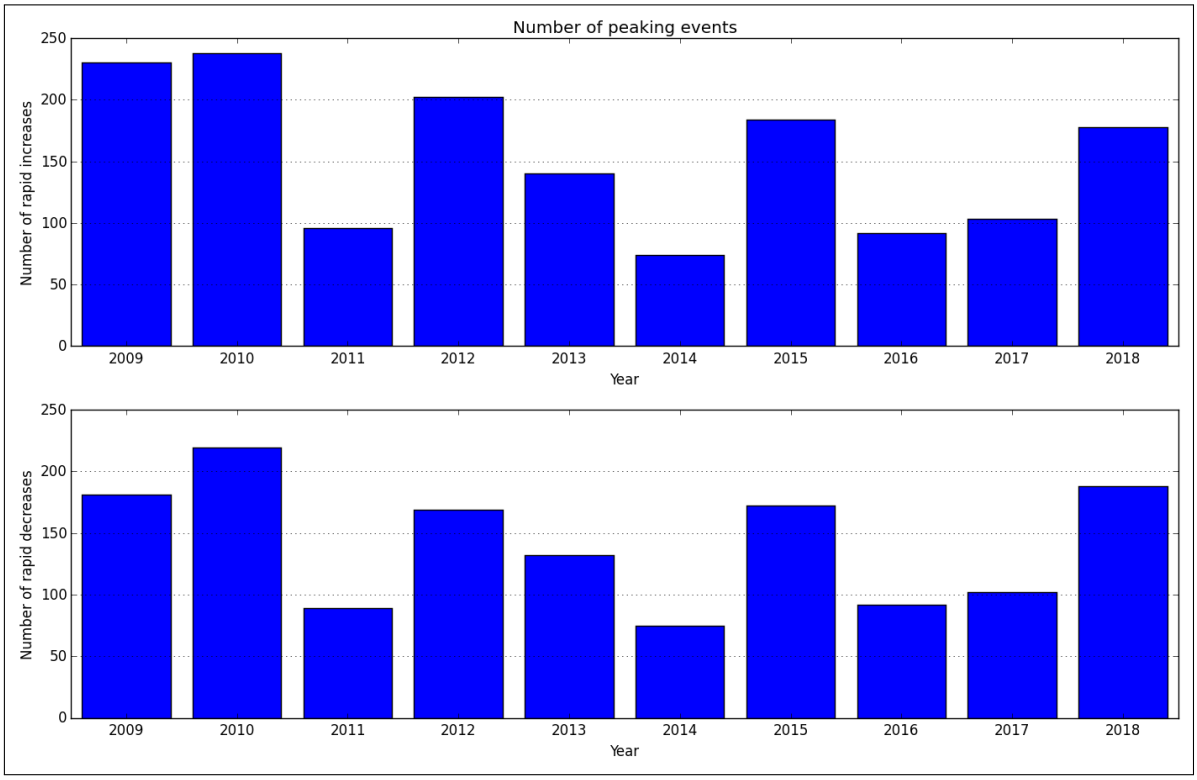

Figure A.9.42: Average annual number of increased/decreased peaks

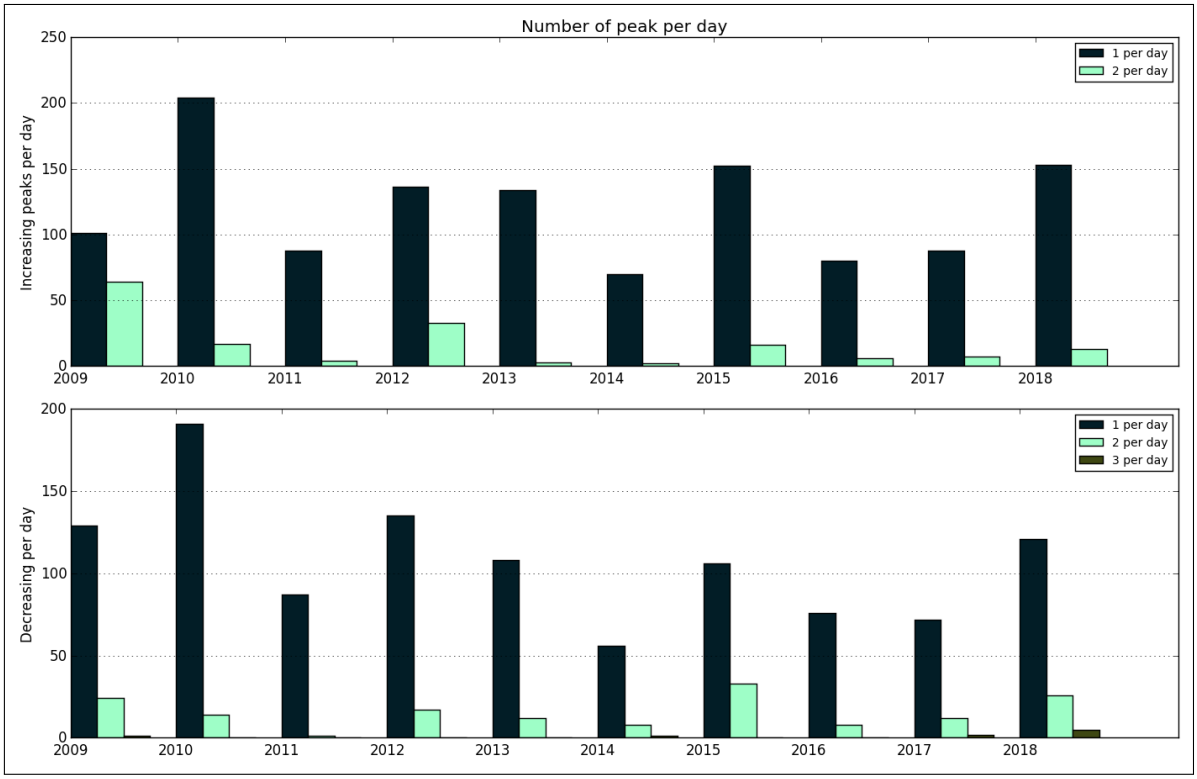

Figure A.9.43: Number of peaks per day

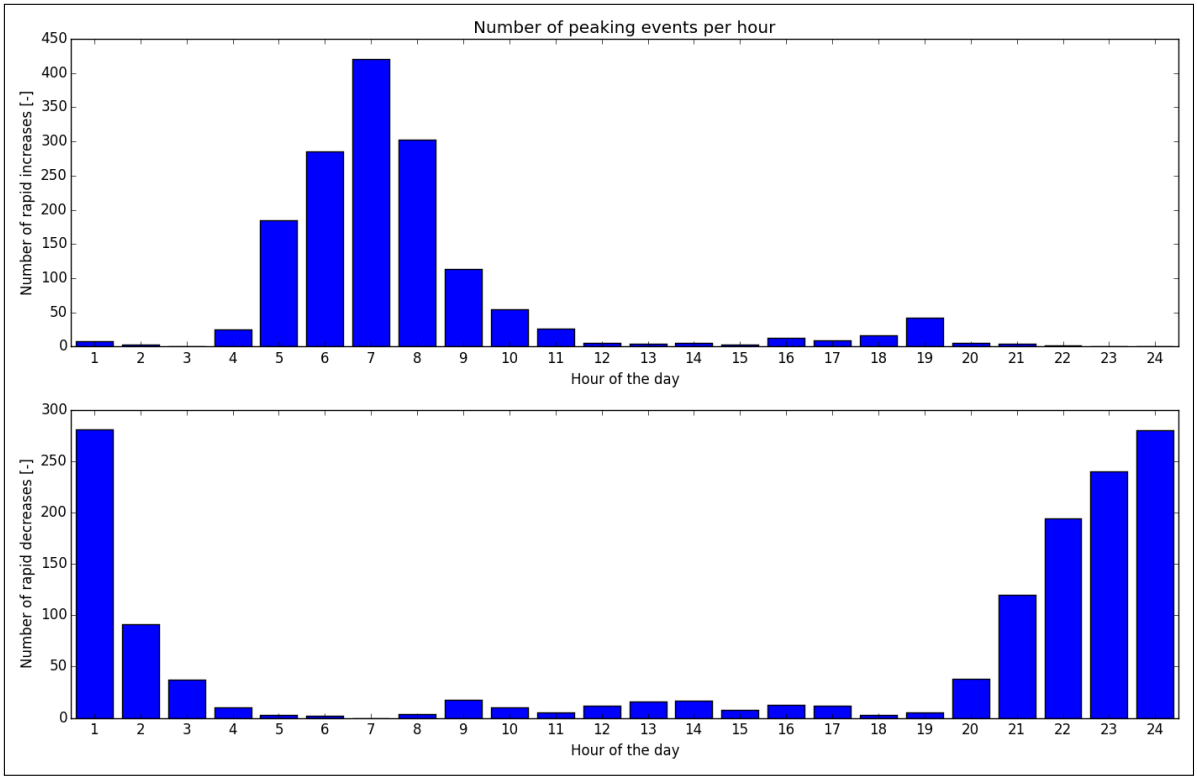

Figure A.9.44: Distribution of peaks throughout day

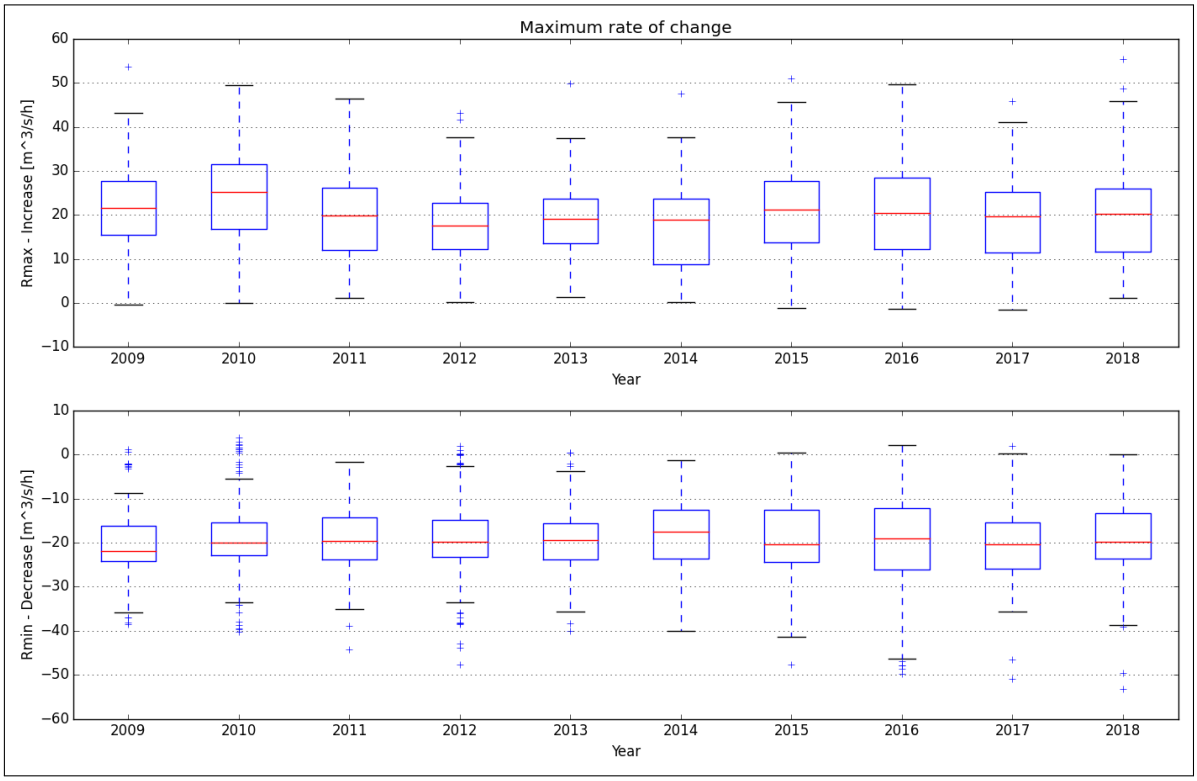

Figure A.9.45: Maximum rate of change

A.10. Hemsil II kraftsasjon

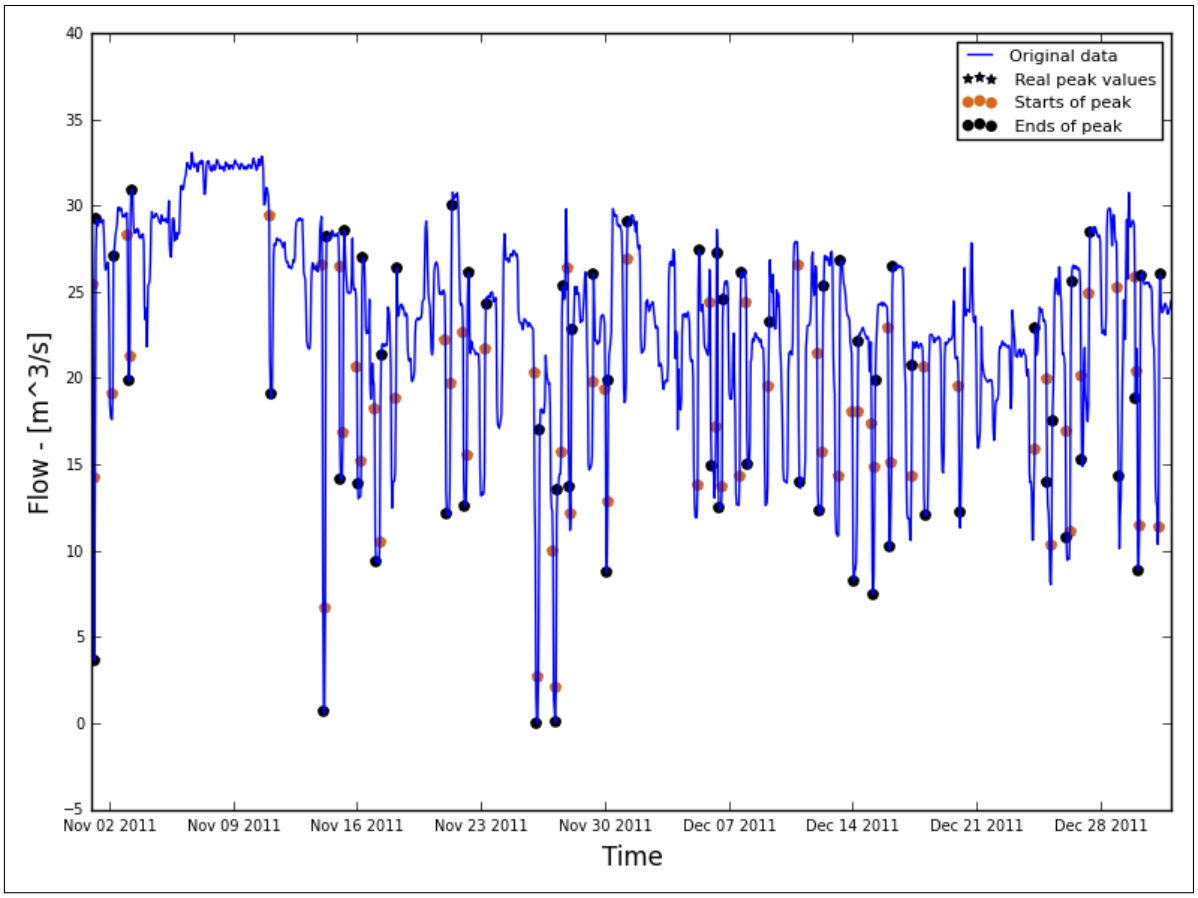

Figure A.10.46: Hydrograph of the last two months of the recorded data

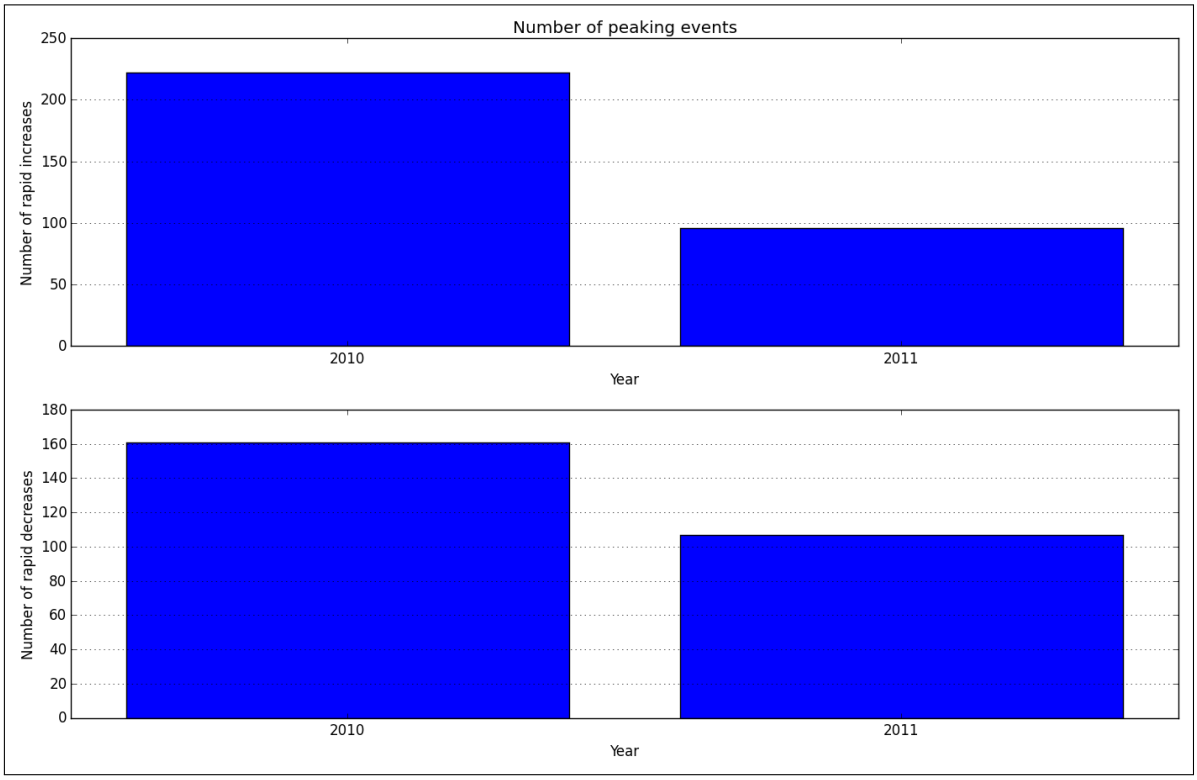

Figure A.10.47: Average annual number of increased/decreased peaks

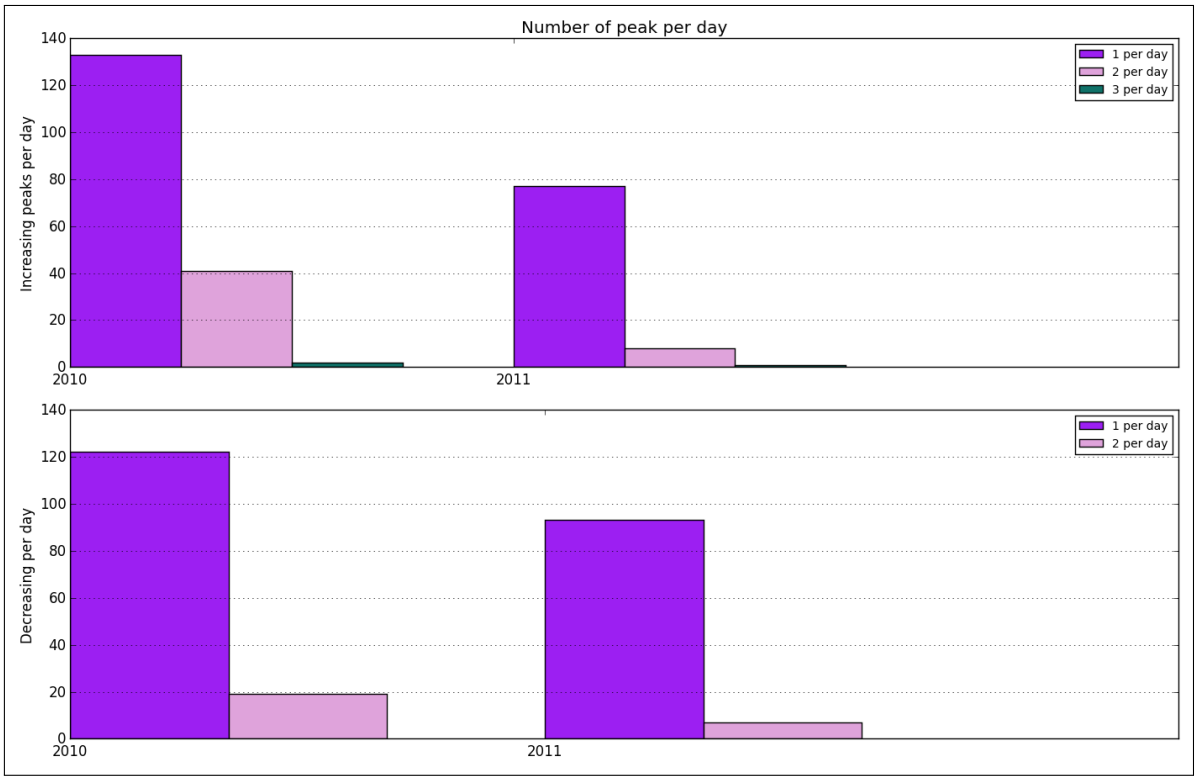

Figure A.10.48: Number of peaks per day

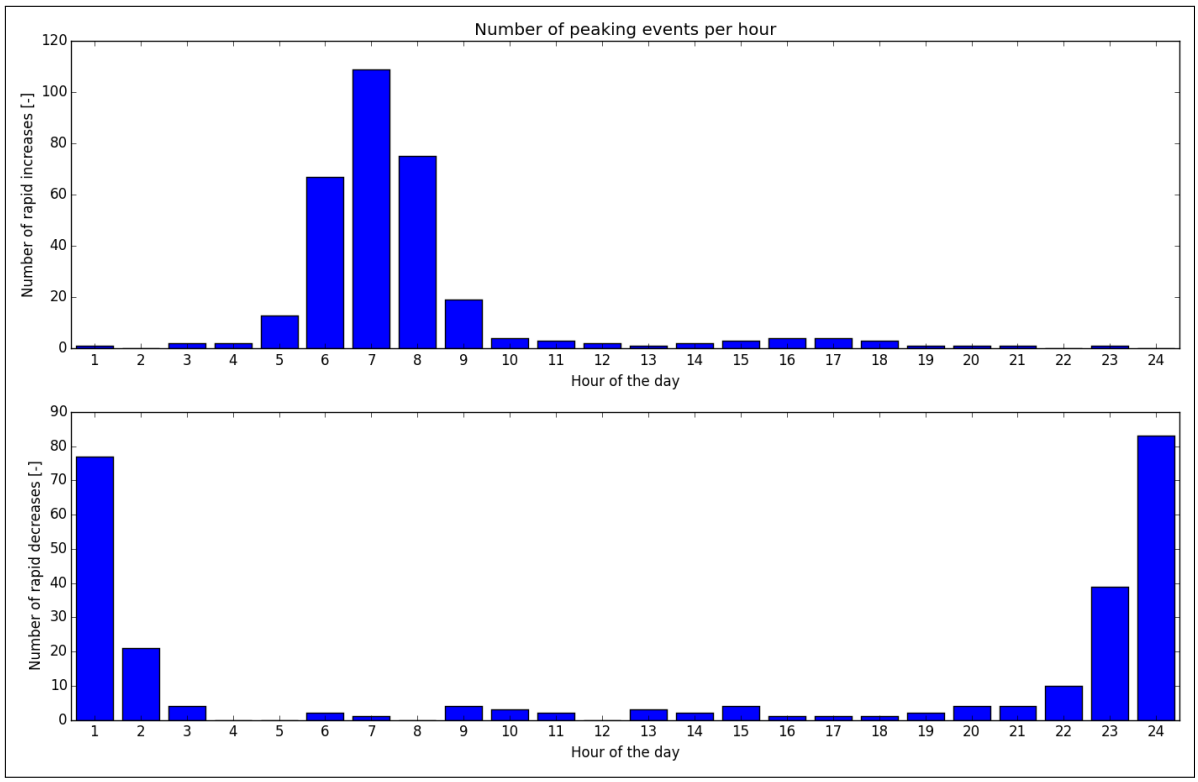

Figure A.10.49: Distribution of peaks throughout day

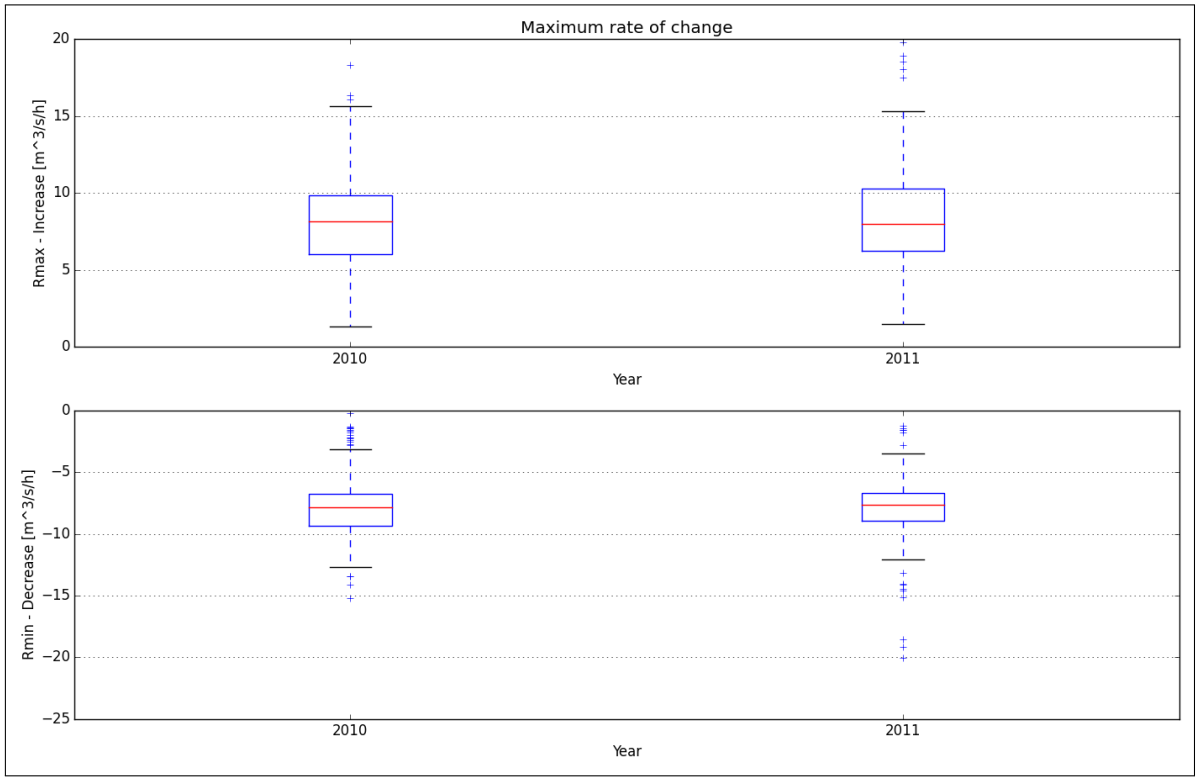

Figure A.10.50: Maximum rate of change

A.11. Storåni

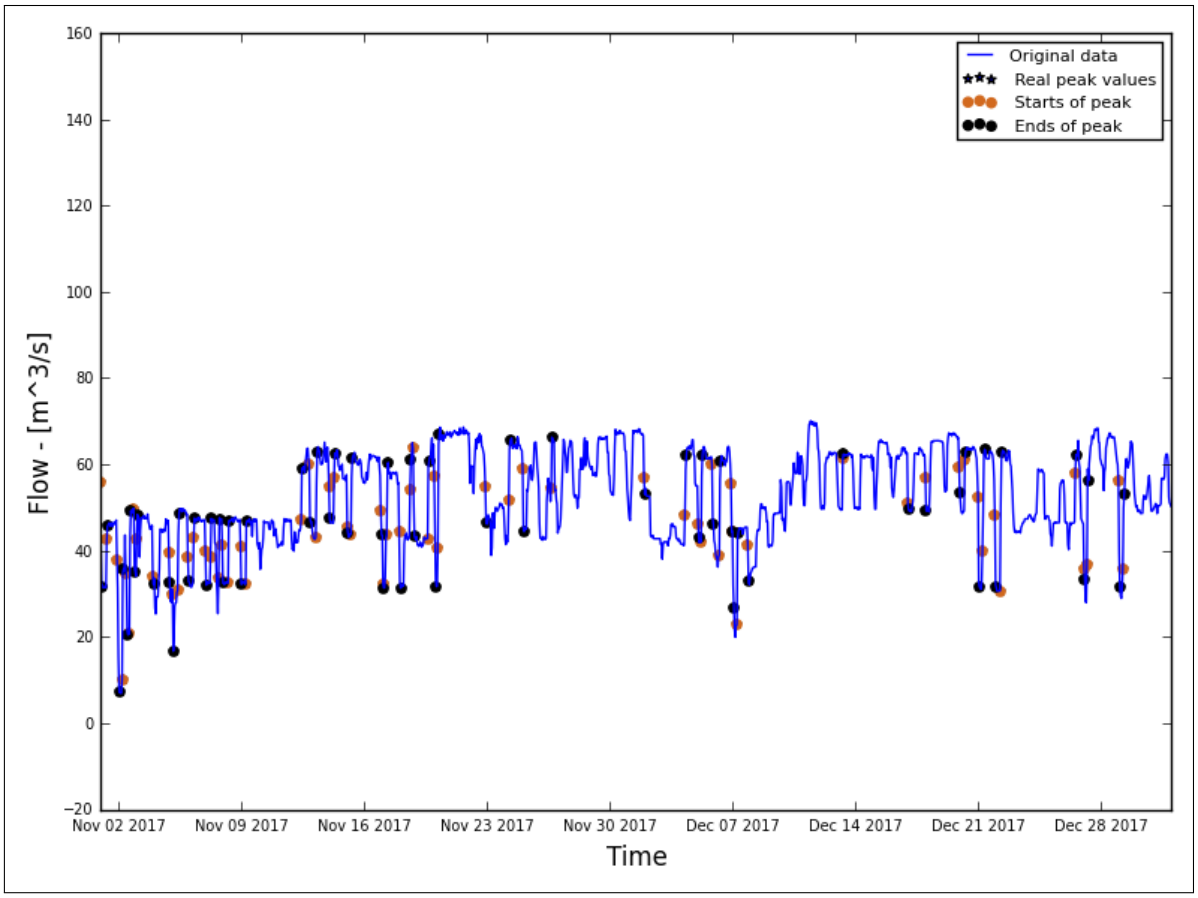

Figure A.11.51: Hydrograph of the last two months of the recorded data

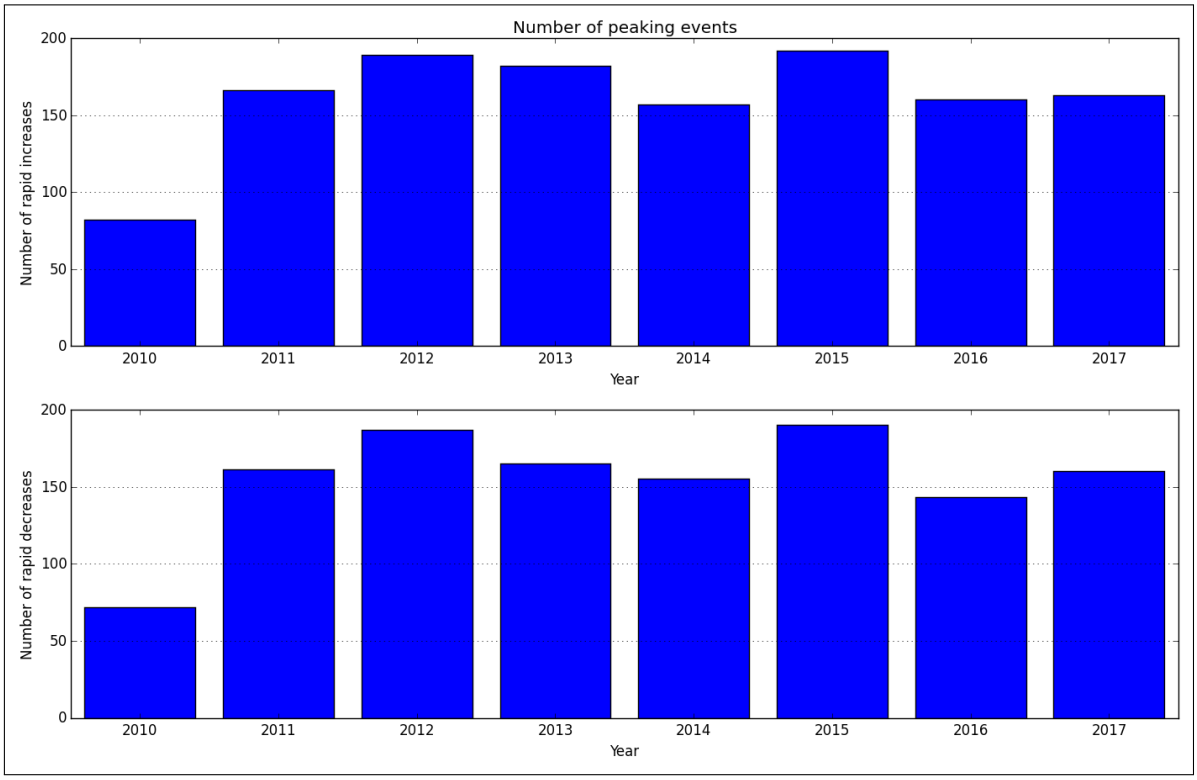

Figure A.11.52: Average annual number of increased/decreased peaks

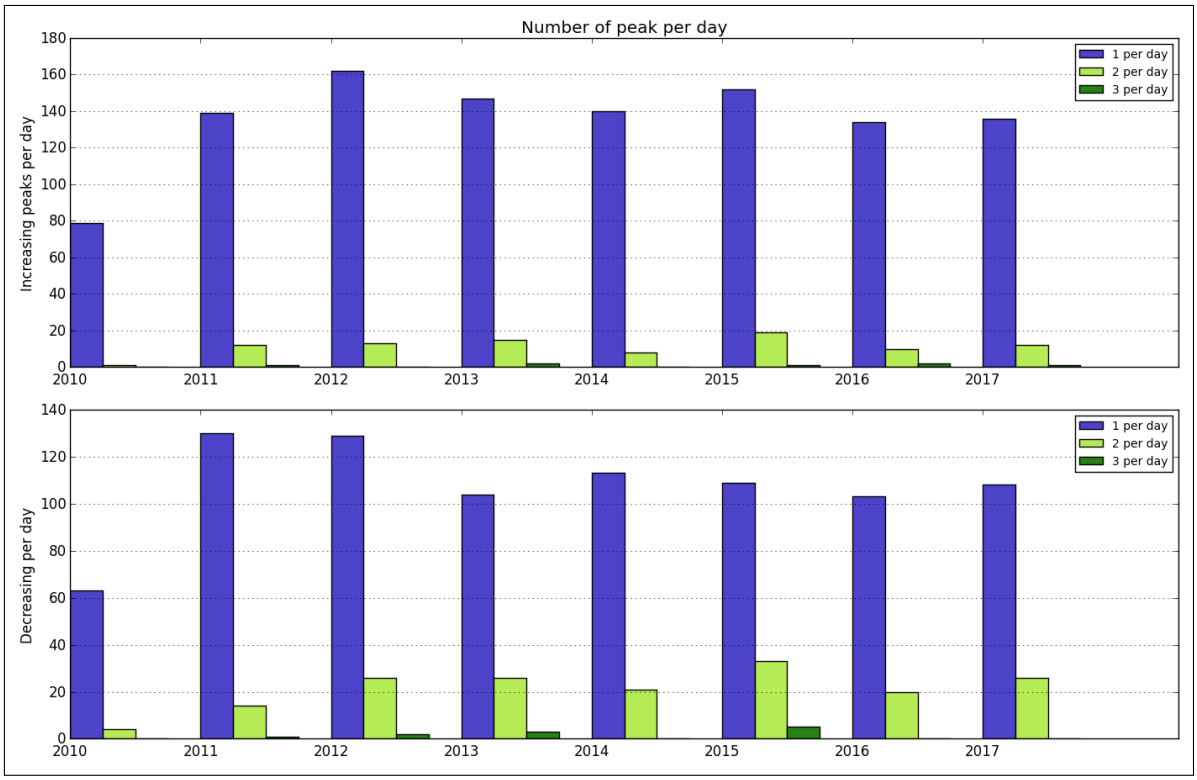

Figure A.11.53: Number of peaks per day

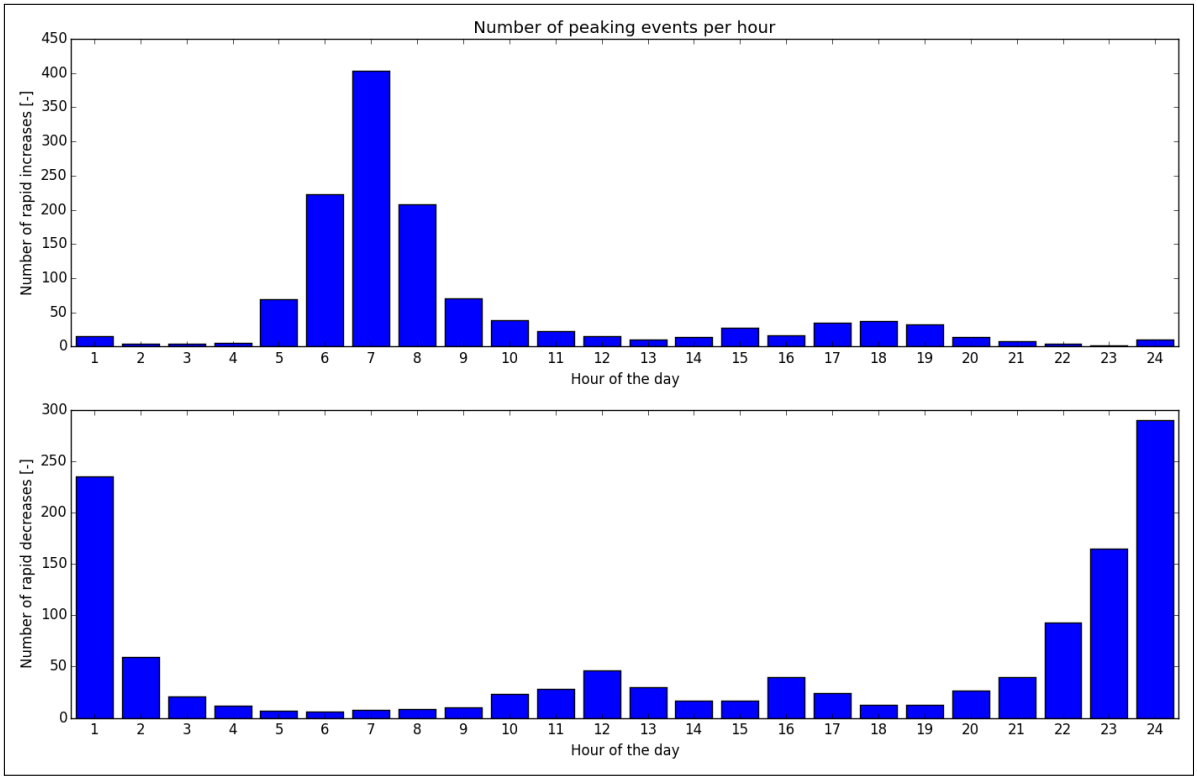

Figure A.11.54: Distribution of peaks throughout day

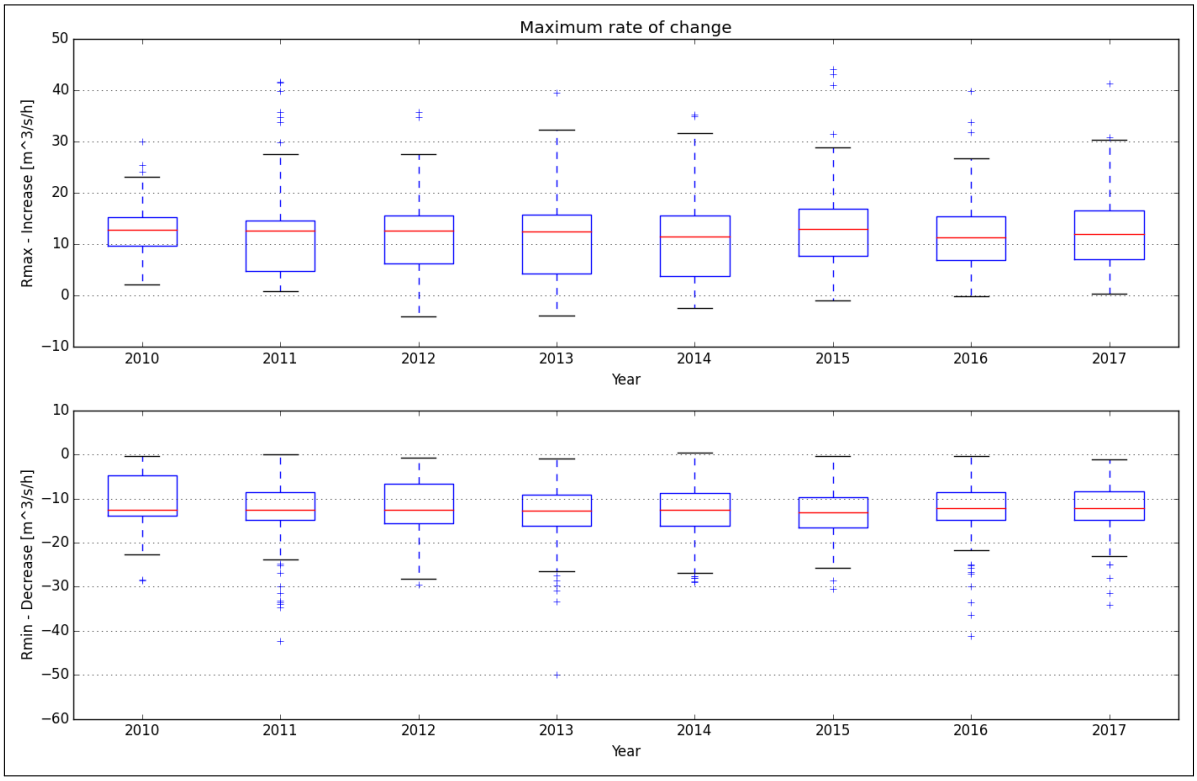

Figure A.11.55: Maximum rate of change

A.12. Laudal

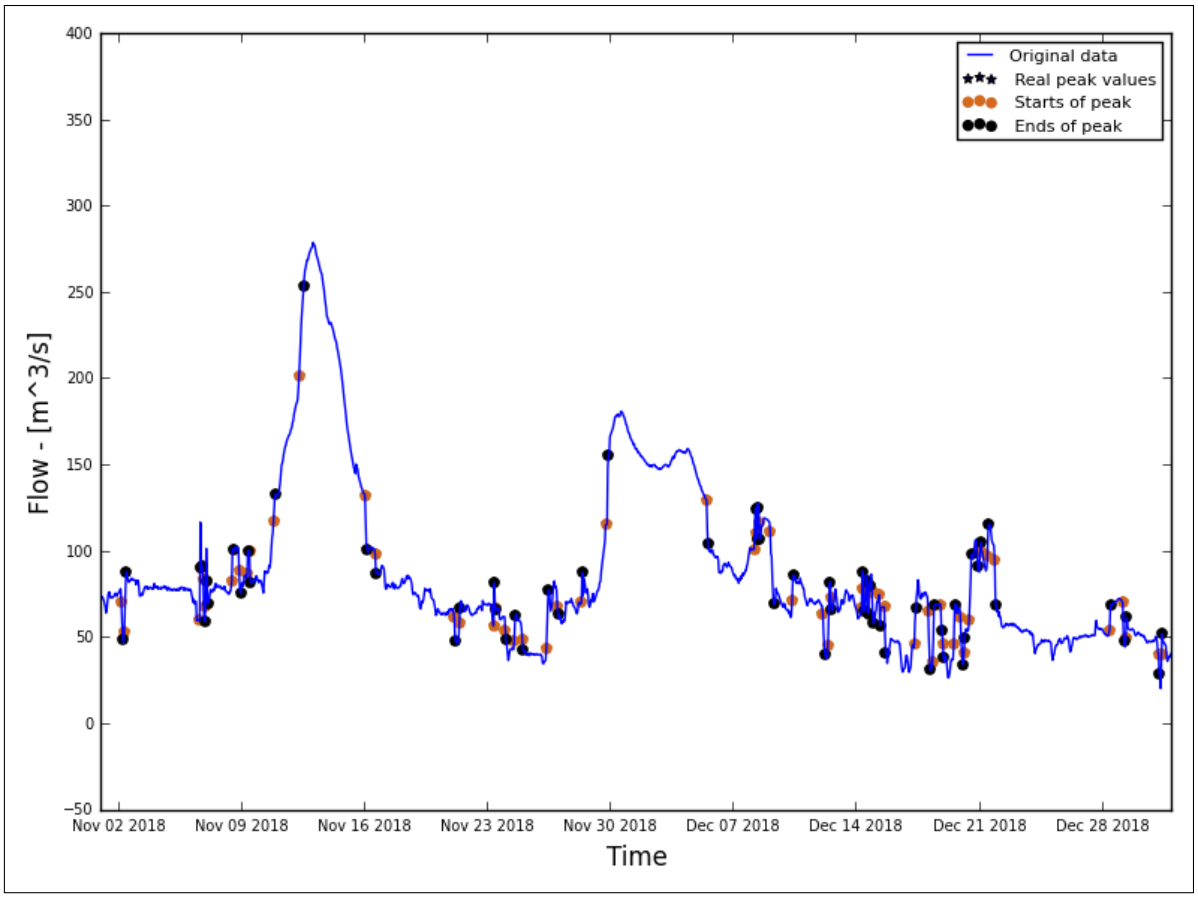

Figure A.12.56: Hydrograph of the last two months of the recorded data

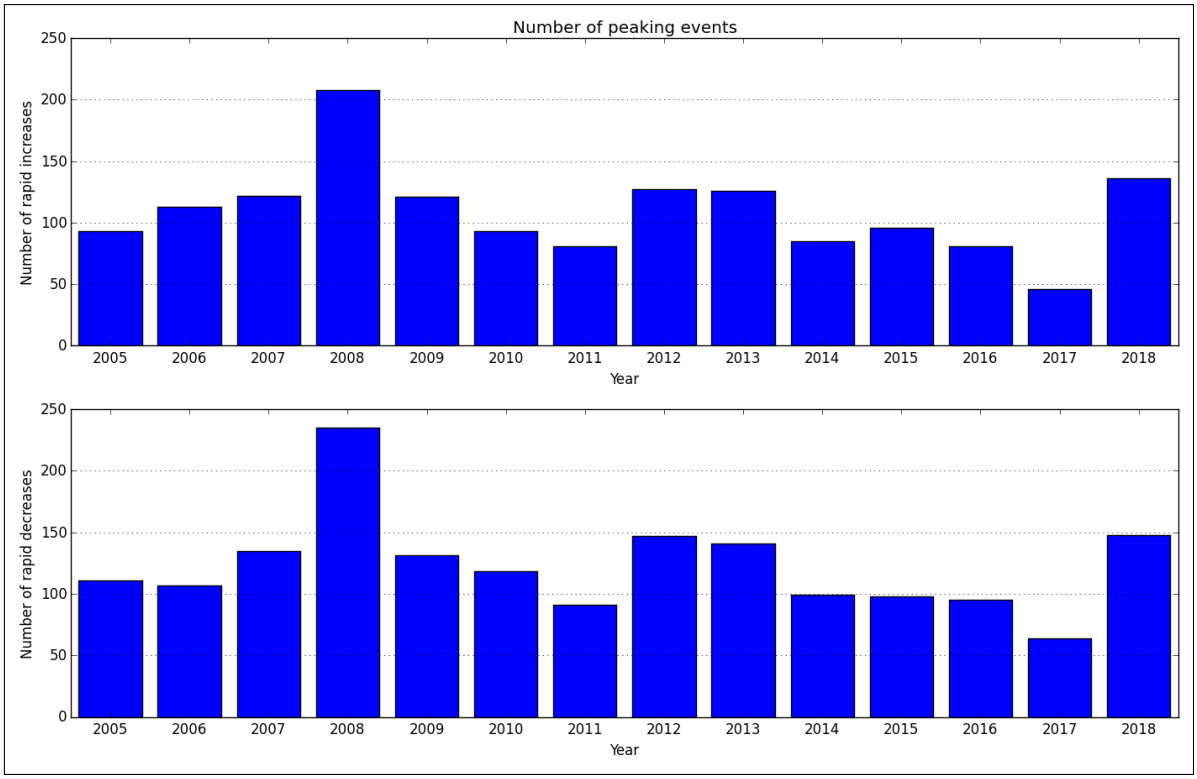

Figure A.12.57: Average annual number of increased/decreased peaks

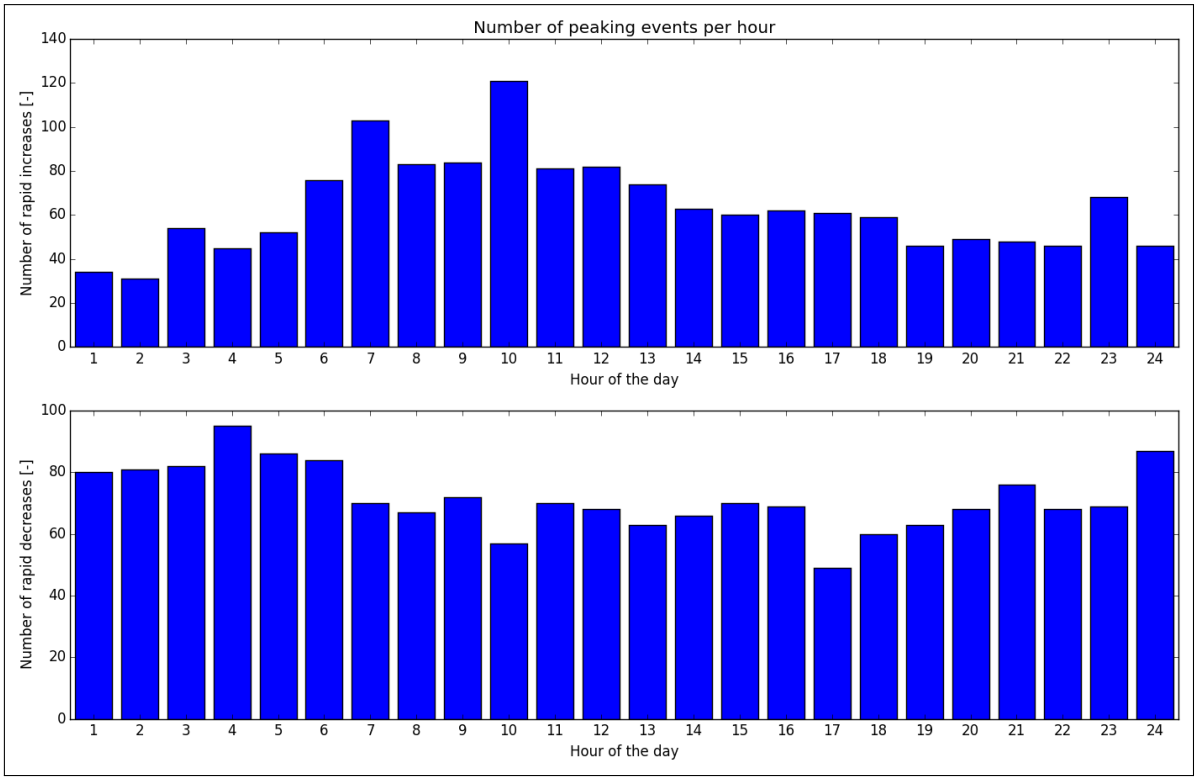

Figure A.12.58: Number of peaks per day

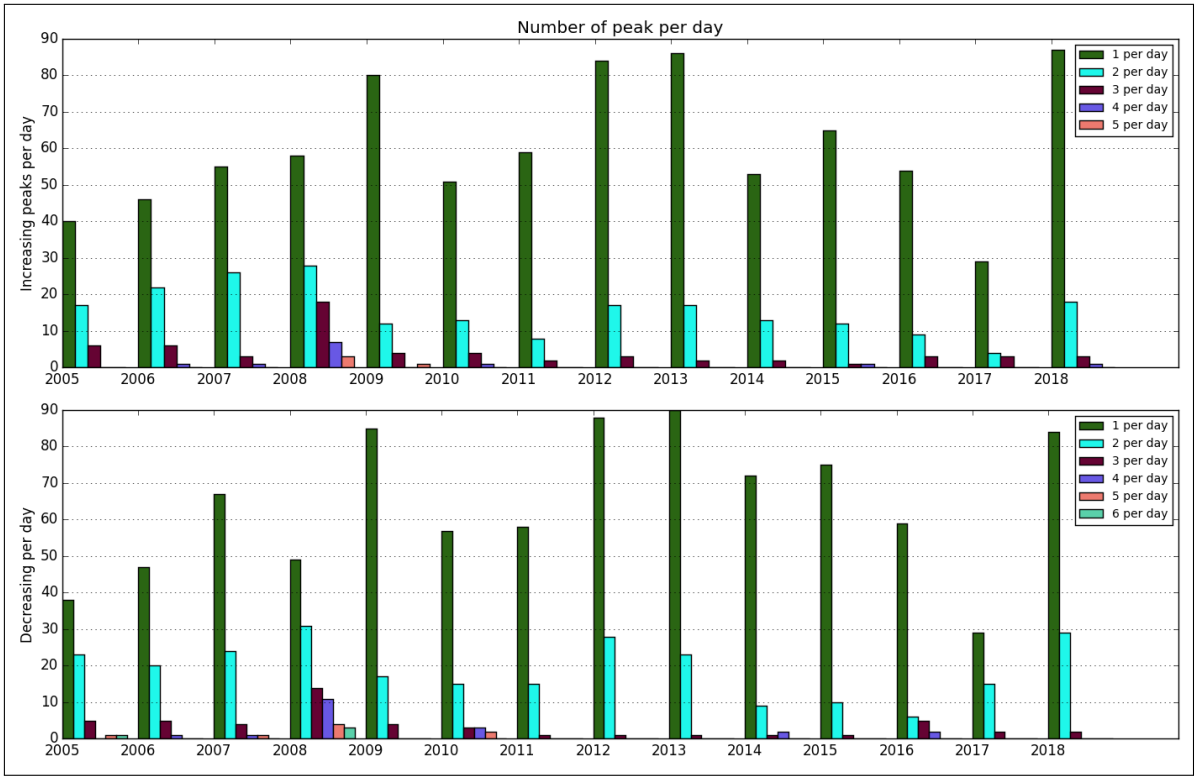

Figure A.12.59: Distribution of peaks throughout day

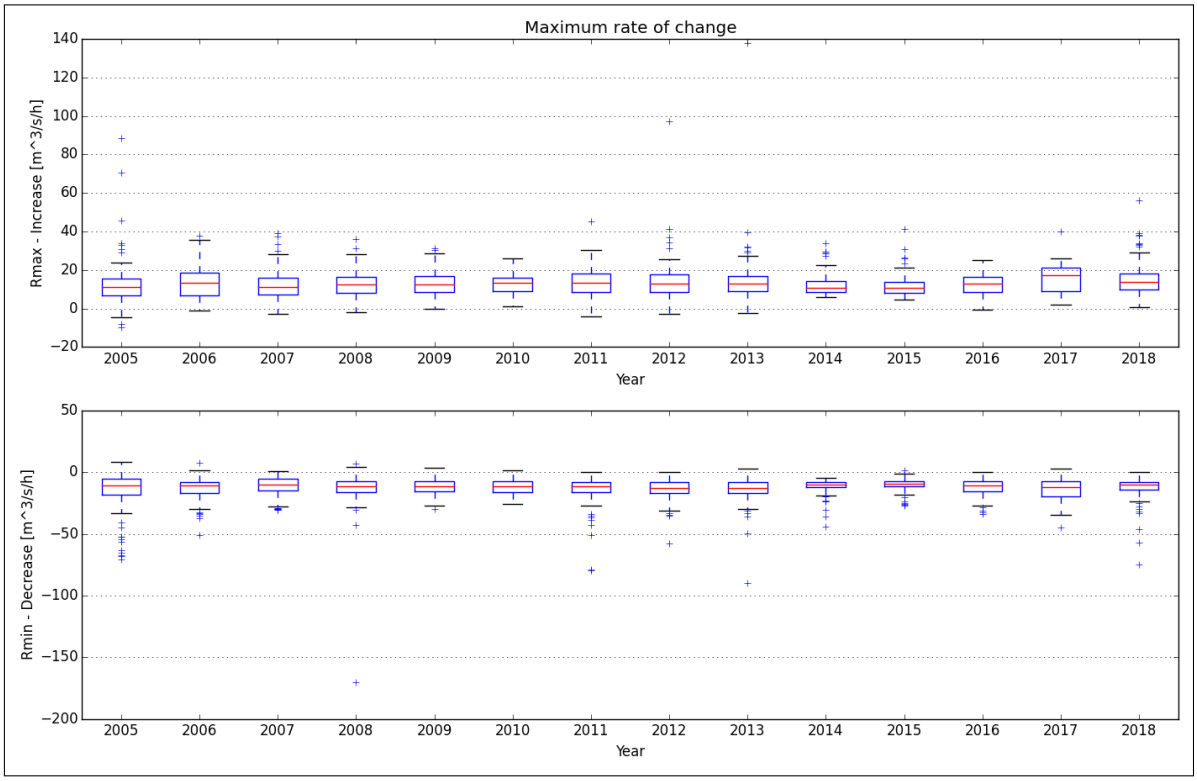

Figure A.12.60: Maximum rate of change

A.13. Solhom

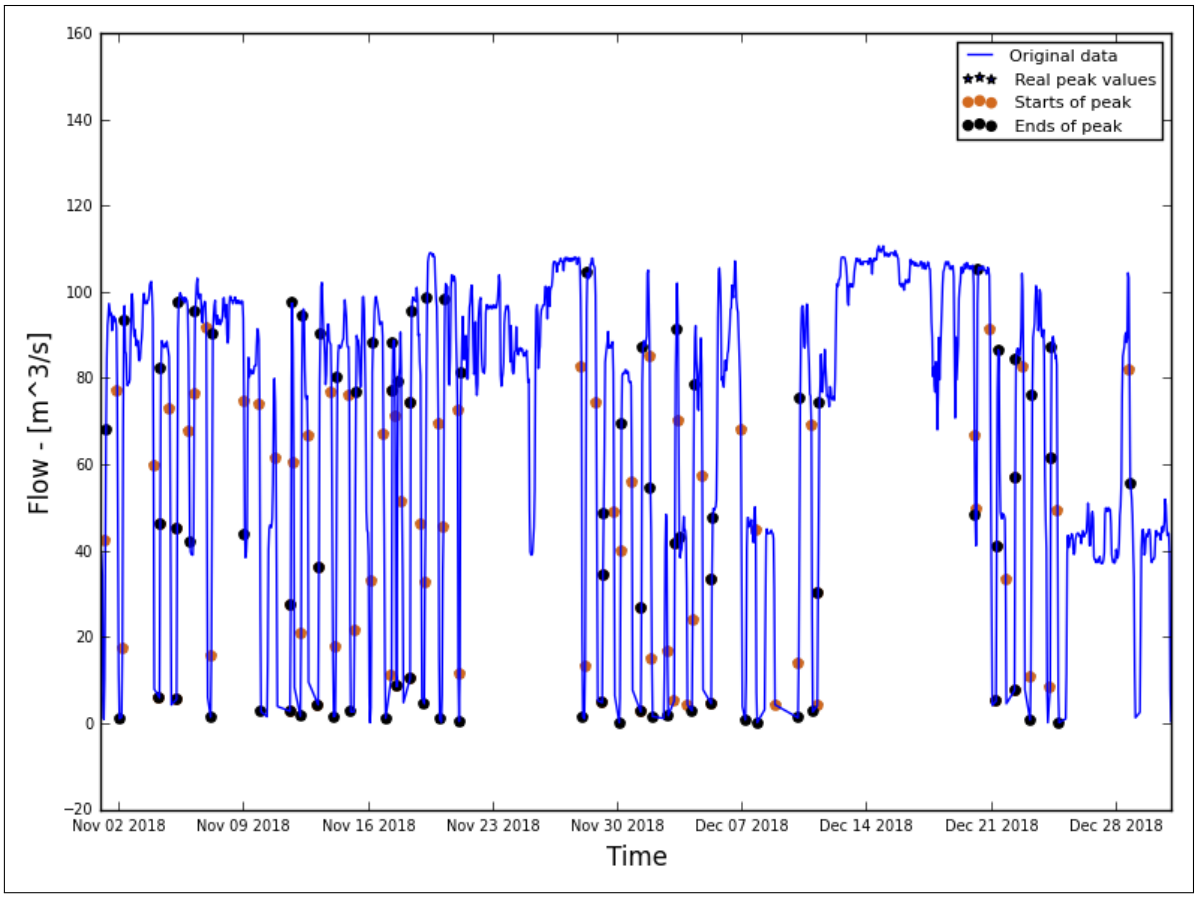

Figure A.13.61: Hydrograph of the last two months of the recorded data

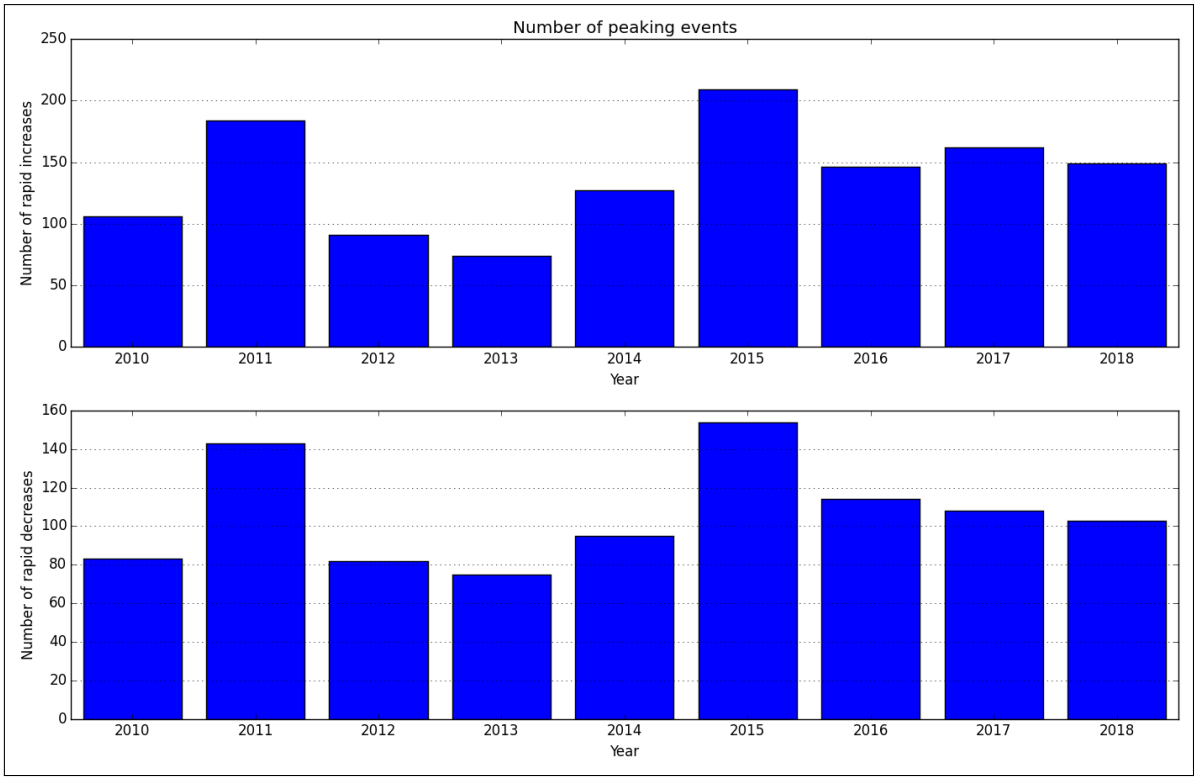

Figure A.13.62: Average annual number of increased/decreased peaks

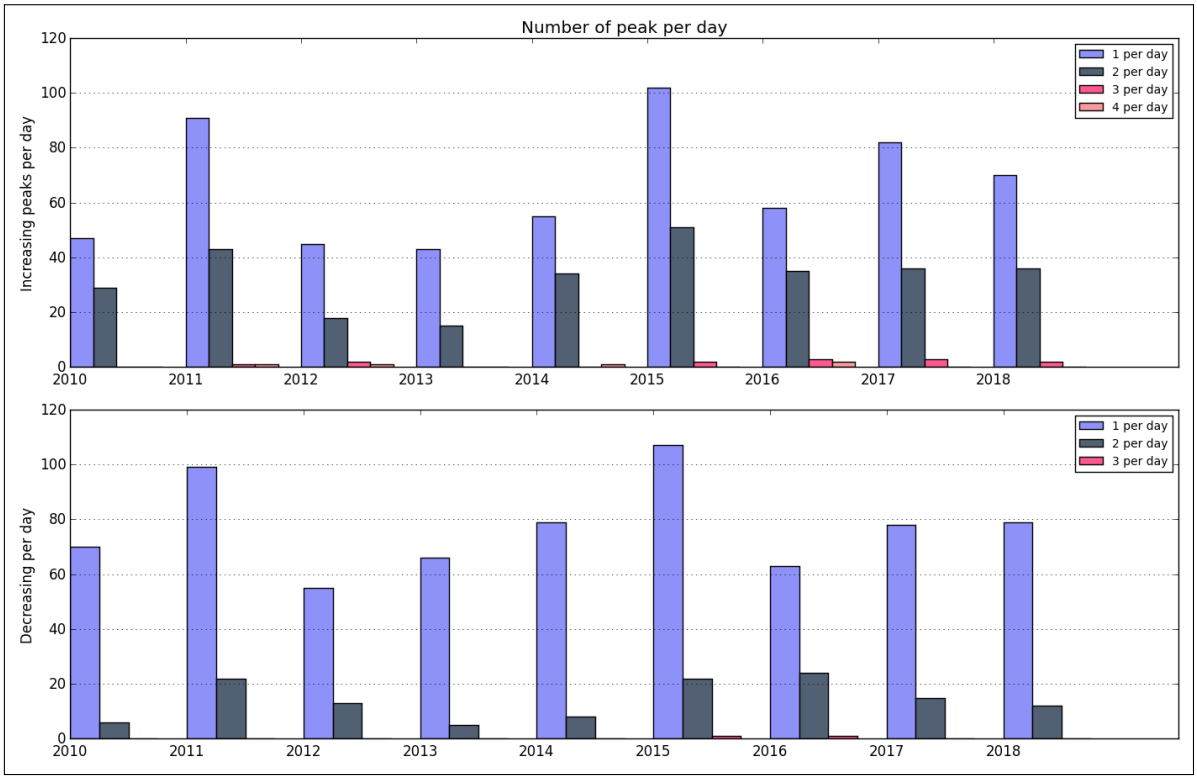

Figure A.13.63: Number of peaks per day

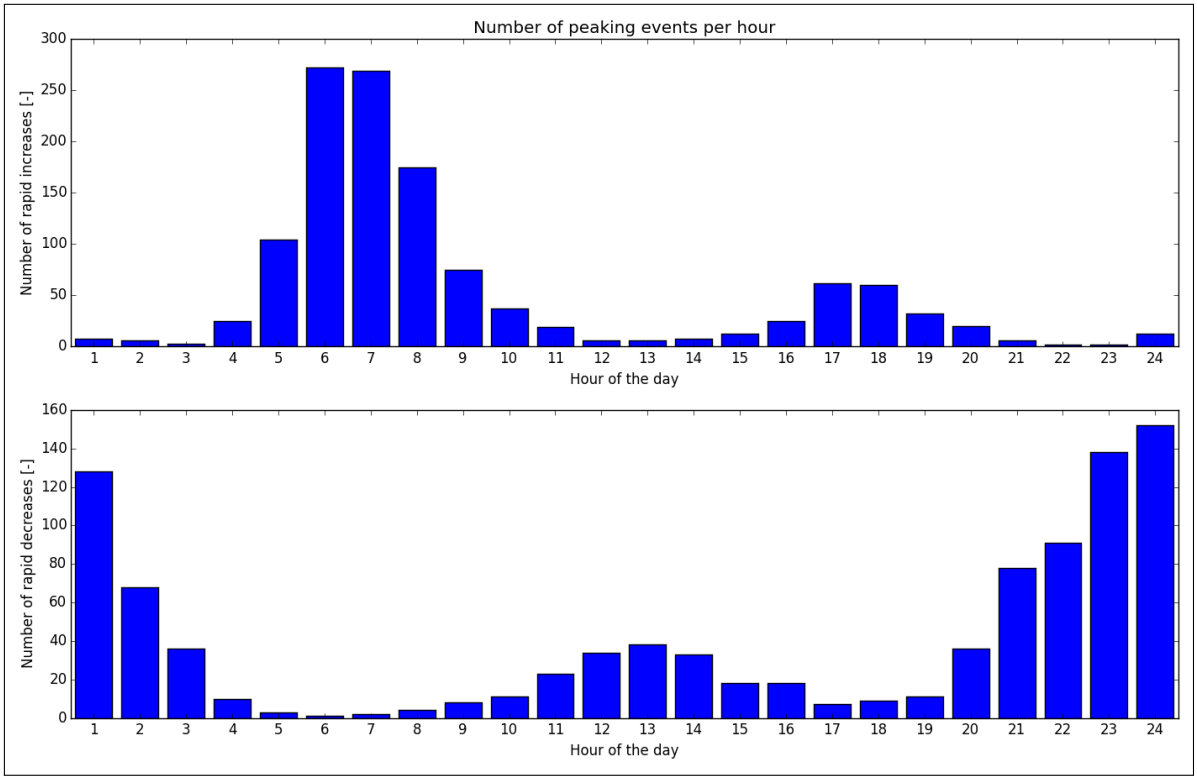

Figure A.13.64: Distribution of peaks throughout day

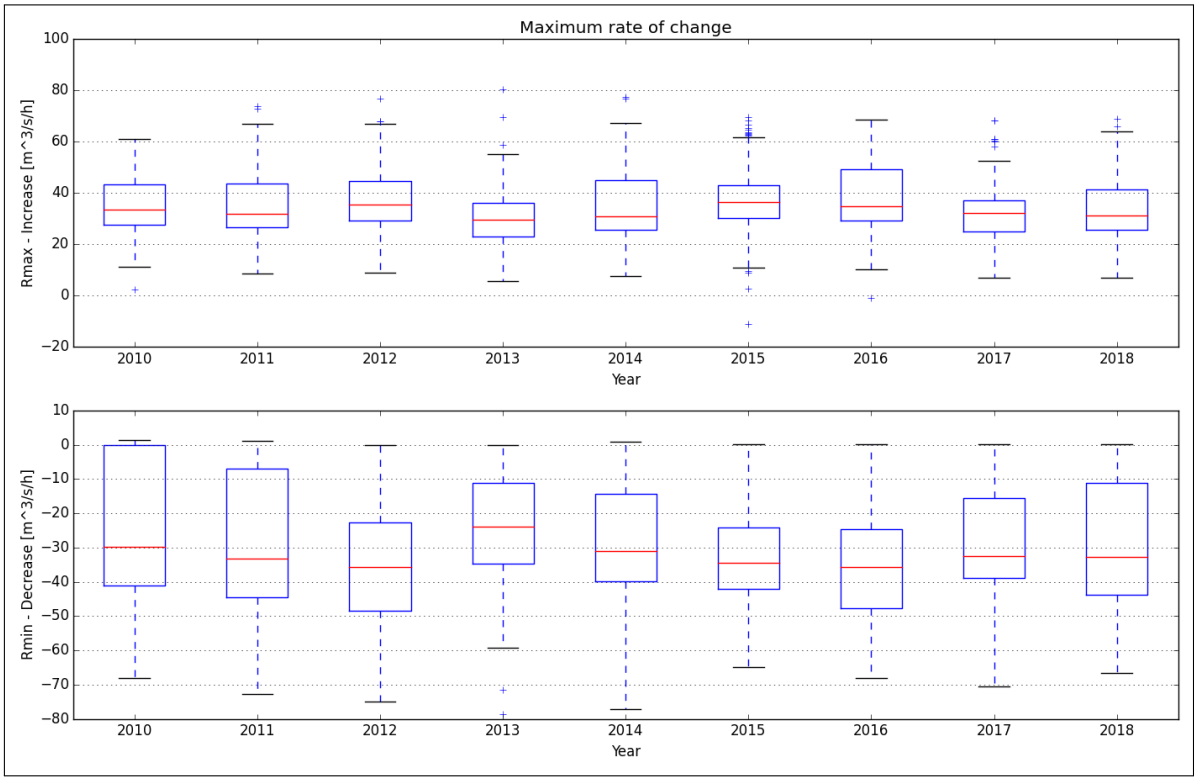

Figure A.13.65: Maximum rate of change

A.14. Åna-Sira

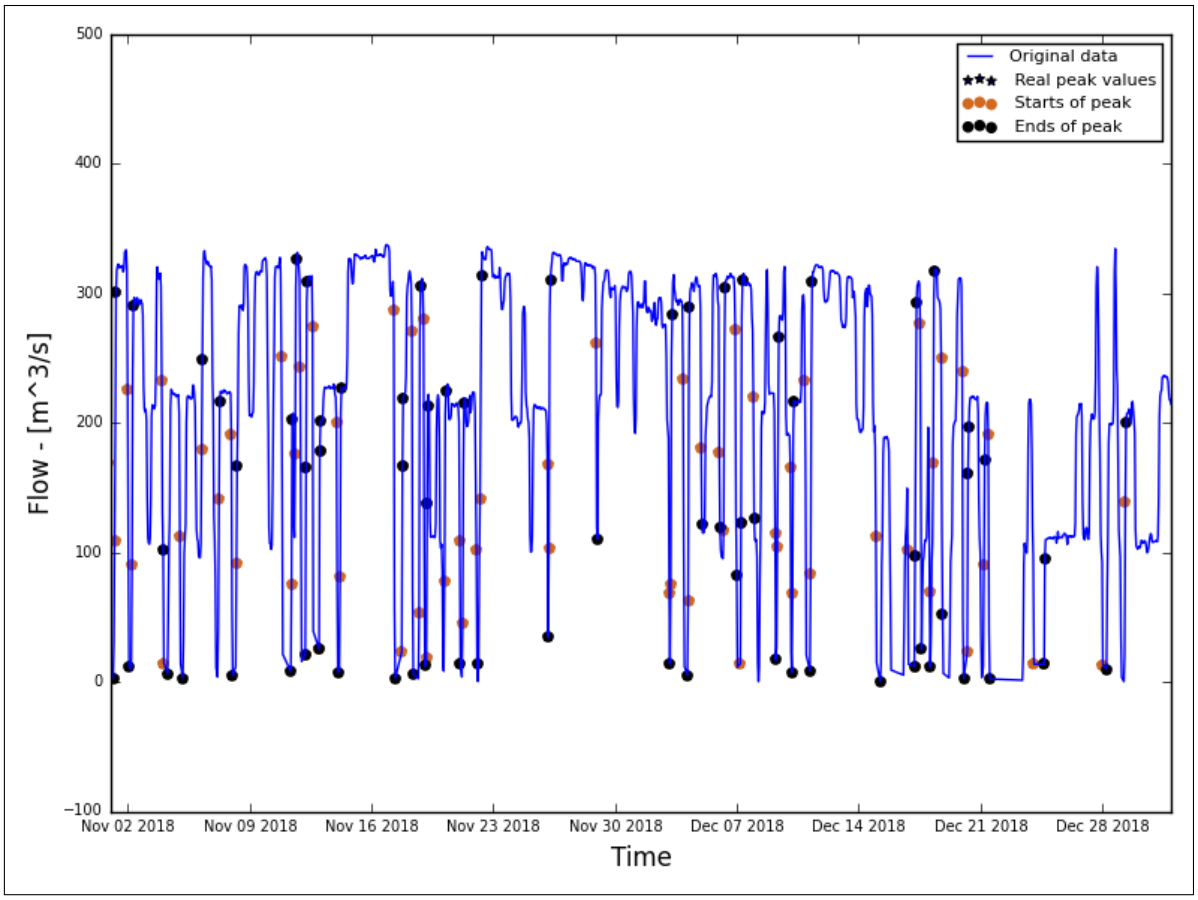

Figure A.14.66: Hydrograph of the last two months of the recorded data

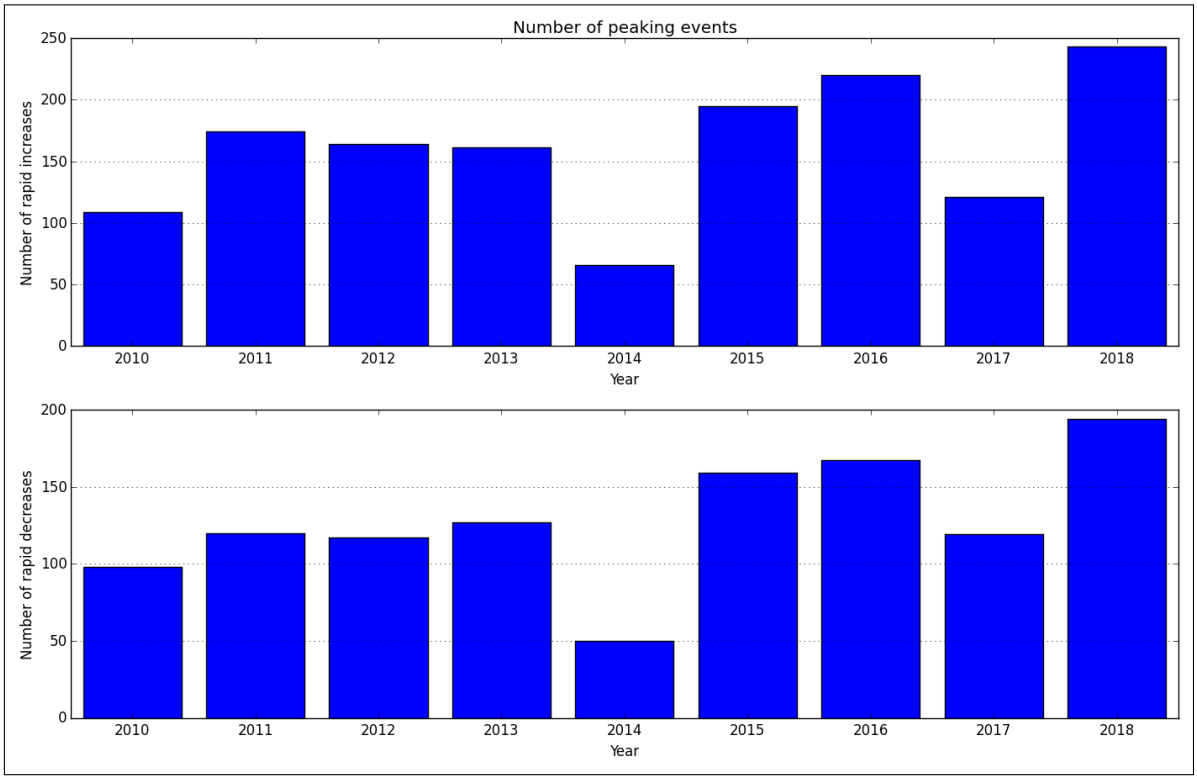

Figure A.14.67: Average annual number of increased/decreased peaks

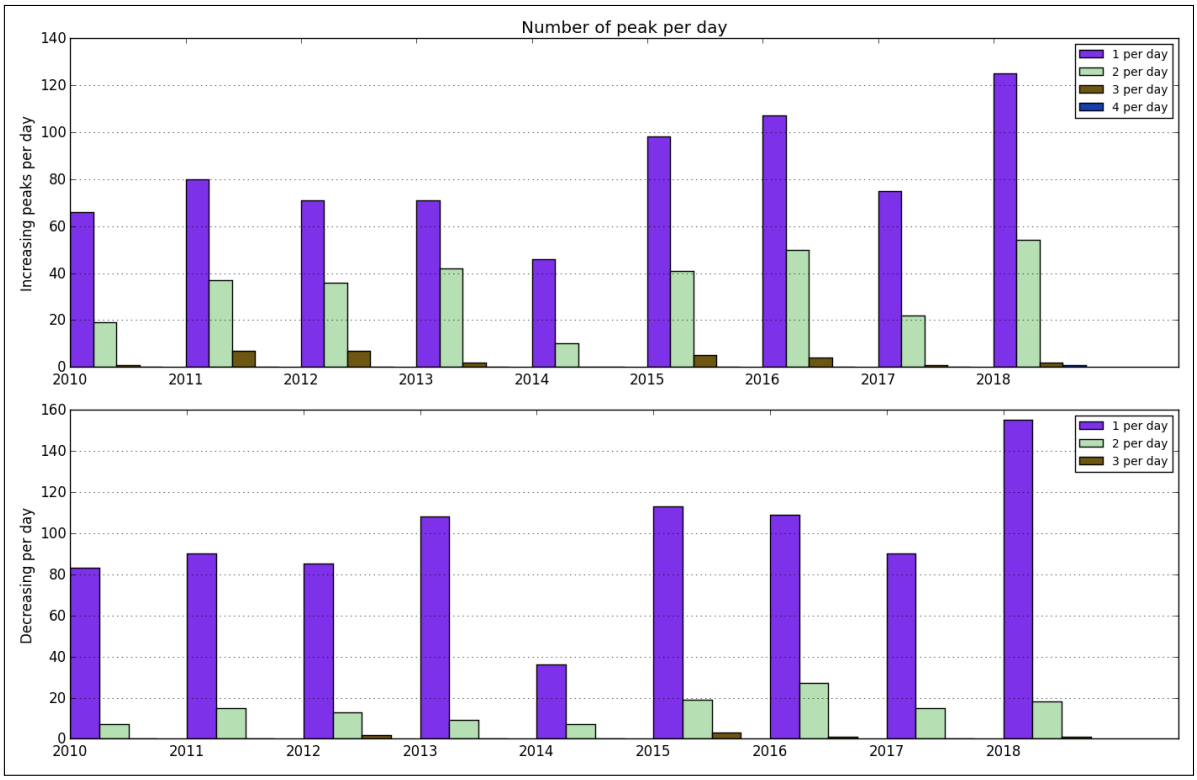

Figure A.14.68: Number of peaks per day

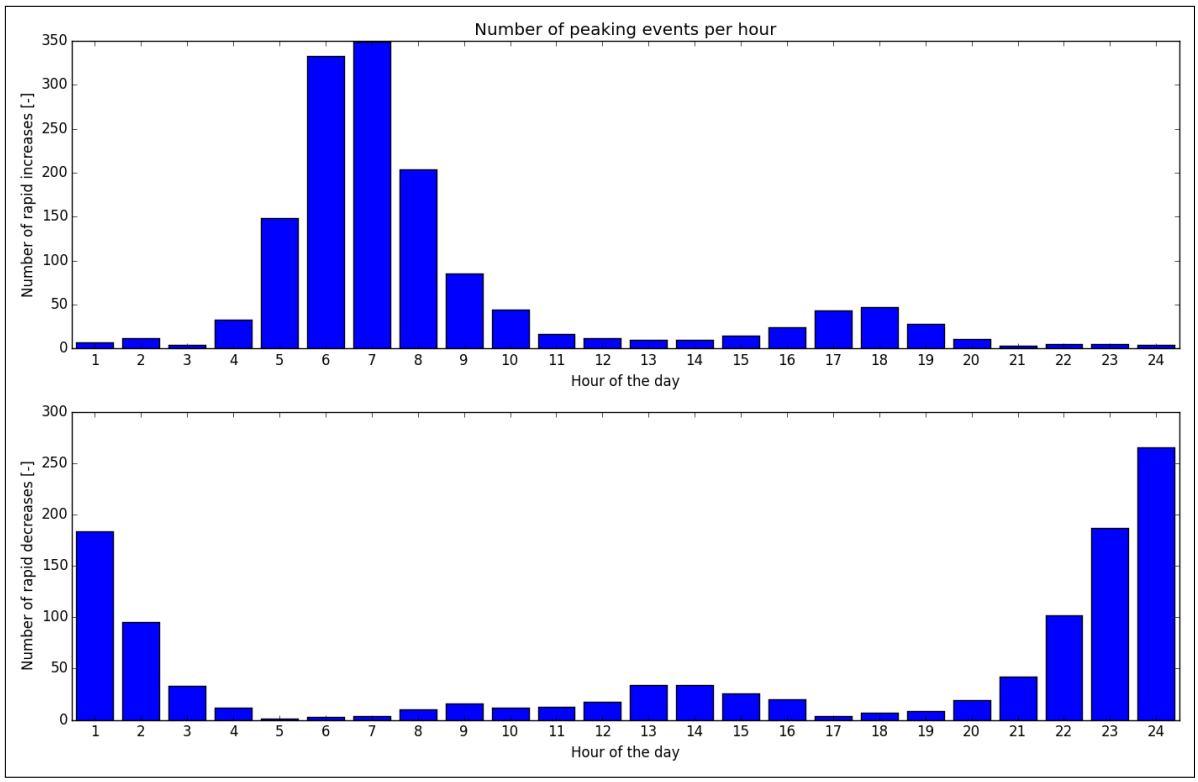

Figure A.14.69: Distribution of peaks throughout day

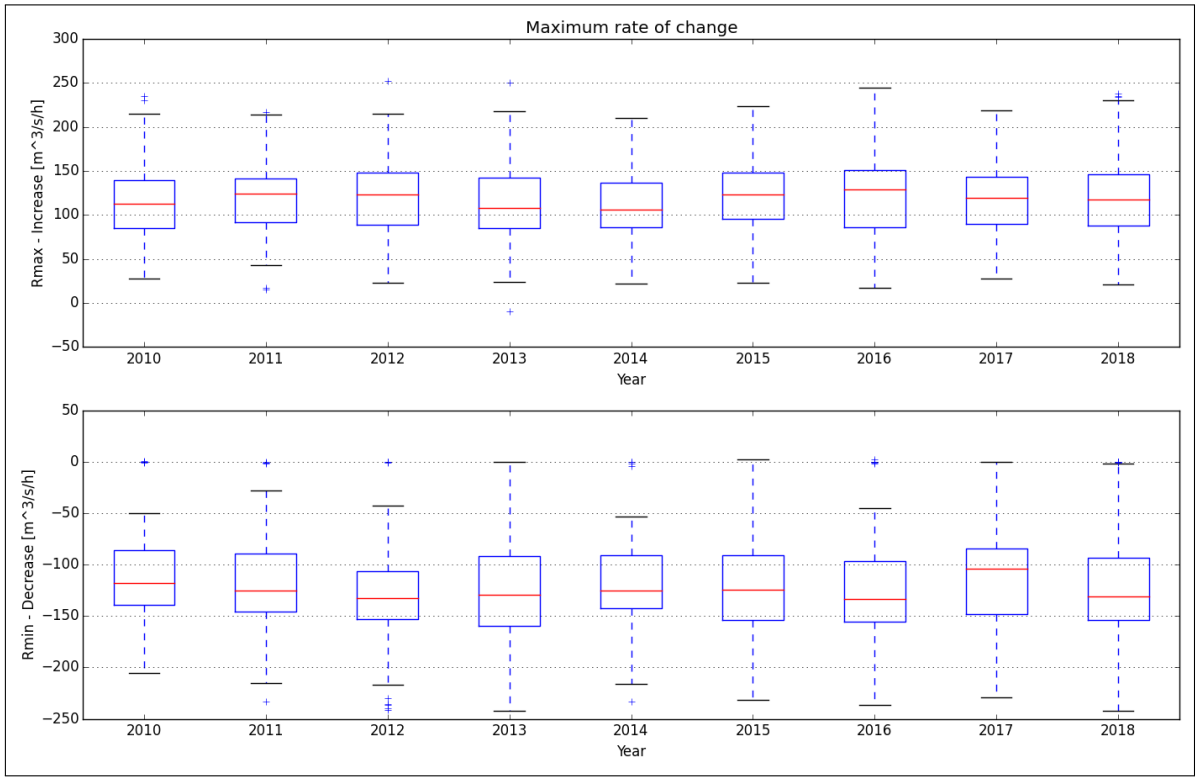

Figure A.14.70: Maximum rate of change

A.15. Tonstad

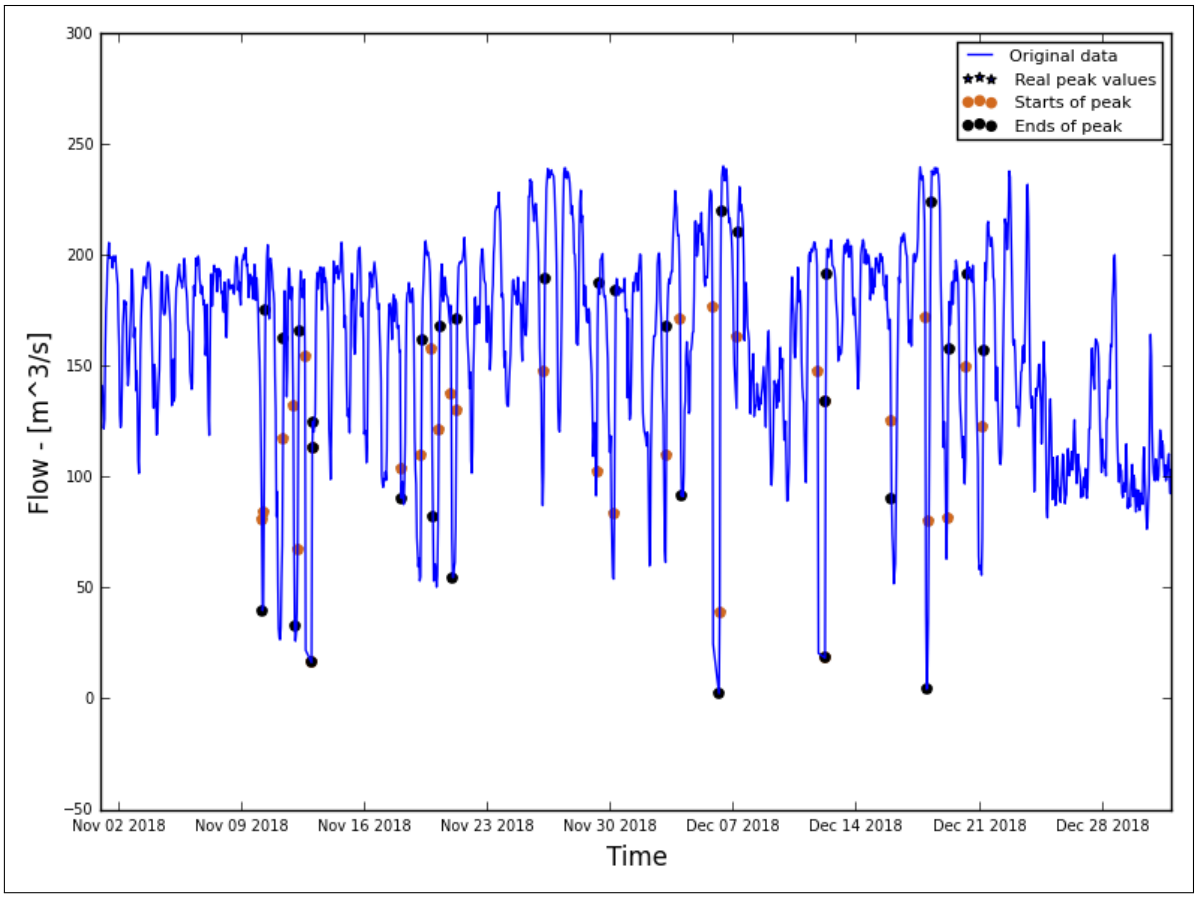

Figure A.15.71: Hydrograph of the last two months of the recorded data

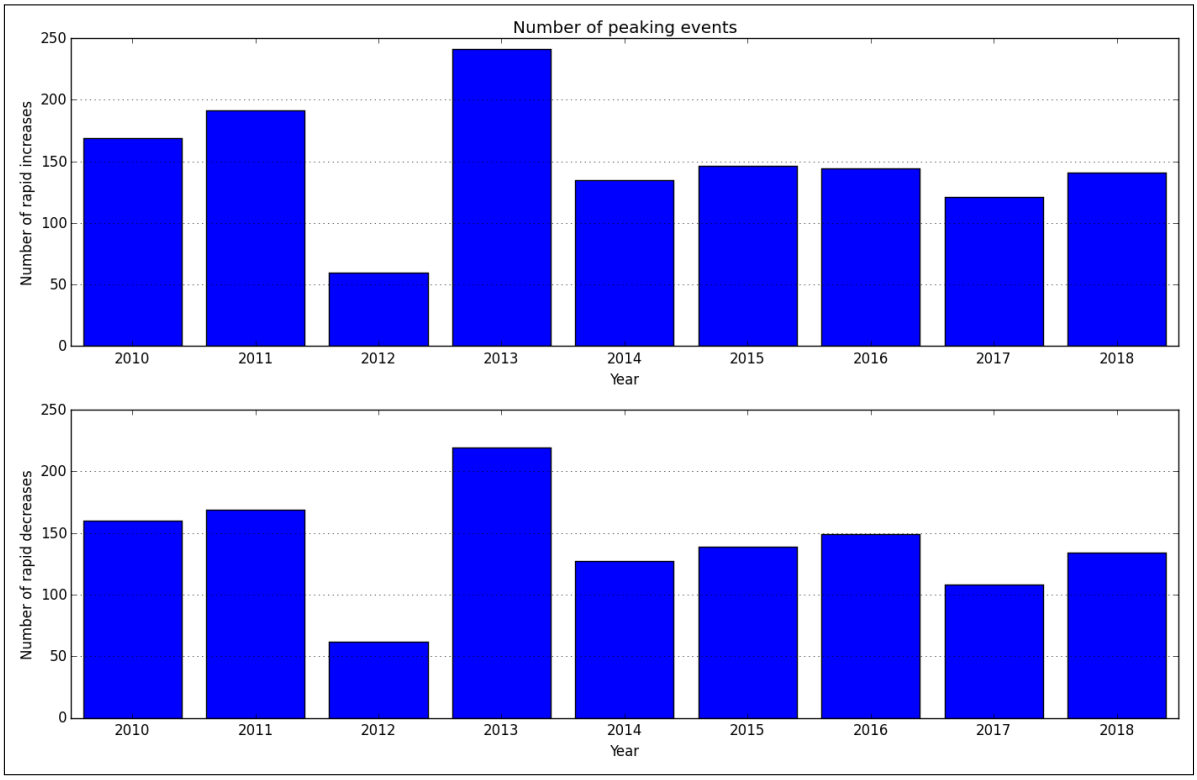

Figure A.15.72: Average annual number of increased/decreased peaks

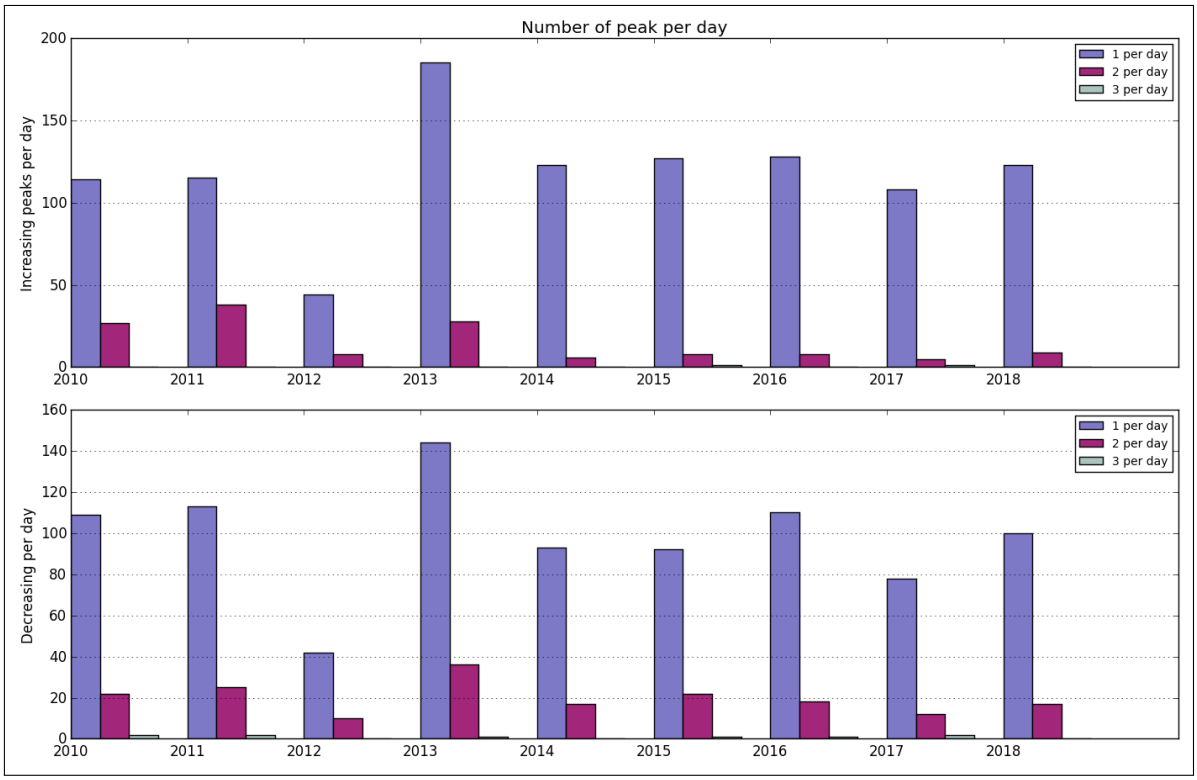

Figure A.15.73: Number of peaks per day

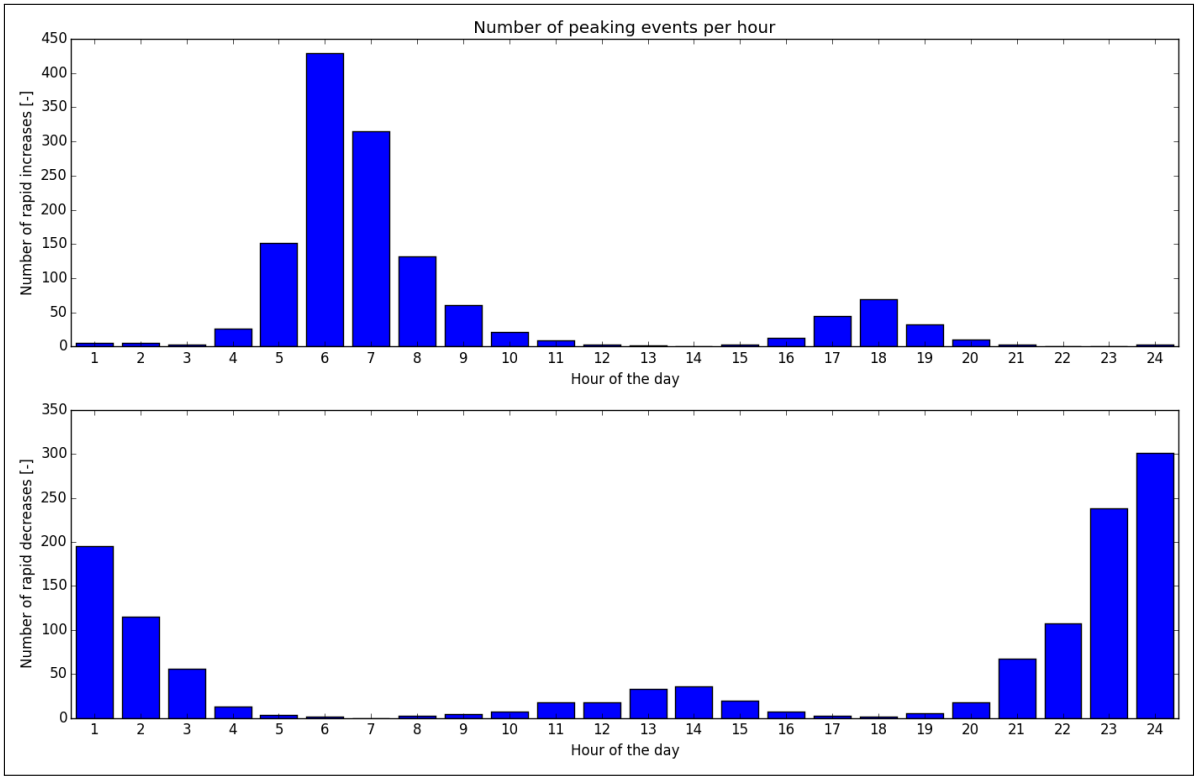

Figure A.15.74: Distribution of peaks throughout day

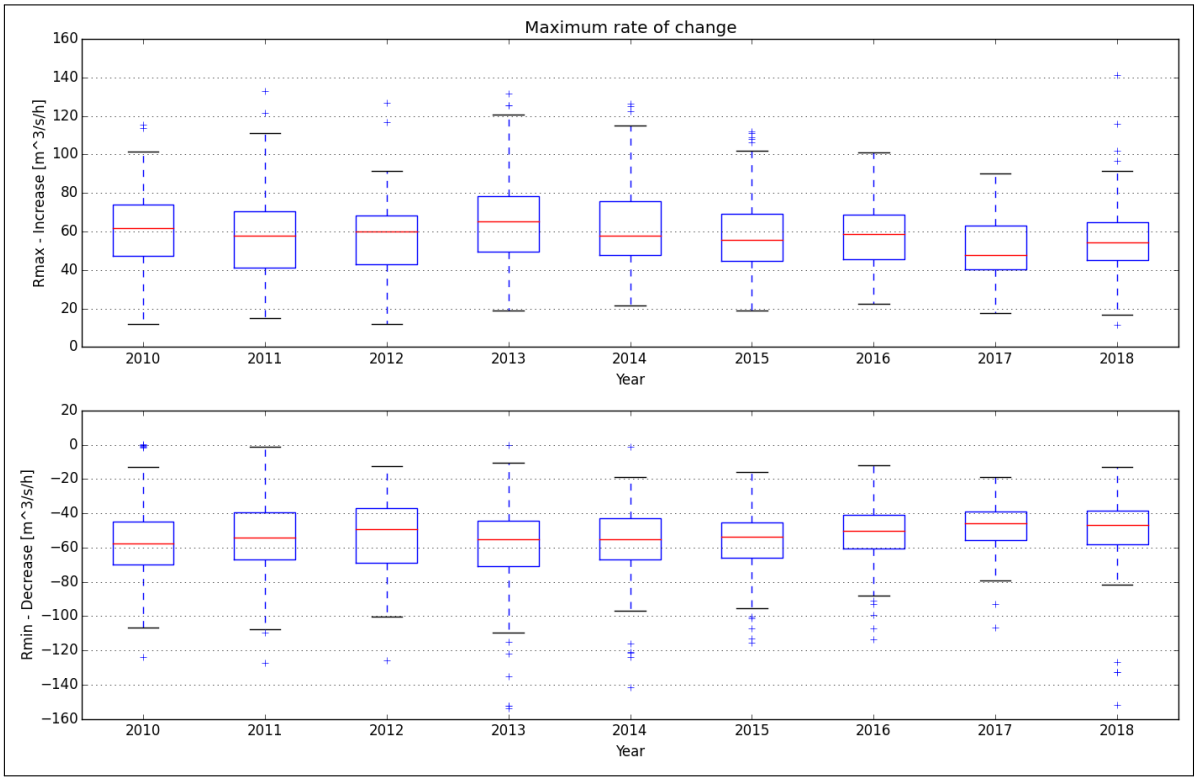

Figure A.15.75: Maximum rate of change

A.16. Borgund

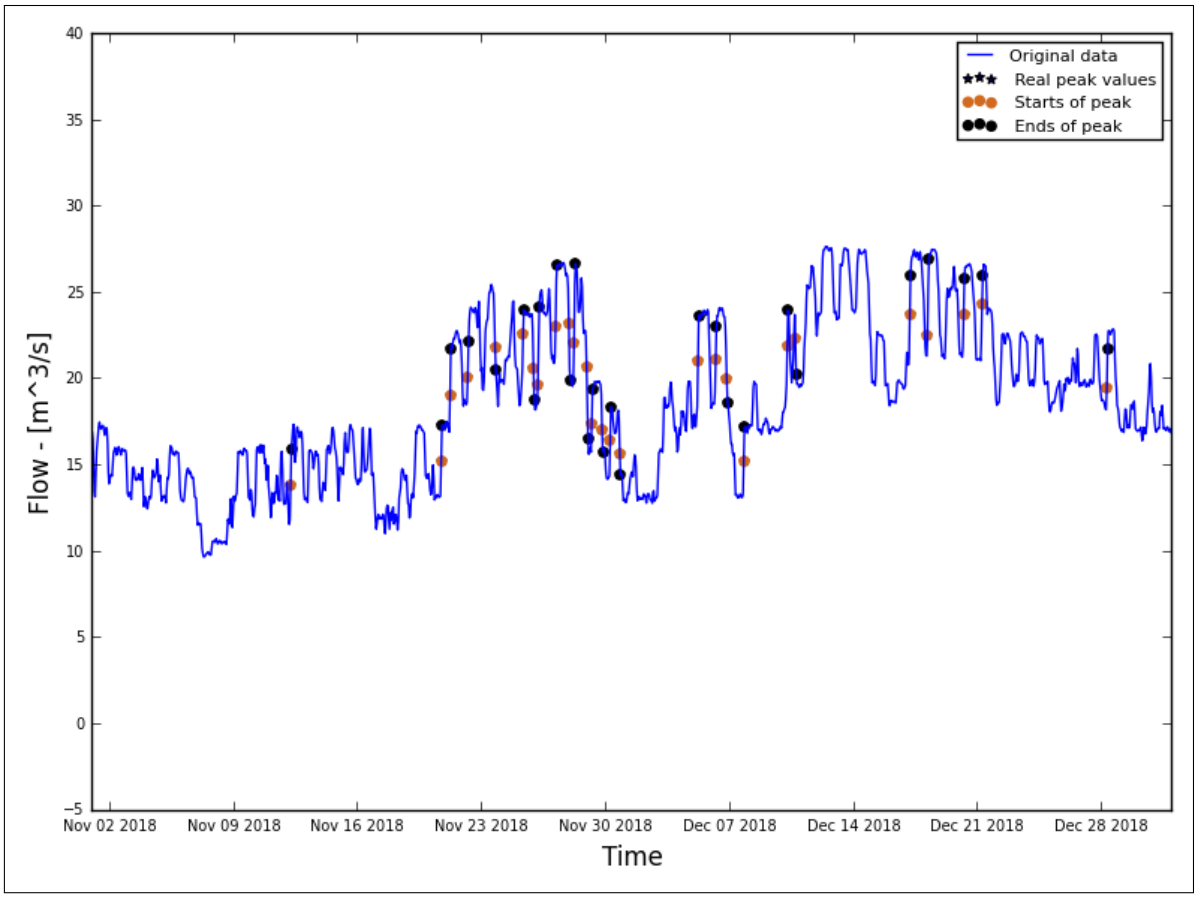

Figure A.16.76: Hydrograph of the last two months of the recorded data

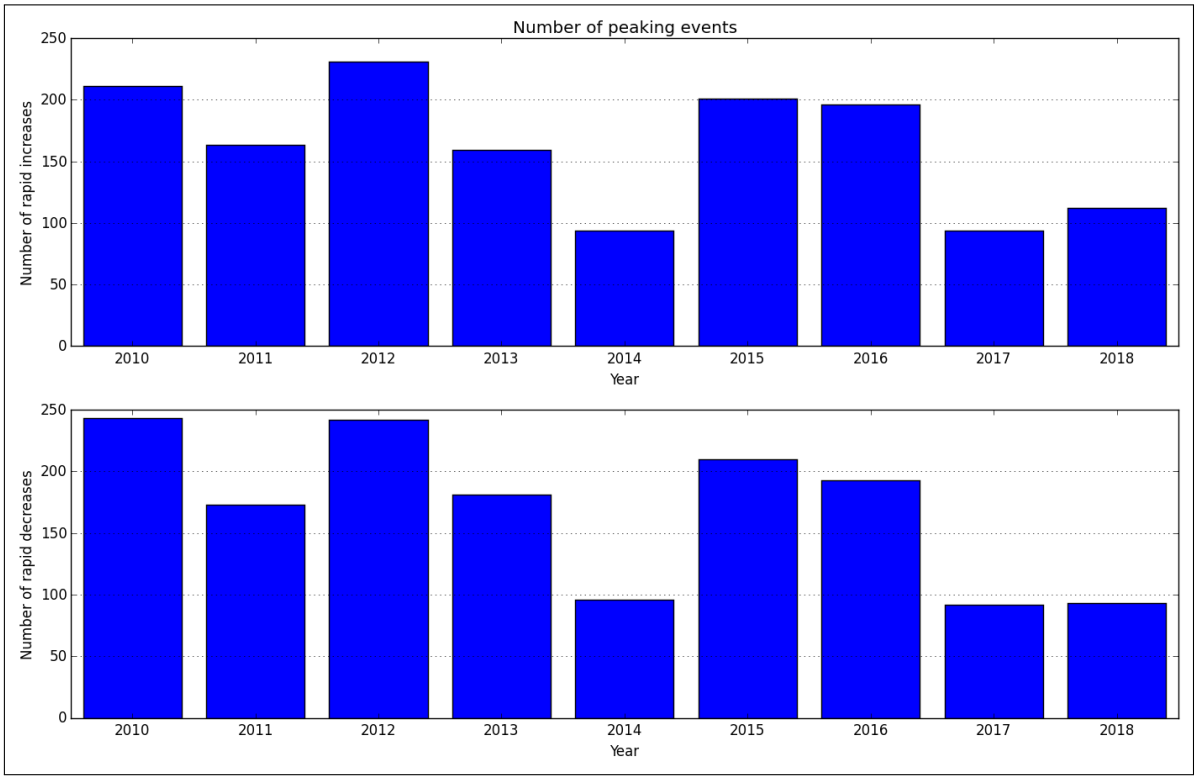

Figure A.16.77: Average annual number of increased/decreased peaks

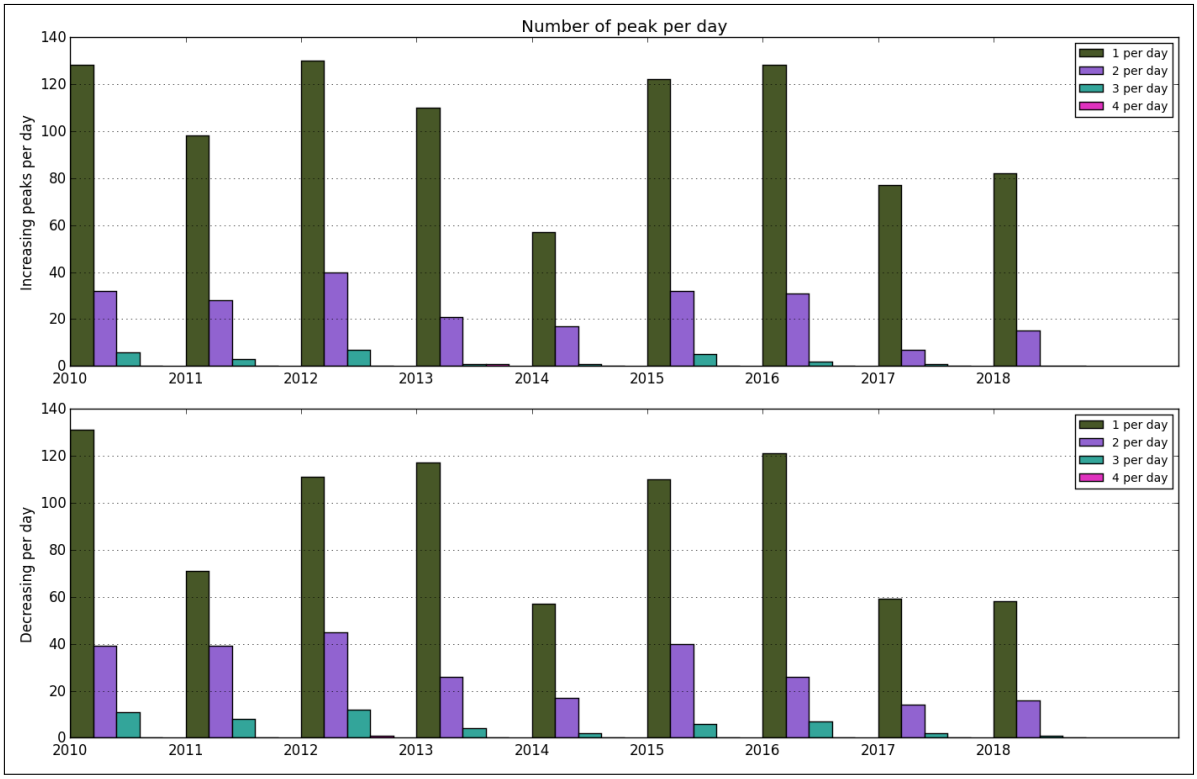

Figure A.16.78: Number of peaks per day

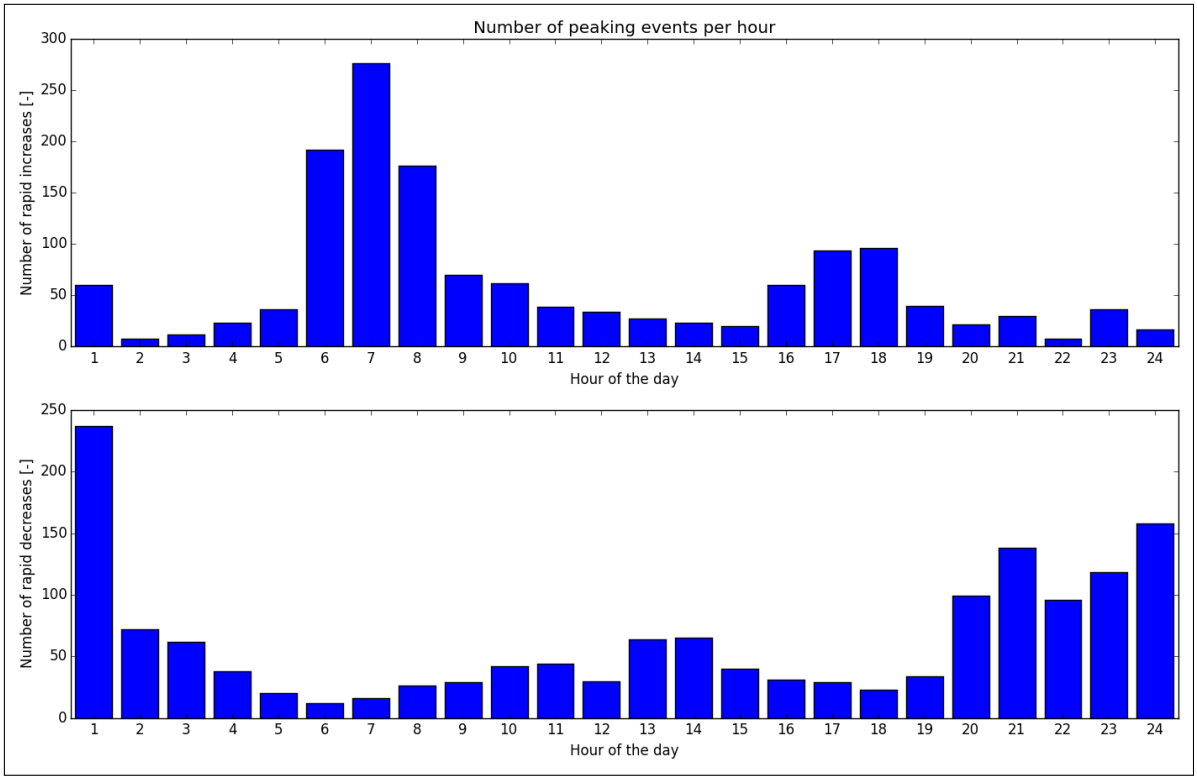

Figure A.16.79: Distribution of peaks throughout day

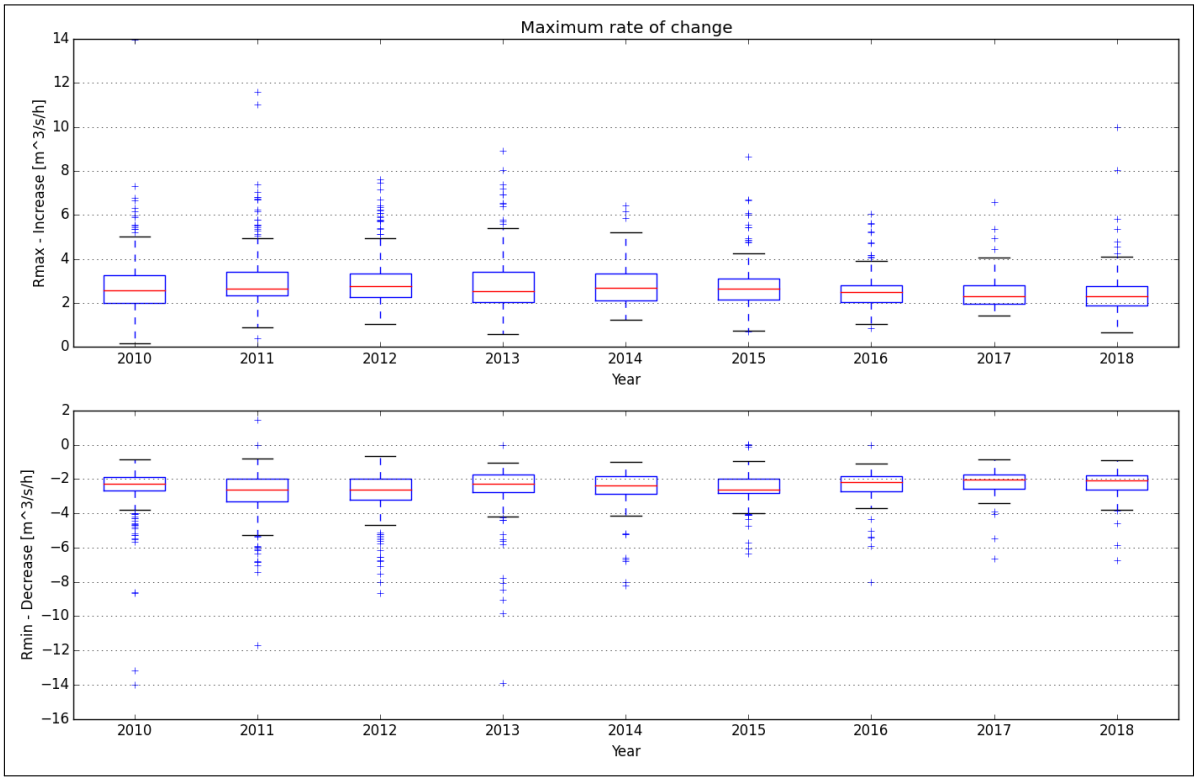

Figure A.16.80: Maximum rate of change

A.17. Stuvane kraftstasjon

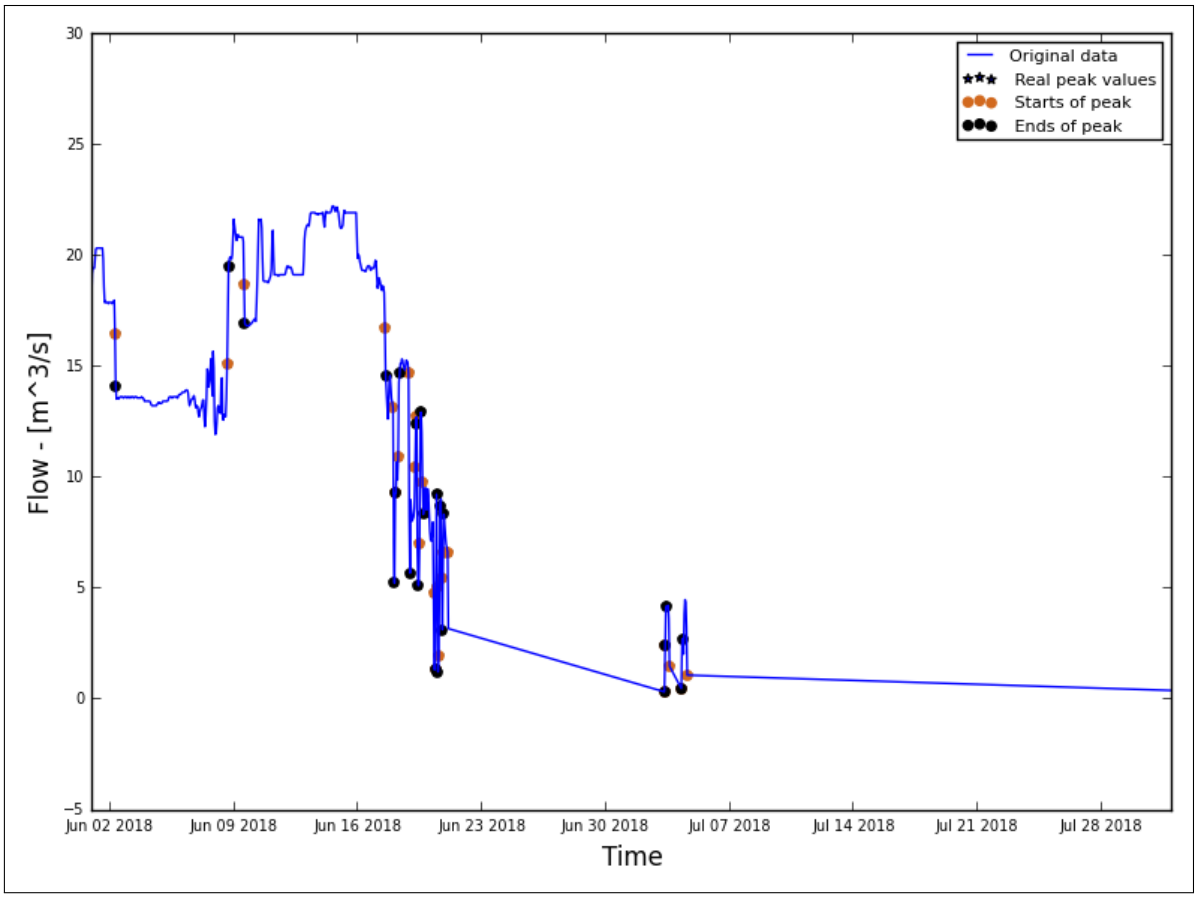

Figure A.17.81: Hydrograph of the last two months of the recorded data

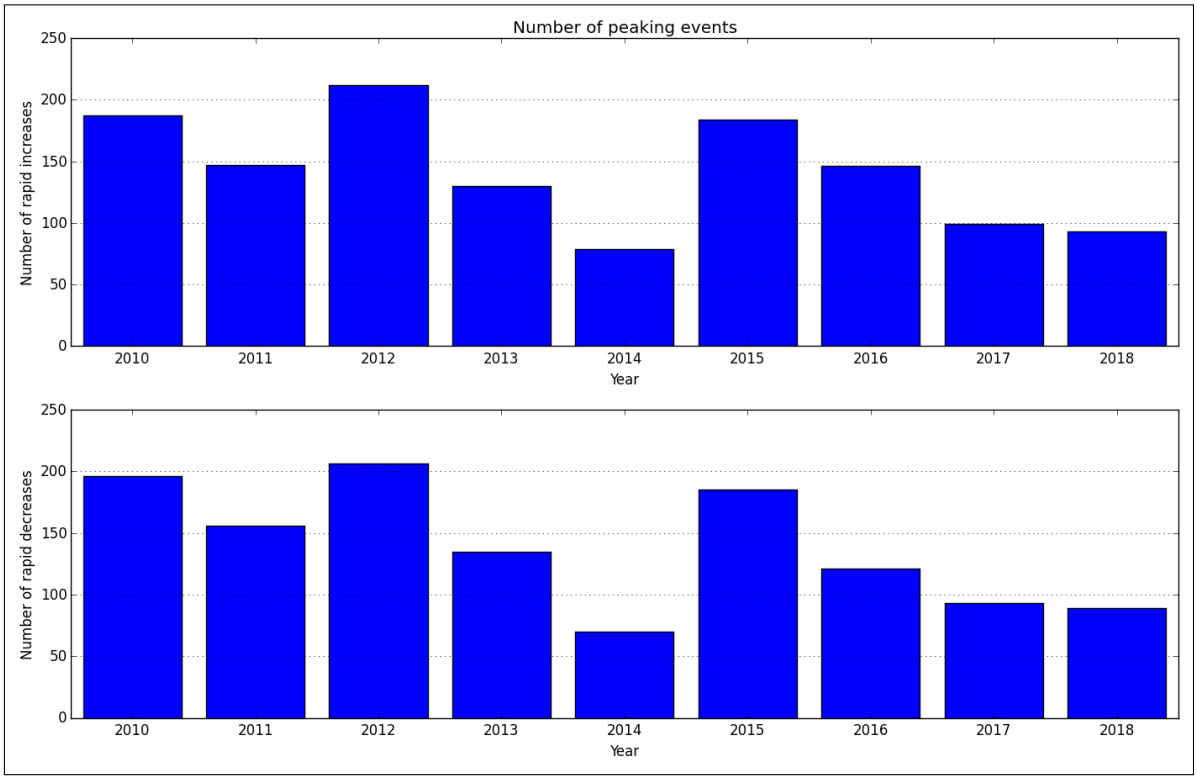

Figure A.17.82: Average annual number of increased/decreased peaks

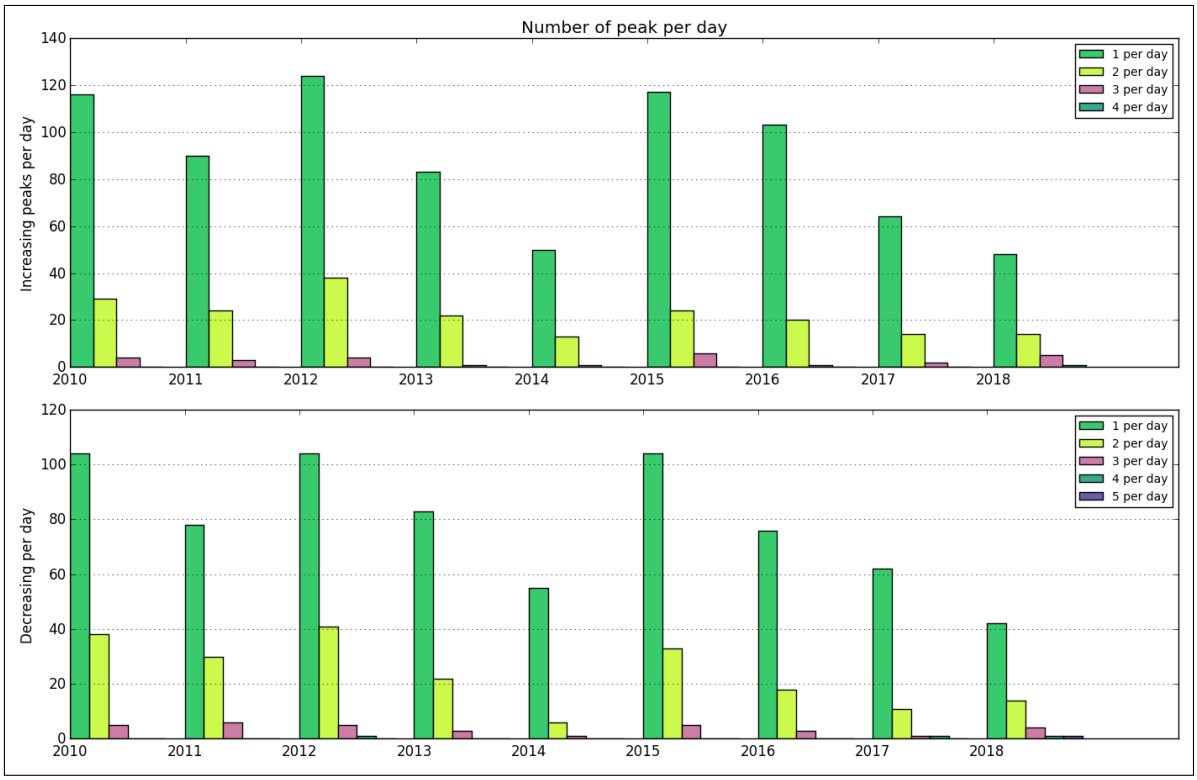

Figure A.17.83: Number of peaks per day

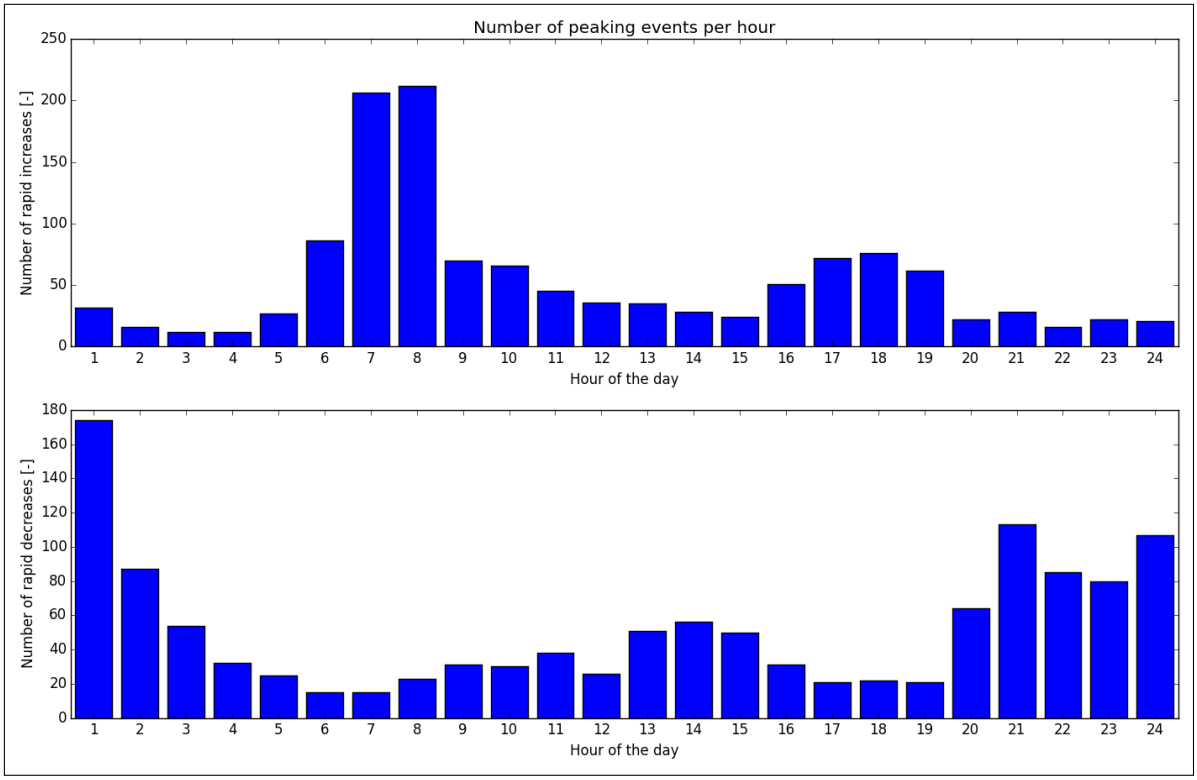

Figure A.17.84: Distribution of peaks throughout day

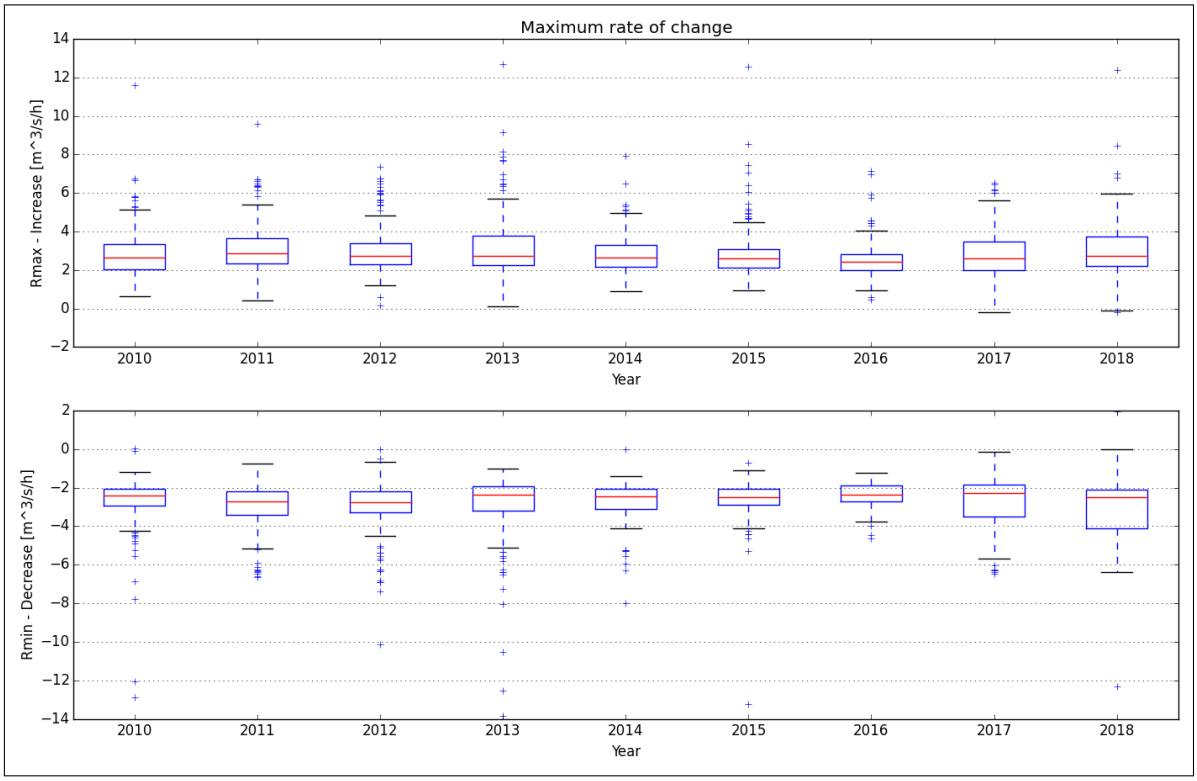

Figure A.17.85: Maximum rate of change

A.18. Skagen kraftstasjon

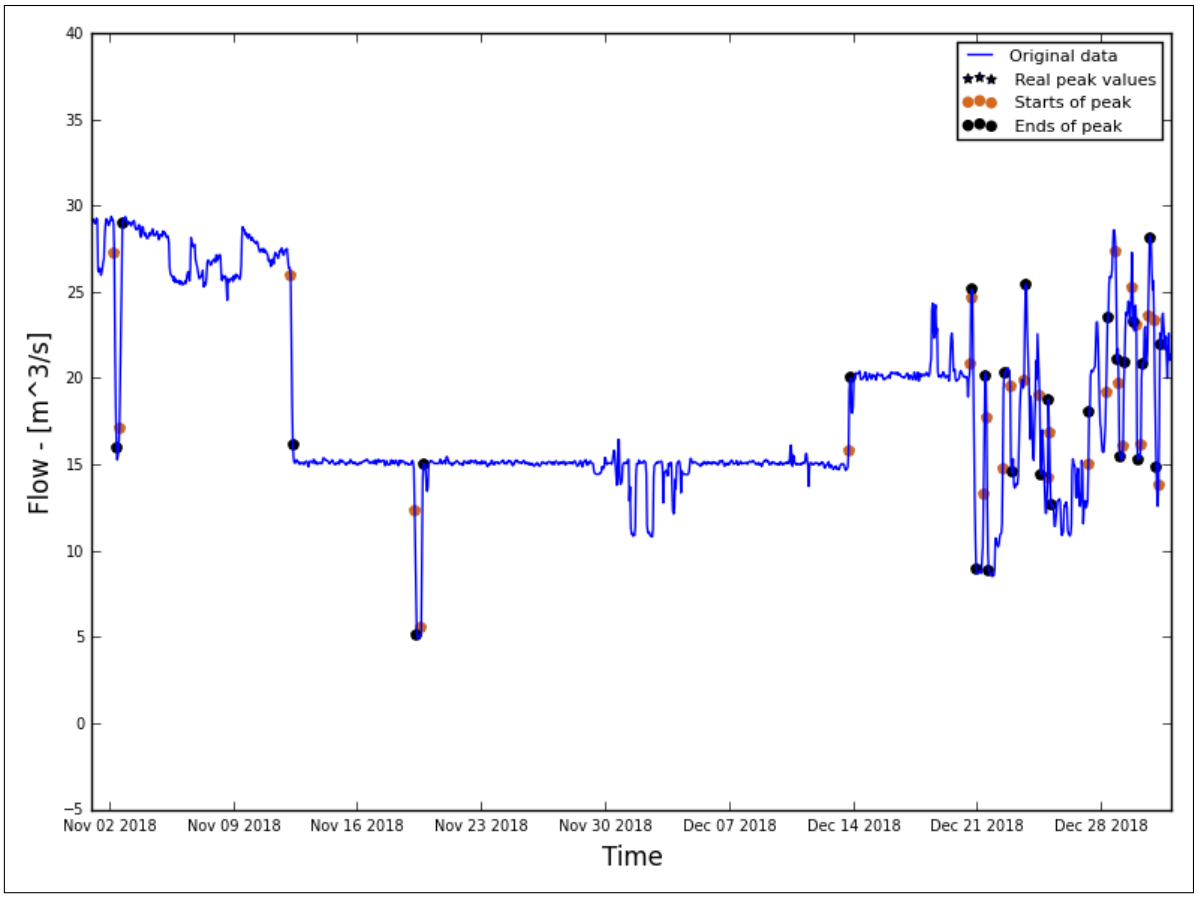

Figure A.18.86: Hydrograph of the last two months of the recorded data

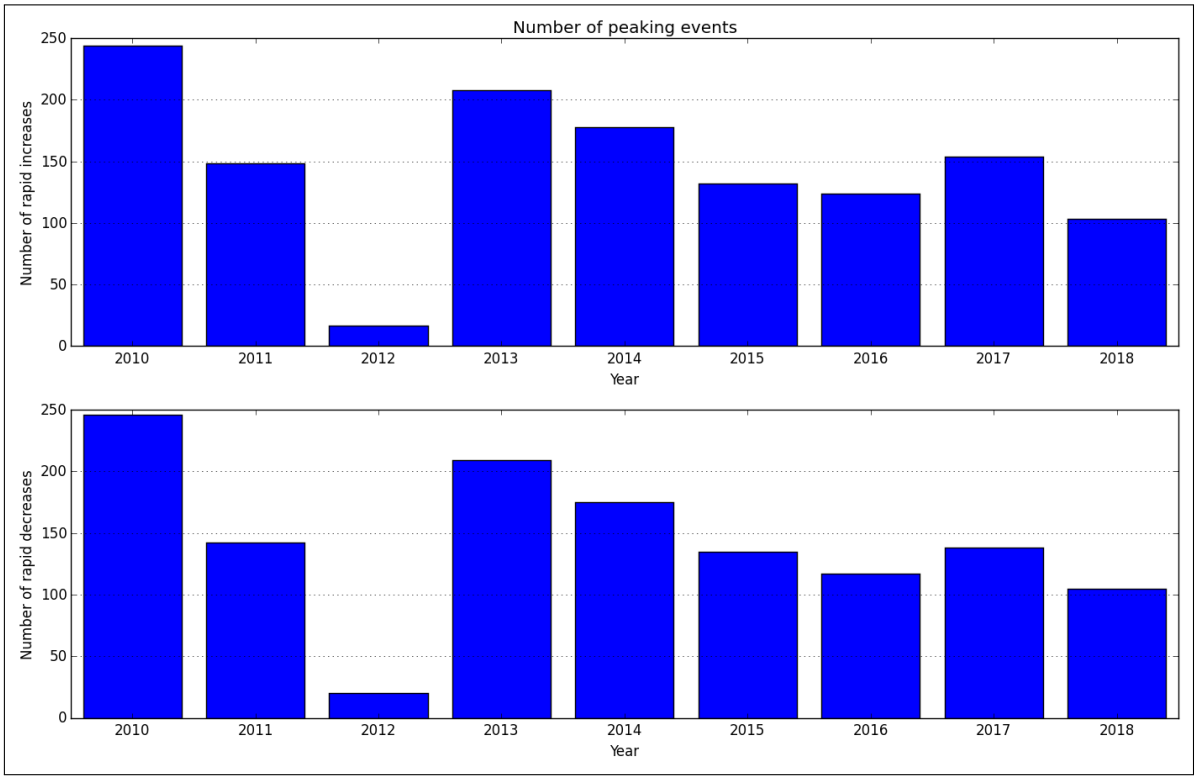

Figure A.18.87: Average annual number of increased/decreased peaks

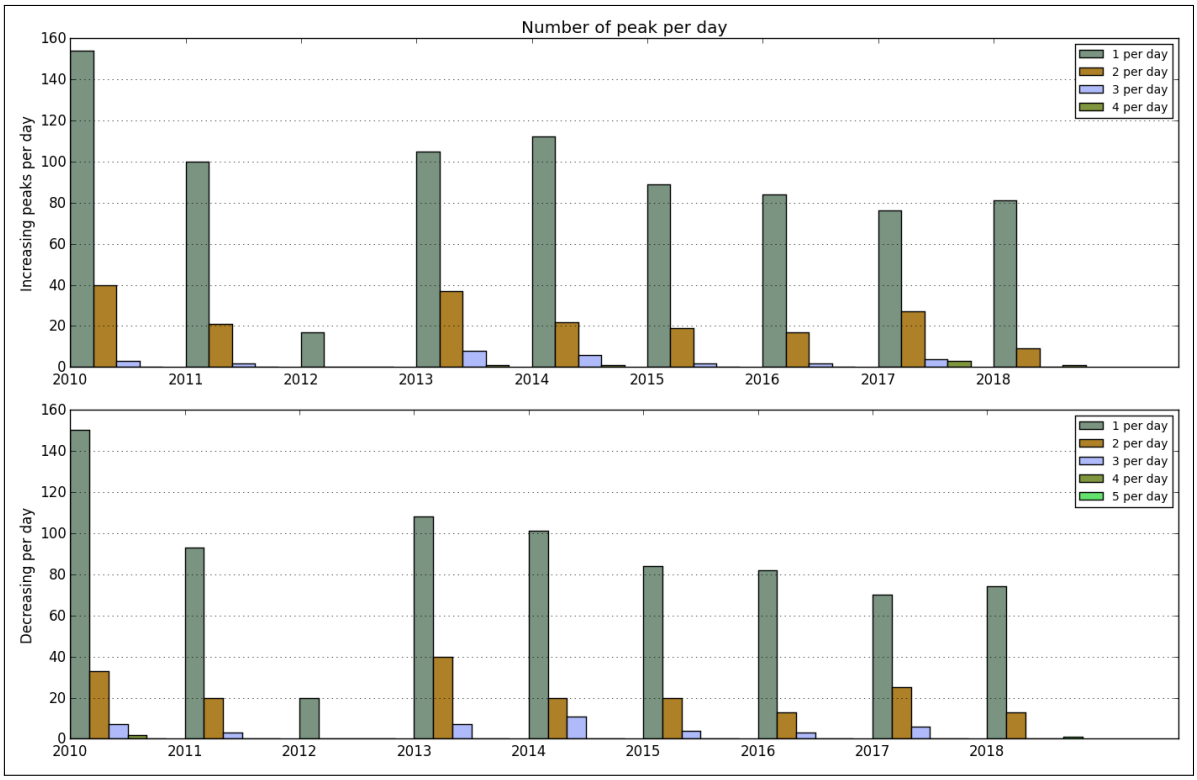

Figure A.18.88: Number of peaks per day

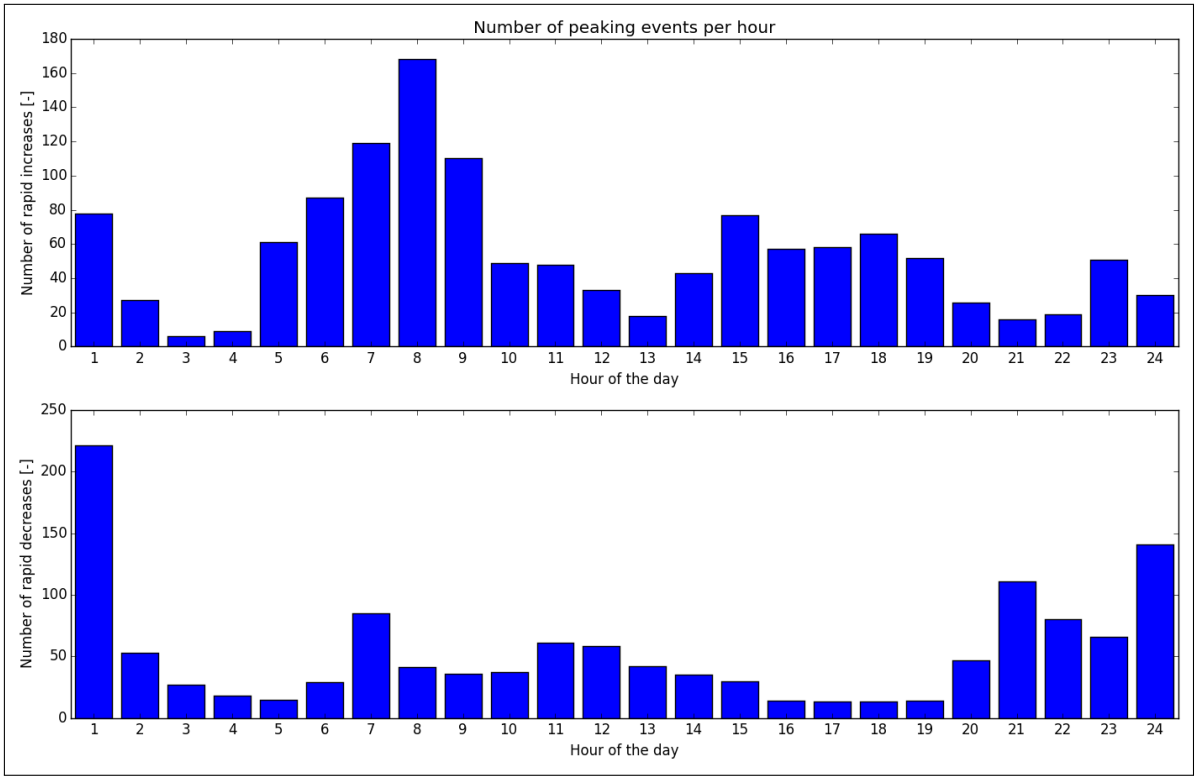

Figure A.18.89: Distribution of peaks throughout day

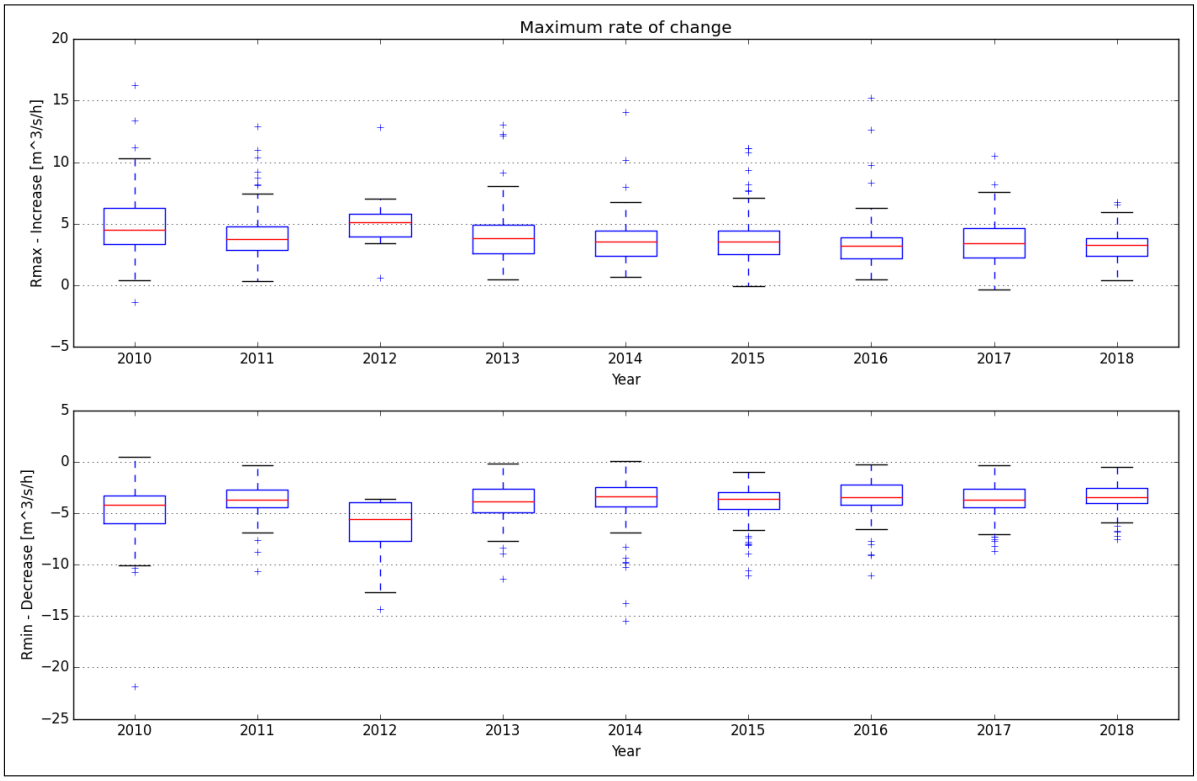

Figure A.18.90: Maximum rate of change

A.19. Årøy

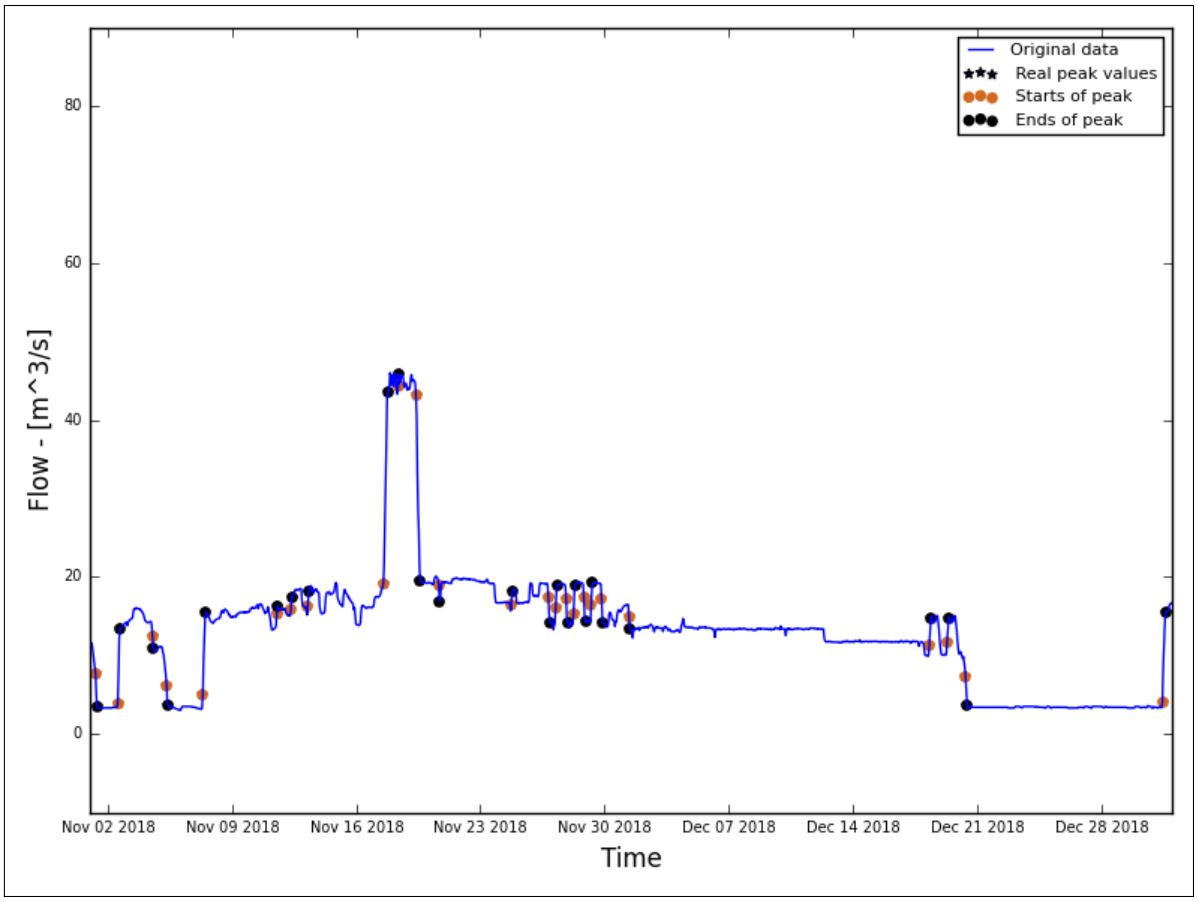

Figure A.19.91: Hydrograph of the last two months of the recorded data

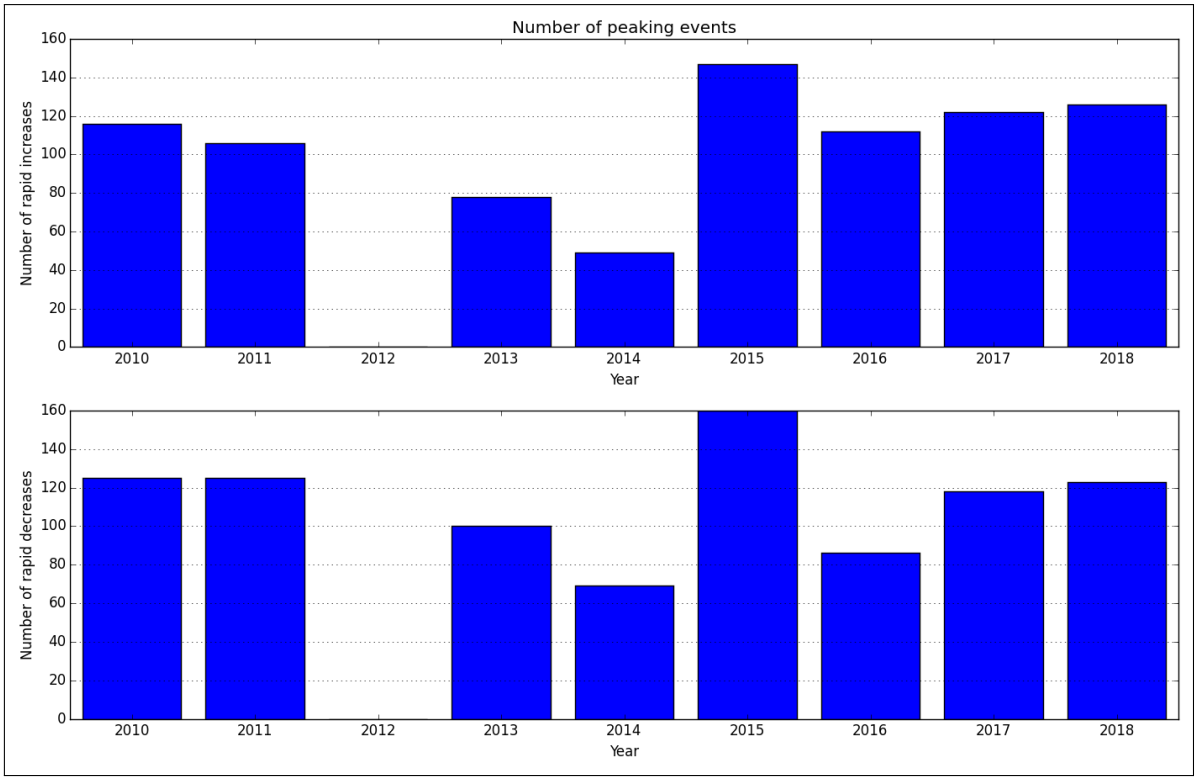

Figure A.19.92: Average annual number of increased/decreased peaks

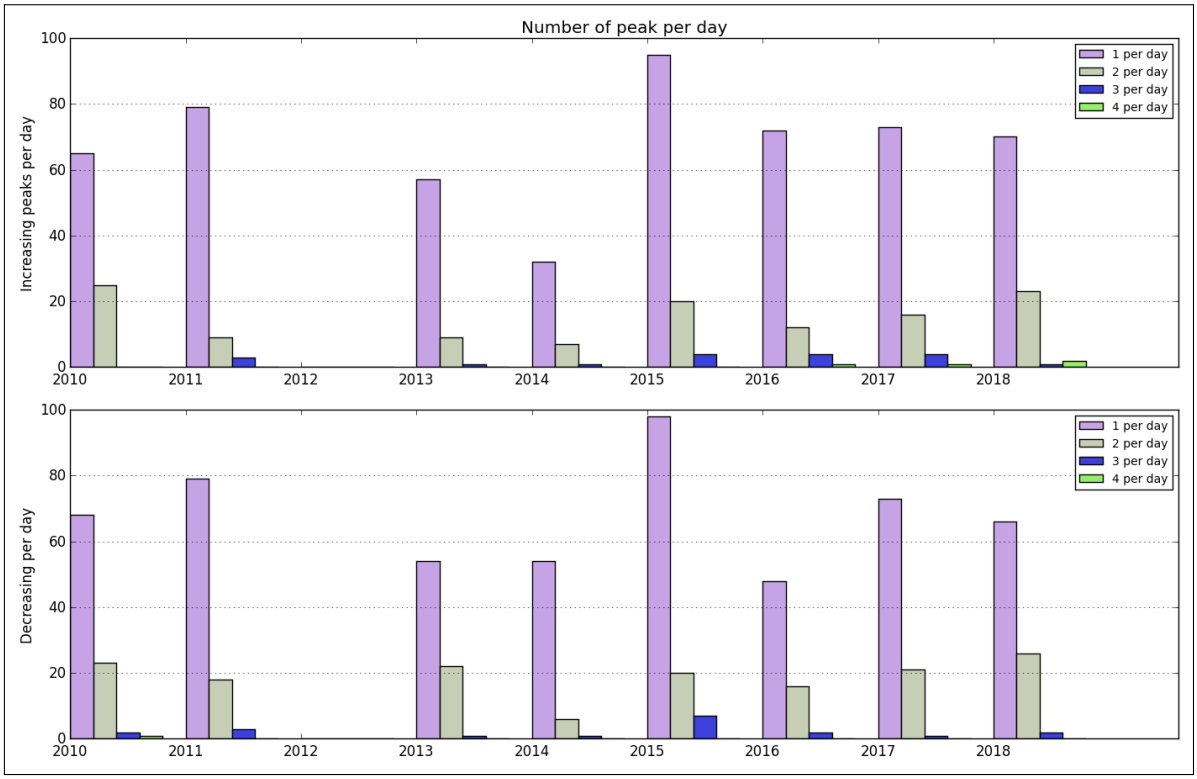

Figure A.19.93: Number of peaks per day

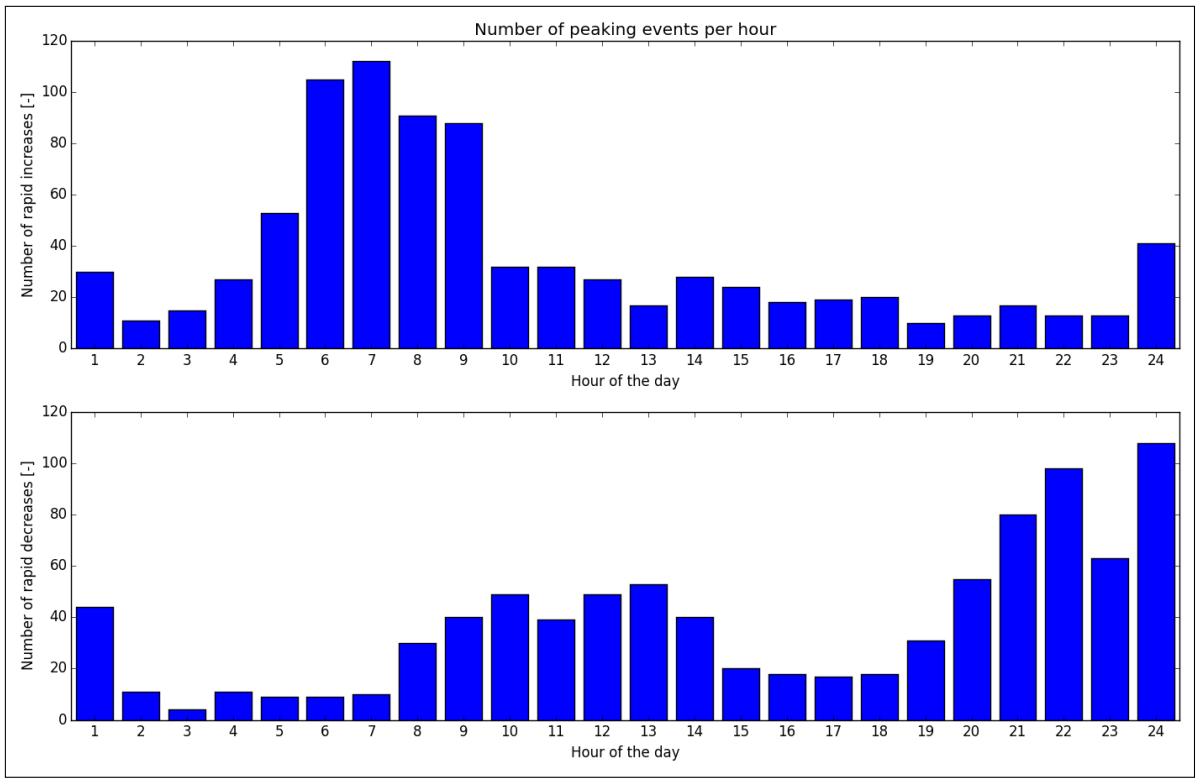

Figure A.19.94: Distribution of peaks throughout day

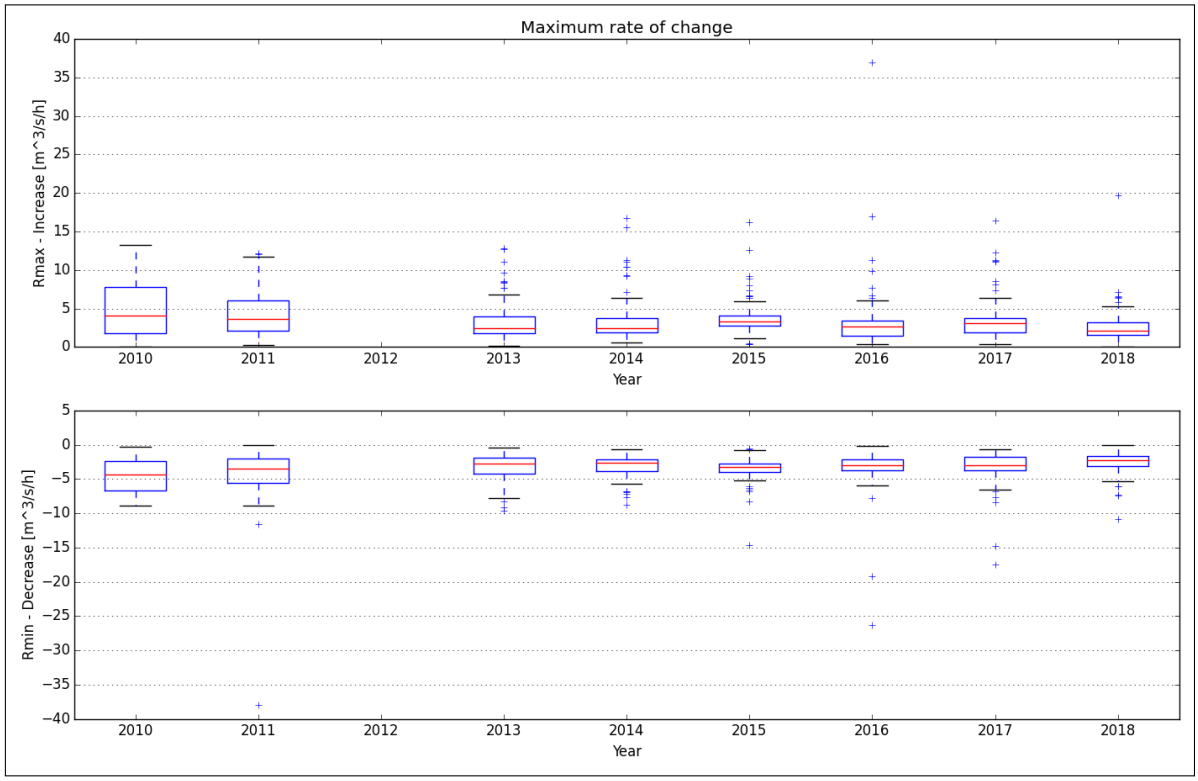

Figure A.19.95: Maximum rate of change

A.20. Mel

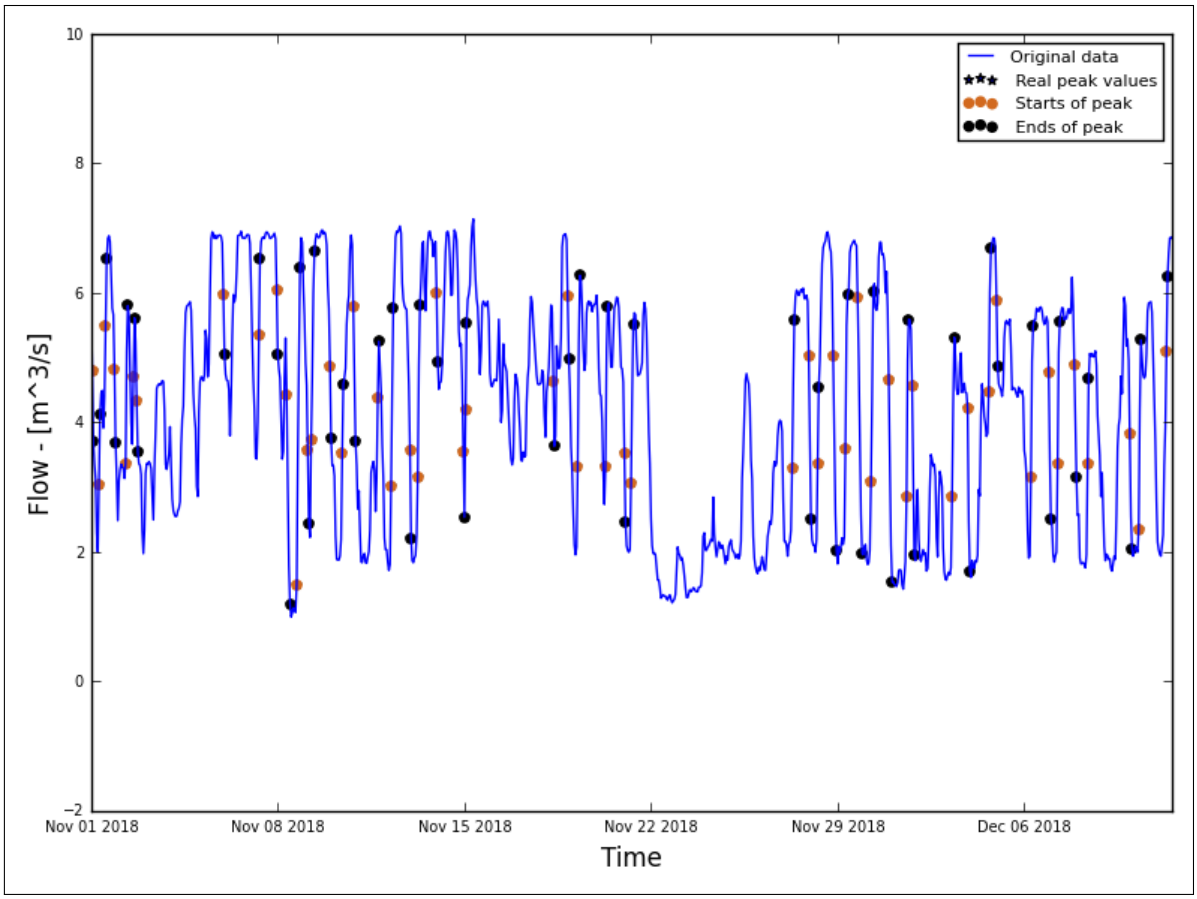

Figure A.20.96: Hydrograph of the last two months of the recorded data

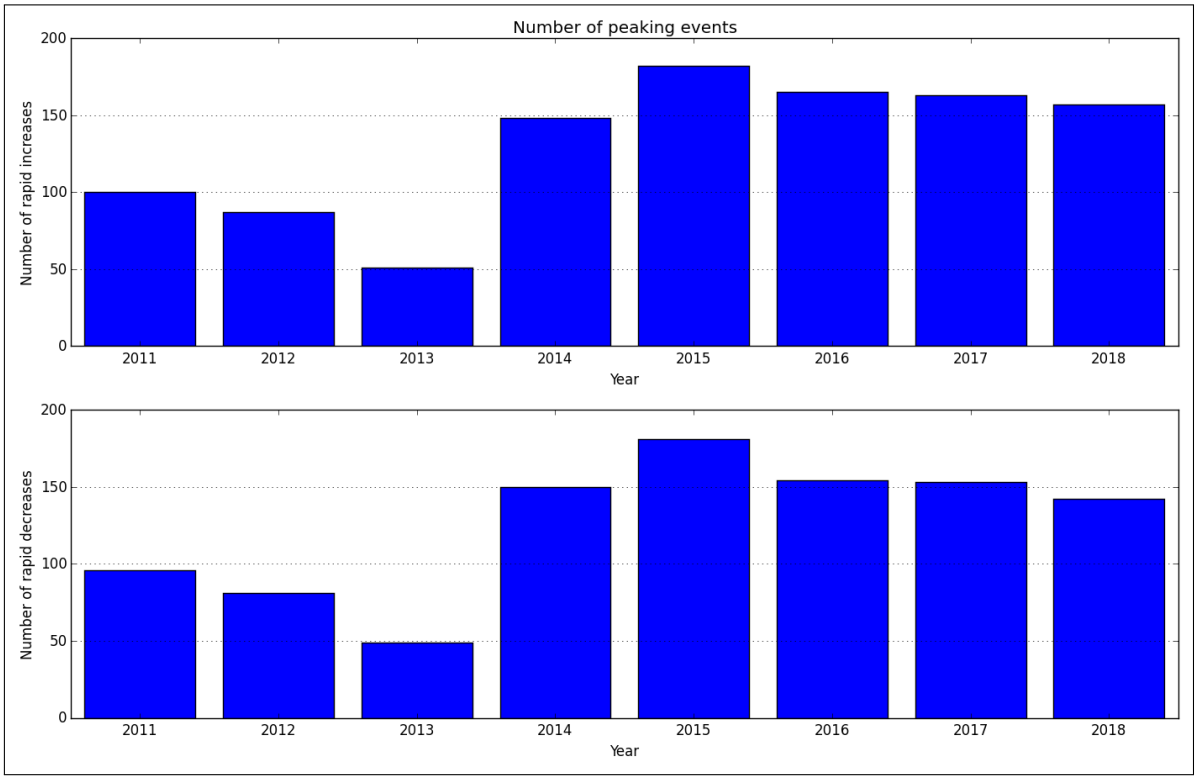

Figure A.20.97: Average annual number of increased/decreased peaks

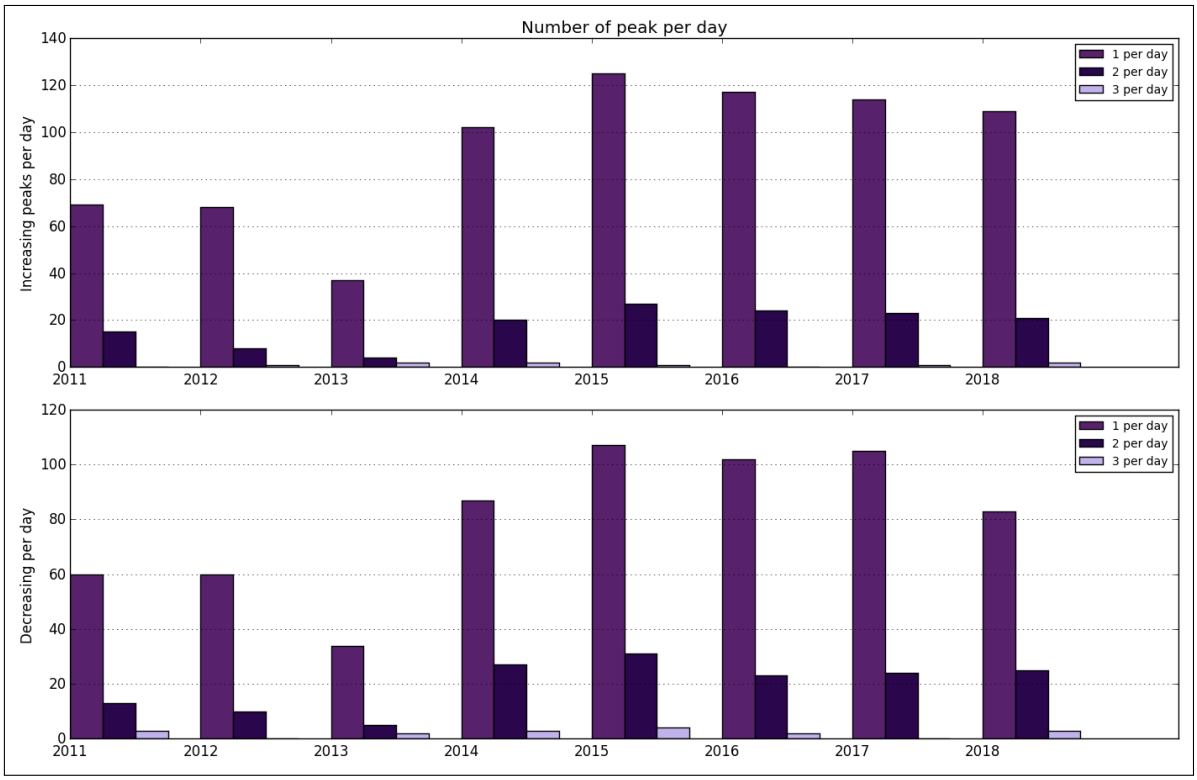

Figure A.20.98: Number of peaks per day

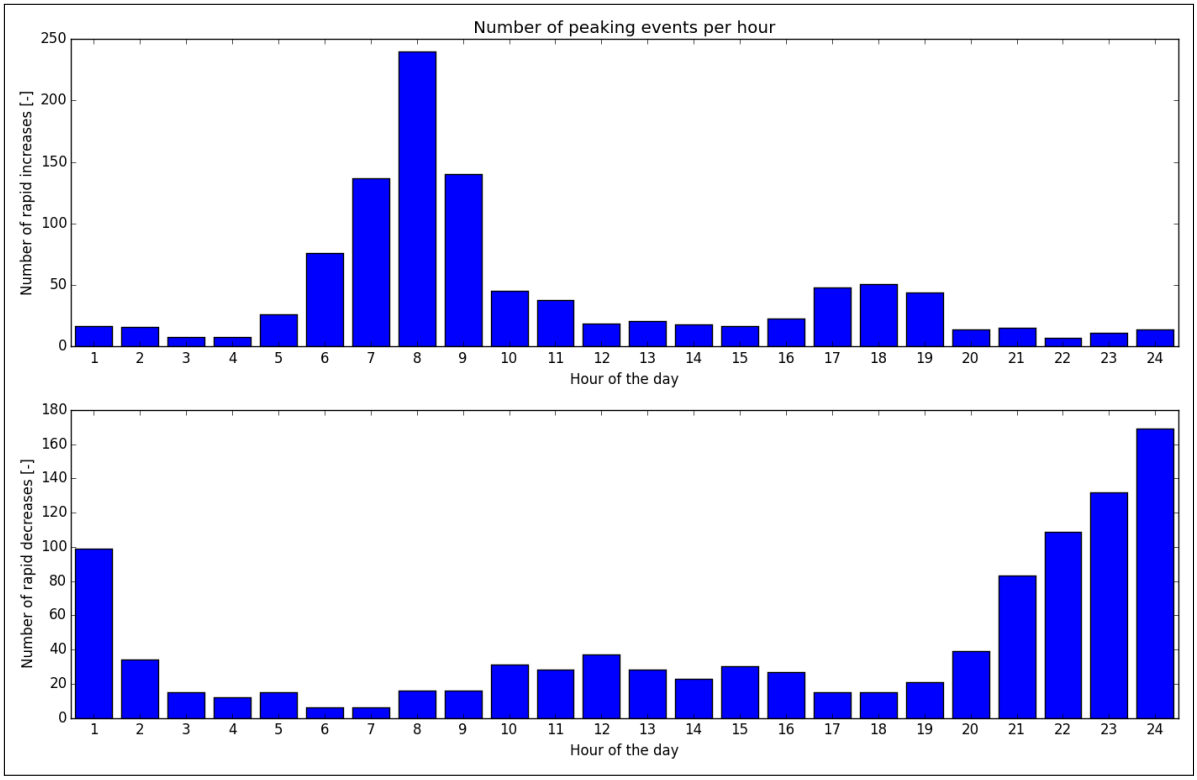

Figure A.20.99: Distribution of peaks throughout day

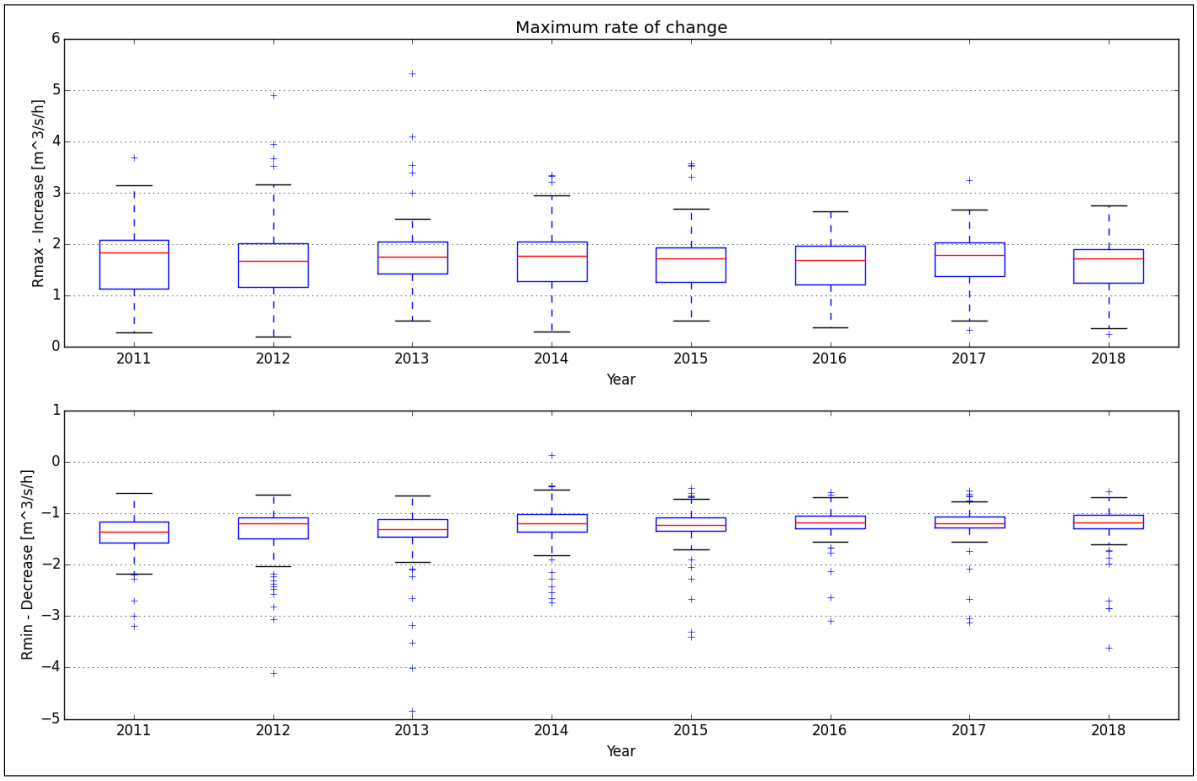

Figure A.20.100: Maximum rate of change

A.21. Driva

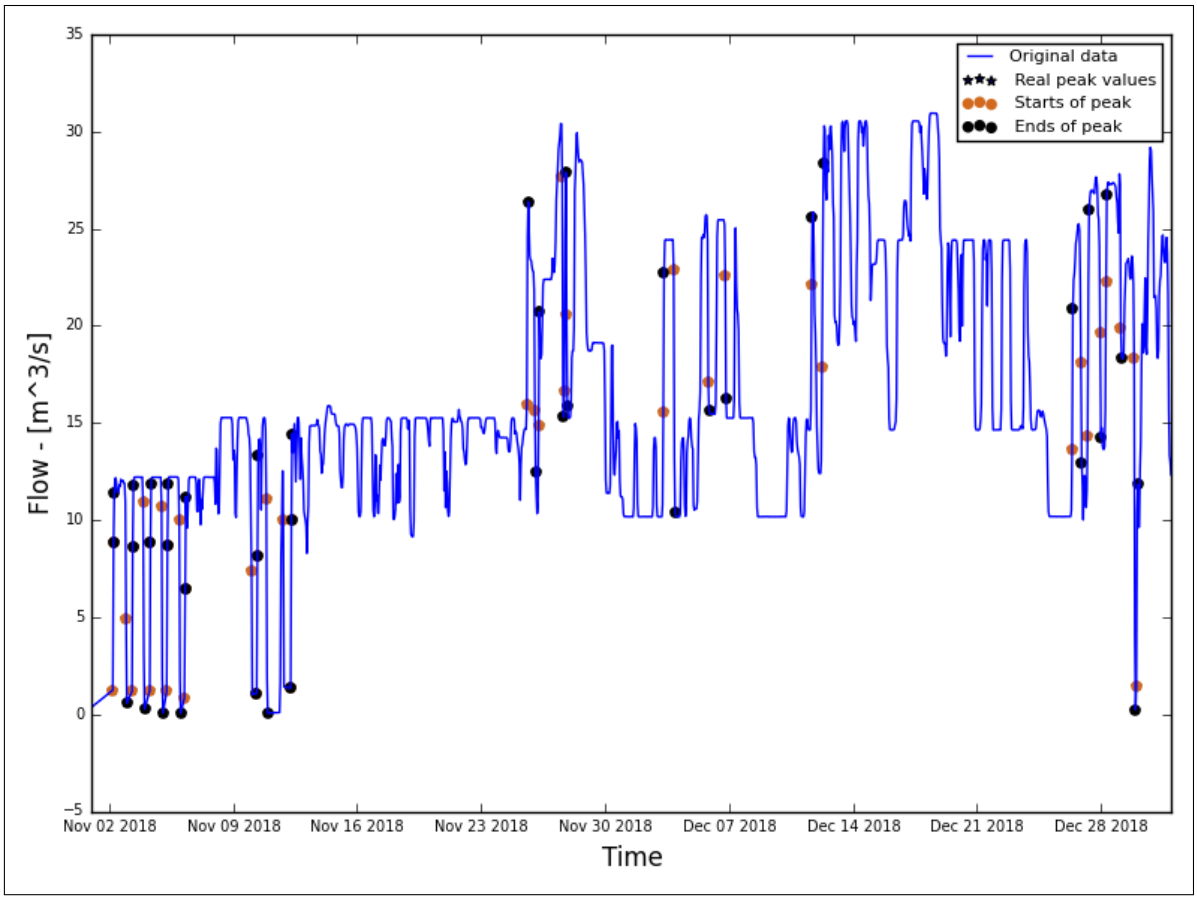

Figure A.21.101: Hydrograph of the last two months of the recorded data

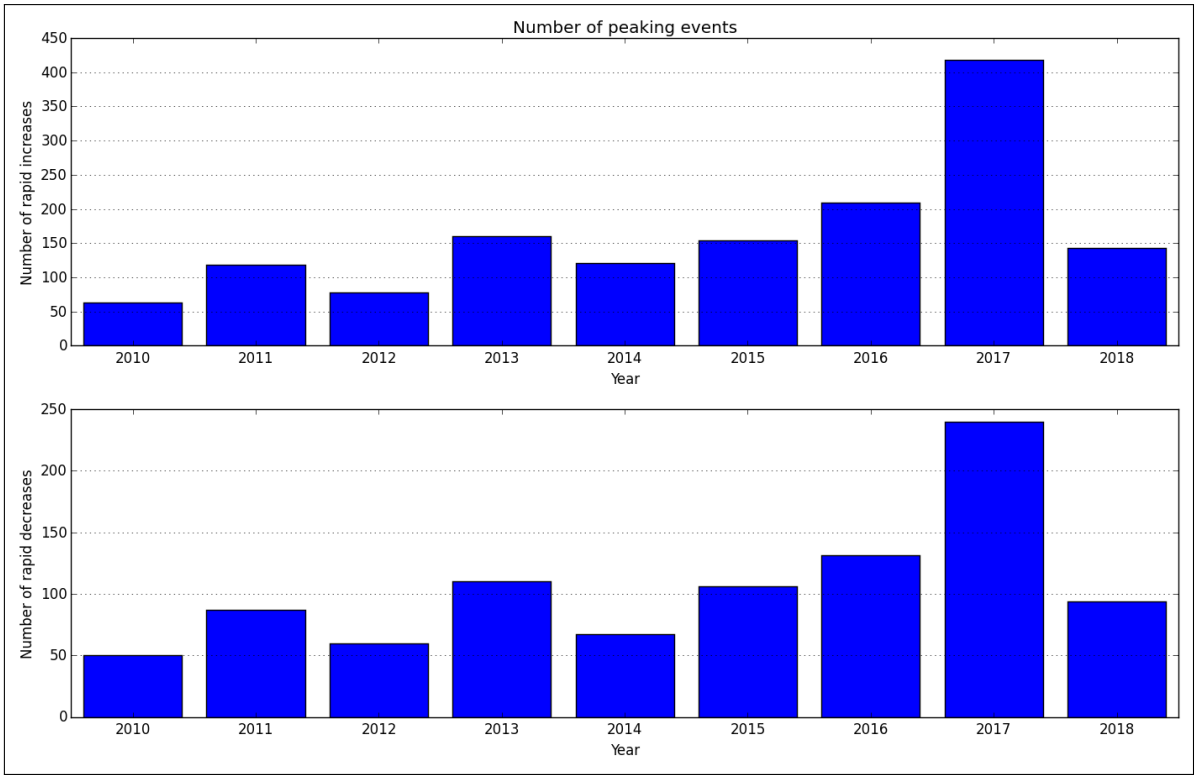

Figure A.21.102: Average annual number of increased/decreased peaks

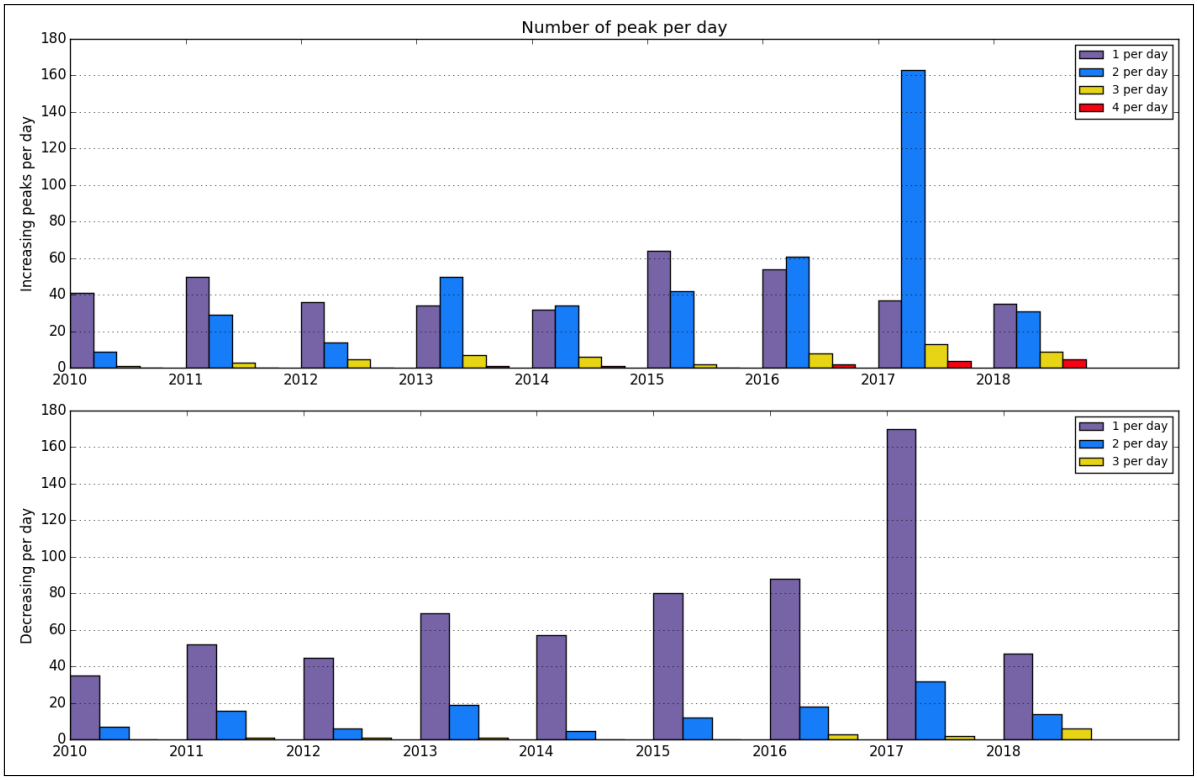

Figure A.21.103: Number of peaks per day

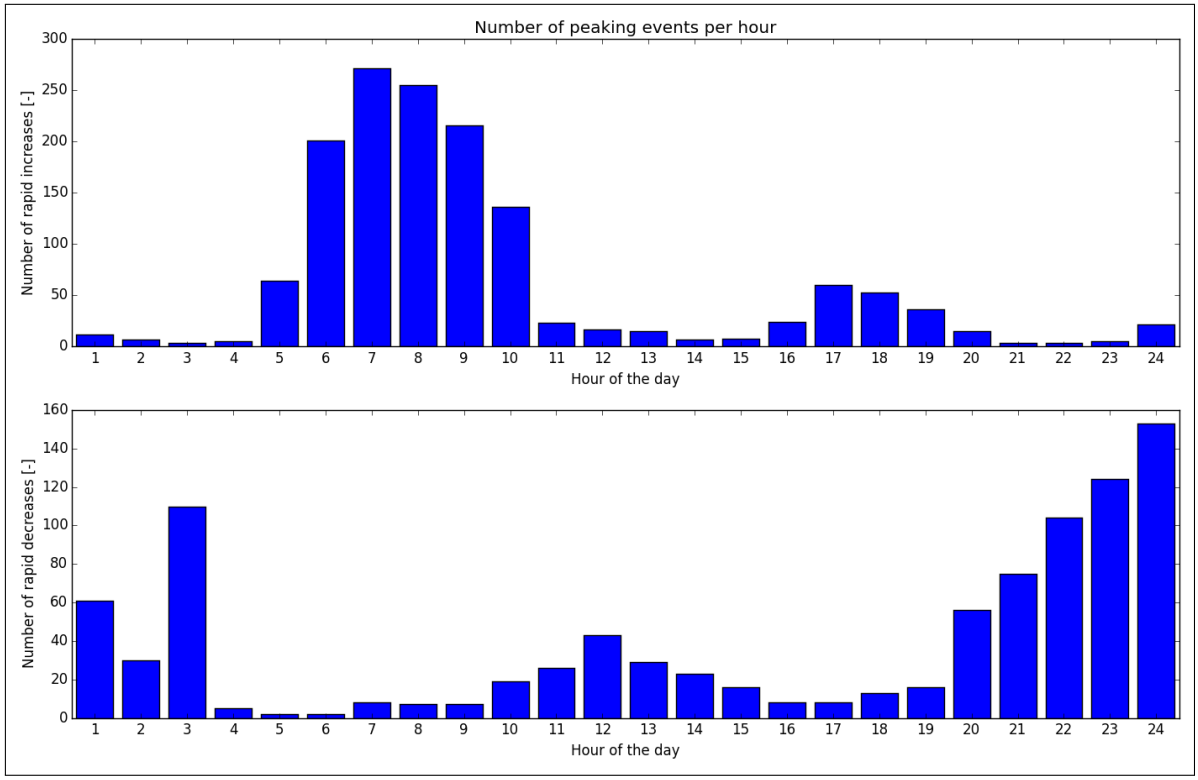

Figure A.21.104: Distribution of peaks throughout day

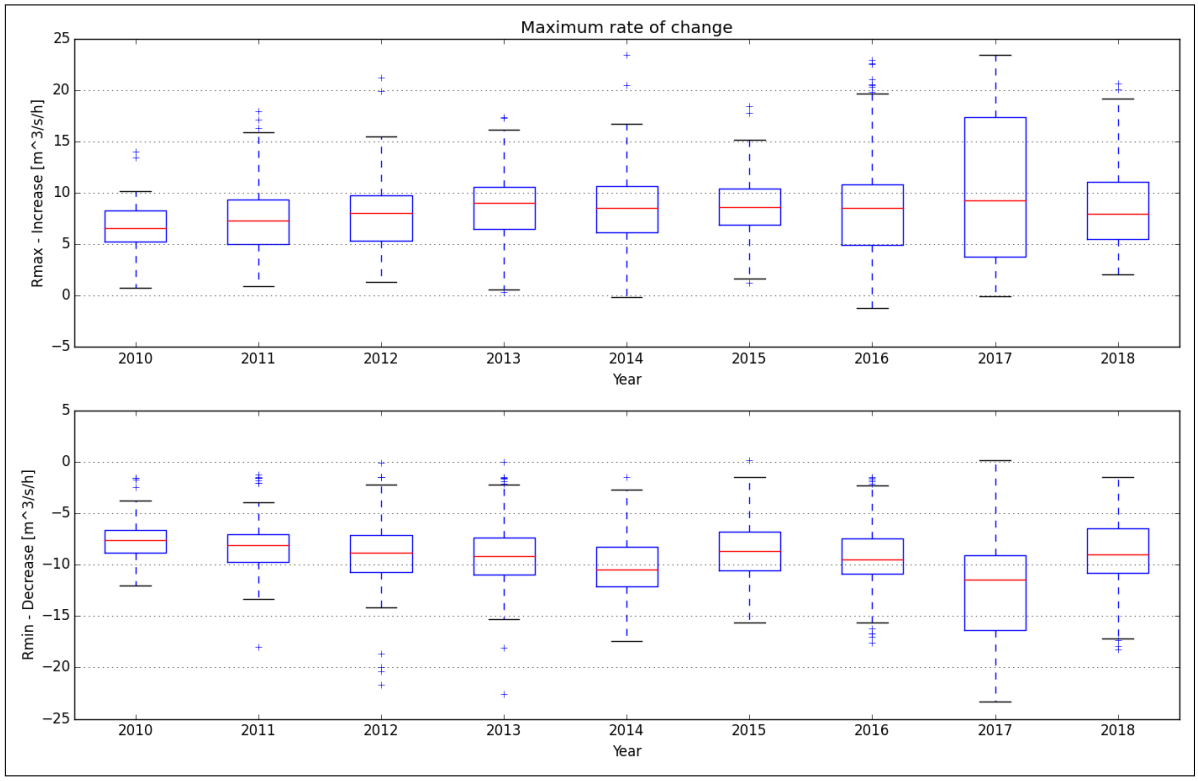

Figure A.21.105: Maximum rate of change

A.22. Søa

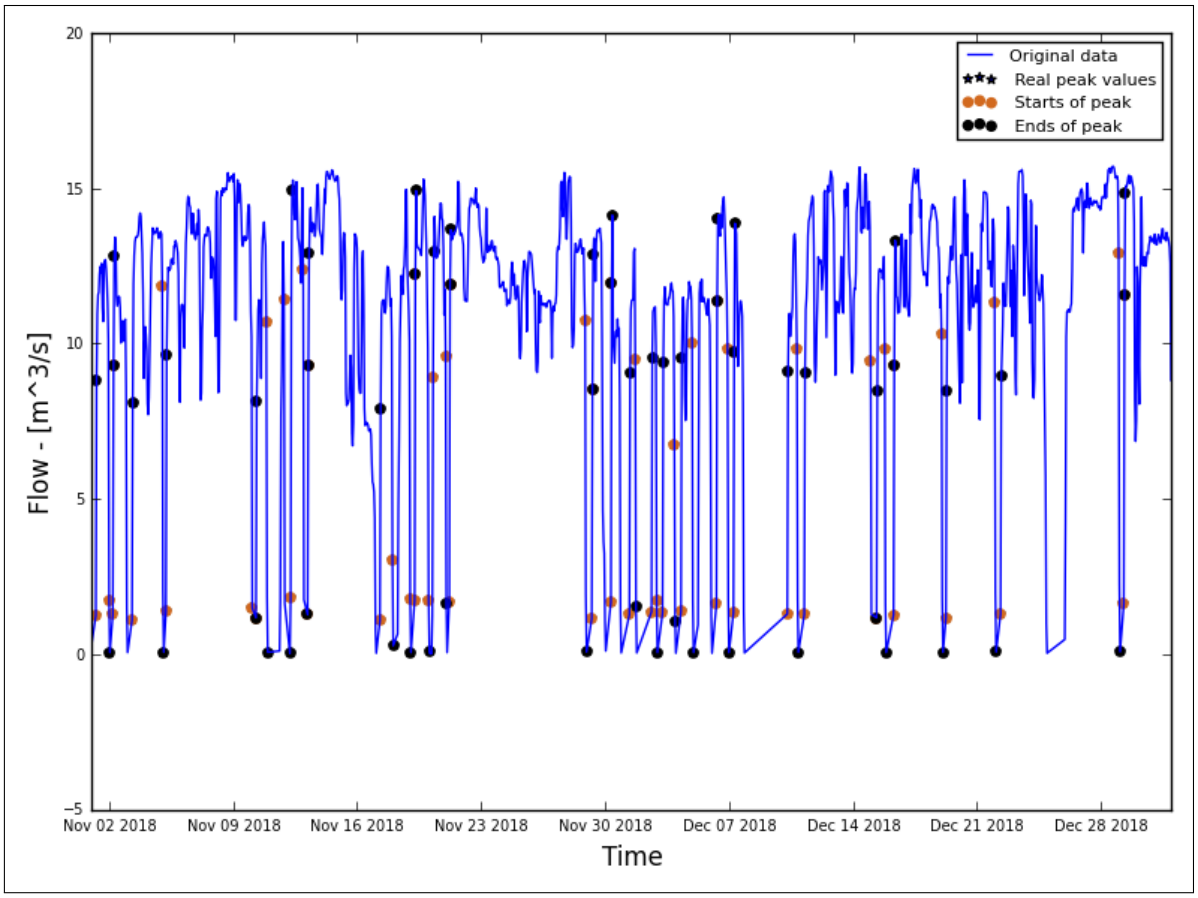

Figure A.22.106: Hydrograph of the last two months of the recorded data

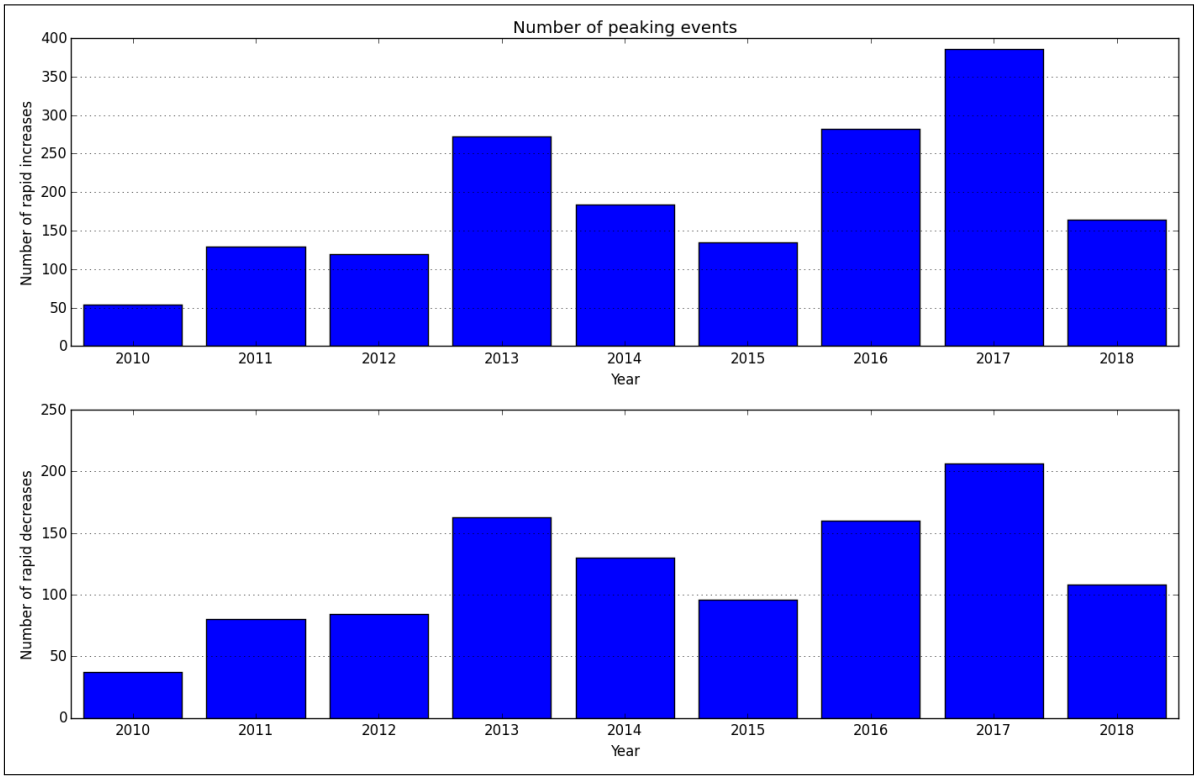

Figure A.22.107: Average annual number of increased/decreased peaks

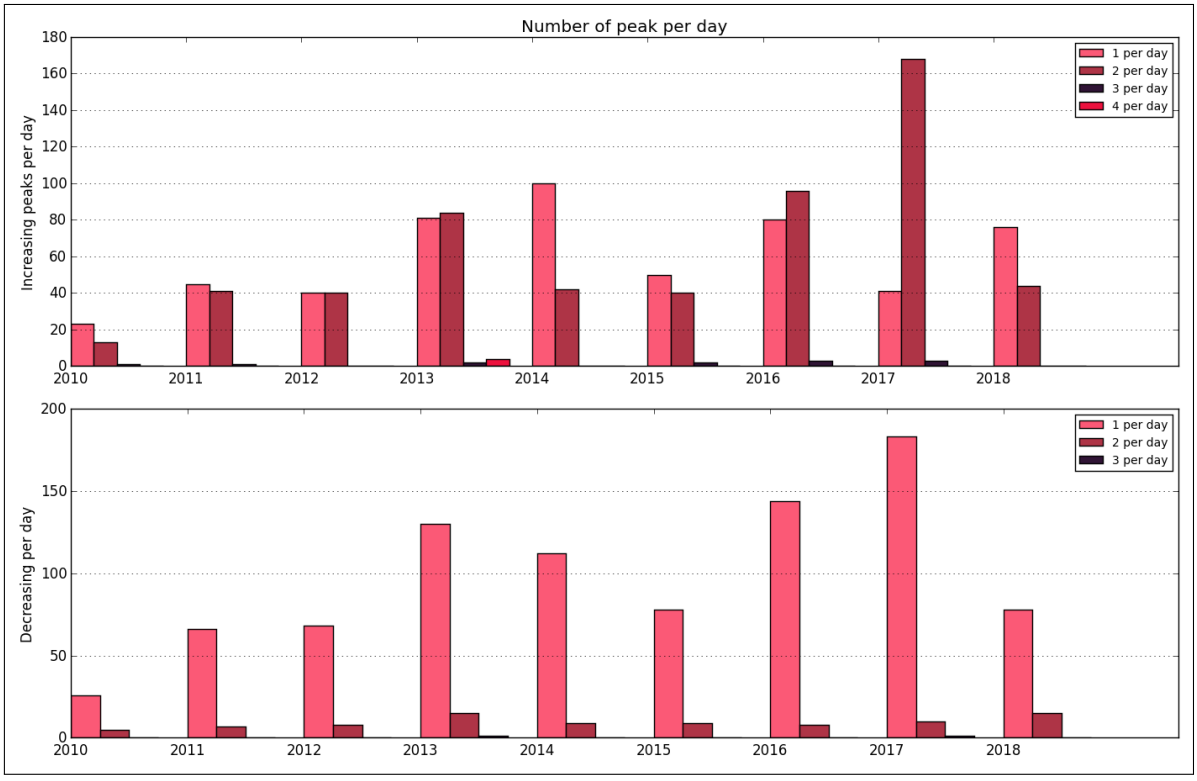

Figure A.22.108: Number of peaks per day

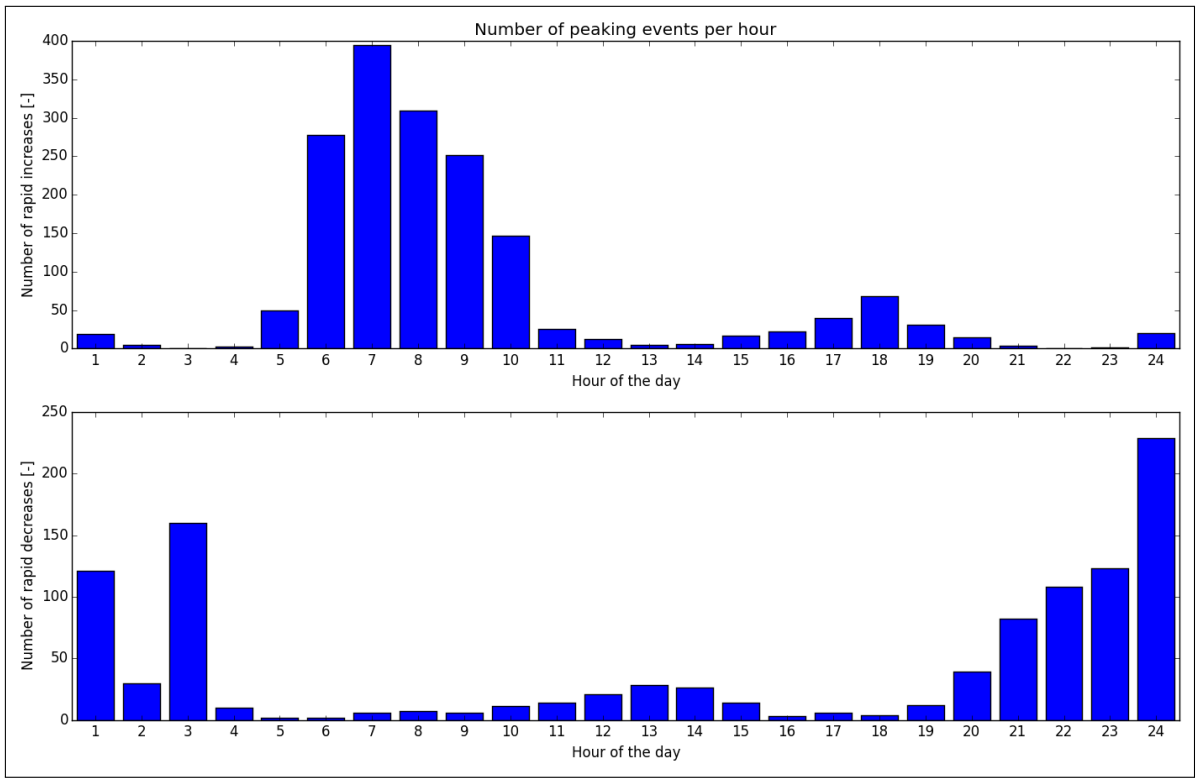

Figure A.22.109: Distribution of peaks throughout day

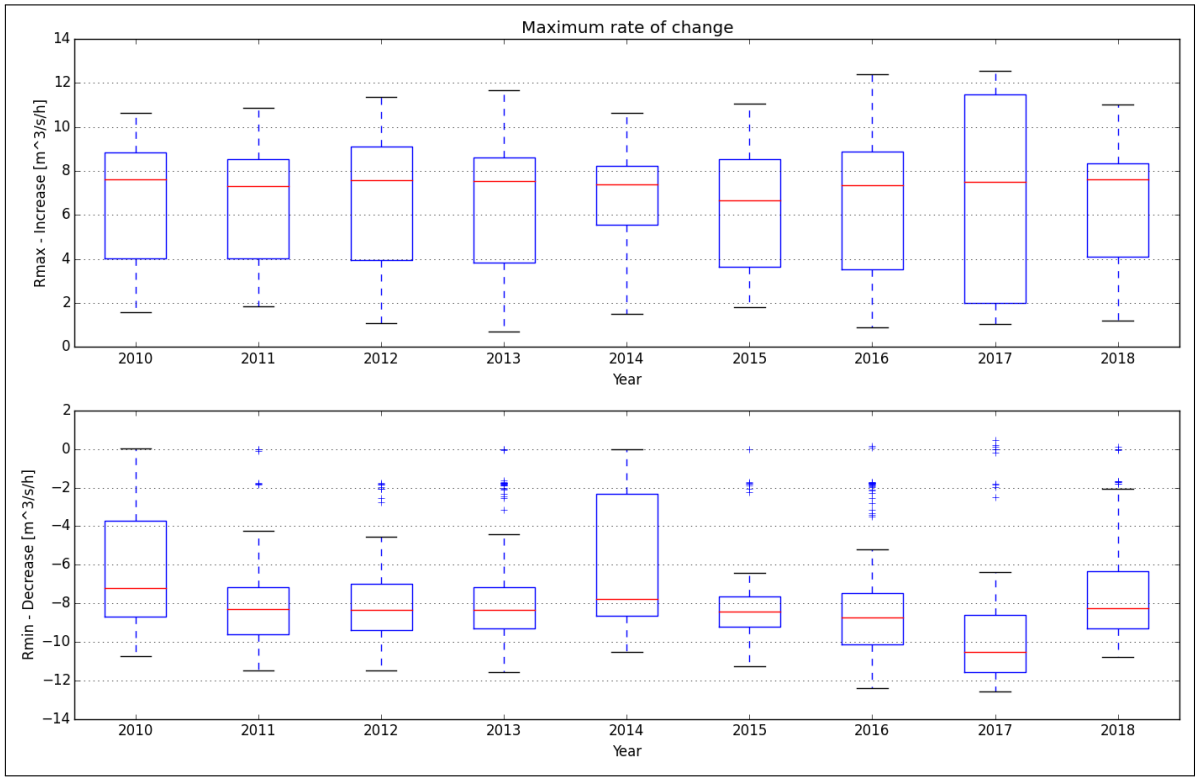

Figure A.22.110: Maximum rate of change

A.23. Svorkmo

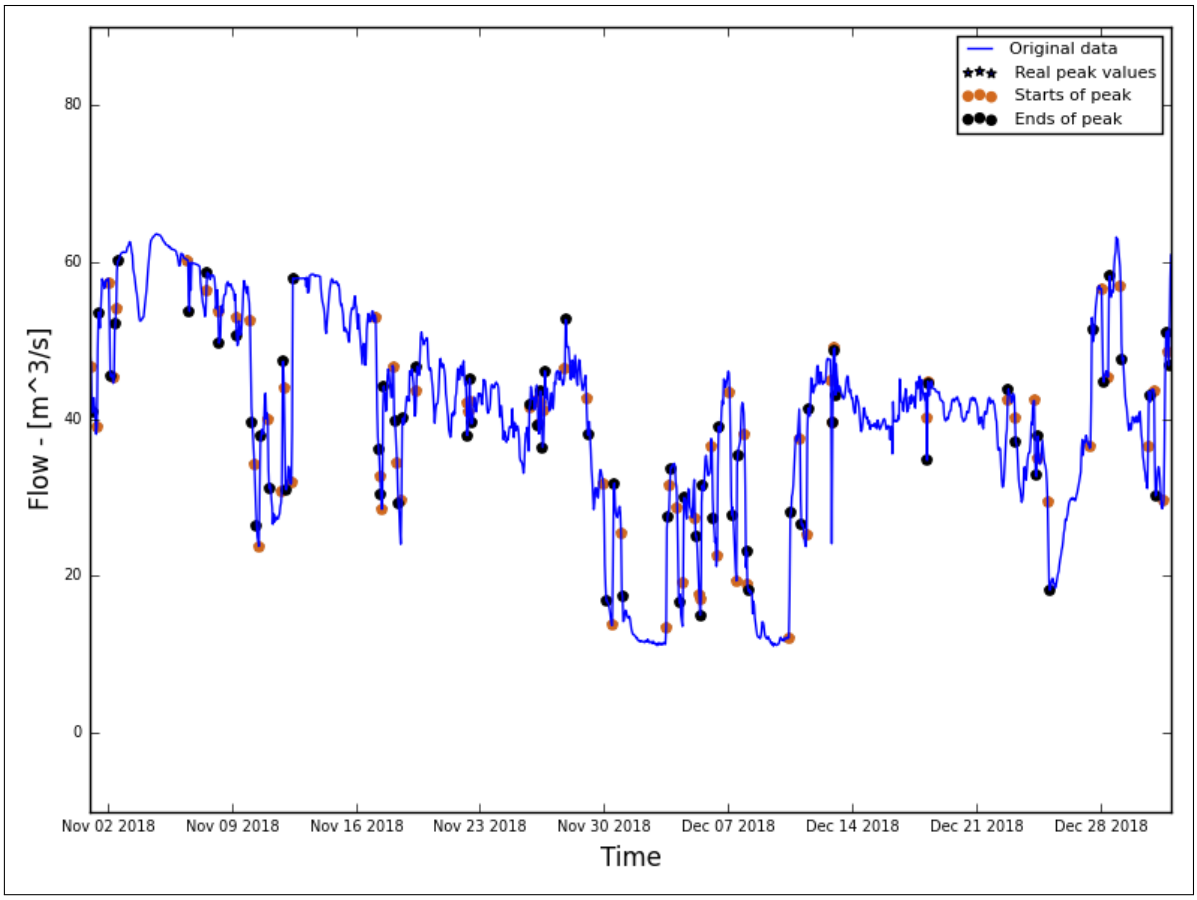

Figure A.23.111: Hydrograph of the last two months of the recorded data

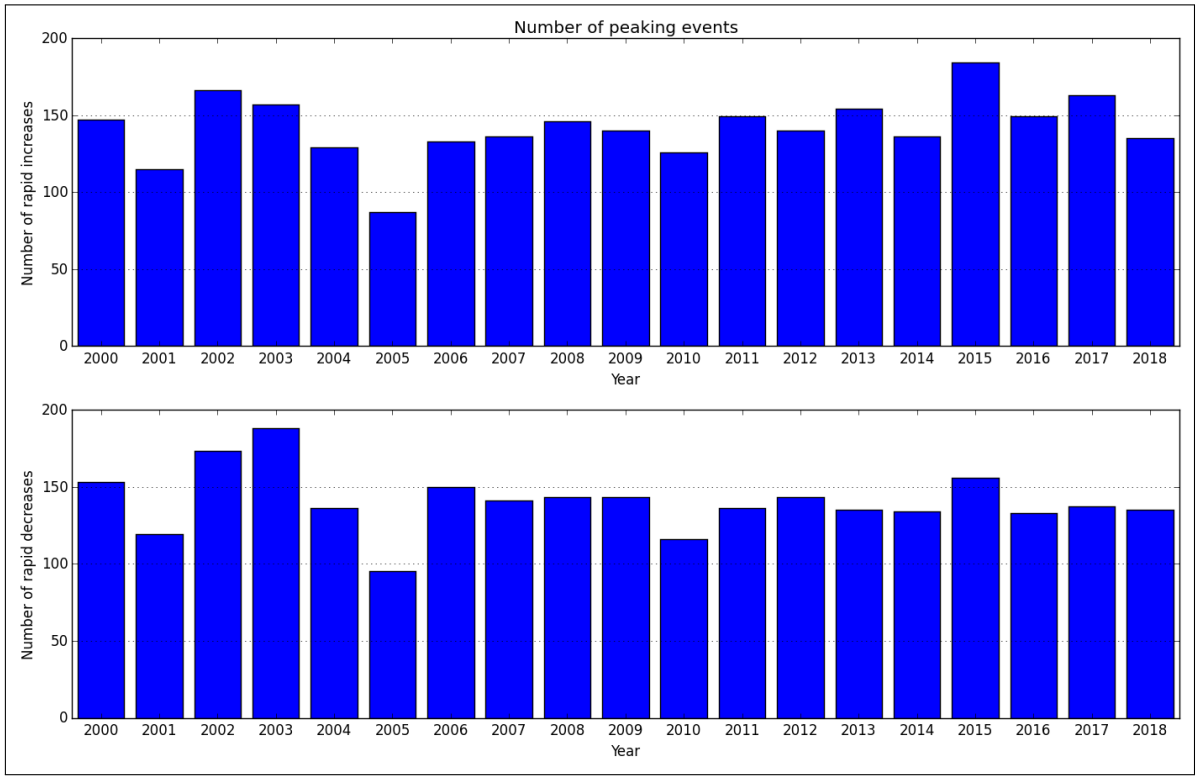

Figure A.23.112: Average annual number of increased/decreased peaks

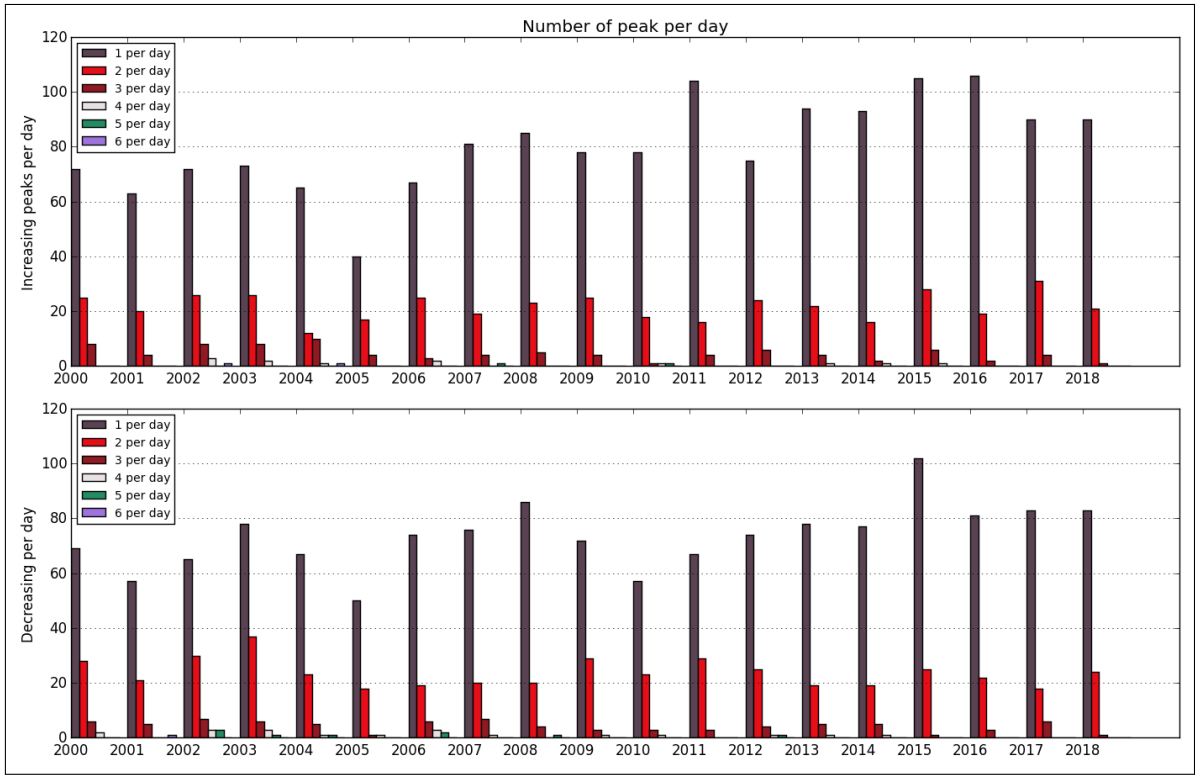

Figure A.23.113: Number of peaks per day

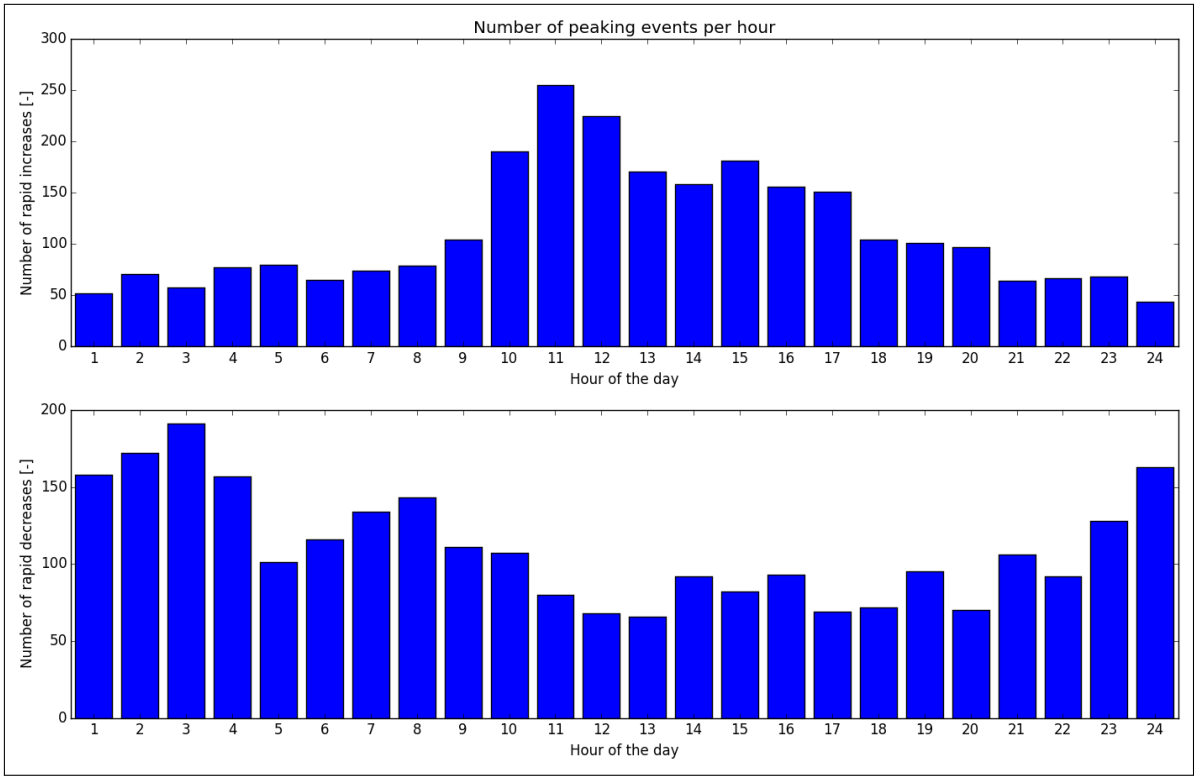

Figure A.23.114: Distribution of peaks throughout day

Figure A.23.115: Maximum rate of change

A.24. Brattset

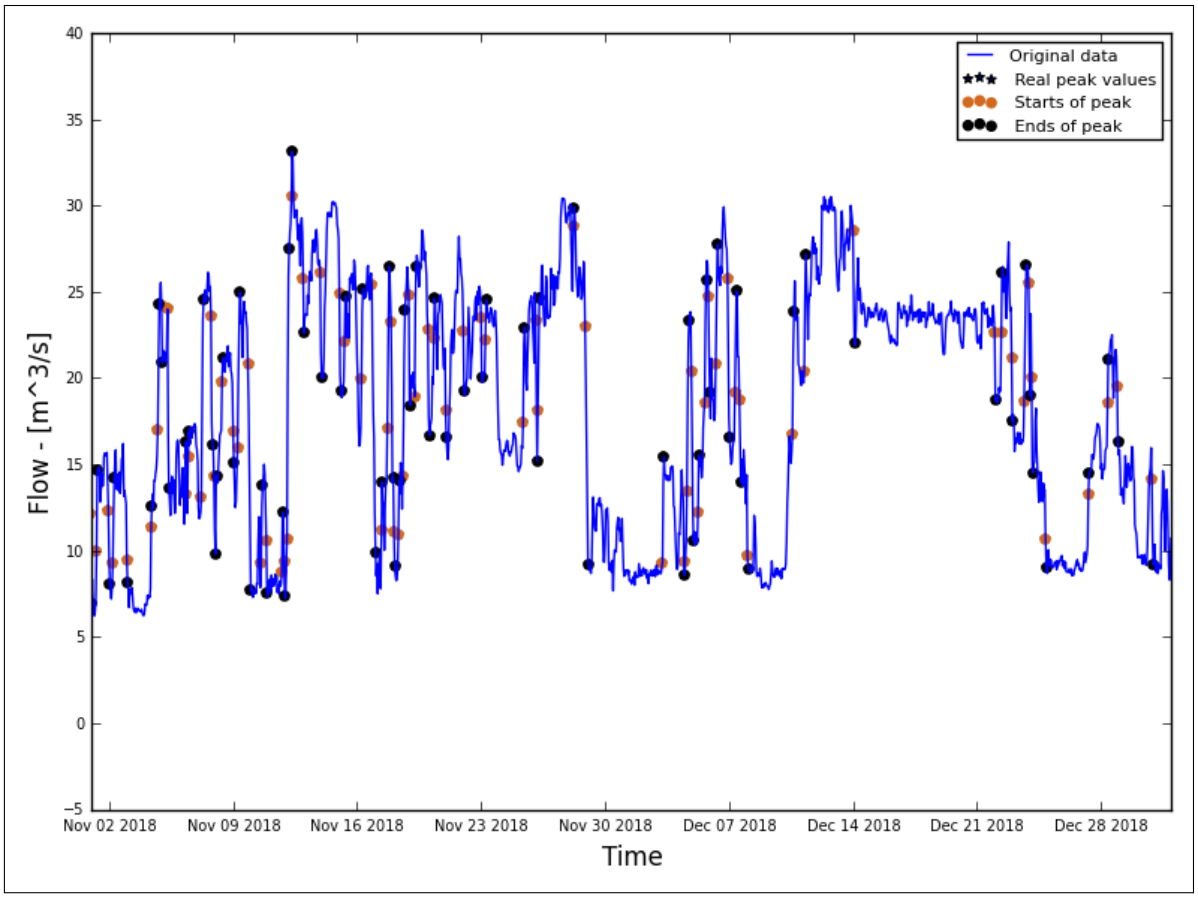

Figure A.24.116: Hydrograph of the last two months of the recorded data

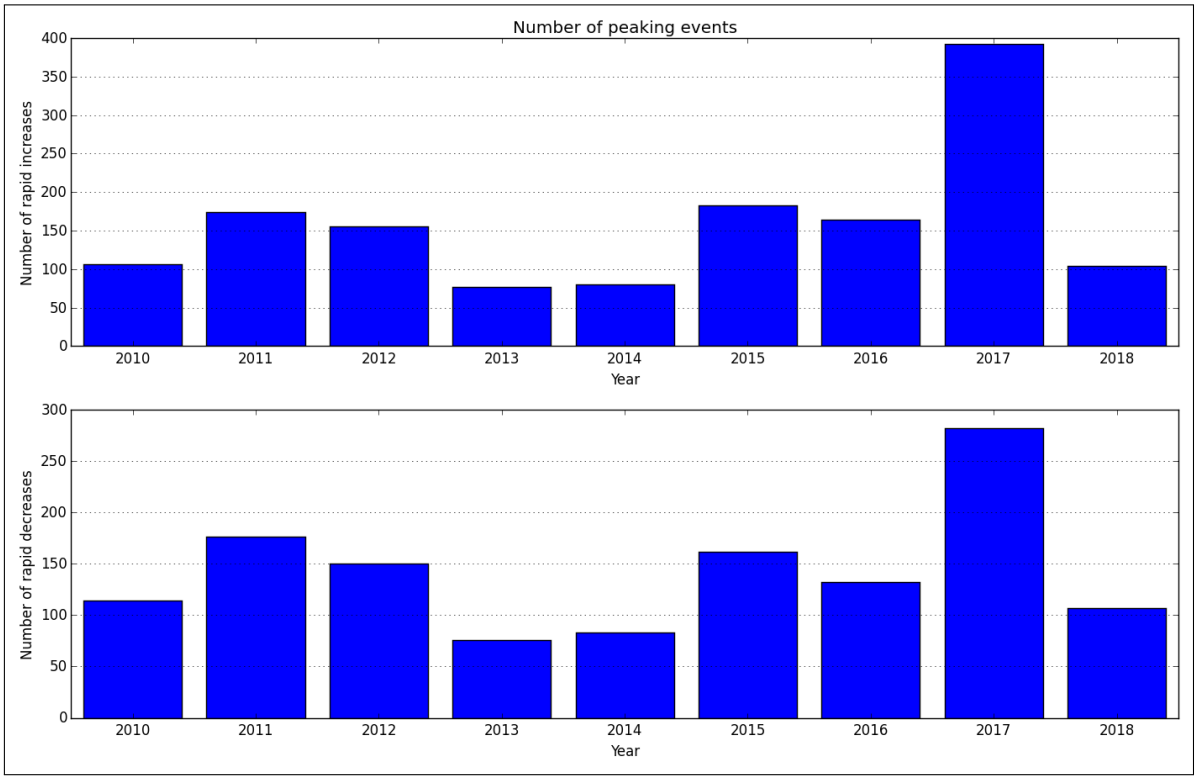

Figure A.24.117: Average annual number of increased/decreased peaks

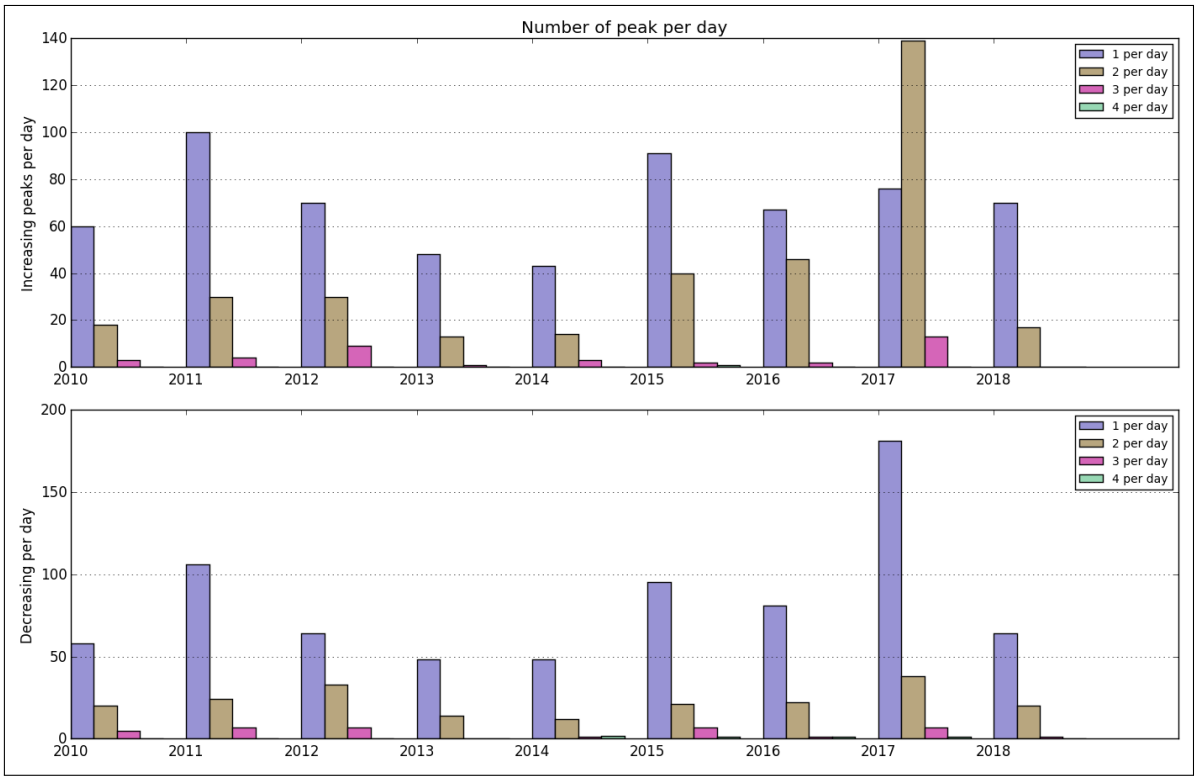

Figure A.24.118: Number of peaks per day

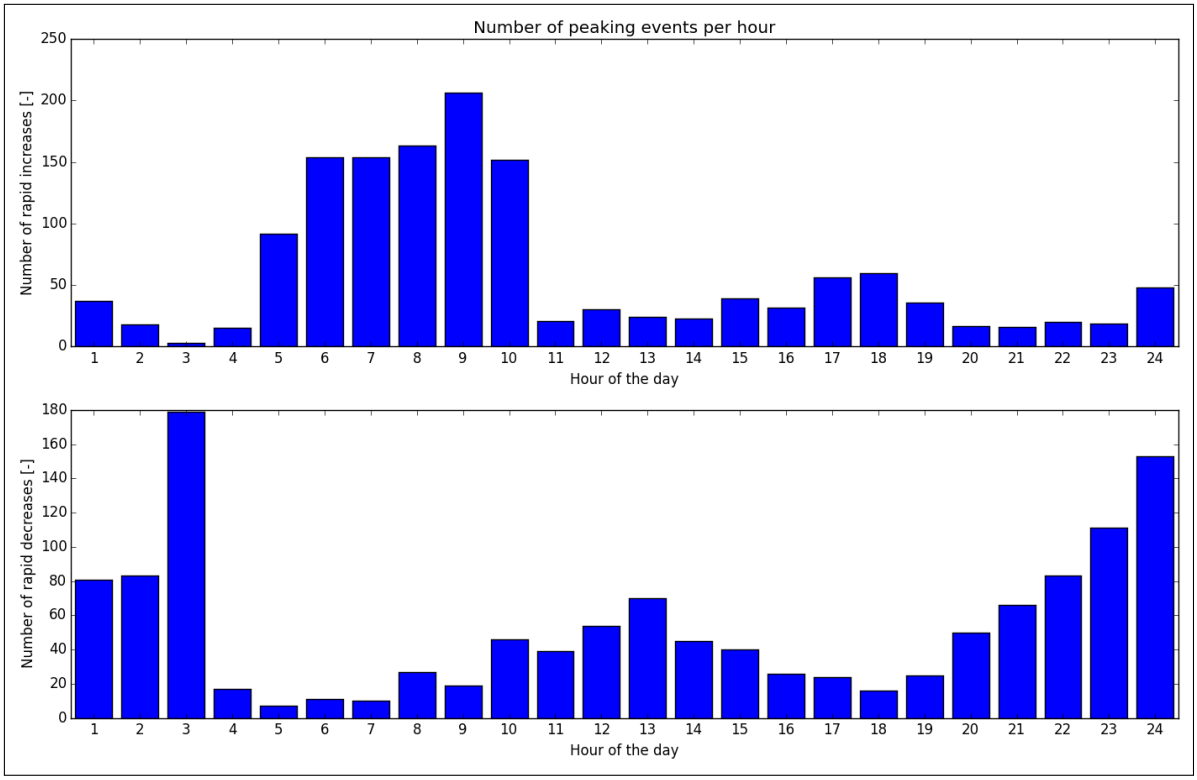

Figure A.24.119: Distribution of peaks throughout day

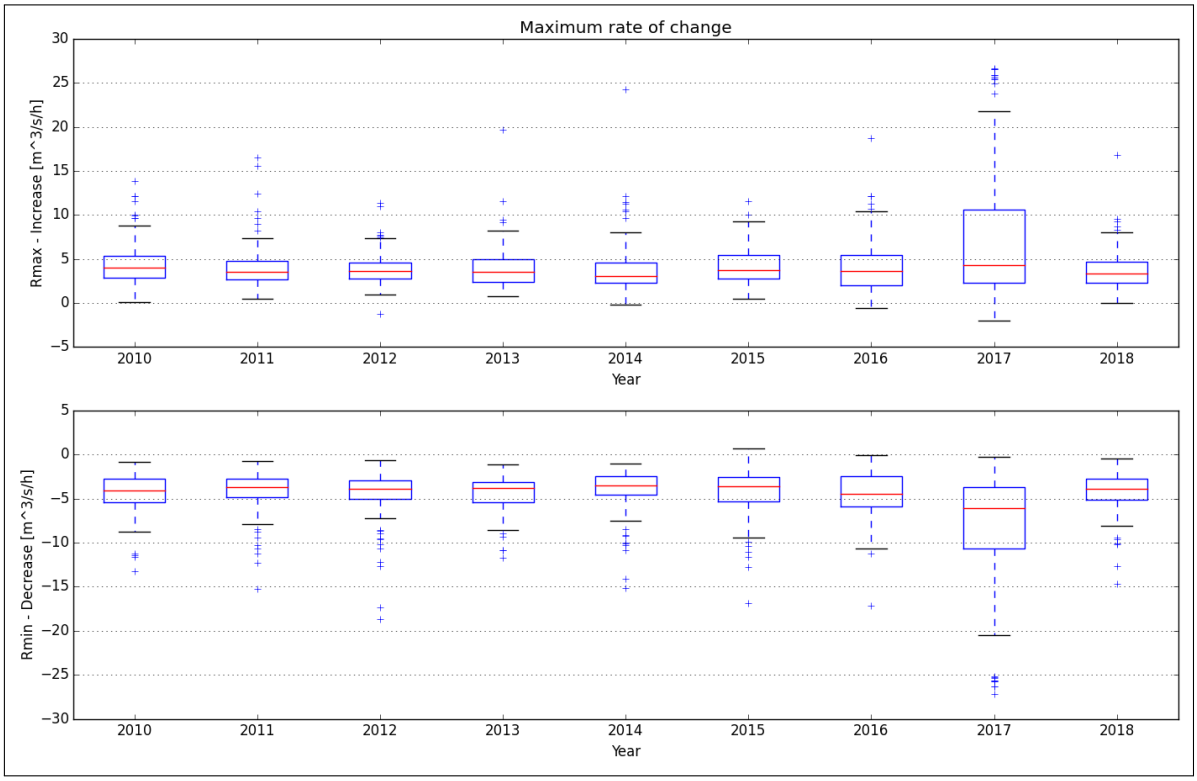

Figure A.24.120: Maximum rate of change

A.25. Grana

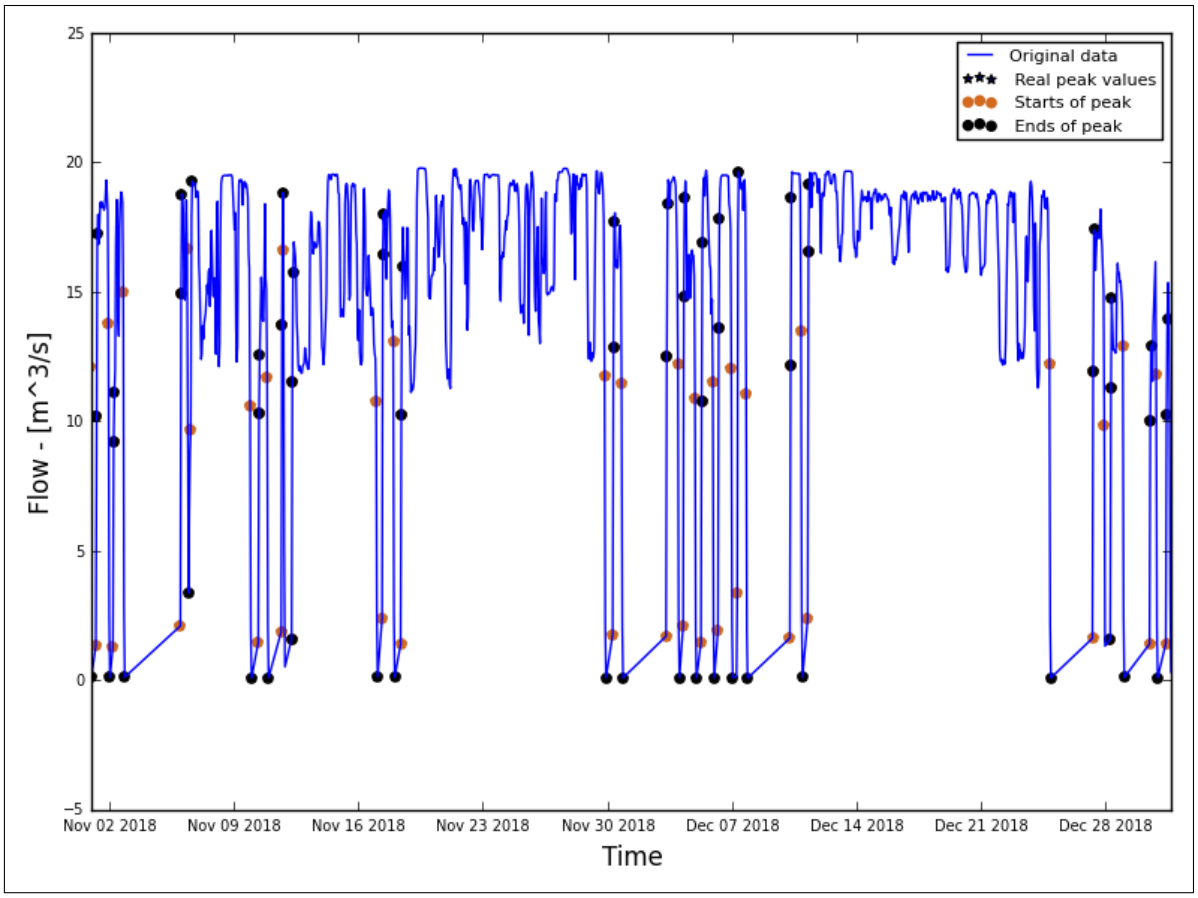

Figure A.25.121: Hydrograph of the last two months of the recorded data

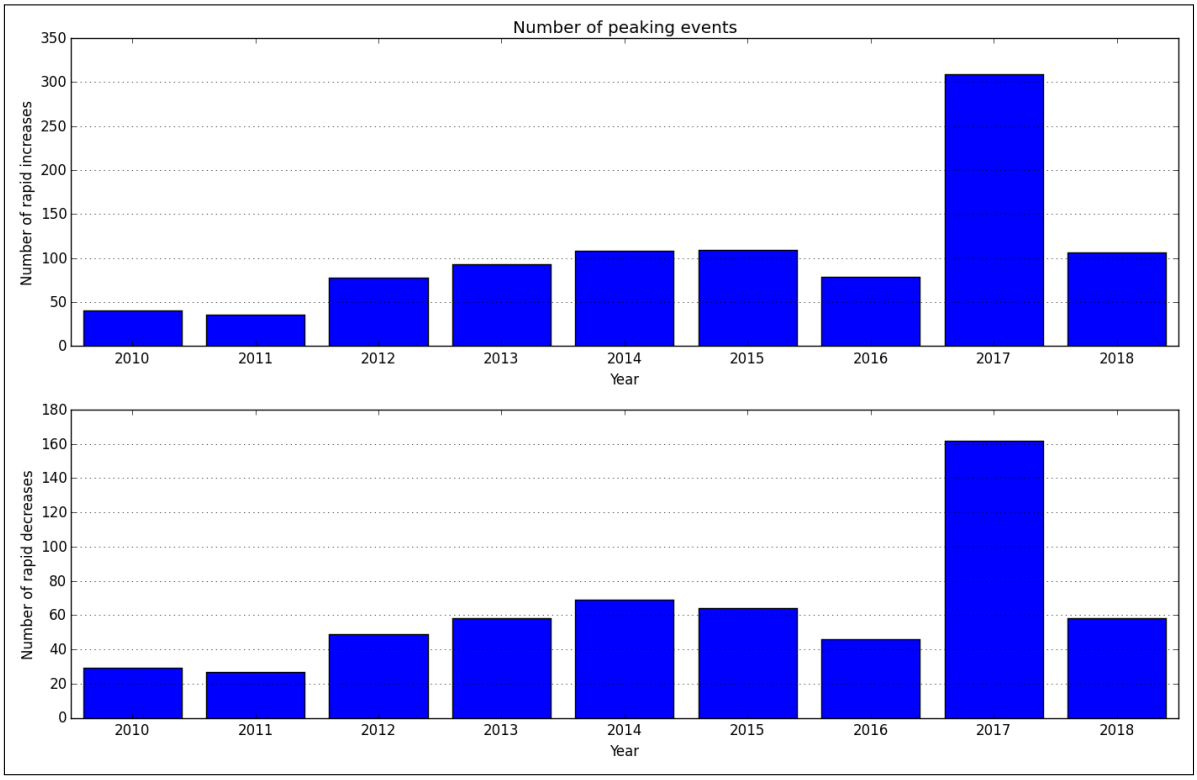

Figure A.25.122: Average annual number of increased/decreased peaks

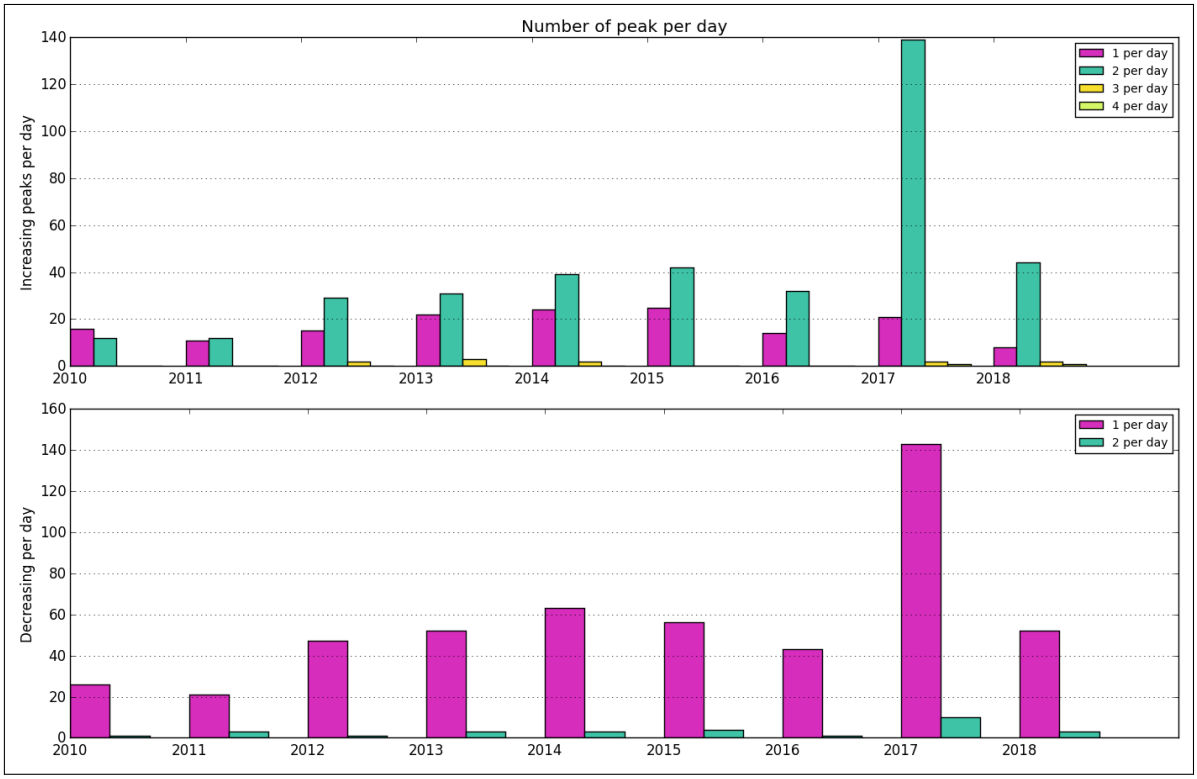

Figure A.25.123: Number of peaks per day

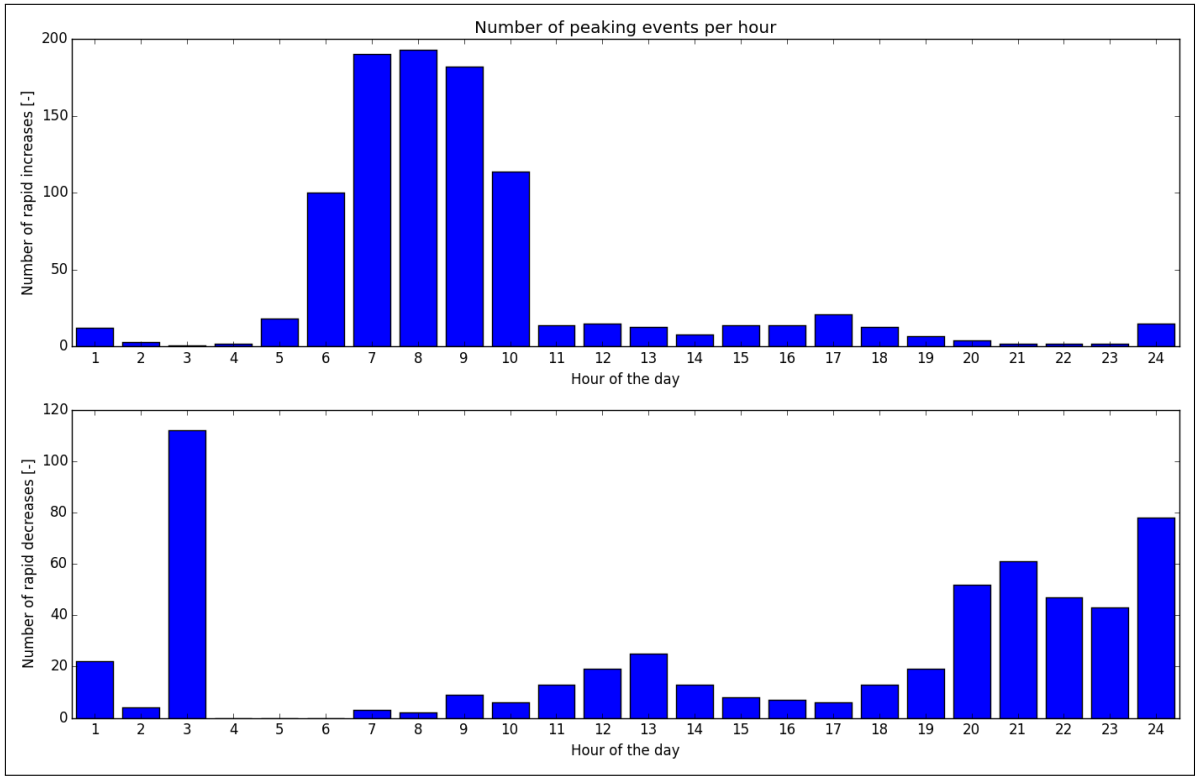

Figure A.25.124: Distribution of peaks throughout day

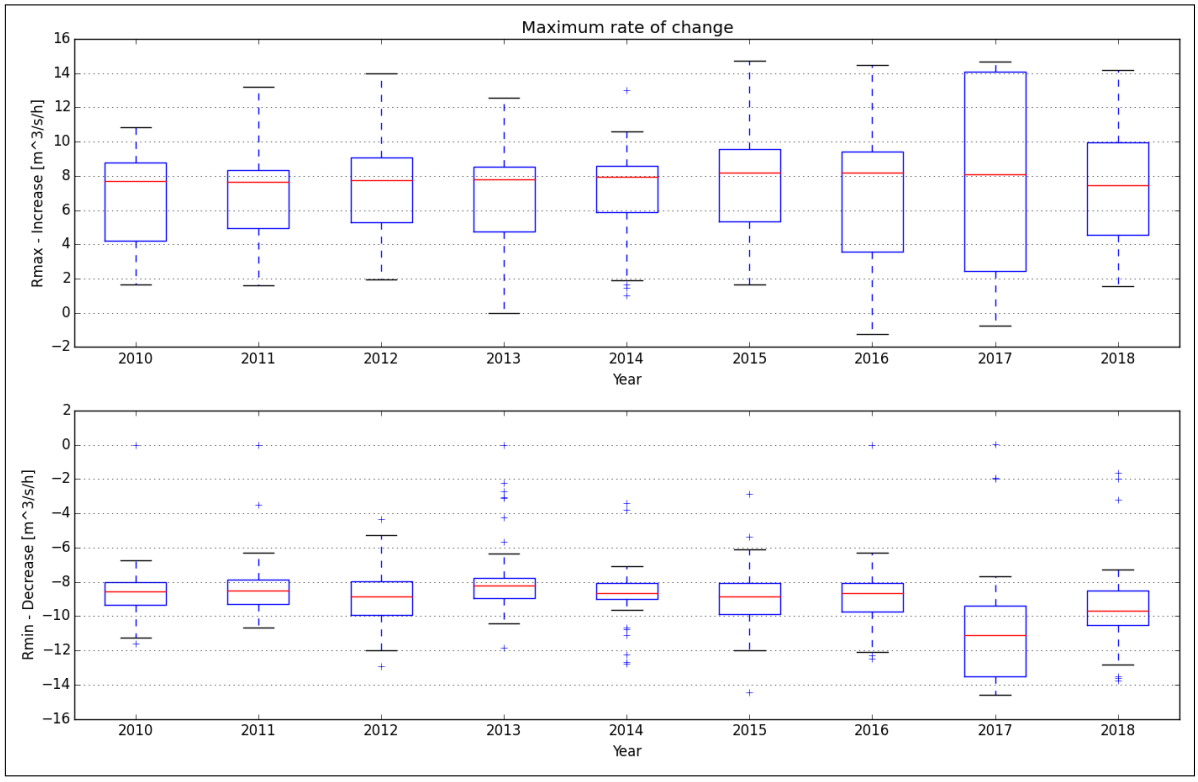

Figure A.25.125: Maximum rate of change

A.26. Litjfossen

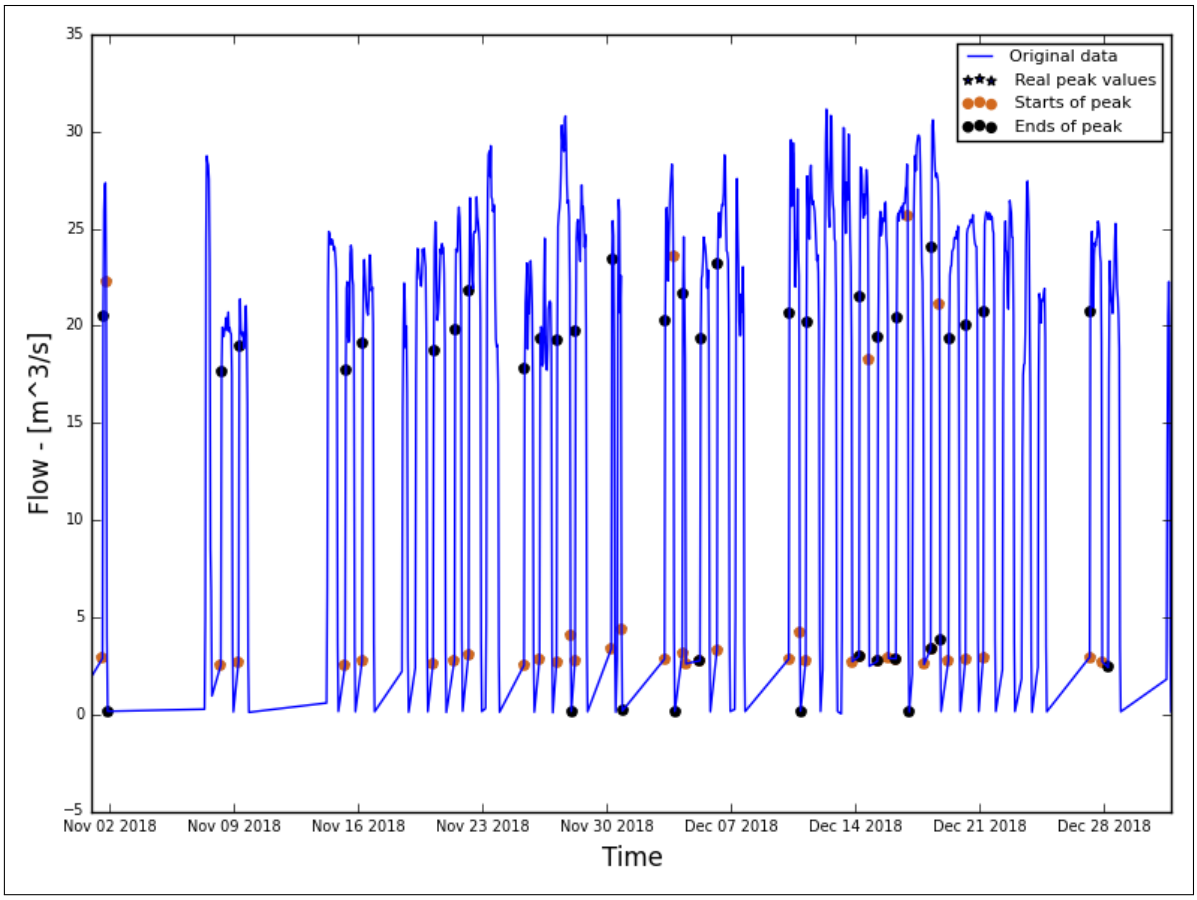

Figure A.26.126: Hydrograph of the last two months of the recorded data

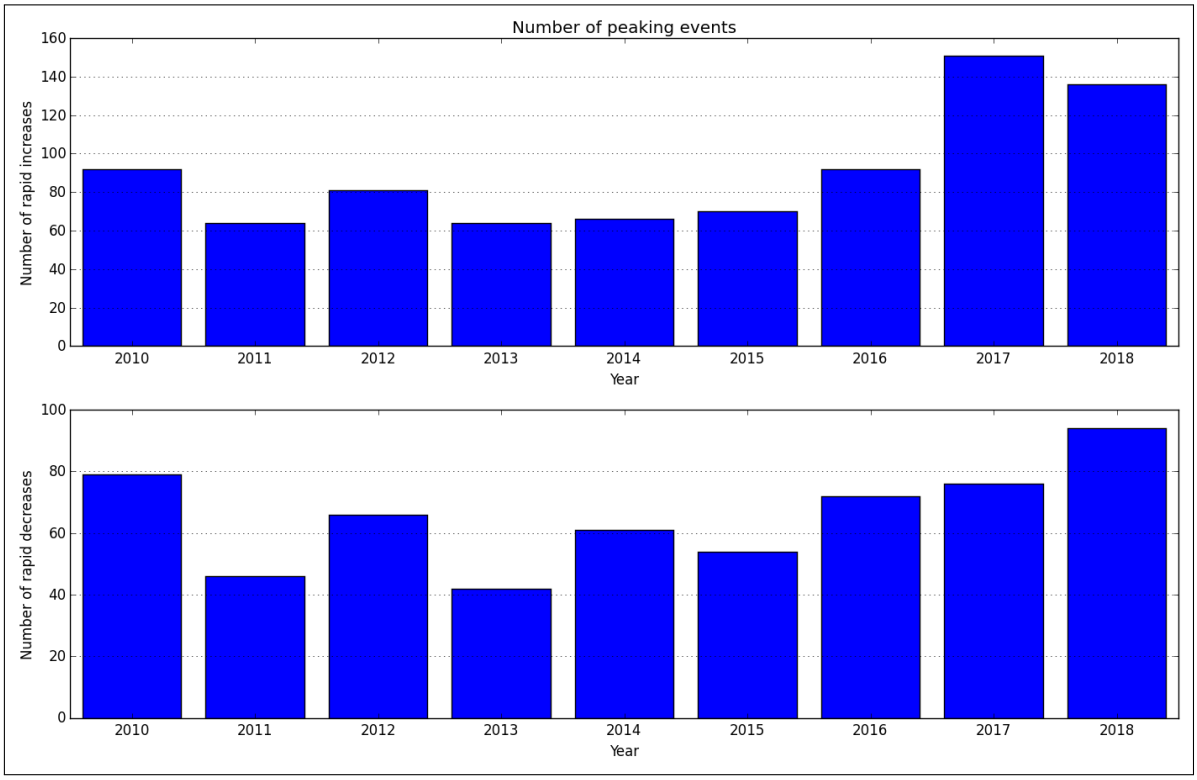

Figure A.26.127: Average annual number of increased/decreased peaks

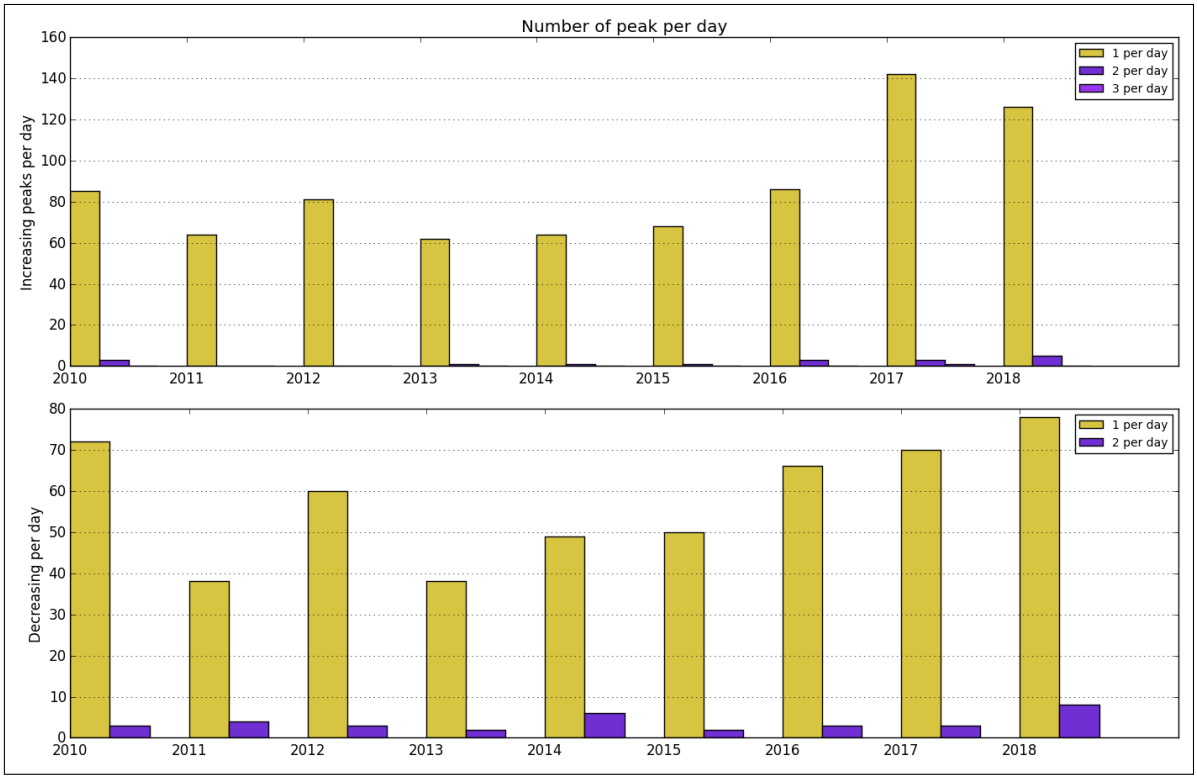

Figure A.26.128: Number of peaks per day

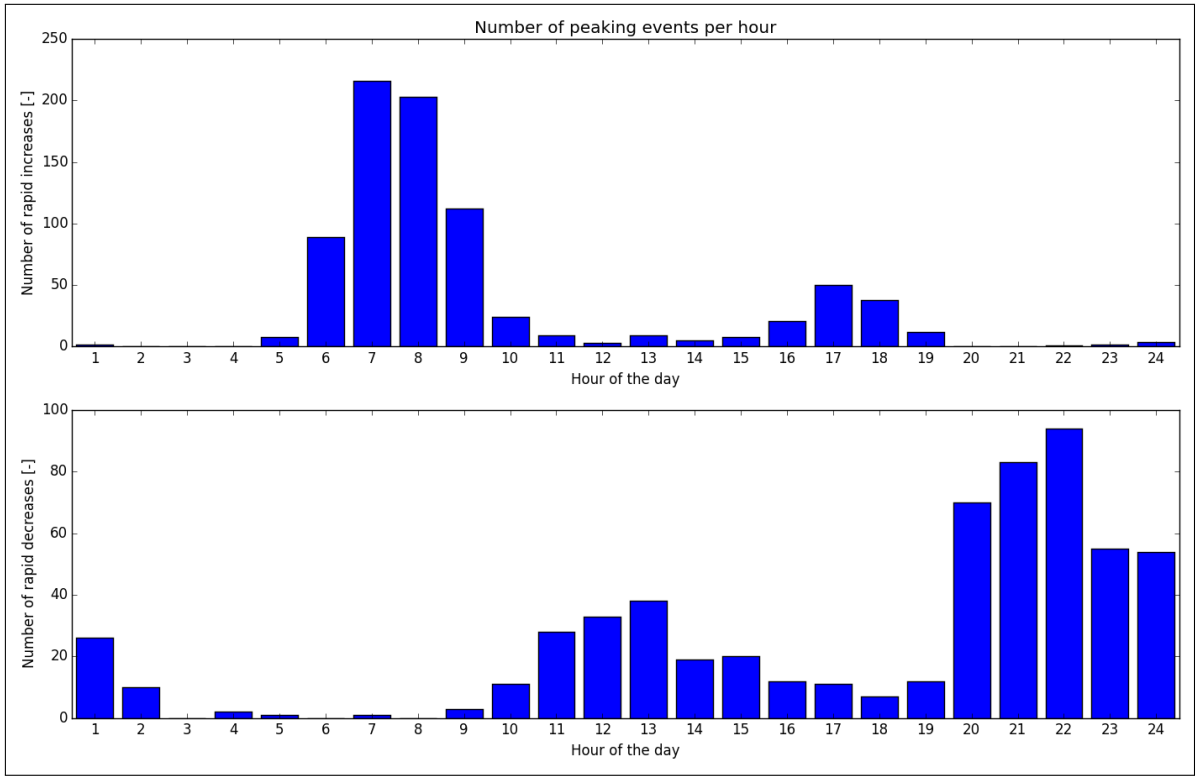

Figure A.26.129: Distribution of peaks throughout day

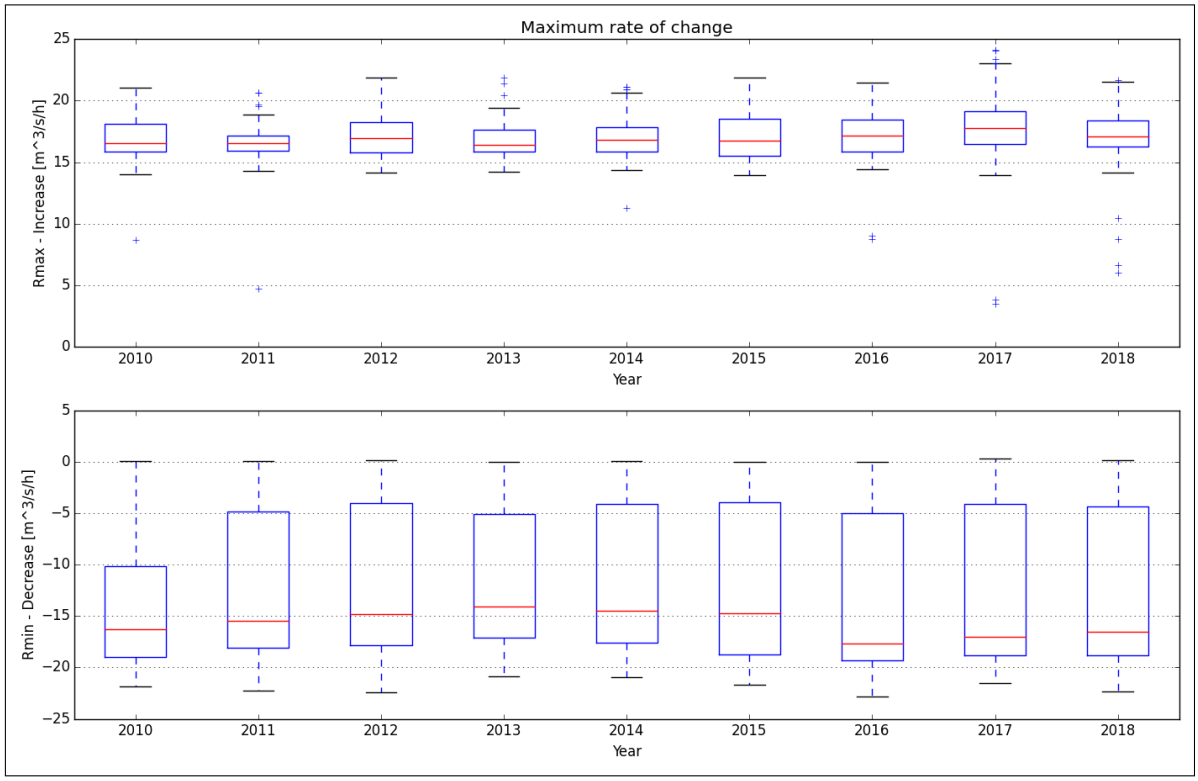

Figure A.26.130: Maximum rate of change

A.27. Ulset

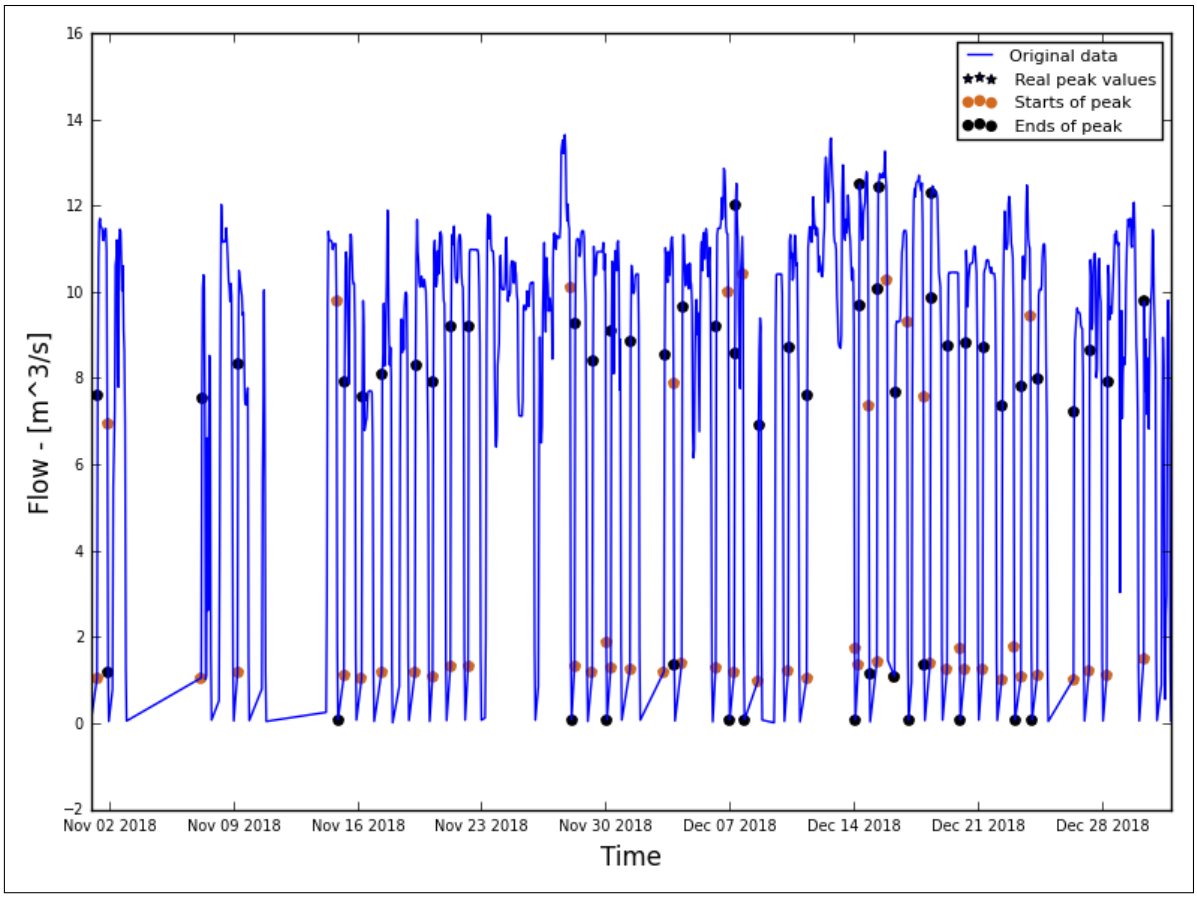

Figure A.27.131: Hydrograph of the last two months of the recorded data

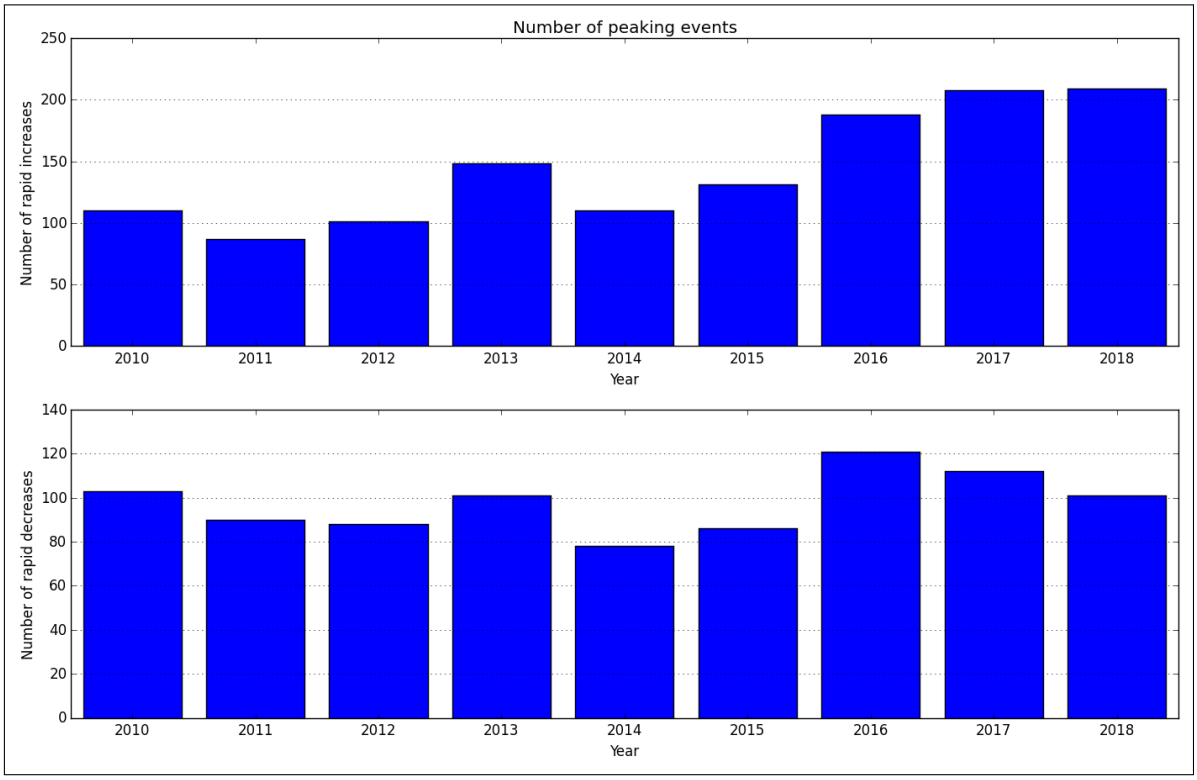

Figure A.27.132: Average annual number of increased/decreased peaks

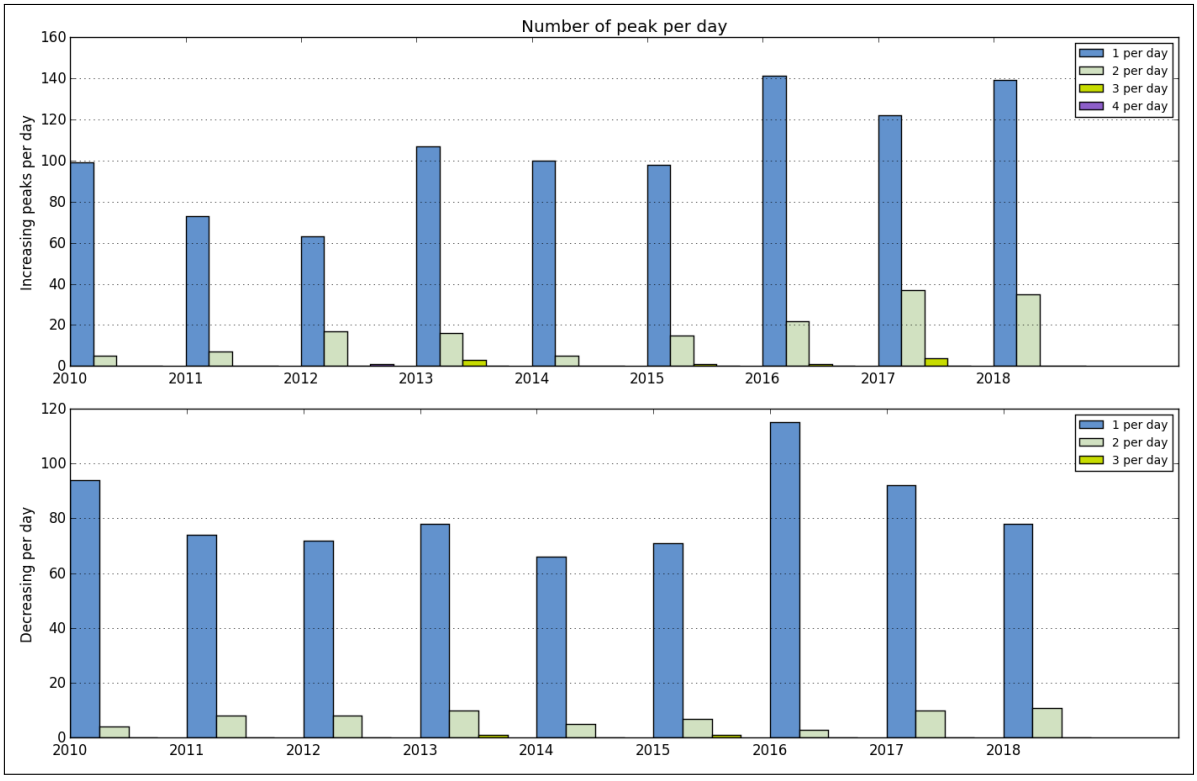

Figure A.27.133: Number of peaks per day

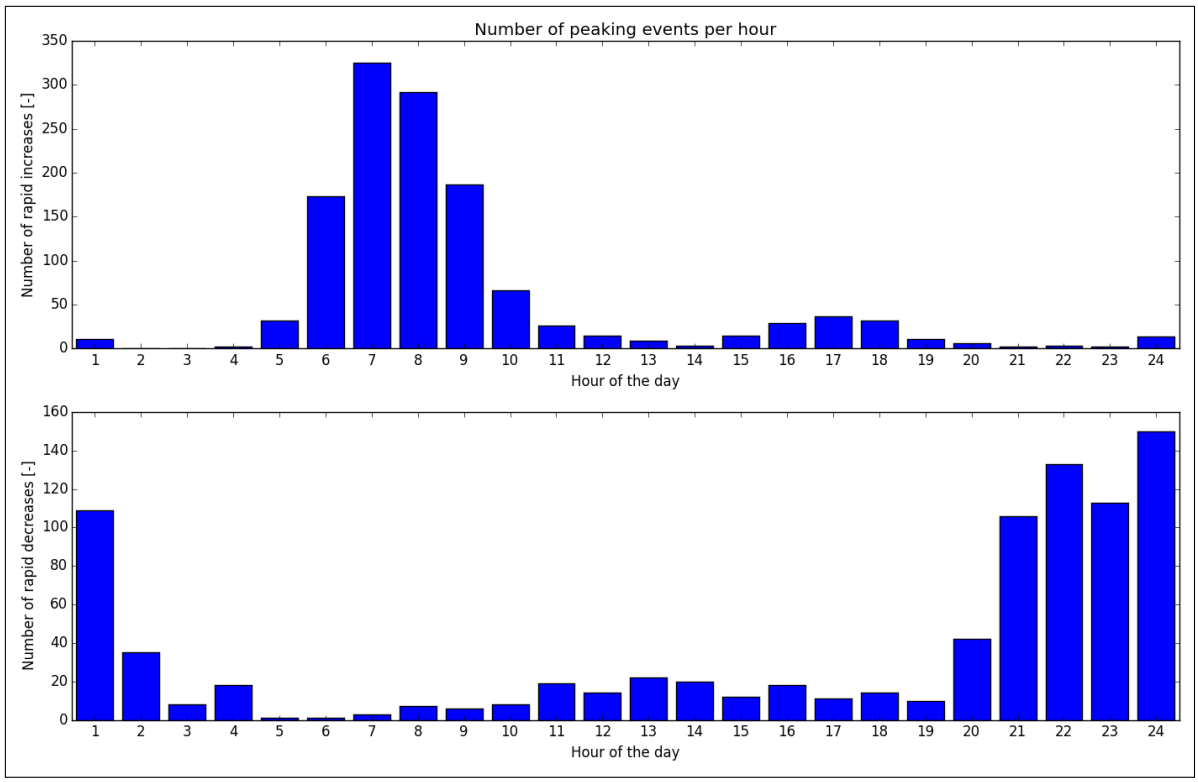

Figure A.27.134: Distribution of peaks throughout day

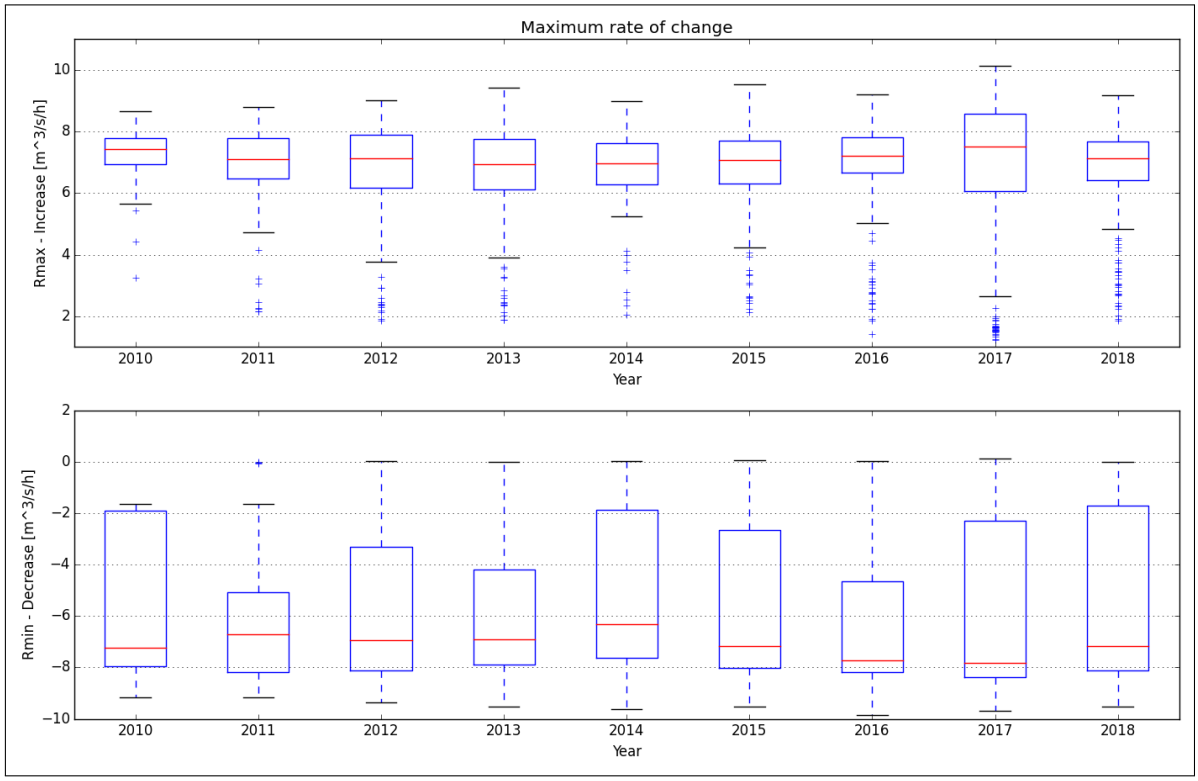

Figure A.27.135: Maximum rate of change

A.28. Sokna

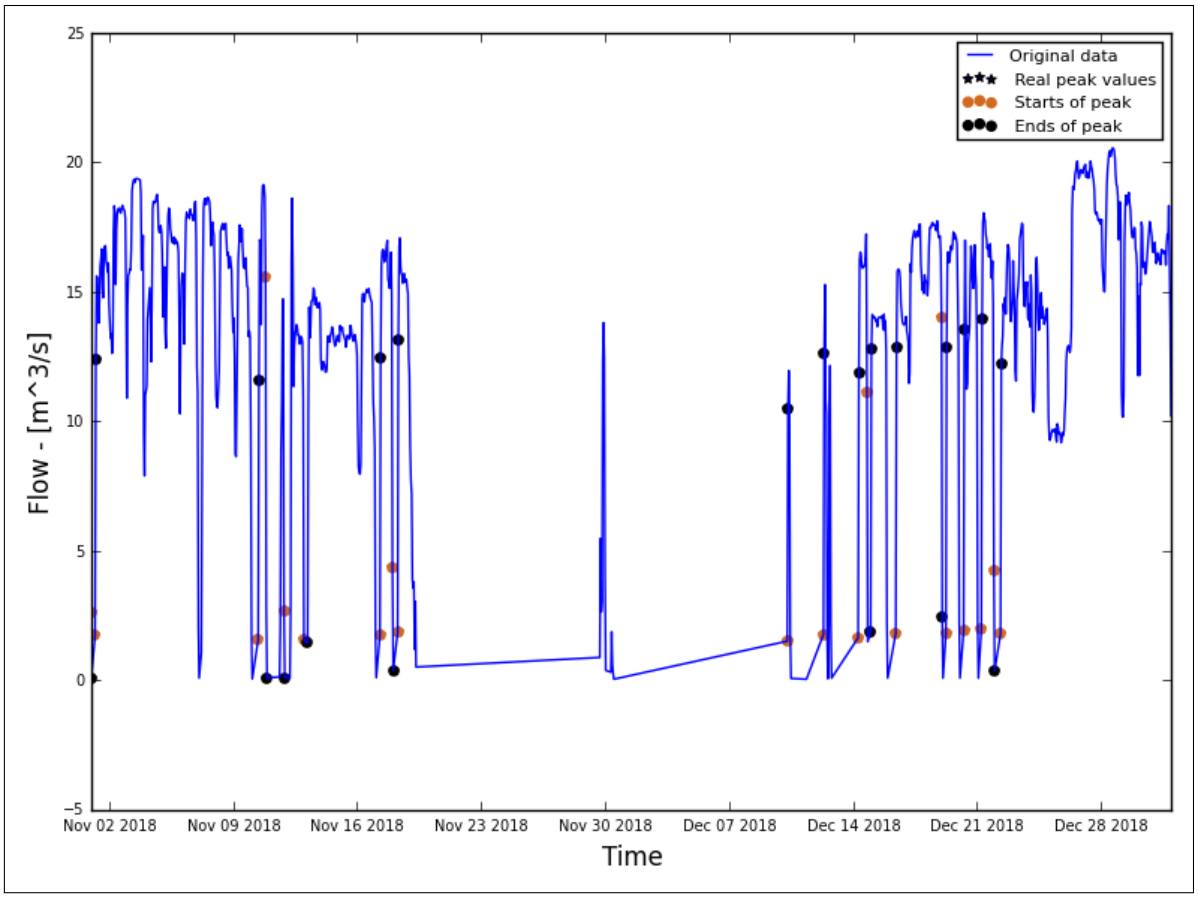

Figure A.28.136: Hydrograph of the last two months of the recorded data

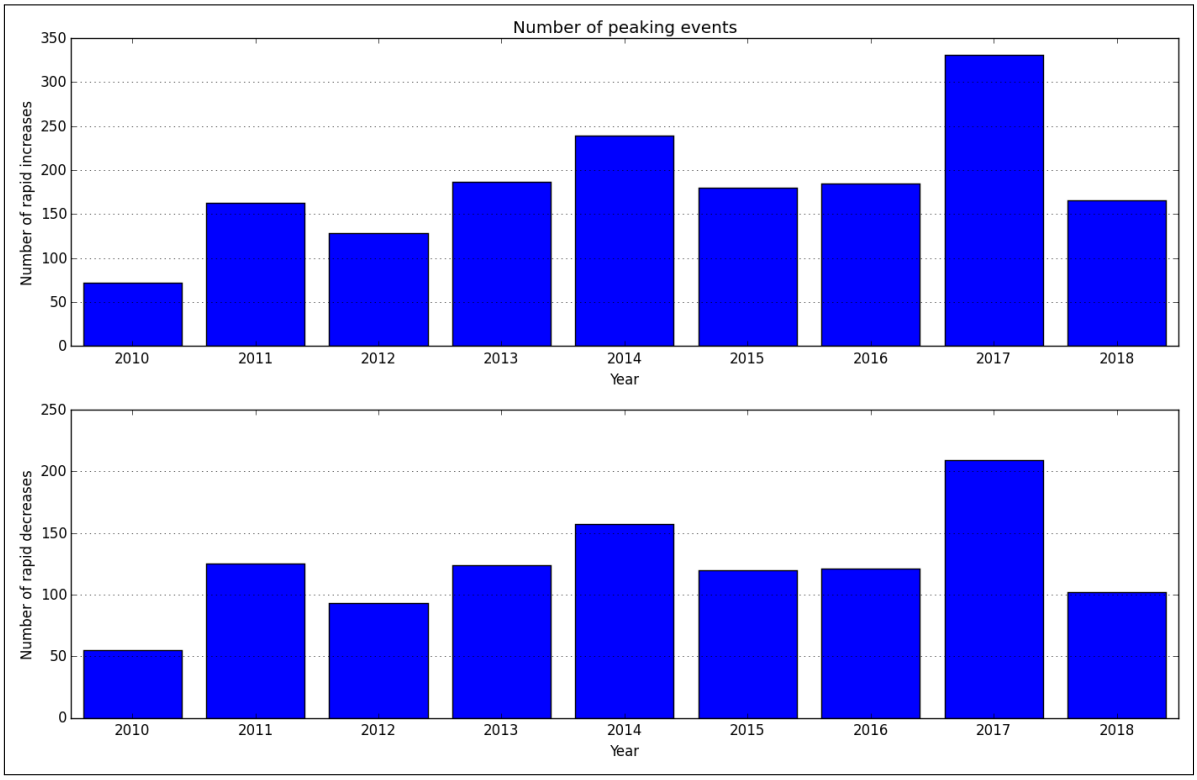

Figure A.28.137: Average annual number of increased/decreased peaks

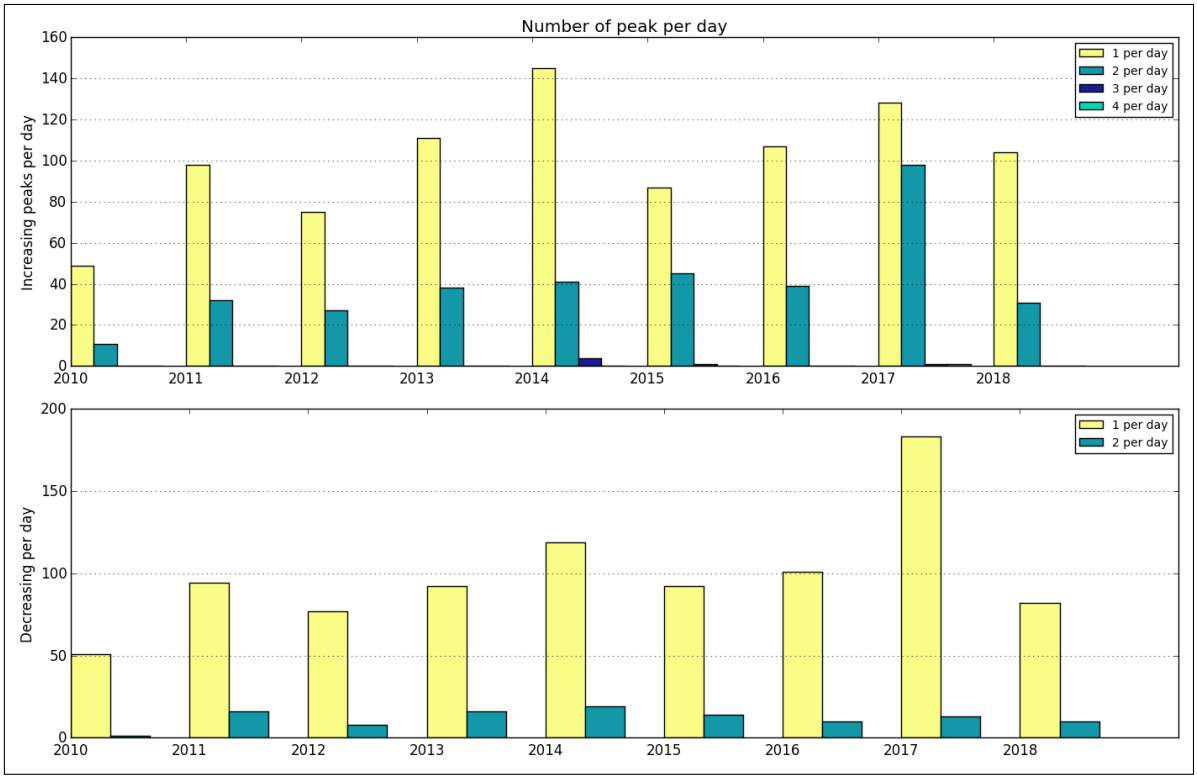

Figure A.28.138: Number of peaks per day

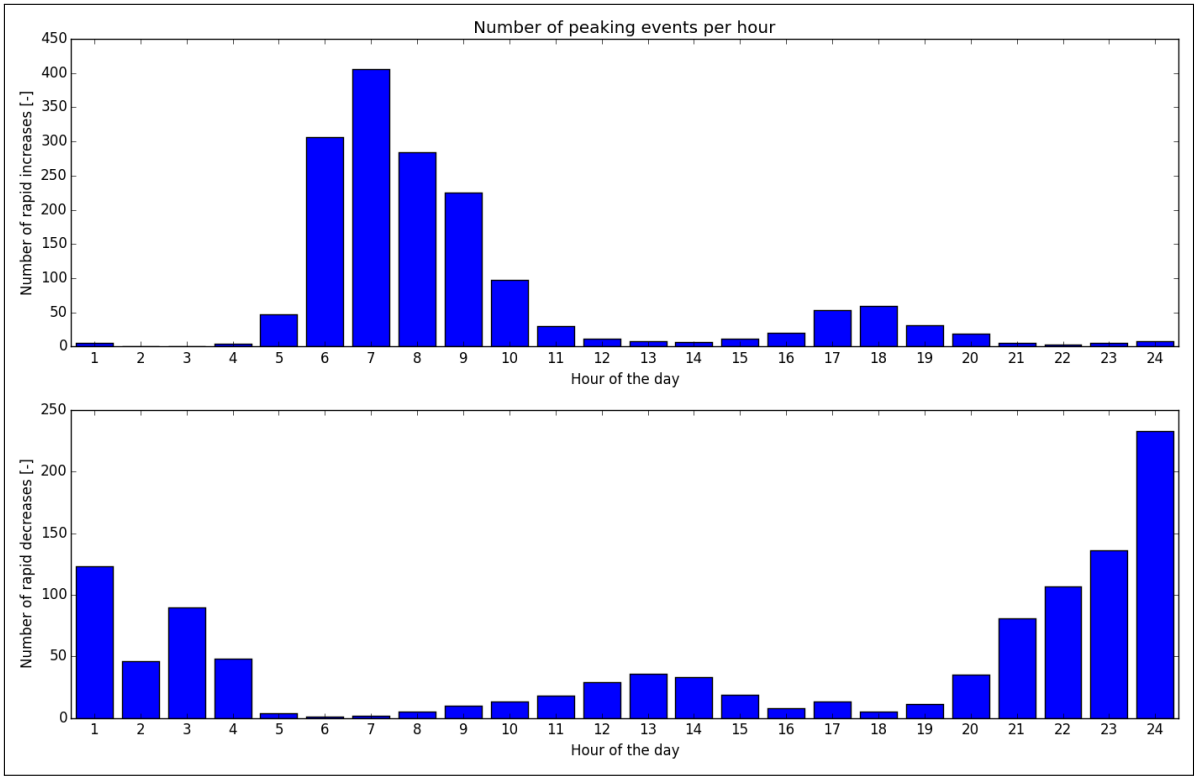

Figure A.28.139: Distribution of peaks throughout day

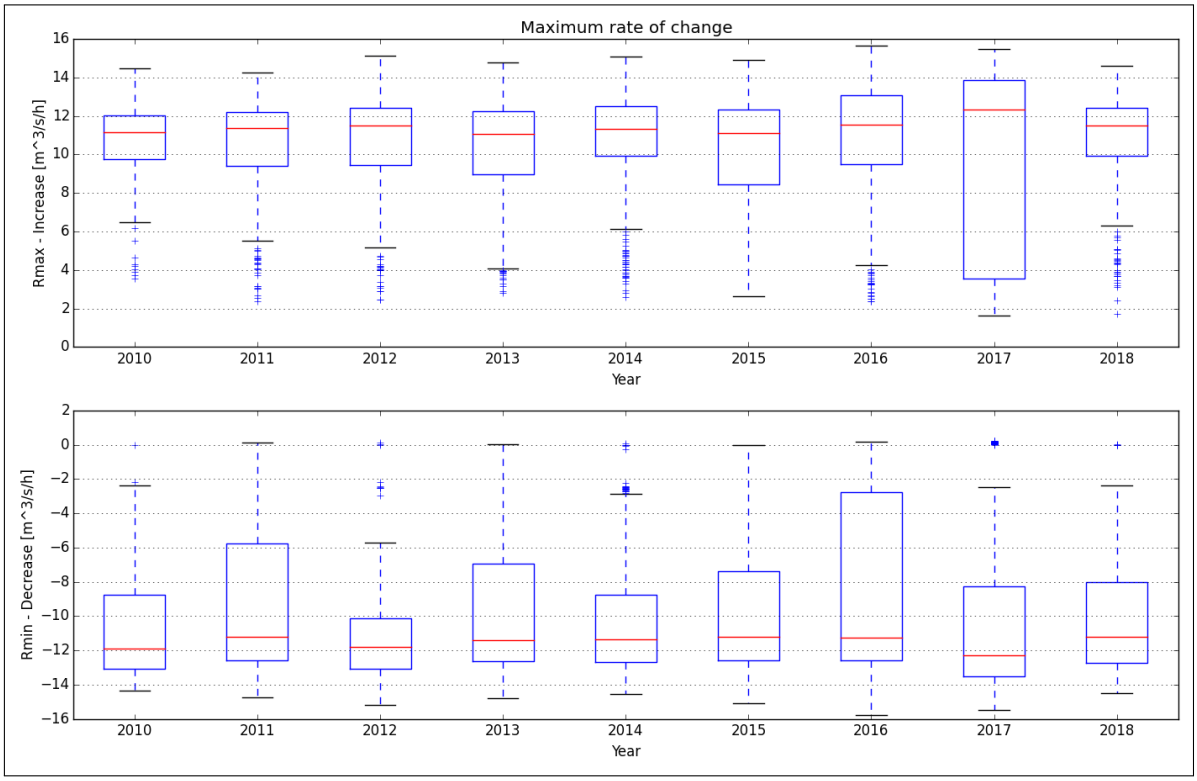

Figure A.28.140: Maximum rate of change

A.29. Fjaermfossen

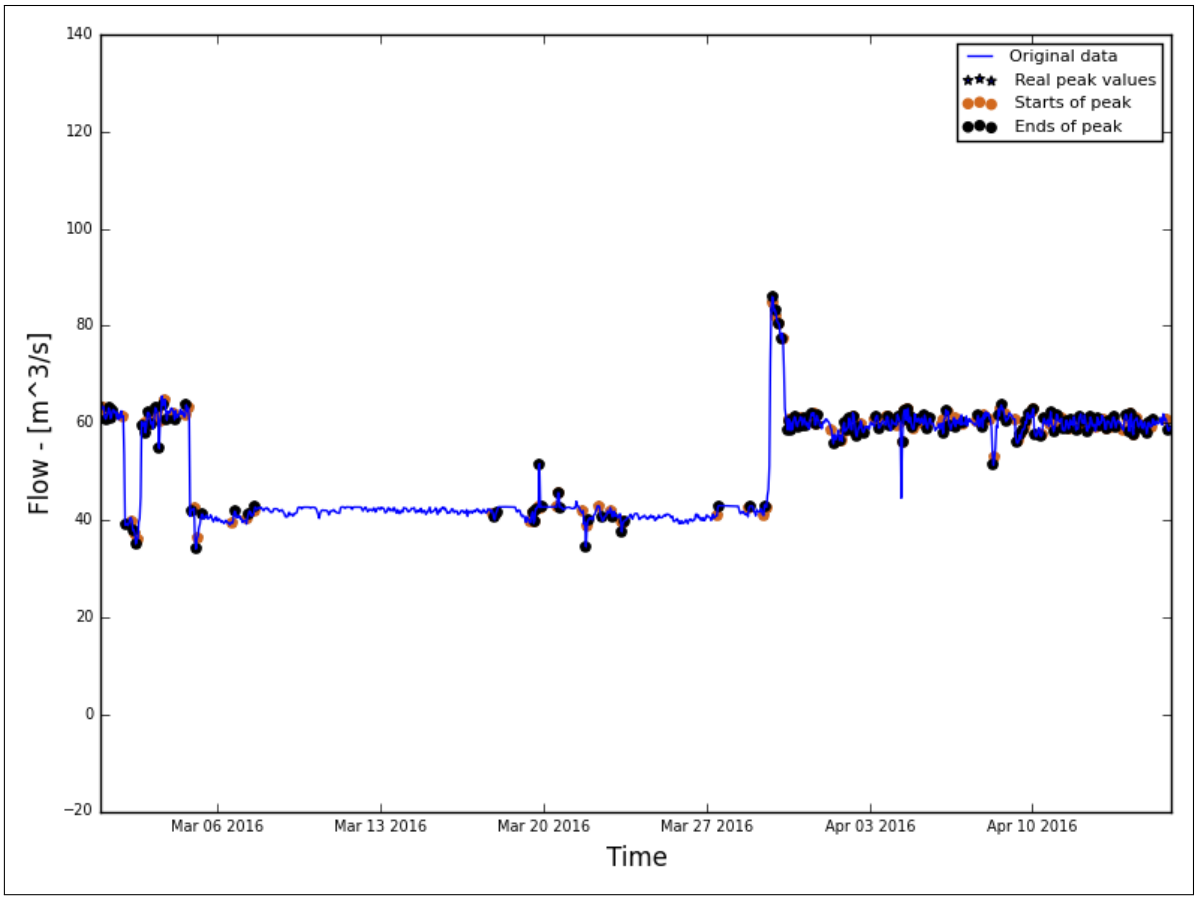

Figure A.29.141: Hydrograph of the last two months of the recorded data

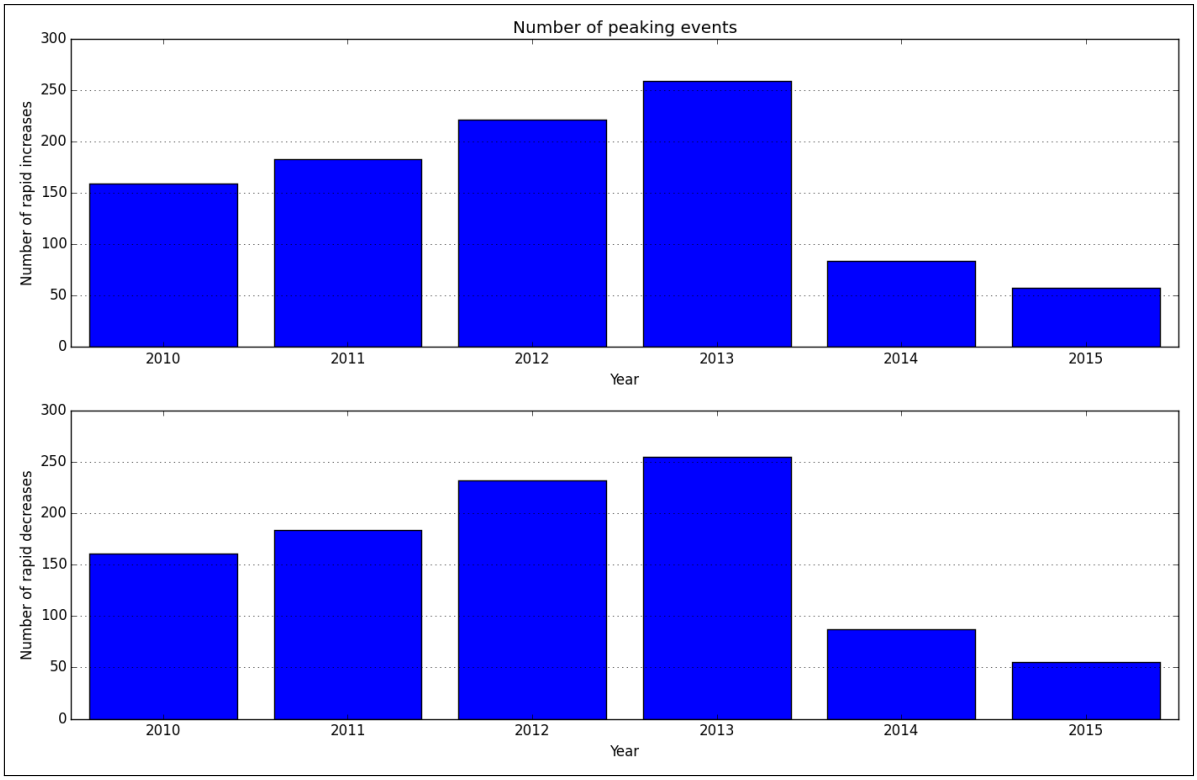

Figure A.29.142: Average annual number of increased/decreased peaks

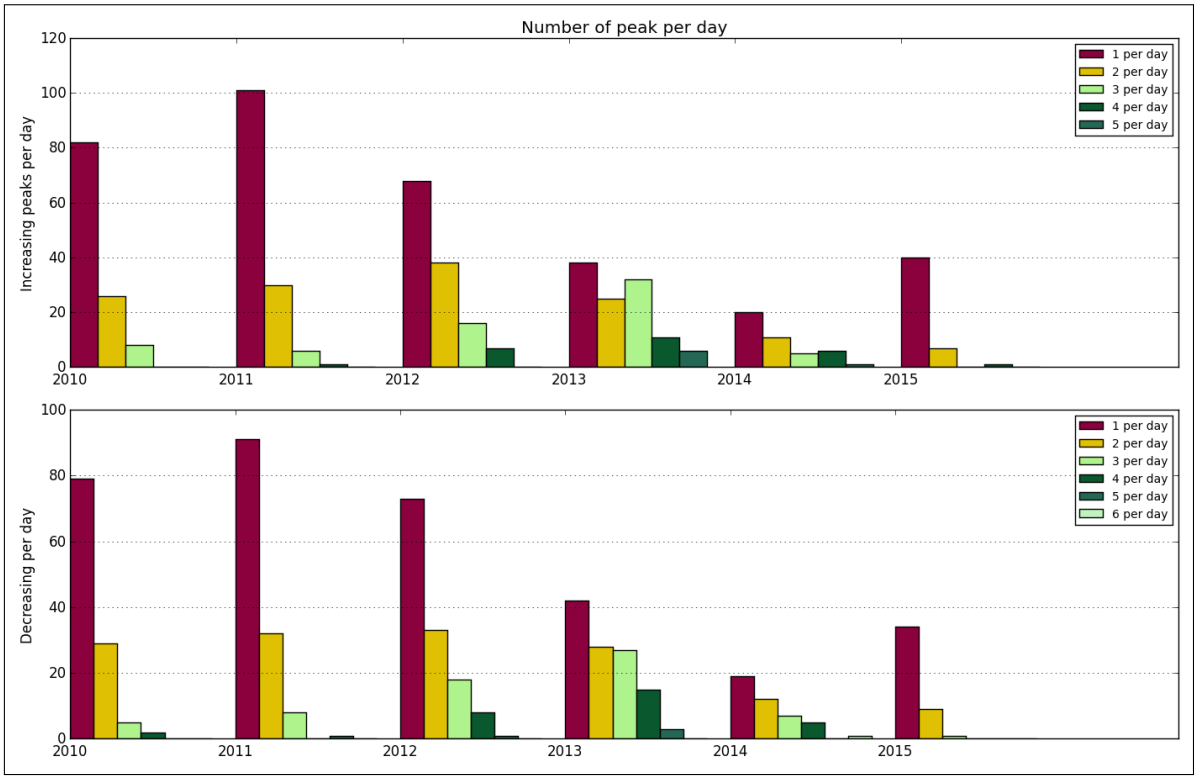

Figure A.29.143: Number of peaks per day

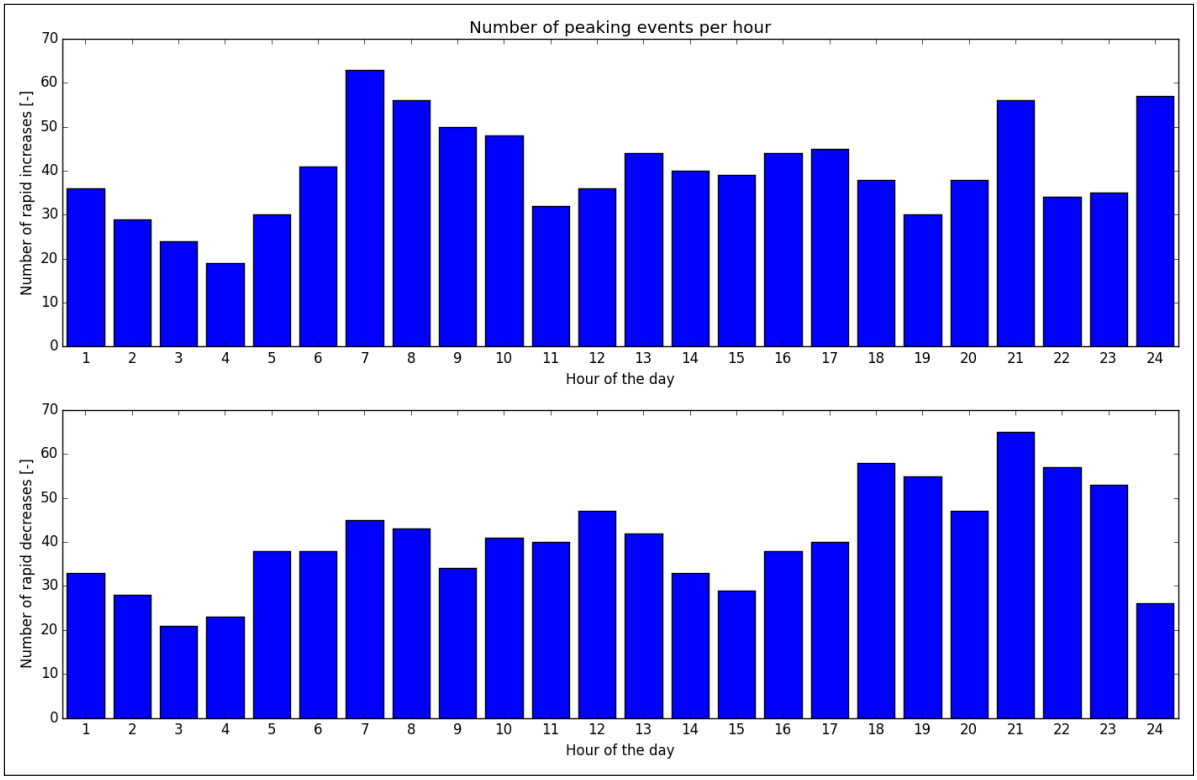

Figure A.29.144: Distribution of peaks throughout day

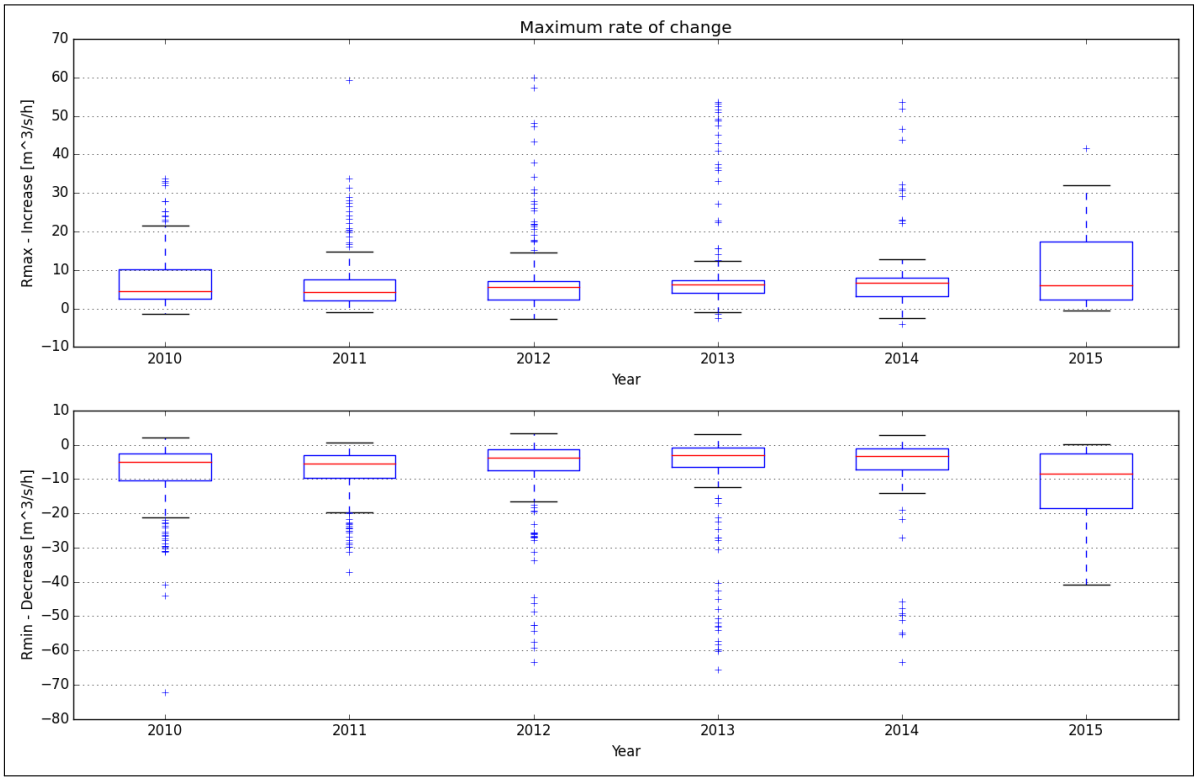

Figure A.29.145: Maximum rate of change

A.30. Bratsberg krv

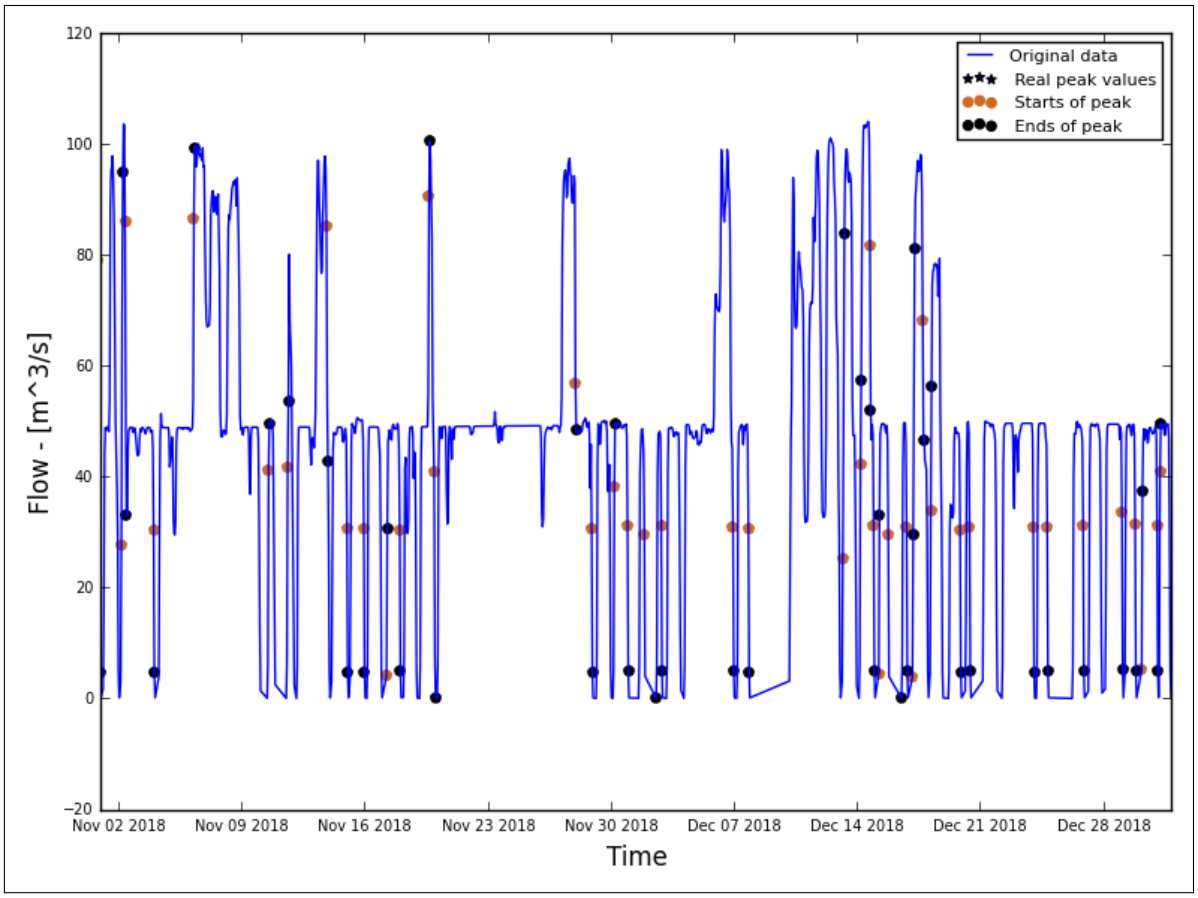

Figure A.30.146: Hydrograph of the last two months of the recorded data

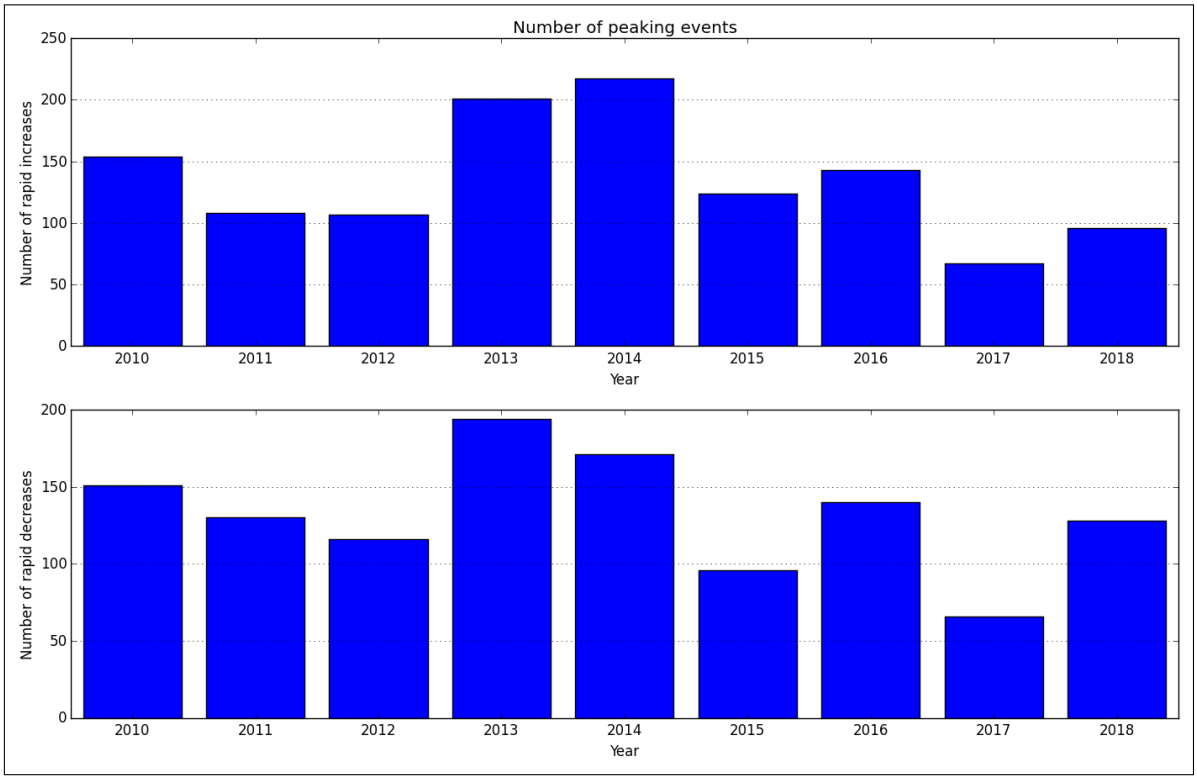

Figure A.30.147: Average annual number of increased/decreased peaks

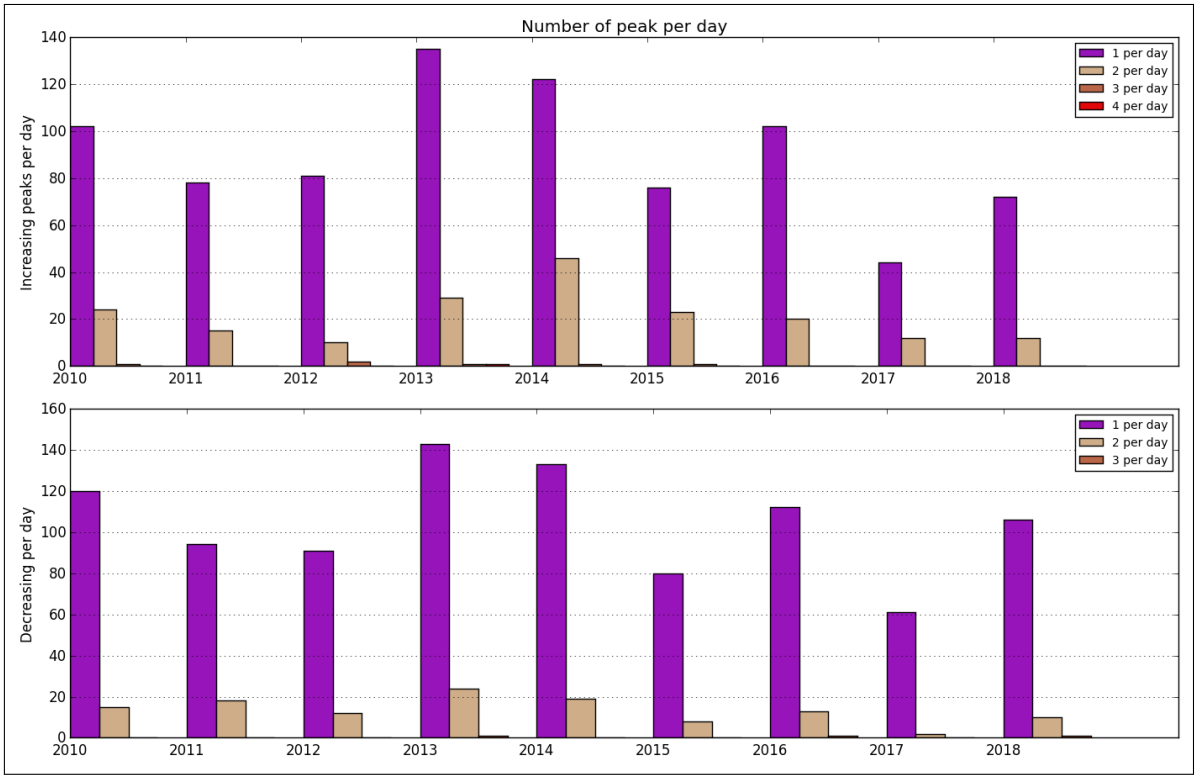

Figure A.30.148: Number of peaks per day

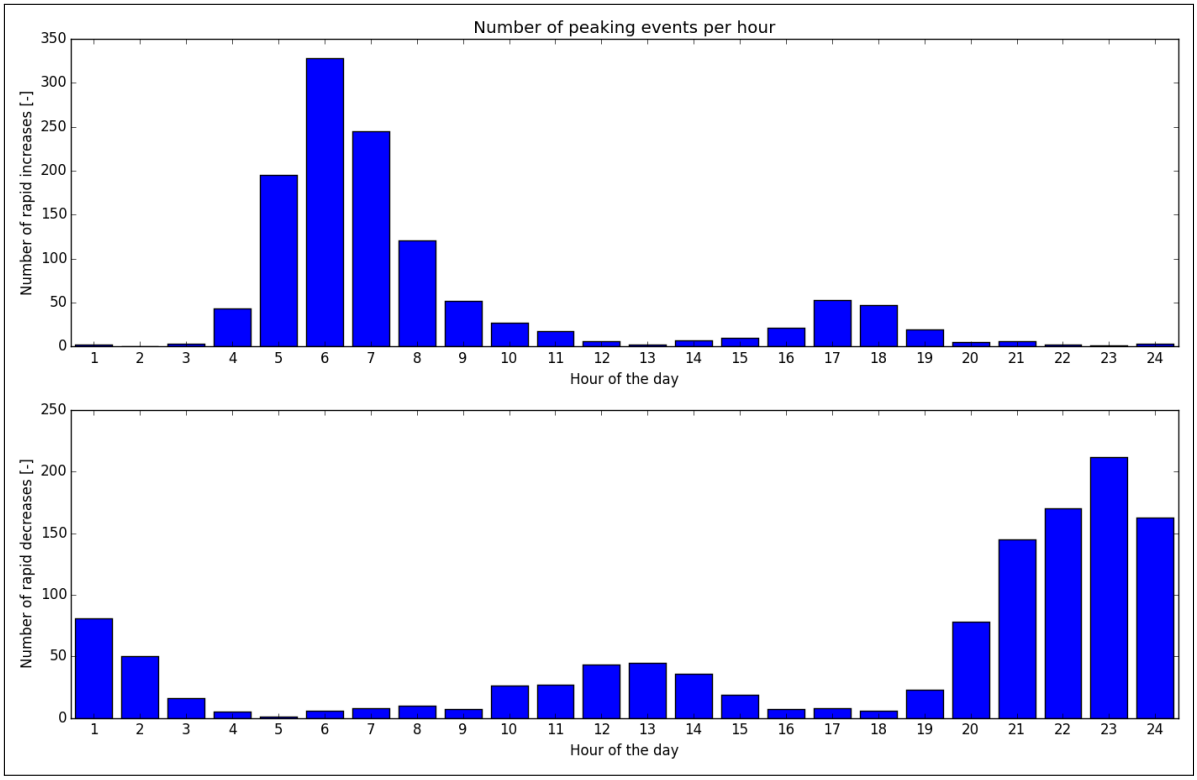

Figure A.30.149: Distribution of peaks throughout day

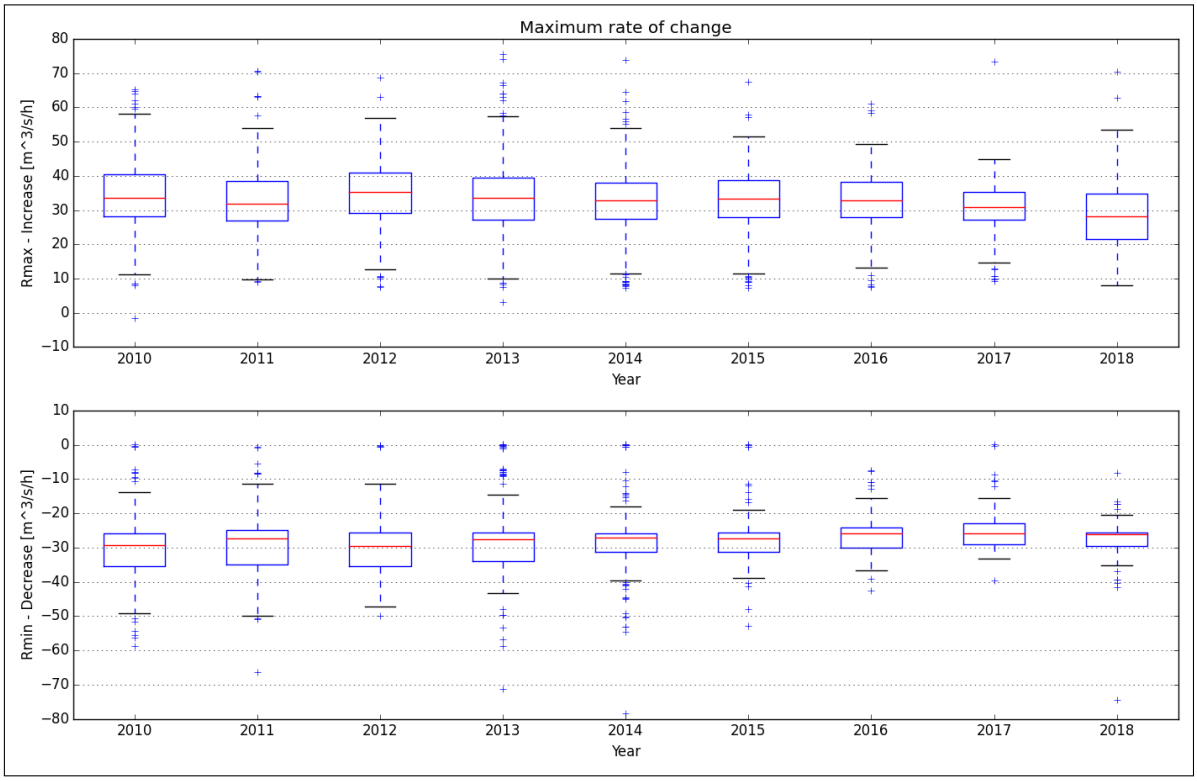

Figure A.30.150: Maximum rate of change

A.31. Meråker kraftverk

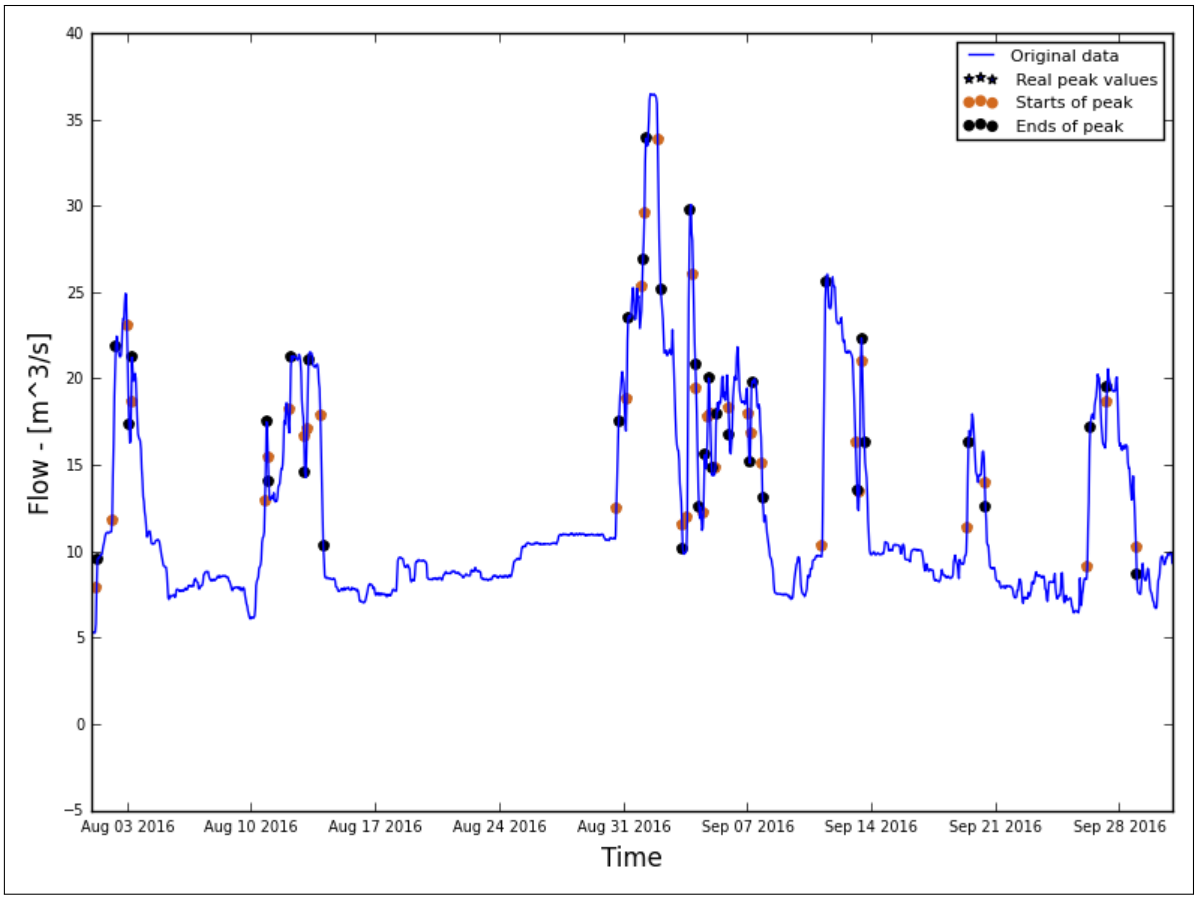

Figure A.31.151: Hydrograph of the last two months of the recorded data

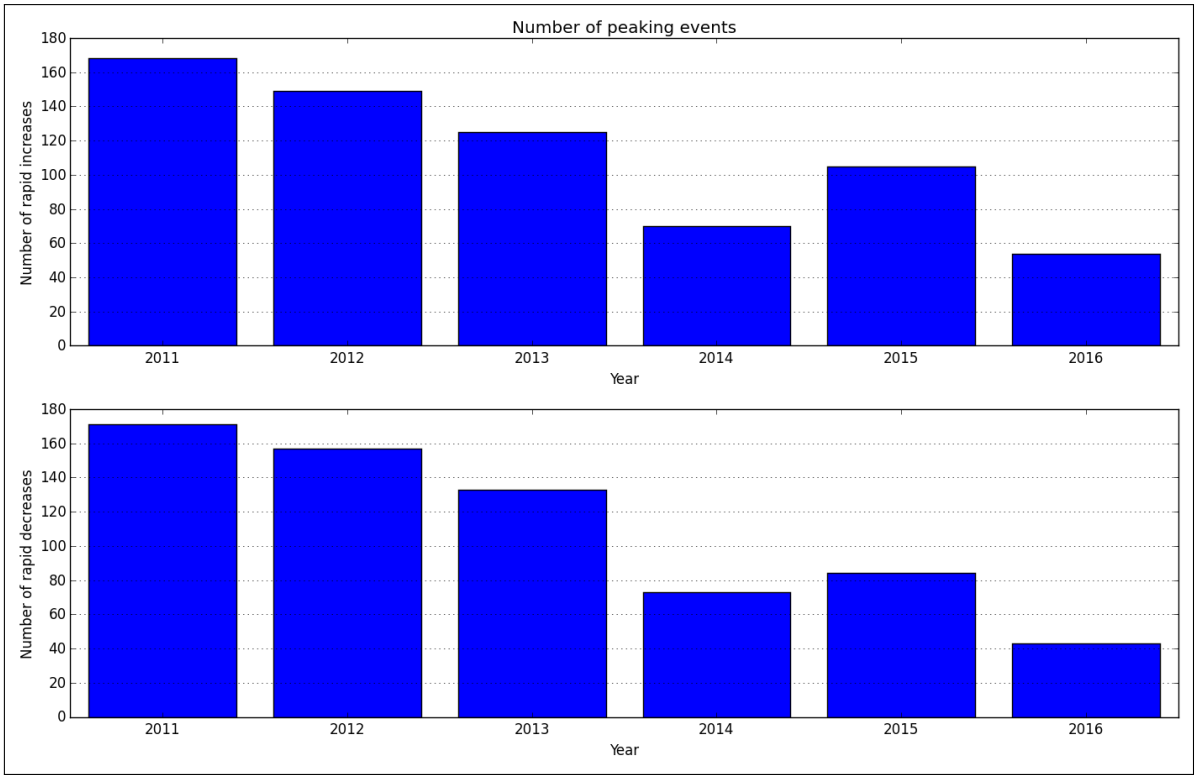

Figure A.31.152: Average annual number of increased/decreased peaks

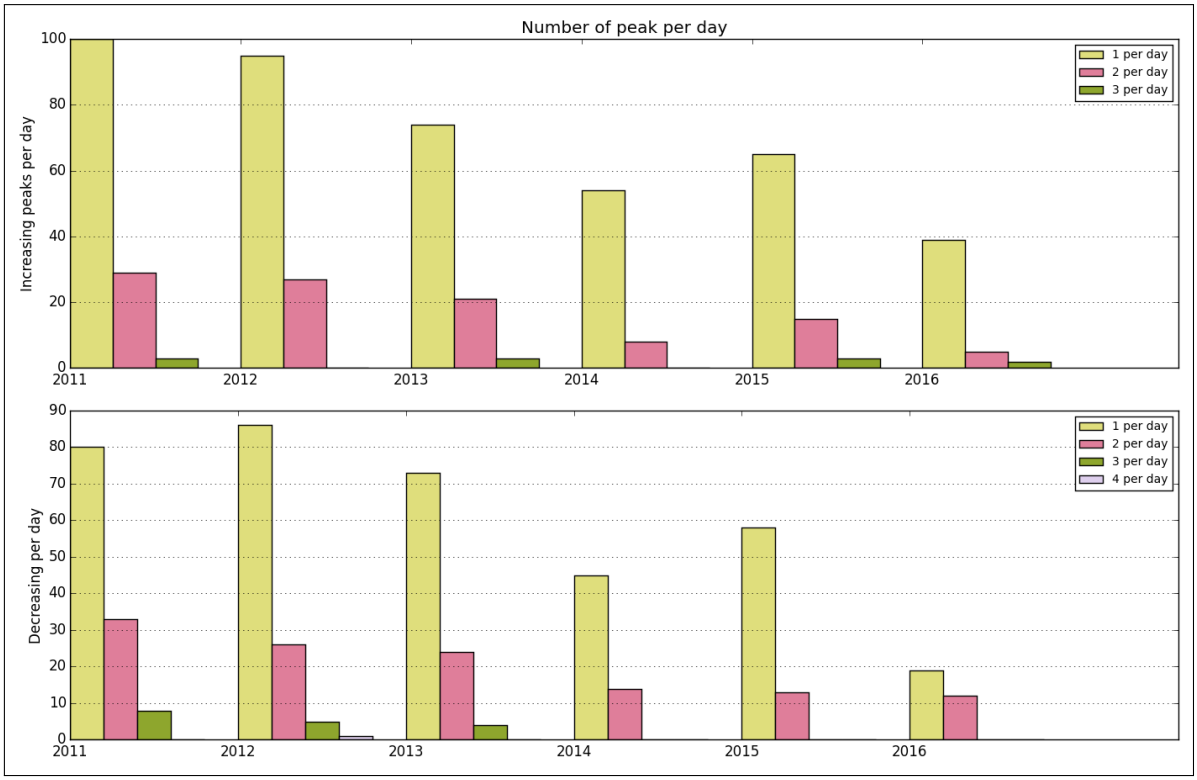

Figure A.31.153: Number of peaks per day

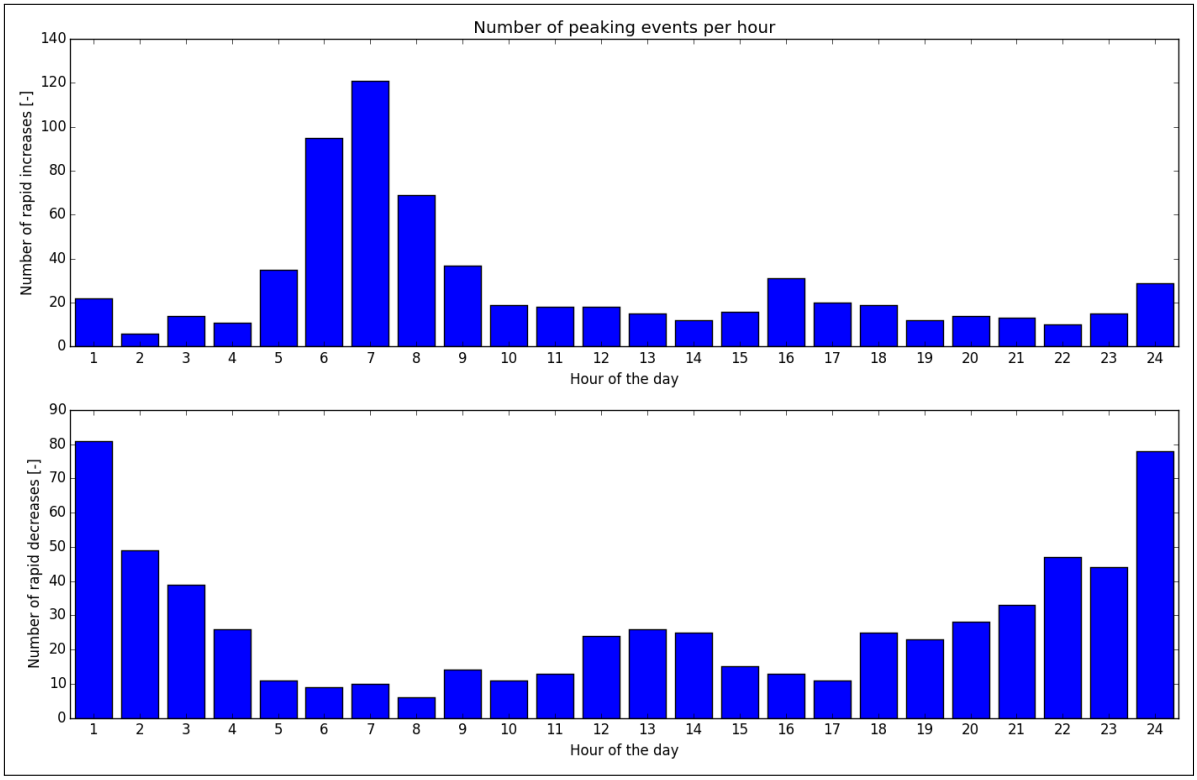

Figure A.31.154: Distribution of peaks throughout day

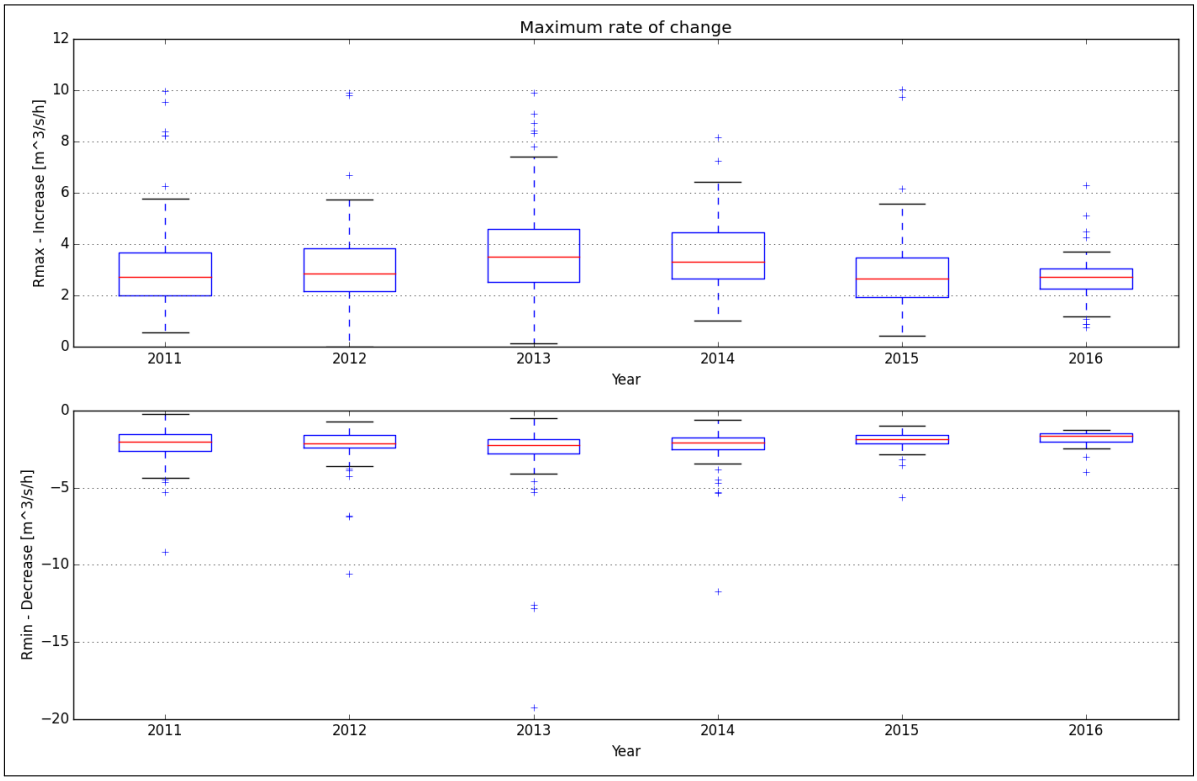

Figure A.31.155: Maximum rate of change

A.32. Follafoss

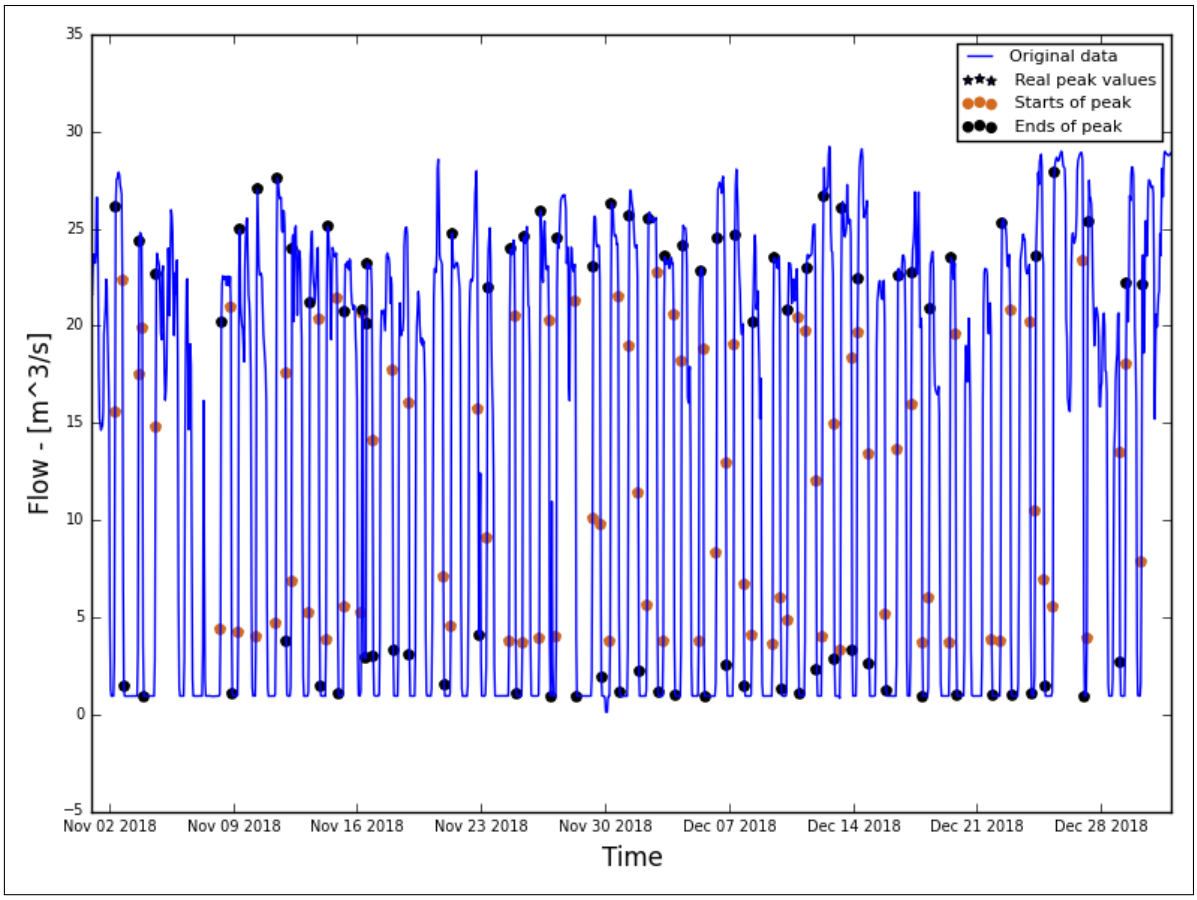

Figure A.32.156: Hydrograph of the last two months of the recorded data

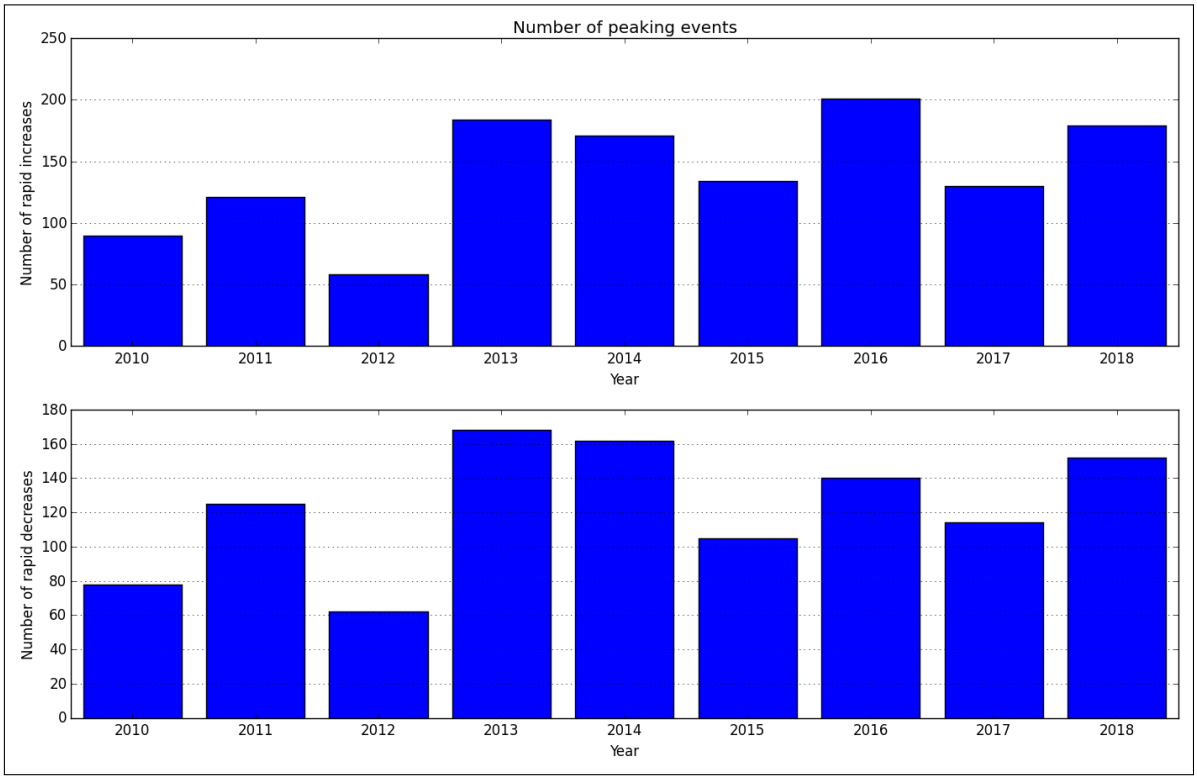

Figure A.32.157: Average annual number of increased/decreased peaks

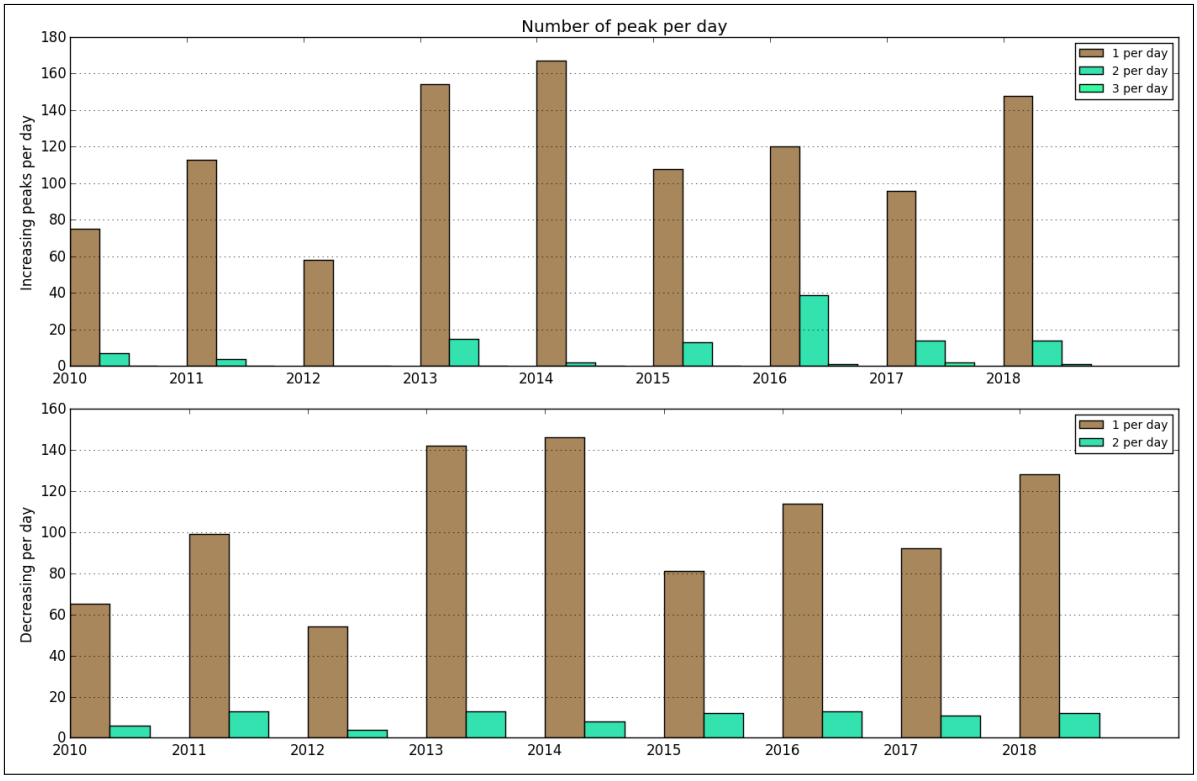

Figure A.32.158: Number of peaks per day

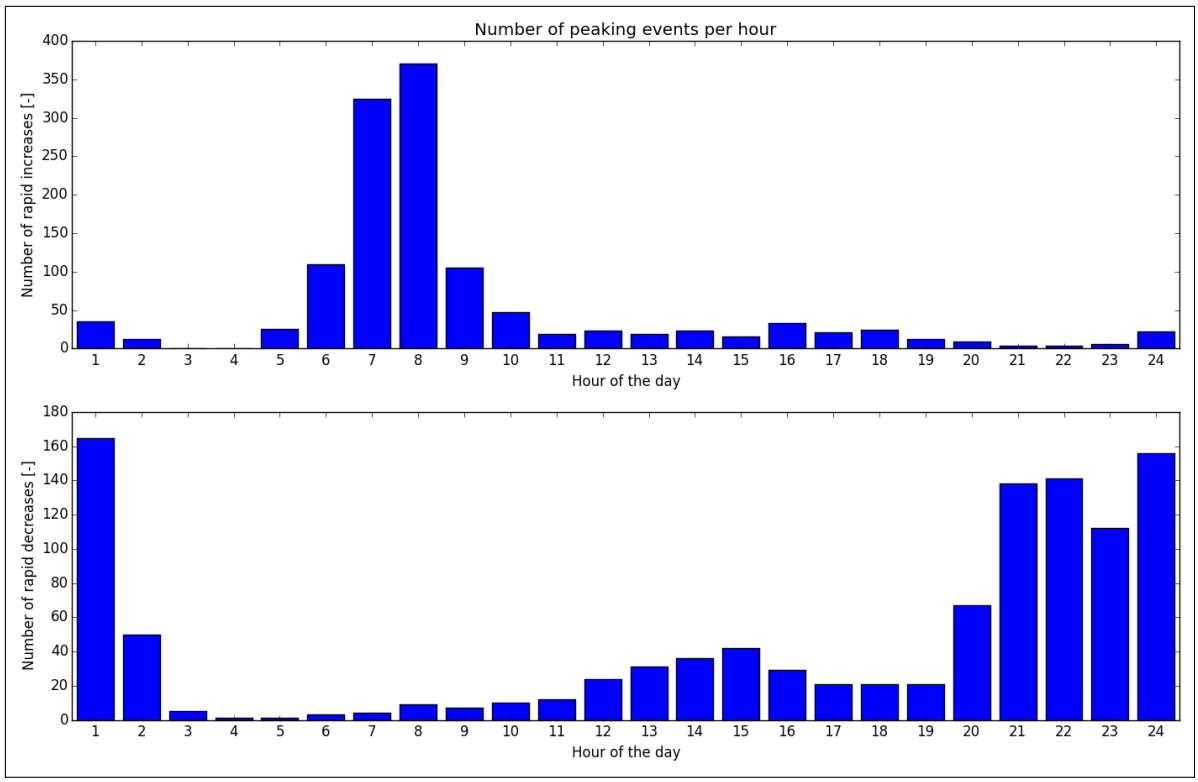

Figure A.32.159: Distribution of peaks throughout day

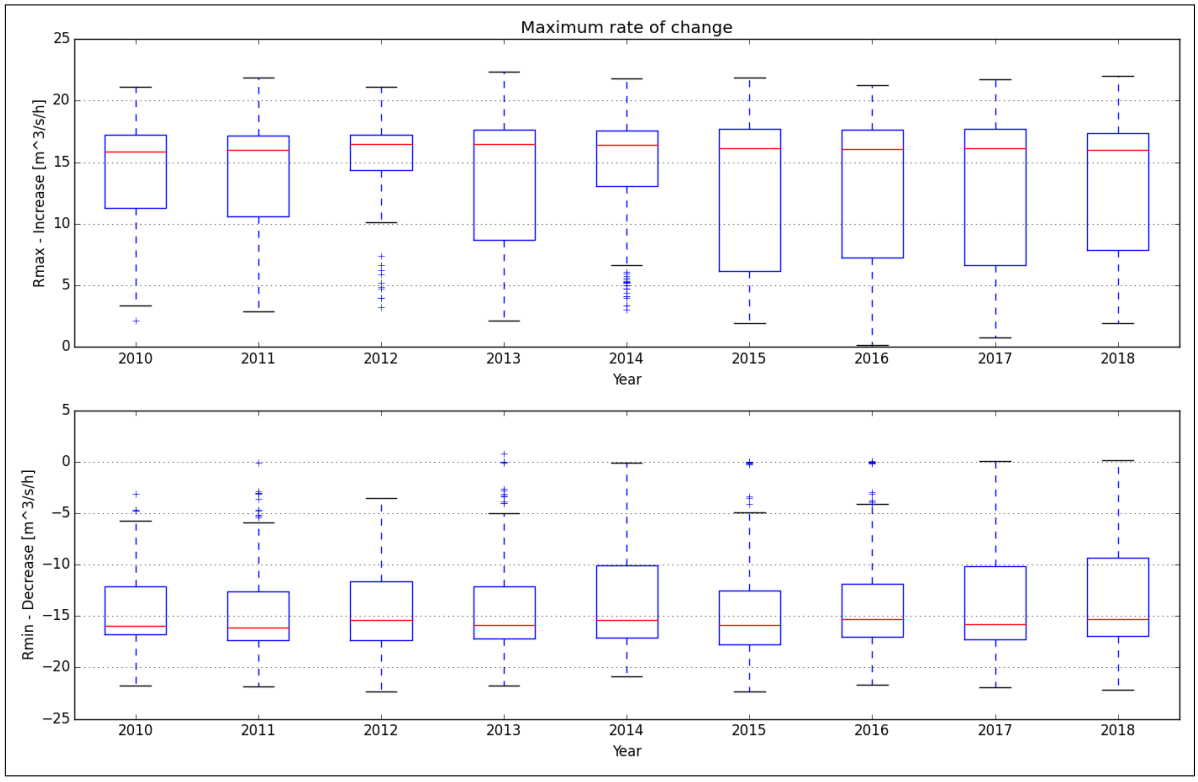

Figure A.32.160: Maximum rate of change

A.33. Svartelva krv

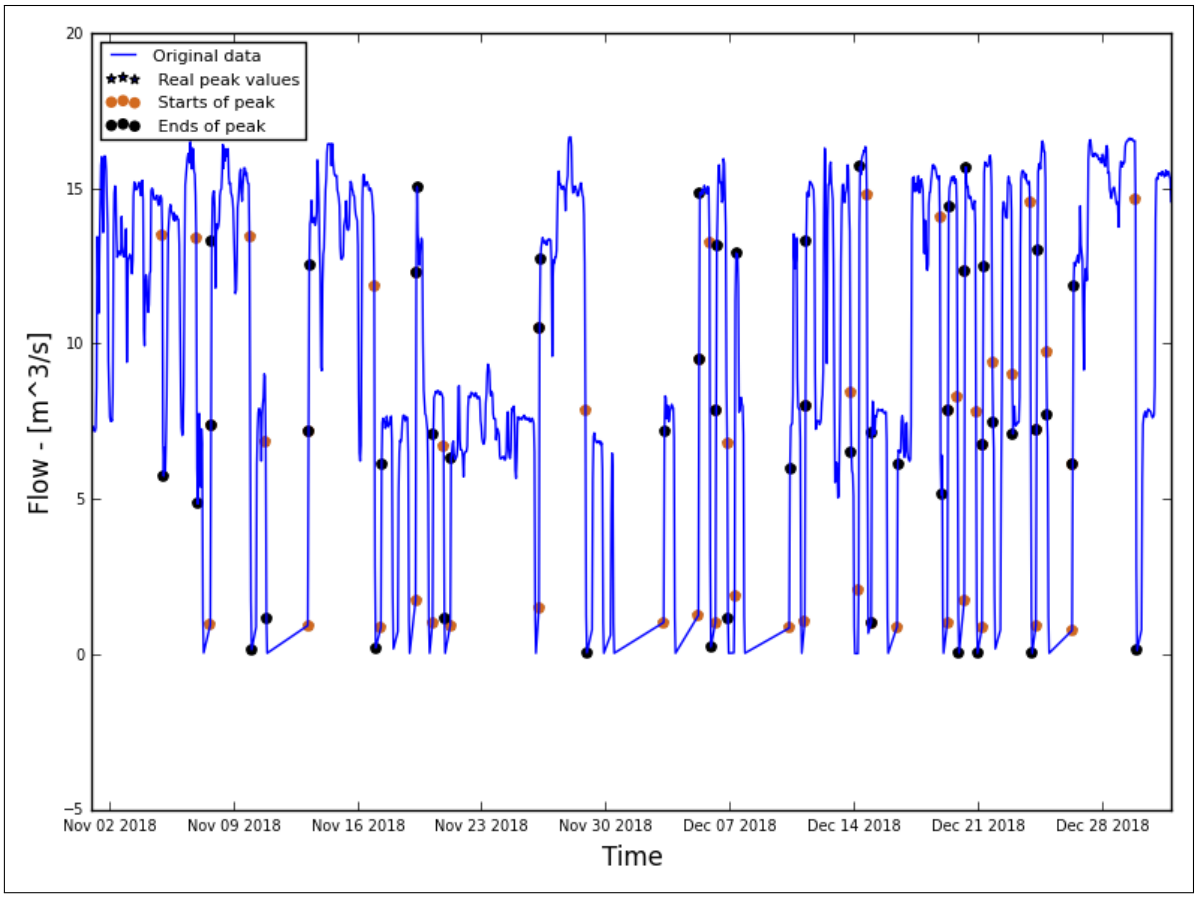

Figure A.33.161: Hydrograph of the last two months of the recorded data

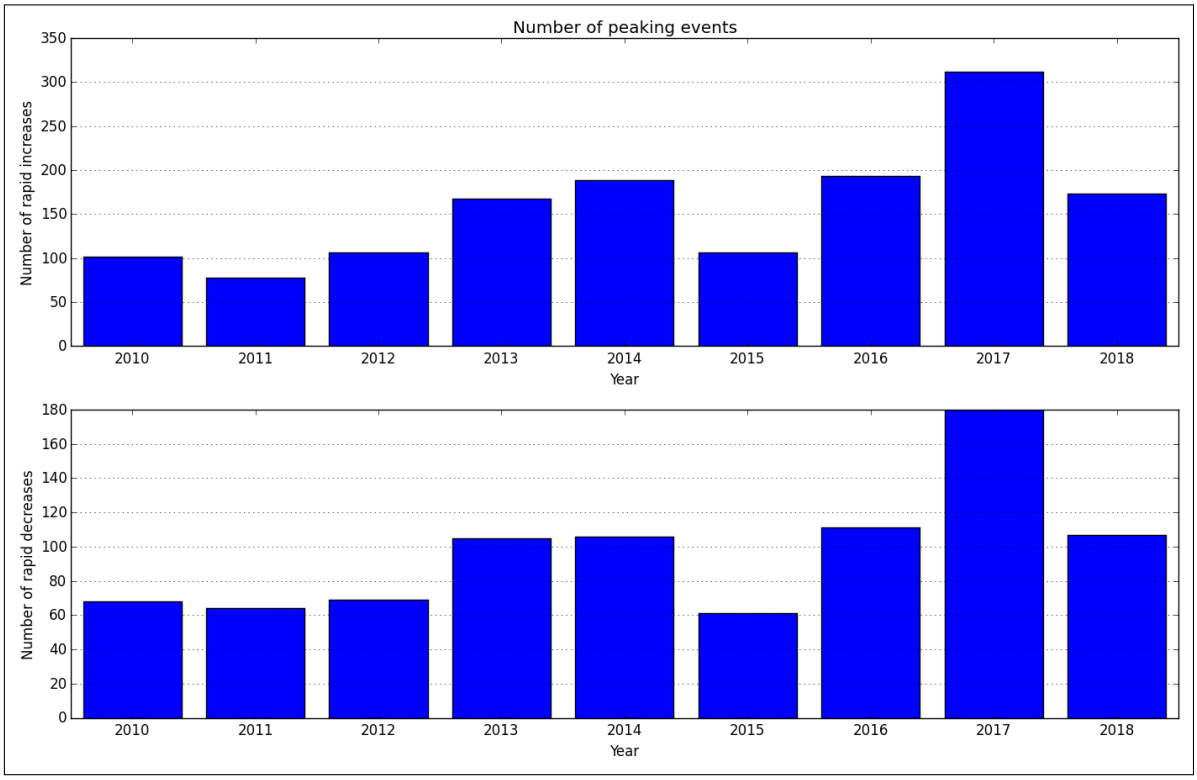

Figure A.33.162: Average annual number of increased/decreased peaks

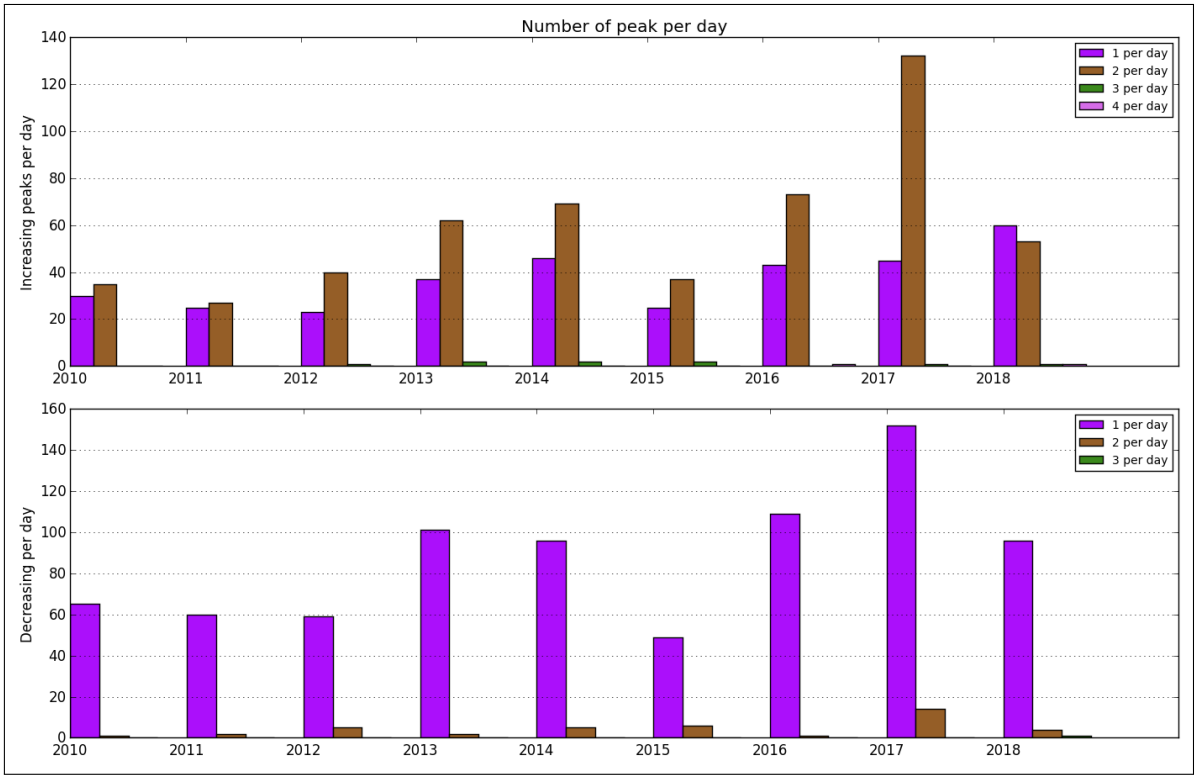

Figure A.33.163: Number of peaks per day

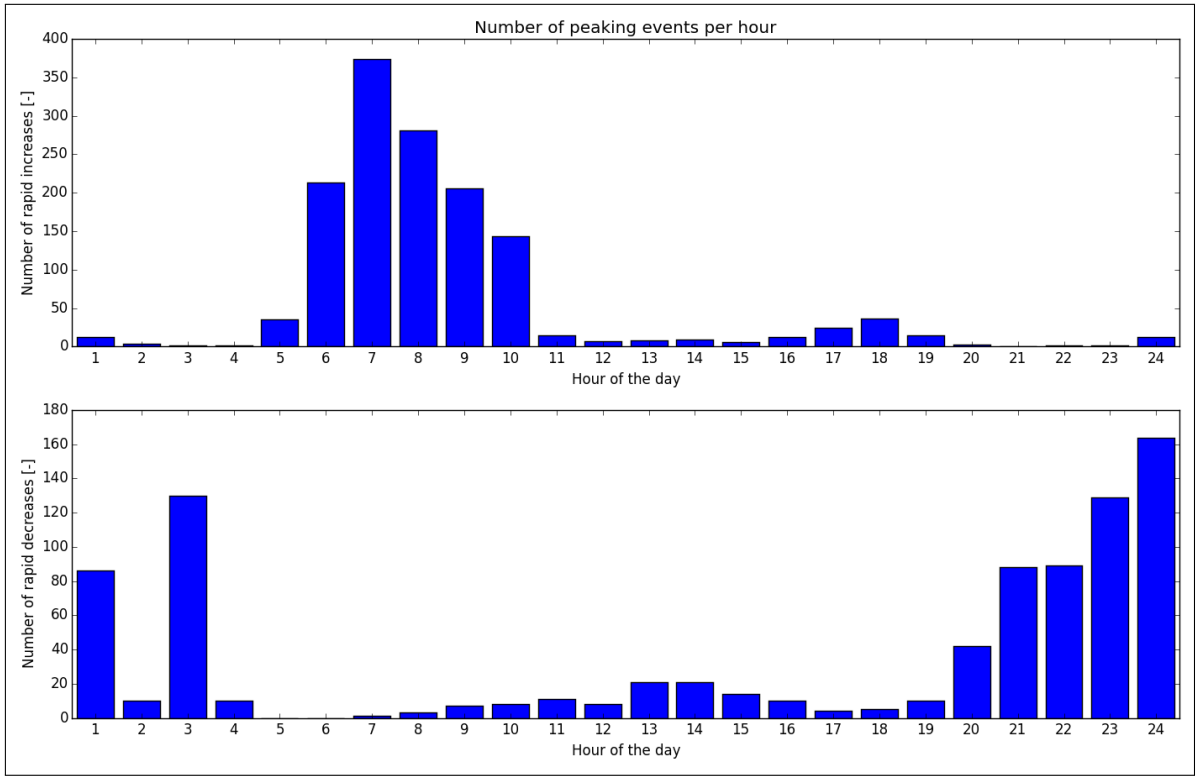

Figure A.33.164: Distribution of peaks throughout day

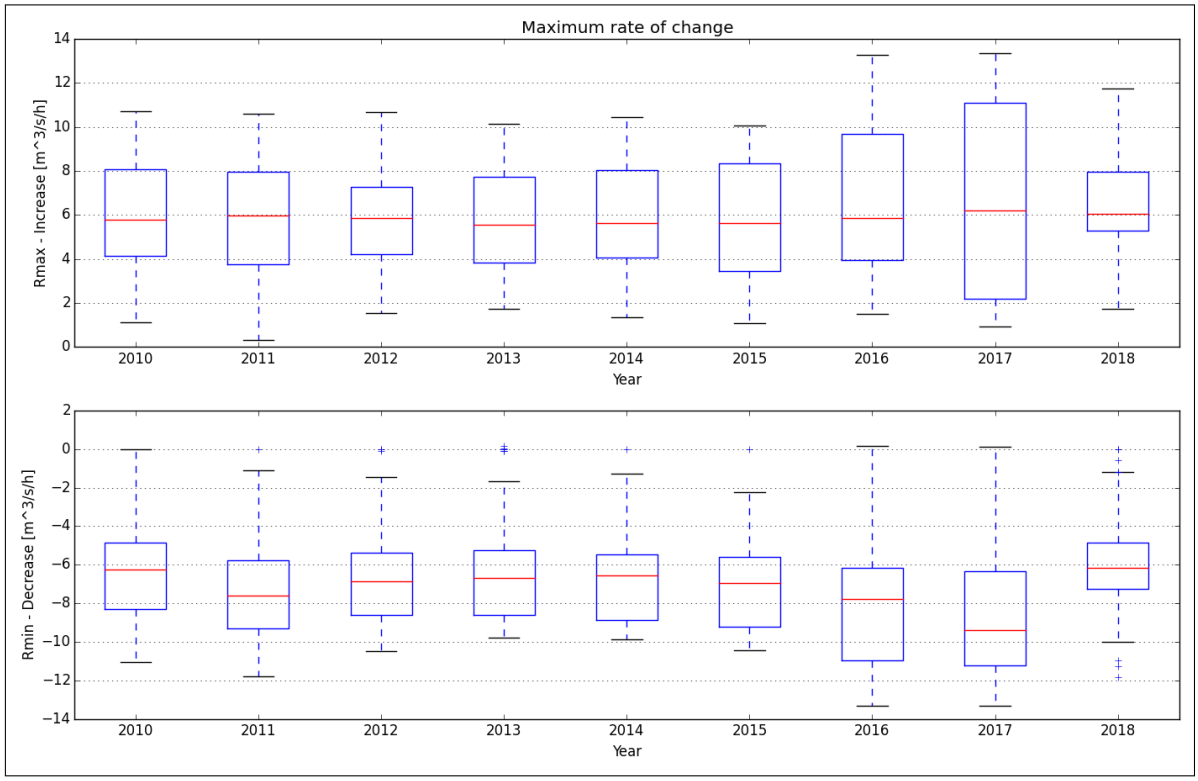

Figure A.33.165: Maximum rate of change

A.34. Mørre

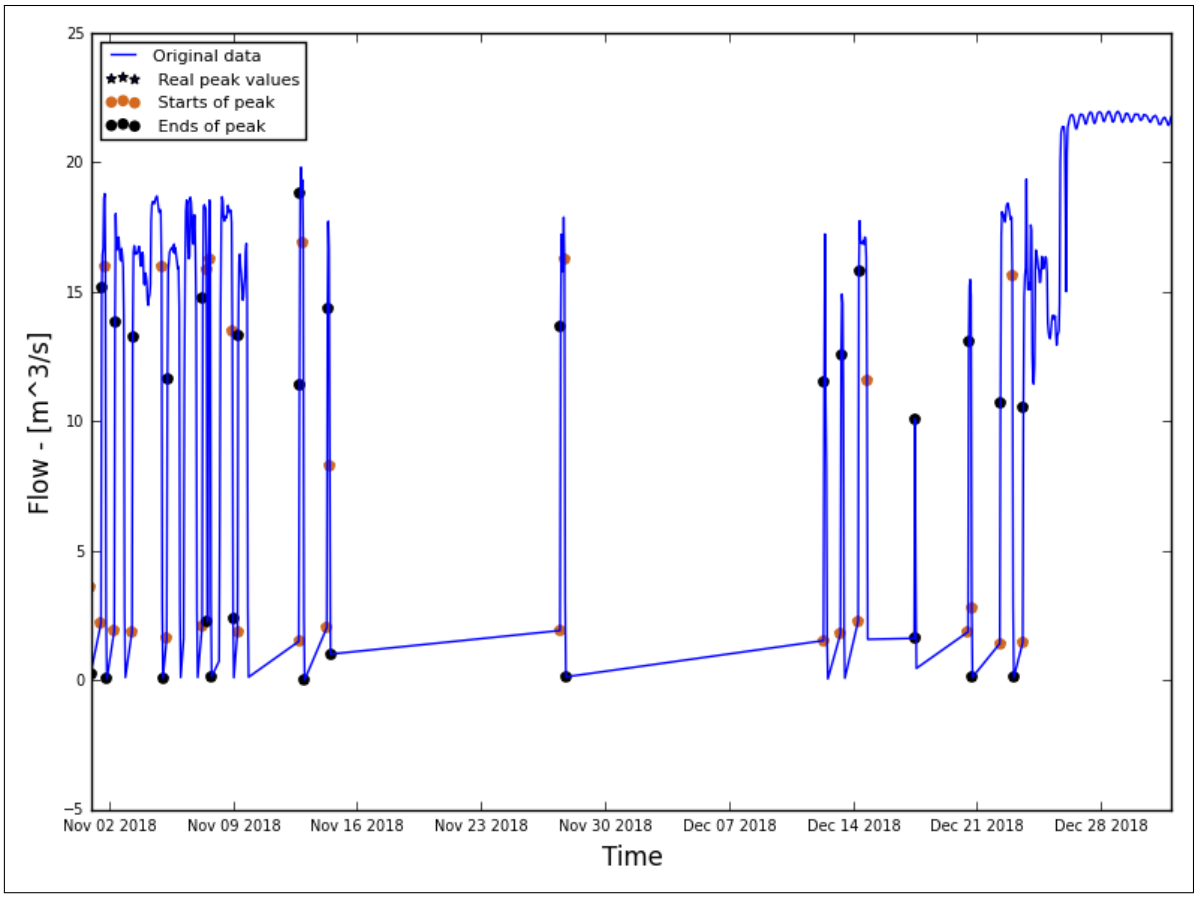

Figure A.34.166: Hydrograph of the last two months of the recorded data

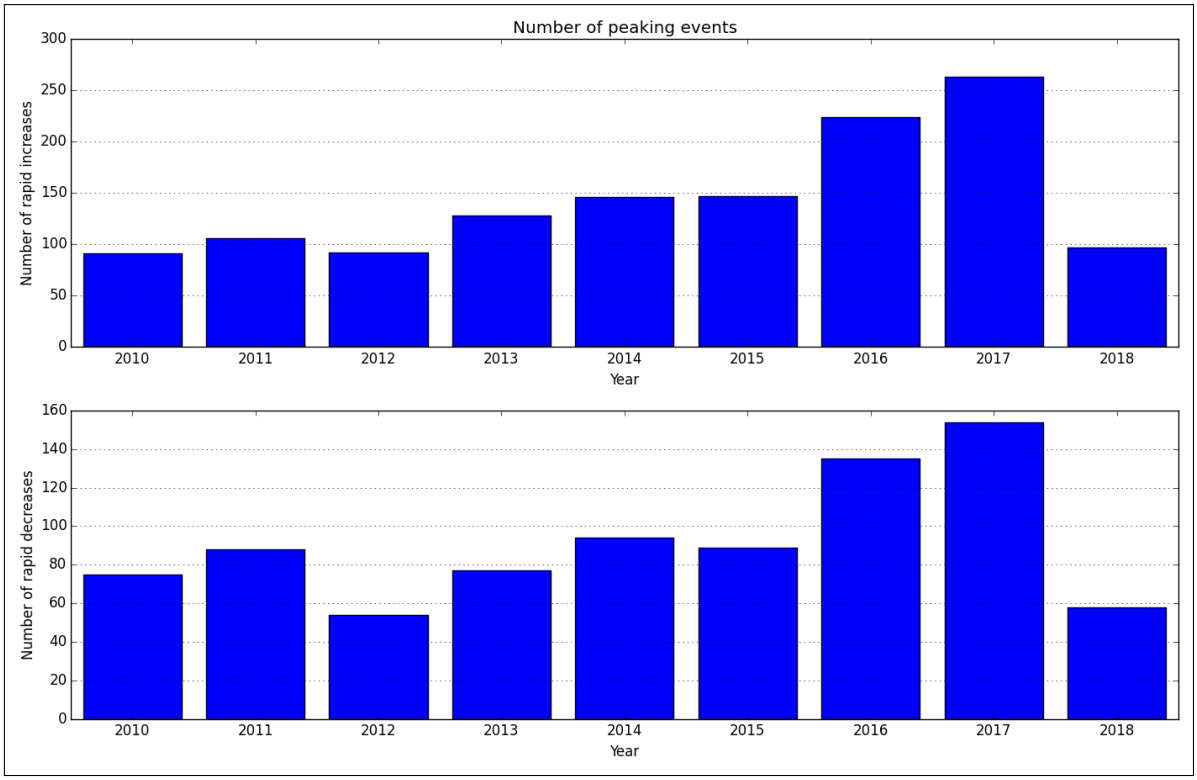

Figure A.34.167: Average annual number of increased/decreased peaks

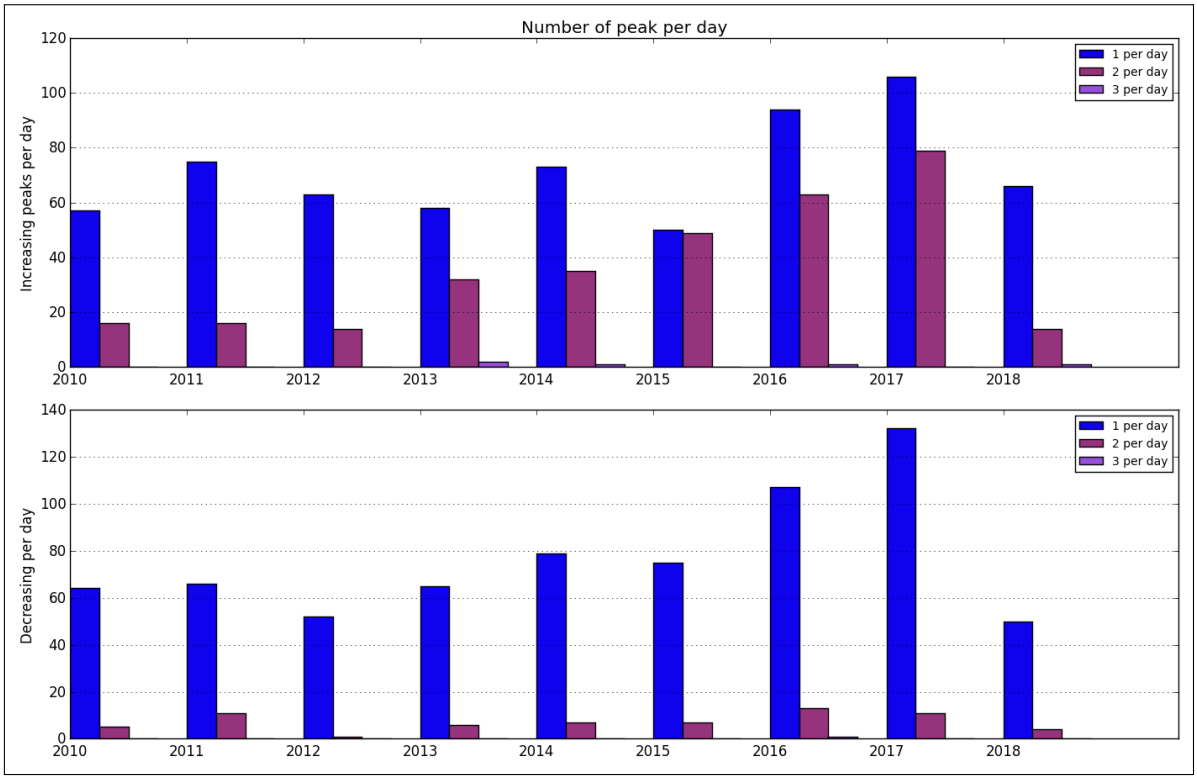

Figure A.34.168: Number of peaks per day

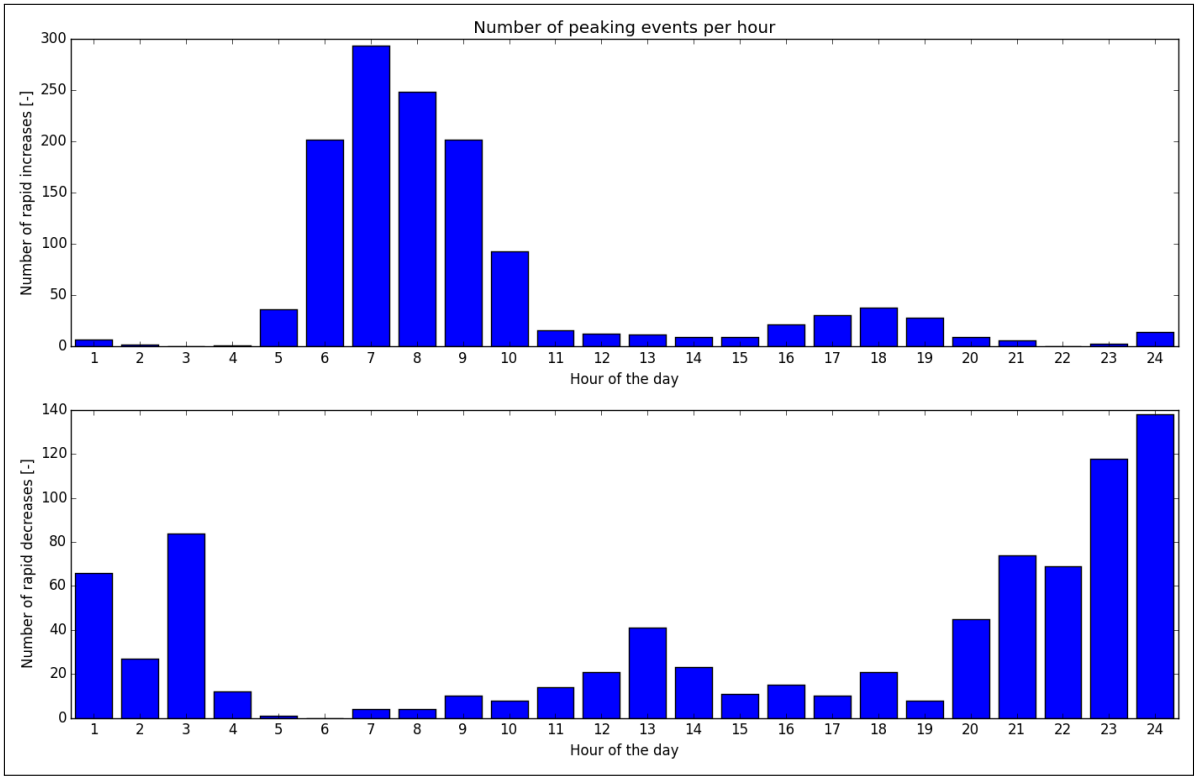

Figure A.34.169: Distribution of peaks throughout day

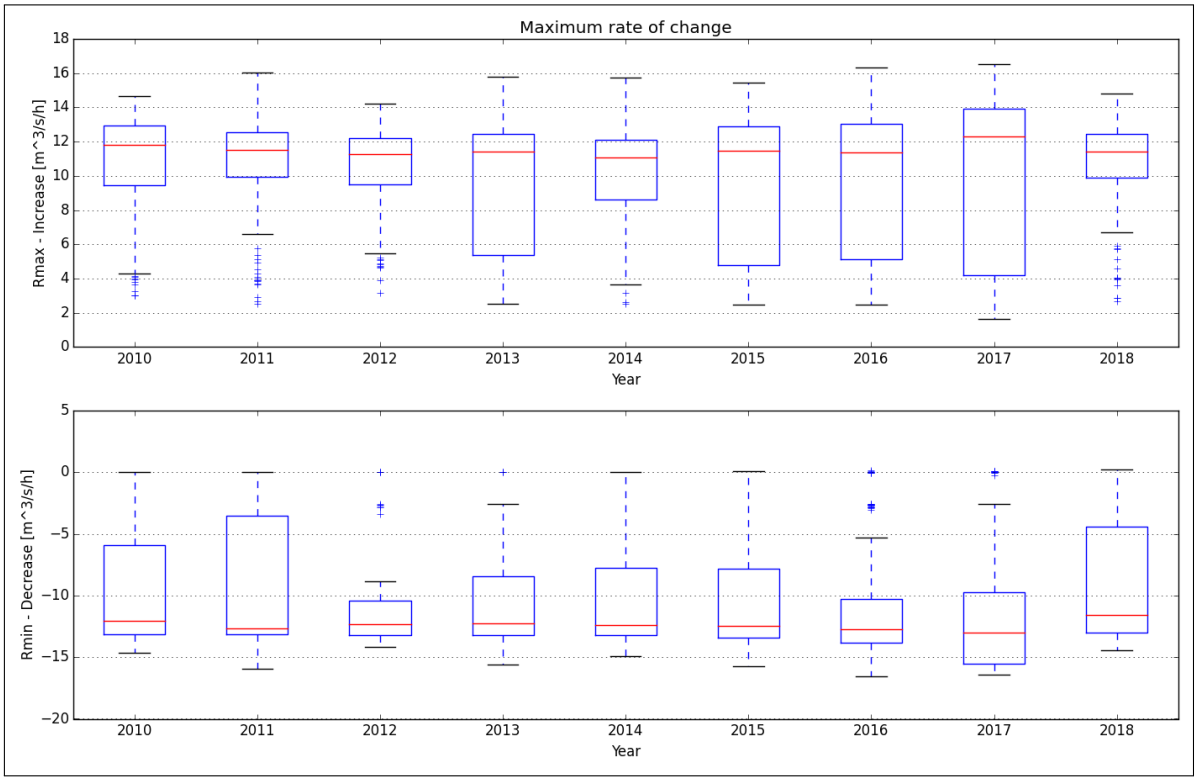

Figure A.34.170: Maximum rate of change

A.35. Bogna

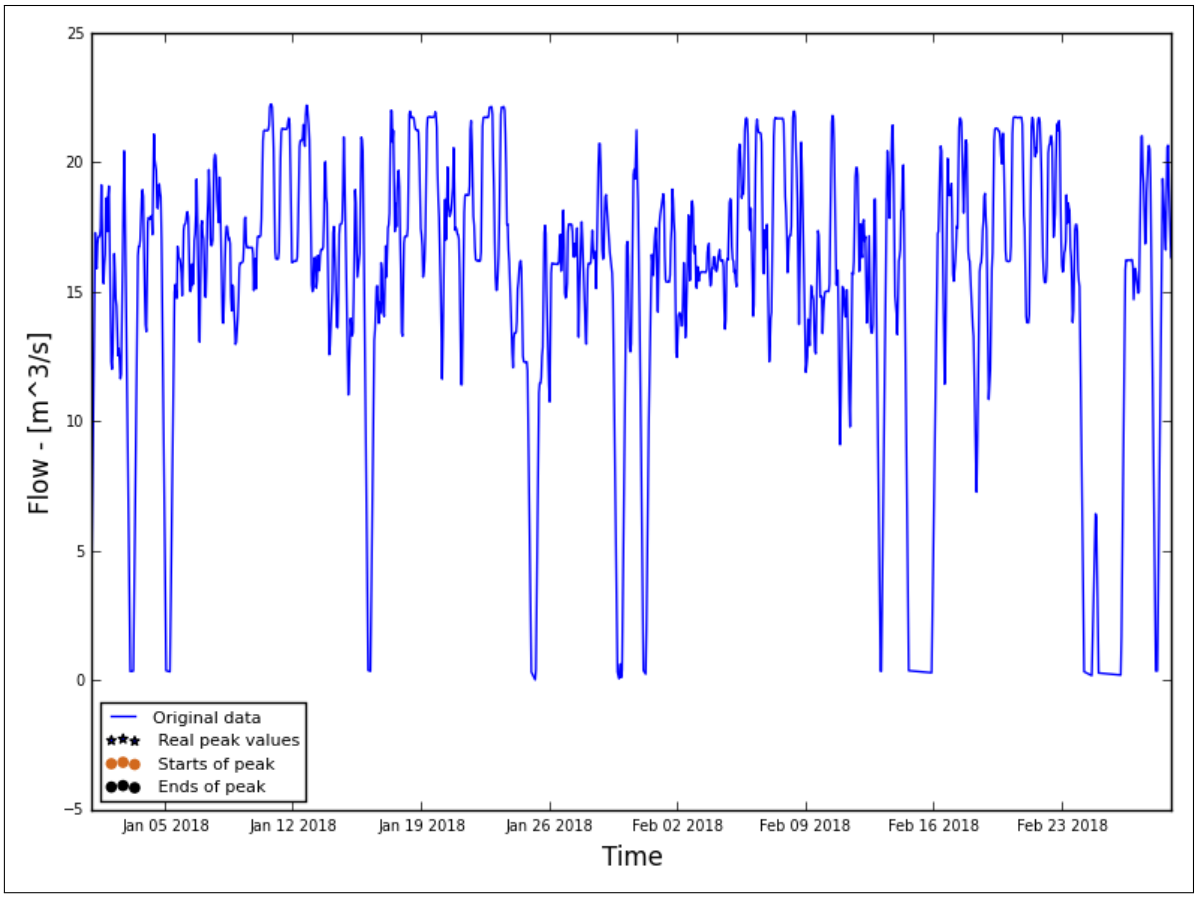

Figure A.35.171: Hydrograph of the last two months of the recorded data

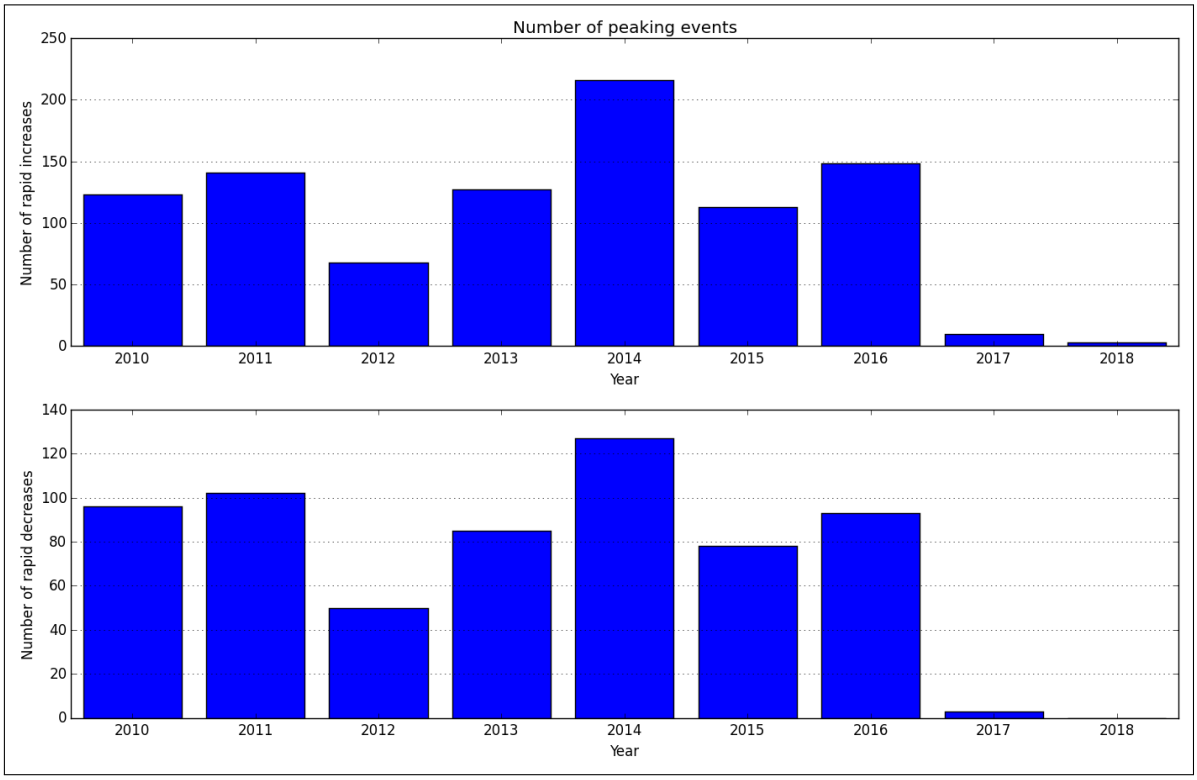

Figure A.35.172: Average annual number of increased/decreased peaks

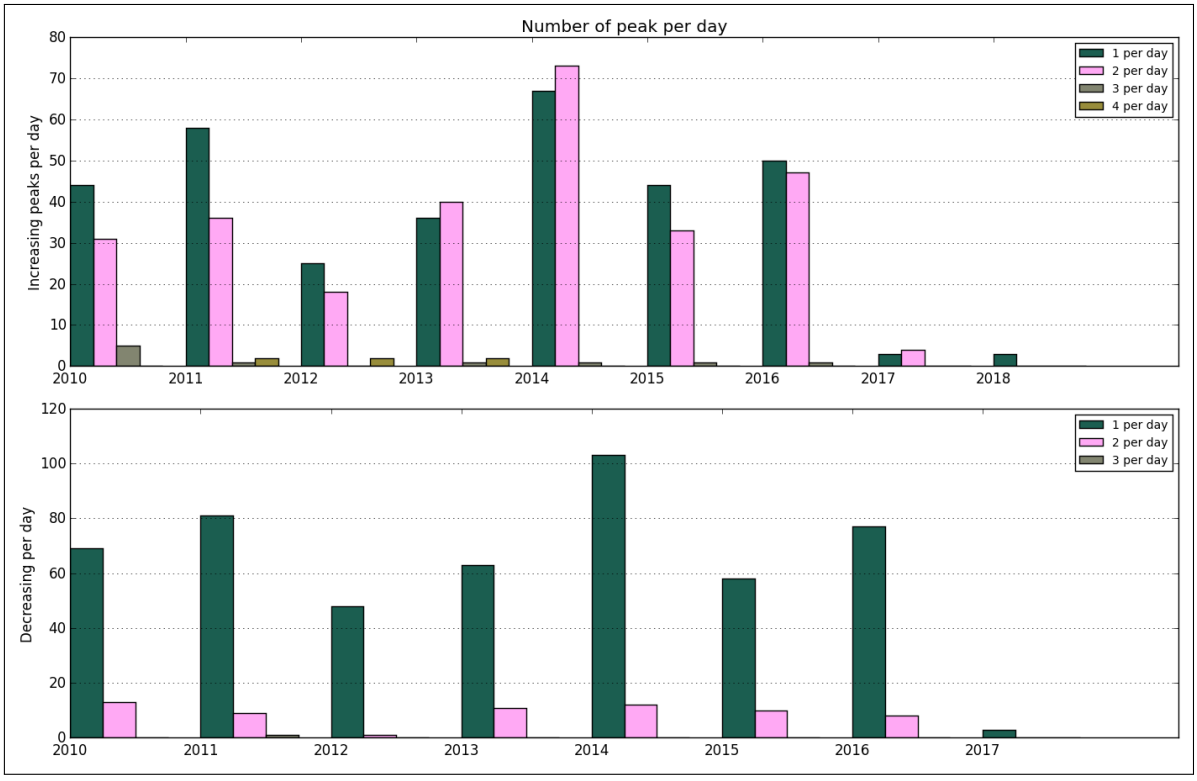

Figure A.35.173: Number of peaks per day

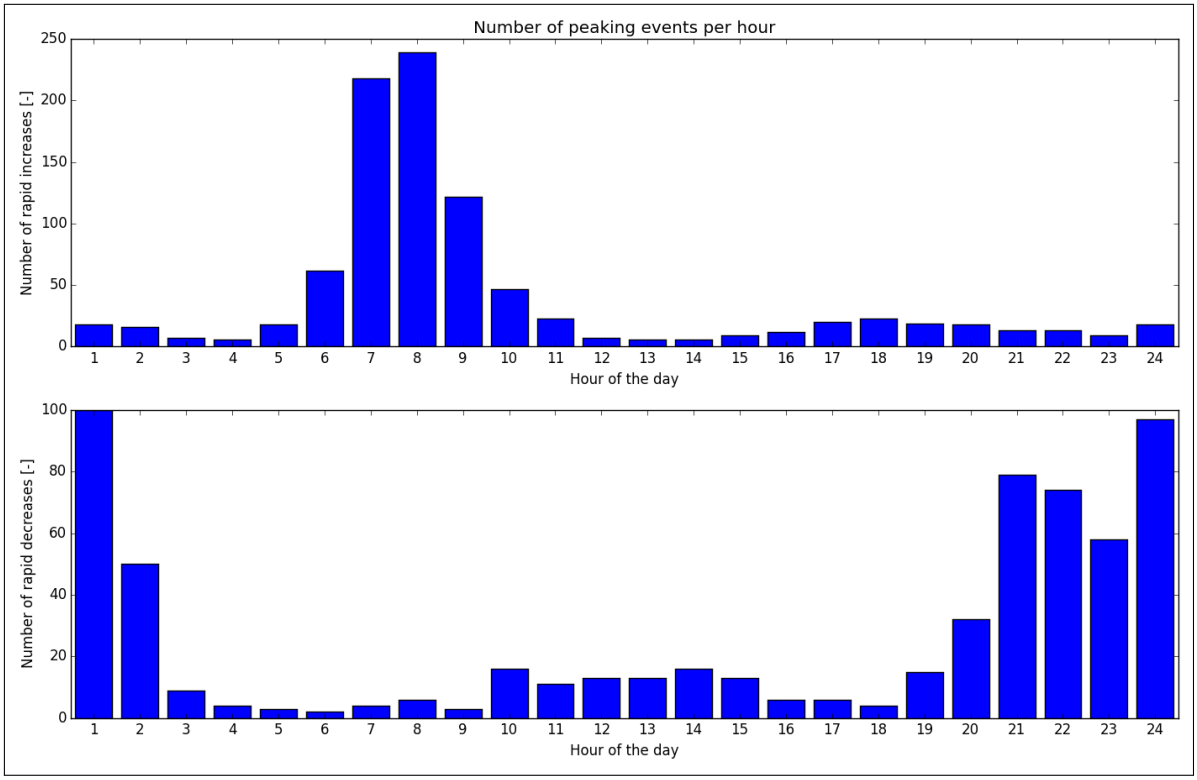

Figure A.35.174: Distribution of peaks throughout day

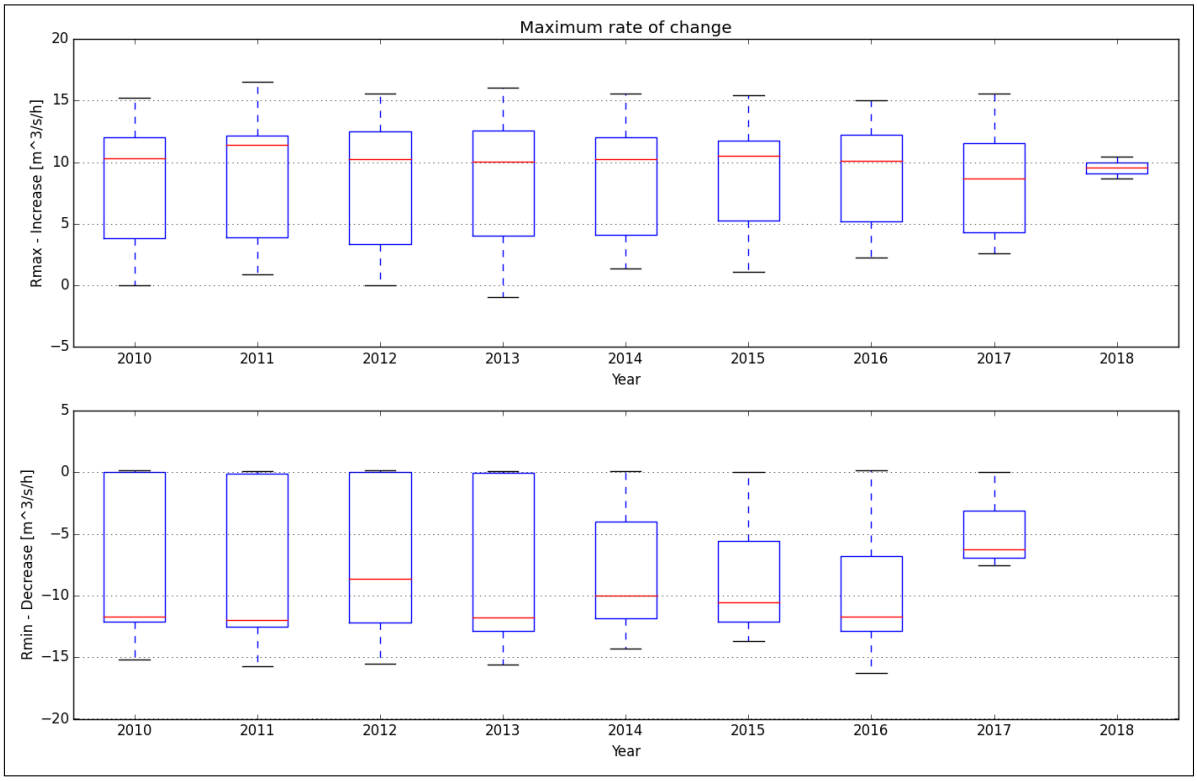

Figure A.35.175: Maximum rate of change

A.36. Kolsvik

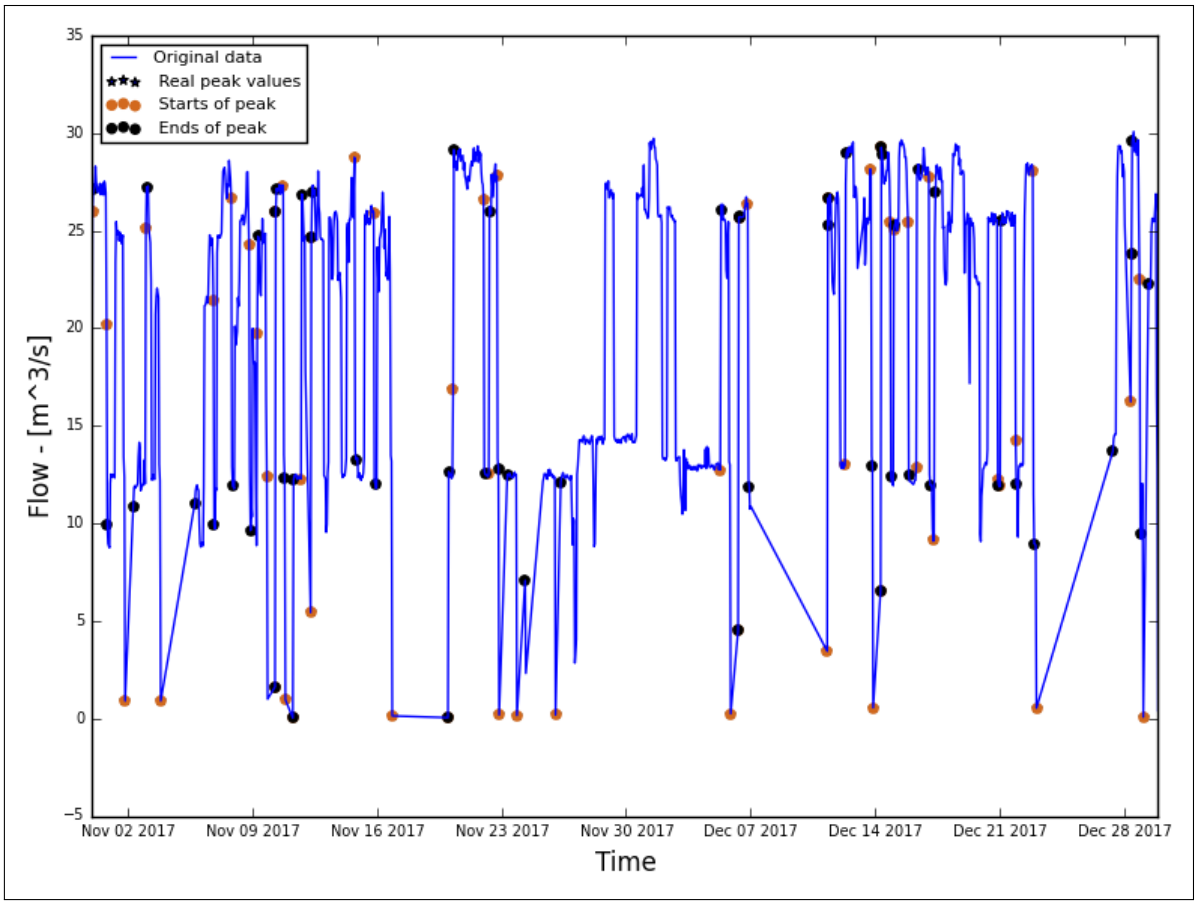

Figure A.36.176: Hydrograph of the last two months of the recorded data

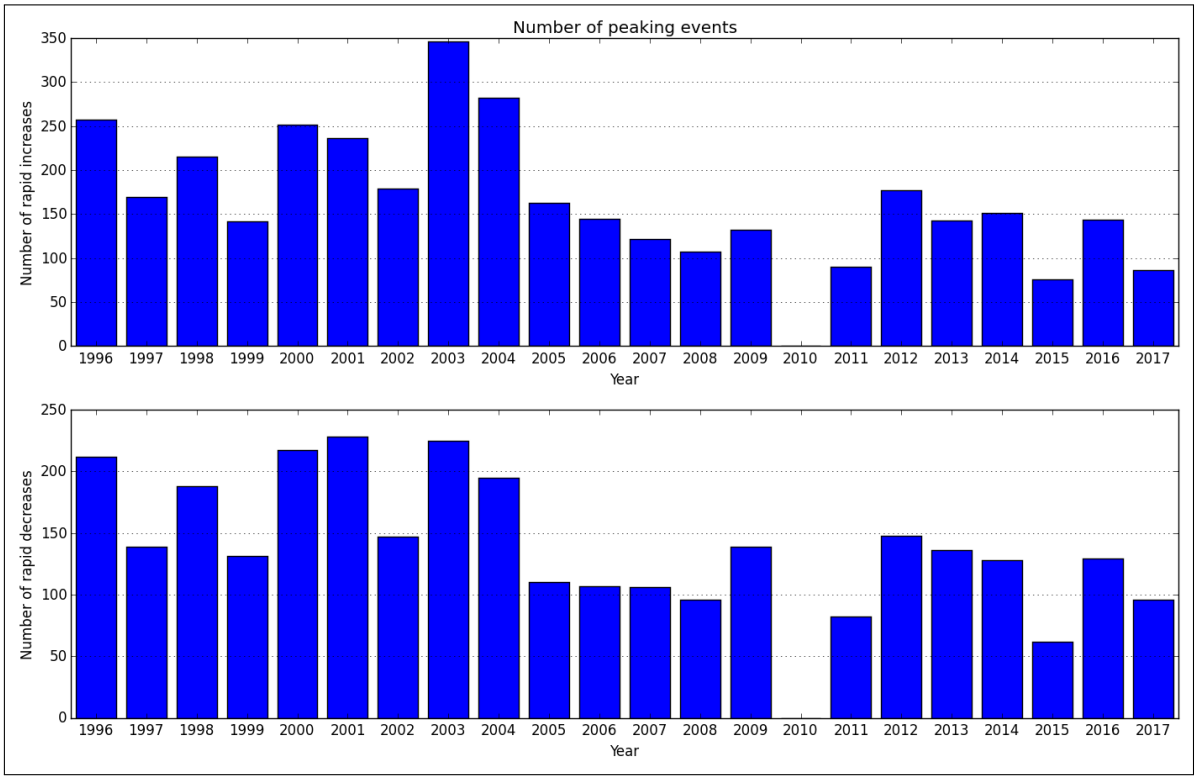

Figure A.36.177: Average annual number of increased/decreased peaks

Figure A.36.178: Number of peaks per day

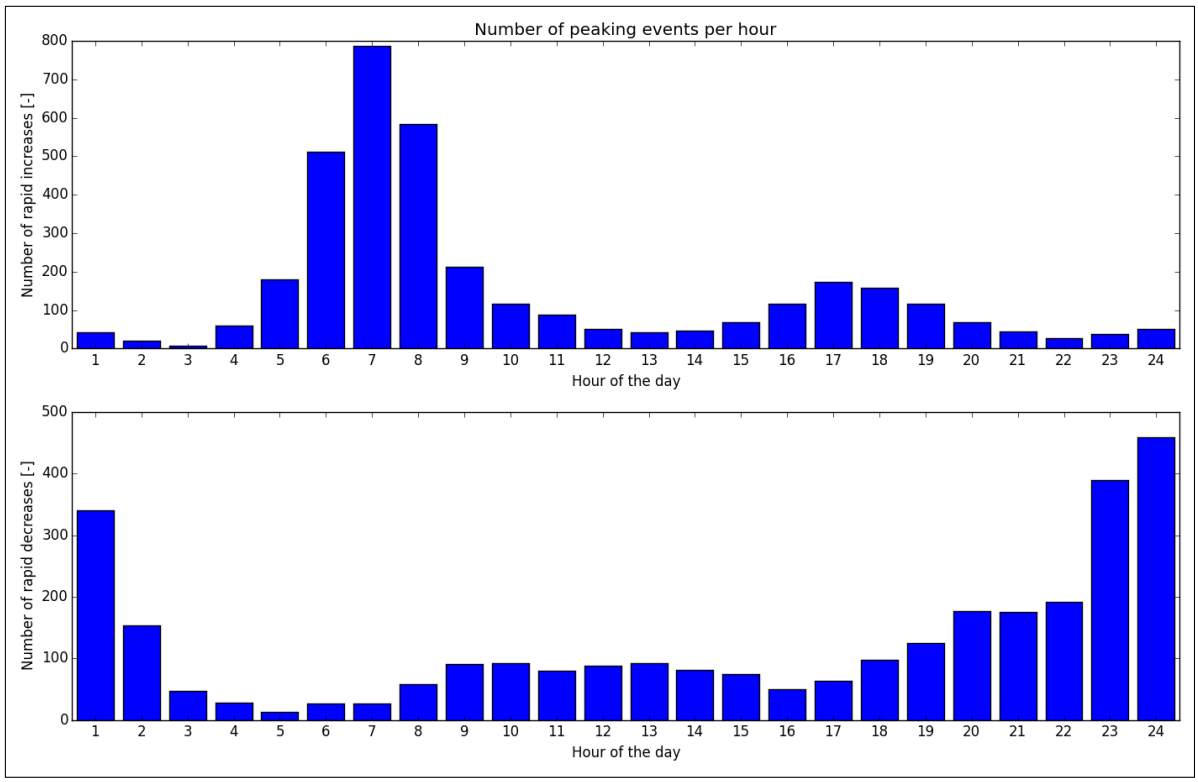

Figure A.36.179: Distribution of peaks throughout day

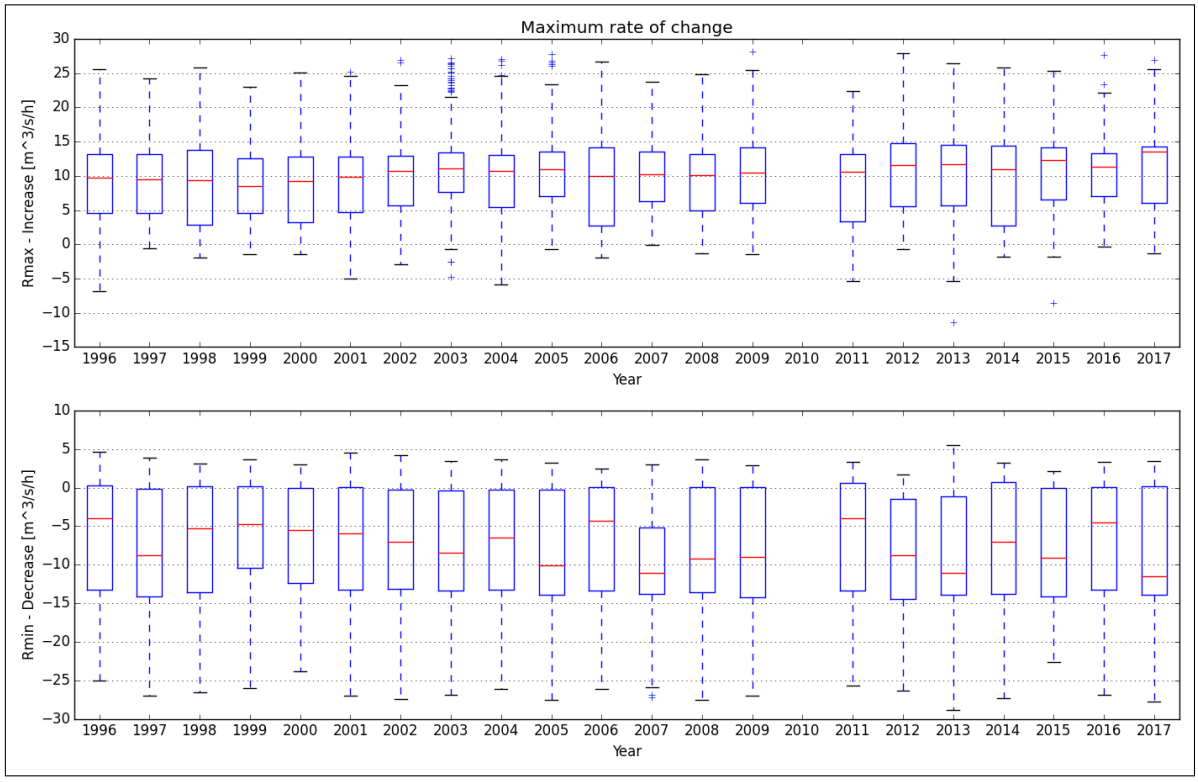

Figure A.36.180: Maximum rate of change

A.37. Lysebotn

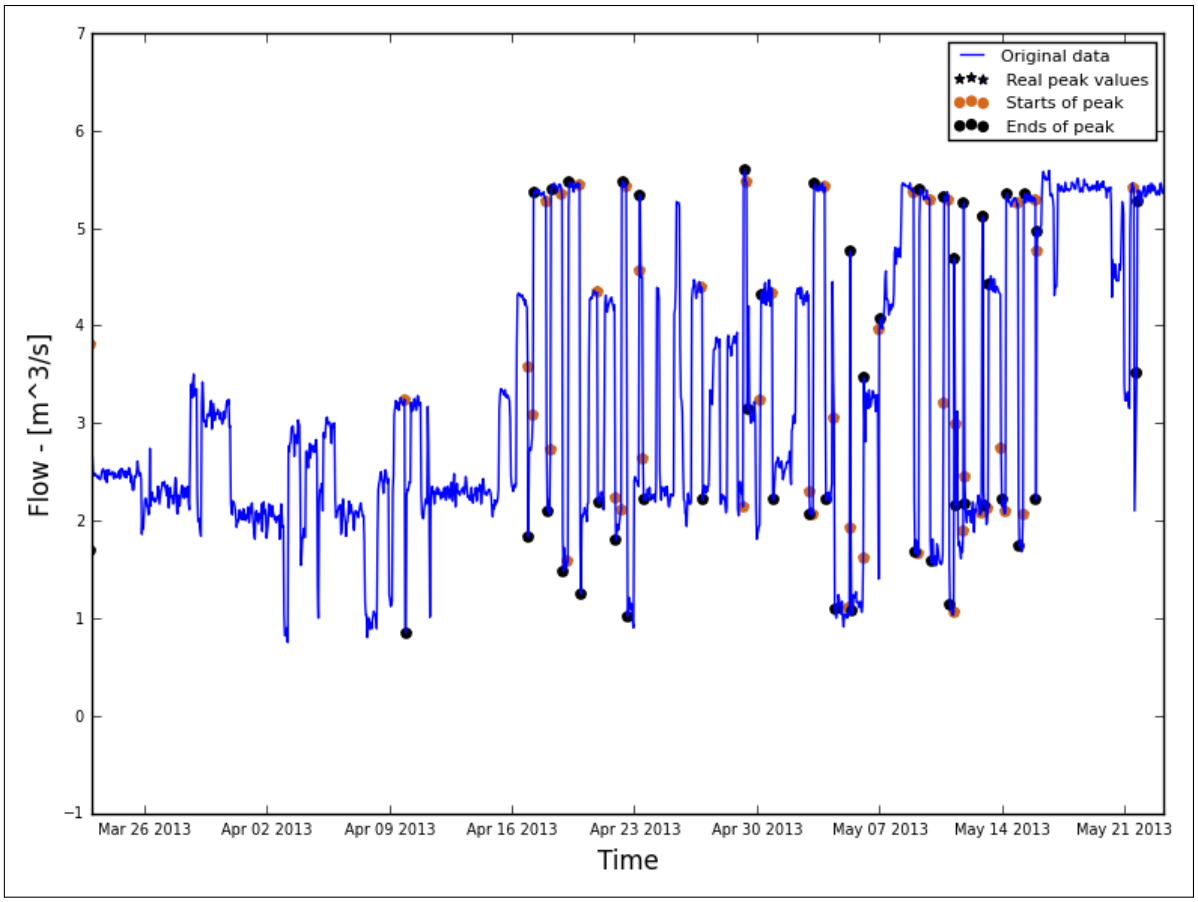

Figure A.37.181: Hydrograph of the last two months of the recorded data

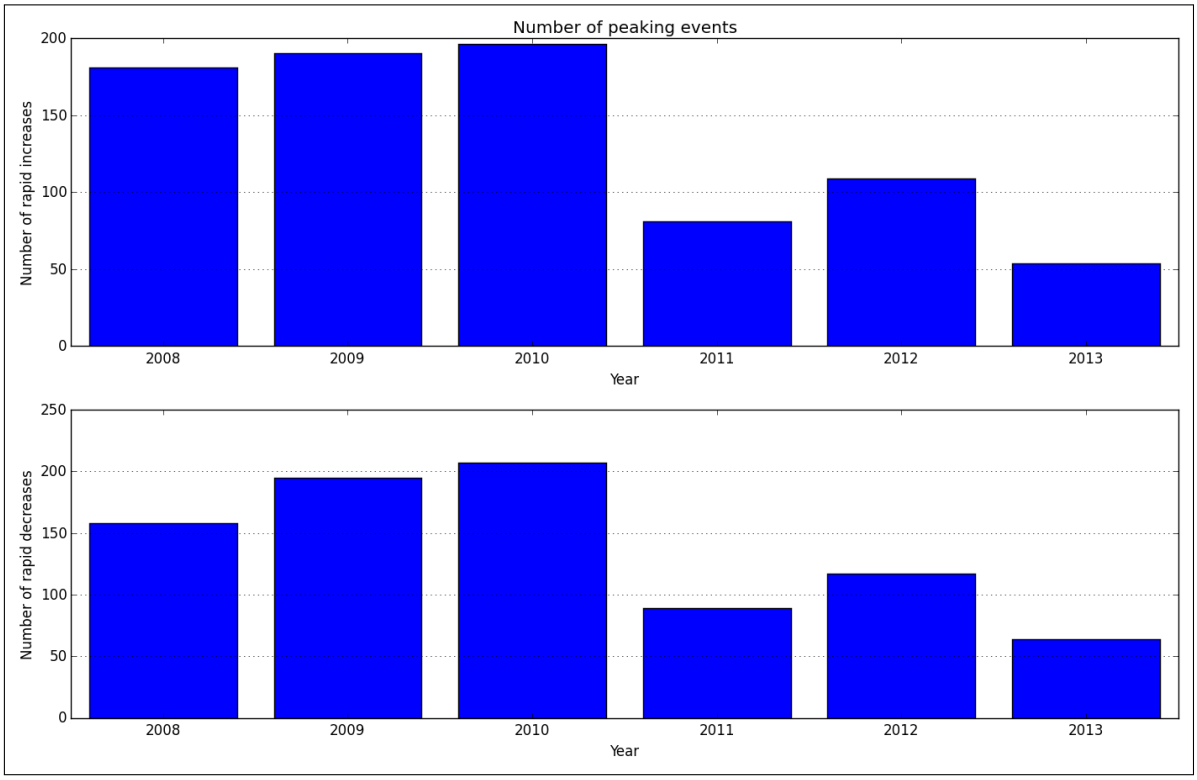

Figure A.37.182: Average annual number of increased/decreased peaks

Figure A.37.183: Number of peaks per day

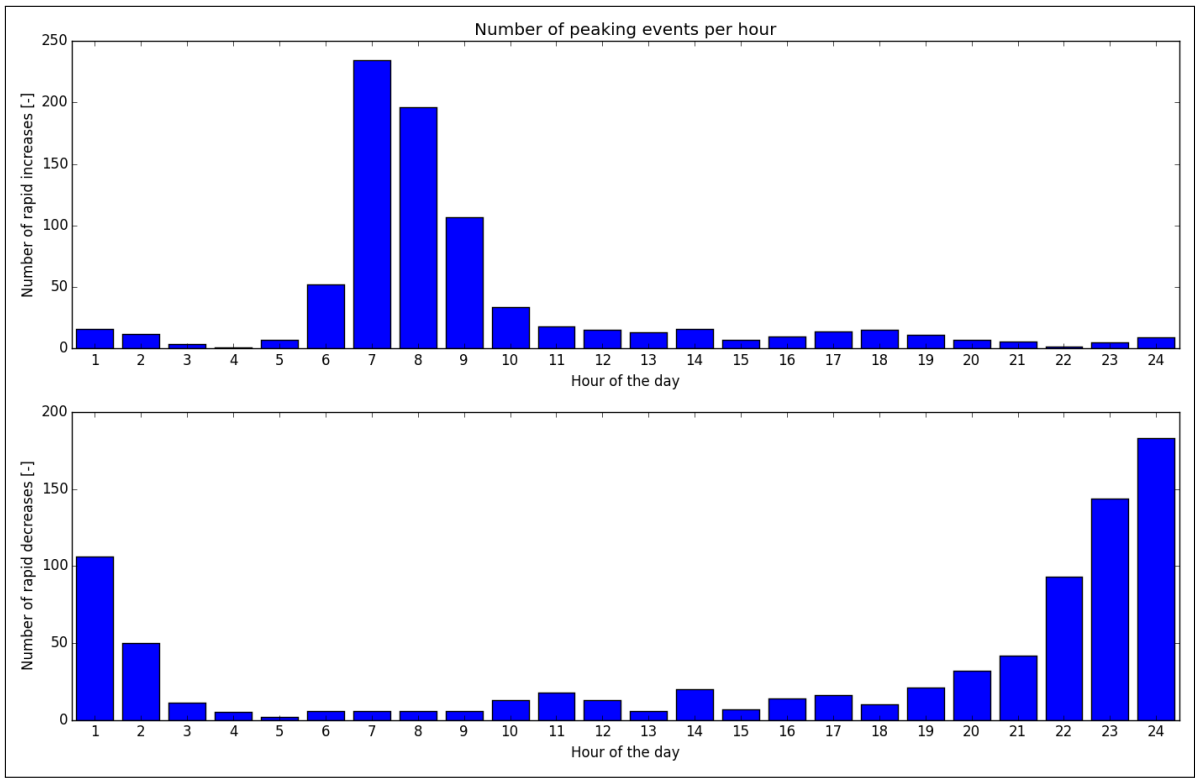

Figure A.37.184: Distribution of peaks throughout day

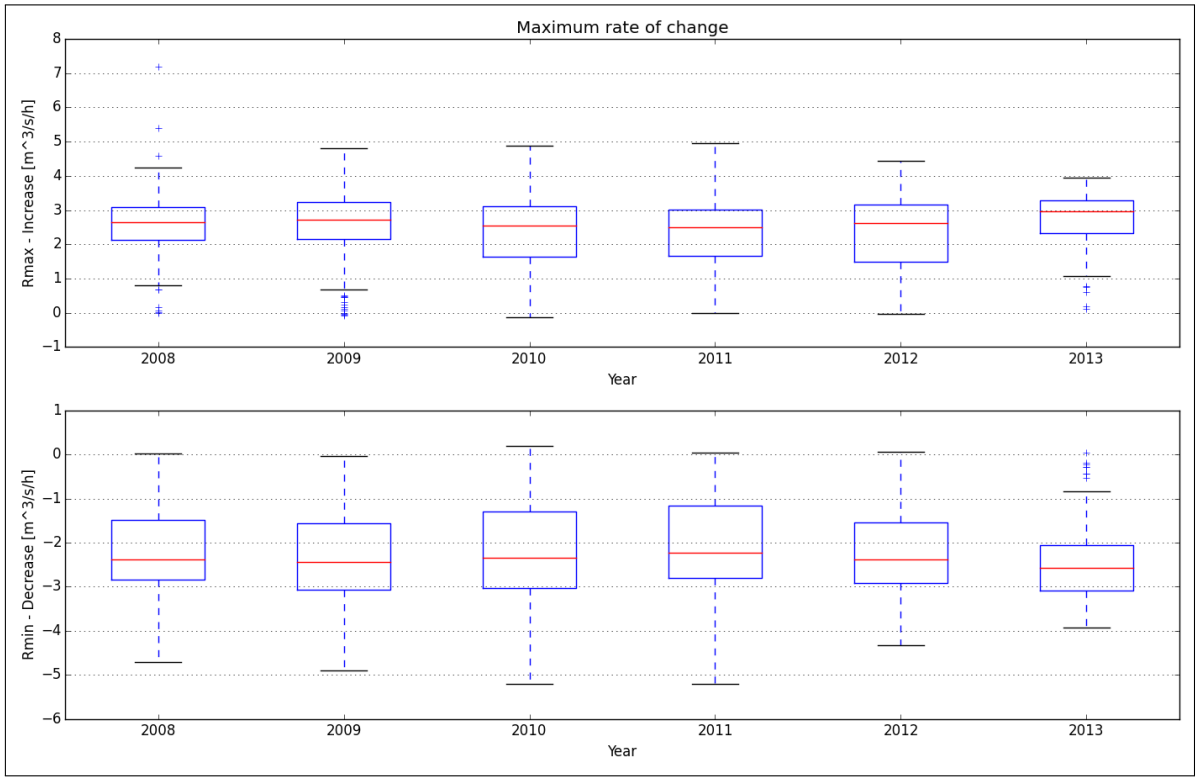

Figure A.37.185: Maximum rate of change

A.38. Straumsmo

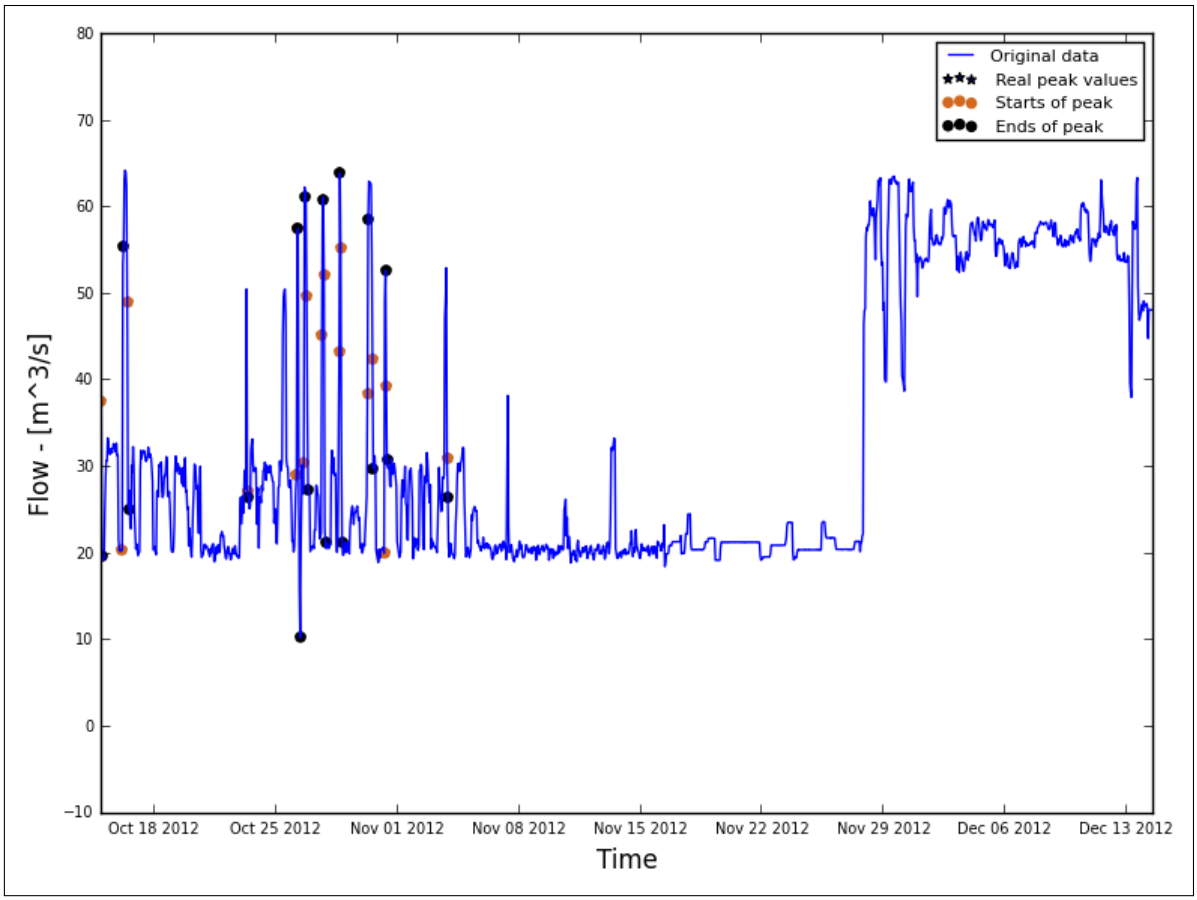

Figure A.38.186: Hydrograph of the last two months of the recorded data

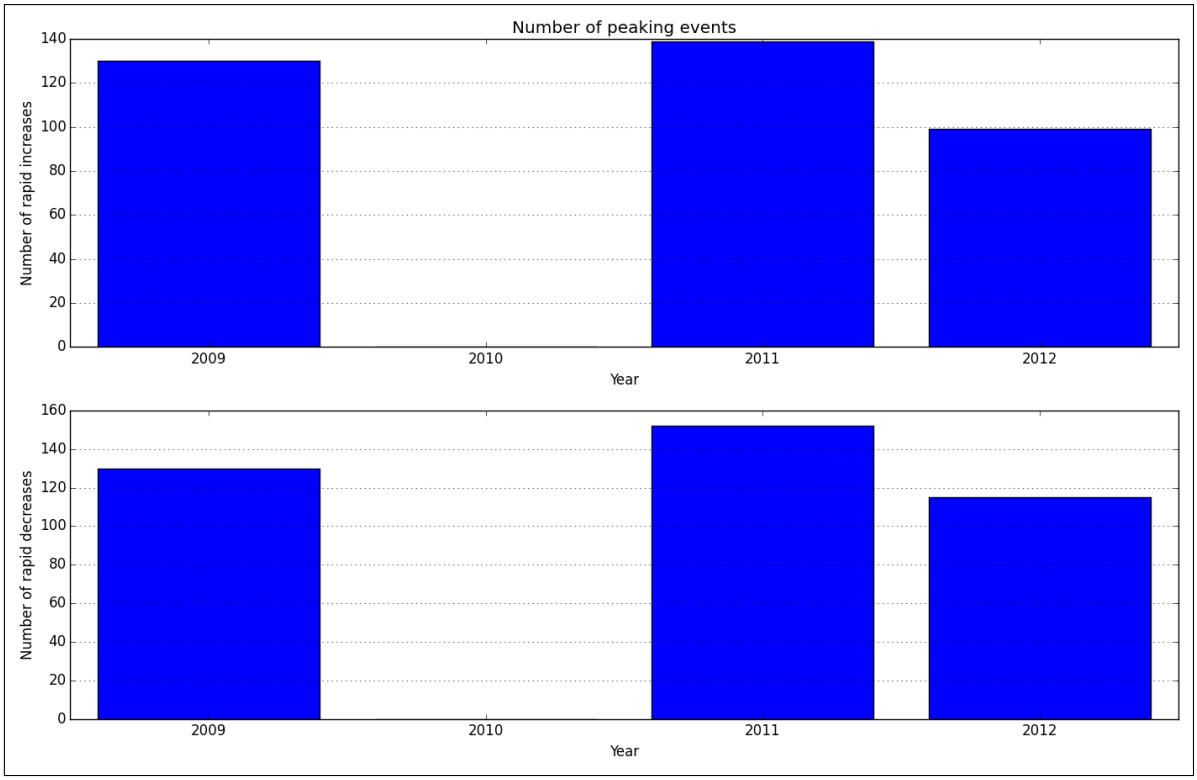

Figure A.38.187: Average annual number of increased/decreased peaks

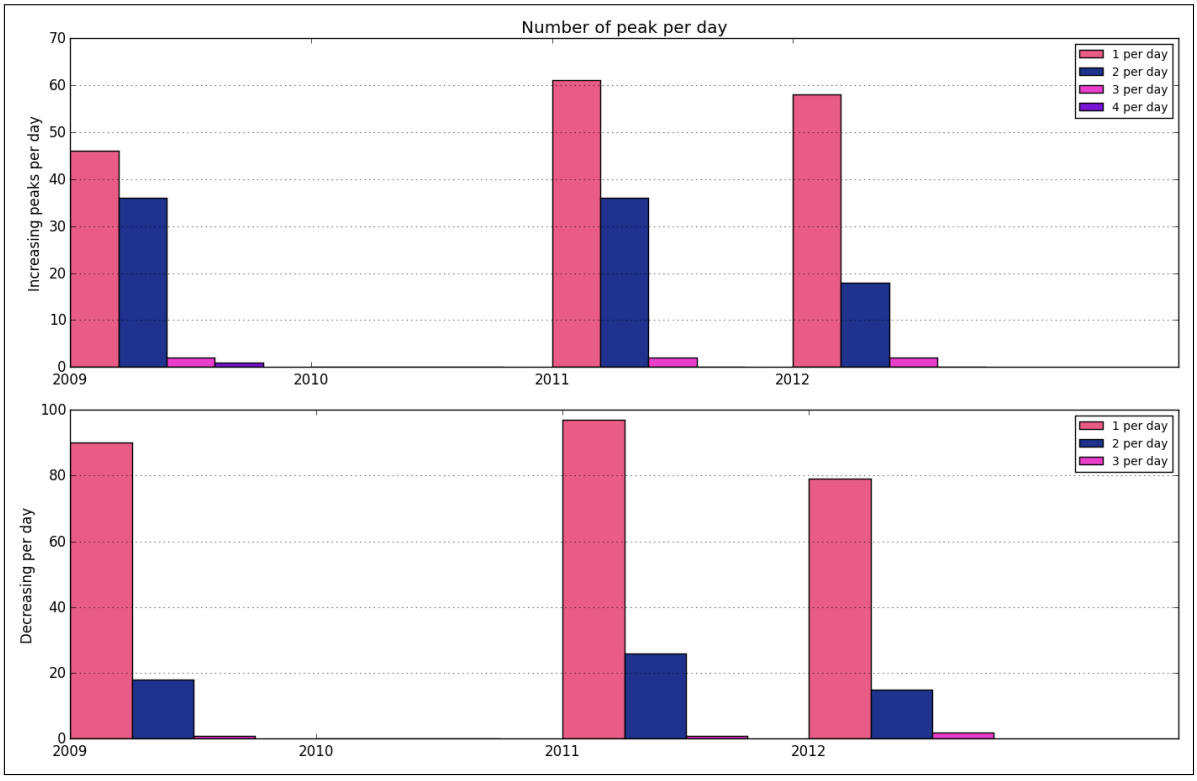

Figure A.38.188: Number of peaks per day

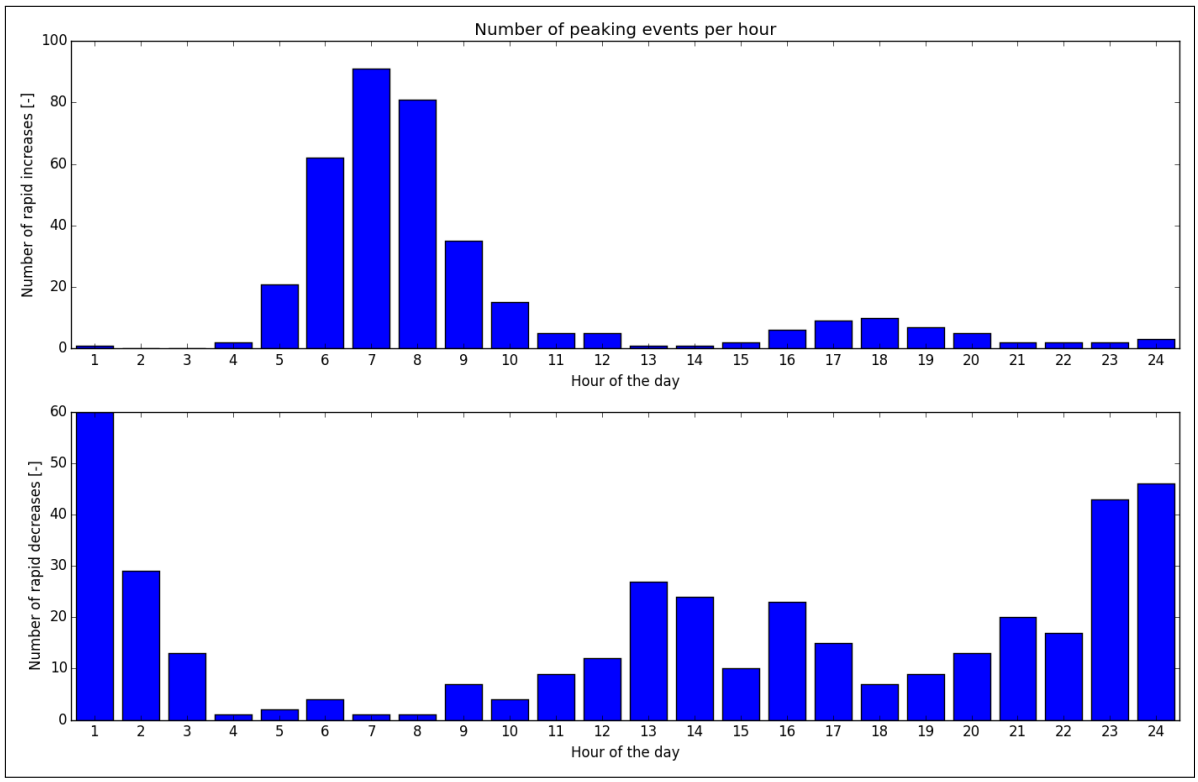

Figure A.38.189: Distribution of peaks throughout day

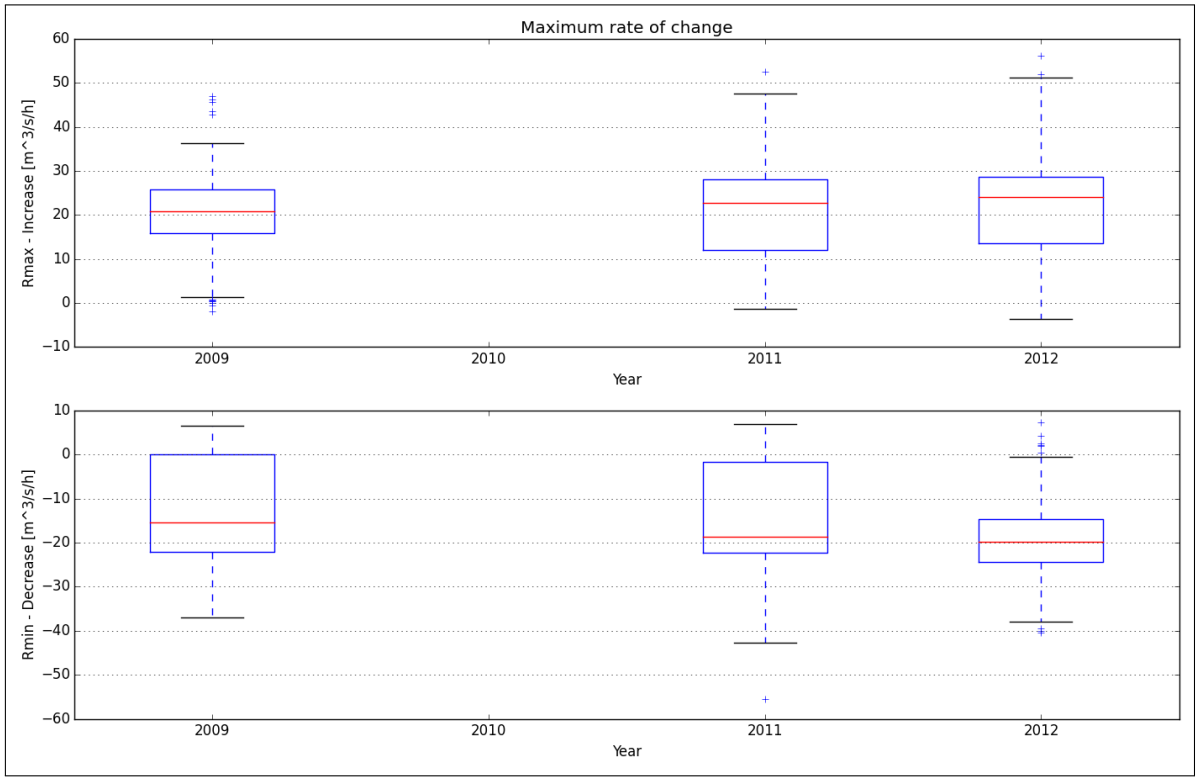

Figure A.38.190: Maximum rate of change

A.39. Dividal

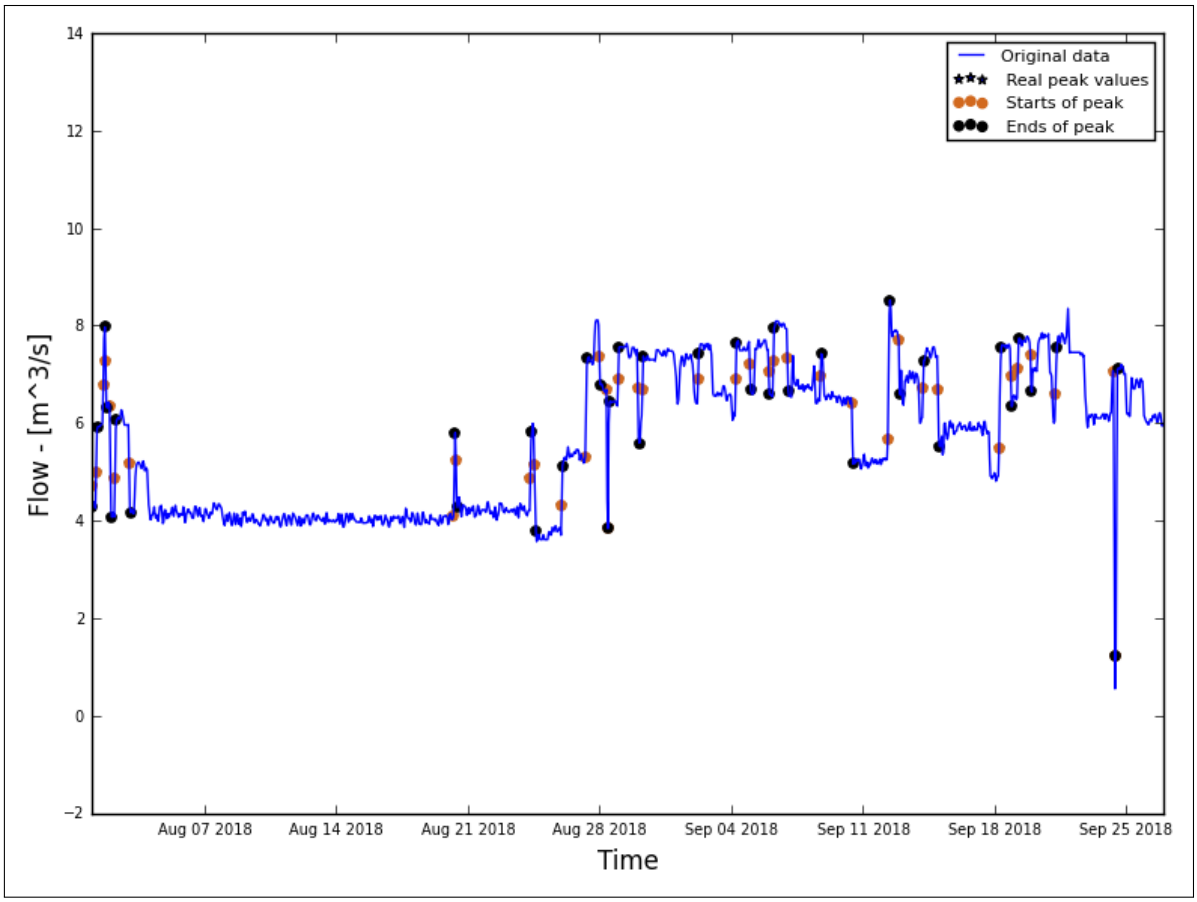

Figure A.39.191: Hydrograph of the last two months of the recorded data

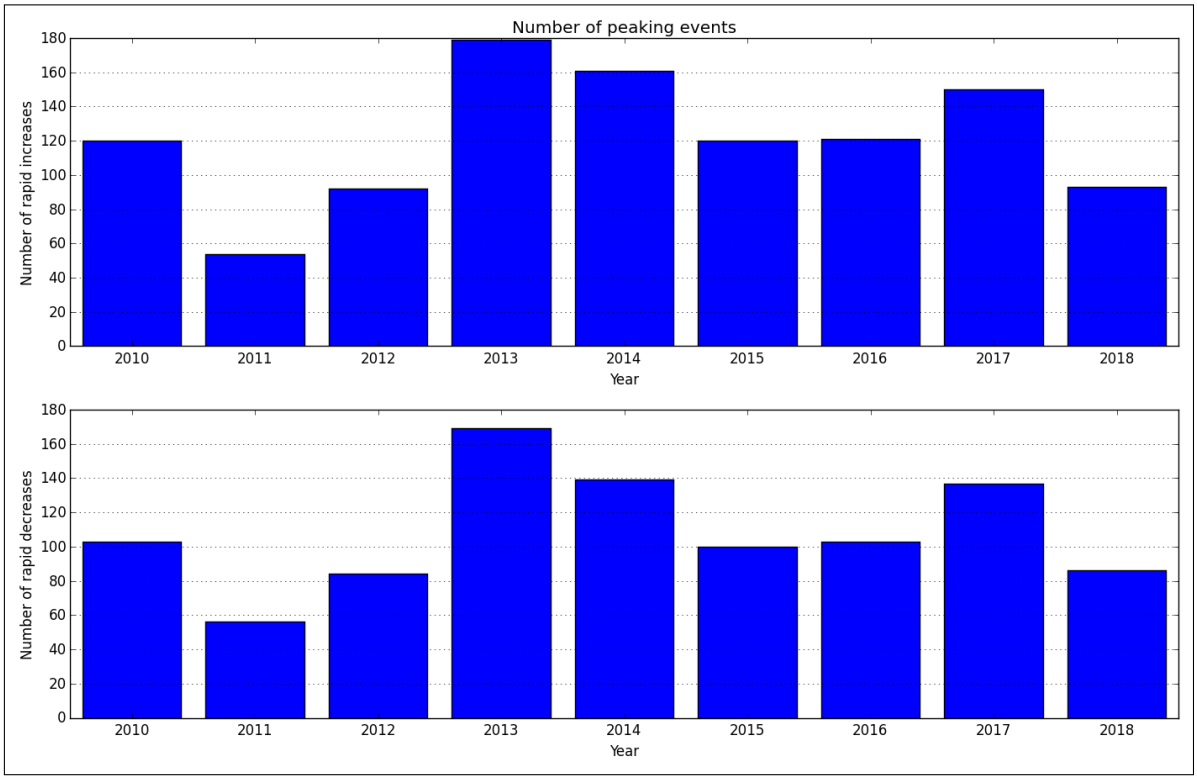

Figure A.39.192: Average annual number of increased/decreased peaks

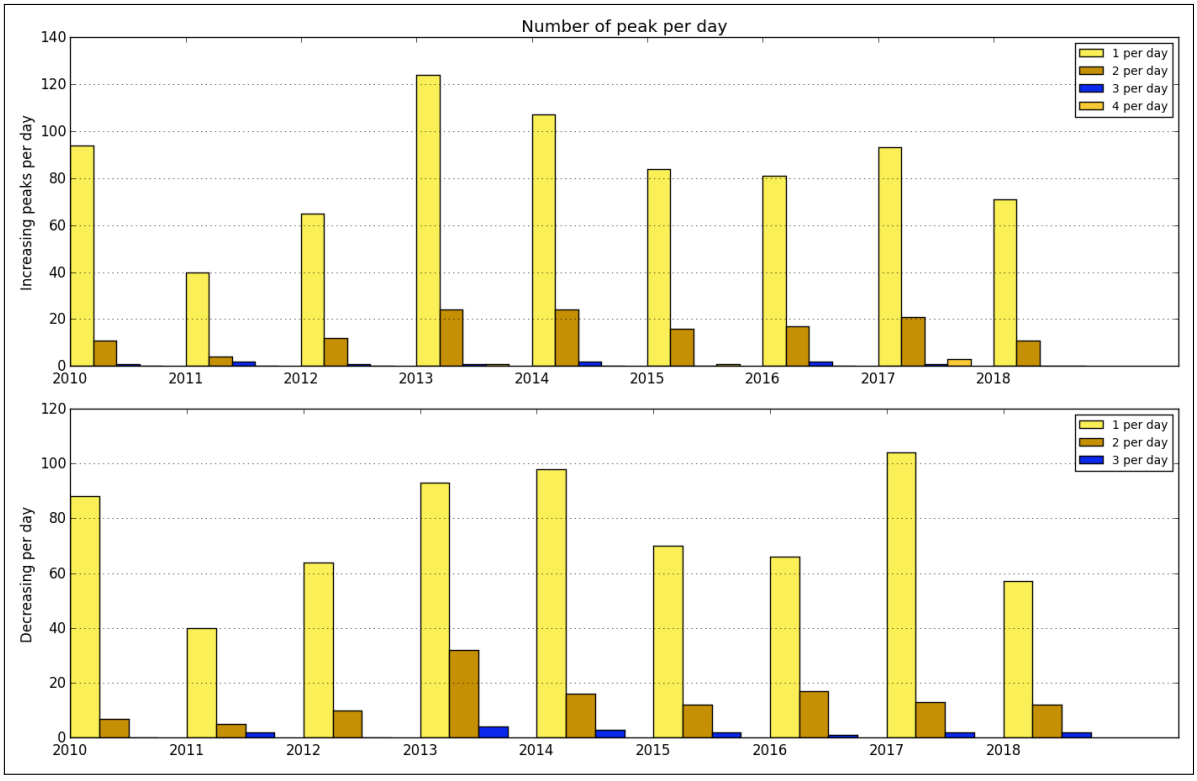

Figure A.39.193: Number of peaks per day

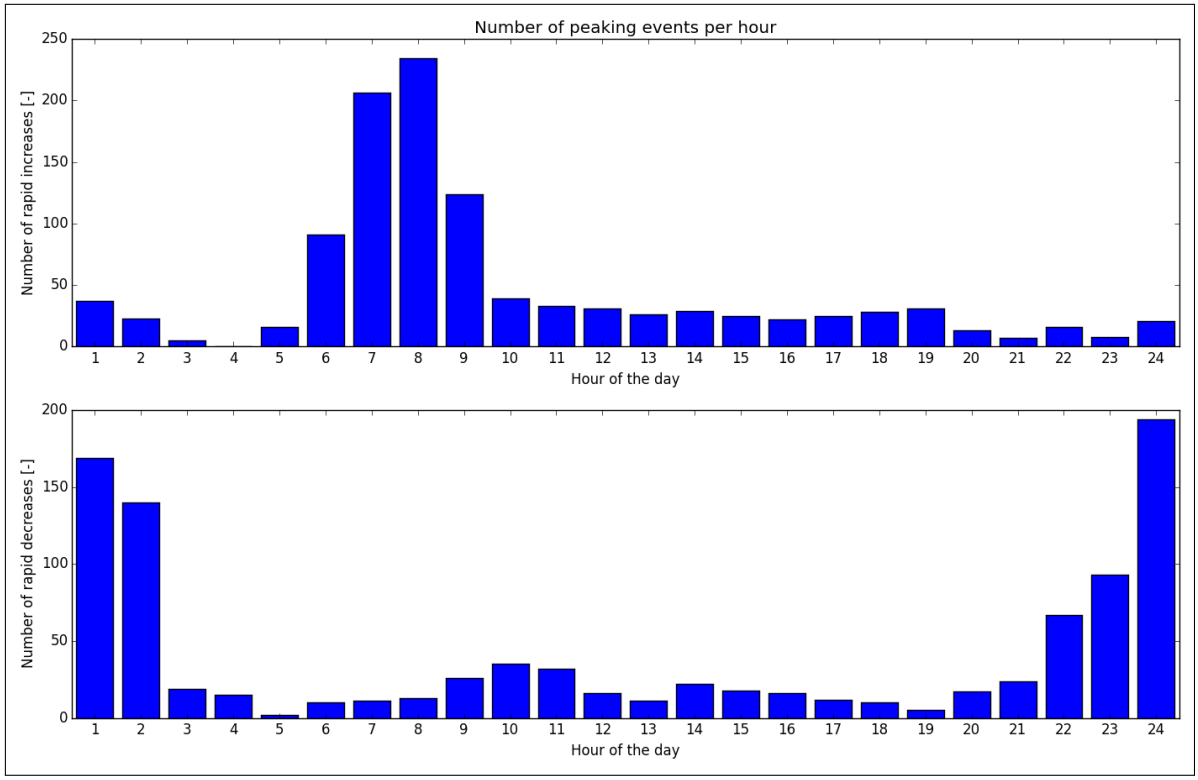

Figure A.39.194: Distribution of peaks throughout day

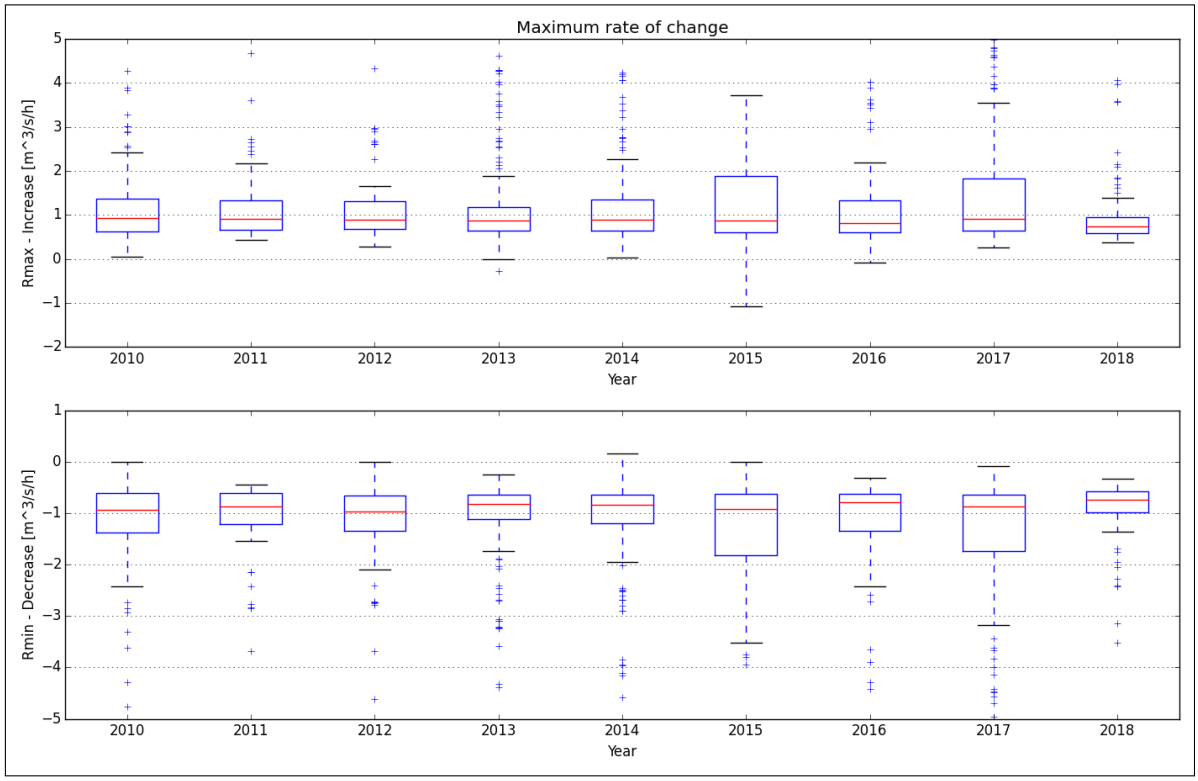

Figure A.39.195: Maximum rate of change

A.40. Skibotn

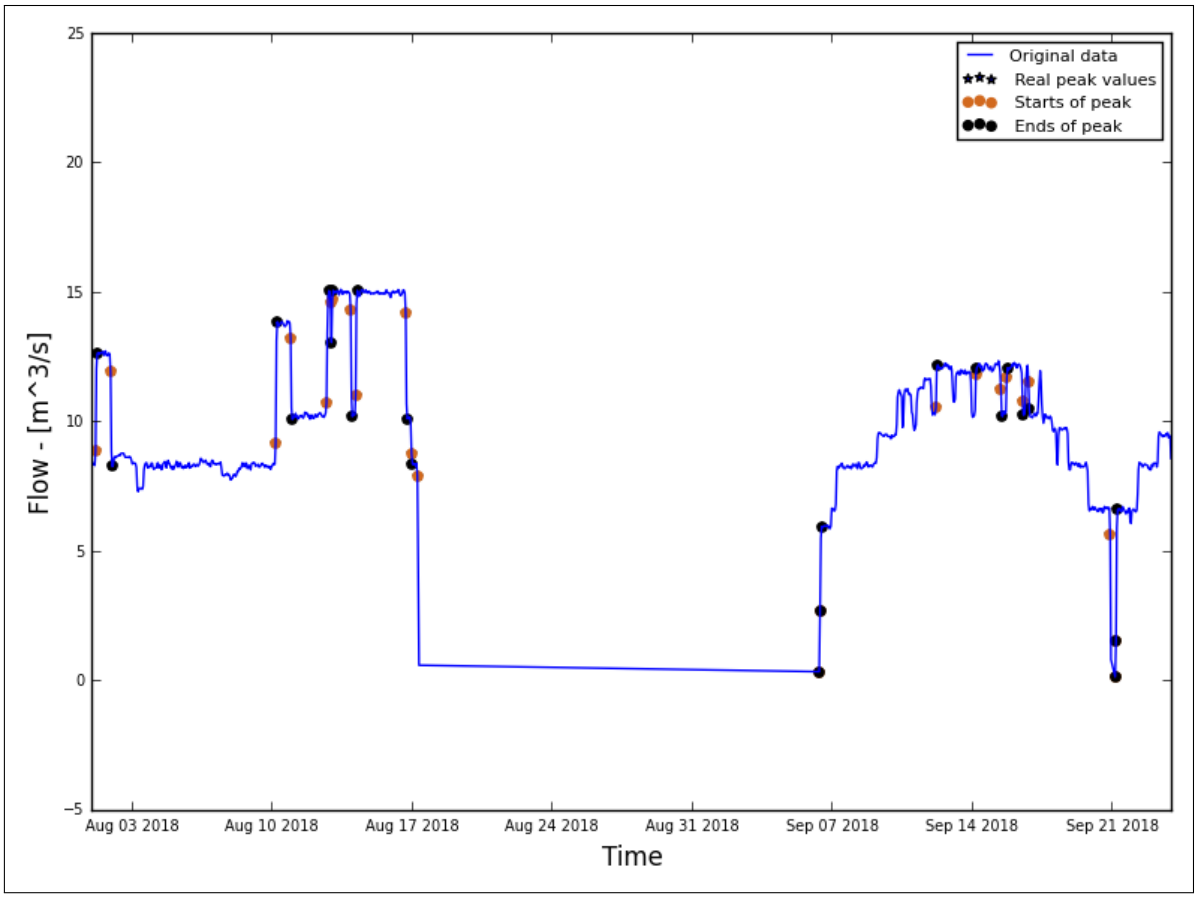

Figure A.40.196: Hydrograph of the last two months of the recorded data

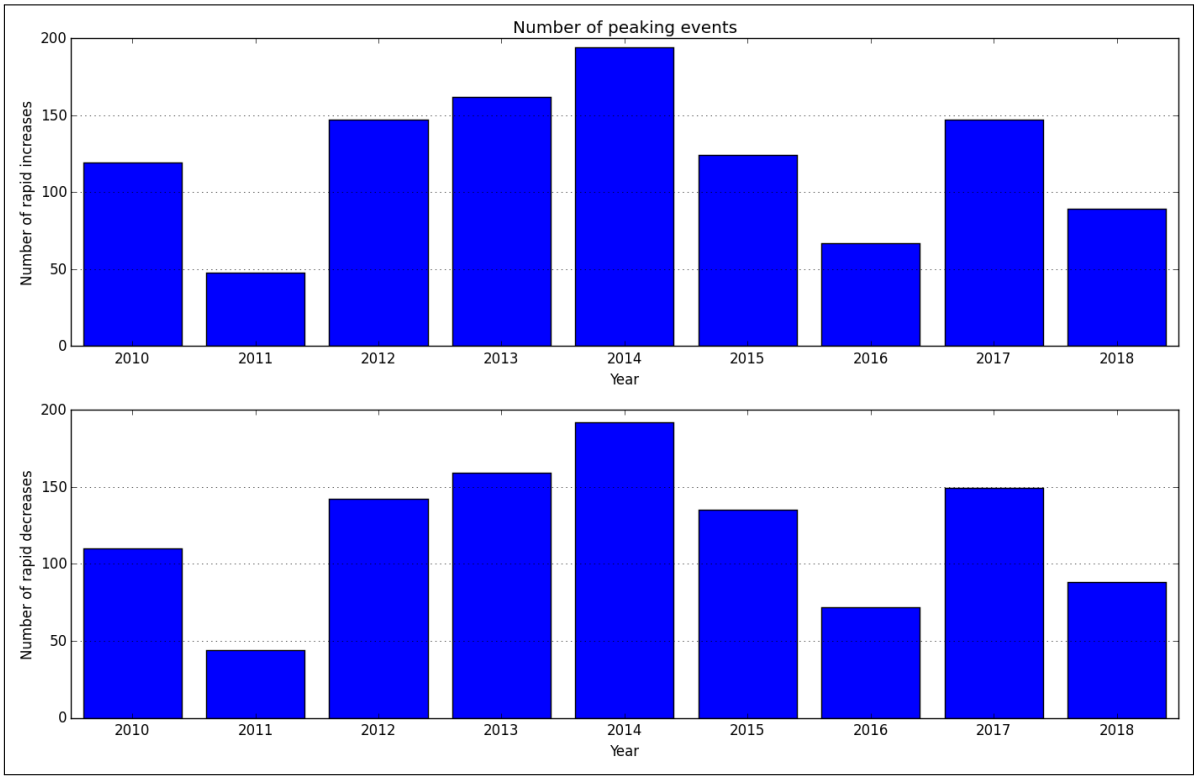

Figure A.40.197: Average annual number of increased/decreased peaks

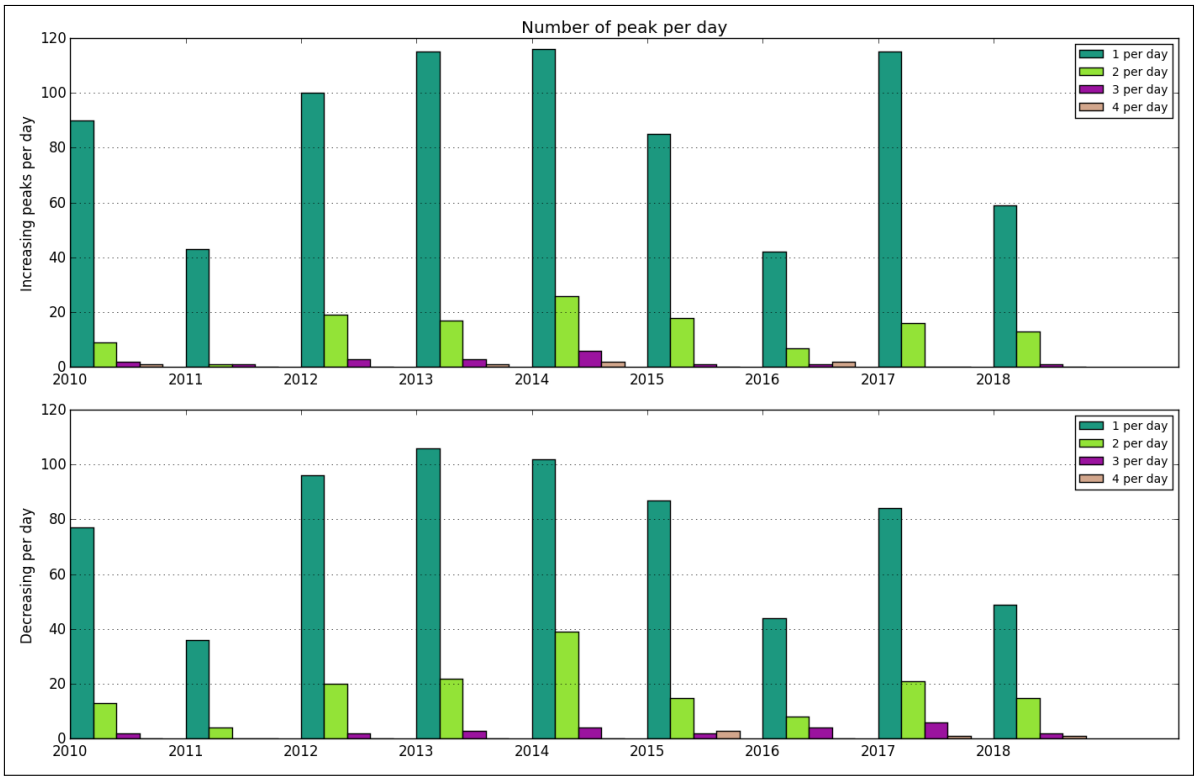

Figure A.40.198: Number of peaks per day

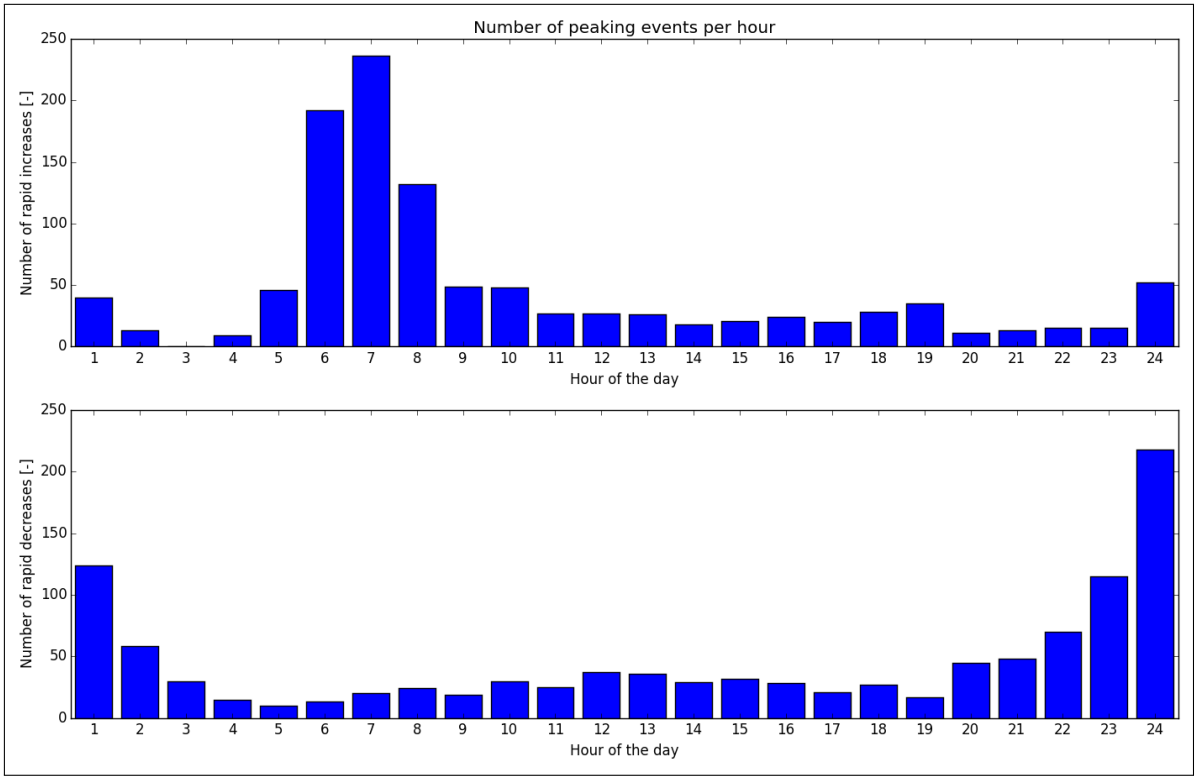

Figure A.40.199: Distribution of peaks throughout day

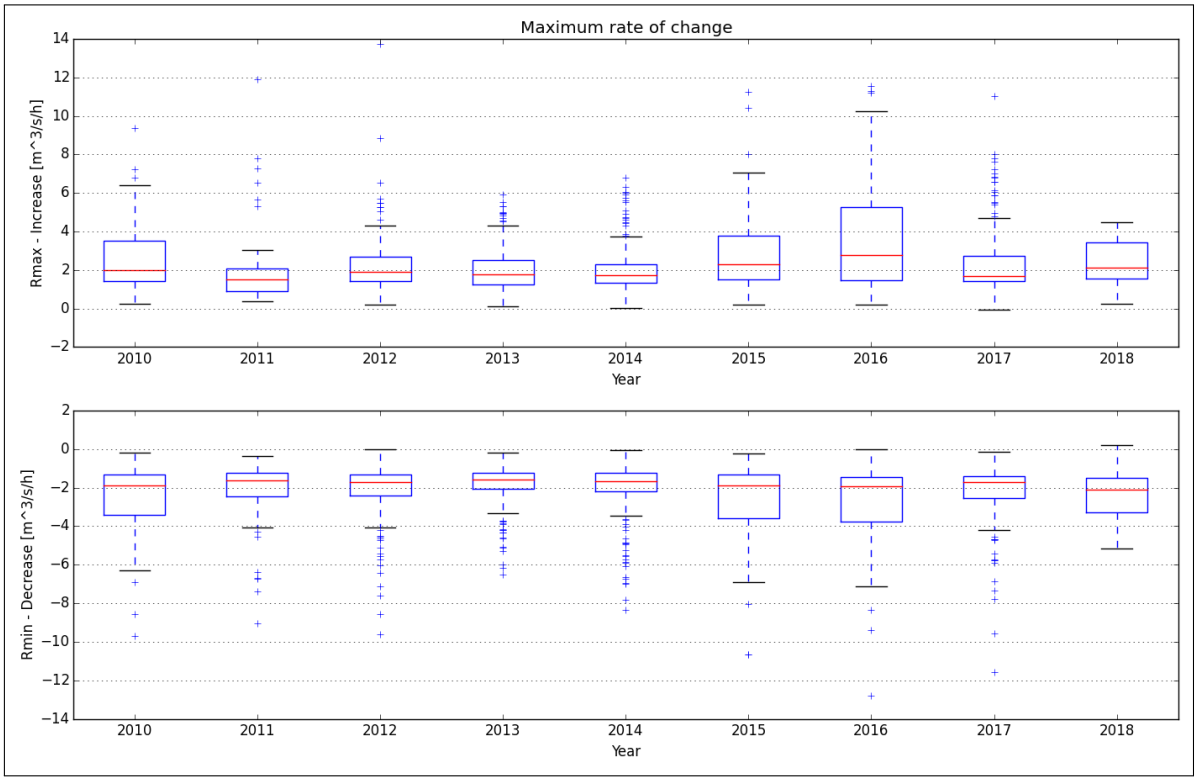

Figure A.40.200: Maximum rate of change

A.41. Alta

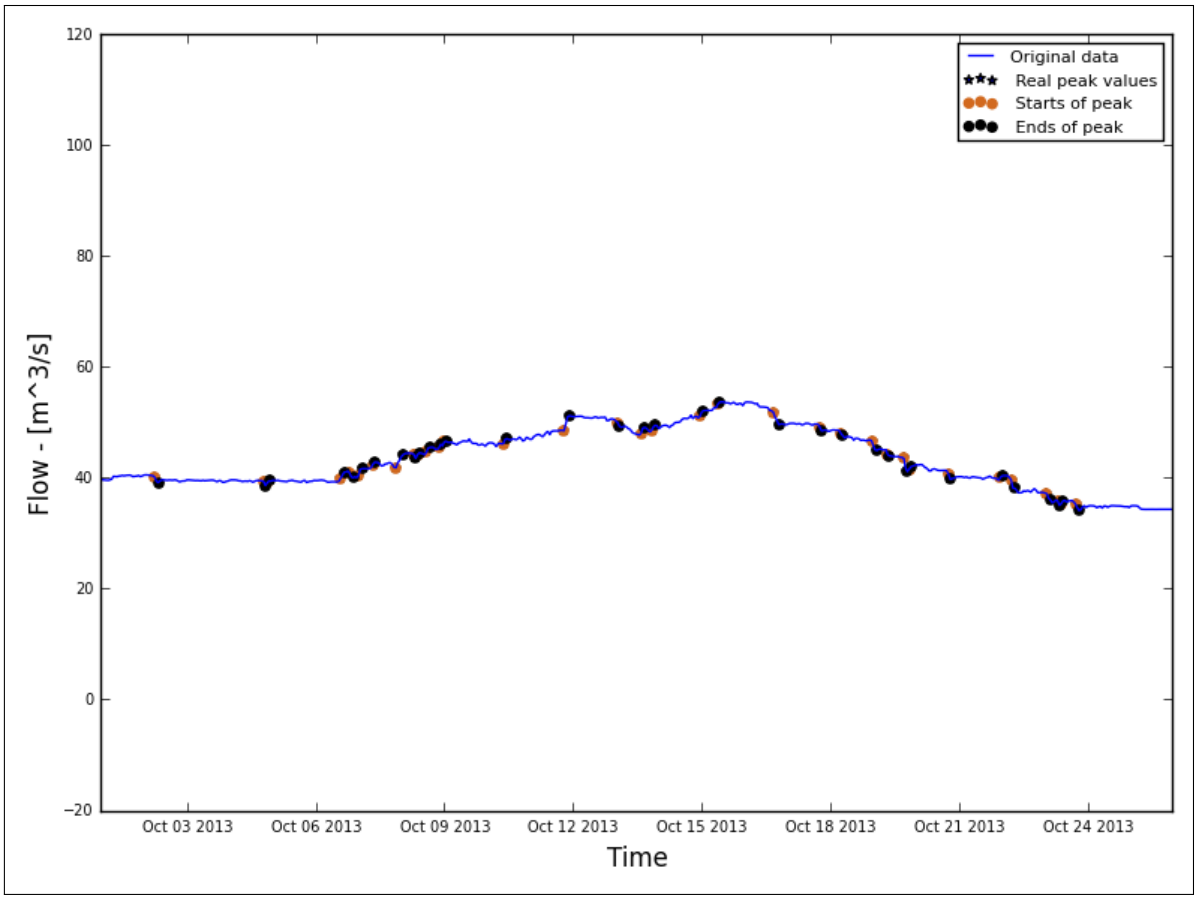

Figure A.41.201: Hydrograph of the last two months of the recorded data

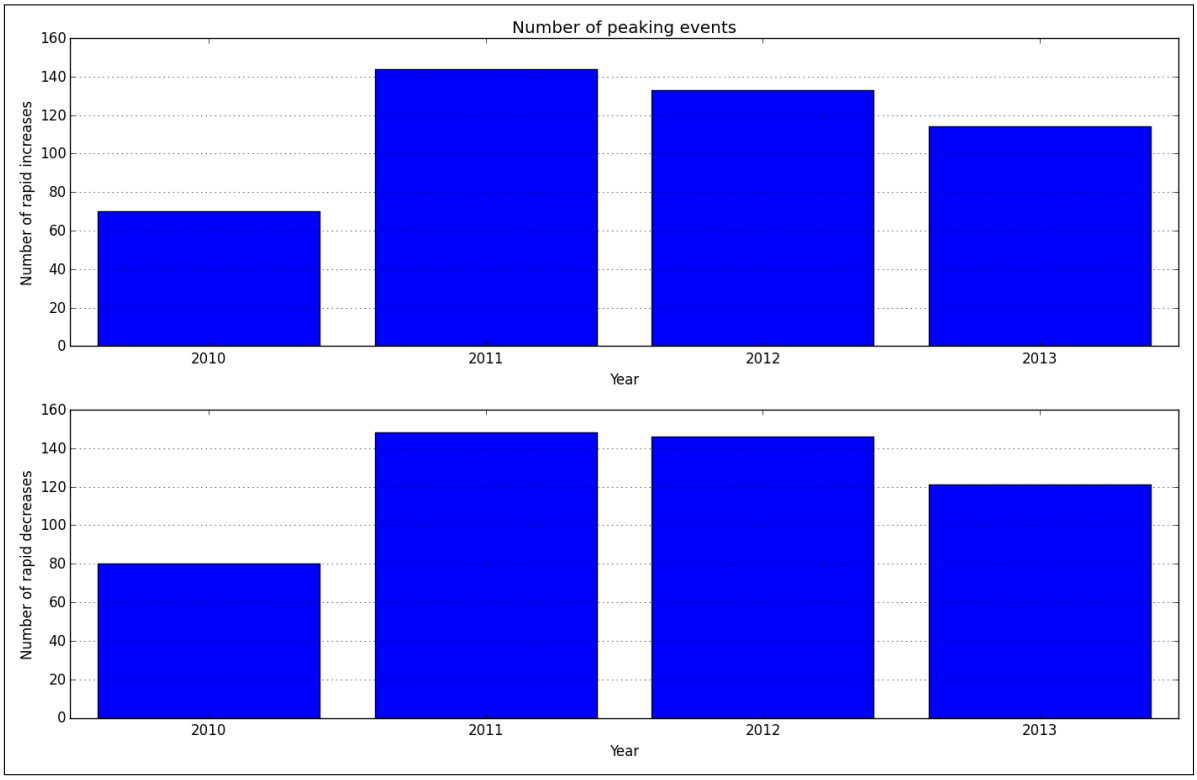

Figure A.41.202: Average annual number of increased/decreased peaks

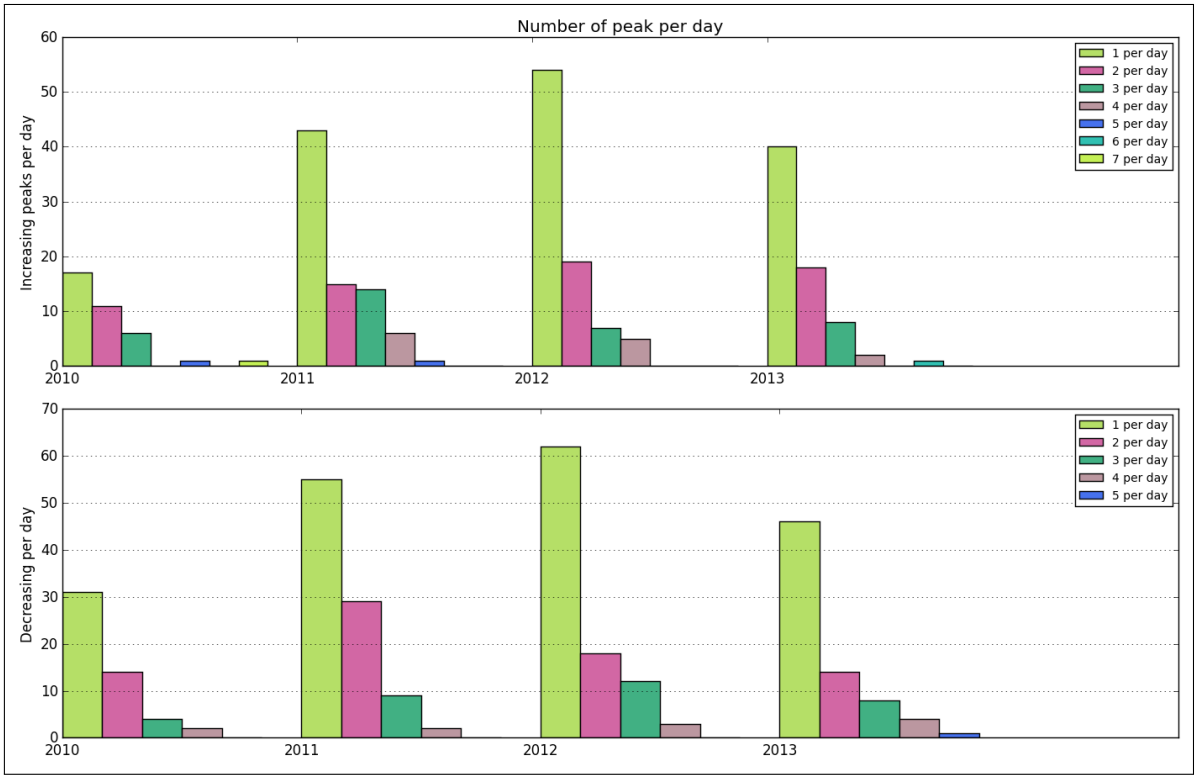

Figure A.41.203: Number of peaks per day

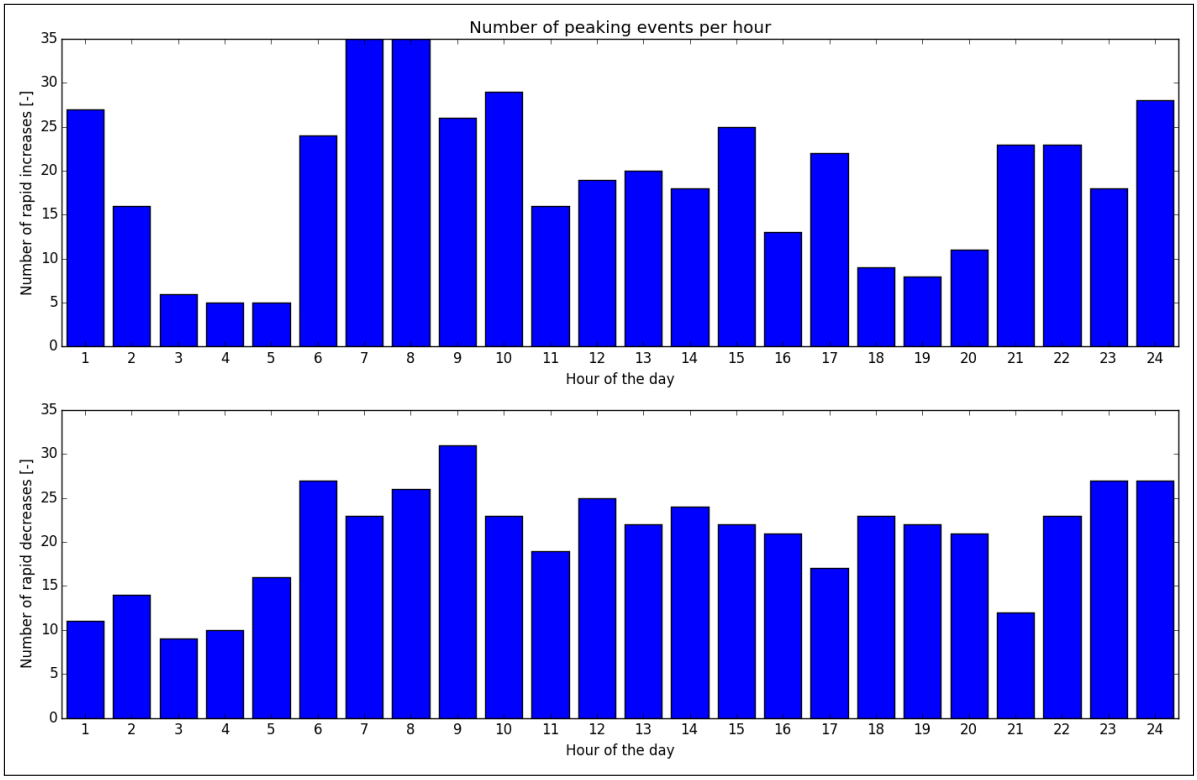

Figure A.41.204: Distribution of peaks throughout day

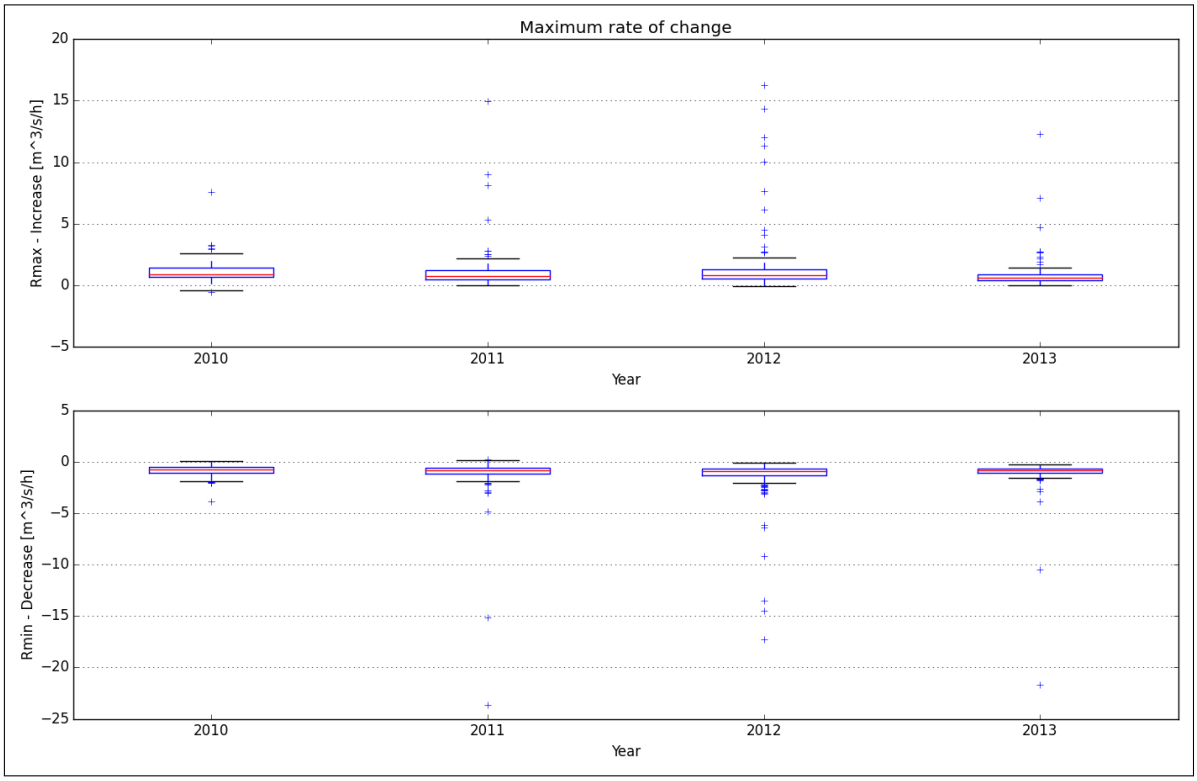

Figure A.41.205: Maximum rate of change

A.42. Kongsfjord

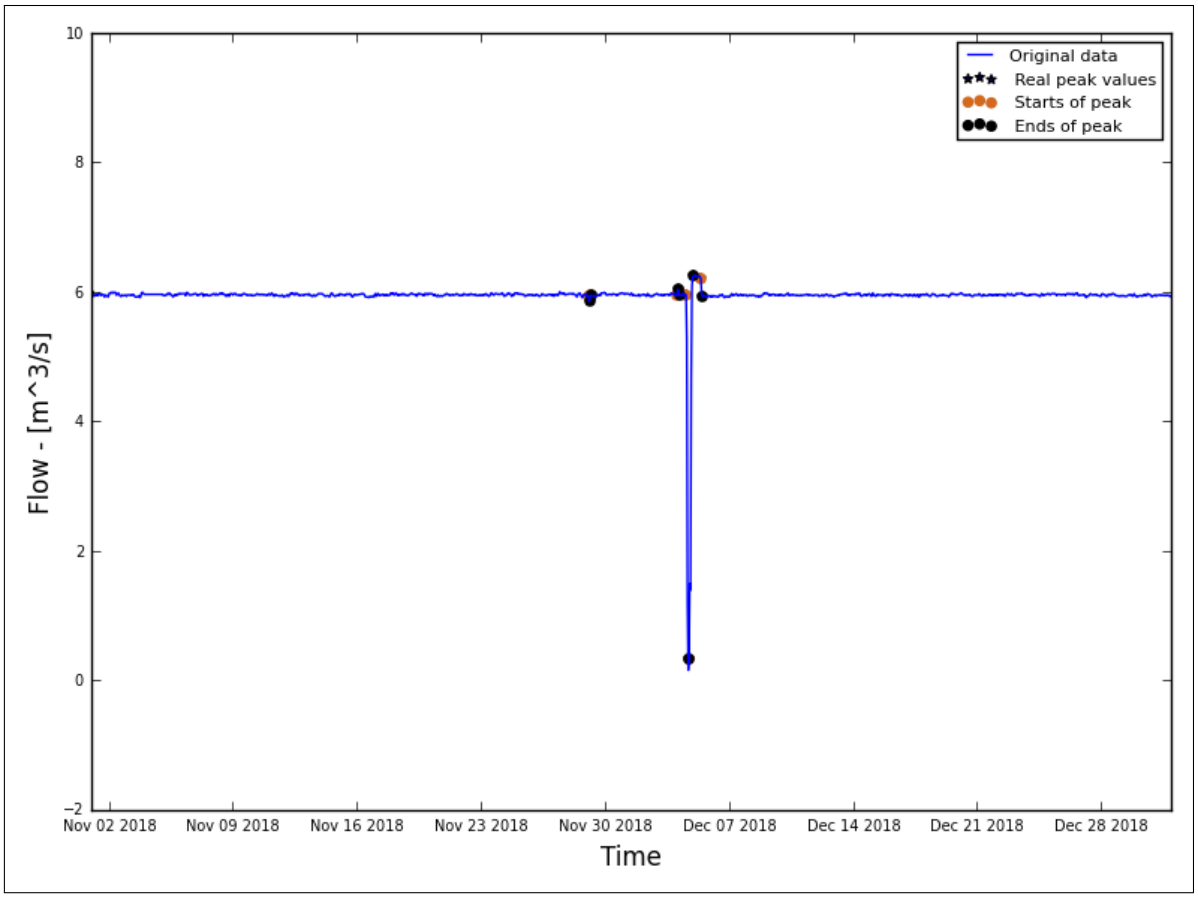

Figure A.42.206: Hydrograph of the last two months of the recorded data

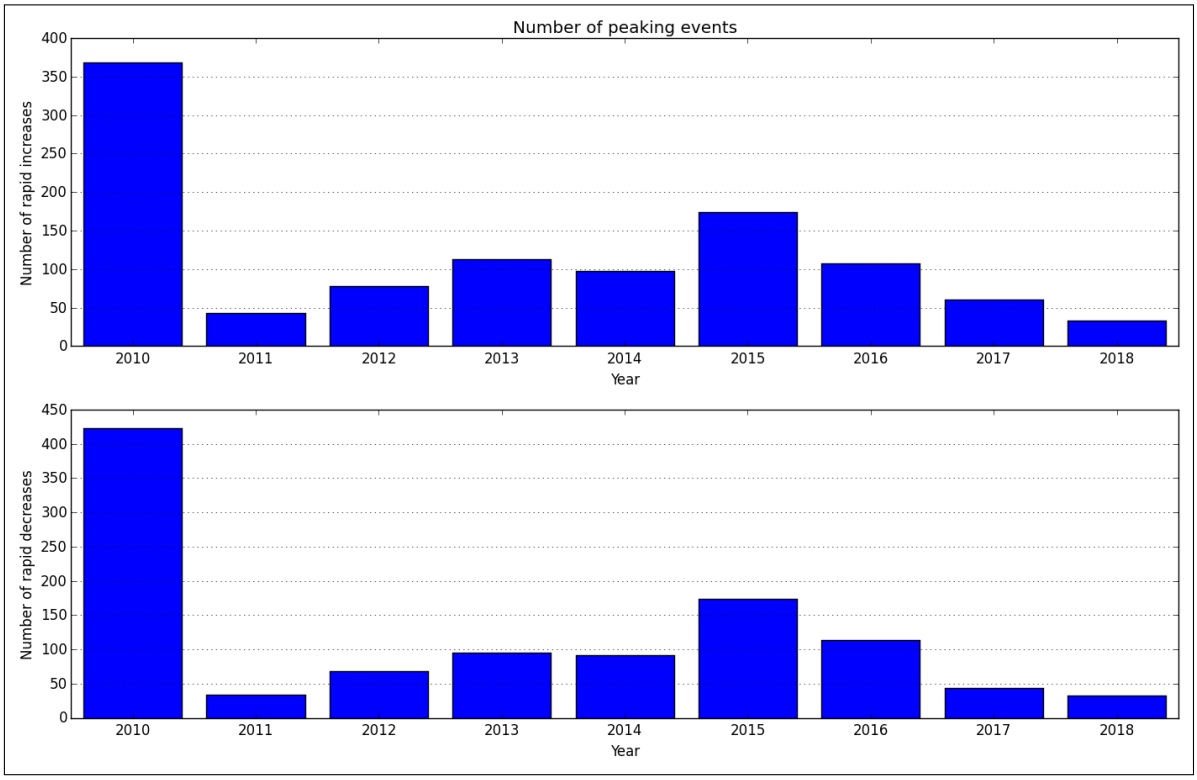

Figure A.42.207: Average annual number of increased/decreased peaks

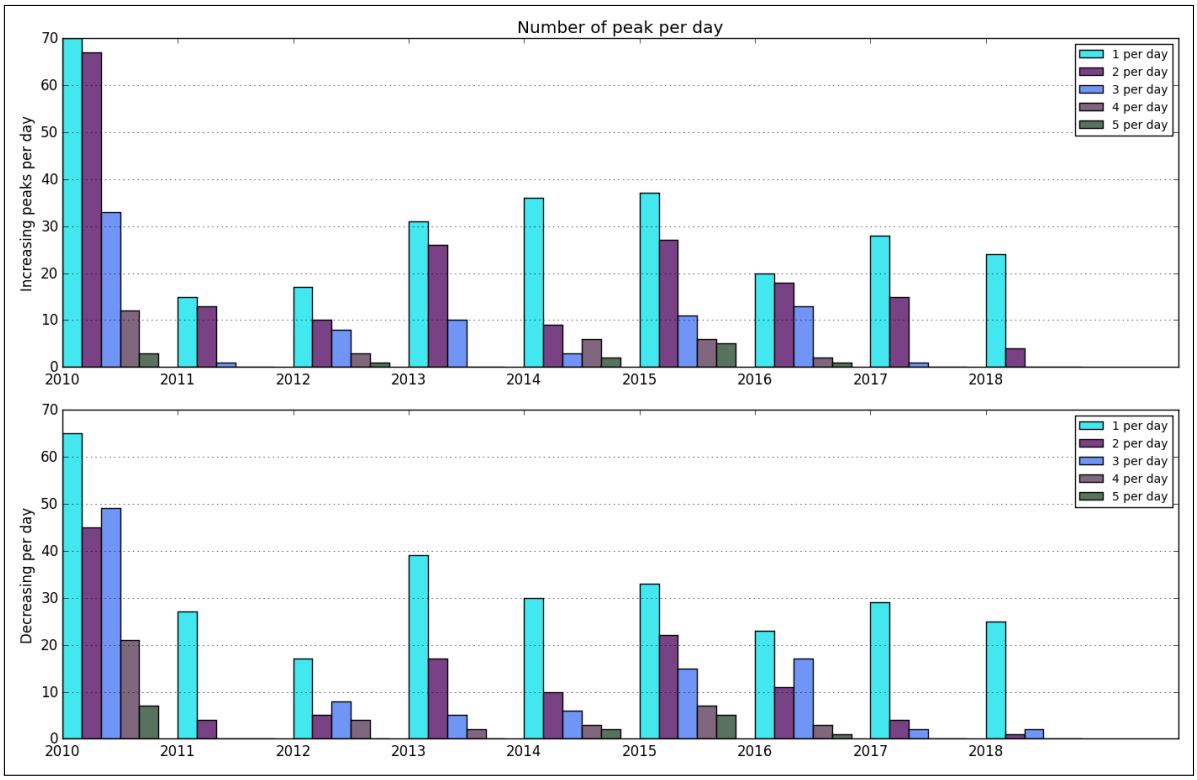

Figure A.42.208: Number of peaks per day

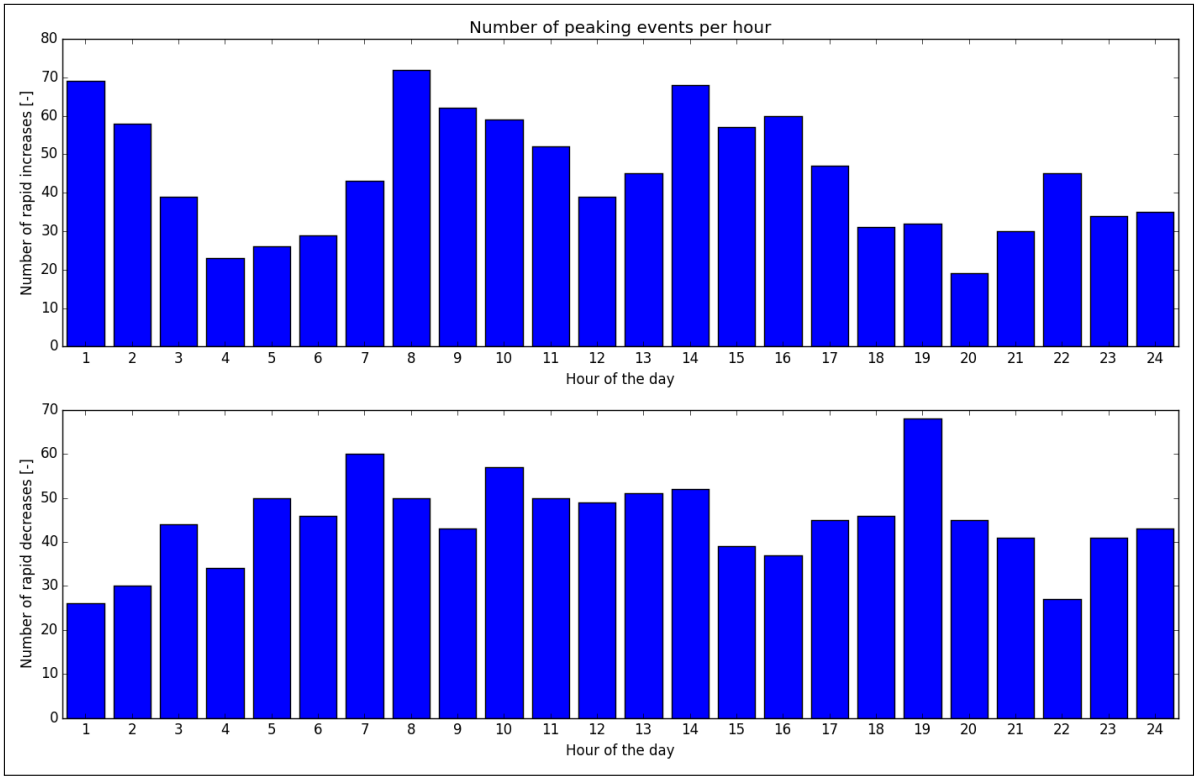

Figure A.42.209: Distribution of peaks throughout day

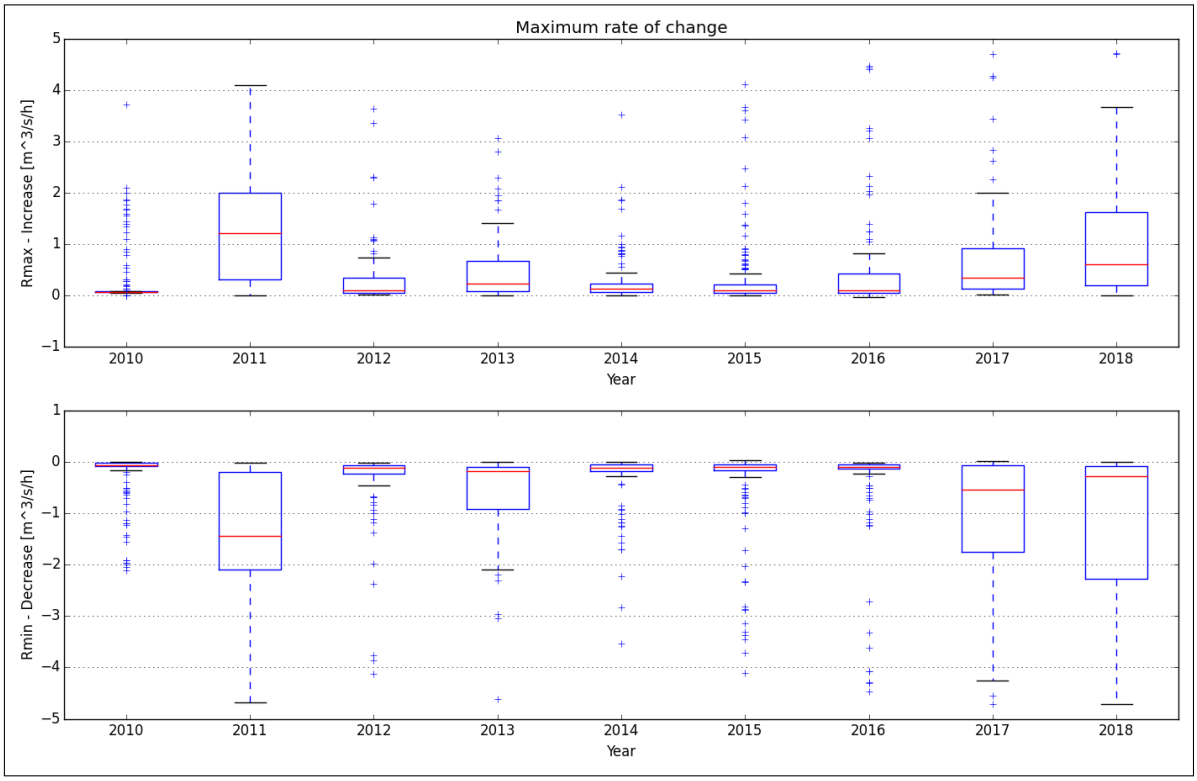

Figure A.42.210: Maximum rate of change

A.43. Skogfoss

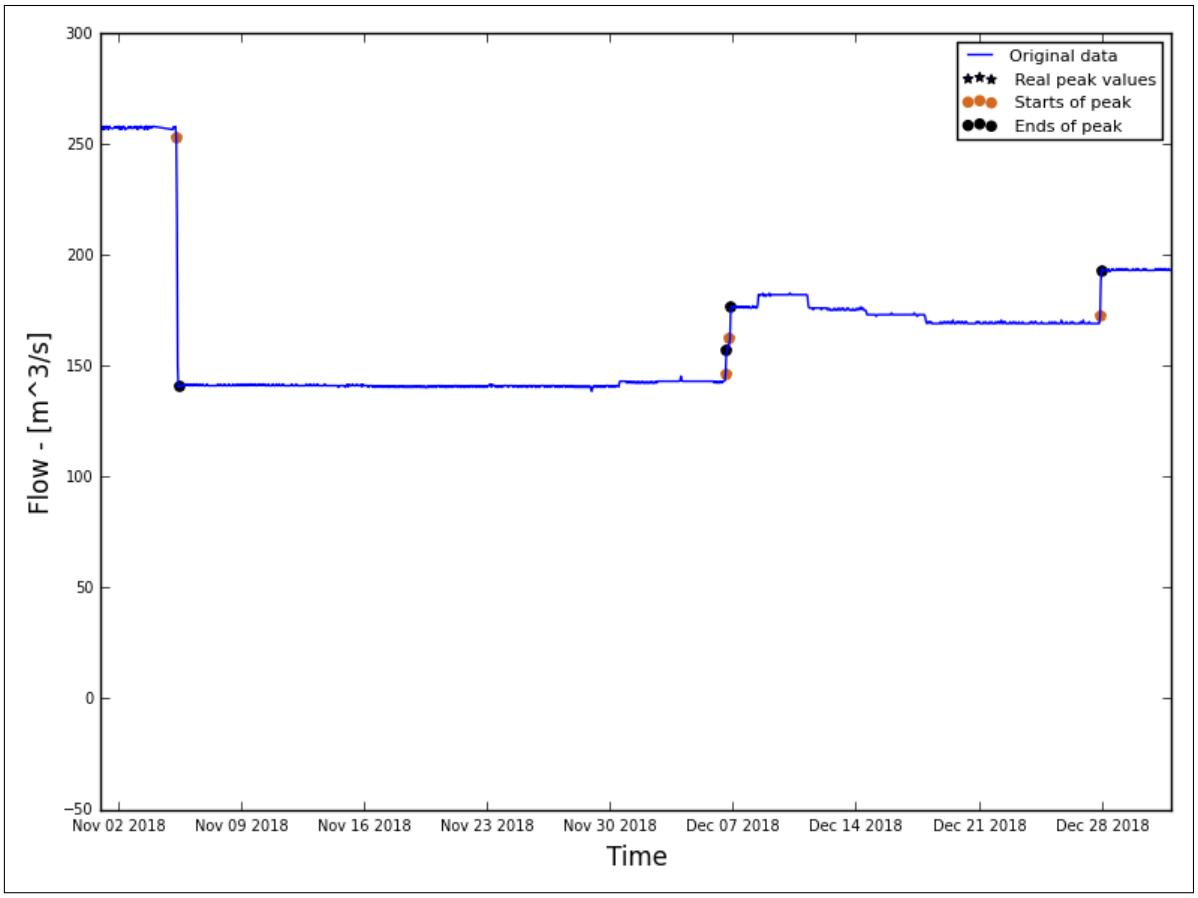

Figure A.43.211: Hydrograph of the last two months of the recorded data

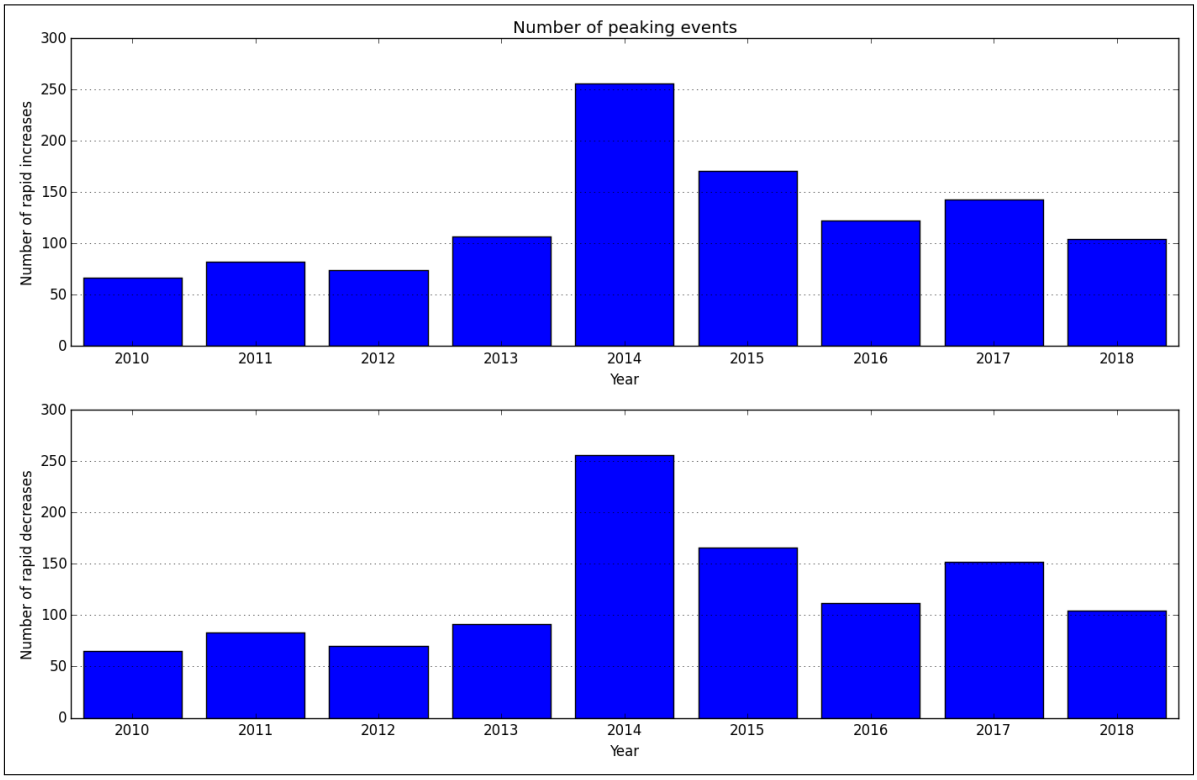

Figure A.43.212: Average annual number of increased/decreased peaks

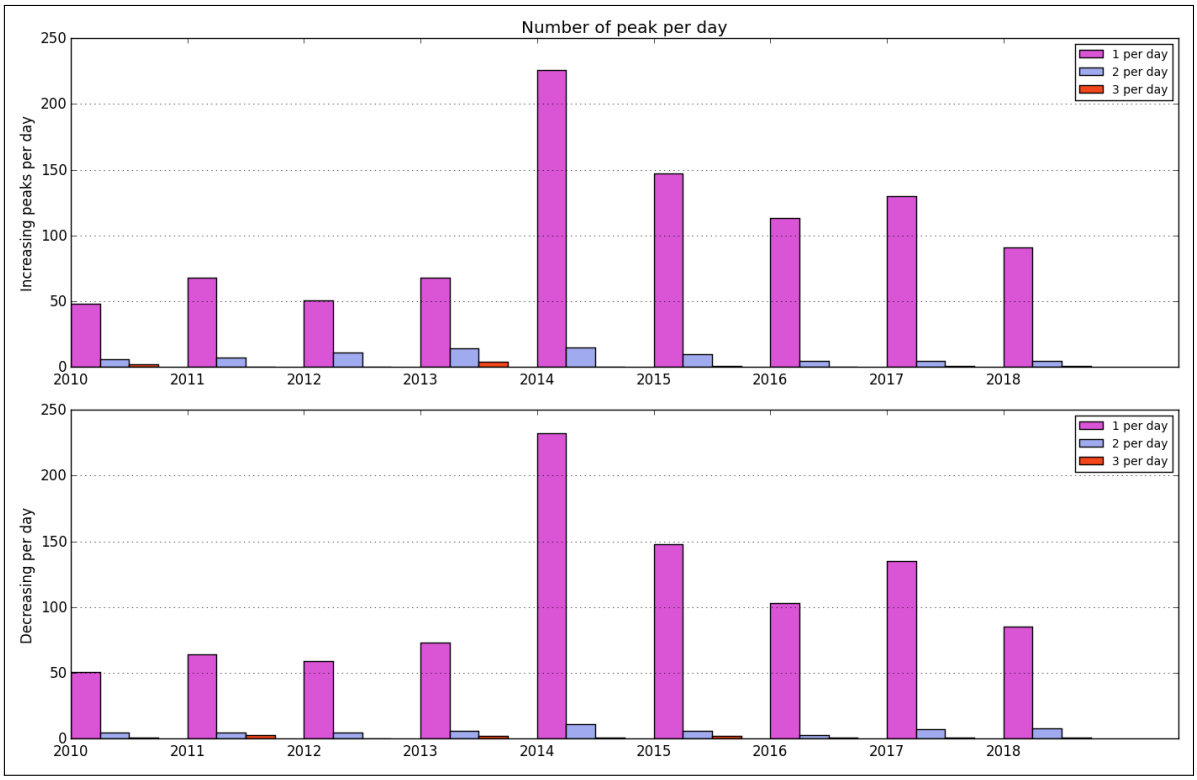

Figure A.43.213: Number of peaks per day

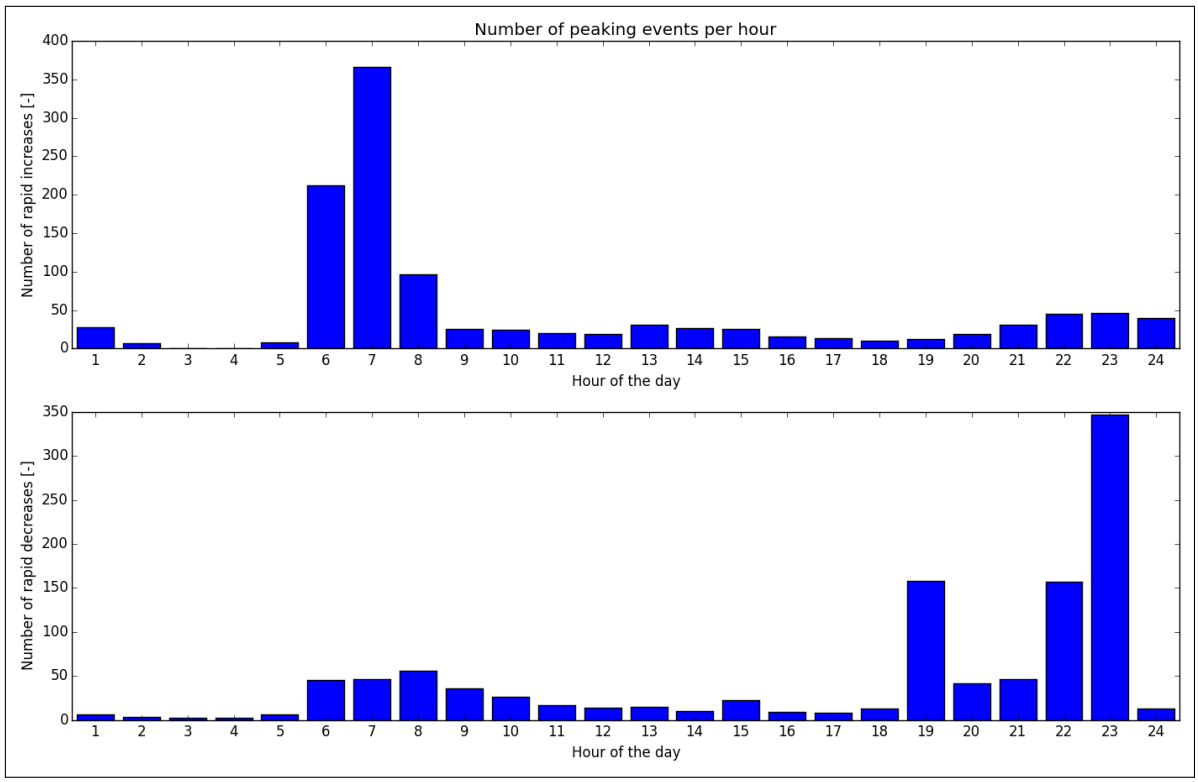

Figure A.43.214: Distribution of peaks throughout day

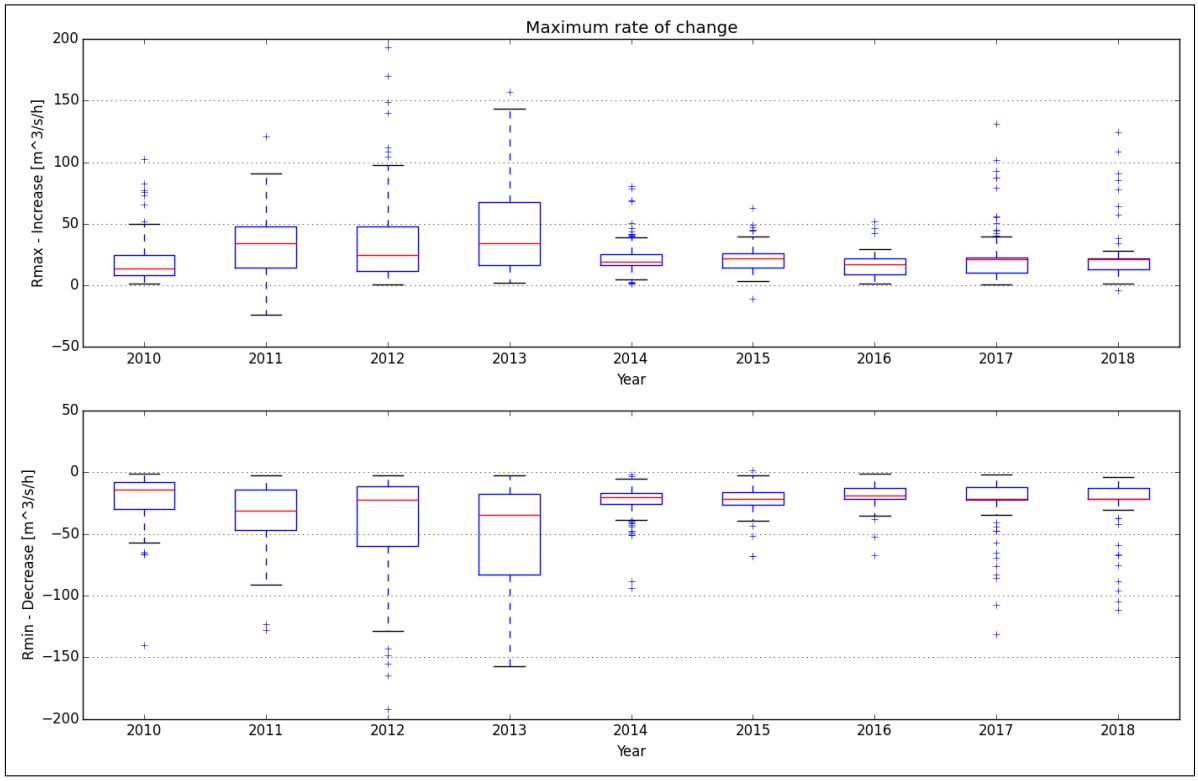

Figure A.43.215: Maximum rate of change

A.44. Hjartal

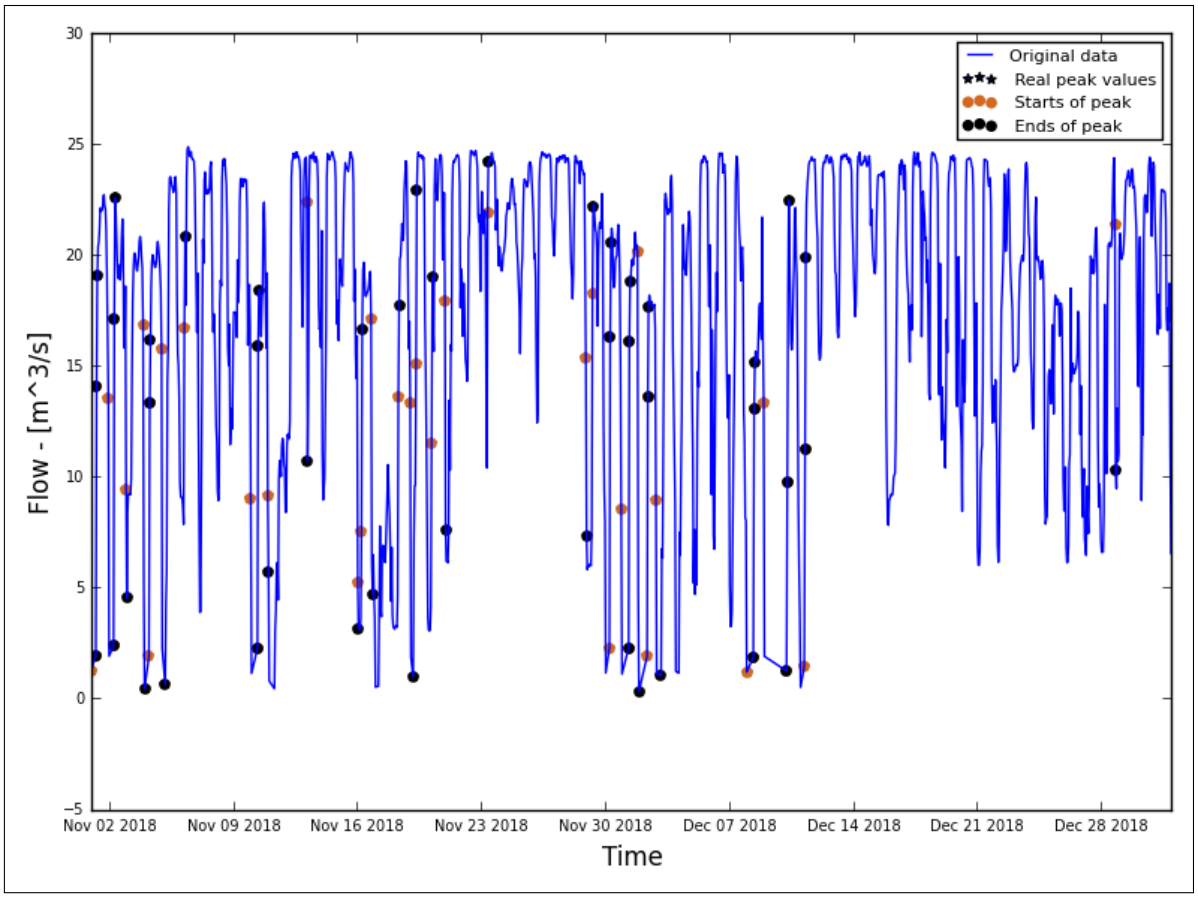

Figure A.44.216: Hydrograph of the last two months of the recorded data

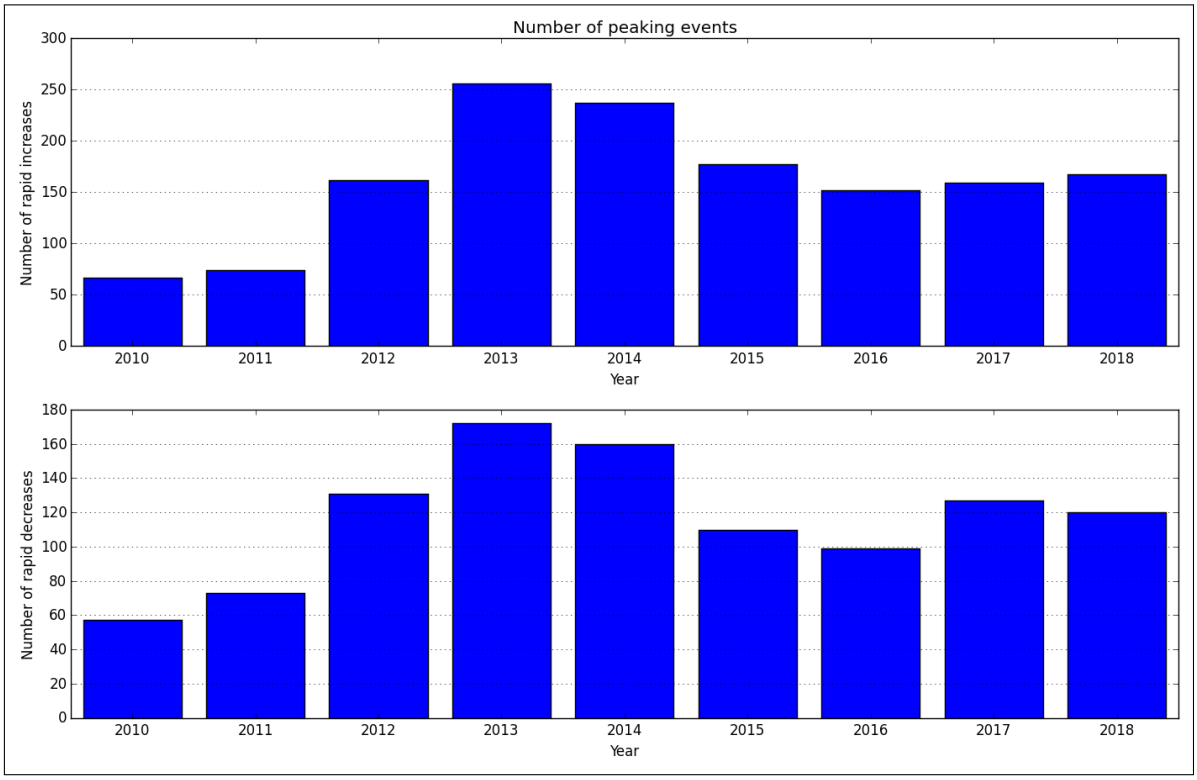

Figure A.44.217: Average annual number of increased/decreased peaks

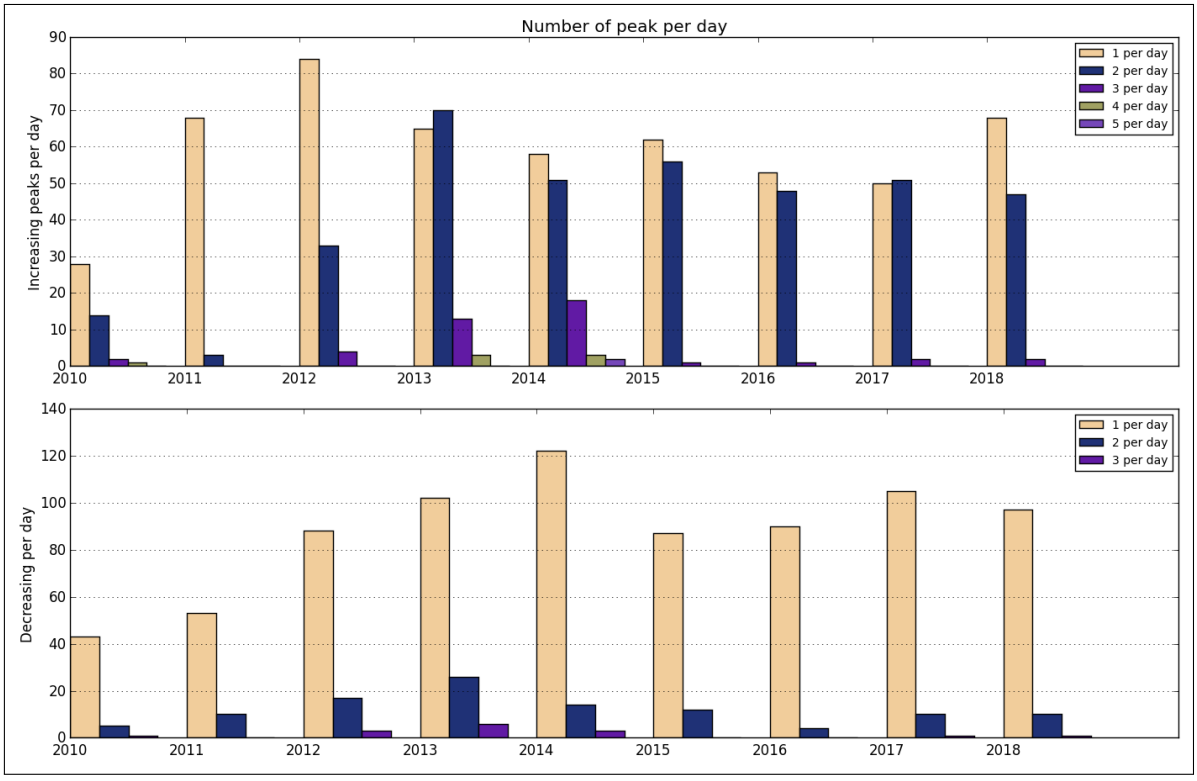

Figure A.44.218: Number of peaks per day

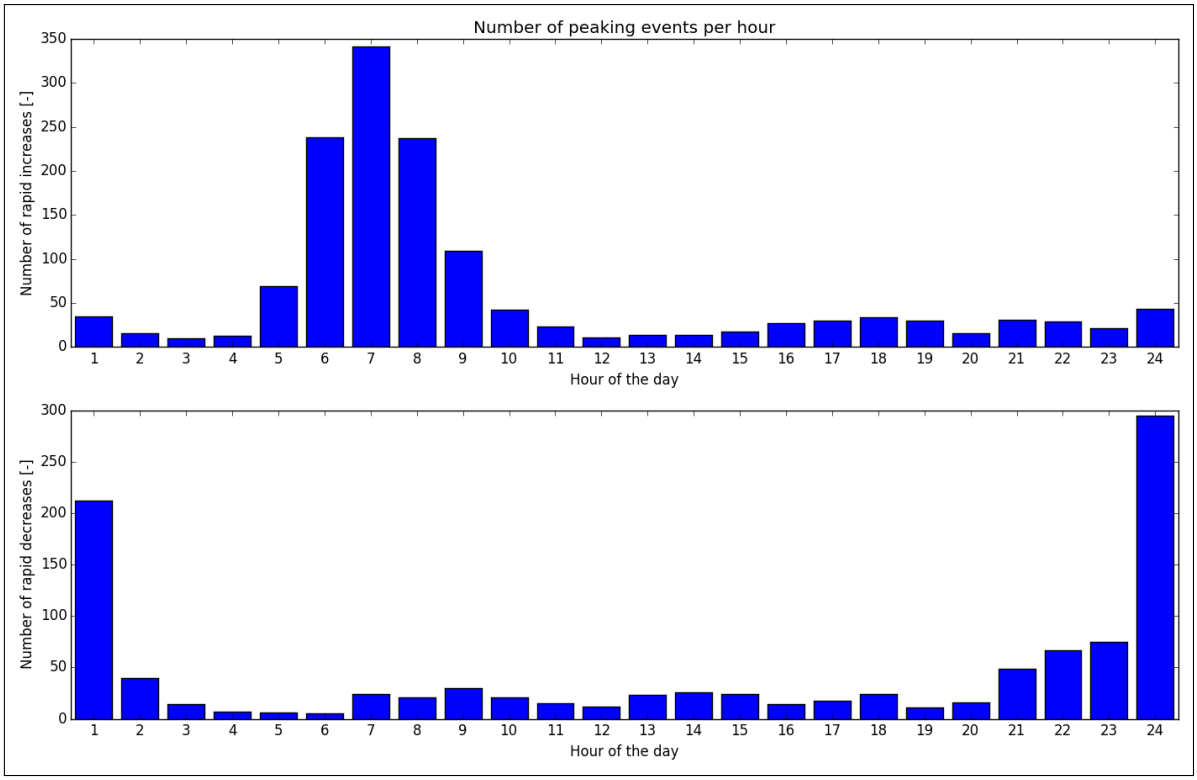

Figure A.44.219: Distribution of peaks throughout day

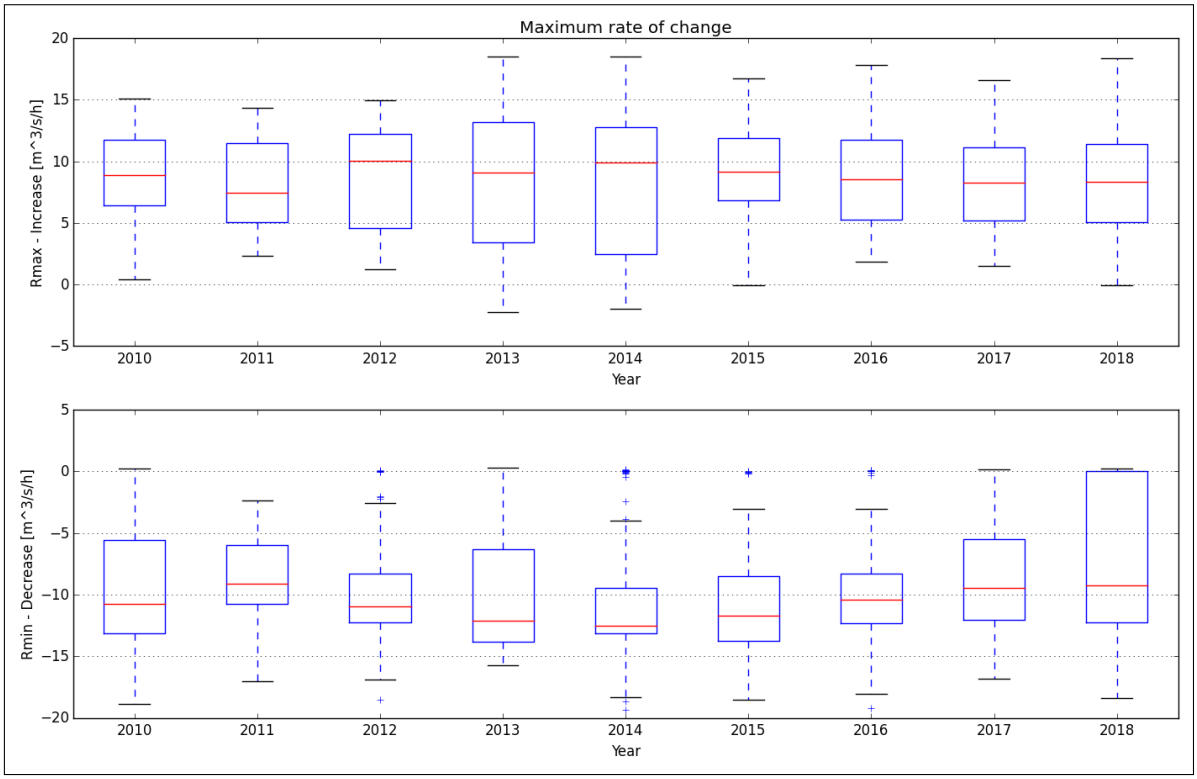

Figure A.44.220: Maximum rate of change

A.45. Usta II

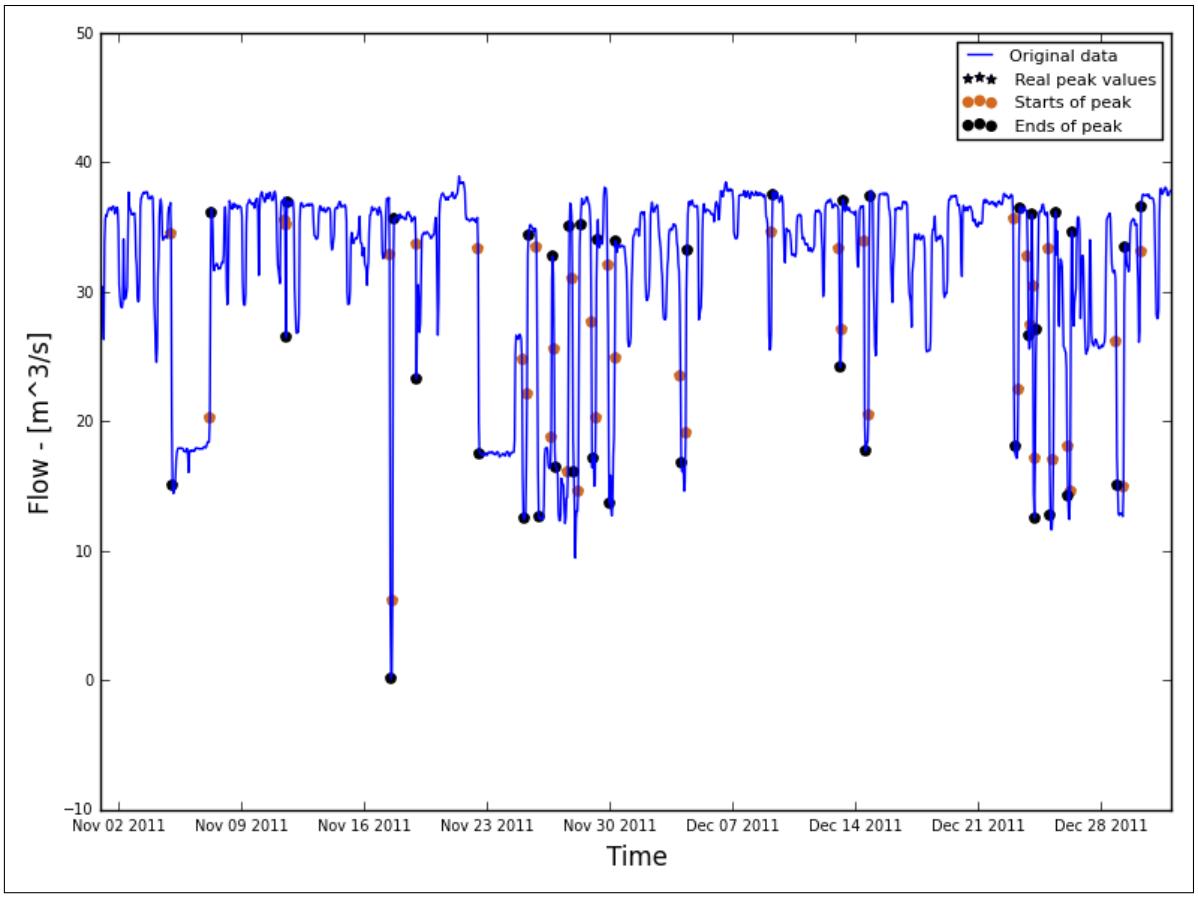

Figure A.45.221: Hydrograph of the last two months of the recorded data

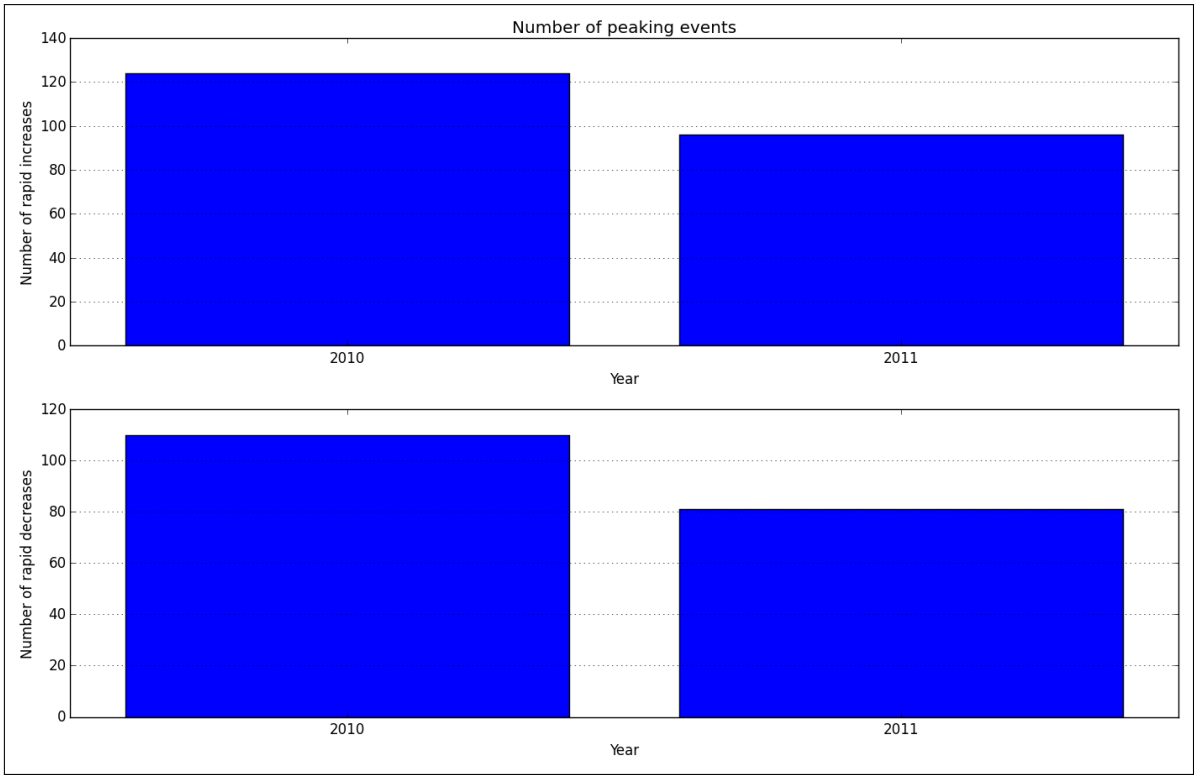

Figure A.45.222: Average annual number of increased/decreased peaks

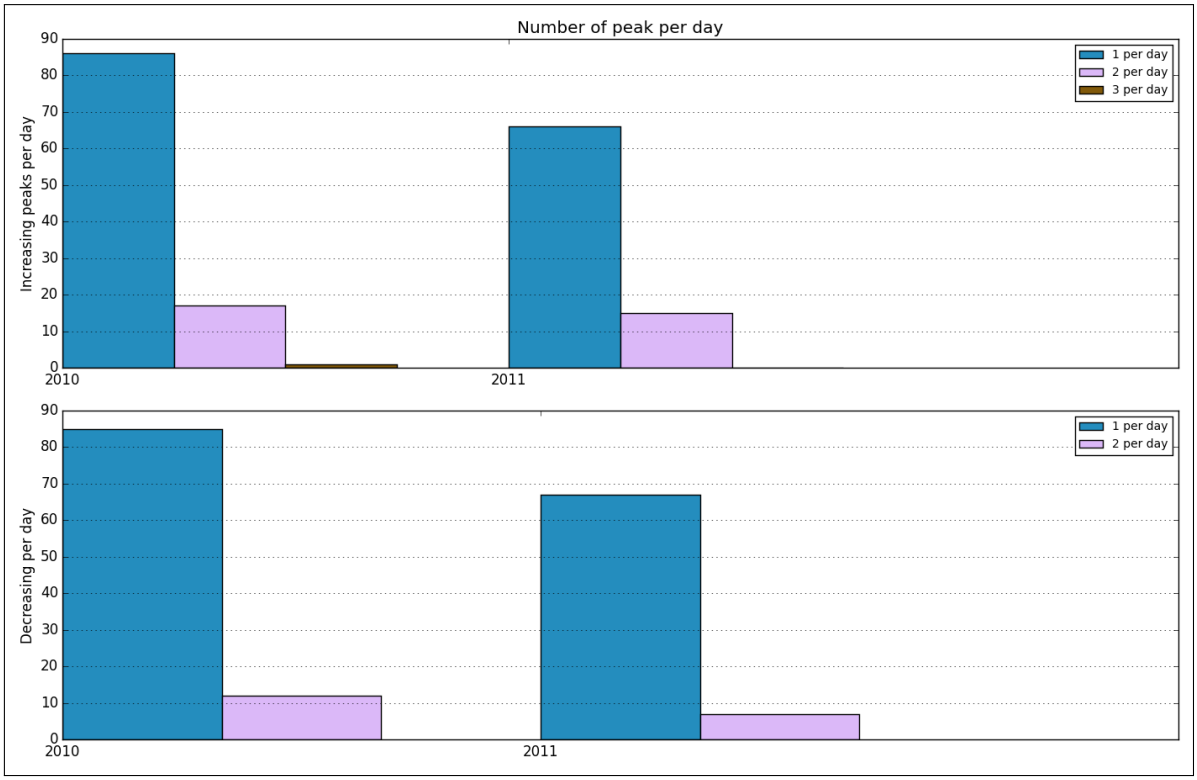

Figure A.45.223: Number of peaks per day

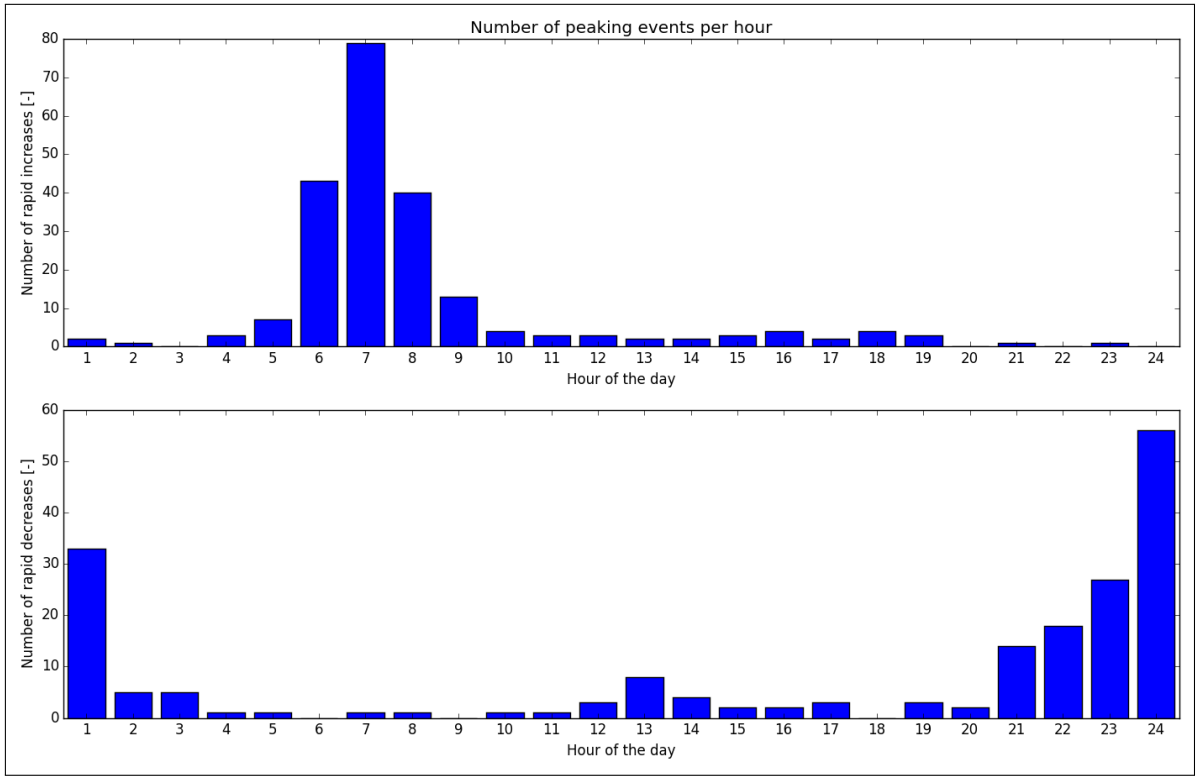

Figure A.45.224: Distribution of peaks throughout day

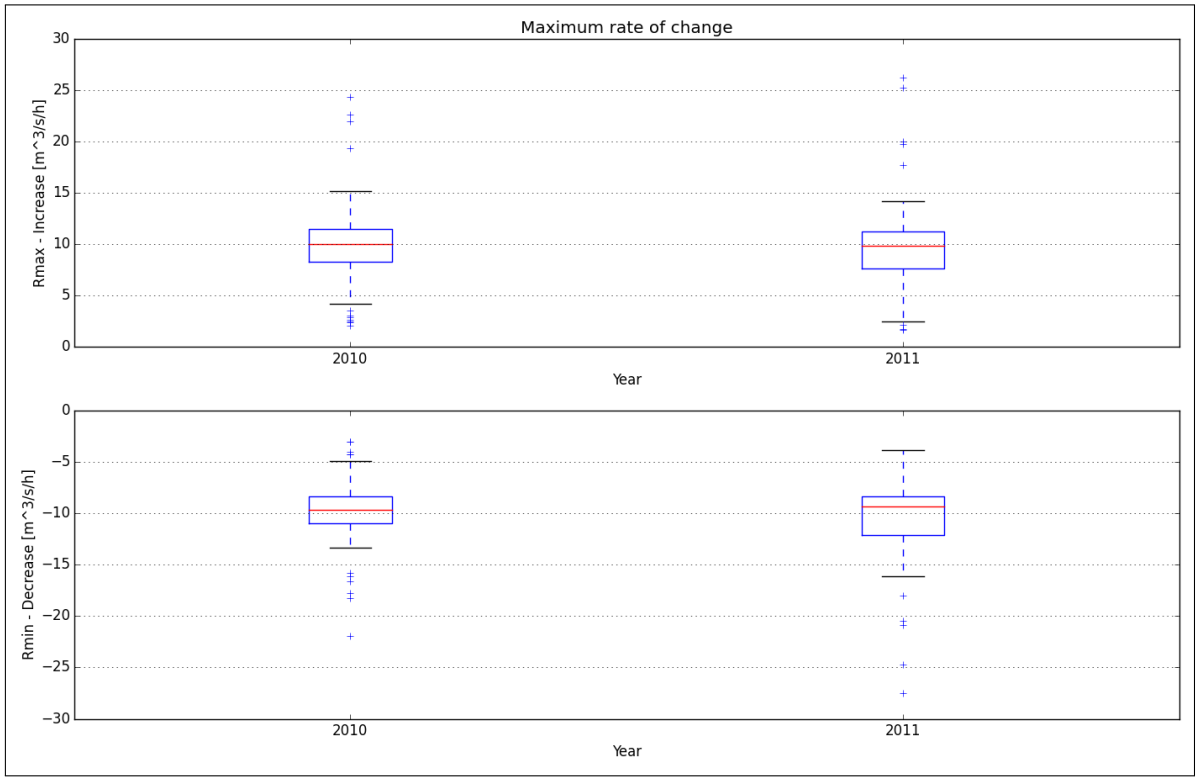

Figure A.45.225: Maximum rate of change

A.46. Bingsfoss

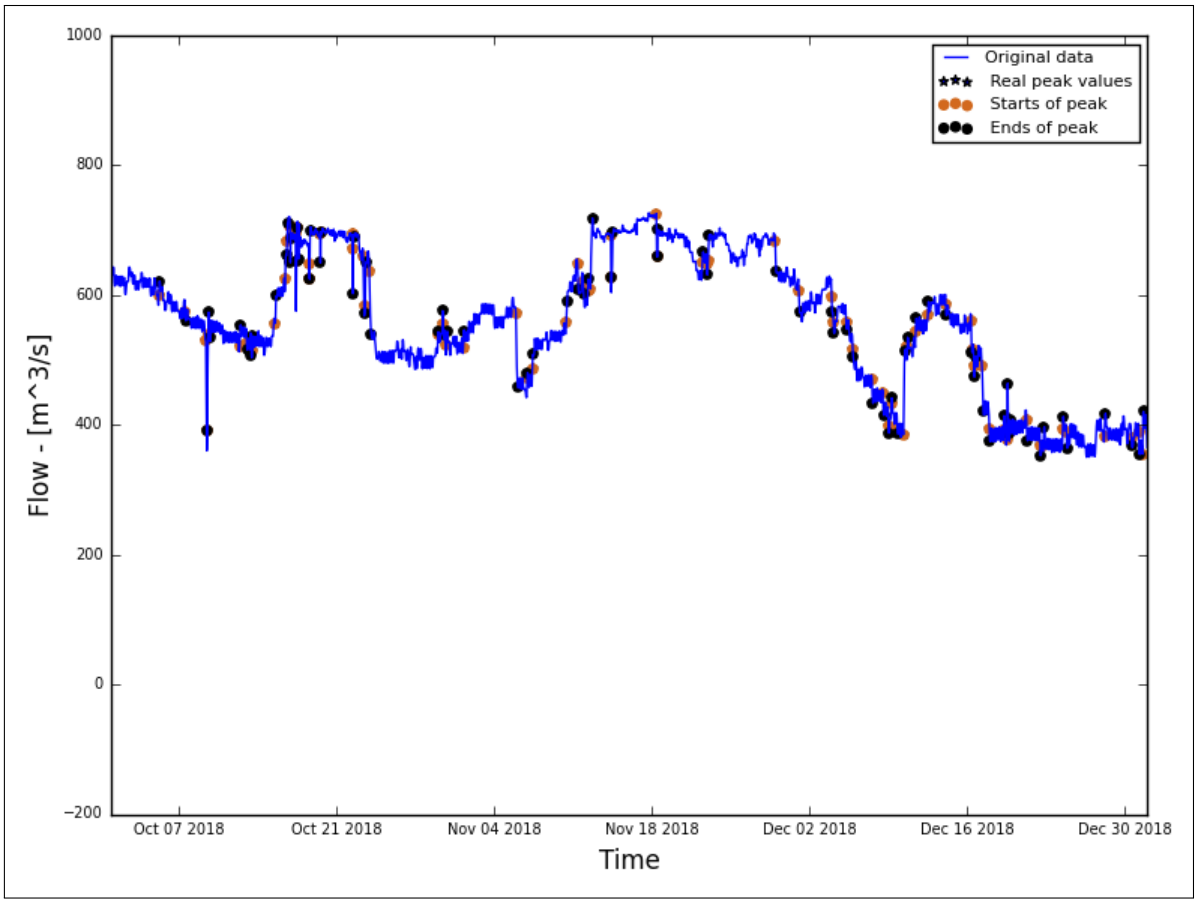

Figure A.46.226: Hydrograph of the last two months of the recorded data

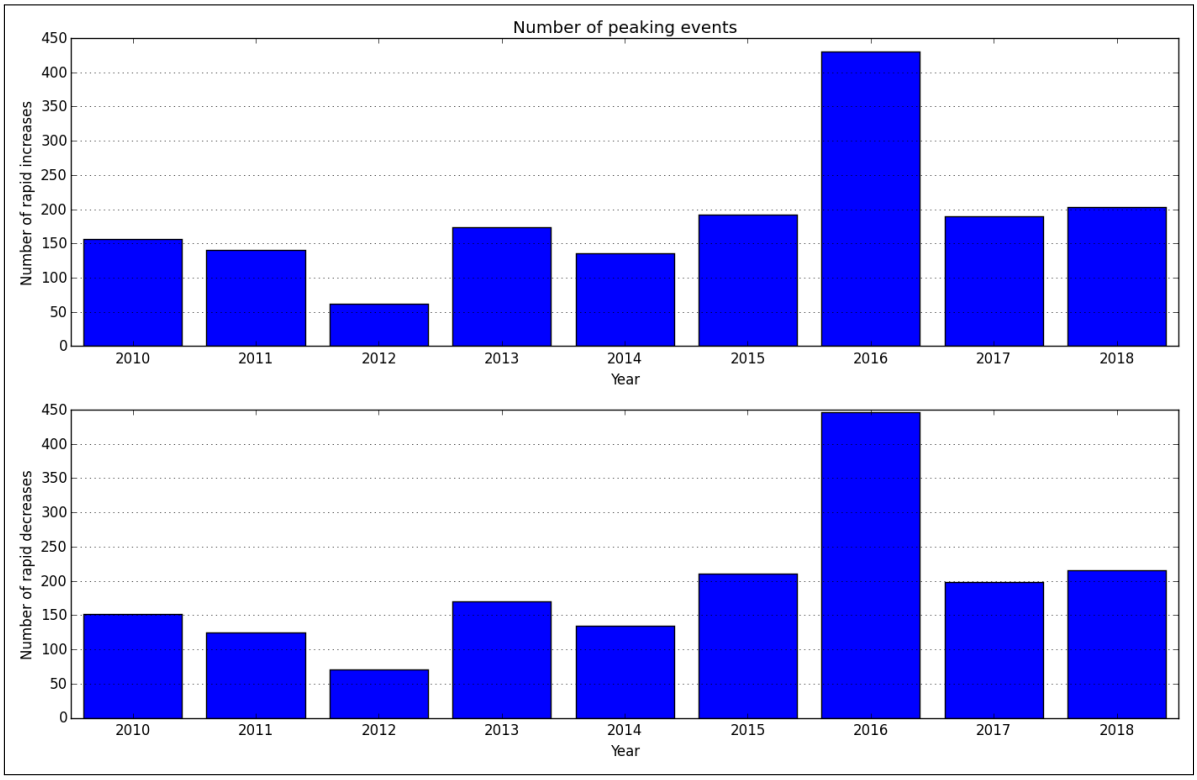

Figure A.46.227: Average annual number of increased/decreased peaks

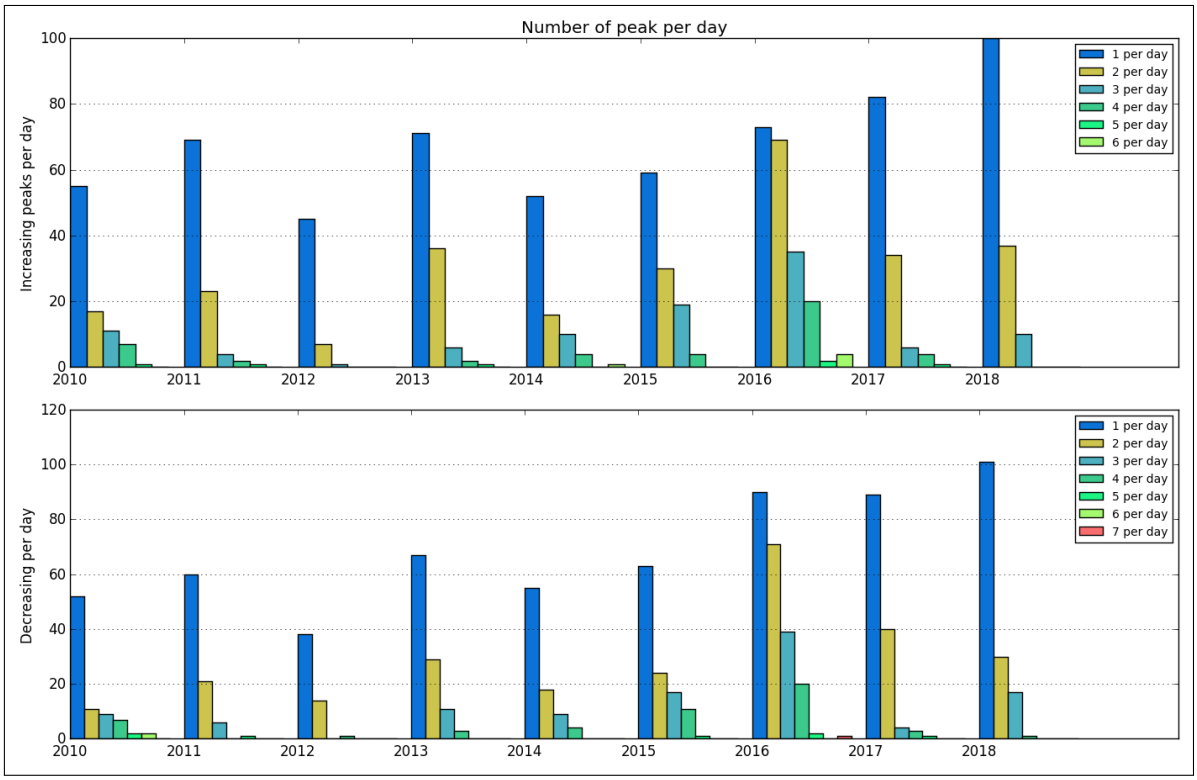

Figure A.46.228: Number of peaks per day

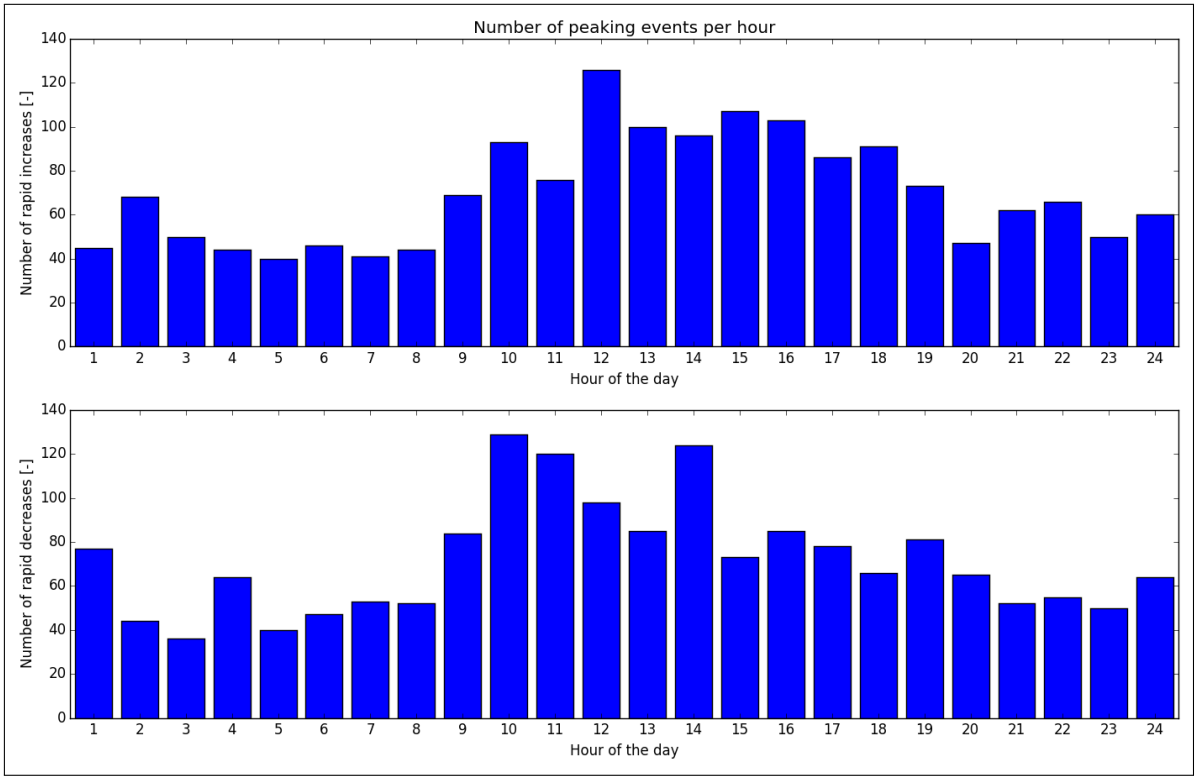

Figure A.46.229: Distribution of peaks throughout day

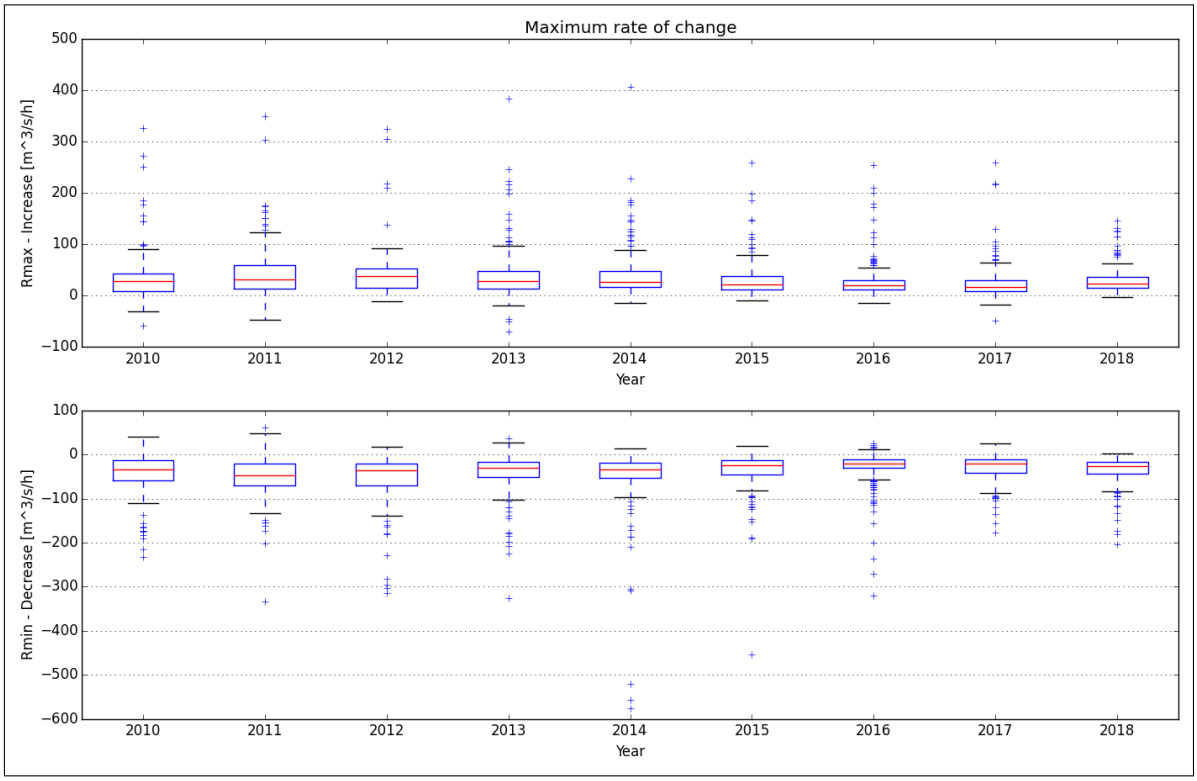

Figure A.46.230: Maximum rate of change

A.47. Dokka

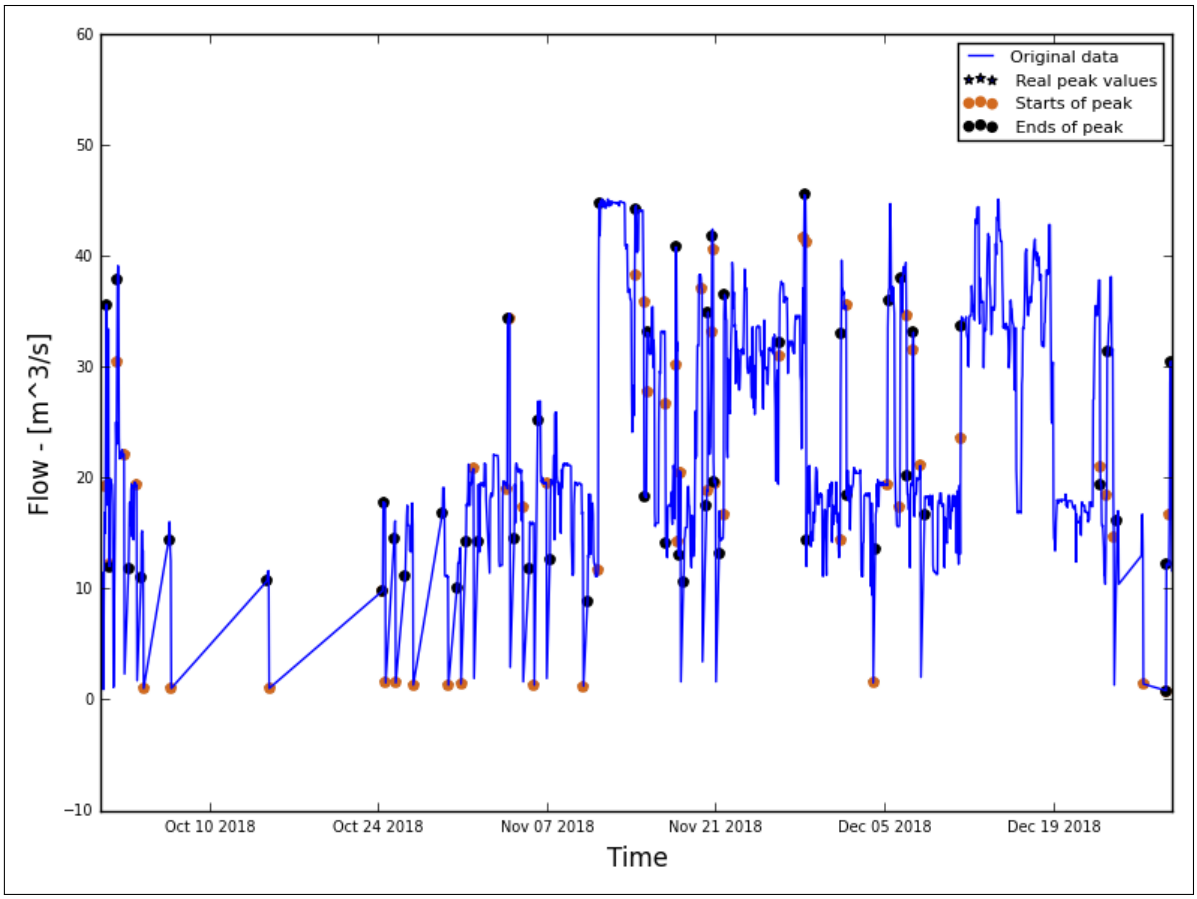

Figure A.47.231: Hydrograph of the last two months of the recorded data

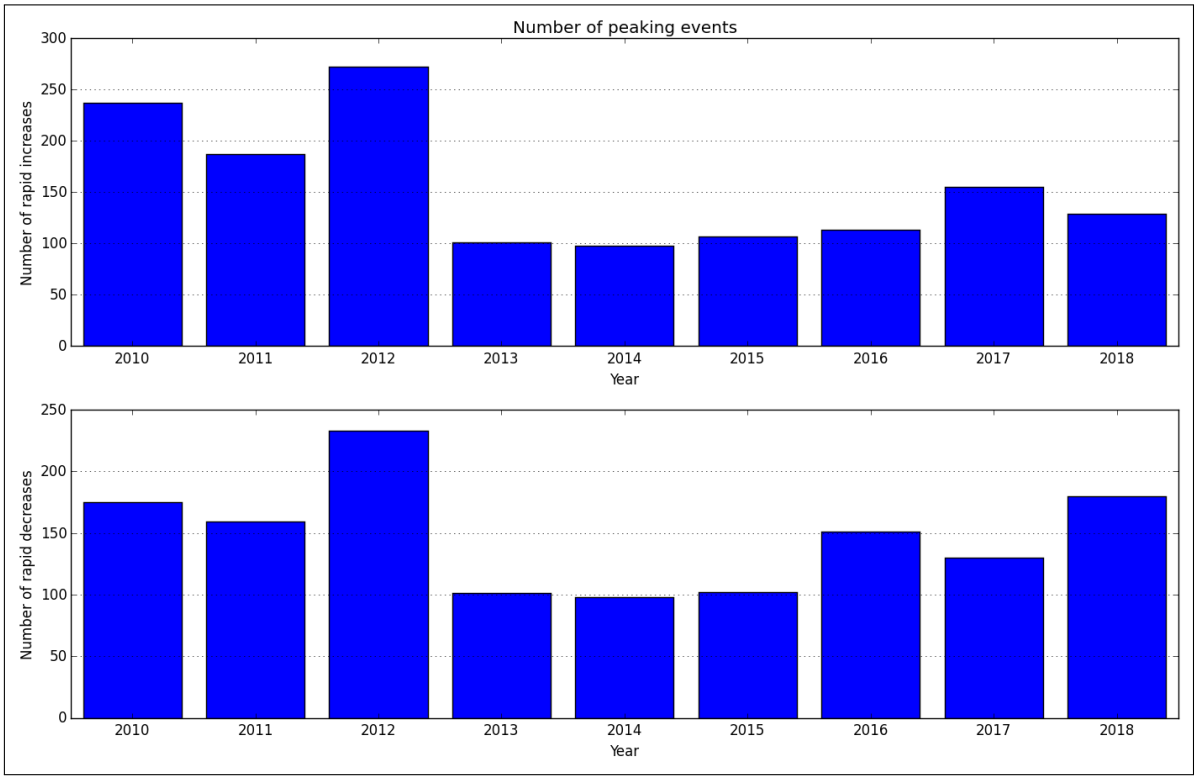

Figure A.47.232: Average annual number of increased/decreased peaks

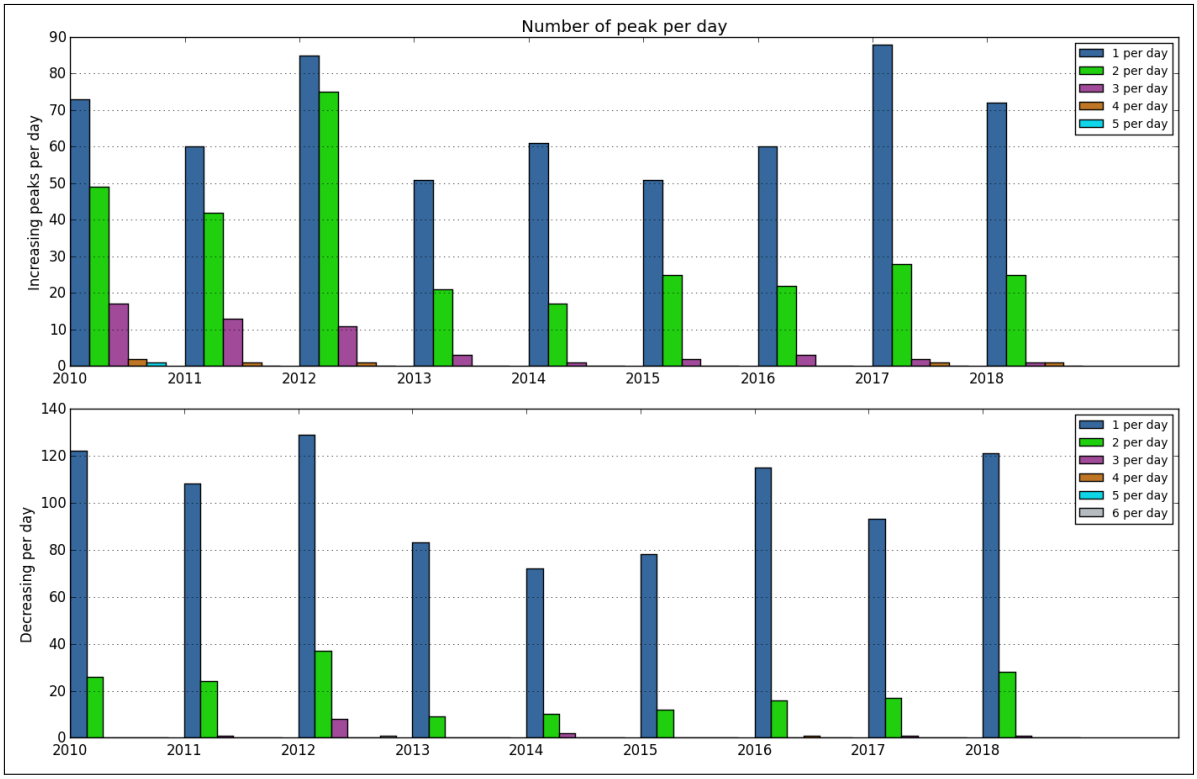

Figure A.47.233: Number of peaks per day

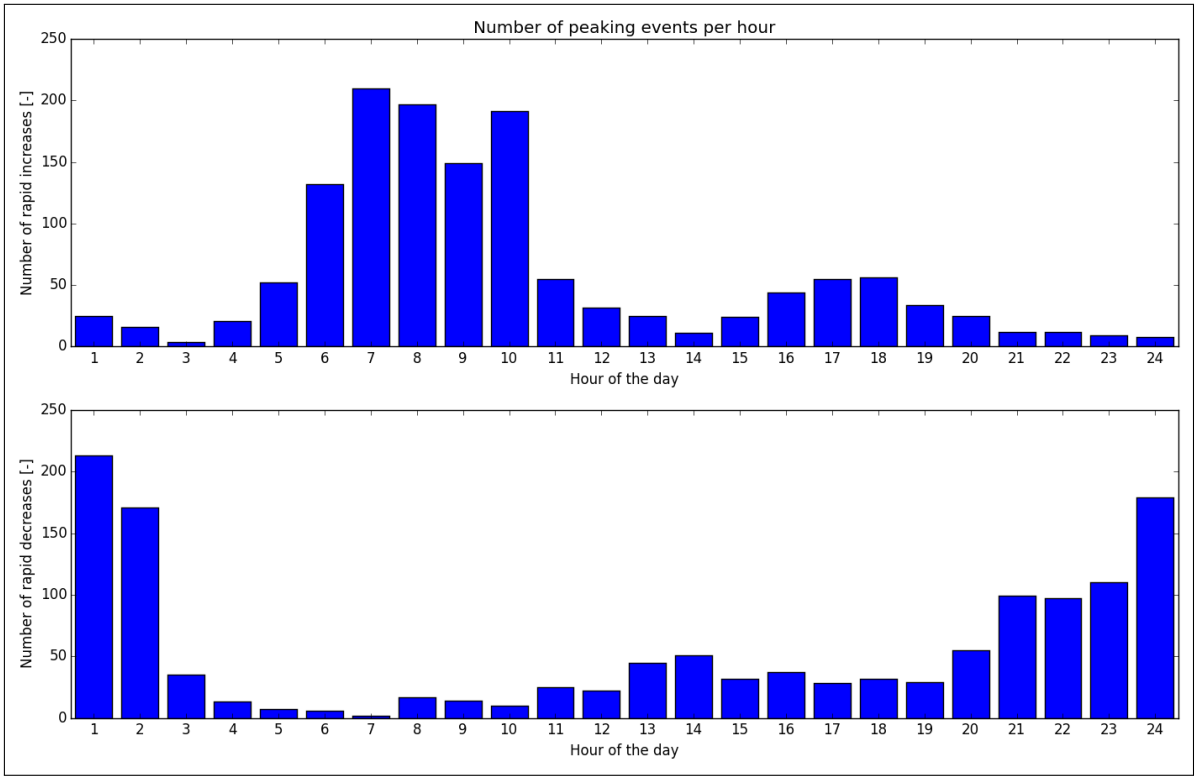

Figure A.47.234: Distribution of peaks throughout day

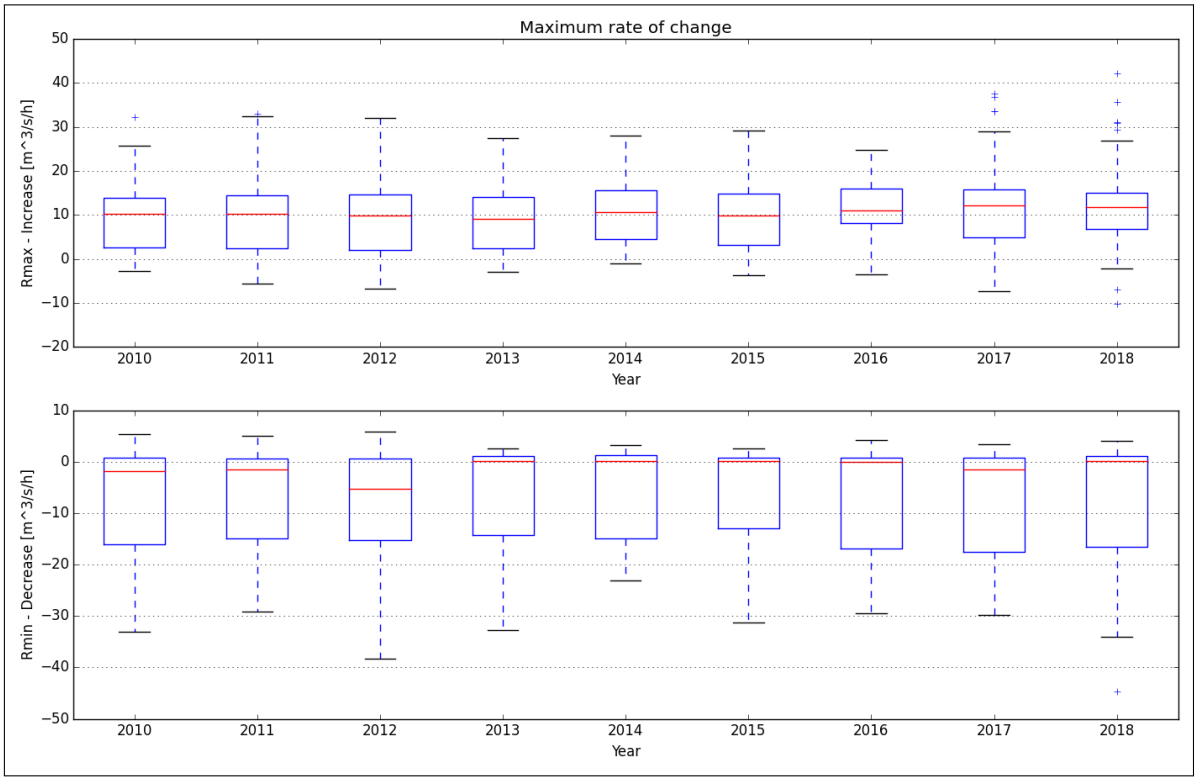

Figure A.47.235: Maximum rate of change

A.48. Funnefoss

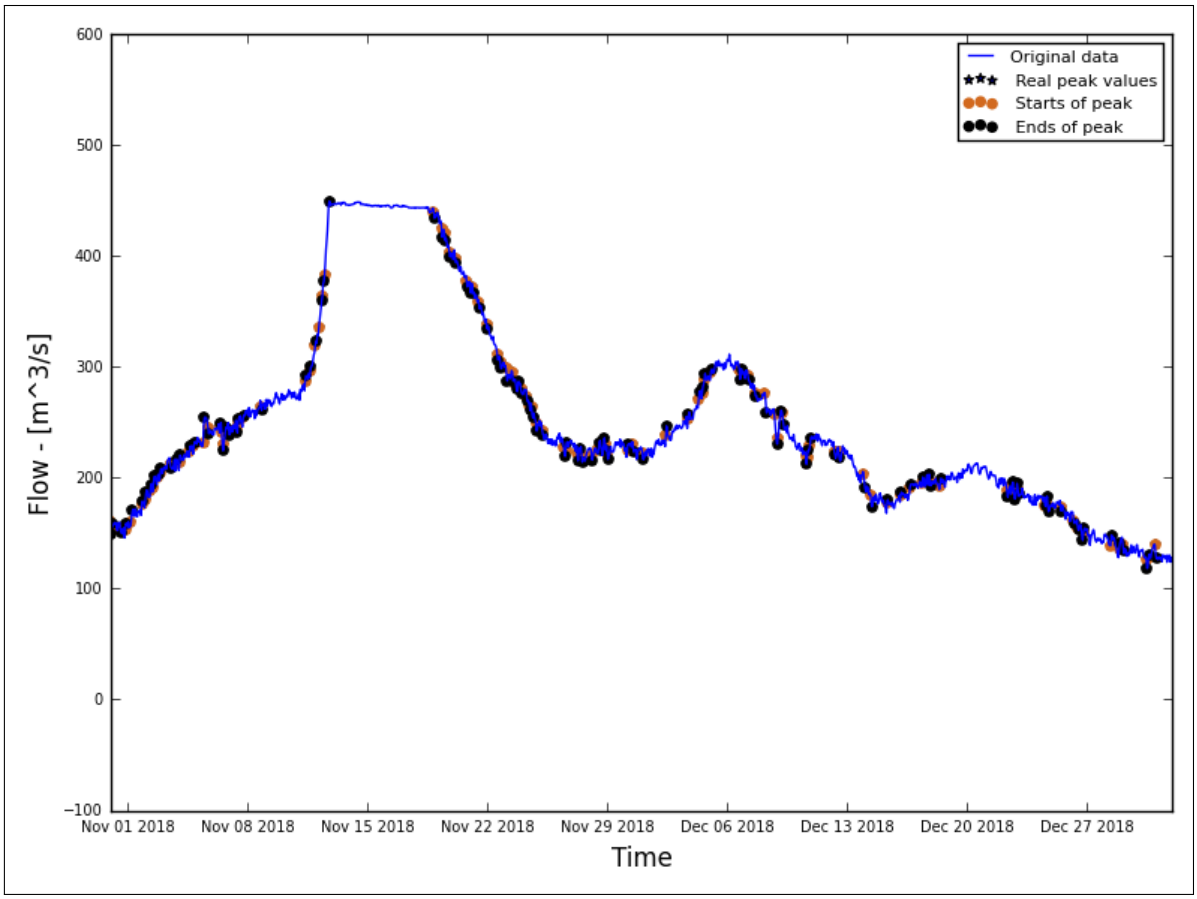

Figure A.48.236: Hydrograph of the last two months of the recorded data

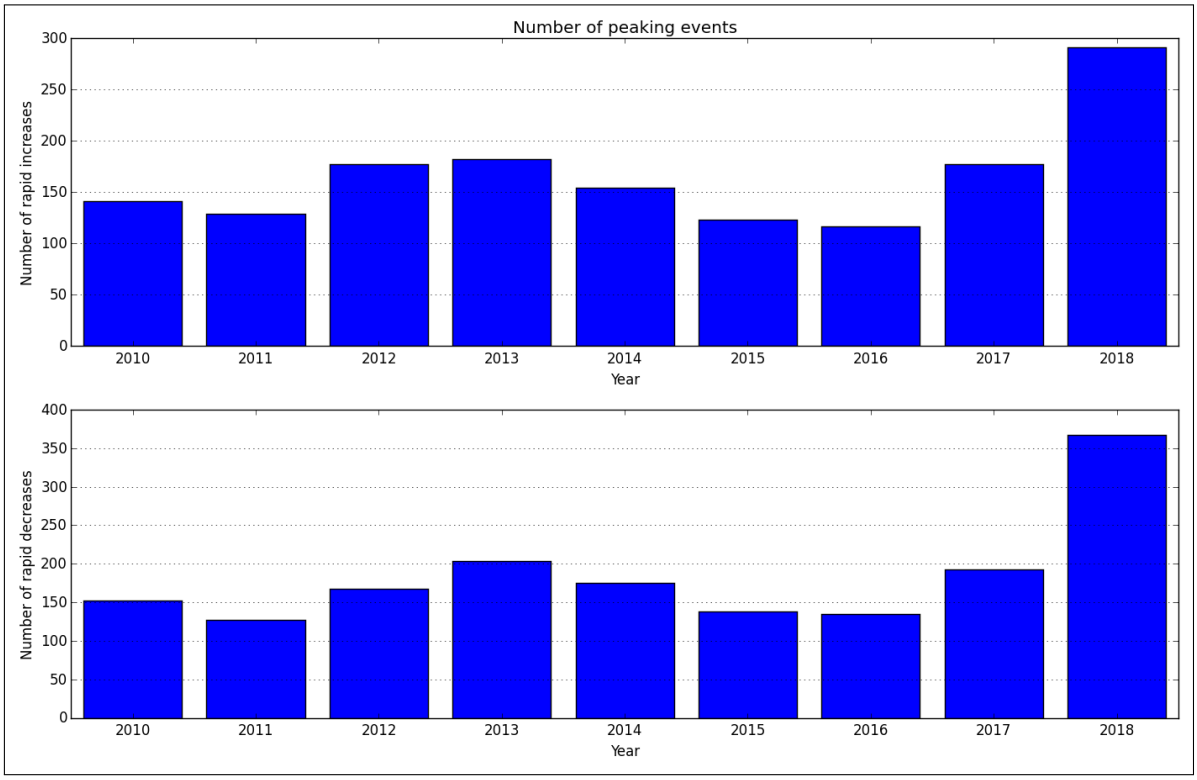

Figure A.48.237: Average annual number of increased/decreased peaks

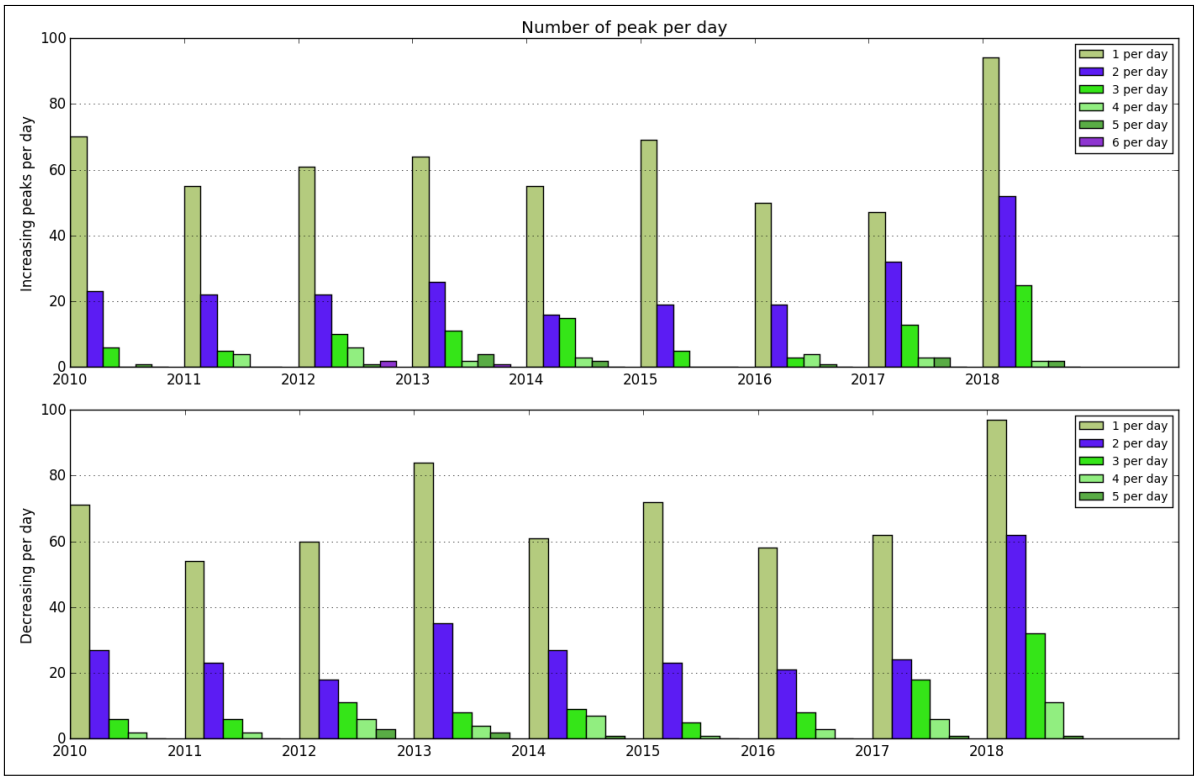

Figure A.48.238: Number of peaks per day

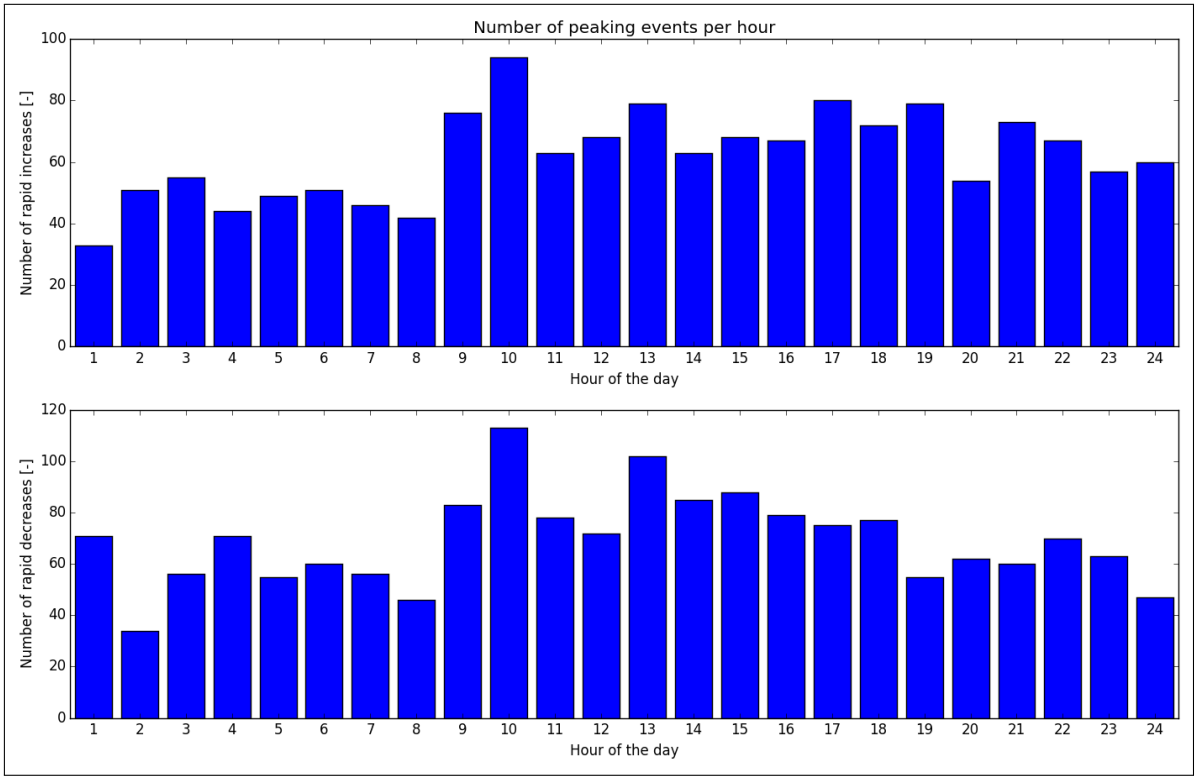

Figure A.48.239: Distribution of peaks throughout day

Figure A.48.240: Maximum rate of change

A.49. Kongsvinger

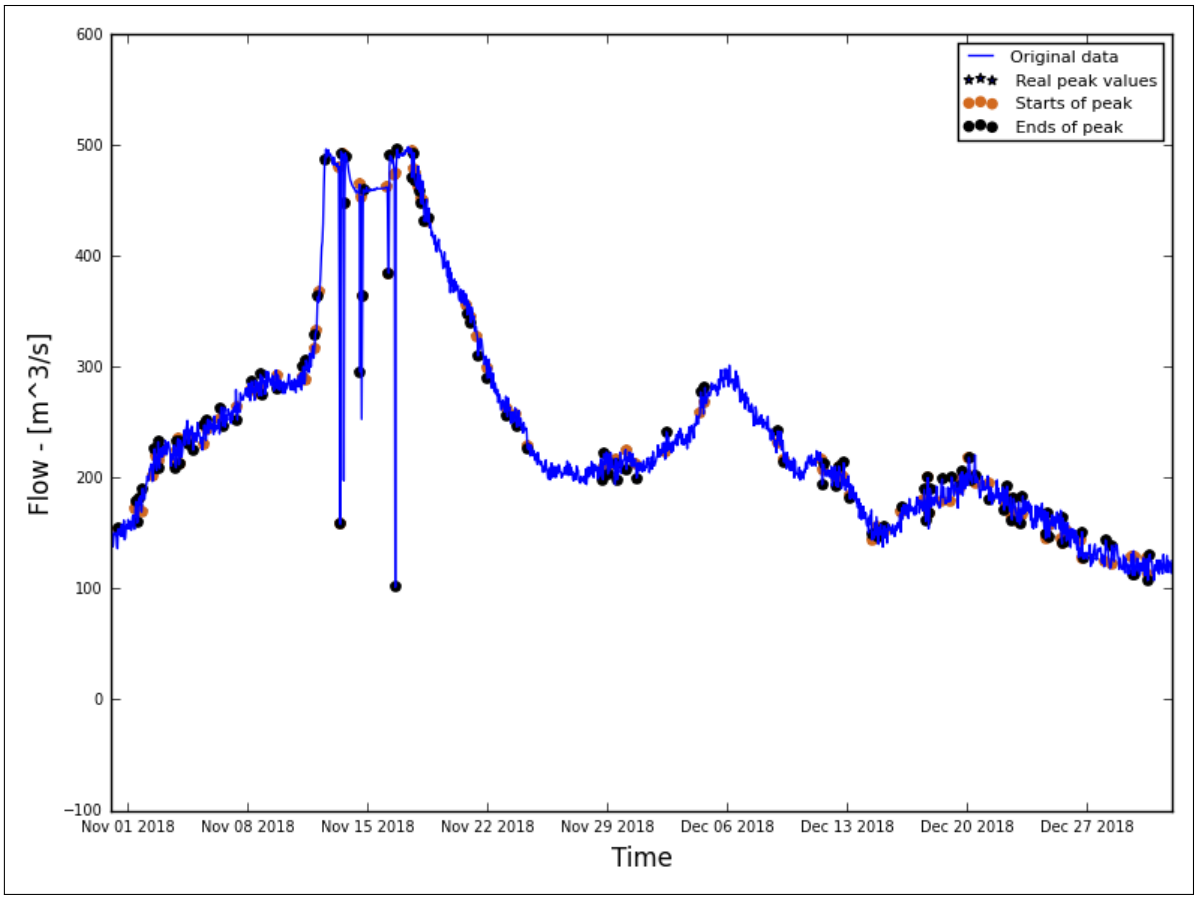

Figure A.49.241: Hydrograph of the last two months of the recorded data

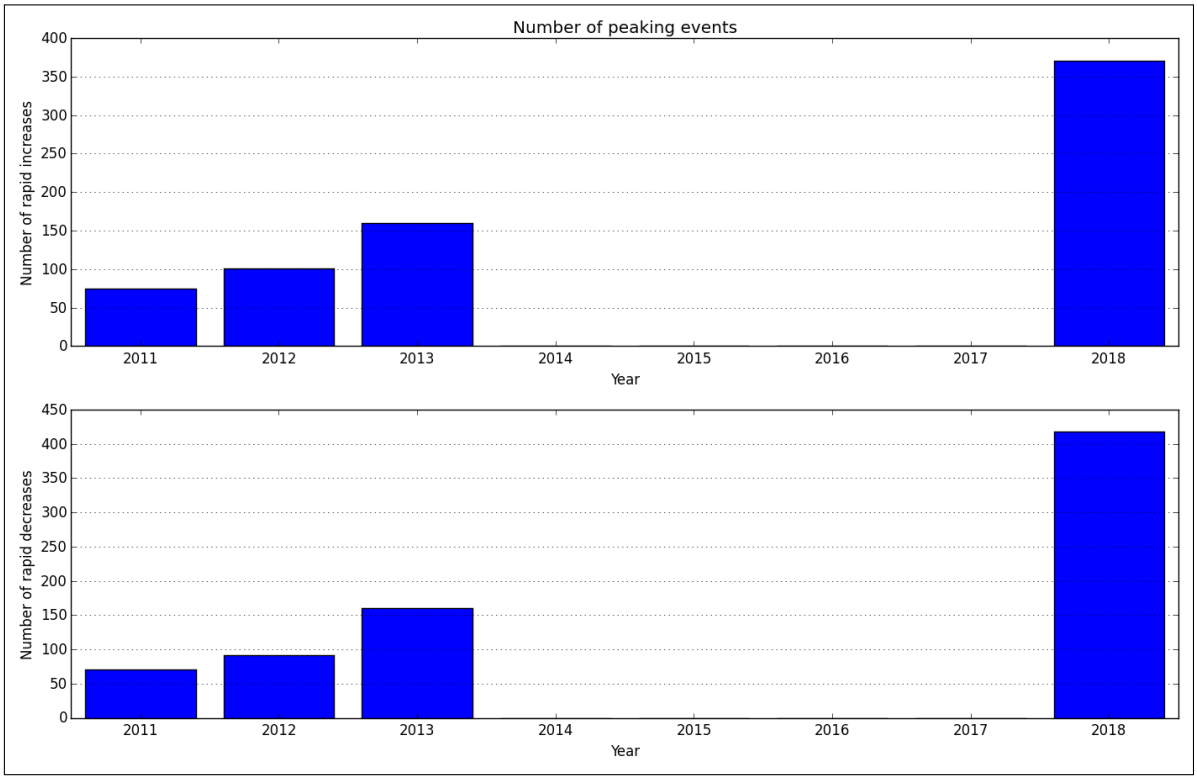

Figure A.49.242: Average annual number of increased/decreased peaks

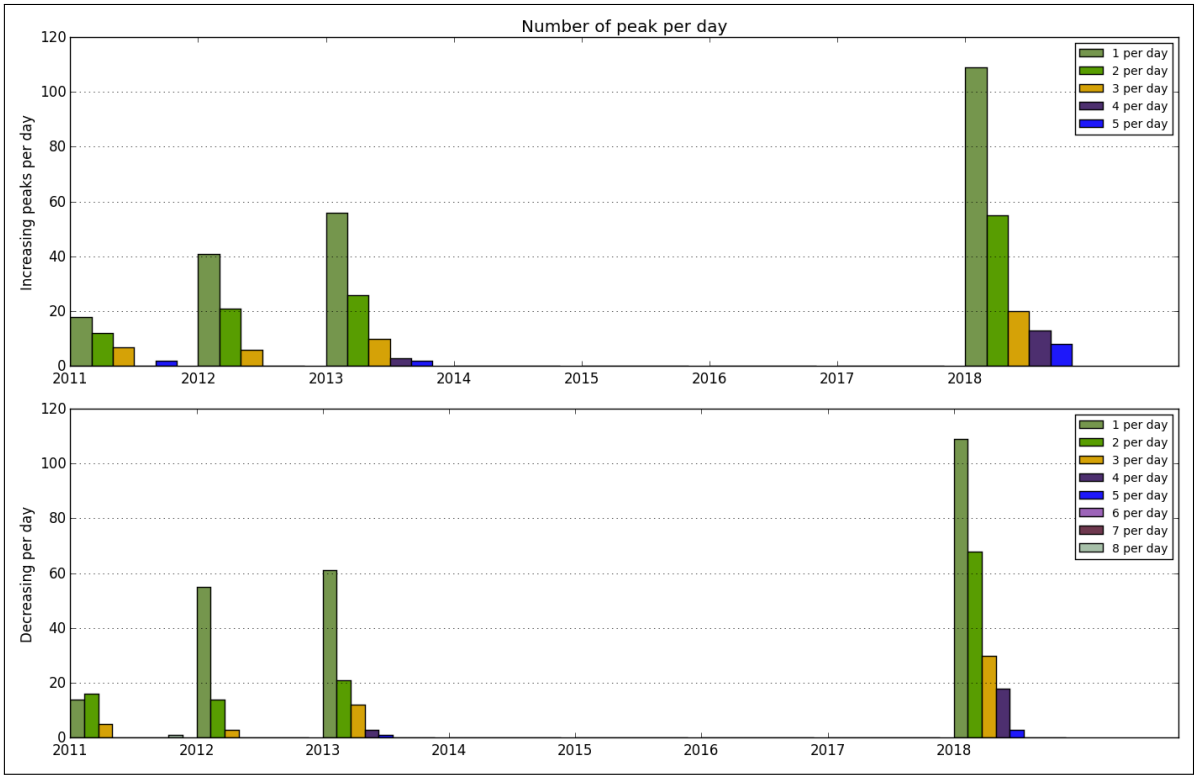

Figure A.49.243: Number of peaks per day

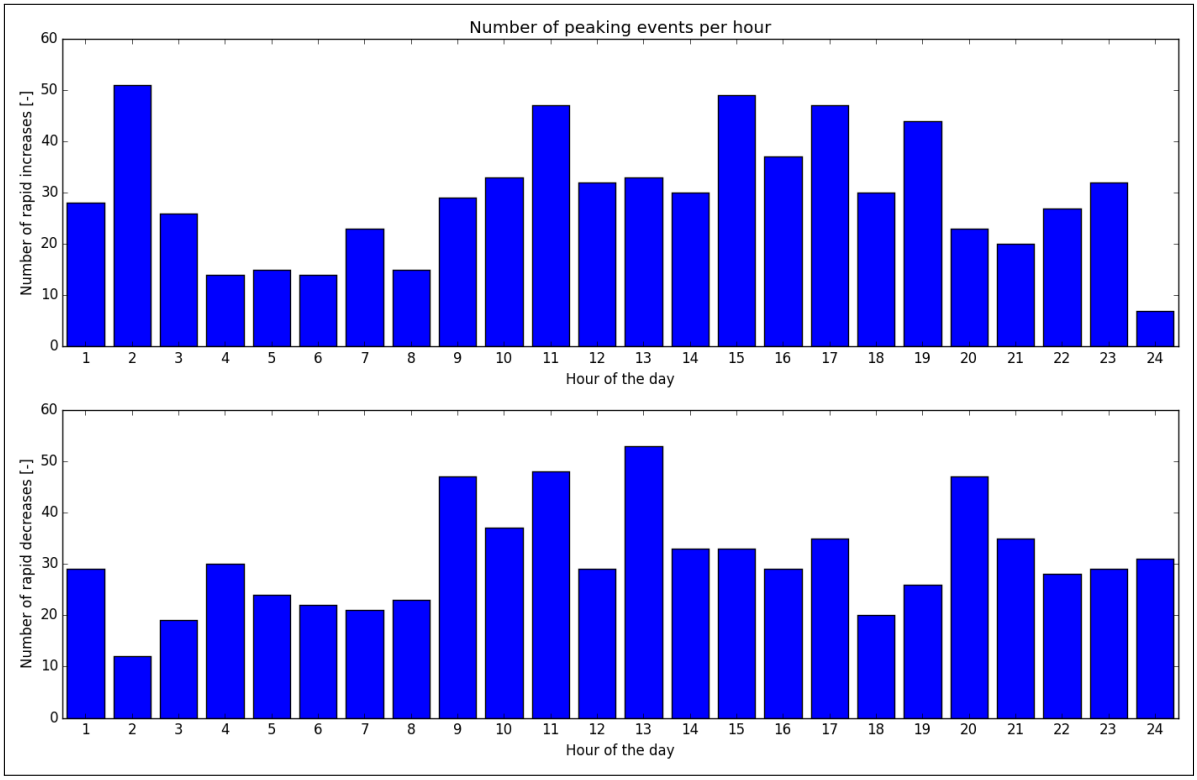

Figure A.49.244: Distribution of peaks throughout day

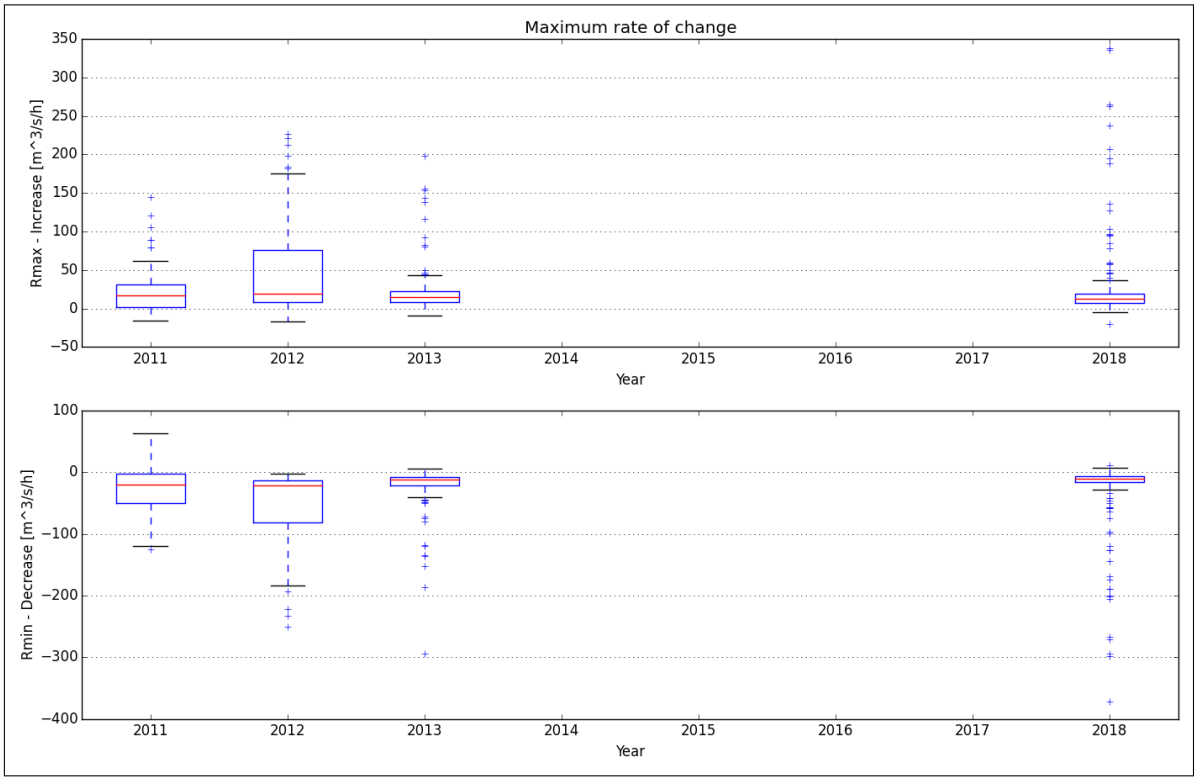

Figure A.49.245: Maximum rate of change

A.50. Lopet

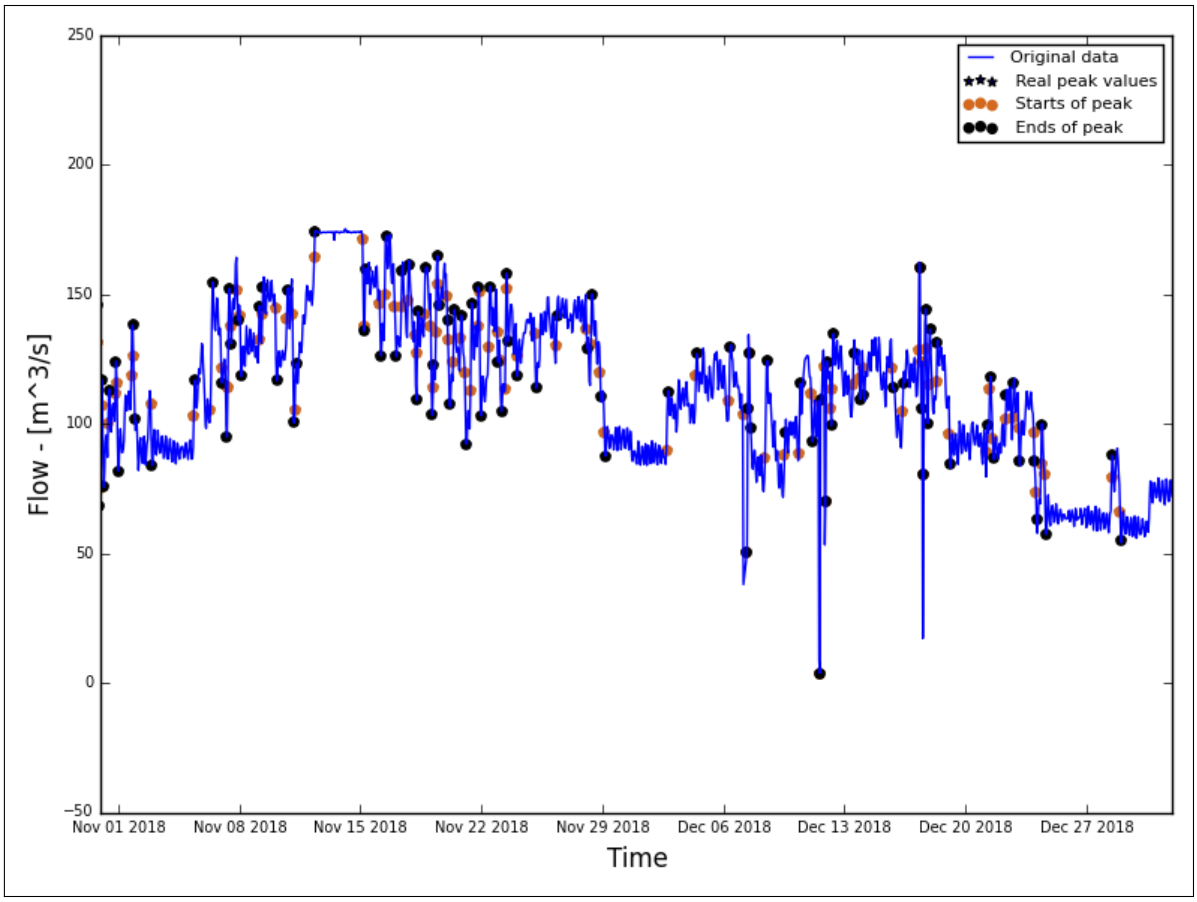

Figure A.50.246: Hydrograph of the last two months of the recorded data

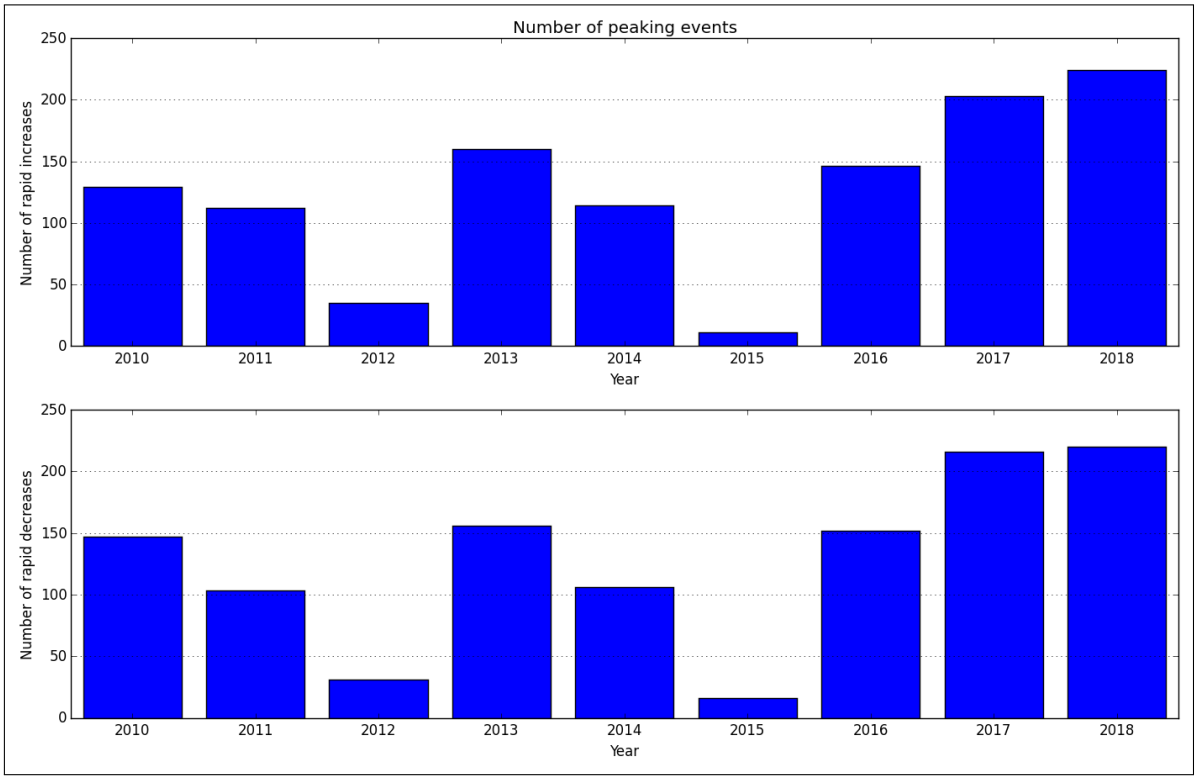

Figure A.50.247: Average annual number of increased/decreased peaks

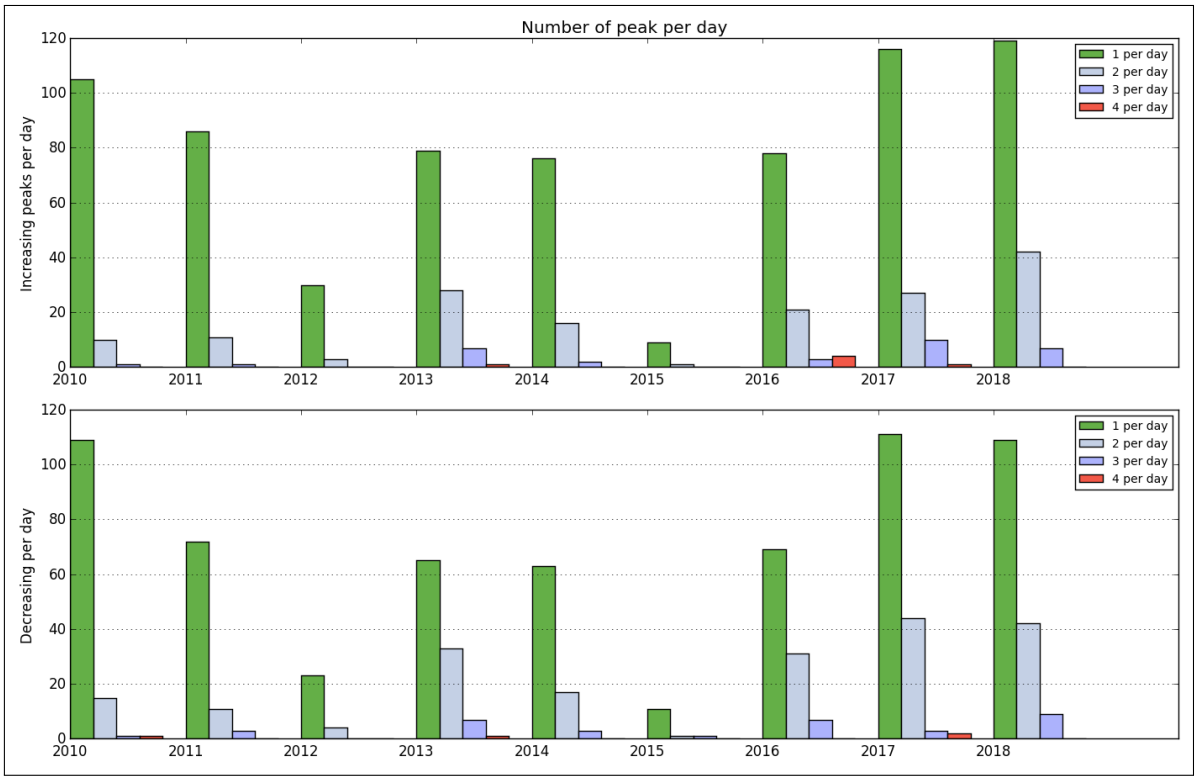

Figure A.50.248: Number of peaks per day

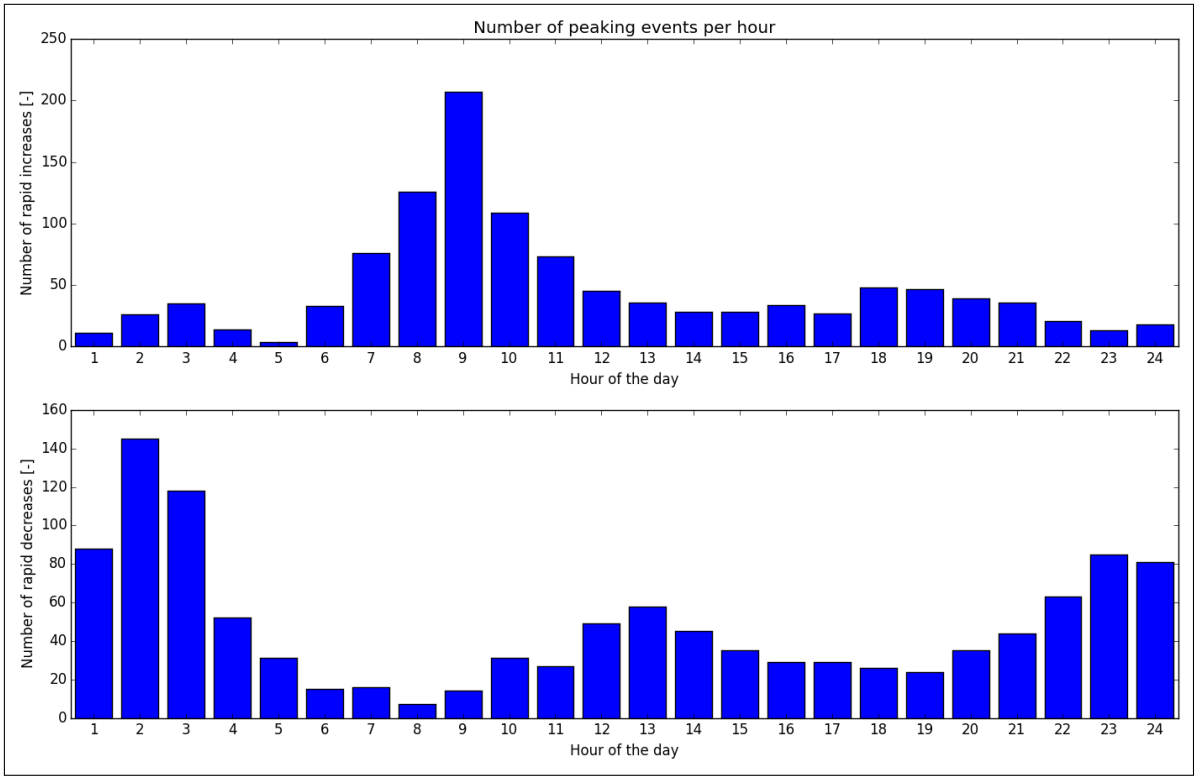

Figure A.50.249: Distribution of peaks throughout day

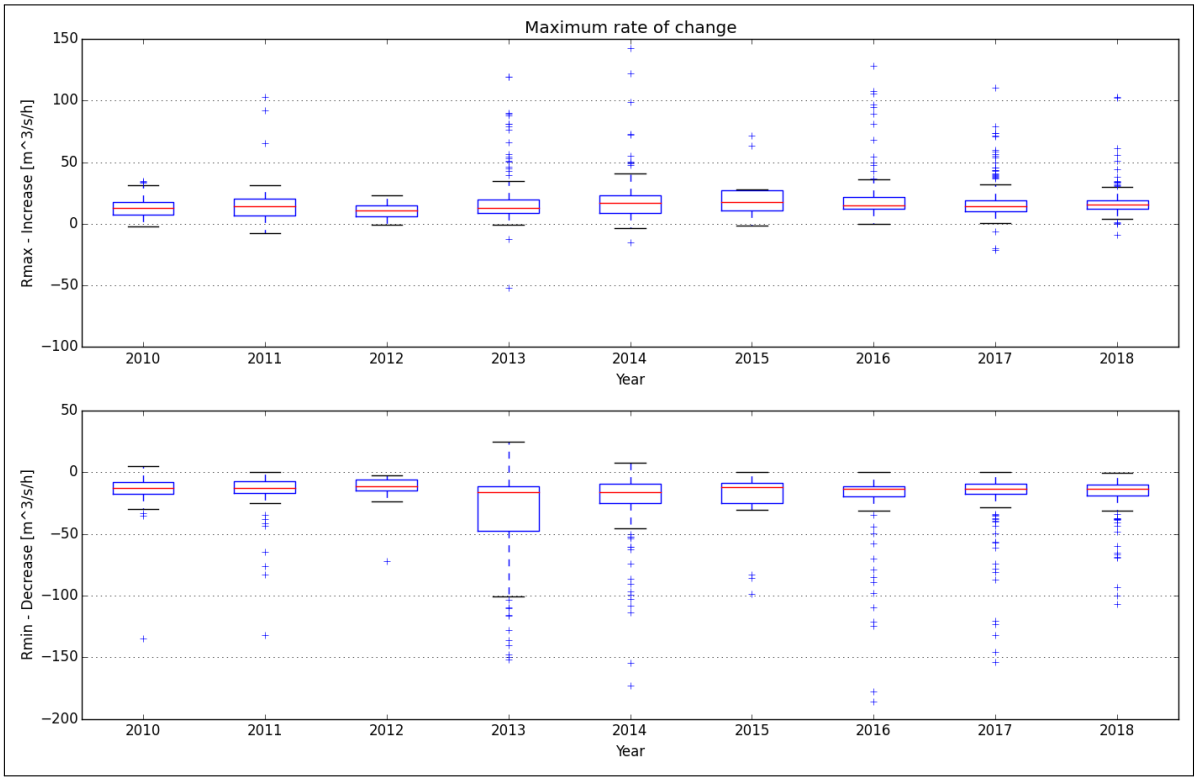

Figure A.50.250: Maximum rate of change

A.51. Mesna

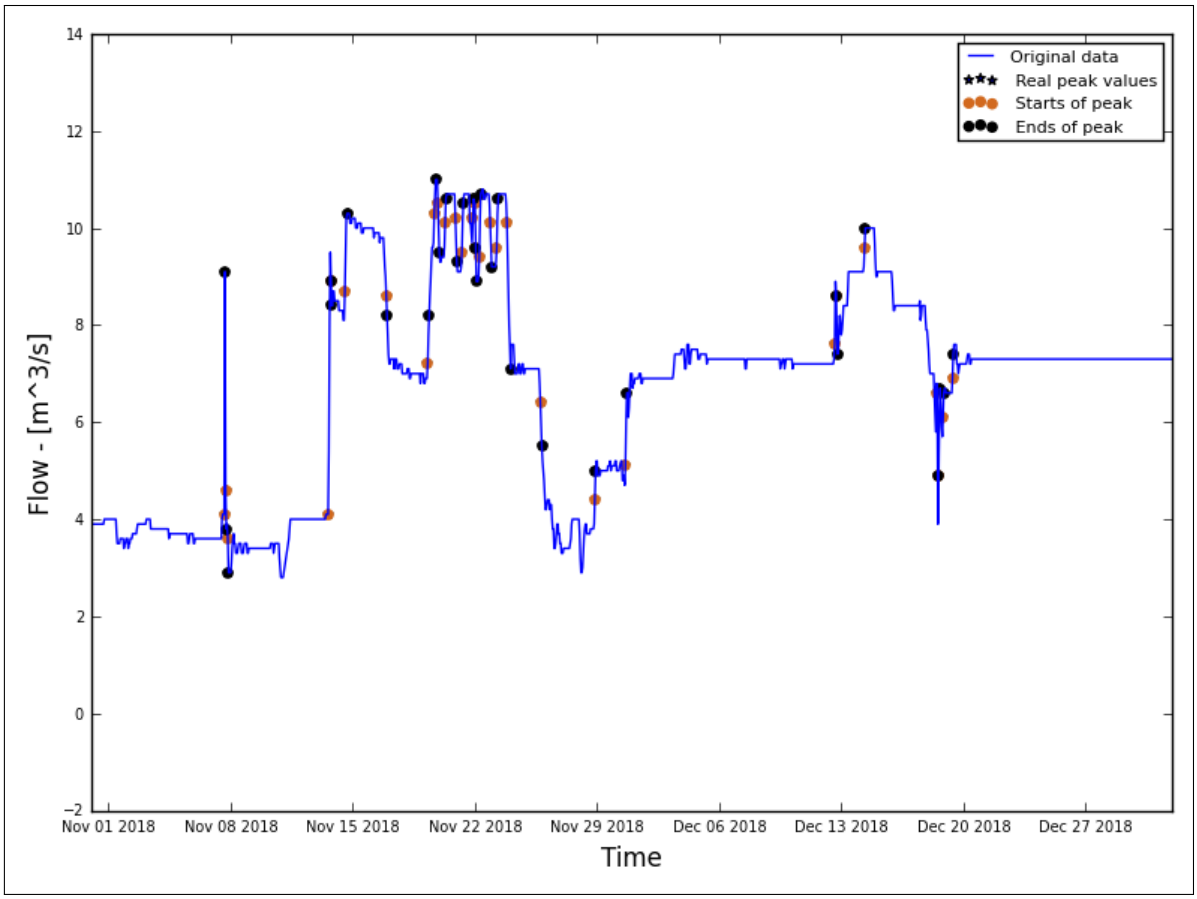

Figure A.51.251: Hydrograph of the last two months of the recorded data

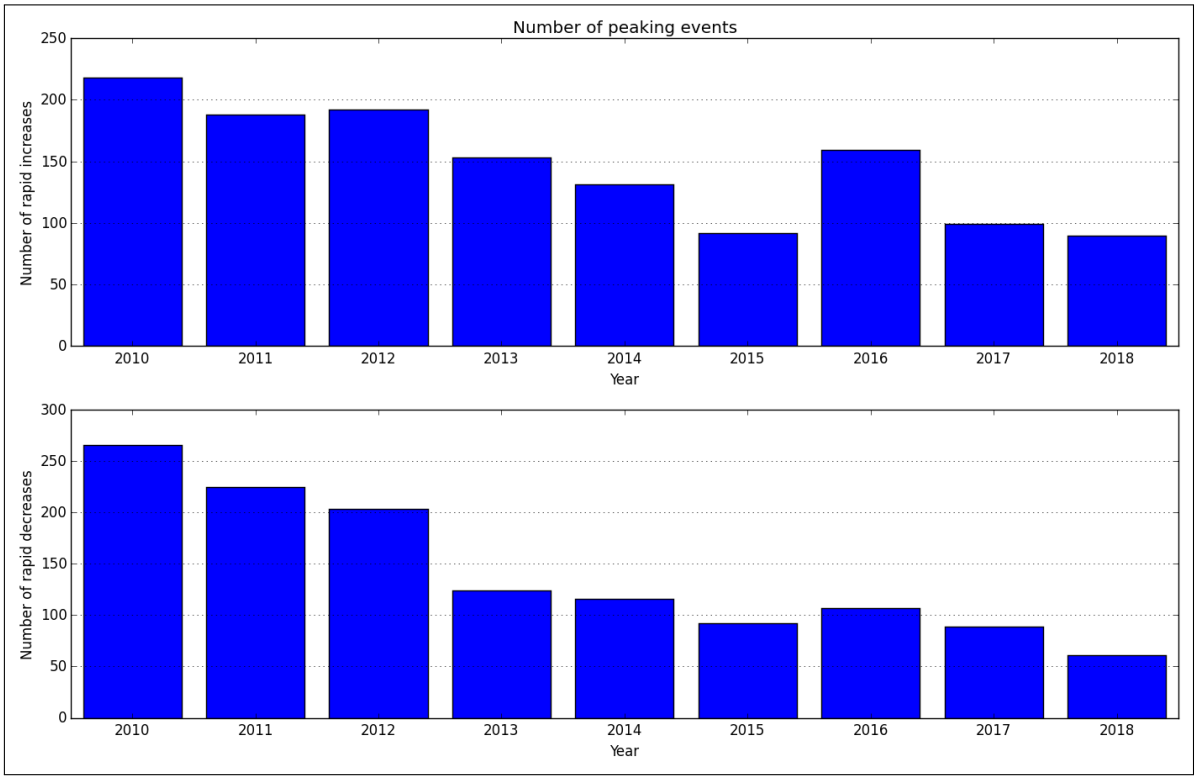

Figure A.51.252: Average annual number of increased/decreased peaks

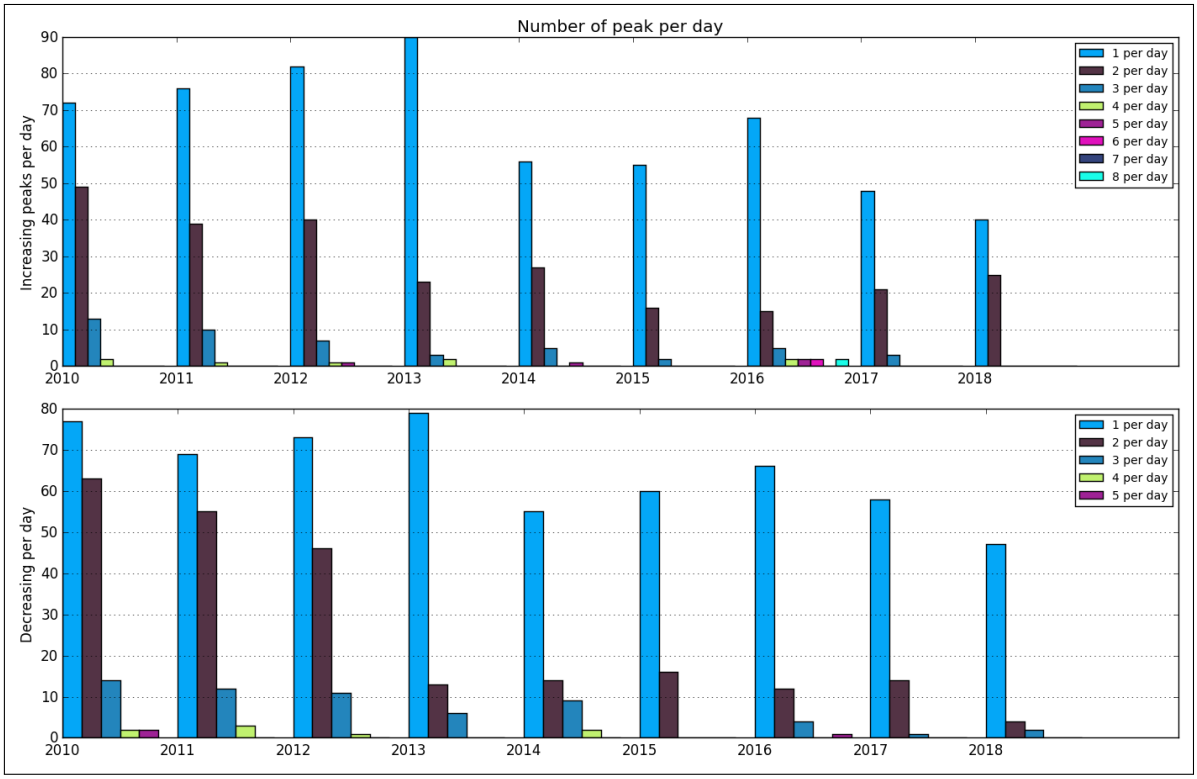

Figure A.51.253: Number of peaks per day

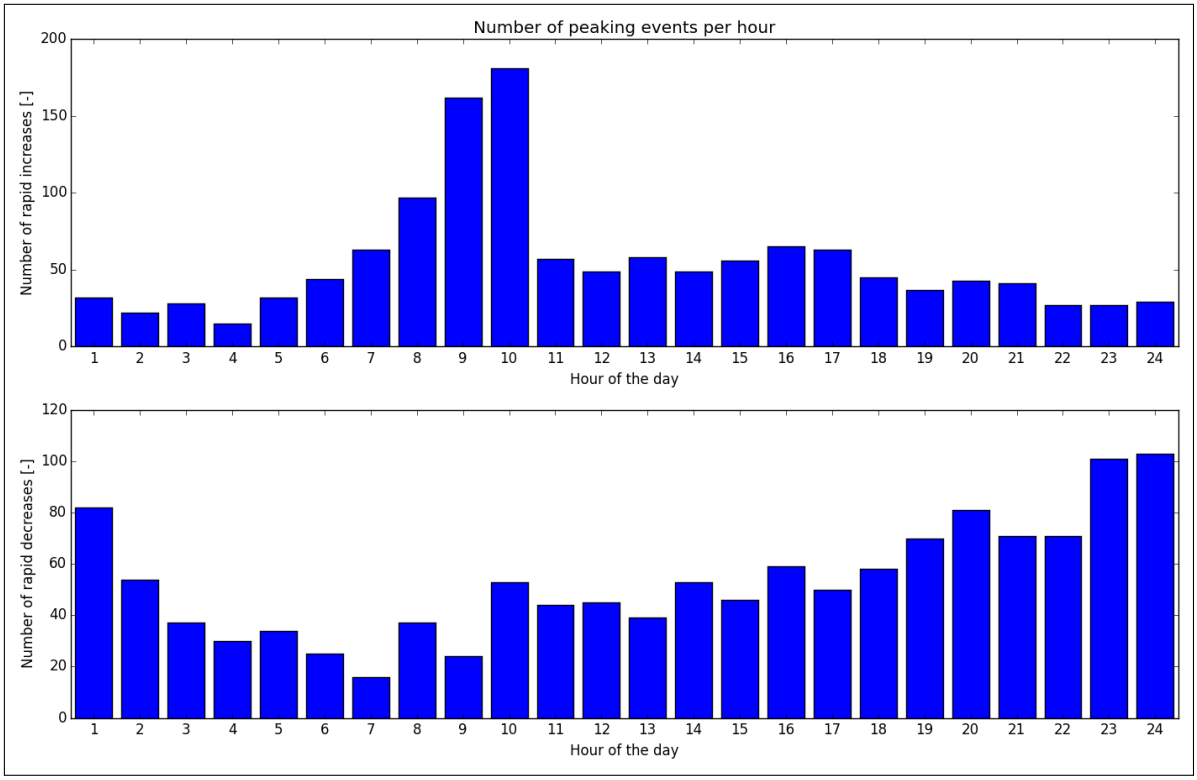

Figure A.51.254: Distribution of peaks throughout day

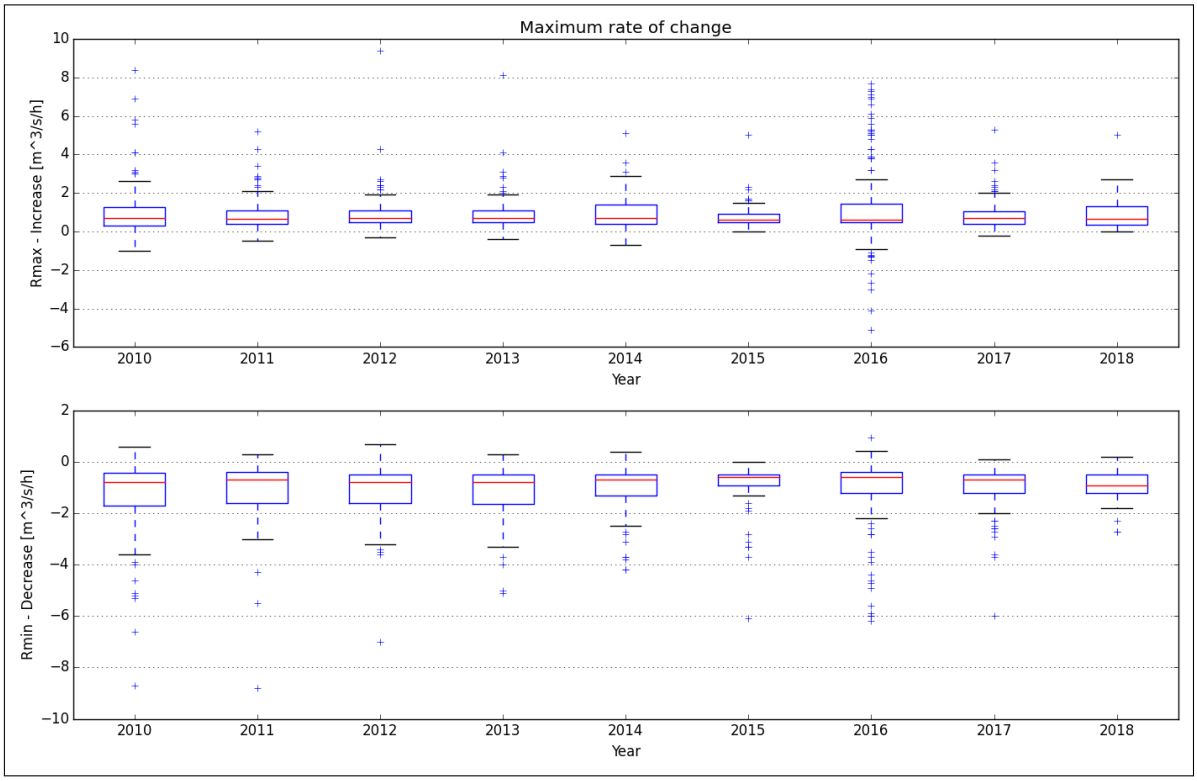

Figure A.51.255: Maximum rate of change

A.52. Raanaafoss

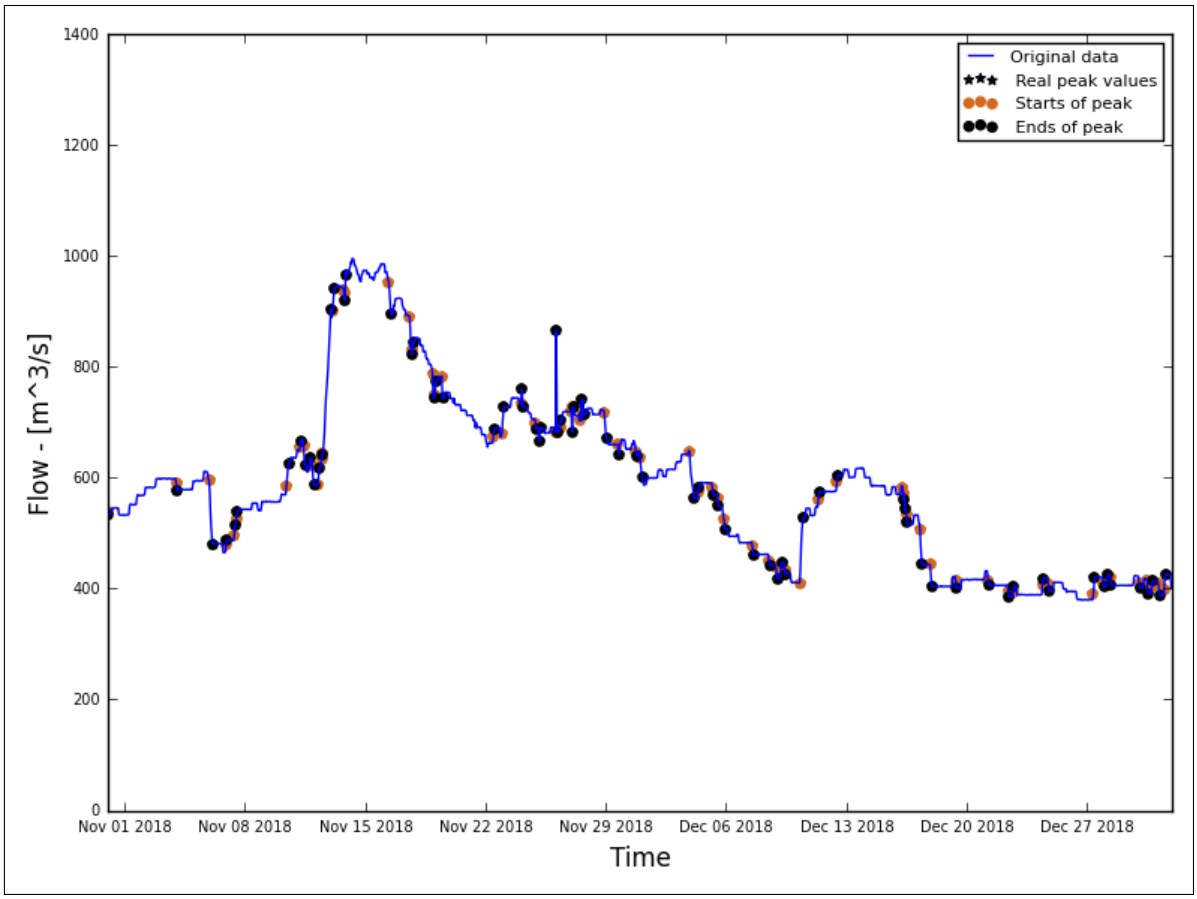

Figure A.52.256: Hydrograph of the last two months of the recorded data

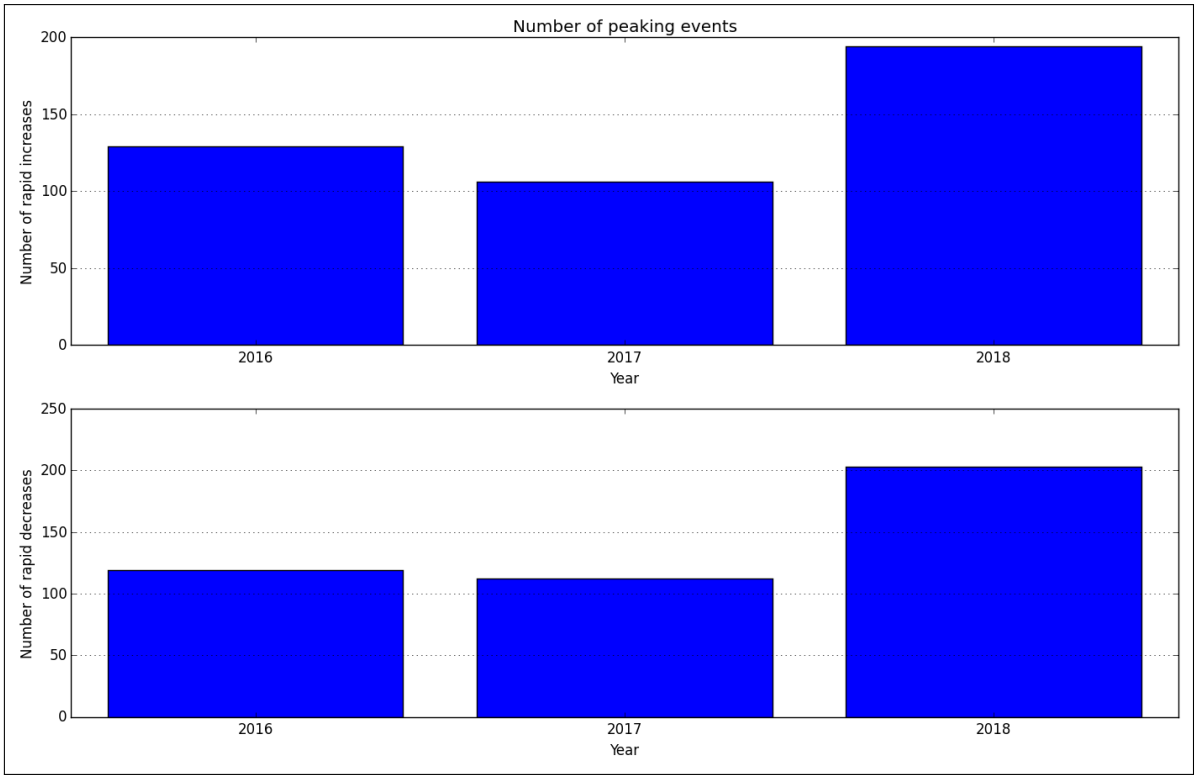

Figure A.52.257: Average annual number of increased/decreased peaks

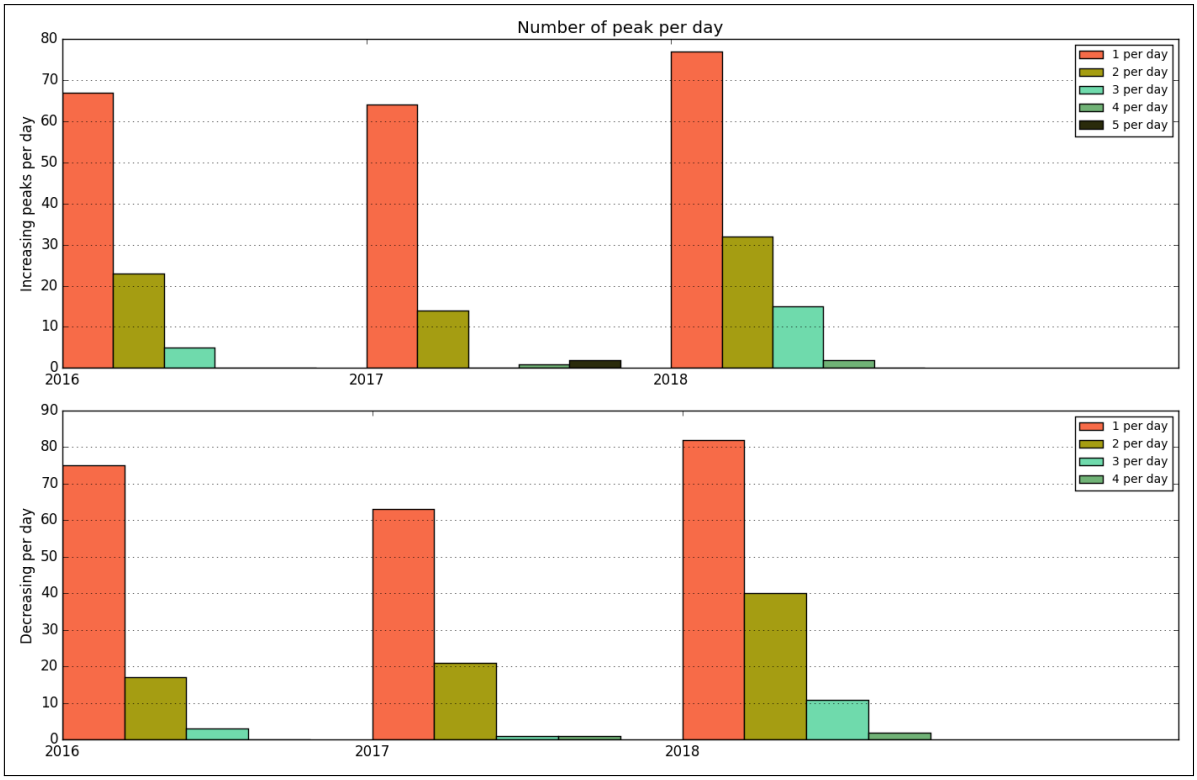

Figure A.52.258: Number of peaks per day

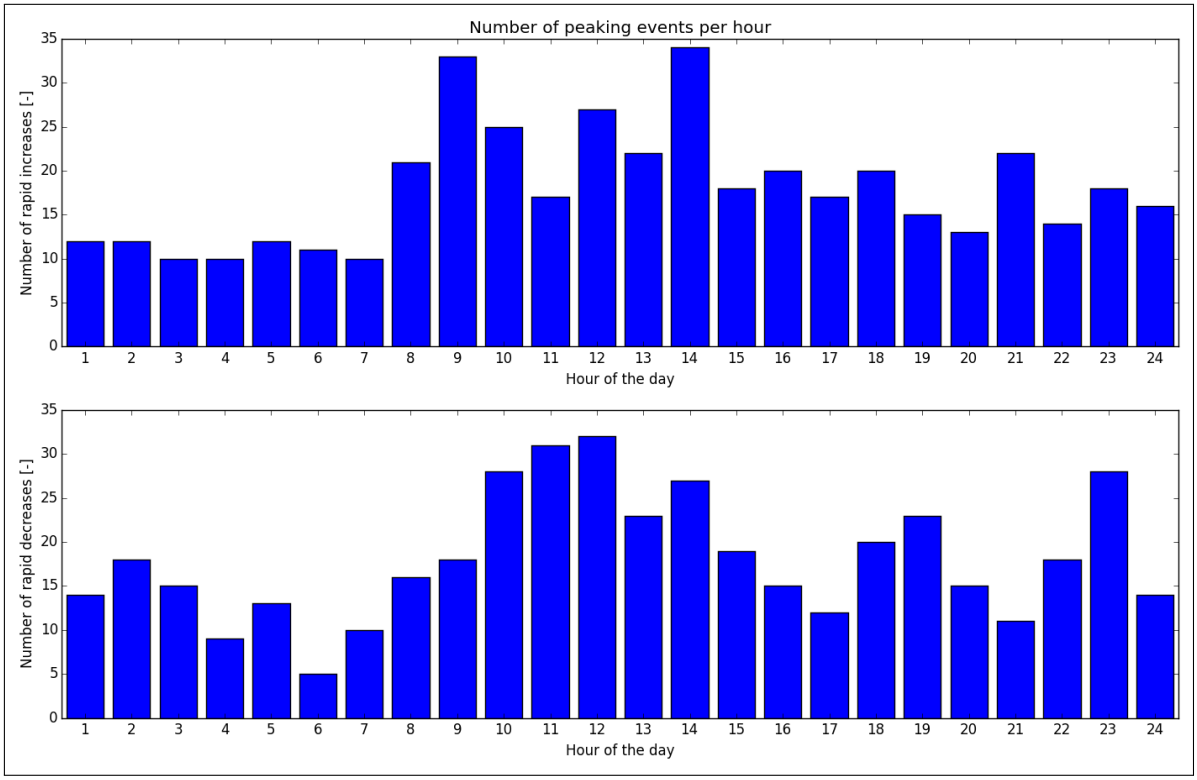

Figure A.52.259: Distribution of peaks throughout day

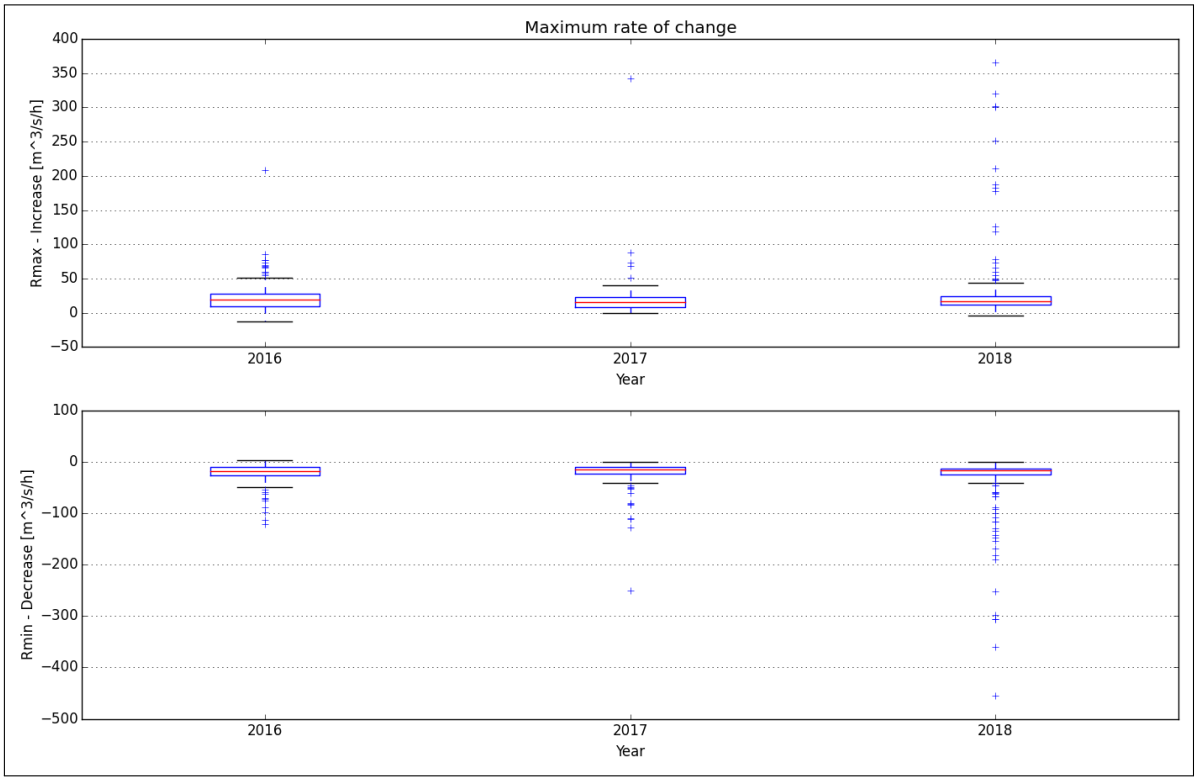

Figure A.52.260: Maximum rate of change

A.53. Skjefstadfoss

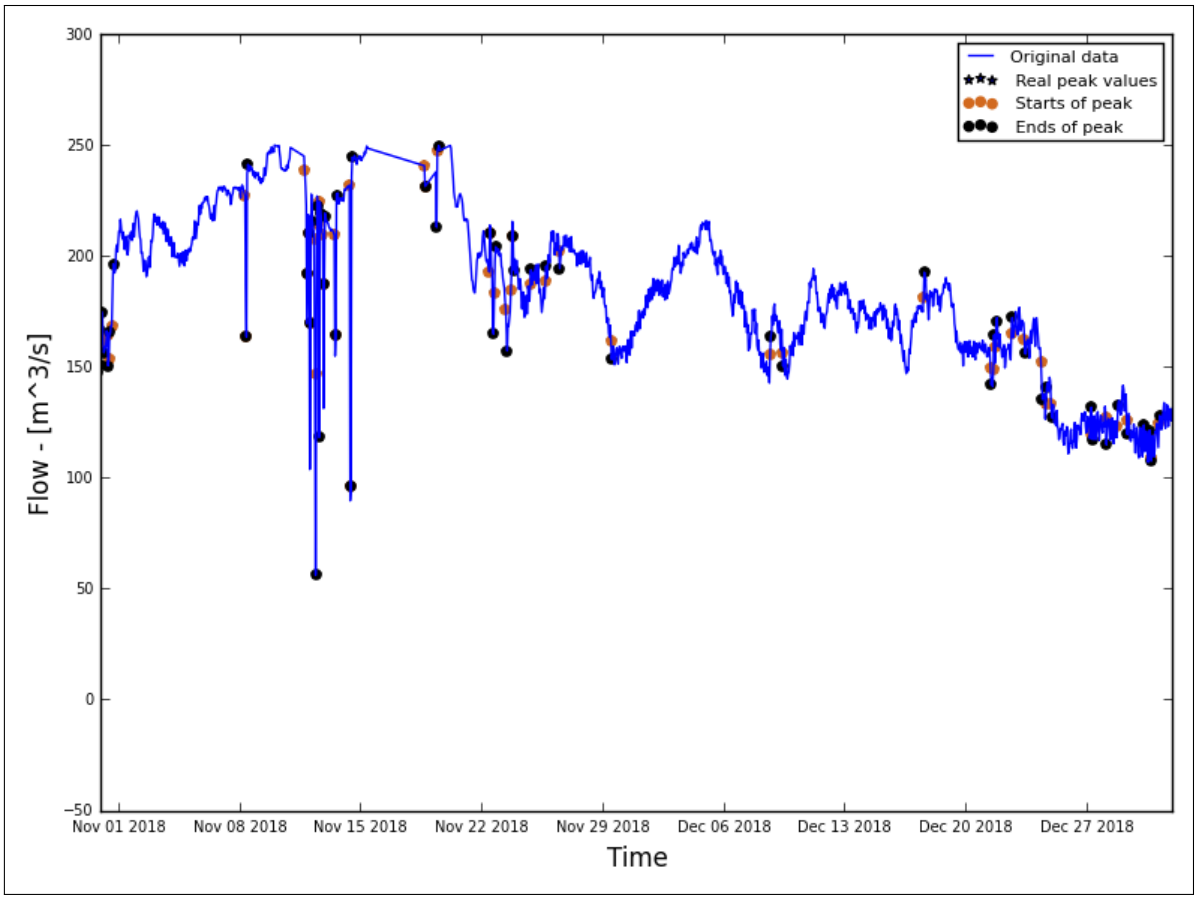

Figure A.53.261: Hydrograph of the last two months of the recorded data

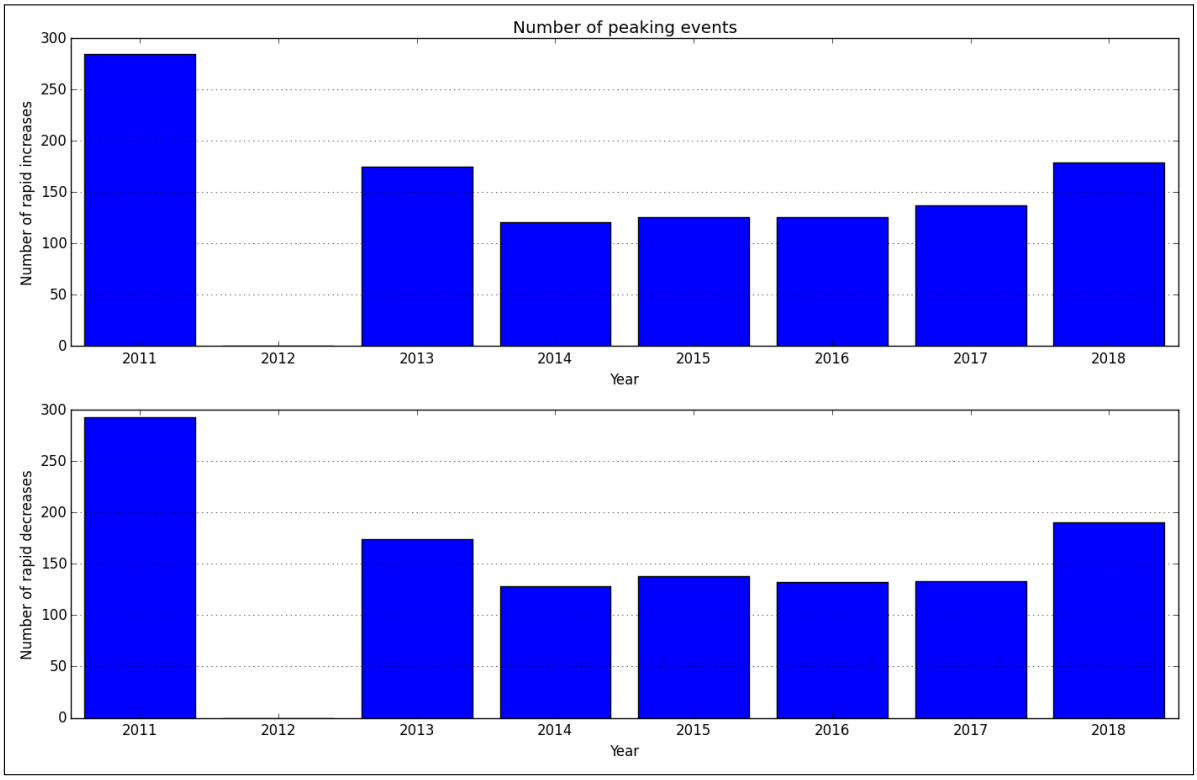

Figure A.53.262: Average annual number of increased/decreased peaks

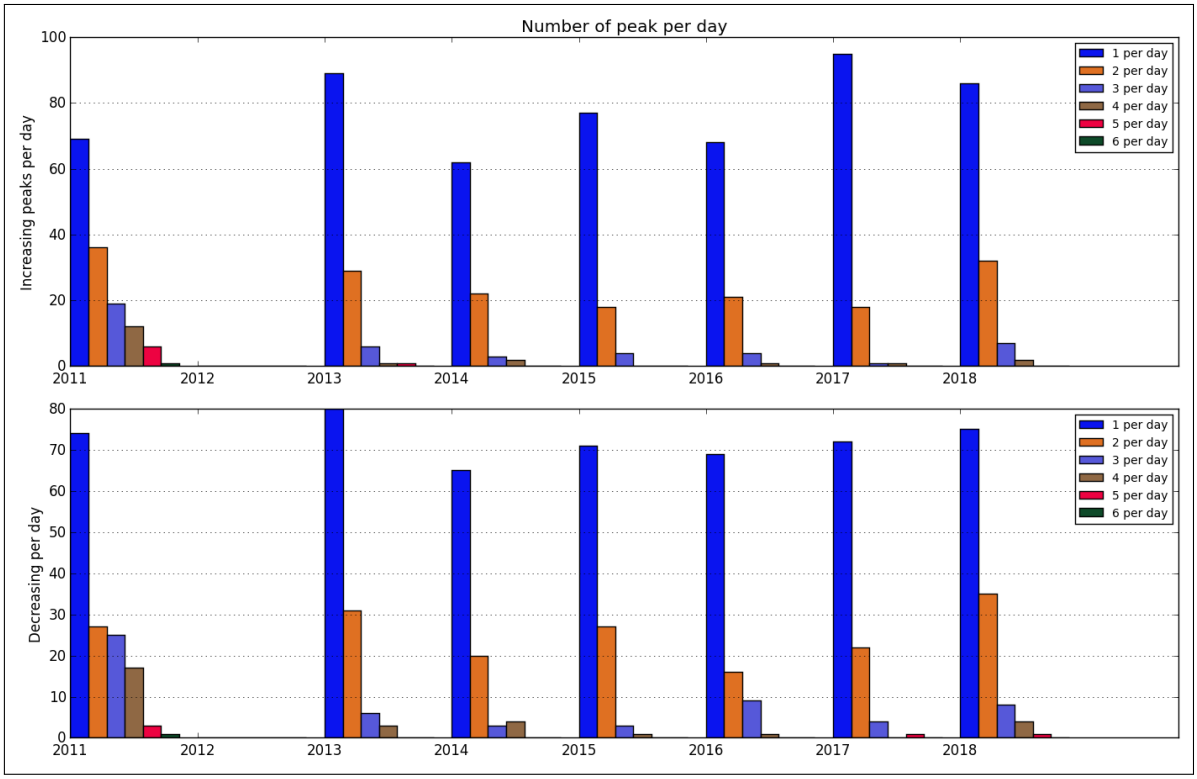

Figure A.53.263: Number of peaks per day

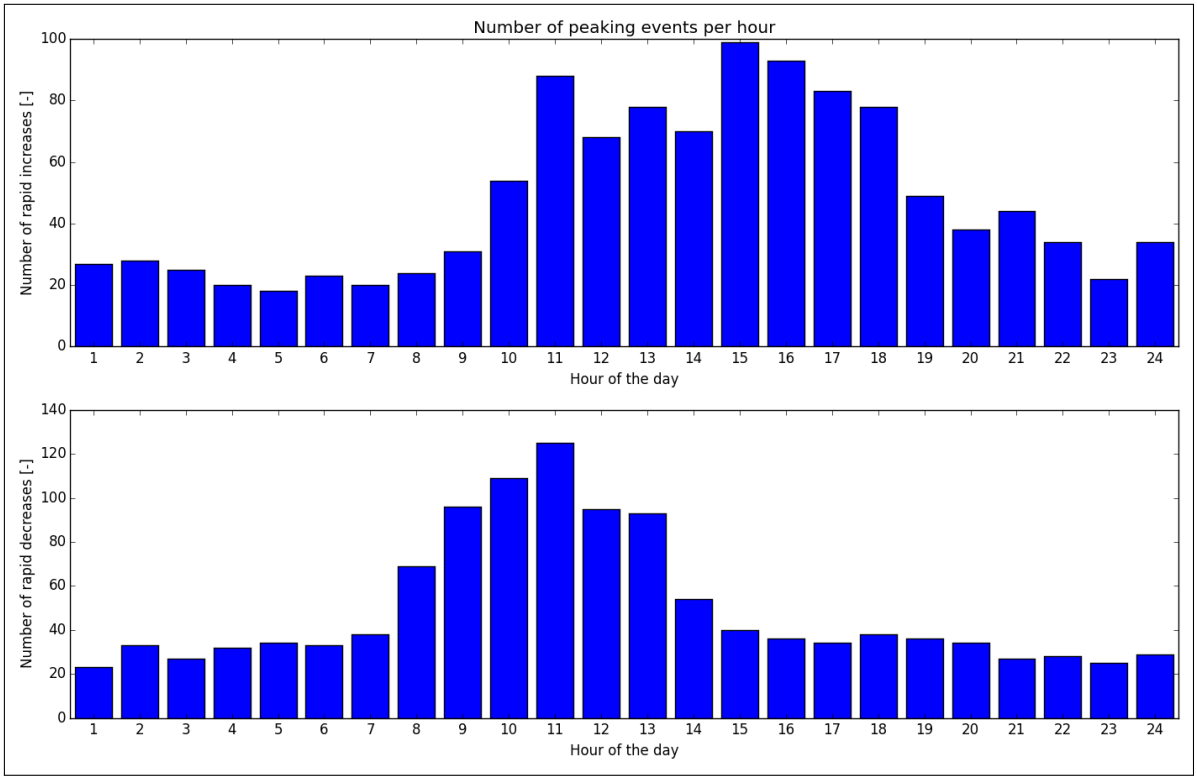

Figure A.53.264: Distribution of peaks throughout day

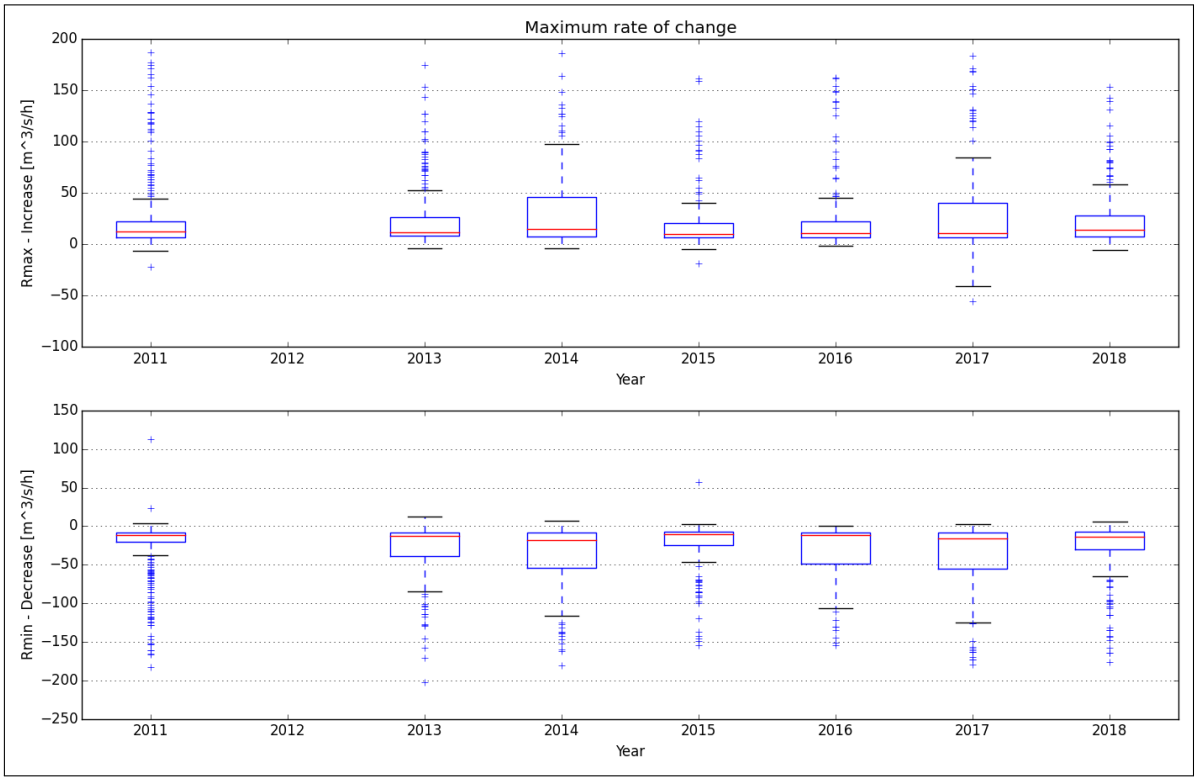

Figure A.53.265: Maximum rate of change

A.54. Einunna

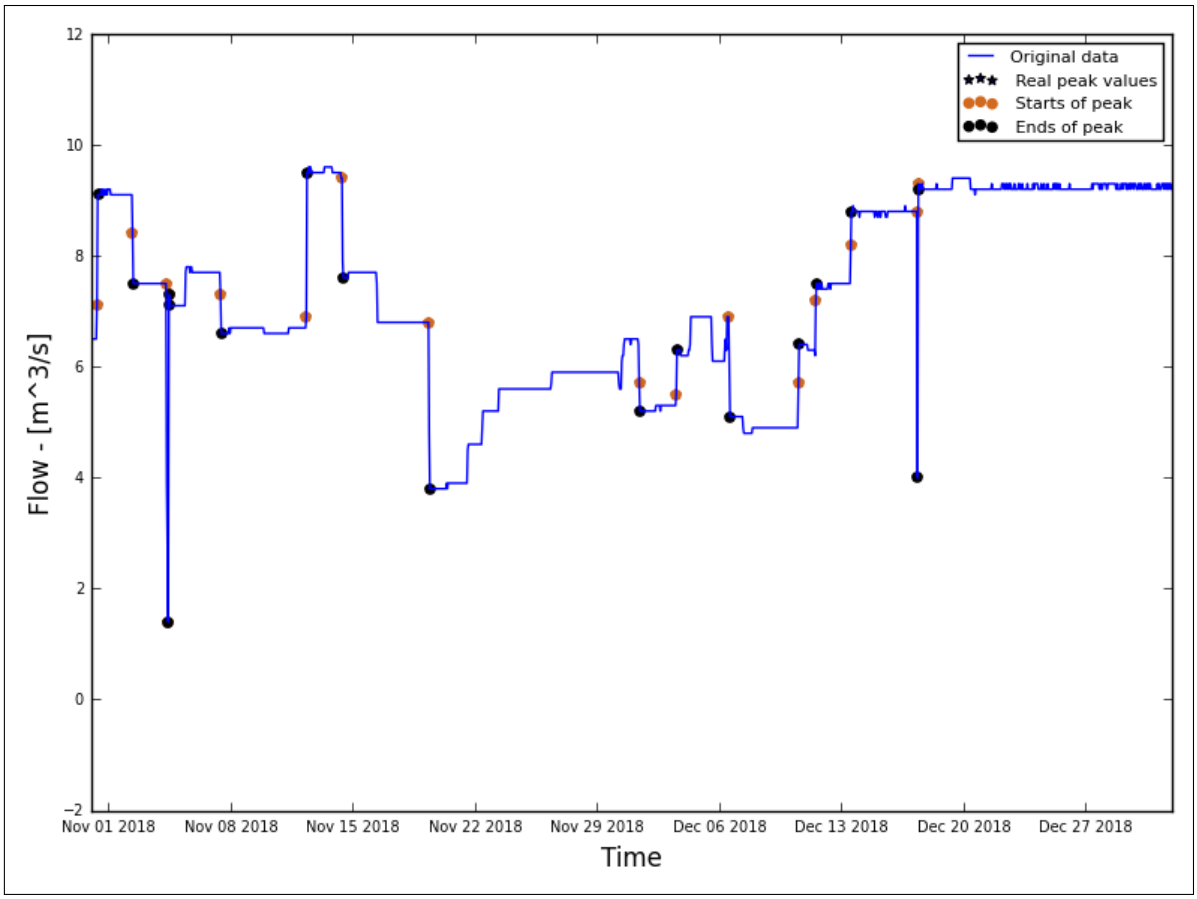

Figure A.54.266: Hydrograph of the last two months of the recorded data

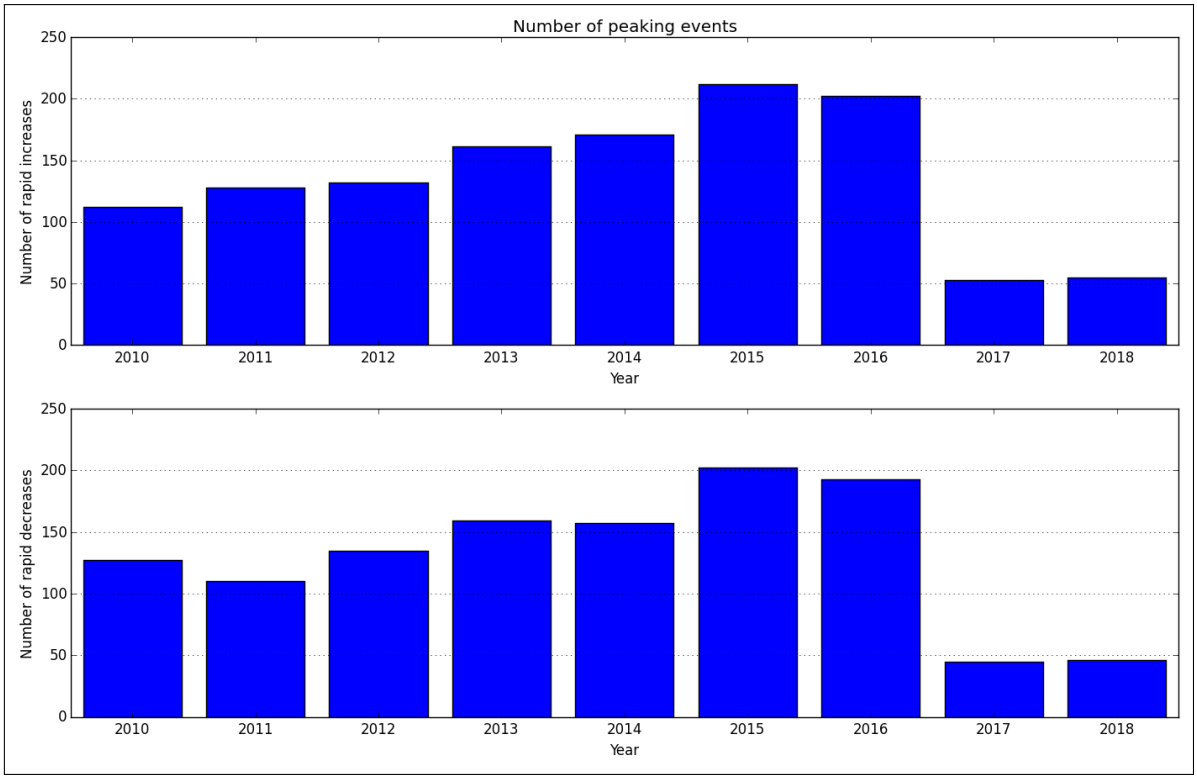

Figure A.54.267: Average annual number of increased/decreased peaks

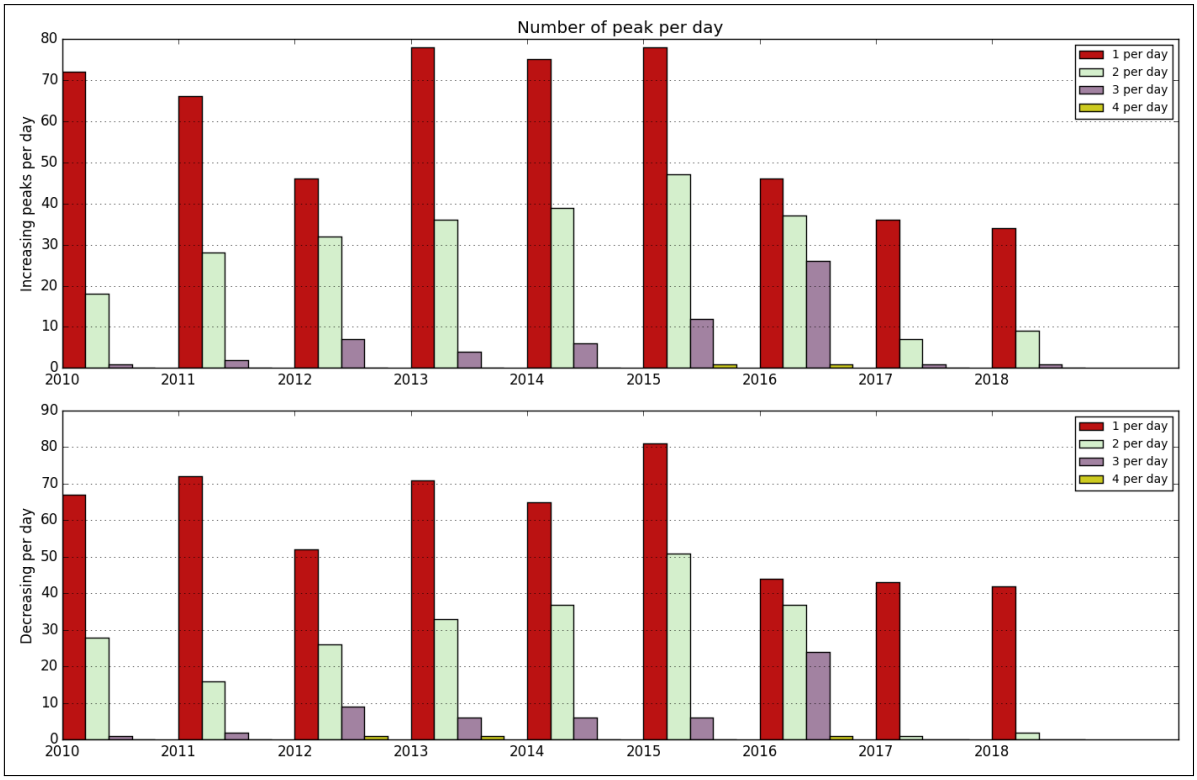

Figure A.54.268: Number of peaks per day

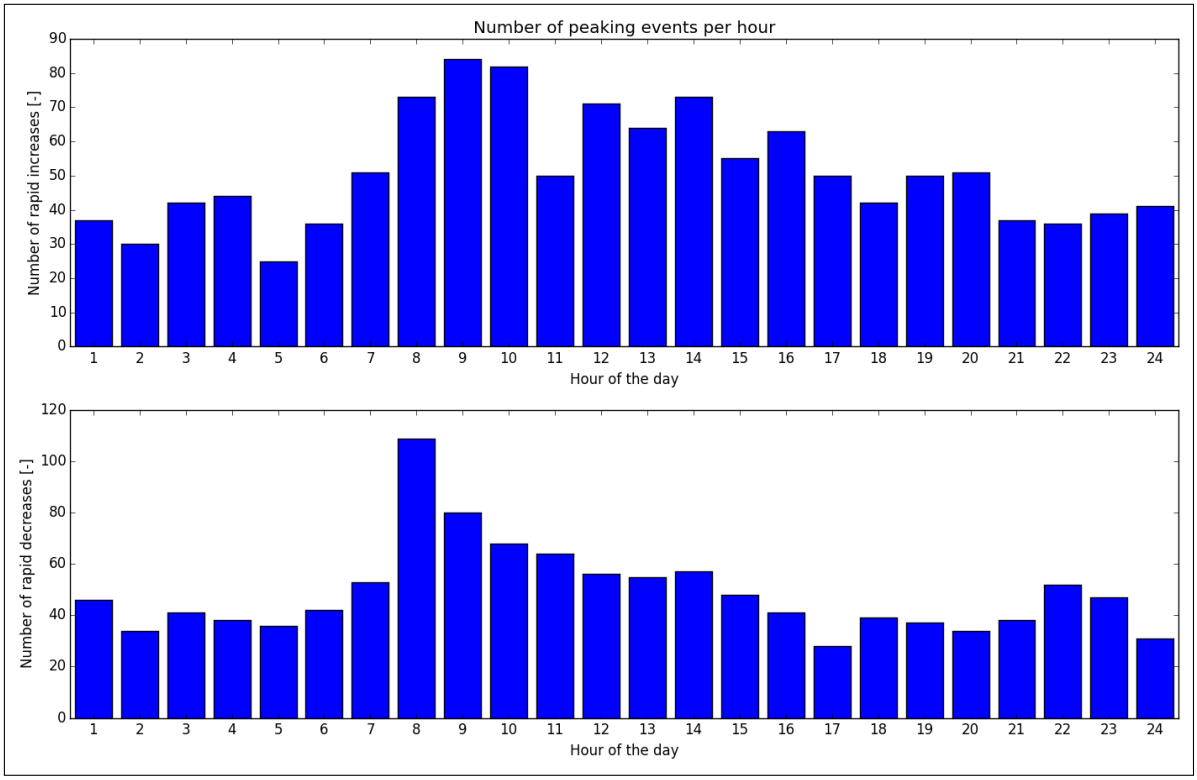

Figure A.54.269: Distribution of peaks throughout day

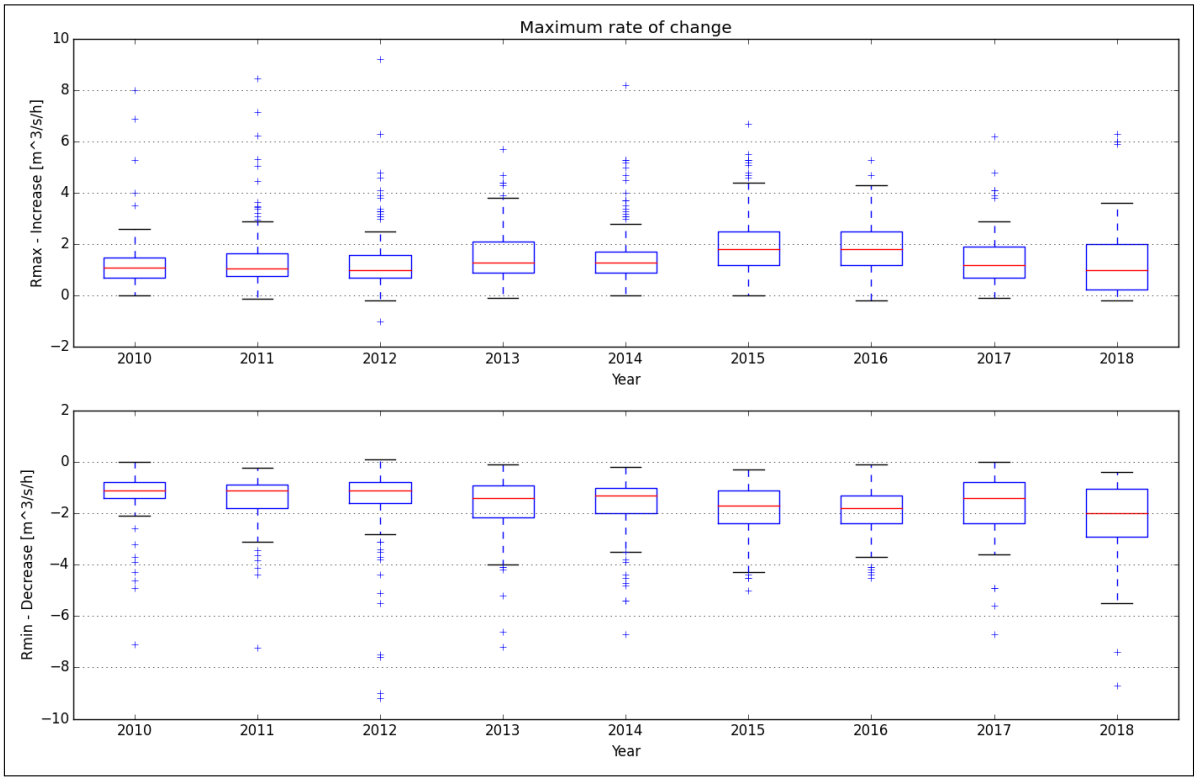

Figure A.54.270: Maximum rate of change

A.55. Savalen

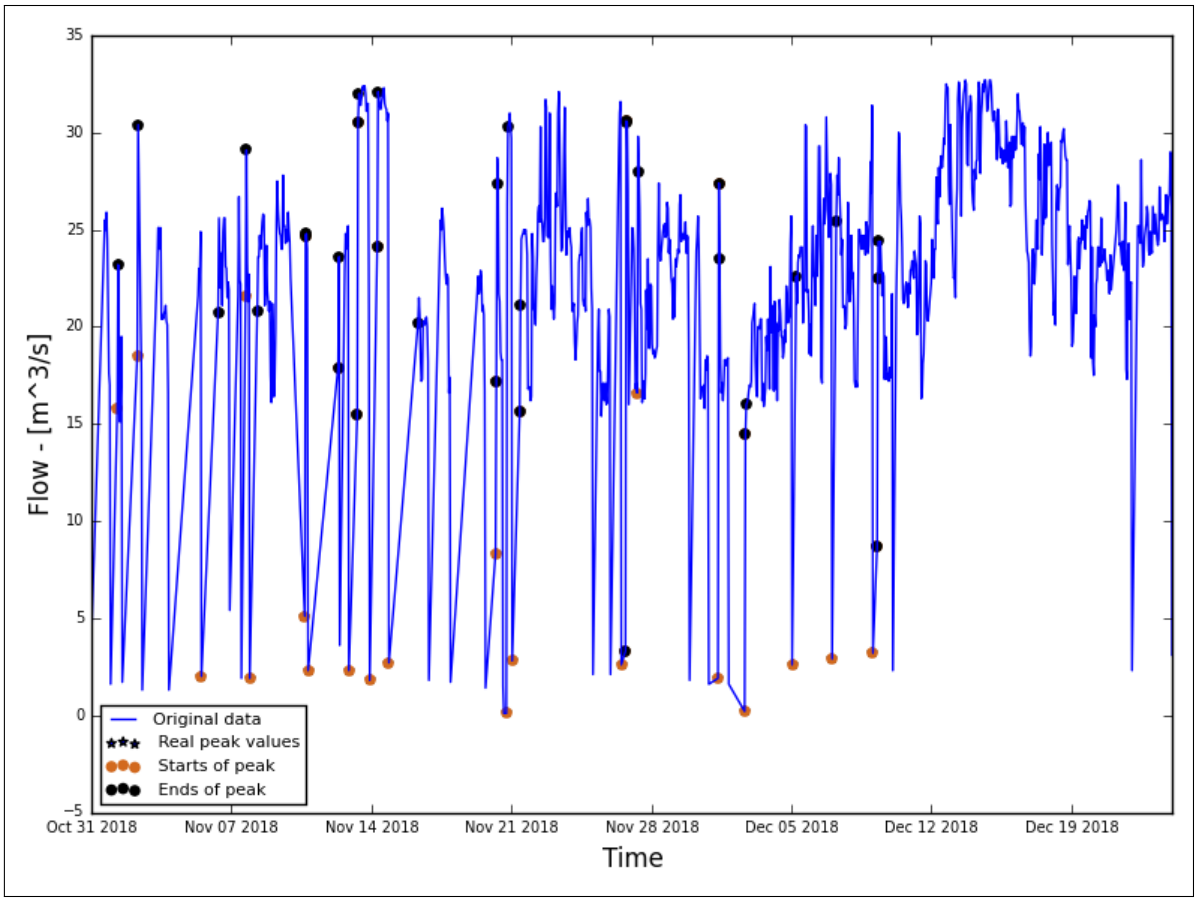

Figure A.55.271: Hydrograph of the last two months of the recorded data

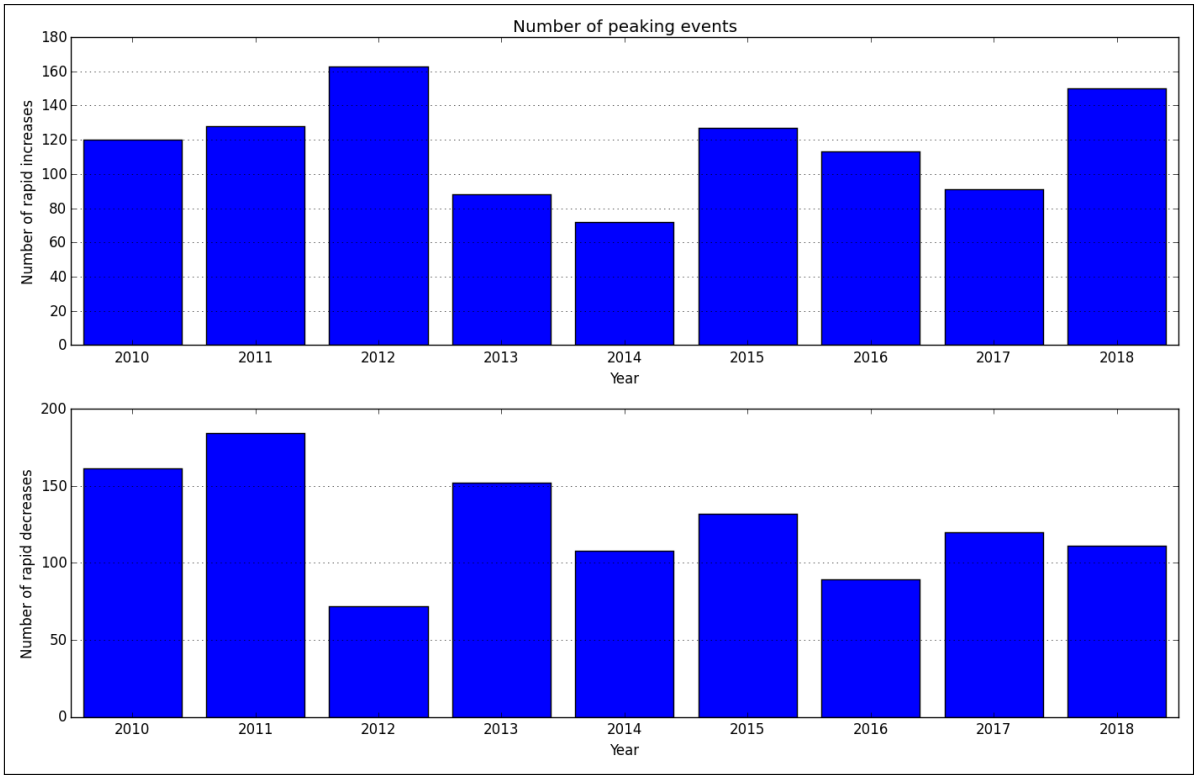

Figure A.55.272: Average annual number of increased/decreased peaks

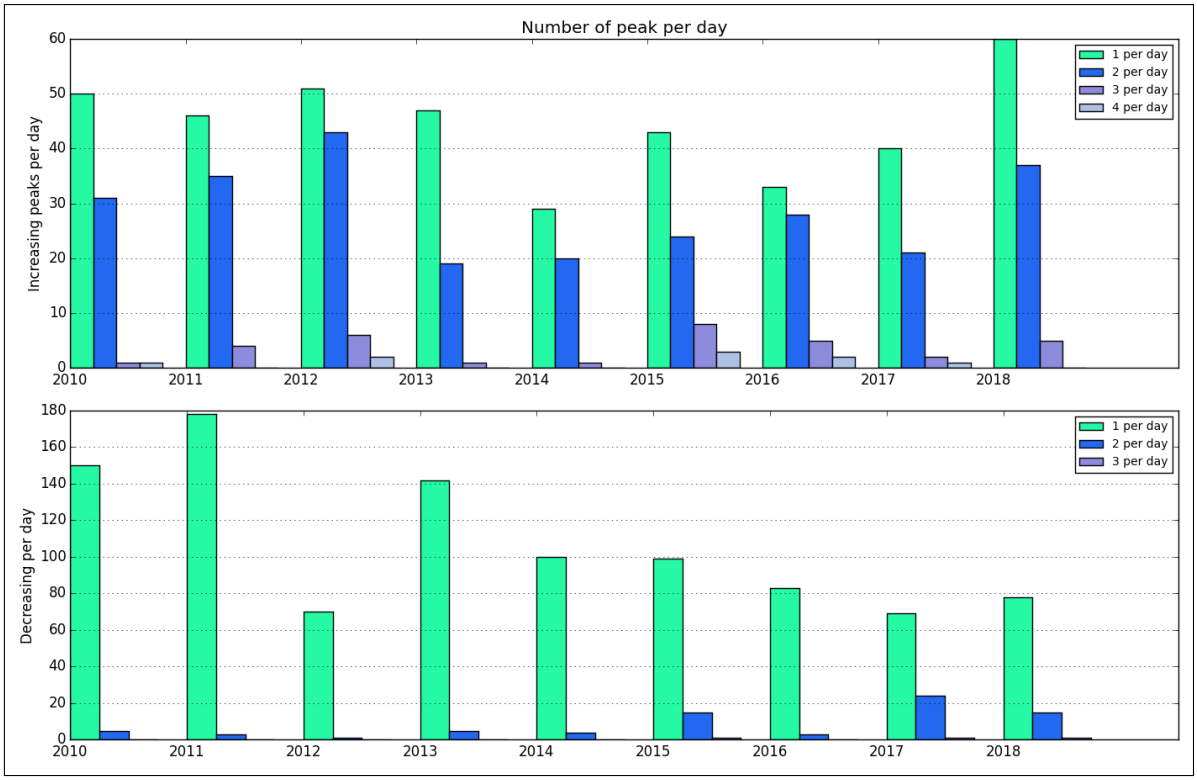

Figure A.55.273: Number of peaks per day

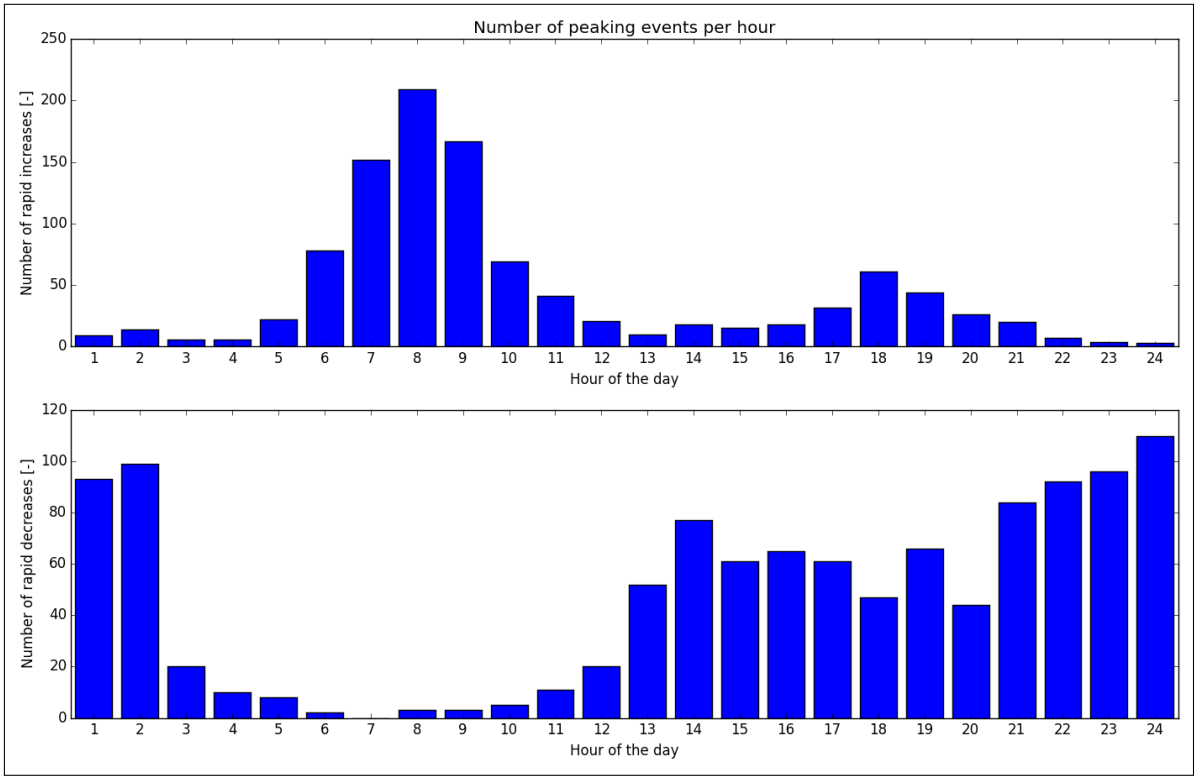

Figure A.55.274: Distribution of peaks throughout day

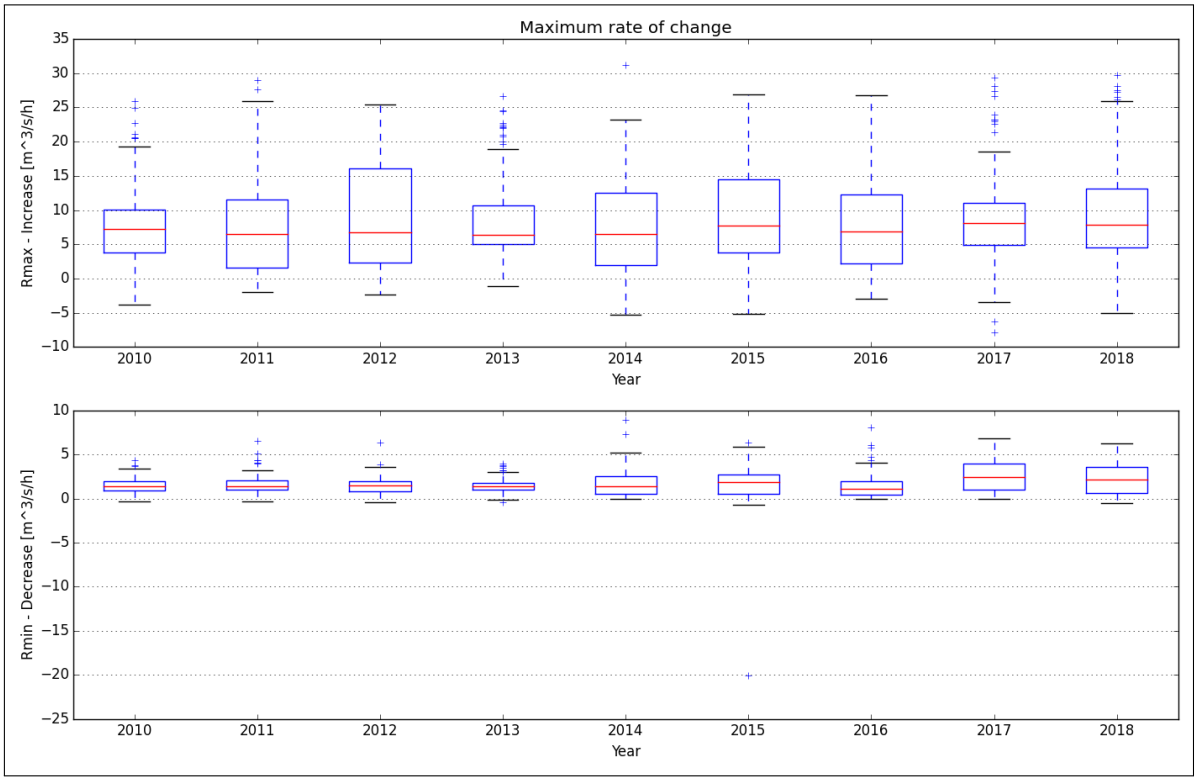

Figure A.55.275: Maximum rate of change

B. STATISTICAL ANALYSIS

B.1. Multiple linear regression results

In this section the results representing our data distribution will be presented. At first section results will show variable distribution when its being fit to a normal distribution Then transformation that was performed to fit it more in order to make it as normal distributed as possible.

B.1.1 Initial normal distribution fitting without transforming

Figures in this section represents variables fitting for a normal distribution without any transformation. Results shows that a transformation is necessary for most of the variables in order to limit the level of skewness.

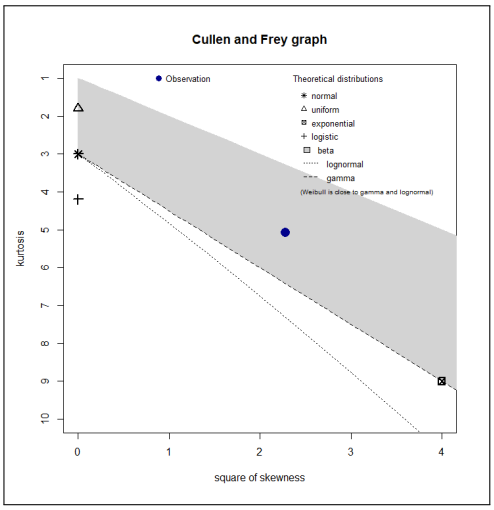

Figure B.1.1: Cullen and Frey graph for HP1

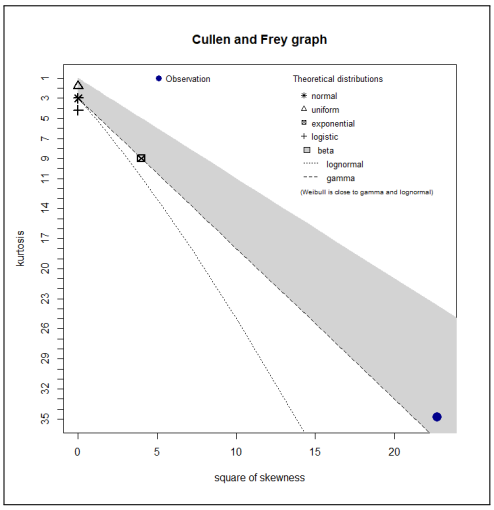

Figure B.1.2: Cullen and Frey graph for HP2

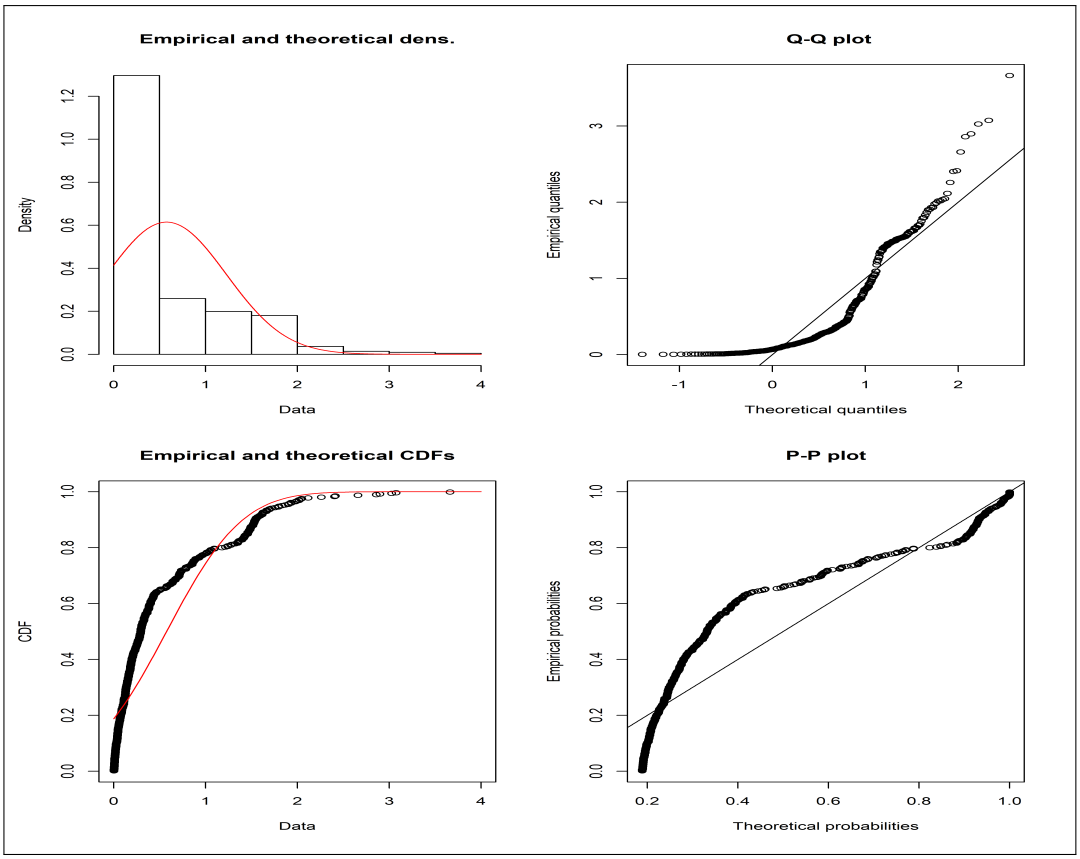

Figure B.1.3: Fitting distribution summary for HP1 before transformation

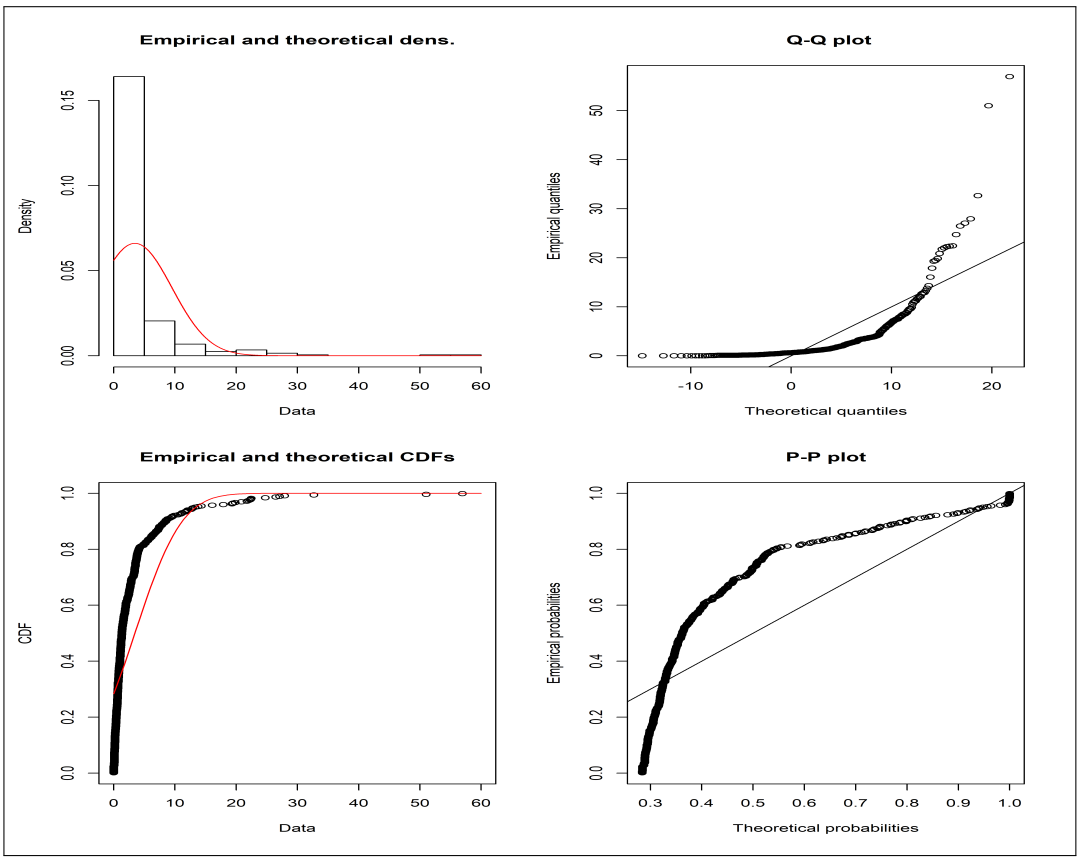

Figure B.1.4: Fitting distribution summary for HP2 before transformation

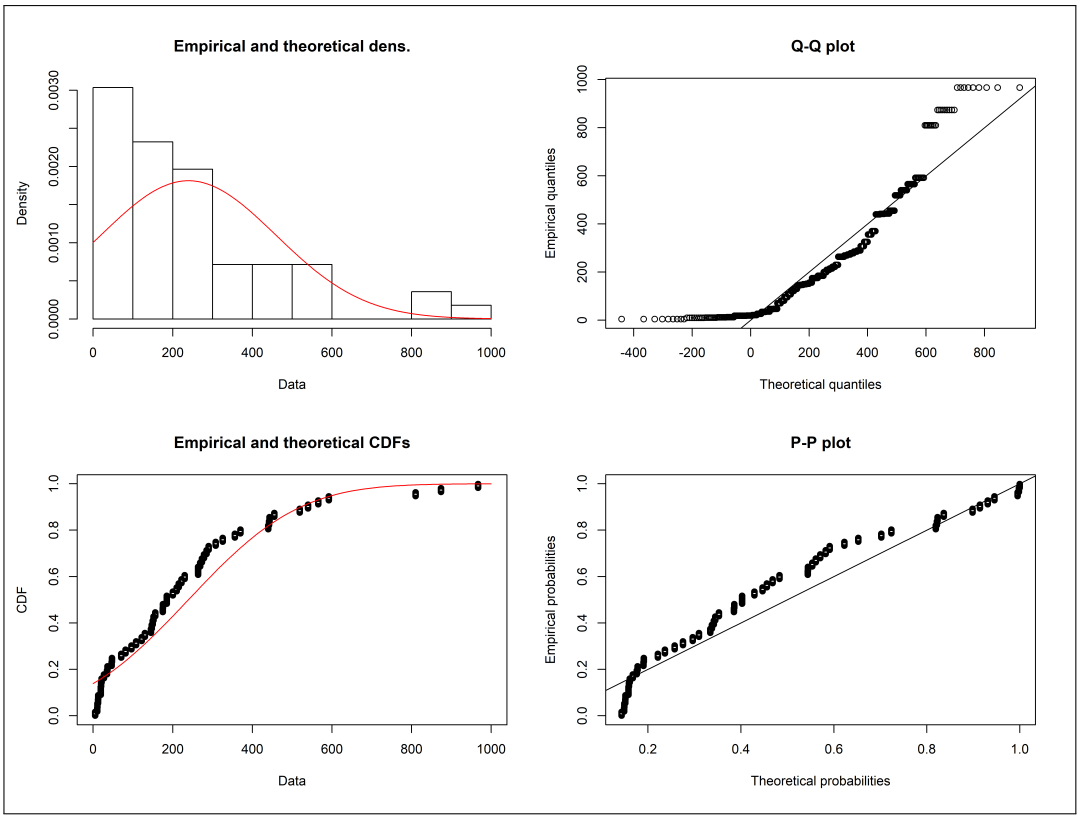

Figure B.1.5: Fitting distribution summary for head of HP before transformation

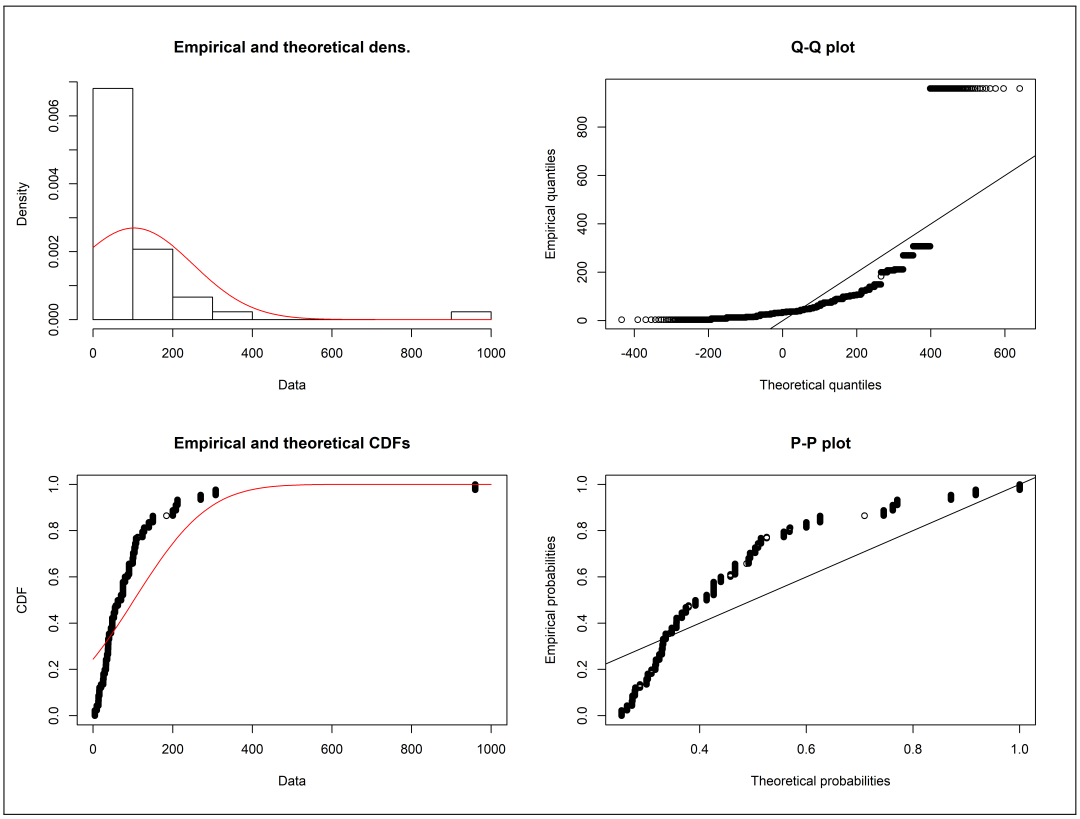

Figure B.1.6: Fitting distribution summary for max capacity of HP before transformation

B.1.2 Final data fitting for normal distribution

After iterative trials in order to fit our variables to be normally distributed as possible figures below shows our normal distribution fitting results with the transformation that was used for each variable.

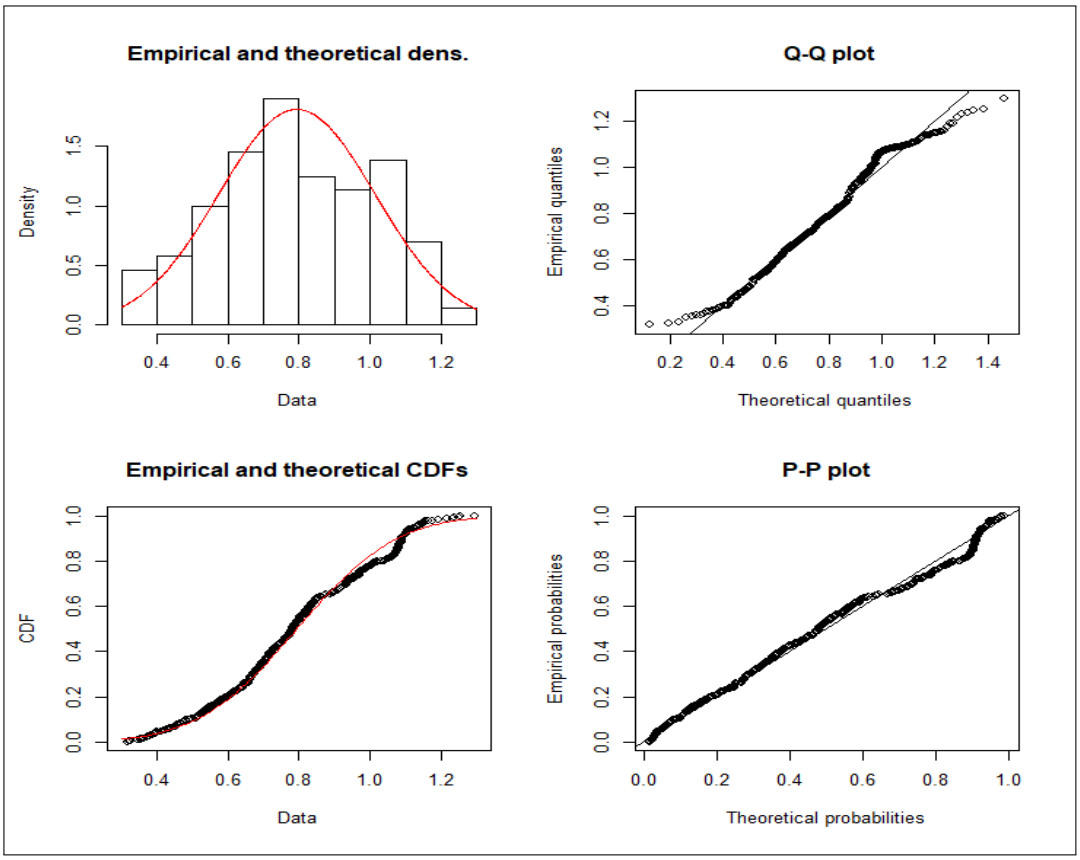

Figure B.1.7: Fitting distribution summary for HP1 after using 5th root transformation

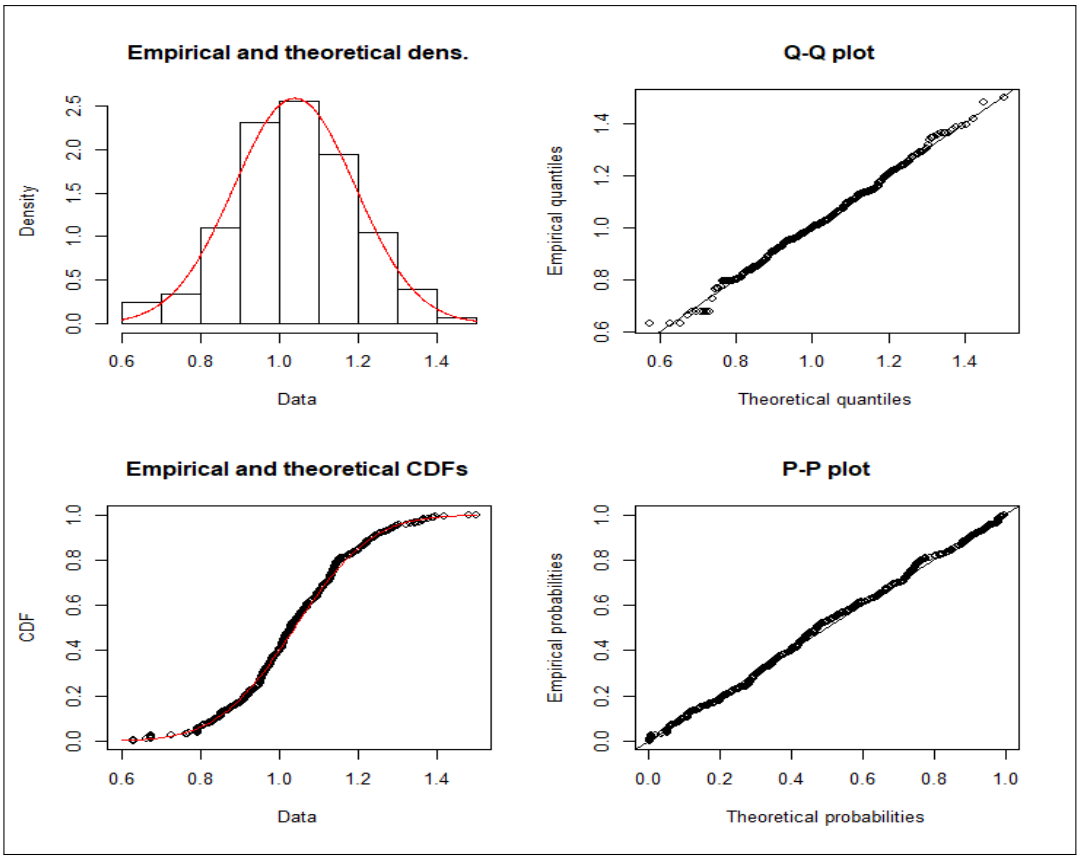

Figure B.1.8: Fitting distribution summary for HP2 after using 10th root transformation

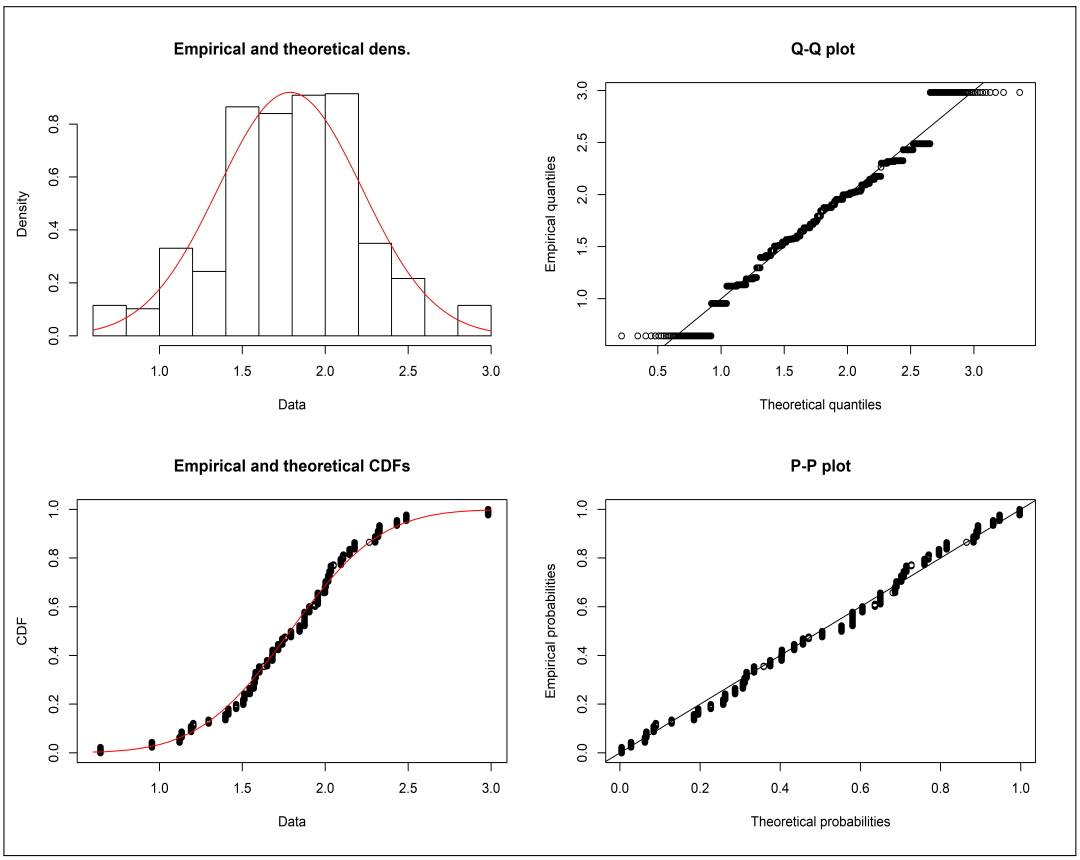

Figure B.1.9: Fitting distribution summary for max capacity after using $\log_{10}$ transformation

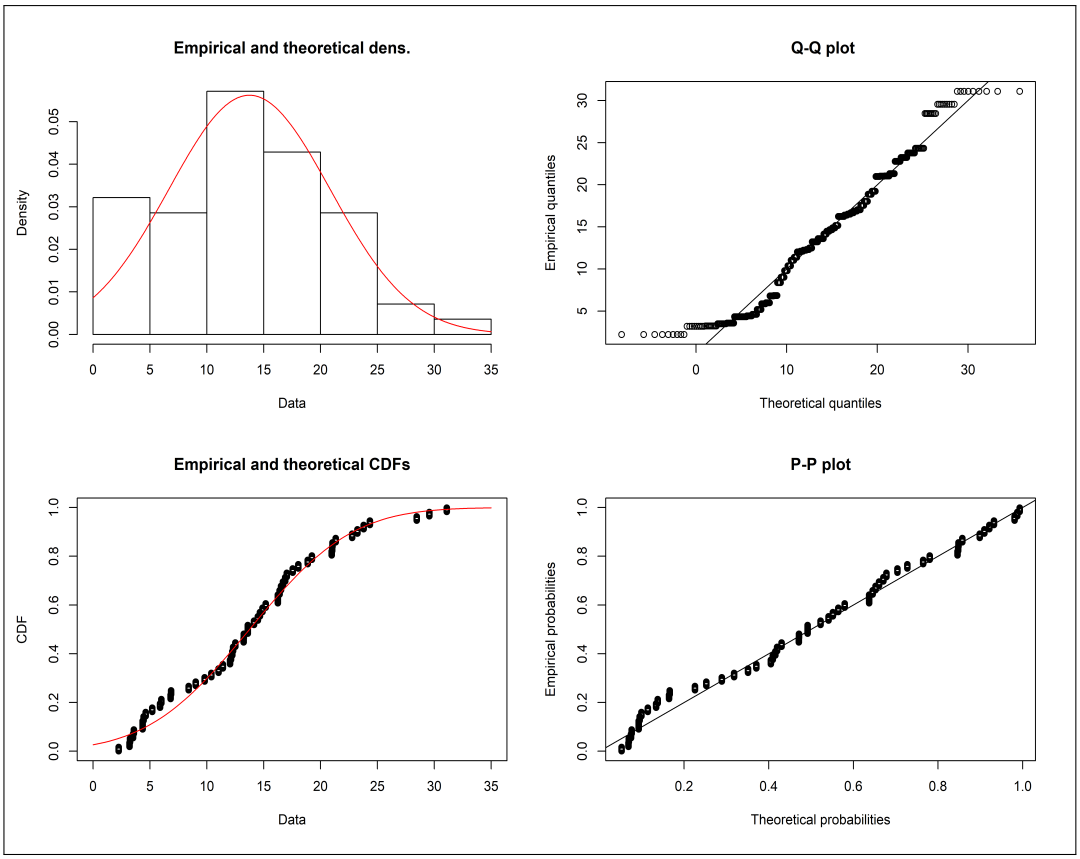

Figure B.1.10: Fitting distribution summary for head after using square root transformation